DIVERSE CATALYTIC ACTIVATION OF SMALLEST CARBOCYCLES TOWARDS VALUABLE CHIRAL AND ACHIRAL ORGANIC SCAFFOLDS

A Thesis Submitted

In Partial Fulfillment of the Requirements

for the Degree of

DOCTOR OF PHILOSOPHY

by

"ARIJIT HAZRA"

(2019CYZ0004)

DEPARTMENT OF CHEMISTRY

INDIAN INSTITUTE OF TECHNOLOGY ROPAR

June, 2024

Arijit Hazra: *Diverse Catalytic Activation of Smallest Carbocycles Towards Valuable Chiral and Achiral Organic Scaffolds*

DEDICATED

TO

MY FAMILY

&

ALMIGHTY

Declaration of Originality

I hereby declare that the work which is being presented in the thesis entitled "**DIVERSE CATALYTIC ACTIVATION OF SMALLEST CARBOCYCLES TOWARDS VALUABLE CHIRAL AND ACHIRAL ORGANIC SCAFFOLDS***"* has been solely authored by me. It presents the result of my own independent investigation/research conducted during the time period from to July, 2019 to May, 2024 under the supervision of Dr. Prabal Banerjee, Associated Professor, IIT Ropar. To the best of my knowledge, it is an original work, both in terms of research content and narrative, and has not been submitted or accepted elsewhere, in part or in full, for the award of any degree, diploma, fellowship, associateship, or similar title of any university or institution. Further, due credit has been attributed to the relevant state-of-the-art and collaborations with appropriate citations and acknowledgments, in line with established ethical norms and practices. I also declare that any idea/data/fact/source stated in my thesis has not been fabricated/ falsified/ misrepresented. All the principles of academic honesty and integrity have been followed. I fully understand that if the thesis is found to be unoriginal, fabricated, or plagiarized, the Institute reserves the right to withdraw the thesis from its archive and revoke the associated Degree conferred. Additionally, the Institute also reserves the right to appraise all concerned sections of society of the matter for their information and necessary action. If accepted, I hereby consent for my thesis to be available online in the Institute's Open Access repository, inter-library loan, and the title & abstract to be made available to outside organizations.

Signature

Name: Arijit Hazra

Entry Number: 2019CYZ0004

Program: PhD.

Department: Chemistry

Indian Institute of Technology Ropar

Rupnagar, Punjab 140001

Date: 12.08.2024

Acknowledgments

Foremost, I am grateful to the Indian Institute of Technology Ropar, Punjab, India for giving me an opportunity to pursue the Ph.D. program. I would like to thank some individuals in my life both from inside the institute and outside of it for their constant support and encouragement throughout this journey. First of all, I express my profound gratitude to my thesis supervisor **Dr. Prabal Banerjee**, Associate Professor, Department of Chemistry, IIT Ropar for providing me a scope to work under his supervision. His constant support, guidance, and motivation helped me continue my research from the beginning. There was a time when I faced some setbacks related to the research work which distressed and demotivated me but he was always there to encourage me and show me the right direction to handle and overcome the issues. Moreover, his belief in me and allowing me to work freely in the lab strengthened my self-confidence and helped me develop experimental skills to execute several projects independently. Other than these, his dedication to research, humanity, and compassionate behavior drives me to perceive the deeper aspects of life. I express my everlasting gratitude towards him.

I am indebted to Ministry of Human Resource and Development (MHRD), Government of India and IIT Ropar for my doctoral research fellowship. I express my sincere thanks to **Prof. Rajeev Ahuja**, Director, IIT Ropar and **Prof. Sarit K. Das,** Ex-Director, IIT Ropar, **Dr. Pushpendra Pal Singh** (Dean Research and Development), **Dr. Arun Kumar** (Dean Student Affairs) **Dr. Dinesh K.S.** (Officiating Registrar) for providing all the required infrastructural facilities for carrying out my research work.

I would also like to thank my doctoral committee members **Dr. Avijit Goswami**, **Dr. Indranil Chatterjee**, **Dr. Srivatsava Naidu**, and chairperson **Dr. T. J. Dhilip Kumar** for their feedback, suggestions, and valuable inputs during the presentations and other times. A special thanks to **Dhilip sir** for the nice collaboration during my research work. I sincerely thank the present head of the department (HOD) **Dr. Tharamani C.N**. and all the other faculty members of the Department of Chemistry for their heartfelt support and invaluable guidance.

I extend my thanks to all the supporting staff of the department of Chemistry **Mr. Nagendra ji**, **Mr. Sushil ji**, and **Ms. Samita Saini** for helping me directly or indirectly in my dissertation work. My special thanks to **Mr. Manish Kumar** (for recording NMR data in time), **Mr. Kamlesh Satpute** (for helping in the analysis of single crystal data), **Mr. Nazre Heyat**, **Dr. Nilotpal**, and **Ms. Hanspreet Kaur** (for recording HRMS data). A special thanks to non-technical supporting staff **Mrs. Poonam Kataria** for always helping me with administrative-related issues. I am also highly thankful to **Dr. Debaprasad Mandal** and his team, for guiding us regarding lab safety.

I am extremely grateful to my senior lab mates **Dr. Priyanka Singh**, **Dr. Rohit Kumar Varsanaya**, **Dr. Raghunath Dey, Dr. Pankaj Kumar**, **Dr. Irshad Maajid Taily**, **Dr. Debarshi Saha**, and **Dr. Navpreet Kaur** for their guidance and support throughout this journey. A special thanks to **Raghu da** for the initial training in the lab works and fruitful discussion regarding research works. Another special thanks to **Debarshi da** for being an elder brother and helping with various research and lab-related problems from the very beginning of this journey. A special thanks to **Navpreet** di for being nice to me from the initial days to the last and also for including me in her research work. I am extremely thankful to other lab members **Rakesh**, **Neeraj**, **Nakshatra**, **Shiv**, **Vikas**, **Rohan**, **Chandan**, **Neelam**, **Umesh**, and **Dr. Nilima** for maintaining a supportive and joyful environment in the laboratory. I also gratefully acknowledge the support of M.Sc students in our lab **Naveen**, **Kritika Singh**, **Sumitra**, **Manish**, **Prince**, **Tanmay**, **Biswadeep**, **Kritika Verma**, **Nidhi**, and

Suman for bringing a happy-go-lucky surrounding in the lab. A special thanks to Tanmay for his hard work and contribution to my research.

The journey of my Ph.D. would not be memorable enough without having friends in the IIT. I am very grateful to all my fellow companions **Rakesh**, **Sandeep**, **Priyank**, **Ritika**, **Akansha**, **Man**, **Saurav**, **Gulshan**, **Ganesh**, **Anoop**, **Vatan**, **Vishal**, **Shambhu**, and **Sweta**. A special thanks to **Rakesh** for some memorable trips, badminton games, and late-night parties. The sense of togetherness that we share inside and outside the campus will be cherished forever. I thank you all from the bottom of my heart for those parties, short trips, and discussions.

I would also like to acknowledge some other seniors and juniors from other research groups at this institute **Dr. Suman da**, **Dr. Sourav da** (for helping in research and also for various fun activities like cooking) **Hrishikesh** (being a nice friend and partner in late night snacks and badminton), **Dr. Prasoon** and **Manisha di** (being companions in some conferences inside and outside of India), **Arnab** and **Arijit** (being partners for worshiping in Saraswati puja), **Himanshu** and **Dr. Pankaj Goutam** (for badminton). A special thanks to **Apoorv** for helping me with computational studies within a very short time in my research.

The greatest strength and support in my life is certainly my family. The journey of the Ph.D. could not have been completed smoothly without the unconditional love, support, encouragement, and blessings of my family members. I am forever grateful to my father **Mr. Ranjit Kumar Hazra** and my mother **Mrs. Manasi Hazra** for the sacrifices they have made throughout their lives for me and our family. It's a blessing to have loving and friendly parents like you who have always given me moral support and freedom to do whatever I wanted in life which made me self-confident and provided me the courage to move forward in life. I also want to thank my two elder brothers **Monojit Hazra** and **Dr. Vivekananda Hazra** for their love, care, support, and various suggestions. I would like to thank my two sister-in-laws **Rupa Mukherjee** and **Supriti Chatterjee** for their care and affection and also to my two adorable nephews **Bilu** and **Biku** for their love and fondness. I also thank my fiancée **Ria Goswami** from the core of my heart for being my best friend and best partner. Without her consistent emotional support throughout these years, the journey of my Ph.D. would not have been easier. I express my profound gratitude to you for your overwhelming love and encouragement in my ups and downs and hope I will be able to be with you forever in every aspect of your life hereafter.

Finally, I would like to thank the almighty for bestowing divine grace during all these years and including so many interesting people in my life.

Arijit Hazra

Certificate

This is to certify that the thesis entitled **"Diverse Catalytic Activation of Smallest Carbocycles Towards Valuable Chiral and Achiral Organic Scaffolds"** submitted by **Arijit Hazra (2019CYZ0004)** for the award of the degree of "**Doctor of Philosophy"** of Indian Institute of Technology Ropar, is a record of bonafide research work carried out under my guidance and supervision. To the best of my knowledge and belief, the work presented in this thesis is original and has not been submitted, either in part or full, for the award of any other degree, diploma, fellowship, associateship or similar title of any university or institution.

In my opinion, the thesis has reached the standard fulfilling the requirements of the regulations relating to the Degree.

Signature of the Supervisor

Dr. Prabal Banerjee

Department of Chemistry

Indian Institute of Technology Ropar

Rupnagar, Punjab 140001

Date: 09/08/2024

Lay Summary

Engineering complex organic scaffolds from simple and small chemical components is an indispensable area of synthetic organic chemistry. Over the years, a huge number of methodological developments have been accomplished in this direction. Though the traditional methods have been employed in the last century which have their own advantages but they are sometimes expensive and deal with some serious environmental threats like the generation of toxic wastes. So, in this 21st century, chemists came up with some environmentally benign techniques like organocatalysis, electrocatalysis, and photoredox catalysis. Keeping the importance of sustainability in mind, some novel synthetic protocols have been developed by utilizing the smallest cyclic organic molecules i.e. cyclopropane and cyclobutane. As these two molecules can be activated by various catalytic approaches, the work in this thesis describes the application of both conventional and modern catalytic techniques for the construction of several valuable organic frameworks. Chapter 1 discusses the two smallest carbocycles along with the different catalytic activation methods that have been utilized over the years. Chapter 2 deals with modern and greener organocatalysis for the activation of *racemic* cyclopropane carbaldehydes towards the construction of enantioenriched heterocycles. The work in Chapter 2A discloses the asymmetric organocatalytic (3+3) cycloaddition of cyclopropane carbaldehydes with aryl hydrazones for the synthesis of chiral tetrahydropyridazine derivatives. A new asymmetric approach for the enantioinduction has been developed and a computational study provides important insights into the mechanism of intriguing aryl migration. Chapter 2B demonstrates the organocatalytic (3+3) cycloaddition of cyclopropane carbaldehydes with *ortho*-substituted nitrones to access chiral oxazinanes. Additionally, *ortho*-hydroxy substituted nitrones lead to the formation of novel tetrahydrochromeno-1,2-oxazine scaffolds. A different kind of asymmetric approach was encountered in this enantioselective transformation. Chapter 3 unfolded the tandem activation of the two smallest carbocycles i.e. cyclopropane diester and 3-ethoxy cyclobutanone to achieve γ-naphthyl butyric acid derivatives. Here, the conventional metal containing Lewis acid catalysis has been employed which can effectively activate both the cyclopropane and cyclobutane derivatives. Chapter 4 represents the Brønsted acid-catalyzed activation of 3-ethoxy cyclobutanones to deliver 2,8-dioxabicyclo[3.3.1]nonane derivatives. While toxic metals or metal-containing catalysts are usually employed for the construction of complex organic scaffolds from this type of cyclobutanones, the designed strategy utilizes the metal-free and mild Brønsted acid to furnish heteroatom-containing bicyclic molecules.

Abstract

Chapter 1. Two smallest carbocycles donor-acceptor cyclopropanes and cyclobutanones and their activation by different catalysis

In organic chemistry, carbocycles are the cyclic molecules where all the atoms composing the cycle are carbon atoms. They are ubiquitous in biologically active molecules, natural products, pharmaceuticals, and organic materials. The construction of intriguing carbocyclic frameworks like fused rings, spirocycles, and carbocycles containing multiple stereocenters always fascinated the synthetic community. The carbocycles can be of various ring sizes and among them, the three and four-membered carbocycles are called cyclopropanes and cyclobutanes respectively. These two carbocycles are the smallest and also among the most studied ones due to their intrinsic properties and reactivities. Over the years, these two smallest carbocycles achieved remarkable attention owing to their prevalence in a large number of bioactive molecules and natural products. Numerous catalytic and non-catalytic strategies have been developed over the past few decades for the construction of several chiral and achiral organic molecular frameworks via activation of these two carbocycles utilizing their strain-releasing reactivity. Different types of cyclopropanes and cyclobutanes are available in the literature according to their substitution pattern. Among them, vicinally substituted donor-acceptor cyclopropanes are the most explored ones. From the beginning of this 20th century, the field of donor-acceptor cyclopropanes experienced a renaissance as different catalytic activation methodologies have been developed so far to construct complex organic scaffolds. Though most of them deal with transition metal containing Lewis acid catalysis, a handful of examples could be found by environmental friendly approach like organocatalysis, whereas modern and sustainable methodologies like electro-organic and photoredox catalysis are rarely studied. Surprisingly, organocatalytic activation of *racemic* donor-acceptor cyclopropanes for the synthesis of chiral heterocyclic frameworks remains unexplored. On the other hand, out of different types of cyclobutanes, 3-donor cyclobutanones are widely studied via transition metal catalysis, Lewis acid catalysis, and even organocatalysis. However, no catalytic activation strategy has been still employed to coalesce the reactivities of the two smallest carbocycles, and catalytic Brønsted acid activation of 3-donor cyclobutanones is also not explored till date.

Chapter 2: Asymmetric Organocatalytic Activation of Cyclopropane Carbaldehydes Towards the Construction of Enantioenriched Heterocycles

Donor-acceptor cyclopropane carbaldehydes have not been previously employed to synthesize enantioenriched heterocyclic scaffolds via secondary amine organocatalysis. Here, we have demonstrated an asymmetric cycloaddition reaction of cyclopropane carbaldehydes with two

different dipolar systems to construct valuable heterocyclic molecules. This chapter is divided into two parts. Chapter 2A will discuss (3+3) cycloaddition of cyclopropane carbaldehydes with aryl hydrazones to obtain chiral tetrahydropyridazine derivatives with good enantioselectivities. Whereas, chapter 2B will further expand the scope of the similar (3+3) cycloaddition with another dipolar system *ortho*-substituted nitrone to furnish enantioenriched oxazinanes.

Chapter 2A: Organocatalytic Activation of Donor−Acceptor Cyclopropanes: A Tandem (3+3)-Cycloaddition/Aryl Migration toward the Synthesis of Enantioenriched Tetrahydropyridazines

The construction of complex chemical entities from simpler building blocks is an essential and evergreen area of organic chemistry. Over the decades, various building blocks have been studied and utilized to access a large number of complex compounds using their typical reactivities. In this realm, donor−acceptor cyclopropane (DAC), a unique three-carbon building block, has been extensively employed to synthesize various important compounds in recent times. An array of cycloadditions of DACs with various dipoles, dienes, and double bonds have been reported. However, these methodologies are pre-eminently associated with metal-containing Lewis acid catalysts. In contrast, their enantioselective versions are less explored. Our laboratory has been working on the reactivity of DACs for more than a decade and developed various methodologies for the one-step synthesis of several carbo- and heterocycles. Keeping the unexplored enantioselective cycloaddition of DACs in mind, we envisioned that a chiral amine organocatalyst could asymmetrically activate cyclopropane carbaldehyde through the iminium ion pathway to render enantioselective cycloaddition. It should be noted that in the previous organocatalytic enantioselective ring-opening reactions, the cyclopropane carbaldehydes are *meso* in nature, and there has been no such report of organocatalytic enantioselective transformations with their racemic versions. In this chapter, we report the first asymmetric (3 + 3)-cycloaddition of *racemic* cyclopropane carbaldehyde with aryl hydrazones via organocatalytic activation. We commenced our optimization study with prolinol organocatalyst and obtained tetrahydropyridazine with an exocyclic double bond, where an intriguing aryl migration occurred just after the cycloaddition. After executing extensive optimization studies, we found that refluxing the reaction in carbon tetrachloride solvent in the presence of 30 mol% of prolinol gave the product in satisfactory yield with excellent enantiomeric excess. A wide variety of chiral tetrahydropyridazines were furnished by changing both the cyclopropane carbaldehydes and aryl hydrazones. From the control experiments, it was established that the enantioinduction from the *racemic* substrates has occurred via an unusual matched/mismatched kinetic resolution. It was also established that the ring-opening of cyclopropane followed a stereospecific S_N2 pathway and the unusual 1,3-aryl migration was concerted and intramolecular in nature. Moreover, these findings were supported by computational studies which also unveiled that the aryl migration proceeds via a four-membered transition state.

Chapter 2B: Organocatalytic (3+3)-cycloaddition of *ortho*-substituted phenyl nitrones with aryl cyclopropane carbaldehydes: A facile access towards the synthesis of enantioenriched 1,2-oxazinanes

Nitrogen-containing enantioenriched heterocycles are ubiquitous structural frameworks that are present in a diverse range of biologically active molecules. Among them, chiral 1,2-oxazinanes gathered significant attention owing to their presence in several natural products which exhibit potent biological activities. Therefore, a number of methodologies flourished over the decades for their enantioselective construction by various research groups; however, most of them involve nitrones as a main precursor. Nitrones are one of the most useful and easily available starting materials for the construction of various biologically important nitrogen and oxygen-containing heterocycles. Especially its ability to undergo the 1,3-dipolar cycloaddition has achieved remarkable attention from synthetic organic chemists for the past few decades. In 2005, Sibi and coworkers reported the first enantioselective (3+3)-cycloaddition of nitrones with cyclopropane dicarboxylates in the presence of $Ni(ClO_4)_2$ and chiral ligand to obtain tetrahydro-1,2-oxazines with high enantiomeric excesses. Henceforth, several groups utilized this moiety for the asymmetric cycloaddition reaction to achieve enantioenriched heterocyclic frameworks, however, most of them are (3+2)-type cycloaddition. Evidently, organocatalytic enantioselective (3+3)-cycloaddition reactions with nitrones are still underexplored. We sought to develop an enantioselective (3+3)-cycloaddition of nitrones by utilizing organocatalysis with an appropriate three-carbon reacting partner. In line with the previous work, in this chapter, we employed cyclopropane carbaldehydes with *ortho*-substituted nitrones in the presence of a prolinol catalyst and obtained the (3+3) cycloadducts in good to moderate enantioselectivities. Here, we started our reaction with the same optimized reaction conditions which were established in Chapter 2A and obtained the desired product with moderate yield and enantioselectivity. Though further screening of various other catalysts, solvents, and additives was performed, none of them were fruitful in improving either the yield or the enantioselectivity further. Then, we started to explore the substrate scope variations for both cyclopropane and *ortho*-substituted nitrones. A range of chiral oxazinane derivatives were obtained with moderate yields and enantioselectivities. In all cases, the corresponding aryl aldehydes were also formed as a side product with a considerable amount, eventually decreasing the yield of the desired cycloadducts. Intriguingly, *ortho*-hydroxy substituted nitrones engendered an additional aryl migration and rendered novel tetrahydrochromeno-1,2-oxazine derivatives with moderate enantiomeric excesses. An unusual type of kinetic resolution was believed to be responsible for the enantioinduction.

Chapter 3: Merging two strained carbocycles: Lewis acid catalyzed remote site-selective Friedel-Crafts alkylation of *in situ* generated *β*-naphthol

Over the years, various strained carbo- and heterocycles have been studied extensively to synthesize a myriad of biologically and pharmaceutically important molecular architectures. However, methodologies exploiting a pair of different strained rings have remained underdeveloped. 3-Donor cyclobutanones are one of the important classes of four-membered carbocycles which can generate 1,4-zwitterionic intermediate in the presence of Lewis acid by regioselective cleavage of C2-C3 bond that further can undergo several transformation reactions. On the other hand, donor-acceptor cyclopropanes (DACs) have also similar strain-releasing reactivity. However, reports of merging DACs with other strained ring molecules are still scarce. In the last decade, our group and Trushkov *et al*. have worked on the reactivity of two different strained rings in the presence of Lewis acids and successfully obtained different heterocyclic frameworks. Encouraged by these affirmative experiences, we aim to utilize the reactivity of the two smallest carbocycles and reported the first tandem activation of donor-acceptor cyclopropane and 3-ethoxy cyclobutanone. Here, the Lewis acid-catalyzed rearrangement of cyclobutanones generated the 1-phenyl 2-naphthol *in situ* which further underwent a remote site-selective Friedel-Crafts alkylation via ring-opening of DAC to provide 1,6-disubstituted *β*-naphthol. After screening several reaction conditions, we found that performing the reaction taking 1:1 equivalent of both the starting materials in dichloromethane solvent at -15 °C in the presence of 20 mol% of $SnCl_4$ is the optimized condition for this transformation. Then, substrate scope evaluation for the cyclopropane diester was executed to achieve a series of *γ*-naphthyl butyric acid derivatives with moderate to good yields. Several control experiments were conducted to get insights into the mechanism. From those, it was confirmed that the reaction was undergoing via *in situ* generation of 1-phenyl 2-naphthol derivative. However, diphenyl substitution on the cyclobutanone was also found to be crucial for the in-between rearrangement reaction. Finally, the site selectivity of the *β*-naphthol was also established for this developed protocol. At last, the gram-scale experiment and some late-stage derivatizations were performed to showcase the synthetic utility of our designed methodology.

Chapter 4: Brønsted acid catalyzed cascade ring-opening/cyclization of 3-ethoxy cyclobutanones to access 2,8-dioxabicyclo[3.3.1]nonane derivatives

The development of new methodologies to architect complex heterocyclic frameworks through small molecule activation has always fascinated the synthetic community. Out of numerous heterocycles embedded with two oxygen atoms, 2,8-dioxabicyclo[3.3.1]nonanes gathered significant attraction as these types of bicyclic moieties constitute several flavonoid compounds that serve as important drugs like procyanidin A1, dracoflavan C, dracoflavan D, ephedrannin B, and diinsinin which shows crucial biological activities like antiviral, anti-inflammatory, antioxidant, enzyme inhibition, and anticancer, etc. Various strategies have been engineered in the past few decades for the construction of this rigid diaryl substituted bicyclic ketals but utilization of small carbocyclic moieties has never been applied. 3-donor cyclobutanones remain distinguished among

the four-membered carbocycles for their unique reactivity and explored for the ring-opening, rearrangement, and cycloaddition reactions mostly under Lewis acid catalysis. However, activation of these four-membered synthons via Brønsted acid (BA) catalysis is still scarce, and to the best of our knowledge, no reports were found on BA-catalyzed direct ring-opening or cyclization with these types of 3-ethoxy cyclobutanones. Herein, we report a Brønsted acid-catalyzed cascade ring-opening/cyclization of 3-ethoxy 2-substituted cyclobutanones with naphthols for the formation of 2,8-dioxabicyclo[3.3.1]nonane derivatives. We started our investigation by employing various Brønsted acids and solvents whereas changing the equivalency of substrate and catalyst loading also became fruitful to get our optimized reaction condition. A range of bicyclic ketal derivatives were synthesized varying both the aryl group of cyclobutanone and *β*-naphthols in this chapter. Apart from β-naphthols, α-naphthol was also found to be tolerated for this reaction but unfortunately, other phenol derivatives and electron-rich arenes failed to give the desired products. The control experiment confirms that these cyclobutanones can also be activated using mild Brønsted acids like PTSA. Further, a gram-scale experiment was conducted to display the practical utility, and also a 15-membered macrocycle was synthesized via ring-closing metathesis as a post-functional modification.

Keywords: Donor-Acceptor Cyclopropane; 3-donor cyclobutanone; Organocatalysis; Kinetic resolution; Lewis acid catalysis; Brønsted acid catalysis;

List of Publications

1. **Arijit Hazra,**[†] Tanmay Kanji,[†] and Prabal Banerjee; Merging Two Strained Carbocycles: Lewis Acid Catalyzed Remote Site-Selective Friedel−Crafts Alkylation of in Situ Generated β-Naphthol. *J. Org. Chem*. **2023**, *88*, 960−971. ([†]equal contribution)

2. **Arijit Hazra**, Raghunath Dey, Apoorv Kushwaha, T. J. Dhilip Kumar, and Prabal Banerjee; Organocatalytic Activation of Donor−Acceptor Cyclopropanes: A Tandem (3 + 3)-Cycloaddition/Aryl Migration toward the Synthesis of Enantioenriched Tetrahydropyridazines. *Org. Lett.* **2023**, *25*, 5470−5475.

3. **Arijit Hazra**, Asit Ghosh, Neeraj Yadav and Prabal Banerjee; Organocatalytic (3+3)-cycloaddition of ortho-substituted phenyl nitrones with aryl cyclopropane carbaldehydes: a facile access to enantioenriched 1,2-oxazinanes. *Chem. Commun.* **2023**, *59*, 11133–11136.

4. Navpreet Kaur, Pankaj Kumar, **Arijit Hazra**, and Prabal Banerjee; Switchable Reactivity of Cyclopropane Diesters toward (3 + 3) and (3 + 2) Cycloadditions with Benzoquinone Esters. *Org. Lett.* **2022**, *24*, 8249−8254.

5. Neeraj Yadav, **Arijit Hazra**, Priyanka Singh, and Prabal Banerjee; Organocatalytic Enantioselective (4+2) Annulation of Cyclopropane Carbaldehydes with 2-Mercapto-1-Arylethanones. *Adv. Synth. Catal*. **2024**, *366*, 1113–1119.

6. **Arijit Hazra**, Tanmay Kanji, and Prabal Banerjee; Brønsted Acid Catalyzed Cascade Ring-Opening/Cyclization of 3-Ethoxy Cyclobutanones to Access 2,8-Dioxabicyclo[3.3.1]nonane Derivatives. *J. Org. Chem.* **2024***, 89,* 8458−8467.

Conferences

1. **CFOS 2022,** IIT Roorkee, December 01 - 04, 2022, *poster presentation* on Organocatalytic deracemization of cyclopropane carbaldehydes: A tandem (3+3)-cycloaddition/aryl migration towards the synthesis of enantioenriched tetrahydropyridazines

2. **CHEMFEST-2023**; 9 March 2023, Dept of Chemistry, IIT Ropar, *Oral talk* on Organocatalytic Deracemization Of Donor-Acceptor Cyclopropane: A Tandem (3+3)-Cycloaddition/Aryl Migration Towards the Synthesis of Enantioenriched Tetrahydropyridazines

3. **23rd Tetrahedron Symposium 2023,** Gothenburg, Sweden, 27-30 June 2023, *Poster presentation* on Organocatalytic deracemization of cyclopropane carbaldehydes: A tandem (3+3)-cycloaddition/aryl migration towards the synthesis of enantioenriched tetrahydropyridazines

4. **JNOST 2023,** 10-12 Oct, 2023, IISER Pune, *Oral talk* on Organocatalytic (3+3)-cycloaddition of ortho-substituted phenyl nitrones with aryl cyclopropane carbaldehydes: A facile access towards the synthesis of enantioenriched 1,2-oxazinanes

5. **RABMC CRICK** symposium 2022, NIPER Mohali, participation

Table of Contents

LIST OF FIGURES

LIST OF SCHEMES

LIST OF TABLES

Notations and Abbreviations

Acronym	Name
A	Acceptor
Å	Angstrom
Ad	Adamantly
MeCN	Acetonitrile
NH_4Cl	Ammonium chloride
Ar	Aryl
$BF_3{\cdot}Et_2O$	Boron trifluoride dietherate
Bn	Benzyl
β	Beta
box	bis(oxazoline)
$Bi(OTf)_3$	Bismuth tris(trifluoromethanesulfonate)
dppb	1,4-Bis(diphenylphosphino)butane
dppp	1,3-Bis(diphenylphosphino)propane
br	Broad
BHT	Butylated hydroxytoluene
CH_2Cl_2 /DCM	Dichloromethane
$CHCl_3$	Chloroform
CCl_4	Carbon tetrachloride
^{13}C	Carbon NMR
$CDCl_3$	Chloroform-D
COSY	Correlation spectroscopy
(CN)CbI	Cyanocobalamin
cod	1,5-Cyclooctadiene
Cp	Cyclopentadienyl

°C	Degree Celsius
cm	Centimeter
$Cu(OTf)_2$	Copper (II) triflоromethanesulphonate
D	Donor
DAC	Donor-acceptor cyclopropane
DABCO	1,4-Diazabicyclo[2.2.2]octane
DBU	1,8-Diazabicyclo[5.4.0]undec-7-ene
DIPEA	*N, N*-Diisopropylethylamine
DMSO	Dimethyl sulphoxide
DMF	Dimethyl formamide
DCB	1,2-Dichlorobenzene
DCE	1,2-Dichloroethane
d	Doublet
dd	Doublet of doublet
ddt	Doublet of doublet of triplet
dq	Doublet of quartet
δ	Delta
DEPT	Distortionless enhancement by polarization transfer
E	Electrophile
EDG	Electron donating group
ee	Enatiomeric excess
equiv.	Equivalent
er	Enantiomeric ratio
Et_2O	Diethyl Ether
EtOAc	Ethyl acetate
ESI	Electronspray ionization

Et	Ethyl
EtOH	Ethanol
EWG	Electron withdrawing group
g	Gram
gem	Geminal
h	Hour
H_2	Hydrogen
^1H	Proton NMR
Hz	Hertz
HFIP	Hexafluoroisopropanol
HME	Heptamethyl cobyrinate
HPLC	High-Performance Liquid Chromatography
HRMS	High Resolution Mass Spectrometry
H_2O	Water
I_2	Iodine
$InCl_3$	Indium (III) chloride
$In(OTf)_3$	Indium(III) trifluoromethanesulfonate
i-PrOH	Isopropanol
FTIR	Fourier Transform Infra-Red
L	Ligand
LA	Lewis acid
LiCl	Lithium chloride
m	Multiplet
Me	Methyl
MS	Molecular Sieves
mL	Millilitre

MHz	Mega Hertz
min	Minute
MeOH	Methanol
MgI_2	Magnesium (II) iodide
Nu	Nucleophile
NMR	Nuclear Magnetic Resonance
N_2	Nitrogen
Ni	Nickel
$NaBH_4$	Sodium borohydride
Na_2CO_3	Sodium carbonate
NaH	Sodium hydride
Na_2SO_4	Sodium sulfate
NOE/NOESY	Nuclear Overhauser effect spectroscopy
OMe	Methoxy
Ph	Phenyl
Pd	Palladium
PTSA	*para*-Toluene sulphonic acid
ppm	Parts per million
Py	Pyridine
q	Quartet
Rf	Retention factor
rt	Room temperature
s	Singlet
S_N2	Bimolecular Nucleophilic Substitution
$Sc(OTf)_3$	Scandium (III) triflоromethanesulphonate
$SnCl_4$	Stannic Chloride

t	Triplet
TfOH	Triflic acid/Trifloromethanesulphonic acid
TFA	Trifluoroacetic acid
PCy_3	Tricyclohexylphosphine
THF	Tetrahydrofuran
Bu_4NPF_6	Tetrabutylammonium hexafluorophosphate
Bu_4NBF_4	Tetrabutylammonium tetrafluoroborate
$TiCl_4$	Titanium tetrachloride
td	Triplet of doublet
TLC	Thin Layer Chromatography
TOF	Time-of-flight
UV	Ultra Violet
V	Volt

Chapter 1

Two smallest carbocycles donor-acceptor cyclopropanes and cyclobutanones and their activation by different catalysis

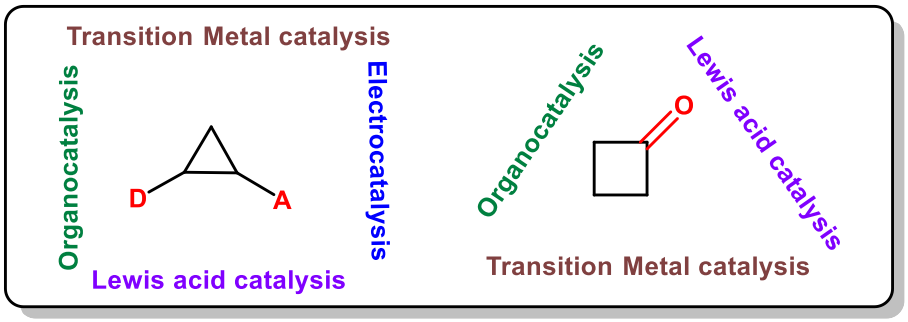

1.1. Two Smallest carbocyclic brothers

"We define organic chemistry as the chemistry of carbon compounds"- August Kekule

In the domain of organic chemistry, carbocycles are the cyclic molecules where all the atoms composing the cycle are carbon atoms. They are ubiquitous in various biologically active molecules, natural products, pharmaceuticals, and organic materials. The construction of intriguing carbocyclic frameworks like fused rings, spirocycles, and carbocycles containing multiple stereocenters always fascinated the synthetic community.[1] The carbocycles are generally three types (a) saturated or alicyclic, (b) aromatic, and (c) partially unsaturated carbocycles.[2] Moreover, depending on the number of carbon atoms, the alicyclic carbocycles can be of various ring sizes which are small carbocycle (3-6 membered), medium carbocycle (7-11 membered), and large carbocycle or macrocycle (more than 12 membered). Among them, three-membered cyclopropanes and four-membered cyclobutanes are the smallest ones and among the most studied carbocycles for their synthesis as well as transformations (Figure 1.1.1). The reactivity and properties of these two carbocycles are somewhat similar and thus regarded as carbocyclic brothers. Intriguingly, chemists have also designed methodologies for the synthesis of these two carbocycles utilizing each other as the precursor via ring expansion and ring-contraction mechanisms. These small chemical entities are present everywhere in the field of modern medicinal chemistry and often exhibit important physicochemical properties. Numerous catalytic and non-catalytic strategies have been developed over the past few decades for the construction of several chiral and achiral organic molecular frameworks via activation of these two carbocycles utilizing their strain-releasing reactivity.

Figure 1.1.1. Types of carbocycles concerning different ring sizes

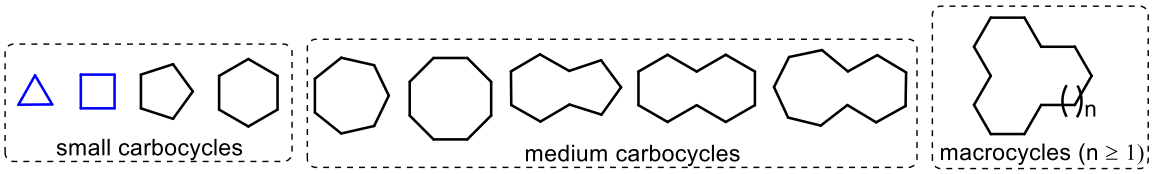

1.2. Cyclopropane: a three-membered strained carbocycle

Cyclopropane, the smallest carbocycle, was synthesized first by August Freund in 1881 by intramolecular Wurtz reaction of 1,3-dibromopropane with sodium.[3] Simple cyclopropane is a colorless gas at room temperature. In 1933, it was started to be used as an anesthetic but later it was known to be extremely flammable and so no longer applied clinically. Releasing this small cycloalkane in a closed area can initiate asphyxiation replacing the oxygen.[4] However, these unique structural motifs have been used for a long time for the synthesis of various complex organic scaffolds due to their distinctive properties. Cyclopropanes seem to be very unstable molecules as they consist of high energy (27.5 kcal/mol) but actually, they are kinetically inert and do not

abandon their cyclic structure easily. The main reason behind this is their peculiar structural properties which can be explained by Coulson-Moffitt's modification of Baeyer strain theory.[5] Though cyclopropane should contain a C-C-C bond angle of 60° which is a large deviation from the ideal sp^3 C-C-C bond angle (109.5°), it consists of a bond angle of 104.5° which attributed to lowering the angle strain and makes a banana or bent bonding in cyclopropane (Figure 1.2.1). Additionally, cyclopropane suffers from torsional (Pitzer) strain due to the coplanar arrangement which arises due to the vicinal C-H bond in its eclipsed conformation (Figure 2). Moreover, contrary to simple hydrocarbons, the C-C bonds in cyclopropane are shorter (1.51 Å) and behave like a double bond which was explained by the Walsh MO model.[6]

Figure 1.2.1. Bonding and strain (angle and torsional) in cyclopropane

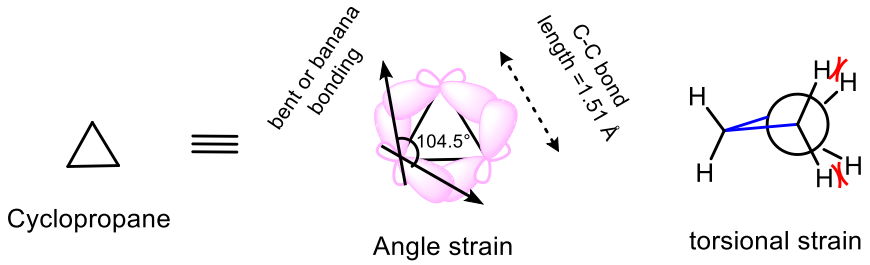

Over the years, these smallest carbocycles achieved remarkable attention owing to their prevalence in a large number of bioactive molecules and natural products.[7] A few of them are (+)-*trans*-chrysanthemic acid (isolated from *Chrysanthemun cinerariaefolium* petals), 1-Aminocyclopropanecarboxylic acid (precursor for phytohormone ethylene), (+)-coronatine (produced by *Pseudomonas syringae* bacterium), (+)-Ptaquiloside (isolated from *Pteridium aquilinum* var. *latiusculum*), tranylcypromine (antidepressant and anxiolytic agent), Grenadamide (isolated from *Lyngbya majuscula* cyanobacterium) (Figure 1.2.2) etc.[8] Other than biological activity, it was also discovered that the presence of cyclopropane cores can enhance the potency of

Figure 1.2.2. Cyclopropane containing natural products and their bioactivities

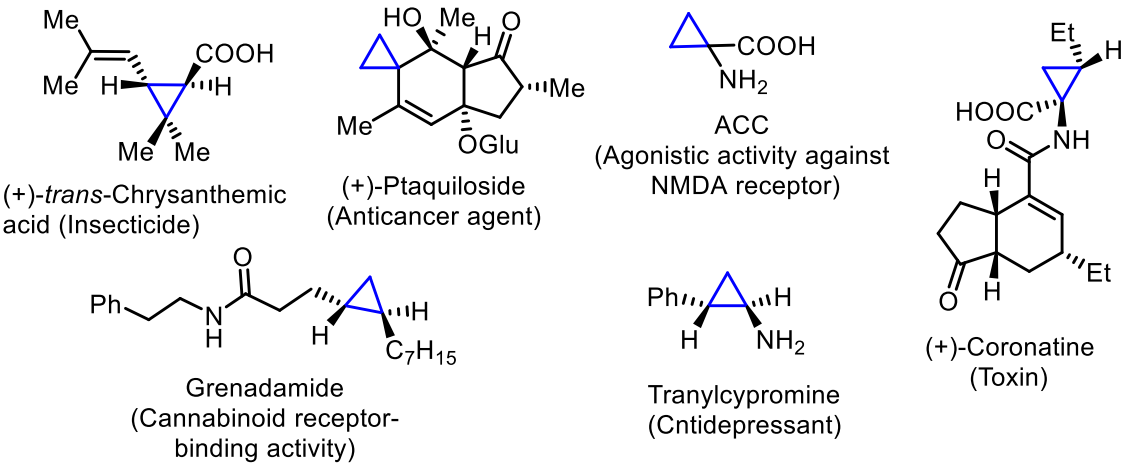

a drug molecule.[5c] Numerous cyclopropanation methodologies[9] have been documented till now for the construction of several types of cyclopropanes and also a plethora of strategies have been discovered for their synthetic transformations[10] as starting materials as well as reactive intermediates towards various racemic and chiral heterocyclic, bicyclic, spirocyclic, and macrocyclic organic frameworks.

1.3. Types of Cyclopropanes

In the past few decades, various types of cyclopropane have been synthesized and modified depending on the reactivity and substituent attached to this smallest carbocycle. As the cyclopropanes are generally inert, so to make them reactive, activating groups are installed in the ring which creates C-C bond polarization to undergo chemical reactions. On that basis, cyclopropanes can be classified majorly into three categories (a) donor cyclopropane, (b) acceptor cyclopropane, and (c) donor-acceptor cyclopropane (Figure 1.3.1). Donor cyclopropanes contain an electron-donating group (alkyl, aryl, vinyl, heteroatom, etc.) attached to one carbon atom of the ring. Whereas in acceptor cyclopropanes, one of the carbon atoms consists of an electron-withdrawing group (carbonyl, cyano, nitro, sulfonyl, etc.). In donor-acceptor cyclopropane, both electron-donating and electron-withdrawing groups are installed on the cyclopropane ring either vicinally or geminally. It is worth mentioning that apart from these three categories, there are also a few other types of cyclopropane present in the literature e.g. cyclopropene[11], cyclopropenone[11], cyclopropanone[12], cyclopropanol[13], and alkylidene cyclopropane[14] (Figure 1.3.1). Among them, vicinally substituted donor-acceptor cyclopropanes are the most reactive ones and as a consequence, they attract paramount interest to the synthetic organic community.

Figure 1.3.1. Classification of cyclopropane

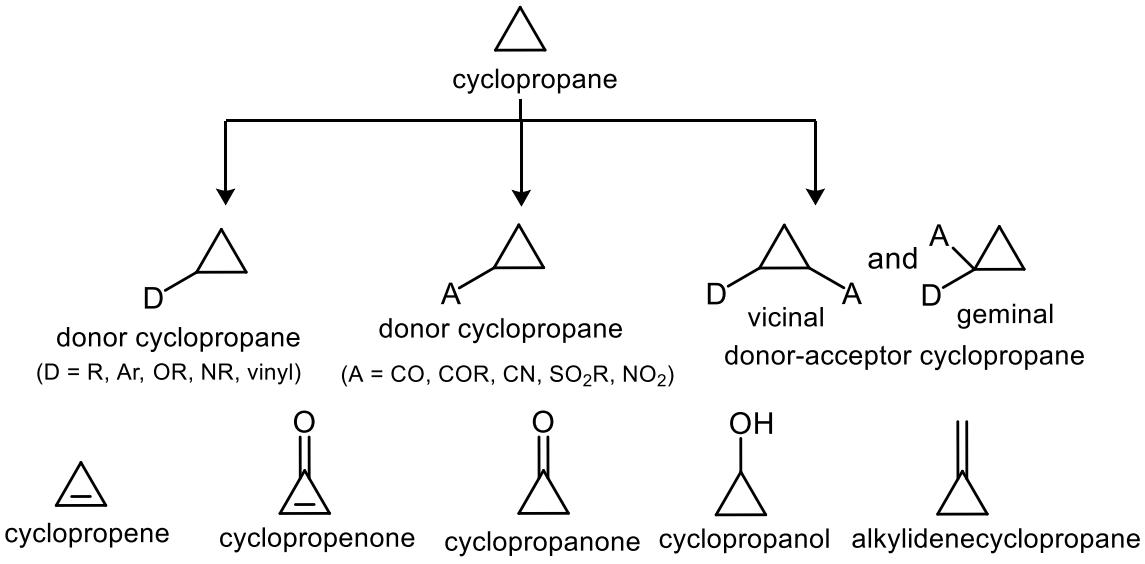

1.4. Various catalytic activation of donor-acceptor cyclopropanes

In the year 1980, a German chemist Hans-Ulrich Reissig[15] pioneered the term 'Donor-Acceptor substituted Cyclopropane' for the first time for those cyclopropanes where a donor group and an acceptor group are substituted at the vicinal position which was later abbreviated as donor-acceptor cyclopropane (DAC). After its appearance in the 1980s, the donor-acceptor cyclopropanes (DACs) were utilized moderately till the beginning of the 21st century but after that, they experienced a renaissance in the arena of modern organic synthesis due to their unique reactivity.[16] The synergistic effect of donor and acceptor groups from the vicinal positions creates a push-pull effect inducing a C-C bond polarization, generating a 1,3-zwitterionic intermediate (Figure 1.4.1) which can undergo several interesting transformations.[17] This type of synergistic effect could not be possible in the

Figure 1.4.1. Reactivity and types of DACs

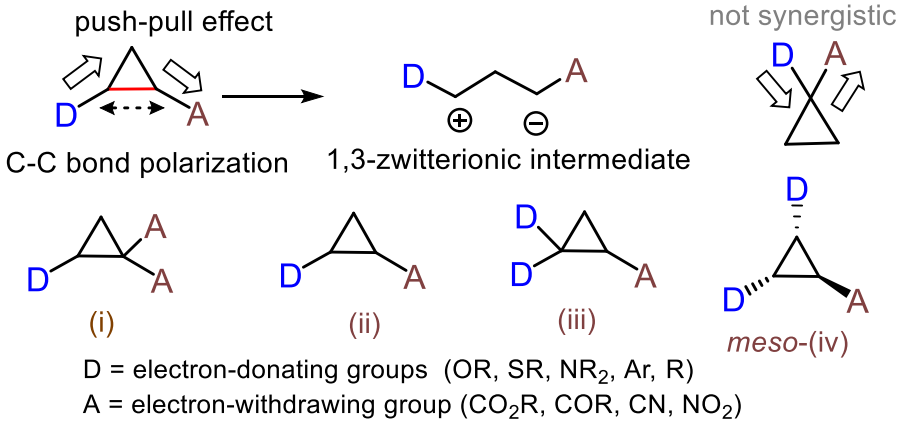

case of geminally donor-acceptor substituted cyclopropanes (Figure 1.4.1). The DACs are generally four types (i) di-acceptor substituted, (ii) mono-acceptor, (iii) di-donor substituted, and (iv) *meso*-cyclopropane (Figure 1.4.1).[18] In most of the cases, it was observed that the impact of the donor group plays a major role in the activation of DACs while installation of an extra group donor or acceptor group can diminish the activation barrier for the ring enlargement.[18] The catalytic activations strategies of the donor-acceptor cyclopropanes are classified into five individual categories which are Lewis acid catalysis, transition metal catalysis, organocatalysis, photoredox catalysis, and electrocatalysis.

1.4.1. Lewis acid catalysis

Lewis acids are those chemical entities that contain vacant orbital(s) to accept electron pairs as depicted by Gilbert Lewis.[19] Usually, when the metals combine with halides to form metal salts they behave as Lewis acids. Though the majority of these acids consist of metals, metalloids (Boron), or semimetal (Silicon) salts can also act as Lewis acids.[20] Over the years a myriad of organic transformations e.g. oxidation, reduction, C-C/C-X bond formation, aldol reaction, and

pericyclic reactions have been accomplished by the catalytic activation of the different Lewis acids.[20, 21] The metal of the Lewis acid coordinates with the electronegative atom of a molecule to form a complex in which the electronegativity of the donor atom increases and as a consequence, the molecule gets highly activated to undergo various bond-forming, bond-breaking, and cycloaddition reactions.[21] The Lewis acid activation of DAC is also similar where the metal center coordinates with the electronegative atom of the acceptor group which enhances the electron-withdrawing capacity of the acceptor group. Eventually, the substituted C-C bond gets sufficiently polarized to undergo either a stereospecific nucleophilic attack or form the 1,3-zwitterionic intermediate for further cyclization, cycloaddition, or rearrangement transformations. Out of different types of DACs, the di-acceptor substituted DACs are explored predominantly due to the presence of two electron-withdrawing groups which can activate the cyclopropane to a greater extent (**I**, Scheme 1.4.1.1.a) than that of a mono-acceptor substituted one ((**II**, Scheme 1.4.1.1.a).

Scheme 1.4.1.1. Lewis acid catalyzed activation of DACs

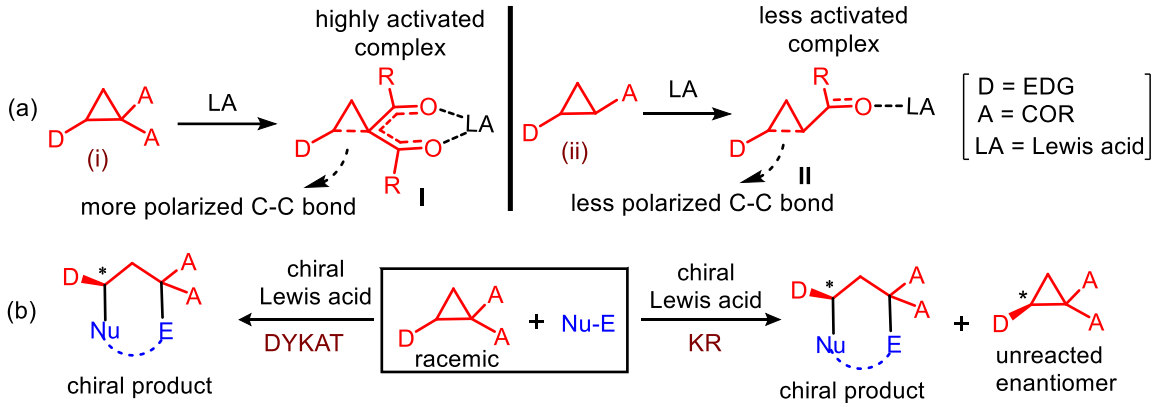

Numerous ring-opening, cyclization, (3+n) cycloaddition, and rearrangement reactions have been reported in the past few decades with the former while studies on the latter one remain limited possibly due to its less reactivity.[22]

After the first Lewis acid-promoted reaction of 2-silyloxycyclopropane by Reissig[23] in 1981, numerous methodologies have been reported till now by the Lewis acid activation of DACs. Among them, one of the most interesting works was done by Kerr *et al.*[24] in 2003 where they employed DAC **1a** and 1,3-dipolar species nitrone **2** in the presence of $Yb(OTf)_3$ to access achiral tetrahydro-1,2-oxazine derivatives **3** (Scheme 1.4.1.2.a). Notably, the DACs are racemic and as a result, all these transformations lead to the formation of achiral molecules only. However, their asymmetric versions can also be achieved by employing the combination of a chiral ligand and the Lewis acid. In this case, the chiral ligand also coordinates with the Lewis acid in complex **I** which creates a sterically hindered environment to facilitate the ring-opening event selectively from one particular face inducing the enantioenrichment. Two common asymmetric approaches generally followed for

the enantioselective conversion of racemic D-A cyclopropanes (a) simple kinetic resolution (KR) and dynamic kinetic asymmetric transformation (DYKAT) (Scheme 1.4.1.1.b).[10, 18] After Sibi's first report[25] of asymmetric reaction of nitrones with DAC, Tang *et al.*[26] in 2007, demonstrated an

Scheme 1.4.1.2. Lewis acid-catalyzed reactions of donor-acceptor cyclopropanes

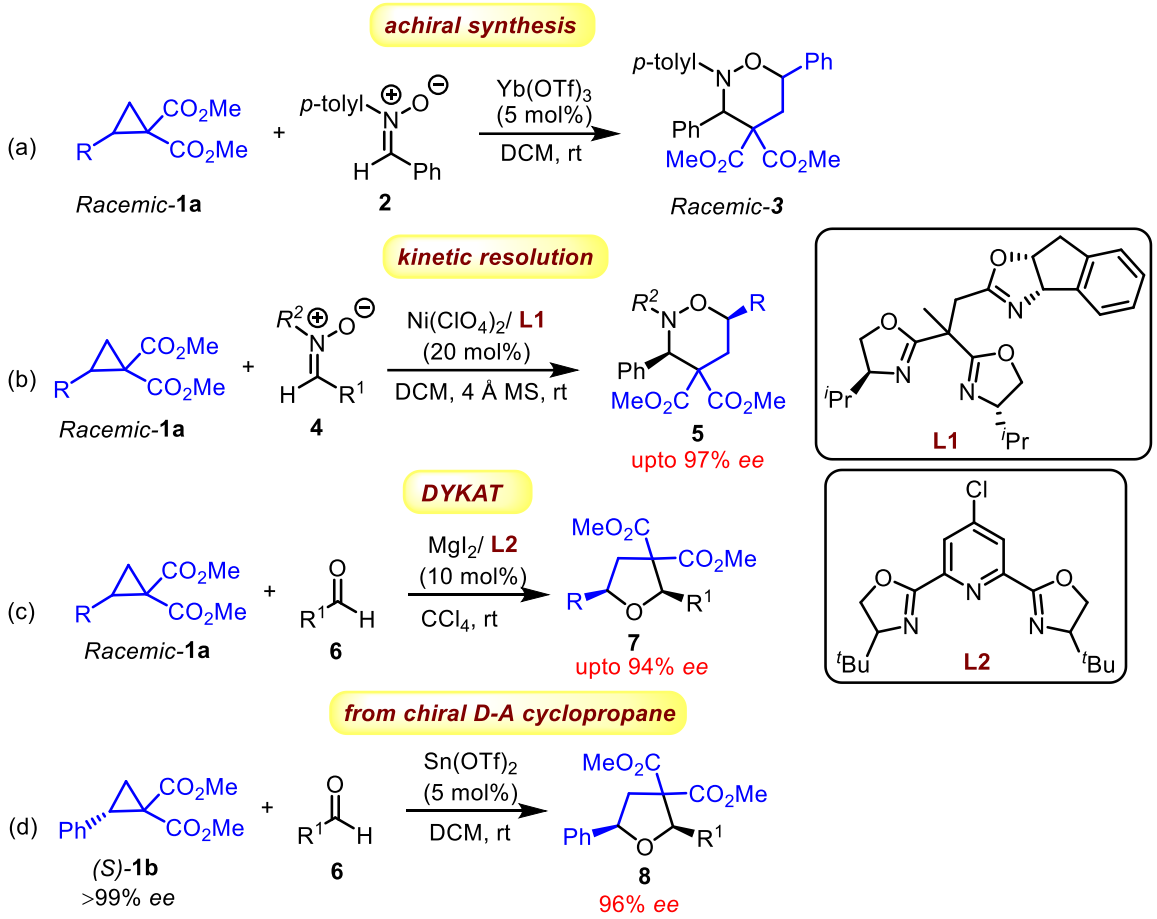

enantioselective (3+3) cycloaddition of *racemic* DACs **1a** with nitrones **4** employing trisoxazoline/$Ni(ClO_4)_2$ catalyst with improved diastereoselectivities (Scheme 1.4.1.2.b). Highly enantioselective products **5** were obtained via a simple kinetic resolution where the remaining cyclopropane could also be recovered with good enantiomeric excess. Later, in 2009, the pioneering work by Johnson *et al.*[27] showcased a remarkable breakthrough in this field developing a (3+2) annulation of the racemic DAC **1a** with aldehydes **6** via dynamic kinetic asymmetric transformation using (pybox)MgI_2 catalyst (Scheme 1.4.1.2.c). In this case, both the enantiomers of electron-rich aryl cyclopropanes get converted to the final product through DYKAT to furnish chiral tetrahydrofuran derivatives **7**. Thereafter, a large number of Lewis acid-catalyzed asymmetric transformation reactions have been reported to date following these two asymmetric approaches. However, apart from these, achiral Lewis acid catalysis with chiral or non-racemic DACs[28] could also lead to the formation of enantioenriched products which was earlier developed by Johnson *et al.*[29] in 2005. The (*S*)-cyclopropane diester **1b** (>99% ee) reacts with aldehyde **6** in the presence of

$Sn(OTf)_2$ to form enantioenriched furan derivatives **8** (Scheme 1.4.1.2.d). The absolute stereochemical information was believed to be transferred via the S_N2 attack of the aldehyde prior to the ring opening of cyclopropane.

1.4.2. Transition metal catalysis

One of the most predominant catalytic methodologies for organic transformations is transition metal catalysis due to its wide versatility and ability to perform unprecedented reactions.[30] Despite the rise of modern and greener methodologies, like organocatalysis, photocatalysis, and electrocatalysis, this traditional approach maintained its popularity and continuously contributed to the synthetic community. However, transition metal-catalyzed activation of donor-acceptor cyclopropanes did not achieve any significant developments. The first transition metal activation of cyclopropane was observed by Tipper[31] in 1955 where the oxidative addition of a transition metal complex into the C-C bond of cyclopropane gave rise to a metallacyclobutane intermediate facilitated by the ring strain release. After that, only two reports were found in the literature on this aspect. Recently, in 2022, Gryko *et al.*[32] reported an activation of cyclopropane **1c** by vitamin B12 which contains Cobalt metal. Here, at first, the Co(III) was reduced to Co(I) in the presence of Zn and NH_4Cl, and after the oxidative addition of Co(I) species to the electrophilic center of DAC **1c** generates Co(III)-complex **III**. This complex then led to the formation of alkyl radical intermediate **IV** via heat or UV irradiation followed by the reaction with olefin **9** to render the product **10**. A reversal in reactivity of DACs was observed here as an electrophilic reagent was regioselectively installed at the electrophilic carbon center of the cyclopropane ring (Scheme 1.4.2.1.a). Another study was reported in the last year by Li and Liu *et al.*[33] where DAC **1d** was activated by copper salts to access ring-opened **12** and cyclized products **13**. In this case, disproportionation of Cu(II) generates Cu(I) which facilitates the homolysis of NFSI **11** to create radical **VI**. The ring-opening of cyclopropane then occurs by the attack of this radical **VI** and forms the intermediate **VII** which after oxidative addition and reductive elimination furnished the open chain products **12**. Alternatively, the radical **VII** could undergo cyclization followed by a single electron transfer (SET) to produce aryl cation **X** which is further transformed into the indane derivative **13** via deprotonation and aromatization (Scheme 1.4.2.1.b).

1.4.3. Organocatalysis

After the emergence in the late 1990s, the domain of organocatalysis experienced exponential growth in the field of asymmetric synthesis and is now considered one of the three pillars of enantioselective synthesis along with the earlier established organometallic and enzymatic catalysis.[34, 35] The overwhelming and expeditious acceptance of this catalysis by chemists is possible as it bestowed some significant advantages over traditional approaches.[35] Organocatalysis deals with small organic molecules which are often naturally available as a single enantiomer, non-

Scheme 1.4.2.1. Transition metal activation of DACs

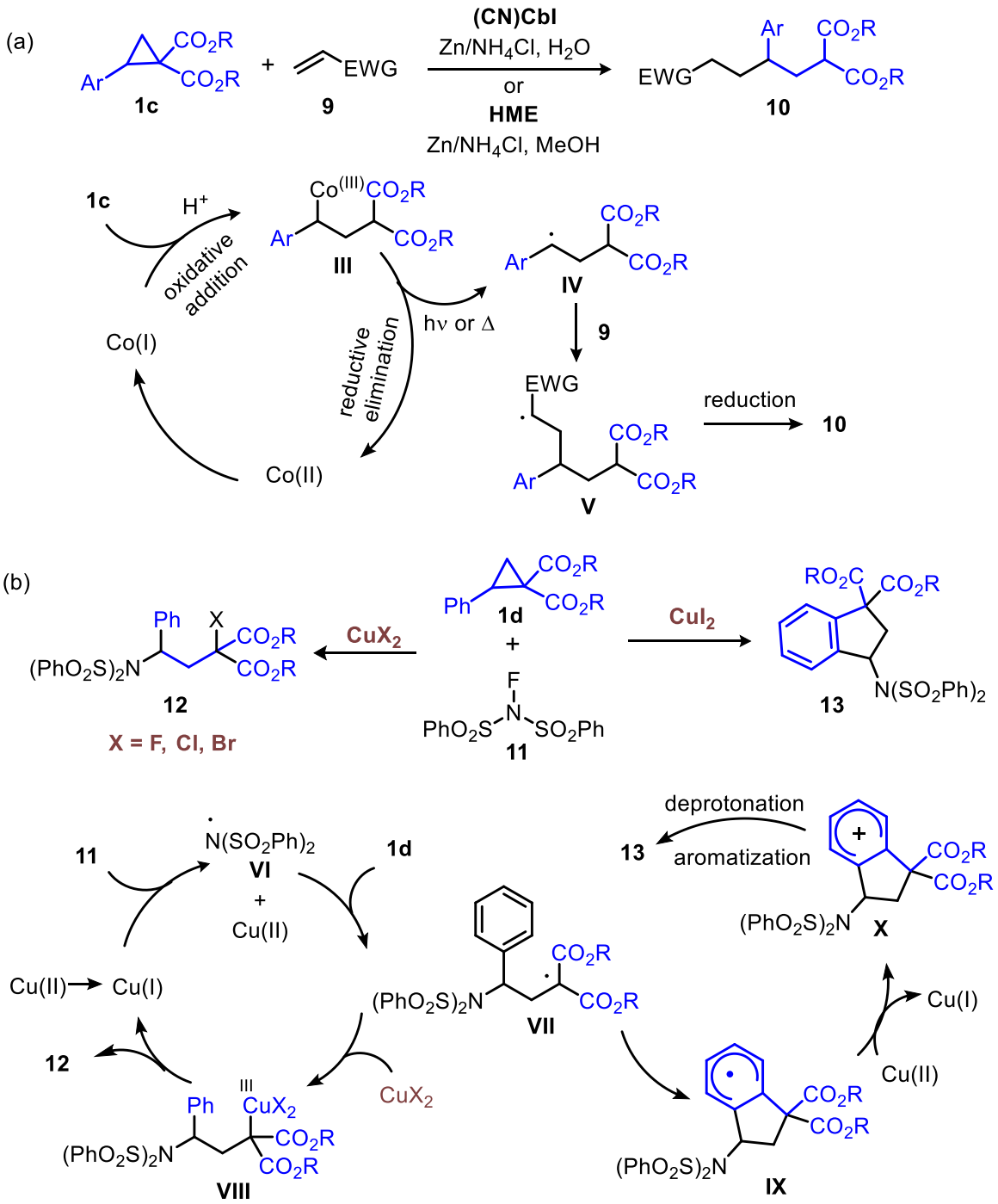

toxic and inexpensive making them commercially convenient and safe both for industry and academic research. Acknowledging the potential of this field, recently in 2021, Professor David W. C. MacMillan and Professor Benjamin List were awarded the *Nobel Prize* in Chemistry for pioneering and developing *asymmetric organocatalysis*. There are generally four types of organocatalysis[36] (i) Lewis bases, (ii) Lewis acids, (iii) Brønsted bases, and (iv) Brønsted acids (Figure 1.4.3.1). While the Lewis base organocatalysts are usually amines like prolines and N-heterocyclic carbenes (NHCs), Lewis acid organocatalysis deals with phase transfer catalysts like

quaternary ammonium salts. On the other hand, Brønsted base organocatalysts are comprised of tertiary amines like cinchona alkaloids and Brønsted acid organocatalysts are generally H-bonding catalysts like thiourea and phosphoric acids.

Figure 1.4.3.1. Types of organocatalysts

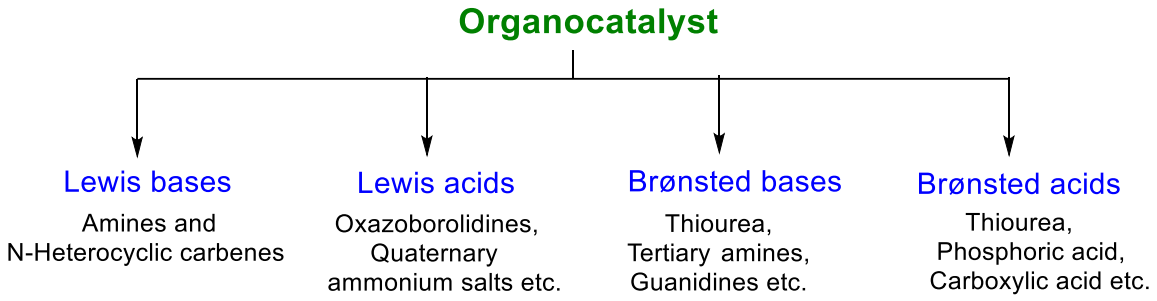

Few of these types of organocatalysts are already utilized for the activation of donor-acceptor cyclopropanes either as a precursor or as reactive intermediates via asymmetric ring-opening, cycloaddition, and cyclization reactions.[10, 18, 22, 37] The first attempt at activating donor-acceptor cyclopropanes was reported by Jørgensen *et al*.[38] in 2009 where asymmetric desymmetrization of a *meso*-cyclopropane cyclopentanones was executed via ring-opening rearrangement reaction. Later, in 2011, Sparr and Gilmour[39] demonstrated the first asymmetric desymmetrization of *meso*-cyclopropane carbaldehydes **1e** by secondary amine catalysis towards enantioselective synthesis of

Scheme 1.4.3.2. Asymmetric secondary amine organocatalytic activation of DACs

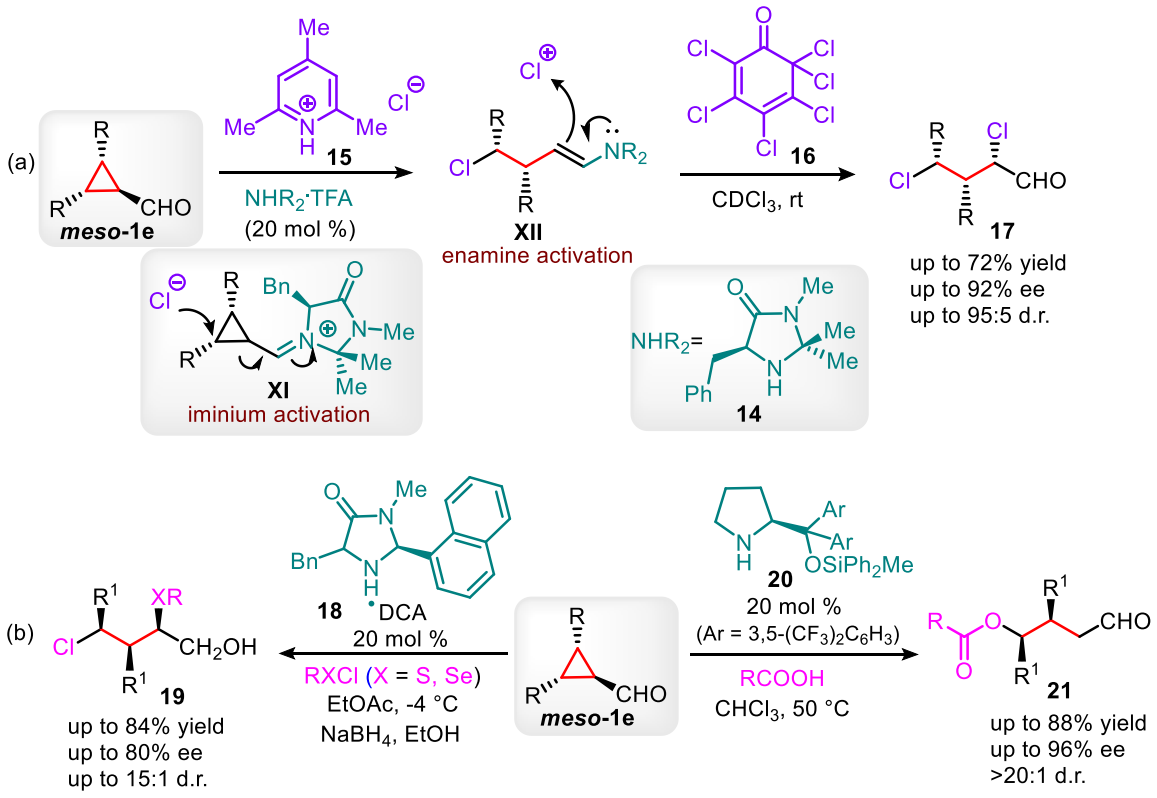

1,3-dichlorides **17** (Scheme 1.4.3.2.a). The iminium activation **XI** of the cyclopropyl aldehyde was achieved by employing MacMillan's catalyst **14** which reacts with the nucleophilic chlorinating agent pyridinium hydrochloride **15** to render the corresponding enamine intermediate **XII**. Further, the addition of an electrophilic chlorinating agent perchlorinated quinone **16** occurred via enamine activation and rendered the enantioenriched dechlorinated product **17**. Later, the same strategy was exploited by Werz *et al.*[40] and Vicario *et al.*[41] independently for the enantioselective dichlorochalcogenation utilizing modified MacMillan's catalyst **18** (Scheme 1.4.3.2.b, left) and asymmetric ring-opening by carboxylates using diaryl prolinol catalyst **20** respectively (Scheme 1.4.3.2.b, right).

Scheme 1.4.3.3. Organocatalytic activation of *in situ* generated DACs

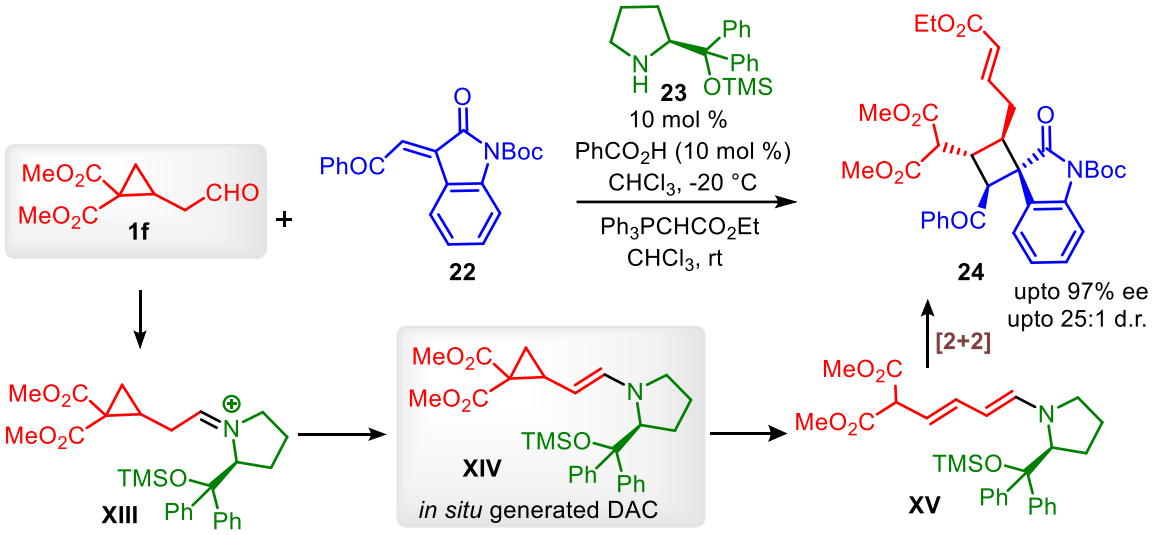

In line with the secondary amine-based organocatalysis, Jørgensen *et al.*[42] reported an unprecedented (2+2) cycloaddition with cyclopropane acetaldehyde **1f** and 3-olefinic oxindoles **22** using diphenyl prolinol catalyst **23** to construct highly stereoselective cyclobutane derivatives **24** (Scheme 1.4.3.3). Initially, the cyclopropane precursor was not a typical DAC, but it was converted into a reactive donor-acceptor cyclopropane intermediate **XIV** *in situ* via enamine activation followed by the tandem ring-opening/cycloaddition which led to the discovery of unusual C-C bond functionalization of cyclopropane ring.

N-heterocyclic carbenes (NHCs) are another type of Lewis base organocatalyst which is also studied for the activation of DACs. In 2017, Vicario *et al.*[43] designed an asymmetric (4+2) annulation of formyl cyclopropane diester **1g** with alkylidene oxindoles **25** catalyzed by chiral triazolium salt **26** as an NHC catalyst (Scheme 1.4.3.4). The NHC first attached to the aldehyde group of cyclopropane to generate the Breslow intermediate **XVI** which acts as a reactive donor-acceptor cyclopropane that further undergoes the strain-driven ring-opening followed by

cycloaddition reaction to render tetrahydropyrano[2,3-*b*]indoles **27** in highly enantioselective manner.

Scheme 1.4.3.4. NHC catalyzed activation of DAC

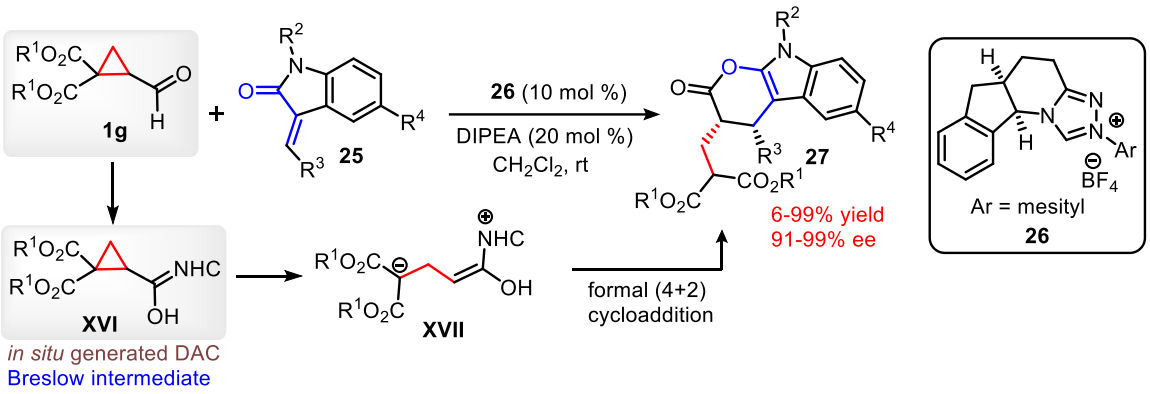

Other than these Lewis base organocatalysis, Brønsted base catalytic activation of DAC was also developed by Jørgensen *et al.*[44] in 2017 where they employed the chiral thiourea derivative which is a bifunctional catalyst and can behave both as Brønsted acid and Brønsted base catalyst. The di-acceptor substituted cyclopropyl ketones **1h** were activated by the Brønsted base **28** via deprotonation to create a reactive DAC intermediate **XVIII** which eventually underwent enantioselective (3+2) cycloaddition with nitroolefin **29** to furnish substituted cyclopentanes **30** (Scheme 1.4.3.5, left). Recently in 2022, a similar strategy of activating DACs was again applied by the same group and performed a reaction with heptafulvenoids **31** to achieve enantioselective (8+3) cycloadducts **32** in good enantioselectivities (Scheme 1.4.3.5, right).[45]

Scheme 1.4.3.5. Brønsted base catalytic activation of *in situ* generated DAC

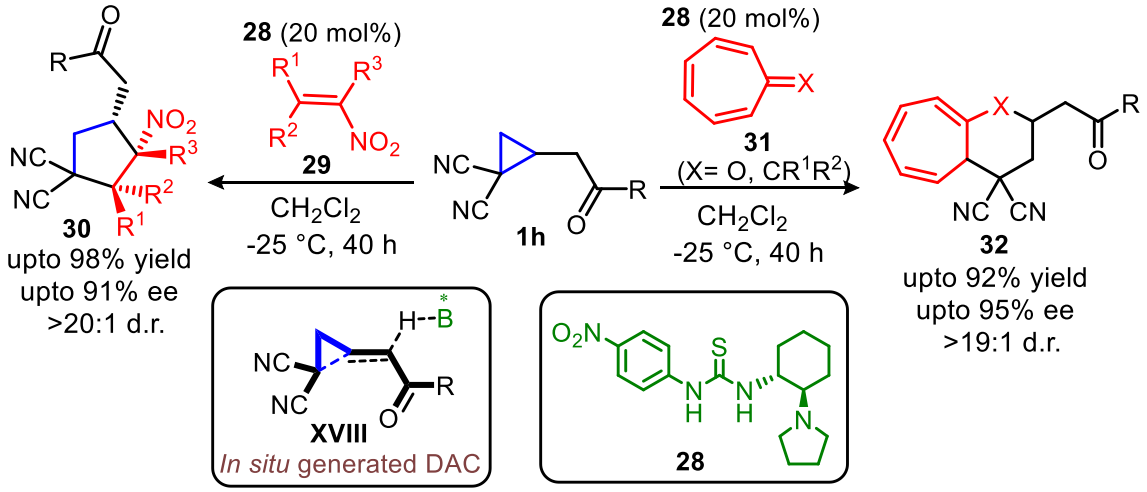

Brønsted acid catalytic activation of DACs was first disclosed by Vicario *et al.*[46] in 2018 with racemic cyclopropyl ketones **1i** in the presence of chiral phosphoric acid **33**. This methodology involves the Brønsted acid-mediated ring-opening of the cyclopropane **1i** engendering a

carbocationic intermediate **XIX** followed by an intramolecular Cloke-Wilson rearrangement to access enantioenriched dihydrofurans **34** (Scheme 1.4.3.6.a). The possible reason for the enantioinduction here is believed to be the hydrogen bonding as well as an ion-pairing interaction between the chiral phosphate ion and the carbocation intermediate. Besides this asymmetric catalysis, some achiral Brønsted acid catalytic activation of DACs was also reported by Banerjee *et al*.[47, 48] from donor-acceptor cyclopropane carbaldehydes **2** (DACCs). In 2019, they displayed a reaction of DACC **2a** with N-Benzyl Anilines **35** in the presence of p-toluenesulfonic acid (PTSA) for the construction of achiral seven-membered heterocyclic scaffolds **36** (Scheme 1.4.3.6.b, left).[47] Here, Brønsted acid activates the aldehyde group of DAC **1j** which induces a polarization of the substituted C-C bond which further undergoes ring opening by the stereospecific nucleophilic

Scheme 1.4.3.6. Brønsted acid catalytic activation of DAC: (a) enantioselective reaction, (b) achiral reaction.

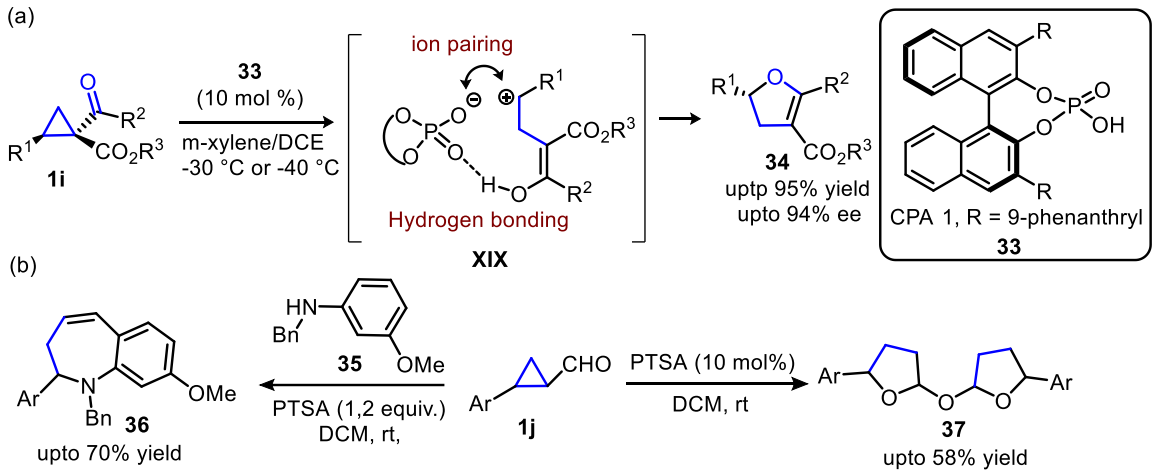

attack of aniline followed by cyclization. Later, in 2021, the same group developed another achiral strategy for the Brønsted acid activation of DACC where a Cloke-Wilson type rearrangement followed by dimerization occurred to render a diastereomeric mixture of oxybis(2-aryltetrahydrofuran) derivatives **37** (Scheme 1.4.3.6.b, right).[48]

1.4.4. Photoredox catalysis

Photoredox catalysis became one of the fastest-growing sustainable catalytic methods to instigate the renaissance of radical chemistry.[49] Over the last few decades, this light-mediated catalysis encompasses numerous exceptional organic transformations. Here, the visible light is irradiated at a particular wavelength where common organic molecules will not absorb but a specially designed photoredox catalyst will. The resulting excited catalytic species can act as a strong oxidant as well as a strong reductant simultaneously and thus effectively induces the subjected substrates or reagents leading to unprecedented organic reactions which are difficult to achieve under thermal conditions.[50] Implementation of this powerful tool for the activation of small molecules has also

begun to be explored in the last decades. Though photoredox activation of relatively less activated cyclopropanes (e.g. donor cyclopropane, acceptor cyclopropane, and nitrocyclopropanes) has already been explored,[51] similar activation of highly activated donor-acceptor cyclopropanes remains underexplored. However, Feng *et al.*[52] recently demonstrated a photoredox catalyzed ring opening/C(sp^3)-heteroatom bond formation strategy where a donor-donor (D-D) cyclopropane **38**

Scheme 1.4.4.1. Photoredox activation of DACs

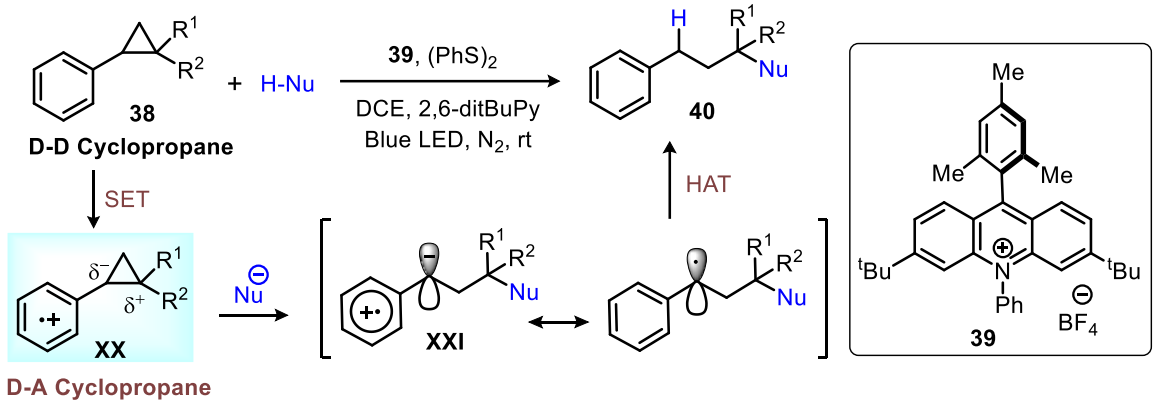

has been converted into a D-A cyclopropane *in situ* by generating aryl cation radical intermediate **XX** via SET oxidation. Further ring-opening by the nucleophilic attack followed by hydrogen atom transfer (HAT) leads to the final product **40** (Scheme 1.4.4.1).

1.4.5. Electrocatalysis

Other than photocatalysis, another catalytic approach that plays a crucial role in the resurgence of radical chemistry is modern electro-organic chemistry. This methodology is environmentally friendly because here the electrons took part in the reaction as traceless reagents as the replacement of hazardous redox reagents.[53] Eventually, electro-organic synthesis became a powerful tool for the organic fraternity in the last two decades and established numerous transformations in an unconventional and sustainable way.[54] But similar to the photoredox catalysis, electrocatalytic activation of DACs also remained underexplored till the end of the last decade. In 2021, Werz *et al.*[55] (Scheme 1.4.5.1, condition a) and Banerjee *et al.*[56] (Scheme 1.4.5.1, condition b) independently reported an electrocatalytic ring cleavage of DACs **1c** via anodic oxidation. Under electrolysis conditions, the oxidation of the aryl ring occurred followed by a homolytic cleavage to form intermediate **XXIII**. This radical intermediate **XXIII** traps the triplet molecular oxygen and subsequent 5-exo trig-cyclization rendered the endoperoxide intermediate **XXV** which after deprotonation furnished the product **41**. In the same year, one more electrocatalytic activation of DAC was studied by the Werz group[57] where a Friedel-Crafts type reactions (Scheme 1.4.5.1, condition c) were executed by reacting arenes with cyclopropane following similar aryl oxidation mechanism.

Scheme 1.4.5.1. Electrocatalytic activation of DACs

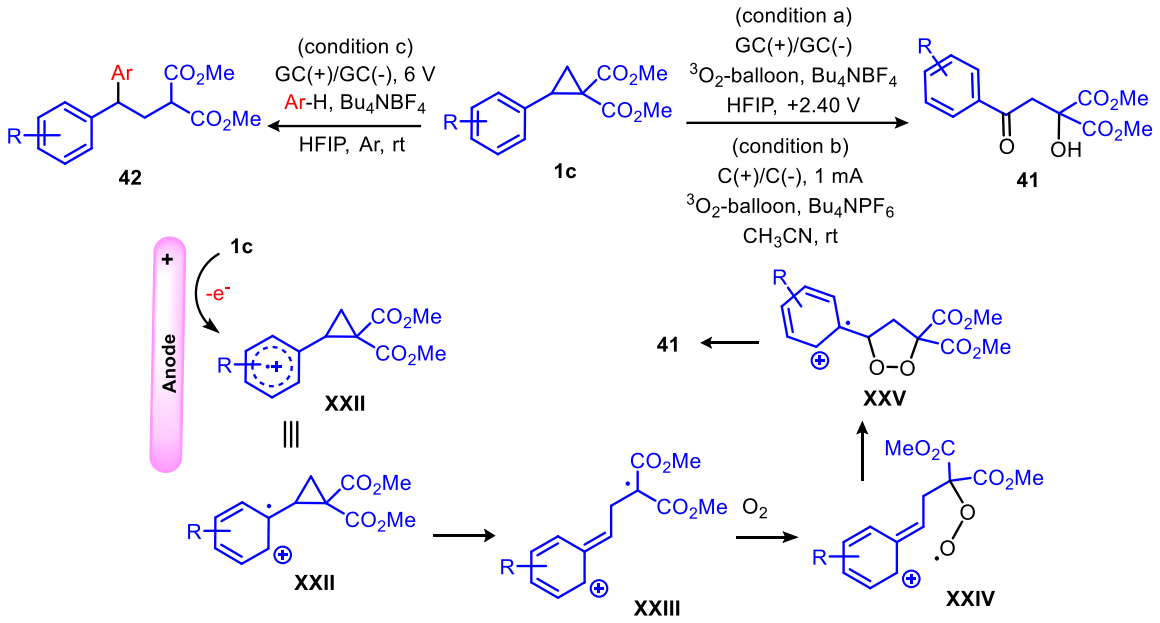

1.5. Cyclobutane: a four-membered strained carbocycle

The second smallest carbocycle is the cyclobutane which was synthesized first in 1907.[58] Cyclobutanes are often regarded as 'big brother' to the cyclopropane as they possess similar reactivity and properties.[59] These are the second strained carbocycles having a strain energy of 26.7 kcal/mol which is almost similar to cyclopropane (27.5 kcal/mol) but much higher than cyclopentane (7.4 kcal/mol). Interestingly, the incorporation of a substituent (e.g. methyl group) on this four-membered ring decreases the ring strain energy slightly. Whereas *gem*-dimethyl substituted cyclobutane enjoys the reduction of ring strain energy of more than 8 kcal/mol due to the Thorpe-Ingold effect[60] (Figure 1.5.1.A). The C-C bond length of cyclobutanone is 1.56 Å which is even longer than that of ethane (1.54 Å). This slight elongation occurs as a result of 1,3 C-C non-bonding repulsions which arises as the cross distance between them is only 2.22 Å (Figure 1.5.1.B). The internal bond angle in the cyclobutane ring is expected to be 90° if it was planar but the actual angle is 88° which is significantly lower than the ideal tetrahedral carbon center (109.5°). This much deviation imposes a high angle strain but at the same time, the torsional strain relieves to some extent to compensate for the slight increase in angle strain. As a result, cyclobutane adopts a

Figure 1.5.1. Strain energy and 3-D structure of cyclobutane; (A) Strain energies of different carbocycles, (B) puckered (i) and eclipsed (ii) structure of cyclobutane

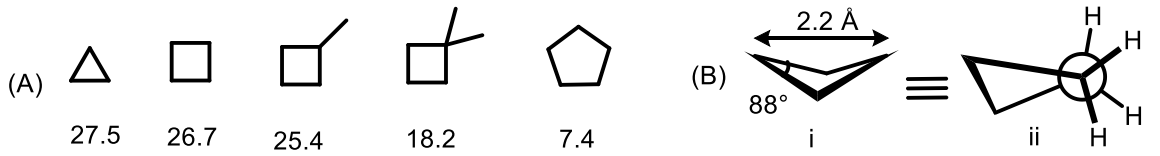

folded structure and remains in the puckered conformation which is energetically the most favorable for these strained carbocycles. Consequently, in cyclobutane, the C-C bonds bear more *p*-character while the C-H bonds bear more *s*-characters and thus they become less reactive than cyclopropane while much more reactive than comparatively inert cyclopentane.

Cyclobutanes have gained significant attraction in the last few decades owing to the easy preparative methods and the inherent strain-driven selective ring cleavage.[61] Though the simple cyclobutane is a colorless gas having no such biological properties, this motif often occurs in natural products mostly found in marine and plant objects e.g. sceptrins (isolated from Agelas sceptrum sea-spong) and *α*-pinene (found in coniferous trees).[58] However, with time the use of this cycloalkane increases substantially in organic and medicinal chemistry because of its unusual structural and physicochemical properties. The introduction of cyclobutane core in the

Figure 1.5.2. Biologically active compounds with cyclobutane core

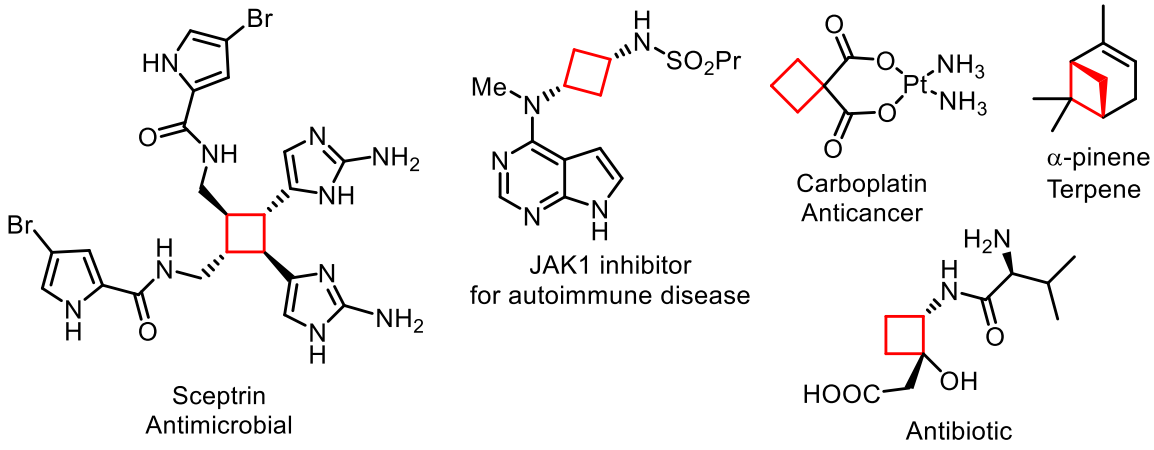

pharmaceutically active compounds also improve their usefulness and are thus utilized in various drug developments. Cyclobutane-containing organic scaffolds show various biological activities (Figure 1.5.2) like anticancer, JAK1 inhibitor, antiviral, antimicrobial, anti-diabetes, etc.[62]

1.6. Types of cyclobutanes

The reactivity of cyclobutane greatly depends on which type of substitution is there on this cyclic ring. In terms of different functional groups, the specific position of the substitution, and various reactivities, cyclobutane could be classified into five different categories- (i) cyclobutanol, (ii) cyclobutanone, (iii) 1-donor 2-acceptor cyclobutane, (iv) cyclobutene, (v) alkylidenecyclobutane (Figure 1.6.1). Similar to the DAC, when an electron-donating (D) and an electron-withdrawing group (A) are substituted vicinally to the cyclobutane ring, it is called 1-donor 2-acceptor cyclobutane or simply donor-acceptor cyclobutane.

Among them, cyclobutanols are generally activated with the transition metal catalysts by *β*-carbon

Figure 1.6.1. Classification of cyclobutane

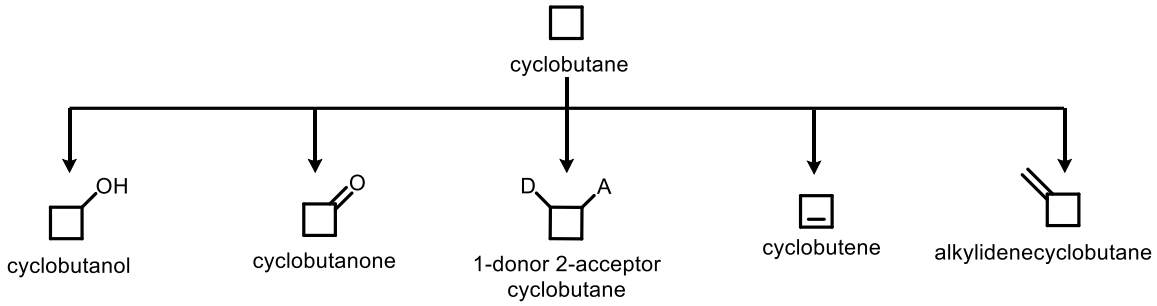

elimination via metal alkoxide formation or by radical pathway via *β*-scission to undergo various ring opening products. On the other hand, reactions of cyclobutanones occur under transition metal catalysis, Lewis acid catalysis, and even under organocatalysis (*vide infra*). The reactivity of donor-acceptor cyclobutanes is similar to the DACs as they could also undergo several cycloaddition reactions in the presence of different Lewis acids. However, depending on the different substitutions on different carbon atoms of the cyclobutenes, they can be activated through transition metal, Brønsted acid, or just employing heat to render ring-opening or cyclization products. Alkylidenecyclobutanes are mostly activated under transition metal catalysis either via oxidative addition or via organometallic addition followed by *β*-carbon elimination similar to the cyclobutanones (*vide infra*).[63]

1.7. Various catalytic activations of cyclobutanones

Cyclobutanones are one of the most exploited classes of four-membered carbocycles. Generally, two types of cyclobutanones are available in the literature, 3-substituted and 2-substituted cyclobutanones (Figure 1.7.1). If there is a substituent at the carbon center of the cyclobutane ring just one carbon away from the carbonyl carbon, it is denoted as 3-substituted cyclobutanone while substitution at the adjacent carbon to the carbonyl carbon is termed as 2-substituted cyclobutanone. When that particular substituent is an electron-donating group, it is called 3-donor or 3-D cyclobutanone.[64] Over the years, various catalytic methods have been employed to activate the cyclobutanone derivatives to construct numerous important organic scaffolds. Depending on the modes of different catalytic activations, the reactivity of cyclobutanones can be categorized into three sections, transition metal catalysis, Lewis acid catalysis, and organocatalysis.

Figure 1.7.1. Types of cyclobutanone

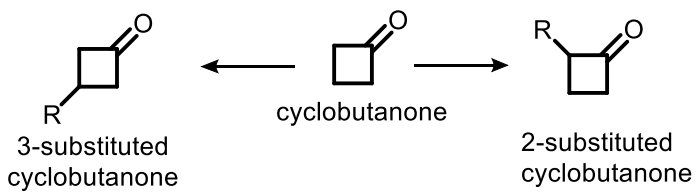

1.7.1. Transition metal catalysis

Transition metals have been used for the activation of cyclobutanones for the last few decades and have developed several methodologies for the construction of complex molecular architectures. Generally, two pathways are followed for the C1-C2 bond cleavage of cyclobutanone.[65] In the first case, an oxidative addition on the C-C bond (the carbonyl carbon and the adjacent carbon) of cyclobutanone **A** occurs by a low-valent transition metal (M) to form a five-membered metallacyclopentanone **B** that could lead to various ring-opening or cyclic products (Scheme 1.7.1.1, path a). However, a subsequent decarbonylation of **B** could also occur to render the cyclopropane derivative **C**. In the other pathway, a nucleophilic 1,2-addition by an organometallic compound (M-R) to the carbonyl group of cyclobutanone **A** could generate metal cyclobutanolate **D** followed by *β*-carbon elimination to furnish ring-opening product **E** which can further undergo various chemical transformations (Scheme 1.7.1.1, path b).

Scheme 1.7.1.1. Activation of cyclobutanone via transition metals

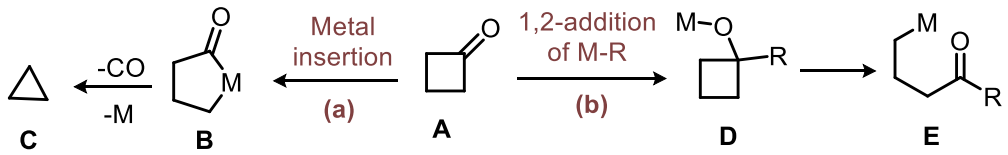

1.7.1.1. Rhodium catalysis: Among the available transition metals rhodium, nickel, and palladium are the most commonly exploited ones for the catalytic activation of cyclobutanones.[63] In the presence of a rhodium catalyst, cyclobutanones generally follow path a (Scheme 1.7.1.1) and eventually undergo various ring contraction and insertion reactions. In the case of ring contraction, cyclobutanones are converted into the other smallest carbocycle i.e. cyclopropanes by the extrusion of the carbonyl group. In 1996, Ito and Murakami[66] discovered this ring contraction strategy via decarbonylation of cyclobutanone **43** by the use of a stoichiometric amount of Wilkinson's catalyst, which was further extended for the catalytic version also modifying the rhodium catalyst to [{Rh(cod)dppb}BF_4] and obtained the cyclopropane **44** in quantitative yield (Scheme 1.7.1.1.a). The rhodium catalyst can also facilitate the insertion-type reaction where alkene or alkyne could be incorporated into the C1-C2 bond of the cyclobutanone. The reaction of 3-(2-styryl) cyclobutanone **45** in the presence of a rhodium catalyst led to the generation of a five-membered rhodacycle (similar to the previous one **XXVI**) via oxidative addition followed by an intramolecular insertion[67] of the tethered C-C double bond into the Rh-C (methylene) bond to produce benzobicyclo[3.2.1]octenone **46** (Scheme 1.7.1.1.b, left) The asymmetric version of this reaction was also executed later by Cramer *et al.*[68] with a different rhodium catalyst using (*R*)-DTMB-SEGPhos as a chiral ligand (Scheme 1.7.1.1.b, right).

Scheme 1.7.1.1.1. Rhodium catalysis, (a) ring contraction; (b) insertion reaction

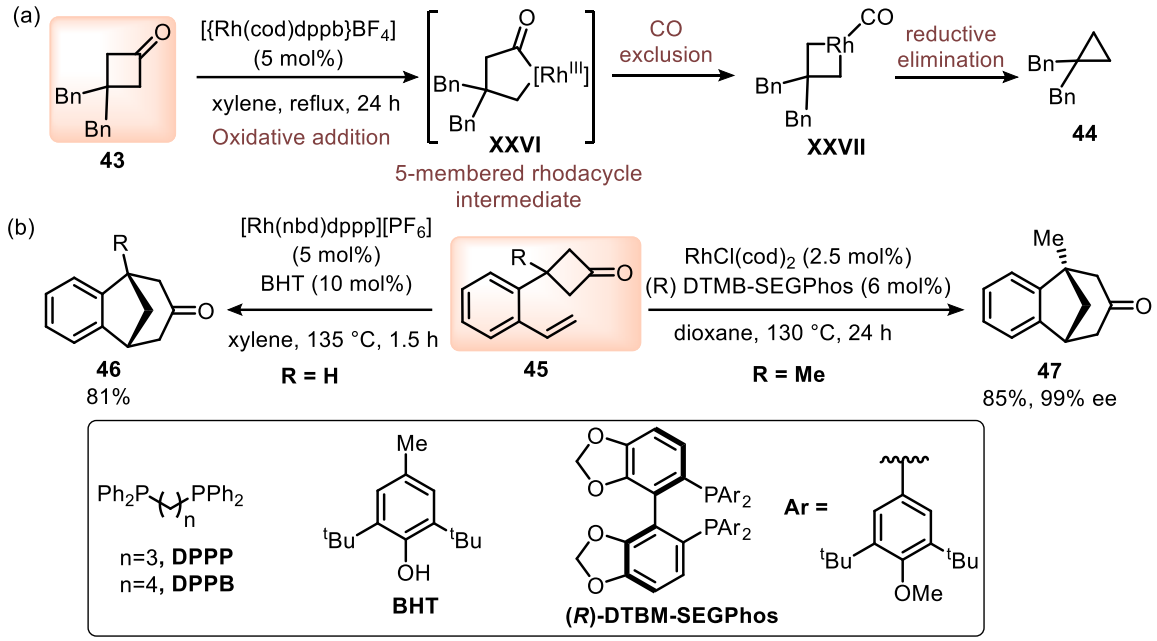

1.7.1.2. Nickel catalysis: Though the intramolecular insertion occurs smoothly via rhodium catalysts, their ability to perform intermolecular insertion becomes tough, on the contrary, nickel catalysts could effectively deliver the intermolecular insertion reactions.[63] In 2005, Murakami *et al*.[69] demonstrated an alkyne **49** insertion to cyclobutanone **48** to render two carbon ring expansion products cyclohexenone **50**. Here, at first, a nickel-catalyzed oxidative cyclization between the carbonyl group of cyclobutanone **48** and alkyne **49** happens to form oxanickelacyclopentene **XXVIII**. A subsequent *β*-carbon elimination engenders the ring-opening of the cyclobutane resulting in a seven-membered nickelacycle **XXIX** which further undergoes reductive elimination to give the desired product **50** (Scheme 1.7.1.2.1).

Scheme 1.7.1.2.1. Nickel catalysis

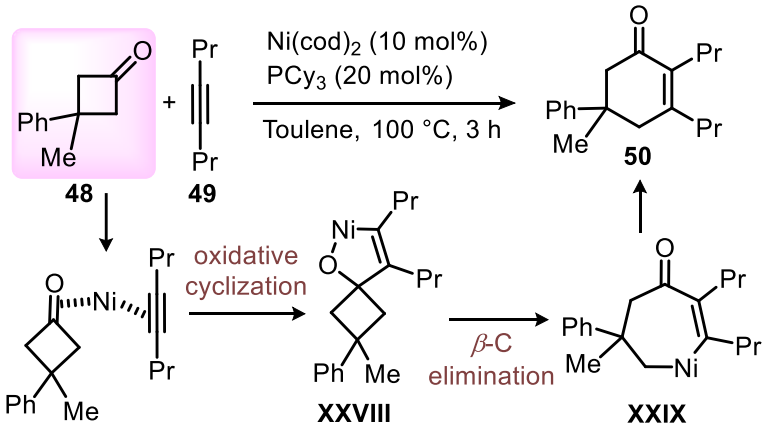

1.7.1.3. Palladium catalysis: Metal-catalyzed insertion of a double or triple bond is somewhat favorable as the π-bond facilitates the insertion of the metal into a C-C σ-bond and also two more

stable σ-bonds are generated at the expense of one π-bond after the insertion. In contrast, these types of kinetic and thermodynamic driving forces are not present in the case of σ-bond metathesis which makes them very difficult to achieve because here the breaking of σ-bonds is required without the participation of any π-bond. In this regard, Murakami *et al.*[70] disclose a palladium-catalyzed intramolecular σ-bond exchange between the C-C bond (cyclobutanone **51**) and the C-Si bond (silacyclobutane). Initially, the palladium (0) is incorporated into the C-Si bond of silacyclobutane via oxidative addition to produce silapalladacycle intermediate **XXX**. This palladium center bearing

Scheme 1.7.1.3.1. Palladium catalysis

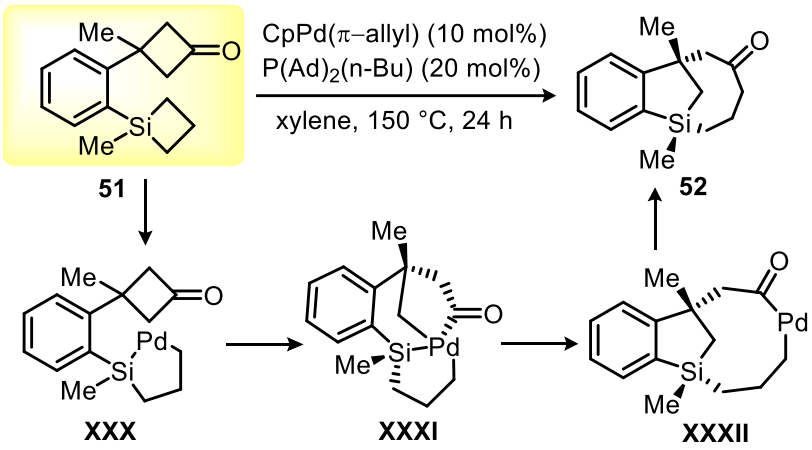

C and Si become electronically rich and thus it undergoes a second oxidative addition with the adjacent C (carbonyl)-C single bond of cyclobutanone moiety which renders a palladium (IV) intermediate **XXXI**. Subsequently, a reductive elimination gives rise to the bicyclic intermediate **XXXII** with C(sp^3)-Si bond formation, and eventually, another reductive elimination leads to the generation of **52** with C(carbonyl)-C(sp^3) σ-bond formation (Scheme 1.7.1.3.1).

1.7.2. Lewis acid catalysis

Another mode of activation of cyclobutanone systems is the Lewis acid catalysis, which generally coordinates to the electronegative atoms e.g. oxygen of the carbonyl group to induce polarization-driven ring cleavage of the four-membered carbocycle. In this regard, the 3-donor cyclobutanones **53** are the most commonly exploited ones for their unique reactivity of generating 1,4-zwitterionic intermediates **XXXIII** (Scheme 1.7.2.1.a). After the coordination of Lewis acid (LA), the combination effect of the electron-withdrawing carbonyl group and electron-donating group (EDG) polarizes the C2-C3 bond (**53a**), and eventually, the regioselective ring opening of the cyclobutanone occurs furnishing the stabilized 1,4-zwitterionic intermediate **XXXIII** which could further undergo various synthetic transformations.[64] This ring cleavage preference at the more substituted C2-C3 bond was first observed by Hasek and Martin[71] in 1963 during the distillation of 4-piperidinocyclobutanone **54** (Scheme 1.7.2.1.b).

Scheme 1.7.2.1. Ring cleavage of 3-donor cyclobutanone

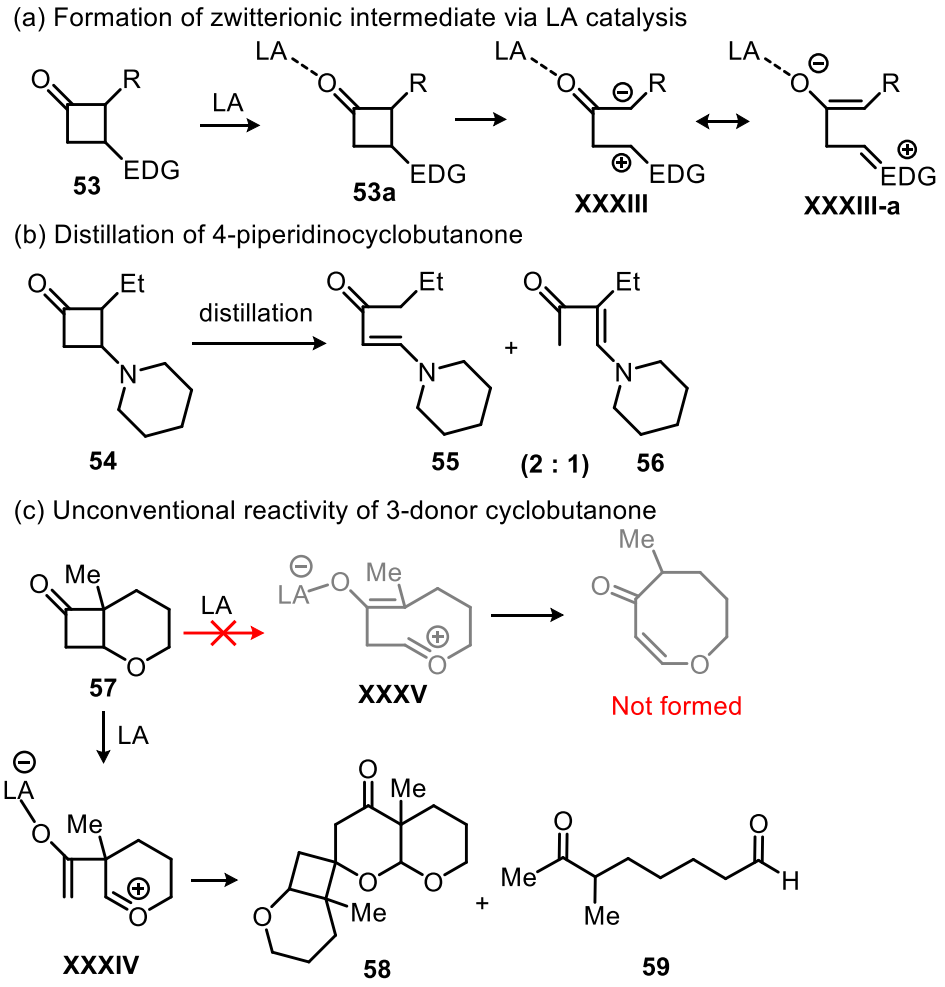

Though most of the reactions of this type of cyclobutanone follow the traditional reactivity,[64] Matsuo *et al*. noticed an abnormality while reporting the first Lewis acid catalyzed (4+2) cycloaddition of 3-ethoxy cyclobutanone with carbonyl compounds.[72] In the presence of Lewis acid, the tetrahydropyran-fused bicyclic cyclobutanone **57** undergoes the less substituted external C2-C3 bond cleavage to form a 1,4-zwitterionic species **XXXIV** alternate to the expected one **XXXV** which further reacts with the starting material and produces a tetracyclic **58** and an acyclic **59** compounds (Scheme 1.7.2.1.c).[72] Utilizing this strategy, they further developed a cross-cycloaddition reaction of bicyclic cyclobutanone **60** with aromatic aldehydes **61** where the corresponding (4+2)-cycloadduct **62** was formed in the presence of $BF_3{\cdot}Et_2O$. On the contrary, monocyclic cyclobutanone **63** showed the conventional reactivity when treated with the same Lewis acid where the aryl aldehydes were incorporated by the cleavage of more substituted C2-C3 bond (Scheme 1.7.2.2.a).[72] Later on, various other annulation reactions were reported with monocyclic cyclobutanones but strikingly in most of those cases, stoichiometric amounts of Lewis acids were employed.[64] Therefore studies on the activation of 3-donor cyclobutanone via catalytic usage of Lewis acid remain limited. Because low catalyst loading might slow the reaction rate which results

in low conversion to the product. Conversely, Rao et al.[73] found that the implementing catalytic amount of Lewis acid was also effective for the activation of 3-ethoxycyclobutane imine **67** which generates after the condensation of cyclobutanone **65** with mono-substituted hydrazine **66** (Scheme 1.7.2.2.b). This imine **67** undergoes an interesting rearrangement reaction via ring opening and cyclization to produce the product **68**.

Scheme 1.7.2.2. LA-activation of 3-donor cyclobutanone, (a) (4+2)-cycloaddition; (b) rearrangement

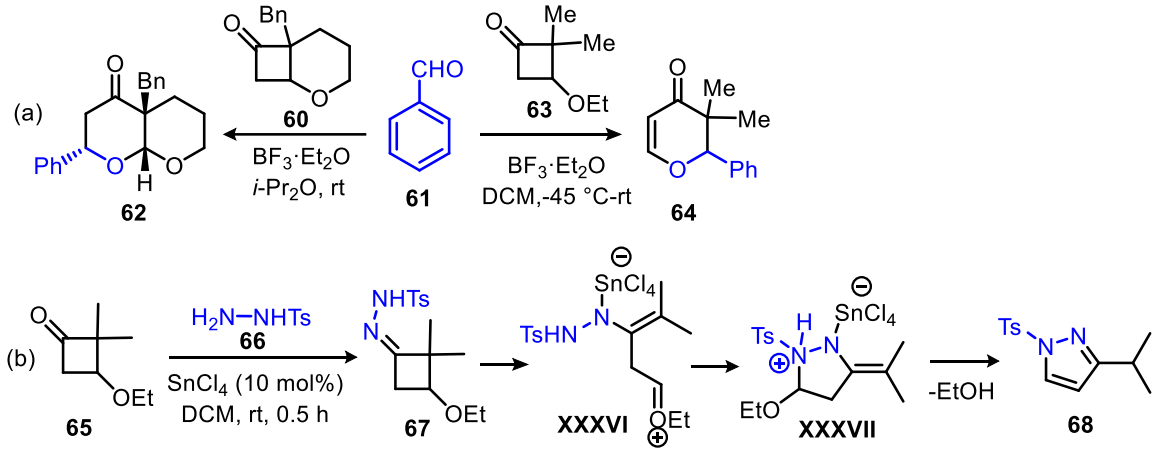

Another catalytic approach for the regiodivergent ring cleavage of cyclobutanone was documented by Cramer *et al.*[74] in 2015 where switching the Lewis acid controls the selective product formation (Scheme 1.7.2.3). An intramolecular formal (4+2) cycloaddition reaction took place between the cyclobutanone moiety and the adjacent carbonyl group of 3-(2-acetylphenyl)cyclobutanone **69** when a catalytic amount of $SnCl_4$ was used. This reaction follows the conventional ring opening that proceeds via the 1,4-zwitterionic intermediate as depicted in scheme 15a. On the other hand, changing the Lewis acid to $Cu(OTf)_2$ delivered the structurally distinct indenylacetic acid **71** from

Scheme 1.7.2.3. LA-catalyzed regiodivergent cyclobutanone cleavage

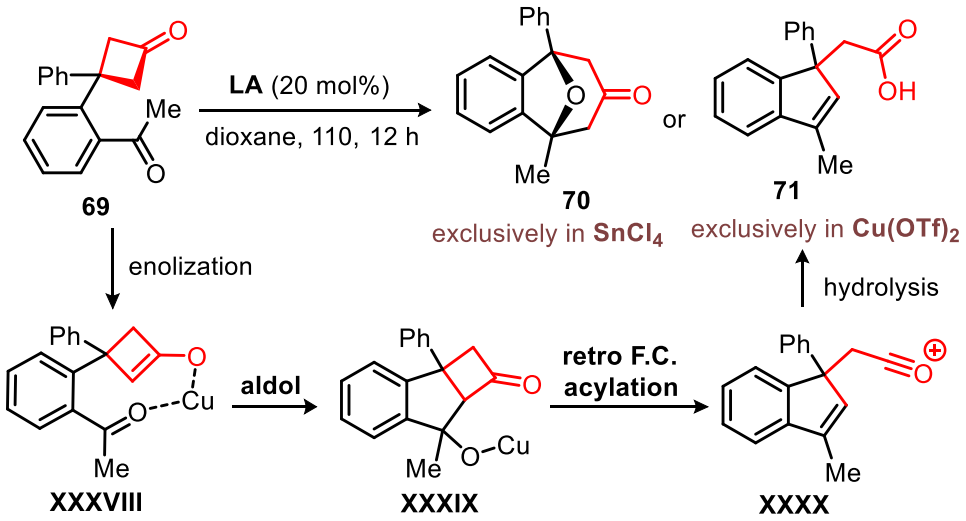

the same precursor **69**. This unprecedented occurrence can be rationalized by a completely different mechanistic pathway. In this case, the soft metal ion Cu(II) enables enolization of the cyclobutanone moiety which subsequently undergoes intramolecular aldol reaction to furnish the intermediate **XXXIX**. After that, a strain-driven retro-Friedel-Crafts acylation followed by the hydrolysis of acylium species **XXXX** generates the indene derivative **71**.

1.7.3. Organocatalysis

Unlike transition metal and Lewis acid catalysis, organocatalytic activation of cyclobutanone has not been that much flourished possibly because of its late appearance as a distinguishable catalytic method in the synthetic community. However, after the emergence of this catalytic field at the very beginning of this century, some notable asymmetric transformations have been developed via the organocatalytic activation of cyclobutanones to date.[75] After the development of an asymmetric Mannich-type reaction from simple cyclobutanone **72** in the presence of a modified proline

Scheme 1.7.3.1. Organocatalytic reactions of cyclobutanones: (a) from simple cyclobutanone, (b) Ring expansion reactions of 2-substituted cyclobutanone

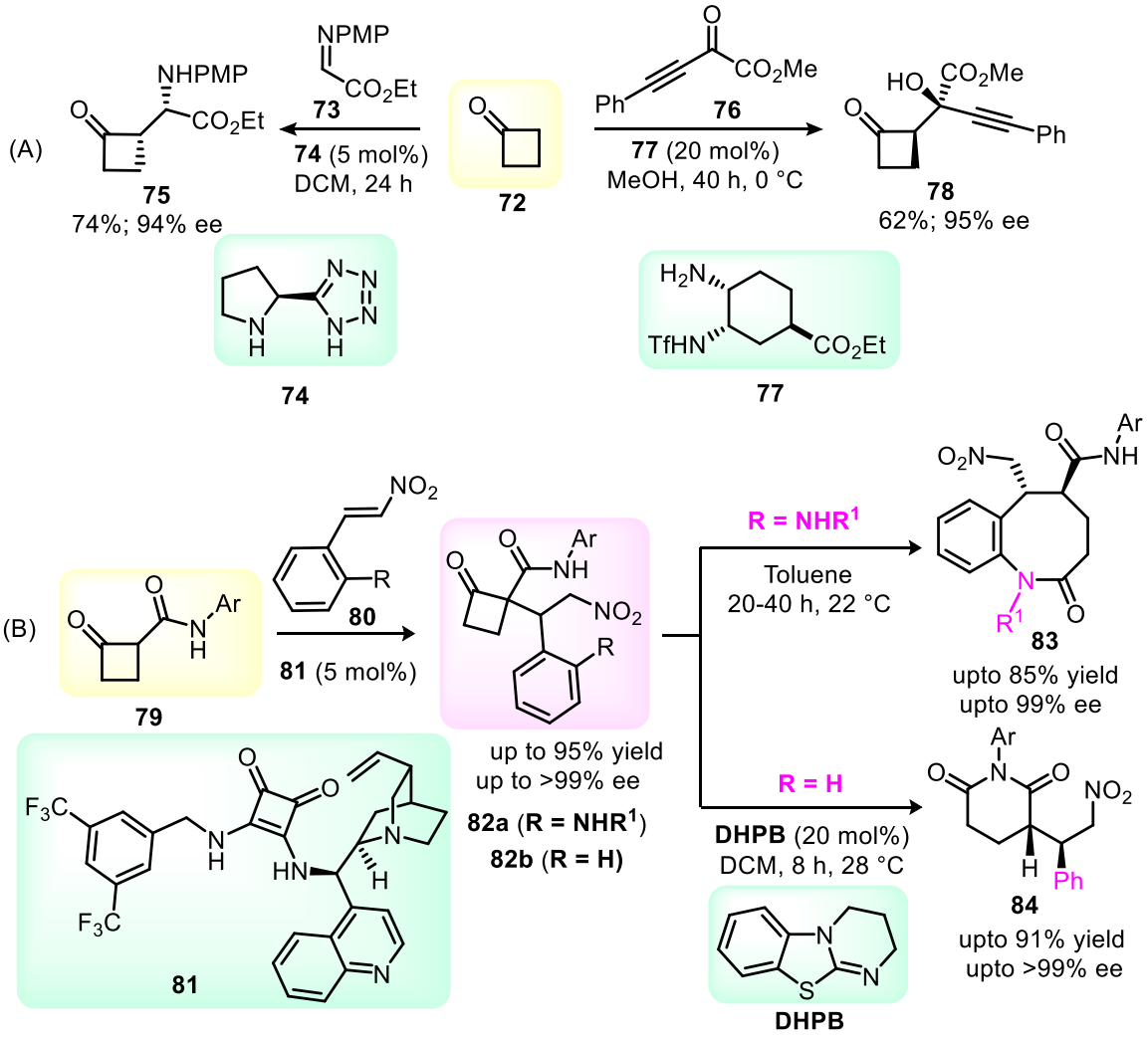

derivative **74** by Ley and his group[76] in 2004 (Scheme 1.7.3.1.A, left), similar cyclobutanone was again exploited for the asymmetric direct aldol reaction catalyzed by chiral *cis*-diamine-based organocatalyst **77** by Maruoka's group[77] in 2012 (Scheme 1.7.3.1.A, right). Activated cyclobutanone, e.g. 2-oxocyclobutane carboxamide **79** could undergo asymmetric Michael reaction[78] with nitro alkene **80** in the presence of catalyst **81** to furnish α, α-disubstituted cyclobutanone **82** which further could take part in various ring expansion reactions (Scheme 1.7.3.1.B). In 2019, Coquerel and Rodriguez together demonstrated two different ring expansion strategies by employing the same bifunctional aminocatalyst **81** from cyclobutanone by incorporating an *ortho*-substitution on the aryl group of nitroalkene. After the formation of the corresponding Michael adducts (**82a** and **82b**), the *ortho*-amino nitrostyrene substituted one **82a** undergoes a four-atom ring expansion[79a] to render eight-membered heterocycle **83**. In contrast, the simple nitrostyrene **82b** undergoes two-atom ring expansion[79b] in the presence of DHPB base to form six-memberd heterocycle **84**.

On the other hand, the enantioselective desymmetrization of 3-donor cyclobutanone was pioneered by Honda *et al*.[80] in the early 1990s through a chiral lithium amide **85** derived aldol reaction. In this strategy, asymmetric deprotonation of cyclobutanone **88** occurred to form chiral enolate which was then converted to the enantioenriched silyl enol ether **87** after reacting with triethylsilyl chloride (TESCl) followed by the addition of valeraldehyde **88** to furnish the corresponding aldol product **89** as a diastereomeric mixture (Scheme 1.7.3.2.a, left). Later, Piras's group,[81] in 2012, extended the same protocol with the help of a proline-based organocatalyst **90** with aromatic aldehydes **91** (Scheme 1.7.3.2.a, right). Here, the enamine intermediate **XXXXI** forms at first, which undergoes

Scheme 1.7.3.2. Desymmetrization of cyclobutanone

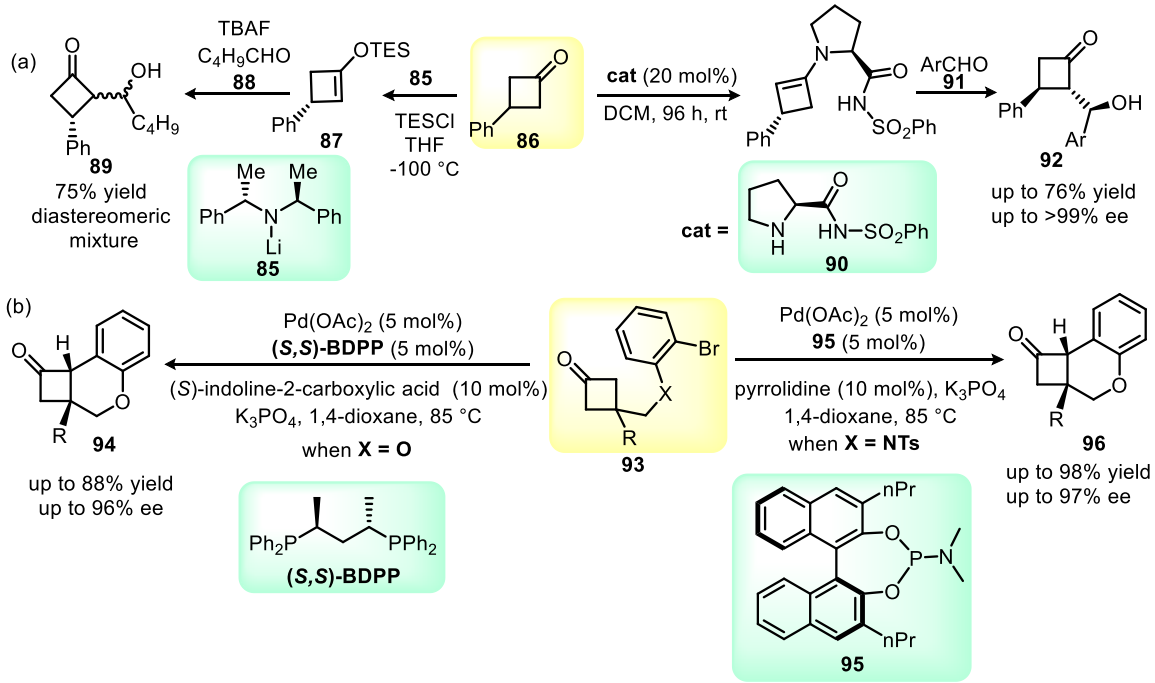

the hydrogen bonding assisted aldol reaction to render the preferred isomer of the product **92**. Later, in 2018, Lu's group[82] developed a synergistic catalytic approach for the desymmetrization of 3-substituted cyclobutanone **93** by employing the combination of palladium and an amine catalyst (Scheme 1.7.3.2.b).

In summary, this chapter discusses the strain-releasing reactivities of the two smallest carbocycles and the application of different catalytic systems to activate DACs and cyclobutanones for constructing chiral and achiral organic frameworks. It discusses that various catalysts can activate these two strained cyclic systems in different ways depending on the substitution pattern. Several distinctive cyclic and acyclic organic scaffolds can be generated from the same strained carbocycle as a precursor by employing diverse catalysts which guided their reactivities in different ways. Though numerous methodologies have flourished over the years, the inception of new ideas to utilize the potential of these small carbocycles using appropriate catalysts can still bring out unprecedented chemical transformations.

1.8. Aim of this thesis

This doctoral thesis aimed to represent the exploration of three different types of catalysis from transition metal containing Lewis acid and metal-free Brønsted acid to green organocatalysis for the activation of the two smallest carbocyclic compounds. The cyclopropane was activated by asymmetric organocatalysis to construct chiral heterocycles. However, tandem activation of both the smallest carbocycles was achieved by Lewis acid catalysis to synthesize achiral acyclic molecules, and Brønsted acid activation of cyclobutane rendered the achiral heterobicyclic scaffolds. The insightful experimental studies for the objectives of the thesis are discussed in the following chapters

Chapter 2A demonstrates the first organocatalytic activation of *racemic* donor−acceptor cyclopropane carbaldehydes for the asymmetric (3 + 3)-cycloaddition with aryl hydrazones followed by an intriguing 1,3-aryl migration toward the synthesis of enantioenriched tetrahydropyridazines via matched/mismatched kinetic resolution.

Chapter 2B discusses the first organocatalytic (3+3)-cycloaddition of ortho-substituted phenyl nitrones with aryl cyclopropane carbaldehydes for the synthesis of enantioenriched 1,2-oxazinanes via an unusual type of kinetic resolution.

Chapter 3 displays the merging of two strained carbocycles by Lewis acid catalysis for the remote site-selective Friedel−Crafts alkylation of *in situ* generated *β*-naphthol for the synthesis of *γ*-naphthyl butyric acid derivatives.

Chapter 4 deals with the Brønsted acid-catalyzed cascade ring-opening/cyclization of 3-ethoxy cyclobutanones to access 2,8-dioxabicyclo[3.3.1]nonane derivatives

1.9. References

1. Hui, C.; Craggs, L.; Antonchick, A. P. *Chem. Soc. Rev.* **2022**, *51*, 8652–8675.

2. Katritzky, A. R.; Ramsden, C. A.; Scriven, E. F. V.; Taylor, R. J. K. Comprehensive Heterocyclic Chemistry III, **2008**, Pages xxi-xxix.

3. Freund, A. *Journal für Praktische Chemie.* **1881**, *26*, 367-377.

4. Sethuraman, K.N.; Jones, J.; Dyer, K.S. Ch 122, Anesthetic-Agent Mass Casualty Incident. In *Ciottone's Disaster Medicine (2nd edition)*; Elsevier, **2016**; 692–695.

5. Coulson, C. A.; Moffit, W. E. J. *Chem. Phys*. **1947**, *15*, 151.

6. Meijere, A. *Angew. Chem. Int. Ed.* **1979**, *18*, 809-826.

7. (a) Ma, S.; Mandalapu, D.; Wang. S.; Zhang, Q. *Nat. Prod. Rep.* **2022**, *39*, 926–945. (b) Ebner, C.; Carreira, E. M. *Chem. Rev.* **2017**, *117*, 11651−11679. (c) Wu, W.; Lin, Z.; Jiang, H. *Org. Biomol. Chem.* **2018**, *16*, 7315–7329.

8. (a) Chen, D. Y.-K.; Pouwer, R. H.; Richard, J.-A.; *Chem. Soc. Rev.* **2012**, *41*, 4631–4642. (b) Sansinenea, E.; Ortiz, A. *Eur. J. Org. Chem*. **2022**, e202200210.

9. (a) Reissig, H.-U. *Angew. Chem. Int. Ed.* **1996**, *35*, 971-973. (b) Lautens, M.; Klute, W.; Tam,

W.; *Chem. Rev*. **1996**, *96*, 49−92. (c) Lebel, H.; Marcoux, J.-F.; Molinaro, C.; Charette, A. B. *Chem. Rev.* **2003**, *103*, 977−1050.

10. Pirenne, V.; Muriel, B.; Waser, J. *Chem. Rev.* **2021**, *121*, 1, 227–263.

11. Raiguru, B. P.; Nayak, S.; Mishra, D. R.; Das, T. Mohapatra, S.; Mishra, N. P.; *Asian J. Org. Chem.* **2020**, *9*, 1088-1132.

12. Jang, Y.; Machín-Rivera, R.; Lindsay, V. N. G. *Synthesis* **2021**, *53*, 3909–3934.

13. Liu, Q.; You, B.; Xie, G.; Wang, X. *Org. Biomol. Chem.* **2020**, *18*, 191-204.

14. Brandi, A.; Cicchi, S.; Cordero, F. M.; Goti, A. *Chem. Rev*. **2014**, *114*, 7317-7420.

15. Reissig, H.-U.; Hirsch, E. *Angew. Chem. Int. Ed.* **1980**, *19*, 813-814.

16. Schneider, T. F. Kaschel, J.; Werz, D. B. *Angew. Chem. Int. Ed*. **2014**, *53*, 5504−5523.

17. Reissig, H. U.; Zimmer, R. *Chem. Rev*. **2003**, *103*, 1151−1196.

18. Xia, Y.; Liu, X.; Feng, X. *Angew. Chem. Int. Ed*. **2021**, *60*, 9192–9204.

19. Lewis, G. N. *J. Am. Chem. Soc.* **1916**, *38*, 4, 762–785.

20. Mamari, H. H. A.; Electrophile and Lewis Acid. Developments and Uses of Lewis Acids: From Conventional Catalysts to Modern Green Catalysts; IntechOpen, 2023; pp 1-21

21. Carey, F. A.; Sundberg, R. J. Advanced Organic Chemistry. 5th ed. Part A: Structure and Mechanisms; Springer, 2007.

22. Banerjee, P.; Biju, A. T. Donor-Acceptor Cyclopropanes in Organic Synthesis. Wiley-VCH: Weinheim, 2024.

23. Reissig, H. U. *Tetrahedron Lett*. **1981**, *22*, 2981 – 2984.

24. Young, I. S.; Kerr, M. A. *Angew. Chem. Int. Ed*. **2003**, *42*, 3023 – 3026.

25. Sibi, M. P.; Ma, Z.; Jasperse, C. P. *J. Am. Chem. Soc*. **2005**, *127*, 5764-5765.

26. Kang, Y. B.; Sun, X. L.; Tang, Y. *Angew. Chem. Int. Ed*. **2007**, *46*, 3918 –3921.

27. Parsons, A. T.; Johnson, J. S. *J. Am. Chem. Soc.* **2009**, *131*, 3122–3123

28. (a) Bao, M.; Doyle, M. P. *Org. Lett*. **2023**, *25*, 3029−3033.

29. Pohlhaus, P. D.; Johnson, J. S. *J. Am. Chem. Soc*. **2005**, *127*, 16014-16015.

30. (a) Trost, B. M. *Science*. **1991**, *254*, 1471-1477. (b) Trost, B. M. *Angew. Chem., Int. Ed.* **1995**, *34*, 259-281.

31. Tipper, C. F. H. *J. Chem. Soc.* **1955**, 2045.

32. Turkowska, J.; Durka, J.; Ociepa, M.; Gryko, D. *Chem. Commun.* **2022**, *58*, 509–512.

33. Liu, L.; Wang, X.; Xiao, W.; Chang, W.; Li, J. *Chem. Eur. J.* **2023**, *29*, e202202544 (1 of 6).

34. (a) Dalko, P. I. Enantioselective Organocatalysis, Wiley-VCH, Weinheim, Germany, 2007. (b) Bertelsen, S.; Jørgensen, K. A. *Chem. Soc. Rev*. **2009**, *38*, 2178–2189. (c) Maruoka, K.; List, B.; Yamamoto, H.; Gong, L.-Z. *Chem. Commun*. **2012**, *48*, 10703. (d) Liu, D. J.; Chen, E. Y.-X. *Green Chem*. **2014**, *16*, 964–981. (e) Abbasov, M. E.; Romo, D. *Nat. Prod. Rep*. **2014**, *31*, 1318–1327. (f) Aleman, J.; Cabrera, S. *Chem. Soc. Rev*. **2013**, *42*, 774-793.

35. MacMillan, D. W. C. Nature. **2008**, *455*, 304–308

36. List, B. *Chem. Rev*. **2007**, *107*, 12, 5413-5415

37. Reyes, E.; Uria, U.; Prieto, L.; Carrillo, L.; Vicario, J. L. *Tetrahedron Chem*. **2023**, *7*, 100041 (1-17).

38. Dickmeiss, G.; Sio, V. D.; Udmark, J.; Poulsen, T. B.; Marcos, V.; Jørgensen, K. A. *Angew. Chem. Int. Ed.* **2009**, *48*, 6650 – 6653.

39. Sparr, C.; Gilmour, R. *Angew. Chem. Int. Ed.* **2011**, *50*, 8391–8395.

40. Wallbaum, J.; Garve, L. K. B.; Jones, P. G.; Werz, D. B. *Chem. Eur. J.* **2016**, *22*, 18756 – 18759.

41. Diaz, E.; Reyes, E.; Uria, U.; Carrillo, L.; Tejero, T.; Merino, P.; Vicario, J. L. *Chem. Eur. J.* **2018**, *24*, 8764–8768.

42. Halskov, K. S.; Kniep, F.; Lauridsen, V. H.; Iversen, E. H.; Donslund, B. S.; Jørgensen, K. A. *J. Am. Chem. Soc.* **2015**, *137*, 1685−1691.

43. Prieto, L.; Sμnchez-Díez, E.; Uria, U.; Reyes, E.; Carrillo, L.; Vicario, J. L. *Adv. Synth. Catal*. **2017**, *359*, 1678–1683.

44. Blom, J.; Vidal-Albalat, A.; Jørgensen, J.; Barløse, C. L.; Jessen, K. S.; Iversen, M. V.; Jørgensen, K. A. *Angew. Chem. Int. Ed.* **2017**, *56*, 11831–11835.

45. McLeod, D. A.; Thøgersen, M. K.; Barløse, C. L.; Skipper, M. L.; Obregón, E. B.; Jørgensen, K. A. *Angew. Chem. Int. Ed*. **2022**, *61*, e202206096 (1-7).

46. Ortega, A.; Manzano, R.; Uria, U.; Carrillo, L.; Reyes, E.; Tejero, T.; Merino, P.; Vicario, J. L. *Angew. Chem. Int. Ed.* **2018**, *57*, 8225 –8229.

47. Dey, R.; Banerjee, P.; *Adv. Synth. Catal*. **2019**, *361*, 2849– 2854.

48. Dey, R.; Rajput, S.; Banerjee, P. *Tetrahedron*. **2020**, *76*, 131080.

49. Romero, N. A.; Nicewicz, D. A. *Chem. Rev*. **2016**, *116*, 10075-10166.

50. Shaw, M. H.; Twilton, J.; MacMillan, D. W. C. *J. Org. Chem.* **2016**, *81*, 6898-6926.

51. (a) Sivanandan, S. T.; Krishna, R. B.; Baiju, T. V.; Mohan, C. *Eur. J. Org. Chem.* **2021**, 6781–6805. (b) Lu, Z.; Shen, M.; Yoon, T. P. *J. Am. Chem. Soc*. **2011**, *133*, 1162-1164. (c) Amador, A. G.; Sherbrook, E. M.; Yoon, T. P. *J. Am. Chem. Soc*. **2016**, *138*, 4722-4725. (d) Amador, A. G.; Sherbrook, E. M.; Lu, Z.; Yoon, T. P. *Synthesis*. **2018**, *50*, 539-547.

52. Ge, L.; Zhang, C.; Pan, C.; Wang, D.-X.; Liu, D.-Y.; Li, Z.-Q.; Shen, P.; Tian, L.; Feng, C. *Nat Commun.* **2022**, *13*, 5938.

53. Zhu, C.; Ang, N. W. J.; Meyer, T. H.; Qiu, Y.; Ackermann, L. *ACS Cent. Sci*. **2021**, *7*, 415−431.

54. (a) Yan, M.; Kawamata, Y.; Baran, P. S. *Chem. Rev.* **2017**, *117*, 13230−13319. (b) Pollok, D.; Waldvogel, S. R. *Chem. Sci*. **2020**, *11*, 12386–12400. (c) Yoshida, J.; Kataoka, K.; Horcajada, R.; Nagaki, A. *Chem. Rev.* **2008**, *108*, 2265–2299. (d) Francke, R.; Little, R. D. *Chem. Soc. Rev*. **2014**, *43*, 2492-2521. (e) Novaes, L. F. T.; Liu, J.; Shen, Y.; Lu, L.; Meinhardt, J. M.; Lin, S. *Chem. Soc. Rev.*, **2021**, *50*, 7941-8002.

55. Kolb, S.; Petzold, M.; Brandt, F.; Jones, P. G.; Jacob, C. R.; Werz, D. B. *Angew. Chem. Int. Ed.* **2021**, *60*, 15928–15934.

56. Saha, D.; Taily, I. M.; Banerjee, P. *Eur. J. Org. Chem.* **2021**, 5053–5057.

57. Kolb, S.; Ahlburg, N. L.; Werz, D. B. *Org. Lett.* **2021**, *23*, 5549-5553.

58. Kolk, M. R.; Janssen, M. A. C. H.; Rutjes, F. P. J. T.; Blanco-Ania, D. *ChemMedChem.* **2022**, *17*, e202200020

59. Seiser, T.; Saget, T.; Tran, D. N.; Cramer, N. *Angew. Chem. Int. Ed.* **2011**, *50*, 7740–7752.

60. Ringer, A. L.; Magers, D. H. *J. Org. Chem.* **2007**, *72*, 2533-2537.

61. (a) Matsuda, T. Reactions of Four-Membered Ring Compounds. Wiley-VCH Verlag GmbH & Co. KGaA, Ch 3, 2016. (b) Wong, H. N. C.; Lau, K.-L.; Tam, K.-F. The Application of Cyclobutane Derivatives in Organic Synthesis. *Top. Curr. Chem.* **1986**, *133*, 83-157.

62. (a) Bauer, M. R.; Fruscia, P. D.; Lucas, S. C. C.; Michaelides, I. N.; Jennifer E. Nelson, J. E.; Storer, R. I.; Whitehurst, B. C. *RSC Med. Chem.* **2021**, *12*, 448–471. (b) Dembitsky, V. M. *J Nat Med.* **2008**, *62*, 1–33.

63. Murakami, M.; Ishida; N. *Chem. Rev.* **2021**, *121*, 264-299.

64. Matsuo, J. *Tetrahedron Lett*. **2014**, *55*, 2589–2595.

65. (a) Souillart, L.; Cramer, N. *Chem. Rev*. **2015**, *115*, 9410-9464. (b) Fumagalli, G.; Stanton, S.; Bower, J. F. *Chem. Rev*. **2017**, *117*, 9404-9432.

66. Murakami, M.; Amii, H.; Shigeto, K.; Ito, Y. *J. Am. Chem. Soc.* **1996**, *118*, 8285-8290.

67. Murakami, M.; Itahashi, T.; Ito, Y. *J. Am. Chem. Soc*. **2002**, *124*, 13976-13977.

68. Souillart, L.; Parker, N.; Cramer, N. *Angew. Chem., Int. Ed*. **2014**, *53*, 3001-3005.

69. Murakami, M.; Ashida, S.; Matsuda, T. *J. Am. Chem. Soc*. **2005**, *127*, 6932-6933.

70. Ishida, N.; Ikemoto, W.; Murakami, M. *J. Am. Chem. Soc*. **2014**, *136*, 5912-5915.

71. Hasek, R. H.; Martin, J. C. *J. Org. Chem.* **1963**, *28*, 1468-1474.

72. Matsuo, J.; Sasaki, S.; Tanaka, H.; Ishibashi, H. *J. Am. Chem. Soc.* **2008**, *130*, 11600–11601.

73. Shan, G.; Liu, P.; Rao, Y. *Org. Lett.* **2011**, *13*, 7, 1746–1749.

74. Souillart, L.; Cramer, N. *Chem. Eur. J*. **2015**, *21*, 1863–1867.

75. (a) Wen, K.-G.; Peng, Y.-Y.; Zeng, X.-P. *Org. Chem. Front*. **2020**, *7*, 2576–2597. (b) Barday, M.; Bouillac, P.; Coquerel, Y.; Amatore, M.; Constantieux, T.; Rodriguez, J. *Eur. J. Org. Chem.* **2021**, 3023–3034.

76. Cobb, A. J. A.; Shaw, D. M.; Ley, S. V. *SYNLETT*, **2004**, *3*, 0558–0560.

77. Moteki, S. A.; Han, J.; Arimitsu, S.; Akakura, M.; Nakayama, K.; Maruoka, K. *Angew. Chem. Int. Ed*. **2012**, *51*, 1187–1190.

78. Mailhol, D.; Duque, M. M. S.; Raimondi, W.; Bonne, D.; Constantieux, T.; Coquerel, Y.; Rodriguez, J. *Adv. Synth. Catal*. **2012**, *354*, 3523–3532.

79. (a) Zhou, Y.; Wei, Y.-L.; Rodriguez, J.; Coquerel, Y. *Angew. Chem. Int. Ed*. **2019**, *58*, 456–460. (b) Wei, Y.-L.; Ren, Y.; Mailhol, D.; Rajzmann, M.; Rodriguez, J.; Coquerel, Y. *Adv. Synth. Catal*. **2019**, *361*, 2992–3001. (c) Yang, W.-L.; Li, W.; Yang, Z.-T.; Deng, W.-P.; *Org. Lett*. **2020**, *22*, 4026-4032; (d) Yang, W.-L.; Wang, Y.-L.; Li, W.; Gu, B.-M.; Wang, S.-W.; Luo, X.; Tian, B.-X.; Deng, W.-P.; *ACS Catal*. **2021**, *11*, 12557-12564.

80. Honda, T.; Kimura, N. *J. Chem. Soc. Chem. Commun*. **1994**, 77–78.

81. Aitken, D. J.; Bernard, A. M.; Capitta, F.; Frongia, A.; Guillot, R.; Ollivier, J.; Piras, P. P.; Secci, F.; Spiga, M. *Org. Biomol. Chem.* **2012**, *10*, 5045–5048.

82. Wang, M.; Chen, J.; Chen, Z.; Zhong, C.; Lu, P. *Angew. Chem. Int. Ed*. **2018**, *57*, 2707–2711.

Chapter 2

Asymmetric Organocatalytic Activation of Cyclopropane Carbaldehydes Towards the Construction of Enantioenriched Heterocycles

Chapter 2: Organocatalytic Activation of Cyclopropane Carbaldehyde

2.1. Introduction

The burgeoning field of organocatalysis paved the way for asymmetric synthesis using small organic molecules and a myriad of enantioselective methodologies have already been developed in this century.[1] As discussed in Chapter 1, various organocatalytic strategies have flourished in the past few years through the activation of donor-acceptor cyclopropane to obtain several cyclic and acyclic organic compounds in an enantioselective manner. However, organocatalytic cycloaddition reaction has not been developed from *racemic* cyclopropane carbaldehydes. So, in this chapter, we present enantioselective (3+3) cycloaddition reaction of cyclopropane carbaldehydes with two different dipolar systems. This chapter is divided into two parts. In Chapter 2A, we have chosen the aryl hydrazone derivatives which can effectively undergo (3+3) cycloaddition with another 1,3-dipolar synthon e.g. donor-acceptor cyclopropane. Here, the cyclopropane carbaldehyde was activated by the secondary amine catalyst via iminium ion formation which further took part in (3+3) cycloaddition with aryl hydrazone derivatives. Additionally, an unusual aryl migration occurred which led to the one-step synthesis of chiral tetrahydropyridazine derivatives with an exocyclic double bond. Furthermore, mechanistic investigations have been performed by density functional theory. Also, a series of control experiments have been conducted to get insights into the actual reason behind the asymmetric induction from a racemic substrate. In Chapter 2B, we have taken nitrone as the 1,3-dipolar system which undergoes a similar type of (3+3) cycloaddition with the cyclopropane carbaldehydes in the presence of the same secondary amine organocatalyst. In this case, the aryl migration could take place if an appropriate substitution was incorporated into the nitrone derivative.

References

1. (a) Enders, D.; Grondal, C.; Huttl, M. R. M. *Angew. Chem. Int. Ed.* **2007**, *46*, 1570–1581. (b) Enders, D.; Niemeier, O.; Henseler, A. *Chem. Rev.* **2007**, *107*, 5606−5655. (c) Mukherjee, S.; Yang, J. W.; Hoffmann, S.; List, B. *Chem. Rev.* **2007**, *107*, 5471−5569. (d) Moyano, A.; Rios, R. *Chem. Rev.* **2011**, *111*, 4703–4832. (e) Volla, C. M. R.; Atodiresei, I.; Rueping, M. *Chem. Rev.* **2014**, *114*, 2390−2431.

Chapter 2A

Organocatalytic Activation of Donor-Acceptor Cyclopropanes: A Tandem (3+3)-Cycloaddition/Aryl Migration towards the Synthesis of Enantioenriched Tetrahydropyridazines

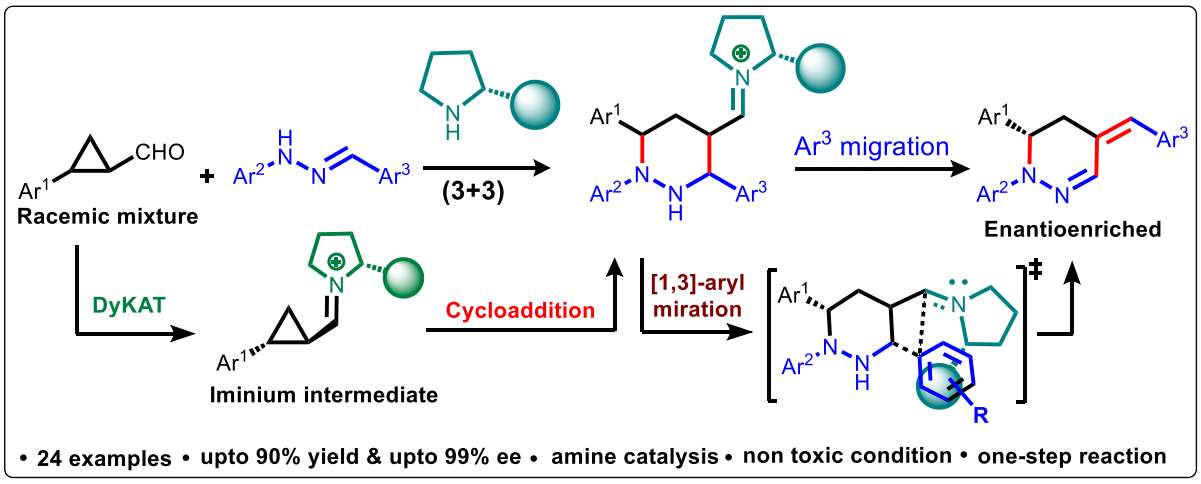

This work was published in *Organic Letters* (A journal of the *American Chemical Society*). Please see citation "Hazra, A.; Dey, R.; Kushwaha, A.; Kumar, T. J. D.; Banerjee, P. *Org. Lett.* **2023**, *25*, 5470−5475."

2.A.1. Introduction

The construction of complex chemical entities from simpler building blocks is an essential and evergreen area of organic chemistry.[1] Over the decades, various building blocks have been studied and utilized to access a large number of complex compounds by using their typical reactivities. In this realm, donor-acceptor cyclopropane (DAC), a unique three-carbon building block, has been extensively employed to synthesize various important compounds in recent times. Especially its ability to generate a reactive 1,3-dipole *in situ* makes it an ideal choice for a large number of dipolar cycloadditions to provide a wide variety of cyclic compounds.[2] An array of cycloadditions of DACs with various dipoles, dienes, and double bonds have been reported.[3] However, these methodologies are pre-eminently associated with metal-containing Lewis acid catalysts, whereas their enantioselective versions are less explored.[4] Most of the reported asymmetric cycloadditions of DACs have been accomplished using a combination of Lewis acid and chiral ligand[5] (Scheme 2.A.1.1.A).

Scheme 2.A.1.1. Enantioselective cycloadditions of cyclopropanes

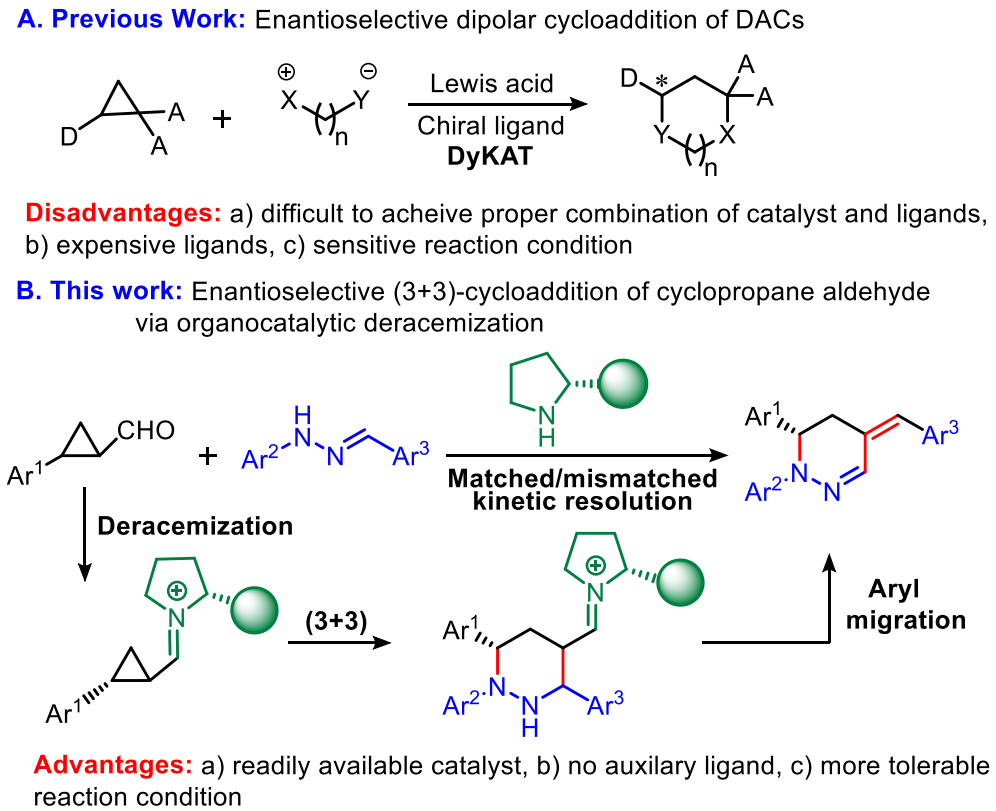

Our laboratory has been working on the reactivity of DACs for more than a decade[6] and developed various methodologies for the one-step synthesis of several carbo- and heterocycles.[7] Keeping the unexplored enantioselective cycloaddition of DACs in mind, we became interested in developing a generalized approach for asymmetric access to biologically important carbo- and heterocycles from

DACs. We envisioned that a chiral amine organocatalyst could asymmetrically activate cyclopropane carbaldehyde through the iminium ion pathway to render enantioselective cycloaddition.[8] In this regard, *in situ* generations of DACs via enamine activation of cyclopropyl acetaldehydes were studied by the research groups of Jørgensen[9] and Vicario.[10] It should be noted that in the previous organocatalytic enantioselective ring-opening reactions, the cyclopropane carbaldehydes are *meso* in nature[8a, 8b, 8c] (which was discussed in Scheme 1.4.3.2, Chapter 1) and there has been no such report of organocatalytic enantioselective transformations with their *racemic* versions. Herein, we report the first asymmetric (3+3)-cycloaddition of *racemic* cyclopropane carbaldehyde with aryl hydrazones for the formation of enantioselective tetrahydropyridazine derivatives via organocatalytic activation (Scheme 2.A.1.1.B).

2.A.2. Result and Discussion

Initially, *trans*-methylenedioxyphenyl cyclopropane carbaldehyde **1a** and benzaldehyde-derived phenyl hydrazone **2a** were chosen as model substrates to find the optimized reaction conditions for the titled (3+3)-cycloaddition (Table 2.A.2.1). We began our study by taking chiral (*S*)-proline **I** as a catalyst and performed the reaction in carbon tetrachloride as a solvent in the presence of 4 Å

Table 2.A.2.1. Optimization of the reaction conditions[a]

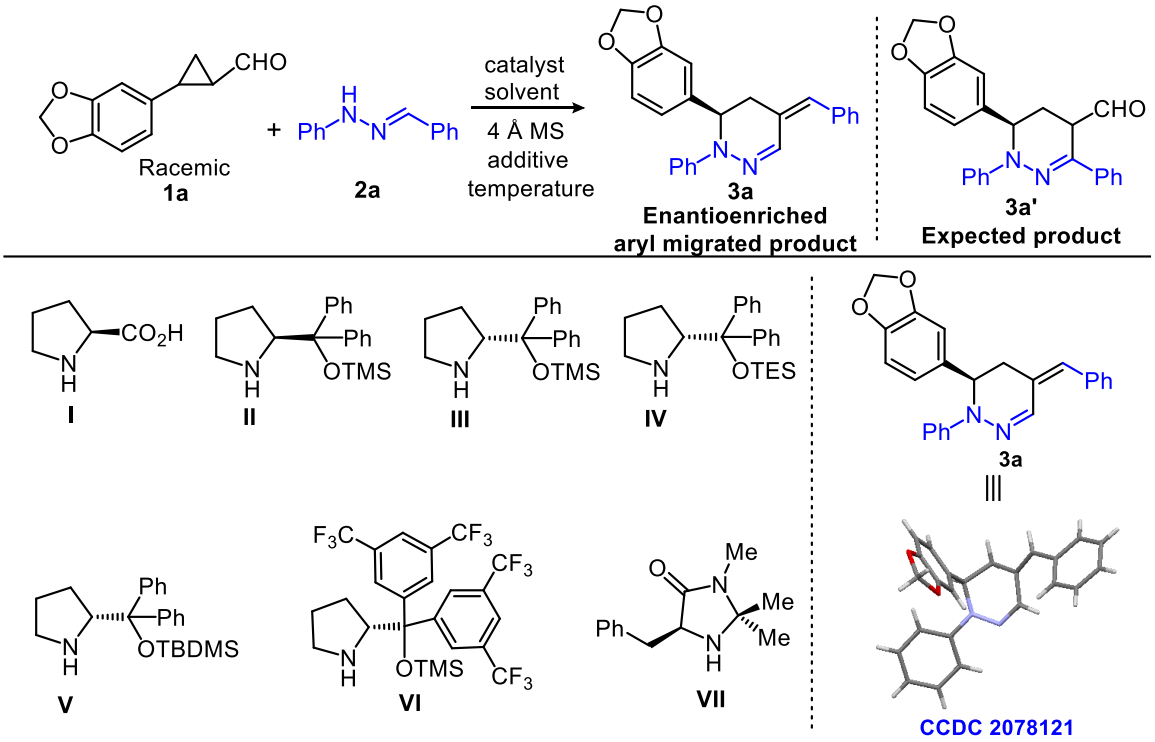

entry	catalyst	solvent	additive	yield (%)[b]	*ee* (%)[c]
1	I	CCl_4	-	n.r.[d]	-
2	II	CCl_4	-	20	95

3	II	DCM	-	18	n.d.[e]
4	II	DCE	-	c.m.[f]	
5	II	$CHCl_3$	-	c.m.[f]	
6	II	THF	-	n.r.[d]	-
7	II	Toluene	-	n.r.[d]	-
8	II	CH_3CN	-	n.r.[d]	-
9	II	CCl_4	$PhCO_2H$	c.m.[f]	-
10	II	CCl_4	CSA	c.m.[f]	-
11	II	CCl_4	PTSA	c.m.[f]	-
12[g]	II	CCl_4	-	60	92 (*R*)
13[g]	**III**	**CCl_4**	**-**	**60**	**97 (*S*)**
14[g]	IV	CCl_4	-	25	85
15[g]	V	CCl_4	-	10	81
16[g]	VI	CCl_4	-	n.r.[d]	-
17[g]	VII	CCl_4	-	n.r.[d]	-
18[g,h]	II	CCl_4	-	40	92
19[g,i]	II	CCl_4	-	35	91
20[g,j]	II	CCl_4	-	n.r.[d]	-
21[k]	II	CCl_4	-	trace	n.d.[e]

[a]Unless specified all the reactions were performed with 1 equiv. of **1a**, 1 equiv. of **2a**, 30 mol% of catalyst in the presence of molecular sieves (4 Å) in 2 mL solvent at room temperature for 24 hour. [b]isolated yields, [c]enantiomeric excess determined by chiral HPLC analysis, [d]n.r. = no desired product formed, [e]n.d. = not determined, [f]c.m. = complex mixture, [g]refluxing for 12 hour, [h]catalyst used = 20 mol%, [i]catalyst used = 40 mol%, [j]without molecular sieves, [k]**1e'** was used instead of **1a**.

molecular sieves at room temperature. However, no desired product was obtained even after 24 hours of the reaction (Table 2.A.2.1, entry 1). Afterward, we changed the catalyst to Jørgensen-Hayashi catalyst **II**,[11] and delightfully, an unprecedented product **3a** was obtained with 20% and 95% of enantioselectivity instead of **3a'** (Table 2.A.2.1, entry 2). The structure and absolute configuration of product **3a** were confirmed by X-ray crystallography. The analysis of the structure indicates a rare [1,3]-aryl migration took place after the cycloaddition (*vide infra*). Thereafter, to improve the yield, the reaction was performed under different solvent systems. While no improvement in the yield was observed in other chlorinated solvents (Table 2.A.2.1, entries 3-5), solvents like tetrahydrofuran, toluene, and acetonitrile proved inefficient for this transformation (Table 2.A.2.1, entries 6-8). As the presence of additive in the asymmetric reaction can efficiently improve the yield and stereoselectivity[12] the reaction was performed under various Brønsted acid additives like $PhCO_2H$, PTSA, and CSA, which resulted in the formation of a complex reaction mixture (Table 2.A.2.1, entries 9-11), presumably, these Brønsted acids activated the cyclopropanes itself to undergo various ring-opening reactions.[13] However, the yield was significantly improved, and a good enantiomeric excess of 92% was obtained by conducting the reaction under refluxing

conditions (Table 2.A.2.1, entry 12). Hereafter, we started to explore other secondary amine-based organocatalysts to upgrade the enantioselectivity. Gratifyingly, our trial with catalyst **III** furnished the product with a similar yield and with enhanced enantioselectivity of 97% (Table 2.A.2.1, entry 13). A range of other secondary amine catalysts was also screened to further improve the enantioselectivity. Whereas catalysts **IV** and **V** delivered the desired products with poor yields and decreased enantioselectivities (Table 2.A.2.1, entries 14-15), catalysts **VI** and **VII** proved to be fatal for this transformation (Table 2.A.2.1, entries 16-17). Notably, a substantial decrease in the yield was observed on increasing or decreasing the catalyst loading while no reaction took place in the absence of the molecular sieves (Table 2.A.2.1, entries 18-20). No diastereomeric mixture was encountered, as confirmed by the crude NMR experiment. Finally, *cis*-configured cyclopropane was also tested, and a trace amount of desired product formation establishes that the *trans*-

Scheme 2.A.2.1. Substrate scope[a]

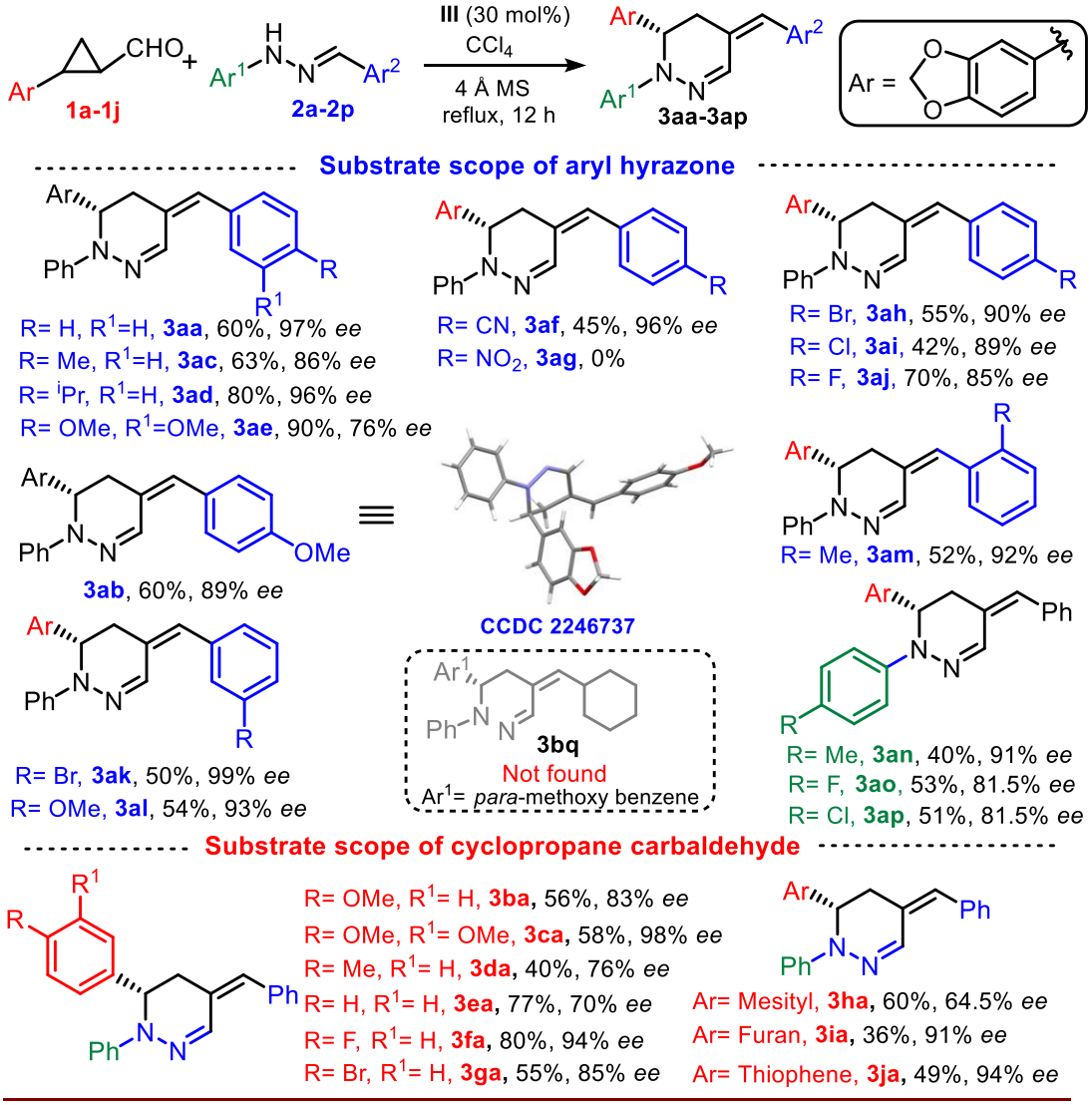

[a]Reaction conditions: **1** (0.2 mmol), **2** (0.2 mmol), **III** (30 mol %), 2 mL of CCl_4, molecular sieves (4 Å), reflux, 12 h, yields represent isolated products; ee values were determined by HPLC analysis.

configuration is essential for this cycloaddition (Table 2.A.2.1, entries 21).

With the optimized conditions, we started to investigate the scopes and limitations of the proposed cycloaddition concerning various substituted aromatic aldehyde-derived phenylhydrazones **2a-2p** (Scheme 2.A.2.1). Various electron-donating, electron-withdrawing, and halogen-containing substituents at the *para*-, *meta*- and *ortho*-position of the Ar^2 ring proved efficient for our proposed transformation giving the desired products (**3aa-3am**) in moderate to excellent yields (42-90%) with good to excellent enantiomeric excesses (76-99%). Only the strongly electron-withdrawing *nitro*-substituted one failed to give the desired product. Following these, substrates containing *para*-substitution on the Ar^1 ring were also exploited, which furnished the products (**3an-3ap**) in moderate yields (40-53%) with good enantioselectivities (81.5-91% *ee*). Eventually, to check the progress of the reaction after the cycloaddition, a reaction was conducted between cyclopropane **1b** and cyclohexancarbaldehyde-derived hydrazone **2q** (Ar^2 was replaced by an aliphatic group). The desired product was not formed, which established only the aryl group could undergo this1,3-shift.

Then we examined the substrate scope with respect to the cyclopropane carbaldehydes (Scheme 2.A.2.1). Moderate to highly electron-rich aryl-substituted cyclopropane carbaldehydes rendered the products (**3ba-3ga**) in moderate to good yields with good to excellent enantioselectivities. To our surprise, sterically hindered mesityl cyclopropane carbaldehyde **1h** also furnished the product **3ha** with a good yield (60%) and satisfying enantioselectivity (64.5% *ee*). It is worth mentioning that heteroatom-bearing aryl cyclopropane carbaldehydes (**1i** and **1j**) also rendered the products (**3ai** and **3aj**) with low to moderate yields (36% and 49%) and excellent enantioselectivities (91% and 94% *ee*).

To gain insights into the mechanism, we have executed some control experiments with each enantiomer[14] of the cyclopropane carbaldehyde (Scheme 2.A.2.2.A). First, we reacted (*R*,*R*)-cyclopropane carbaldehyde-**1e** with hydrazone **2a** in the presence of the *racemic* catalyst and obtained (*R*)-product ***ent*-3ea** with an excellent enantiomeric excess (94% *ee*) which confirms that the ring-opening reaction undergoes via the stereospecific S_N2 pathway. Then we performed the reaction in the presence of only (*S*)-catalyst and obtained ***ent*-3ea** with exceptionally high enantioselectivity (>99% *ee*), but with (*R*)-catalyst, the reaction was slow, and the product was formed in a trace amount of yield with poor enantioselectivity (<5%, 40% *ee*) (Case A, Scheme 2.A.2.2.A). Next, we repeated the same set of experiments with the other enantiomer of the cyclopropane (*S*,*S*)-**1e,** and an almost similar outcome was found (Case B, Scheme 2.A.2.2.A). These experiments stipulated that each enantiomer of the substrate favors one particular enantiomer of the catalyst, which suggests a matched/mismatched type scenario[15] between the two enantiomers of the racemates. An alternative approach for this transformation could be enantioconvergent transformation, in which each enantiomer of the substrate undergoes different routes for the

synthesis of the same enantioenriched product. But in the presence of a *racemic* catalyst (*R*,*R*)-**1e** produces ***ent*-3ea**, while (*S*,*S*)-**1e** furnished **3ea** (Scheme 2.A.2.2.A), which excludes the possibility of enantioconvergence.[16]

Scheme 2.A.2.2. Control experiments and plausible mechanism. (A) Experiments with chiral cyclopropane carbaldehydes; (B) Cross-rearrangement experiment; (C) Correlation between product ee and catalyst ee; (D) Enantiomeric excess as a function of time; (E) Racemization study of chiral cyclopropane; (F) Plausible mechanistic diagram

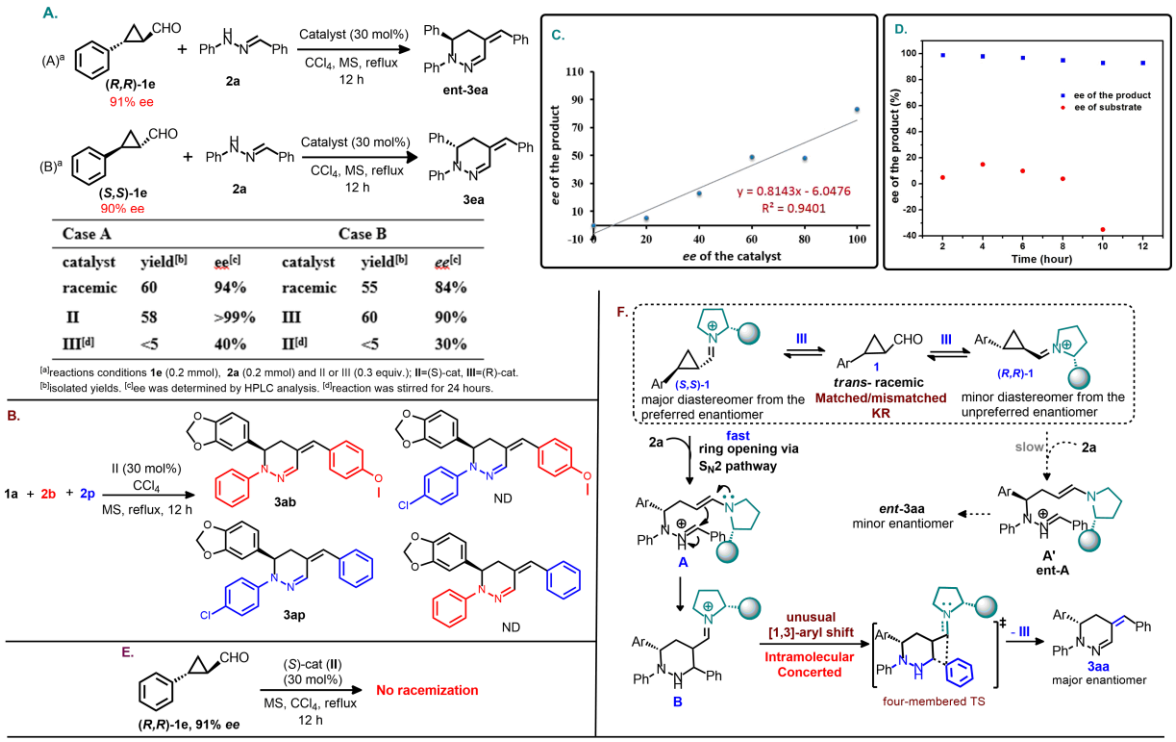

Further, we have also checked the dependence of product *ee* as a function of catalyst *ee* (Scheme 2.A.2.2.C). A linear correlation between them clearly excludes the involvement of more than one catalyst molecule in the catalytic cycle[17]. Later, we checked the enantiomeric excess of the substrate as well as the product as a function of time where the *racemic* **1a** is reacted with **2a** in the presence of (*S*)-catalyst (**II**) in the optimized reaction conditions (Scheme 2.A.2.2.D). In this experiment, an initial increase of enantiomeric excess in favor of (*R*,*R*)-cyclopropane was detected, which indicates that the other isomer (*S*,*S*)-cyclopropane started decomposing due to the mismatched condition. Eventually, an enantiomeric excess in favor of the (*S*,*S*)-cyclopropane was noticed just before the completion of the reaction since the matched isomer was almost converted to the product while the mismatched one still remained to some extent due to the slow kinetics. Moreover, when the enantiopure cyclopropane (**1a**) was treated with the (*S*)-catalyst (**II**) under the optimized conditions, no racemization was noticed, which excludes the DKR pathway (Scheme 2.A.2.2.E).[18b] Complete consumption of starting material and more than 50% yield in some cases ruled out the possibility of a simple kinetic resolution. Noticeably, in most of the cases, the yields are around 50%, and in a

few cases where yields are high, albeit of moderate enantiomeric excesses, eliminate the occurrence of Dynamic Kinetic asymmetric Transformation. So, this unusual phenomenon hinted towards a unique type of matched/mismatched kinetic resolution.

Next, to know the mode of this [1,3]-rearrangement, a control experiment has been carried out combining 0.2 mmol of **1a**, 0.10 mmol of **2b,** and 0.10 mmol of **2p** under standard conditions Scheme 2.A.2.2.B). The rearranged products **3ab** and **3ap** were obtained in 26% and 24% yield, respectively, whereas no cross-rearrangement products were detected. This study disclosed that this unusual [1,3]-aryl shift undergoes[19] via an intramolecular and concerted rearrangement pathway.[19b] Moreover, this aryl migration could happen either via Friedel-Crafts type reaction or via *ipso*-type substitution. Here, the *ipso*-substitution has been confirmed unambiguously by Single Crystal X-Ray analysis of **3ab,** which reveals the bond connectivity of the migrating aryl ring remains the same before and after the migration.

Further insights into this interesting aryl migration have also been investigated by computational studies. All calculations are performed with ONIOM (wB97XD/6-31G(d,p): PM6) using the Gaussian 09 software (Appendix B). The solvent effect has been included using the PCM model (CCl_4). Computational calculations also depict that the initial ring opening of the cyclopropane undergoes the nucleophilic attack of hydrazone via the S_N2 pathway, which after subsequent cyclization, gave the six-membered cyclic intermediate **B**. It was also revealed that to facilitate the *ipso*-type substitution this unusual 1,3-aryl migration was proceeding via an unprecedented four-membered transition state (**B_TS**).

Based on all experimental results and literature precedences[15], a plausible mechanistic diagram is shown in Scheme 2.A.2.2.F. At first, the *racemic* cyclopropane carbaldehyde binds with the catalyst **III** to form the iminium intermediates. Moreover, in the presence of catalyst **III** one enantiomer of the cyclopropane (*S*,*S*-**1**) reacted faster (matched case) with hydrazone (**2**) via S_N2 attack to form the major intermediate (**A**) while the other one (*R*,*R*-**1**) experienced slow transformation (mismatched case) towards the minor intermediate (**A'**) along with decomposition (which could be rationalized from Scheme 2.A.2.2.A and Scheme 2.A.2.2.D) following a matched/mismatched type kinetic resolution. Subsequently, this enamine intermediate (**A**) took part in the cyclization to give the intermediate (**B**). Eventually, the *ipso*-type 1,3-aryl migration took place via a four-membered TS followed by the elimination of the catalyst led to the formation of the desired product **3aa**.

For additional synthetic utilization, the exocyclic double bond of **3ba** was selectively reduced through a hydrogenation[5c] by Pd-C catalyst, and a new stereogenic center was generated. The relative stereochemistry of **4ba** was determined by the NOE experiment (Scheme 2.A.2.3).

Scheme 2.A.2.3. Synthetic transformation

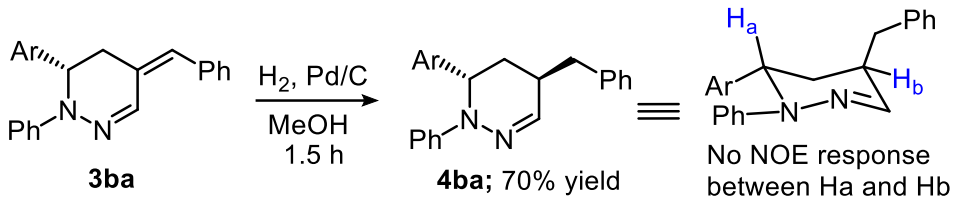

2.A.3. Conclusion

In conclusion, we report the first organocatalytic activation of cyclopropane carbaldehydes for the enantioselective (3+3)-cycloaddition to access a range of enantioenriched tetrahydropyridazines. An unconventional type of matched/mismatched kinetic resolution was believed to be reason behind this asymmetric transformation. The control experiment and computational studies disclosed the intriguing [1,3]-aryl migration proceeds in an intramolecular and concerted manner. Further exploration of organocatalytic enantioselective cycloaddition of cyclopropane carbaldehydes is still under the scope of our investigation.

2.A.4. Experimental section

2.A.4.1. General Information

All reactions were carried out under inert atmosphere with oven-dried glasswares. All solvents and reagents were obtained from commercial sources and were purified following the standard procedure prior to use. Powdered molecular sieves (4Å MS) were dried at 200 °C under vacuum prior to use. Thin-layer chromatography was performed on Merck precoated silica gel 60 F254 aluminum sheets with detection under UV light at 254 nm and charring with *p*-anisaldehyde solution. Chromatographic purifications were performed with silica gel (230-400 mesh) and melting points were taken on Stuart digital melting point apparatus. Nuclear magnetic resonance (NMR) spectroscopy was performed using JEOL 400 MHz and HRMS was recorded on Waters Xevo G2-XS (Q-TOF). The ^{1}H NMR and ^{13}C NMR spectra were recorded in $CDCl_3$. Chemical shifts of ^{1}H and ^{13}C NMR spectra are expressed in parts per million (ppm). All coupling constants are absolute values and are expressed in Hertz. The description of the signals includes the following: s = singlet, d = doublet, dd = doublet of doublet, t = triplet, dt = doublet of triplet, q = quartet, dq = doublet of quartet, br = broad, and m = multiplet. Optical rotations were measured on an Anton Paar MCP 200, $[\alpha]^{D}$ values are given in $deg \cdot cm^{3} \cdot g^{-1} \cdot dm^{-1}$; concentration (c) in g $(100\ mL)^{-1}$. The enantiomeric excess (*ee*) values of the products were determined by High Performance Liquid Chromatography (Waters modular system) using Daicel Chiralpak IC, ODH, ADH and ASH columns as chiral stationary phase. Structural assignments were made with additional information from gCOSY experiments.

Scheme 2.A.4.2. Reaction of *racemic* cyclopropane with the catalyst

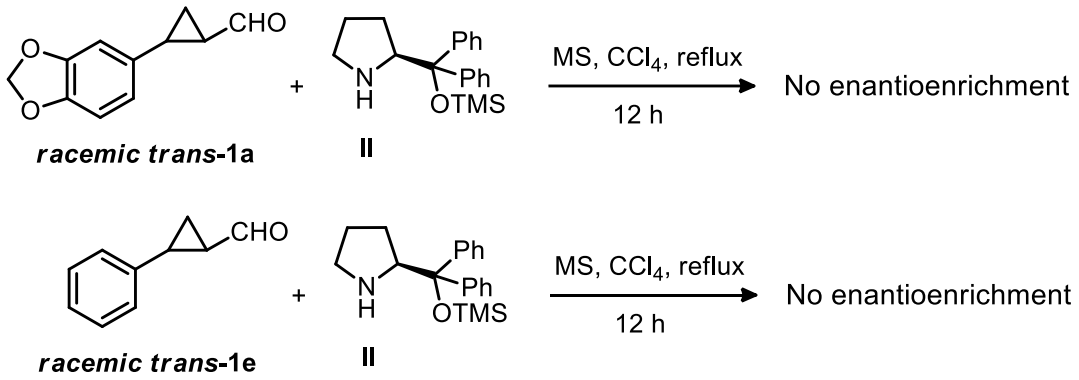

These experiments suggested that this proposed cycloaddition reaction is not happening via a simple kinetic resolution (SKR) and the requirement of an external nucleophile is needed for the enantioselective transformation. In our study, the hydrazone acts as a nucleophile and attack the cyclopropane via the S_N2 pathway for the ring opening and an enantioenriched intermediate was formed followed by the production of chiral products.

2.A.4.3. General procedure for the preparation of *trans*-2-Aryl cyclopropane carbaldehydes (1)[20]

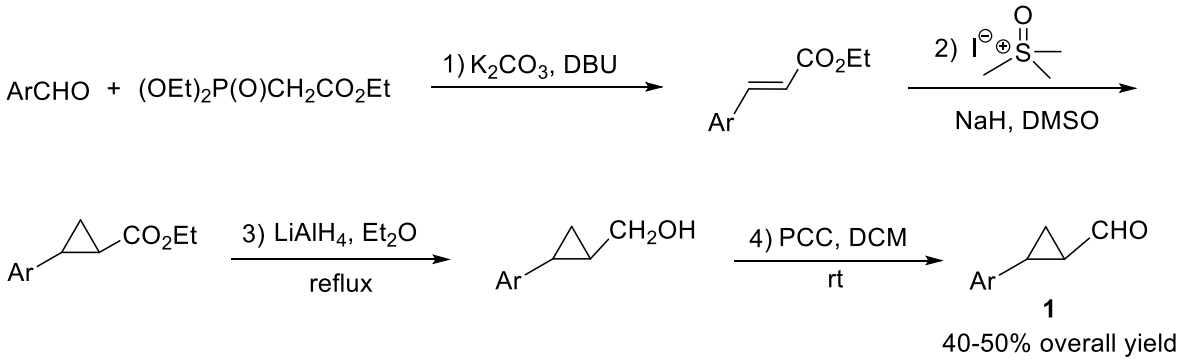

1) To a mixture of triethyl phosphonoacetate (1.1 equiv.), DBU (0.035 equiv.), and finely ground K_2CO_3 (2 equiv.) was added ArCHO (1 equiv.) and the resulting mixture was stirred using a magnetic stirrer for 4 h at room temperature under an argon atmosphere. Ethyl acetate was added to the crude mixture, and the solid was filtered off. The solid was rinsed with ethyl acetate, and the combined filtrate was concentrated. The resulting oil was distilled under reduced pressure using a bulb-to-bulb apparatus (10 mm Hg/240 °C) to give the corresponding alkene (yield 84%) (E:Z = 99:1).

2) A suspension of TMSOI (1.2 equiv.) and NaH (1.5 equiv.) in anhydrous DMSO (15 mL) was stirred for 1 h. A DMSO solution (14 mL) of alkene (14 mmol, 1 equiv) was added at 0 °C. The reaction mixture was stirred at 55 °C (oil bath) for 24 h. Another suspension of TMSOI (0.3 equiv.) and NaH (0.3 equiv.) in DMSO (10 mL) was added to the reaction mixture, and the reaction was

stirred at 65 °C (oil bath) for 84 h. The solution was poured into a brine solution and extracted with ethyl acetate. Combined organic layer was washed with water and dried over $MgSO_4$, concentrated and purified by silica gel column chromatography (EtOAc/hexane) to afford corresponding cyclopropane derivative as a white solid (60-80% yield).

3) To a stirred solution of LAH (1.5 equiv.) in 7 mL diethyl ether was added dropwise a solution of cyclopropane ester (0.90 mmol, 1equiv.) in 3 mL diethyl ether under N_2 atmosphere. After addition was completed the reaction mixture was refluxed (oil bath) for another 6 h. The reaction mixture was then cooled to rt, and the excess LAH was destroyed by water. 15 mL of 10% H_2SO_4 and 8 mL of ether was added and the aqueous layer was extracted several times with diethyl ether. The combined organic layer was washed with water and 5% $NaHCO_3$, dried over $MgSO_4$ and concentrated in a rotary evaporator (90-95% yield). Without any further purification, the crude material (a colorless oil) was used for next step.

4) To a solution of cyclopropane alcohol (6.8 mmol, 1 equiv.) in dry DCM (14 mL), PCC (2 equiv.) was added in a portion-wise manner through a solid addition tube under N_2 atmosphere. After 3 h reaction mixture was filtered through a small plug of celite and concentrated in vacuo. The crude mixture was purified by silica gel column chromatography using ethyl acetate in hexane as an eluent. Starting from aryl aldehyde the 2-arylcyclopropanecarbaldehydes was obtained in 40-55% overall yield.

All the cyclopropanes **1a-1j** are known and prepared according to the above mentioned general procedure[20] and **1e'** is also known and prepared according to the literature procedure[20b].

2-(benzo[*d*][1,3]dioxol-5-yl)cyclopropanecarbaldehyde (1a)

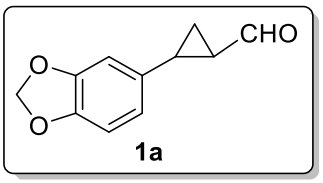

^{1}H NMR (400 MHz): δ 9.30 (d, J = 4.6 Hz, 1H), 6.73 (d, J = 8.2 Hz, 1H), 6.62 (d, J = 8.0 Hz, 1H), 6.57 (s, 1H), 5.93 (s, 2H), 2.60-2.55 (m, 1H), 2.12-2.04 (m, 1H), 1.71-1.66 (m, 1H), 1.49-1.43 (m, 1H)

***trans*-2-(4-methoxyphenyl)cyclopropane-1-carbaldehyde (1b)**

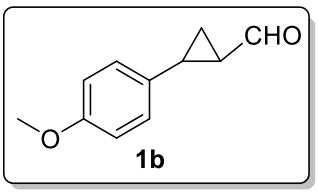

^{1}H NMR (400 MHz): δ 9.30 (d, J = 4.9 Hz, 1H), 7.05 (d, J = 8.7 Hz, 2H), 6.83 (d, J = 8.7 Hz, 2H), 3.79 (s, 3H) 2.63-2.56 (m, 1H), 2.13-2.06 (m, 1H), 1.73-1.67 (m, 1H), 1.51-1.45 (m, 1H)

***trans*-2-(3,4-dimethoxyphenyl)cyclopropanecarbaldehyde (1c)**

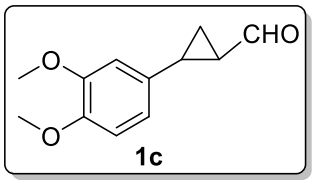

^{1}H NMR (400 MHz): δ 9.28 (d, J = 4.5 Hz, 1H), 6.77 (d, J = 8.3 Hz, 1H), 6.65 (d, J = 8.2 Hz, 2H), 3.85 (s, 3H), 3.83 (s, 3H), 2.62-2.55 (m, 1H), 2.13-2.06 (m, 1H), 1.71-1.65 (m, 1H), 1.51-1.46 (m, 1H)

***trans*-2-(*p*-tolyl)cyclopropane-1-carbaldehyde (1d)**

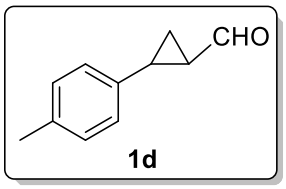

^{1}H NMR (400 MHz): δ 9.30 (d, J = 4.5 Hz, 1H), 7.11 (d, J = 8.0 Hz, 2H), 7.01 (d, J = 8.2 Hz, 2H), 2.63-2.57 (m, 1H), 2.32 (s, 3H), 2.16-2.10 (m, 1H), 1.74-1.68 (m, 1H), 1.54-1.48 (m, 1H)

***trans*-2-phenylcyclopropane-1-carbaldehyde (1e)**

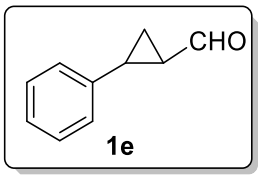

^{1}H NMR (400 MHz): δ 9.32 (d, J = 4.5 Hz, 1H), 7.33-7.27 (m, 2H), 7.25-7.20 (m, 1H), 7.13-7.09 (m, 2H), 2.66-2.60 (m, 1H), 2.21-2.15 (m, 1H), 1.77-1.71 (m, 1H), 1.57-1.51 (m, 1H)

***cis*-2-phenylcyclopropane-1-carbaldehyde (1e')[2]**

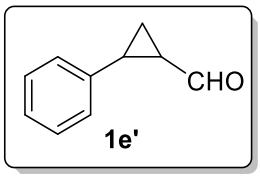

^{1}H NMR (400 MHz): δ 8.66 (d, J = 6.6 Hz, 1H), 7.33-7.20 (m, 5H), 2.82 (q, J = 8.3, 15.9 Hz, 1H), 2.16-2.09 (m, 1H), 1.90-1.86 (m, 1H), 1.61-1.56 (m, 1H)

***trans*-2-(4-fluorophenyl)cyclopropane-1-carbaldehyde (1f)**

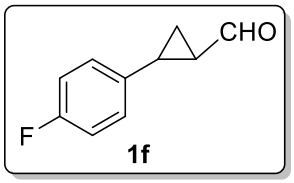

^{1}H NMR (400 MHz): δ 9.32 (d, J = 4.5 Hz, 1H), 7.10-7.05 (m, 2H), 6.98 (t, J = 8.7 Hz, 2H), 2.64-2.58 (m, 1H), 2.15-2.09 (m, 1H), 1.74-1.69 (m, 1H), 1.51-1.45 (m, 1H)

***trans*-2-(4-bromophenyl)cyclopropane-1-carbaldehyde (1g)**

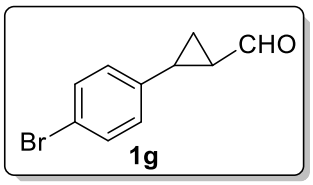

^{1}H NMR (400 MHz): δ 9.31 (d, J = 4.3 Hz, 1H), 7.39 (d, J = 8.6 Hz, 2H), 6.97 (d, J = 8.7 Hz, 2H), 2.60-2.54 (m, 1H), 2.16-2.09 (m, 1H), 1.75-1.69 (m, 1H), 1.50-1.45 (m, 1H)

***trans*-2-mesitylcyclopropane-1-carbaldehyde (1h)**

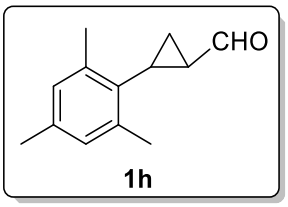

^{1}H NMR (400 MHz): δ 9.28 (d, J = 5.4 Hz, 1H), 6.85 (s, 2H), 2.45-2.39 (m, 1H), 2.33 (s, 6H), 2.25 (s, 3H), 1.98-1.91 (m, 1H), 1.82-1.76 (m, 1H), 1.40-1.34 (m, 1H)

***trans*-2-(furan-2-yl)cyclopropane-1-carbaldehyde (1i)**

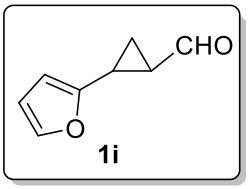

^{1}H NMR (400 MHz): δ 9.36 (d, J = 4.3 Hz, 1H), 7.27-7.25 (m, 1H), 6.30-6.28 (m, 1H), 6.10 (d, J = 3.3 Hz, 1H), 2.65-2.59 (m, 1H), 2.32-2.26 (m, 1H), 1.69-1.64 (m, 1H), 1.62-1.56 (m, 1H)

***trans*-2-(thiophen-2-yl)cyclopropane-1-carbaldehyde (1j)**

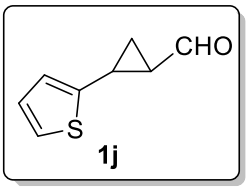

^{1}H NMR (400 MHz): δ 9.38 (d, J = 4.1 Hz, 1H), 7.13-7.11 (m, 1H), 6.92-6.90 (m, 1H), 6.85-6.84 (m, 1H), 2.84-2.78 (m, 1H), 2.25-2.20 (m, 1H), 1.79-1.74 (m, 1H), 1.55-1.50 (m, 1H)

2.A.4.4. General procedure for the preparation of aryl hydrazones (2)[21]

To a solution of aldehyde (4.6 mmol, 1.0 equiv) in dry DCM (10 ml) was added phenyl hydrazine (4.6 mmol, 1.0 equiv) and anhydrous $MgSO_4$ (4.6 mmol, 1.0 equiv). The resulting mixture was stirred at room temperature until the reaction was completed (monitored by TLC). Filtration with DCM as eluent and evaporation of the solvent under reduced pressure afforded the desired hydrazones as yellowish solids (80-90%).

All the hydrazones are known in literature[3b-3i] and prepared according to the above mentioned general procedure.

(*E*)-1-benzylidene-2-phenylhydrazine (2a)

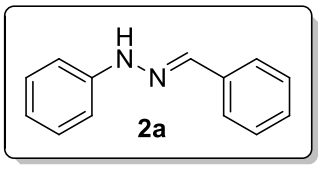

^{1}H NMR (400 MHz): δ 7.69 (s, 1H), 7.66 (d, J = 8.6 Hz, 2H), 7.62 (bs, 1H), 7.37 (t, J = 14.8 Hz, 2H), 7.32-7.26 (m, 3H), 7.12 (d, J = 8.7 Hz, 2H), 6.87 (t, J = 14.5Hz, 1H)

(*E*)-1-(4-methoxybenzylidene)-2-phenylhydrazine (2b)

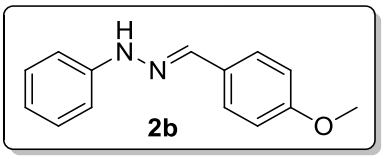

^{1}H NMR (400 MHz): δ 7.66 (s, 1H), 7.60 (d, J = 8.4 Hz, 2H), 7.50 (bs, 1H), 7.28-7.25 (m, 2H), 7.09(d, J = 7.9 Hz, 2H), 6.91(d, J = 8.5 Hz, 2H), 6.85 (t, J = 14.7Hz, 1H), 3.84 (s, 3H)

(*E*)-1-(4-methylbenzylidene)-2-phenylhydrazine (2c)

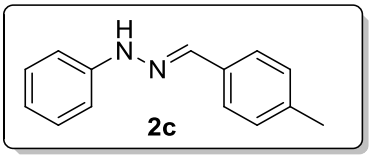

^{1}H NMR (400 MHz): δ 7.67 (s, 1H), 7.56 (d, J = 8.0 Hz, 2H), 7.29-7.25 (m, 2H), 7.18 (d, J = 7.9 Hz, 2H), 7.11 (d, J = 7.8 Hz, 2H), 6.86 (t, J = 14.6 Hz, 1H), 2.36 (s, 3H)

(*E*)-1-(4-isopropylbenzylidene)-2-phenylhydrazine (2d)

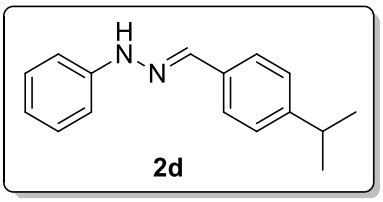

^{1}H NMR (400 MHz): δ 7.68 (s, 1H), 7.59 (d, J = 8.0 Hz, 2H), 7.29-7.22 (m, 4H), 7.11 (d, J = 7.9 Hz, 2H), 6.86 (t, J = 14.3 Hz, 1H), 2.92 (sept, 1H), 1.27 (s, 3H), 1.25 (s, 3H)

(*E*)-1-(3,4-dimethoxybenzylidene)-2-phenylhydrazine (2e)

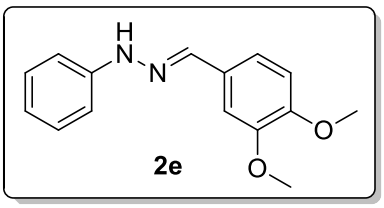

^{1}H NMR (400 MHz): δ 7.57 (s, 1H), 7.50 (bs, 1H), 7.34 (d, J = 1.9 Hz, 1H), 7.26-7.22 (m, 2H), 6.99 (d, J = 8.2 Hz, 1H), 6.84-6.79 (m, 2H), 3.92 (s, 3H), 3.86 (s, 3H)

(*E*)-4-((2-phenylhydrazono)methyl)benzonitrile (2f)

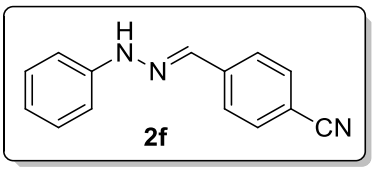

^{1}H NMR (400 MHz): δ 7.90 (bs, 1H), 7.73 (d, J = 8.2 Hz, 2H), 7.63 (t, J = 8.7 Hz, 3H), 7.30 (t, J = 15.2 Hz, 2H), 7.14 (d, J = 8.3 Hz, 2H), 6.93 (t, J = 14.6 Hz, 1H)

(*E*)-1-(4-nitrobenzylidene)-2-phenylhydrazine (2g)

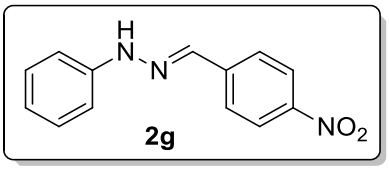

^{1}H NMR (400 MHz): δ 8.22 (d, J = 8.4 Hz, 2H), 7.98 (s, 1H), 7.77 (d, J = 8.7 Hz, 2H), 7.70 (s, 1H), 7.32 (t, J = 15.4 Hz, 2H), 7.15 (d, J = 7.8 Hz, 2H), 6.95 (t, J = 14.6 Hz, 1H)

(*E*)-1-(4-bromobenzylidene)-2-phenylhydrazine (2h)

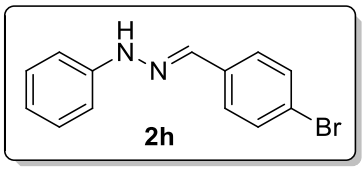

^{1}H NMR (400 MHz): δ 7.67 (bs, 1H), 7.62 (s, 1H), 7.53-7.47 (m, 4H), 7.30-7.26 (m, 2H), 7.11 (d, J = 8.6 Hz, 2H), 6.89 (t, J = 14.6 Hz, 1H)

(*E*)-1-(4-chlorobenzylidene)-2-phenylhydrazine (2i)

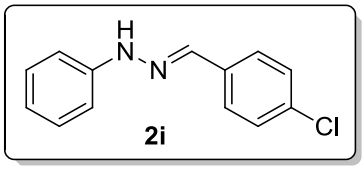

^{1}H NMR (400 MHz): δ 7.65 (bs, 1H), 7.63 (s, 1H), 7.58 (d, J = 8.6 Hz, 2H), 7.33 (d, J = 8.7 Hz, 2H), 7.30 (t, J = 15.5 Hz, 2H), 7.11 (d, J = 7.8 Hz, 2H), 6.88 (t, J = 14.7 Hz, 1H)

(*E*)-1-(4-fluorobenzylidene)-2-phenylhydrazine (2j)

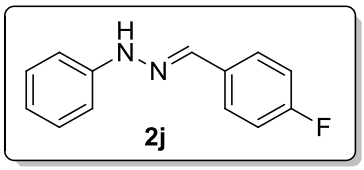

^{1}H NMR (400 MHz): δ 7.64 (s, 1H), 7.63-7.59 (m, 3H), 7.26 (t, J = 19.5 Hz, 2H), 7.09-7.02 (m, 4H), 6.86 (t, J = 14.5 Hz, 1H)

(*E*)-1-(3-bromobenzylidene)-2-phenylhydrazine (2k)

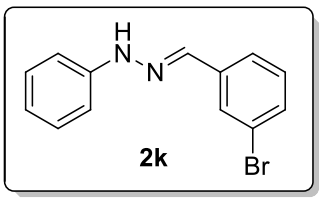

^{1}H NMR (400 MHz): δ 7.82 (s, 1H), 7.70 (s, 1H), 7.58 (s, 1H), 7.53 (d, J = 7.7 Hz, 1H), 7.40 (d, J = 7.7 Hz, 1H), 7.31-7.20 (m, 3H), 7.11 (d, J = 8.3 Hz, 2H), 6.90 (t, J = 14.6 Hz, 1H)

(*E*)-1-(3-methoxybenzylidene)-2-phenylhydrazine (2l)

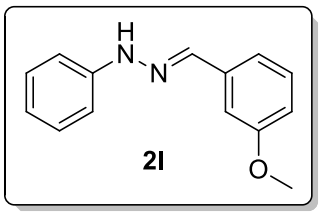

^{1}H NMR (400 MHz): δ 7.57 (bs, 1H), 7.50 (s, 1H), 7.29-7.25 (m, 4H), 7.17(d, J = 7.6 Hz, 2H), 7.10 (d, J = 8.0 Hz, 1H), 6.90-6.84 (m, 2H), 3.84 (s, 3H)

(*E*)-1-(2-methylbenzylidene)-2-phenylhydrazine (2m)

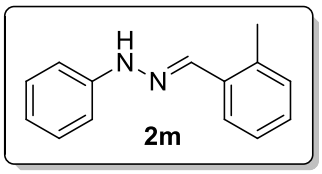

^{1}H NMR (400 MHz): δ 7.94 (s, 1H), 7.84-7.82 (m, 1H), 7.67 (bs, 1H), 7.30-7.17 (m, 5H), 7.11 (d, J = 8.3 Hz, 2H), 6.87 (t, J = 7.3 Hz, 1H), 2.49 (s, 3H)

(*E*)-1-benzylidene-2-(*p*-tolyl)hydrazine (2n)

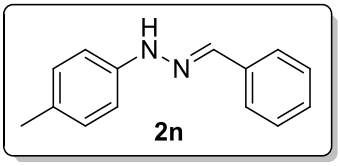

^{1}H NMR (400 MHz): δ 7.67-7.64 (m, 3H), 7.36 (t, J = 7.7 Hz, 2H), 7.29 (d, J = 7.5 Hz, 1H), 7.09 (d, J = 8.2 Hz, 2H), 7.02 (d, J = 8.3 Hz, 2H), 2.29 (s, 3H)

(*E*)-1-benzylidene-2-(4-fluorophenyl)hydrazine (2o)

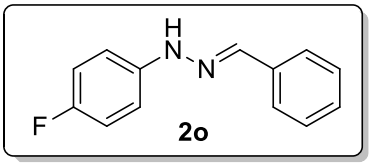

^{1}H NMR (400 MHz): δ 7.68-7.64 (m, 3H), 7.37 (t, J = 7.5 Hz, 2H), 7.32-7.28 (m, 1H), 7.08-7.04 (m, 2H), 7.00-6.96 (m, 2H)

(*E*)-1-benzylidene-2-(4-chlorophenyl)hydrazine (2p)

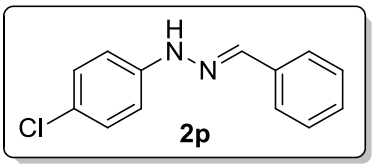

^{1}H NMR (400 MHz): δ 7.67-7.64 (m, 3H), 7.38 (t, J = 7.5 Hz, 2H), 7.33-7.29 (m, 1H), 7.23 (d, J = 8.7 Hz, 2H), 7.05 (d, J = 8.4 Hz, 2H)

(*E*)-1-(cyclohexylmethylene)-2-phenylhydrazine

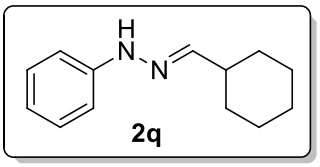

^{1}H NMR (400 MHz): δ 7.26-7.20 (m, 2H), 6.98-6.96 (m, 3H), 6.82-6.79 (m, 1H), 2.30-2.24 (m, 1H), 1.89-1.75 (m, 5H), 1.35-1.21 (m, 5H)

2.A.4.5. Representative procedure for the Organocatalytic (3+3)-cycloaddition reaction between Donor-Acceptor Cyclopropane carbaldehydes (1) and aryl hydrazones (2)

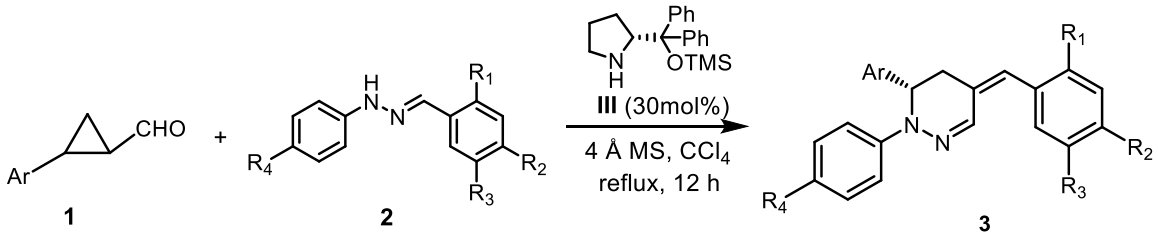

To a round-bottom flask equipped with a magnetic stir bar was charged with cyclopropane carbaldehyde (0.2 mmol, 1 equiv.), aryl hydrazone (0.2 mmol, 1 equiv.), activated 4 Å MS (200 mol%), and Jørgensen-Hayashi Catalyst **III** (0.06 mmol, 0.3 equiv.) under nitrogen atmosphere. CCl_4 (2 mL) was added as a solvent to the reaction mixture and was stirred under reflux conditions (oil bath) for 12 hour. After the completion of the reaction (as monitored by TLC), the reaction mixture was passed through a small pad of Celite, and the solvent was removed under reduced

pressure by a rotary evaporator. Then the crude product was further purified by column chromatography on silica gel with EtOAc/hexane as eluent.

Racemic products were prepared according to the representative procedure **4** by using the *racemic* catalyst.

(*S,Z*)-6-(benzo[*d*][1,3]dioxol-5-yl)-4-benzylidene-1-phenyl-1,4,5,6-tetrahydropyridazine(3aa)

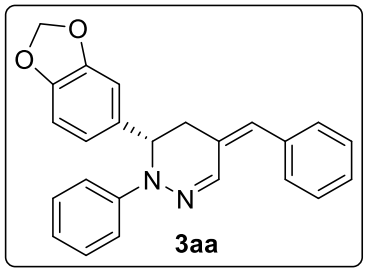

3aa

Reaction Time: 12 h; **1a** (0.050 g, 0.26 mmol); **2a** (0.051 g, 0.26 mmol); **3aa** (0.057 g, 0.15 mmol); **Purification:** Purified by silica gel column chromatography using 3% ethyl acetate in hexane as eluent; **Yield**: 60%; **Nature**: Yellow solid; **Melting point**: 110 °C; $[\alpha]_D^{25}$ = -818.20 (c = 0.6, $CHCl_3$); **HPLC:** Chiralpak IC, *i*-PrOH/hexanes = 10/90, flow rate = 0.5 mL/min, I = 367 nm; t_R = 9.94 min (major), 11.91 min (minor); ***ee* = 97%**; **^{1}H-NMR (400 MHz)** : δ 7.50 (s, 1H), 7.35-7.20 (m, 9H), 6.89 (t, *J* = 13.0 Hz, 1H), 6.72 (d, *J* = 8.1 Hz, 1H), 6.65-6.62 (m, 2H), 6.19 (bs, 1H), 5.90 (d, *J* = 6.4 Hz, 2H), 5.33 (d, *J* = 5.6 Hz, 1H), 3.18 (dd, *J* = 14.5, 5.6 Hz, 1H), 2.66 (d, *J* = 14.4Hz, 1H); **^{13}C-NMR (100 MHz)** : δ 148.1, 146.7, 146.1, 136.0, 133.7, 132.7, 129.8, 129.4, 129.1, 128.4, 127.5, 123.3, 120.6, 119.2, 114.0, 108.6, 106.5, 101.1, 57.2, 34.8; **IR (Neat)**: 2922, 1596, 1492, 1338, 1244, 1129, 1038, 994, 932, 750 cm^{-1}; **HRMS (ESI, Q-TOF)** m/z: $[M+H]^+$ calculated for $C_{24}H_{21}N_2O_2$ 369.1603, Found 369.1602.

(*S,Z*)-6-(benzo[*d*][1,3]dioxol-5-yl)-4-(4-methoxybenzylidene)-1-phenyl-1,4,5,6-tetrahydropyridazine (3ab)

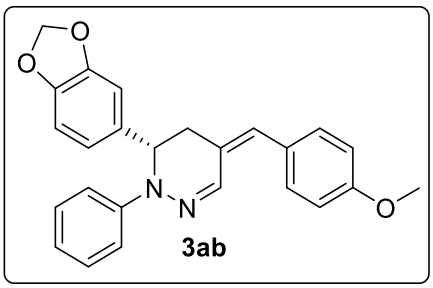

3ab

Reaction Time: 12 h; **1a** (0.050 g, 0.26 mmol); **2b** (0.058 g, 0.26 mmol); **3ab** (0.062 g, 0.15 mmol); **Purification:** Purified by silica gel column chromatography using 10% ethyl acetate in hexane as eluent; **Yield**: 60%; **Nature**: Yellow solid; **Melting point**: 160 °C; $[\alpha]_D^{25}$ = -323.54 (c = 1.5, $CHCl_3$); **HPLC:** Chiralcel OD-H, *i*-PrOH/hexanes = 5/95, flow rate = 0.5 mL/min, I = 387 nm; t_R = 15.67 min (major), 26.31 min (minor); ***ee* = 89%**; **^{1}H-NMR (400 MHz)** : δ 7.50 (s, 1H), 7.30-7.24 (m, 6H), 6.90 (m,3H), 6.74 (d, *J* = 7.9 Hz, 1H), 6.66 (m, 2H), 6.16 (bs, 1H), 5.92 (d, *J* = 6.8 Hz, 2H), 5.34 (m, 1H), 3.84 (s, 3H), 3.19 (dd, *J* = 14.3, 5.5 Hz, 1H), 2.65 (d, *J* = 14.1Hz, 1H); **^{13}C-NMR (100 MHz)**: δ 159.1, 148.0, 146.7, 146.2, 133.9, 133.0, 130.7, 129.5, 129.0, 128.6, 121.8, 120.4, 119.2, 113.9, 113.8, 108.5, 106.6, 101.1, 57.2, 55.4, 34.8; **IR (Neat)**: 2923, 1598, 1497, 1337, 1296, 1252, 1175, 1130, 1036, 992, 933, 800, 750, 691 cm^{-1}; **HRMS (ESI, Q-TOF)** m/z: $[M+H]^+$ calculated for $C_{25}H_{23}N_2O_3$ 399.1709, Found 399.1696

(*S*,*Z*)-6-(benzo[*d*][1,3]dioxol-5-yl)-4-(4-methylbenzylidene)-1-phenyl-1,4,5,6-tetrahydropyridazine (3ac)

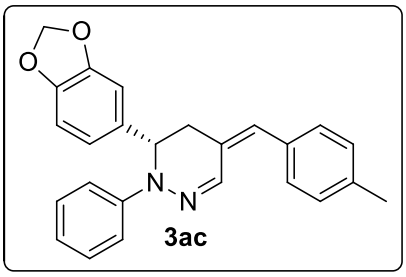

3ac

Reaction Time: 12 h; **1a** (0.050 g, 0.26 mmol); **2c** (0.055 g, 0.26 mmol); **3ac** (0.063 g, 0.16 mmol); **Purification:** Purified by silica gel column chromatography using 8% ethyl acetate in hexane as eluent; **Yield**: 63%; **Nature**: Yellow solid; **Melting point**: 145 °C; $[\alpha]_D^{25}$ = -680.84 (c = 0.9, $CHCl_3$); **HPLC:** Chiralpak IC, *i*-PrOH/hexanes = 10/90, flow rate = 0.3 mL/min, I = 364 nm; t_R = 16.89 min (major), 21.35 min (minor); ***ee* = 86%**; **^{1}H-NMR (400 MHz)** : δ 7.54 (s, 1H), 7.29-7.15 (m, 8H), 6.91 (t, *J* = 13.0 Hz, 1H), 6.73 (d, *J* = 7.8 Hz, 1H), 6.67-6.64 (m, 2H), 6.18 (bs, 1H), 5.91 (d, *J* = 5.5 Hz, 2H), 5.34 (d, *J* = 5.4 Hz, 1H), 3.2 (dd, *J* = 14.4, 5.6 Hz, 1H), 2.65 (d, *J* = 14.2 Hz, 1H), 2.37 (s, 3H); **^{13}C-NMR (100 MHz)**: δ 148.0, 146.7, 146.2, 137.5, 133.9, 133.1, 133.0, 129.8, 129.3, 129.1, 129.0, 122.6, 120.5, 119.2, 114.0, 108.6, 106.6, 101.1, 57.2, 34.9, 21.3; **IR (Neat)**: 2923, 2854, 1597, 1496, 1441, 1338, 1295, 1235, 1131, 1039, 992, 936, 750 cm^{-1}; **HRMS (ESI, Q-TOF)** m/z: $[M+H]^+$ calculated for $C_{25}H_{23}N_2O_2$ 383.1760, Found 383.1745

(*S*,*Z*)-6-(benzo[*d*][1,3]dioxol-5-yl)-4-(4-isopropylbenzylidene)-1-phenyl-1,4,5,6-tetrahydropyridazine (3ad)

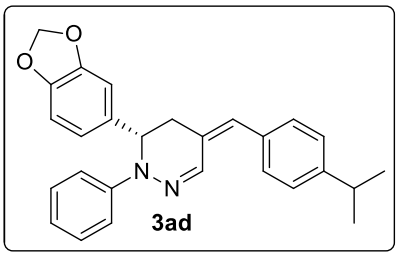

3ad

Reaction Time: 12 h; **1a** (0.050 g, 0.26 mmol); **2d** (0.062 g, 0.26 mmol); **3ad** (0.085 g, 0.21 mmol); **Purification:** Purified by silica gel column chromatography using 8% ethyl acetate in hexane as eluent; **Yield**: 80%; **Nature**: Yellow solid; **Melting point**: 156 °C; $[\alpha]_D^{25}$ = -317.40 (c = 0.5, $CHCl_3$); **HPLC:** Chiralcel OD-H, *i*-PrOH/hexanes = 5/95, flow rate = 0.5 mL/min, I = 361 nm; t_R = 8.16 min (major), 14.41 min (minor); ***ee* = 96%**; **^{1}H-NMR (400 MHz)** : δ 7.56 (s, 1H), 7.30-7.21 (m, 8H), 6.91 (t, *J* = 13.0 Hz, 1H), 6.73 (d, *J* = 7.9 Hz, 1H), 6.67-6.64 (m, 2H), 6.18 (bs, 1H), 5.91 (d, *J* = 6.6 Hz, 2H), 5.35 (d, *J* = 5.5 Hz, 1H), 3.19 (dd, *J* = 14.3, 5.5 Hz, 1H), 2.93 (m, 1H), 2.66 (d, *J* = 14.5 Hz, 1H), 1.28 (s, 3H), 1.26 (s, 3H); **^{13}C-NMR (100 MHz)**: δ 148.5, 148.0, 146.7, 146.2, 133.8, 133.6, 129.8, 129.4, 129.1, 126.5, 122.7, 120.5, 119.2, 114.0, 108.6, 106.6, 101.1, 57.3, 34.9, 34.0, 24.0; **IR (Neat)**: 2960, 2896, 1596, 1494, 1339, 1241, 1129, 1040, 994, 933, 750 cm^{-1}; **HRMS (ESI, Q-TOF)** m/z: $[M+H]^+$ calculated for $C_{27}H_{27}N_2O_2$ 411.2073, Found 411.2057

(*S*,*Z*)-6-(benzo[*d*][1,3]dioxol-5-yl)-4-(3,4-dimethoxybenzylidene)-1-phenyl-1,4,5,6-tetrahydropyridazine (3ae)

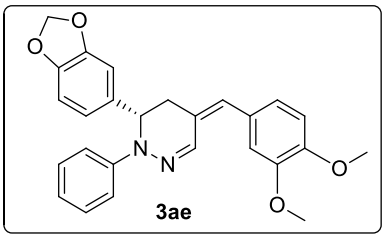

Reaction Time: 12 h; **1a** (0.050 g, 0.26 mmol); **2e** (0.066 g, 0.26 mmol); **3ae** (0.099 g, 0.23 mmol); **Purification:** Purified by silica gel column chromatography using 15% ethyl acetate in hexane as eluent; **Yield**: 90%; **Nature**: Yellow solid; **Melting point**: 90 °C; $[\alpha]_D^{25}$ = -305.91 (c = 0.9, $CHCl_3$); **HPLC:** Chiralpak IC, *i*-PrOH/hexanes = 10/90, flow rate = 1.0 mL/min, I = 369 nm; t_R = 19.31 min (major), 22.75 min (minor); ***ee* = 76%; ^{1}H-NMR (400 MHz)** : δ 7.52 (s, 1H), 7.26-7.19 (m, 5H), 6.90-6.79 (m, 4H), 6.71 (d, *J* = 7.8 Hz, 1H), 6.64-6.62 (m, 2H), 6.12 (bs, 1H), 5.89 (d, *J* = 5.7 Hz, 2H), 5.31 (d, *J* = 5.7 Hz, 1H), 3.88 (s, 3H), 3.87 (s, 3H), 3.16 (dd, *J* = 14.6, 6.3 Hz, 1H), 2.62 (d, *J* = 14.2 Hz, 1H); **^{13}C-NMR (100 MHz)**: δ 148.7, 148.0, 146.7, 146.2, 133.9, 133.0, 129.6, 129.1, 122.3, 122.2, 120.6, 119.2, 114.0, 112.3, 111.0, 108.6, 106.6, 101.1, 57.3, 56.0, 34.9; **IR (Neat)**: 2923, 2853, 1596, 1495, 1461, 1255, 1131, 1037 cm^{-1}; **HRMS (ESI, Q-TOF)** m/z: $[M+H]^+$ calculated for $C_{26}H_{24}N_2O_4$ 429.1814, Found 429.1816

(*S*,*Z*)-4-((6-(benzo[*d*][1,3]dioxol-5-yl)-1-phenyl-5,6-dihydropyridazin-4(1H)-ylidene)methyl)benzonitrile (3af)

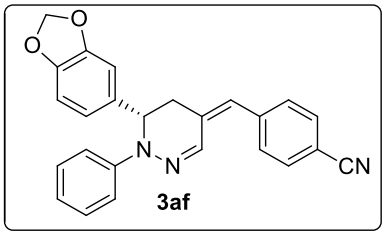

Reaction Time: 12 h; **1a** (0.050 g, 0.26 mmol); **2f** (0.057 g, 0.26 mmol); **3af** (0.046 g, 0.11 mmol); **Purification:** Purified by silica gel column chromatography using 12% ethyl acetate in hexane as eluent; **Yield**: 45%; **Nature**: Yellow solid; **Melting point**: 120 °C; $[\alpha]_D^{25}$ = -619.83 (c = 0.4, $CHCl_3$); **HPLC:** Chiralcel OD-H, *i*-PrOH/hexanes = 10/90, flow rate = 0.8 mL/min, I = 383 nm; t_R = 15.17 min (major), 41.99 min (minor); ***ee* = 96%**; **^{1}H-NMR (400 MHz)** : δ 7.60 (d, *J* = 8.0 Hz, 2H), 7.37 (m, 3H), 7.28-7.21 (m, 4H), 6.92 (t, *J* = 13.5 Hz, 1H), 6.73 (d, *J* = 7.7 Hz, 1H), 6.63-6.60 (m, 2H), 6.13 (bs, 1H), 5.91 (d, *J* = 6.8 Hz, 2H), 5.35 (d, *J* = 4.6 Hz, 1H), 3.20 (dd, *J* = 14.6, 5.6 Hz, 1H), 2.68 (d, *J* = 14.5 Hz, 1H); **^{13}C-NMR (100 MHz)**: δ 148.2, 146.9, 145.9, 140.7, 133.0, 132.2, 131.0, 129.8, 129.1, 127.0, 126.3, 121.2, 119.1, 114.2, 108.7, 106.4, 101.2, 57.1, 34.8; **IR (Neat)**: 2922, 2852, 1597, 1493, 1257, 1039, 809, 751 cm^{-1}; **HRMS (ESI, Q-TOF)** m/z: $[M+H]^+$ calculated for $C_{25}H_{20}N_3O_2$ 394.1556, Found 394.1533

(*S*,*Z*)-6-(benzo[*d*][1,3]dioxol-5-yl)-4-(4-bromobenzylidene)-1-phenyl-1,4,5,6-tetrahydropyridazine (3ah)

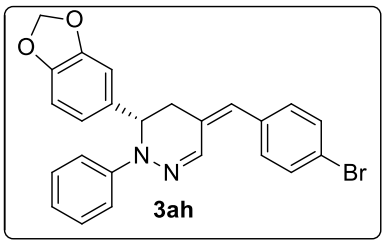

3ah

Reaction Time: 12 h; **1a** (0.050 g, 0.26 mmol); **2h** (0.071 g, 0.26 mmol); **3ah** (0.065 g, 0.14 mmol); **Purification:** Purified by silica gel column chromatography using 3% ethyl acetate in hexane as eluent; **Yield**: 55%; **Nature**: Yellow solid; **Melting point**: 115 °C; $[\alpha]_D^{25}$ = -652.90 (c = 0.4, $CHCl_3$); **HPLC:** Chiralcel OD-H, *i*-PrOH/hexanes = 5/95, flow rate = 0.5 mL/min, I = 400 nm; t_R = 11.66 min (major), 27.97 min (minor); ***ee* = 90%**; **^{1}H-NMR (400 MHz)** : δ 7.45-7.42 (m, 3H), 7.27-7.20 (m, 4H), 7.14 (d, *J* = 8.3 Hz, 2H), 6.9 (t, *J* = 13.4 Hz, 1H), 6.71 (d, *J* = 7.8 Hz, 1H), 6.63-6.60 (m, 2H), 6.08 (bs, 1H), 5.89 (d, *J* = 6.8 Hz, 2H), 5.32 (d, *J* = 5.7 Hz, 1H), 3.15 (dd, *J* = 14.3, 5.5 Hz, 1H), 2.64 (d, *J* = 14.2 Hz, 1H); **^{13}C-NMR (100 MHz)**: δ 148.1, 146.8, 146.0, 134.9, 133.5, 132.0, 131.5, 130.9, 129.1, 128.2, 124.0, 121.4, 120.8, 119.1, 114.1, 108.6, 106.5, 101.2, 57.1, 34.8; **IR (Neat)**: 2921, 2852, 1597, 1488, 1459, 1376, 1237, 1040, 750 cm^{-1}; **HRMS (ESI, Q-TOF)** m/z: $[M+H]^+$ calculated for $C_{24}H_{20}BrN_2O_2$ 447.0708, Found 447.0702

(*S*,*Z*)-6-(benzo[*d*][1,3]dioxol-5-yl)-4-(4-chlorobenzylidene)-1-phenyl-1,4,5,6-tetrahydropyridazine (3ai)

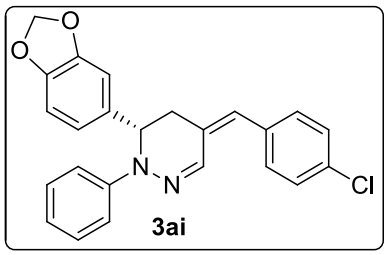

3ai

Reaction Time: 12 h; **1a** (0.050 g, 0.26 mmol); **2i** (0.060 g, 0.26 mmol); **3ai** (0.044 g, 0.11 mmol); **Purification:** Purified by silica gel column chromatography using 3% ethyl acetate in hexane as eluent; **Yield**: 42%; **Nature**: Yellow solid; **Melting point**: 114 °C; $[\alpha]_D^{25}$ = -629.02 (c = 0.8, $CHCl_3$); **HPLC:** Chiralcel OD-H, *i*-PrOH/hexanes = 5/95, flow rate = 0.5 mL/min, I = 400 nm; t_R = 11.33 min (major), 23.92 min (minor); ***ee* = 89%**; **^{1}H-NMR (400 MHz)** : δ 7.47 (s, 1H), 7.34-7.24 (m, 8H), 6.94 (t, *J* = 13.7 Hz, 1H), 6.76 (d, *J* = 7.7 Hz, 1H), 6.66 (m, 2H), 6.16 (bs, 1H), 5.94 (d, *J* = 6.8 Hz, 2H), 5.37 (d, *J* = 5.7 Hz, 1H), 3.2 (dd, *J* = 14.2, 5.5 Hz, 1H), 2.69 (d, *J* = 14.5Hz, 1H); **^{13}C-NMR (100 MHz)**: δ 148.1, 146.8, 146.1, 134.5, 133.5, 133.3, 132.0, 130.6, 129.1, 128.6, 128.2, 124.0, 120.8, 119.2, 114.1, 108.6, 106.5, 101.2, 57.1, 34.8; **IR (Neat)**: 2920, 2851, 1596, 1488, 1337, 1255, 1091, 1039, 992, 935, 804, 749, 509 cm^{-1}; **HRMS (ESI, Q-TOF)** m/z: $[M+H]^+$ calculated for $C_{24}H_{20}ClN_2O_2$ 403.1213, Found 403.1187

(*S*,*Z*)-6-(benzo[*d*][1,3]dioxol-5-yl)-4-(4-fluorobenzylidene)-1-phenyl-1,4,5,6-tetrahydropyridazine (3aj)

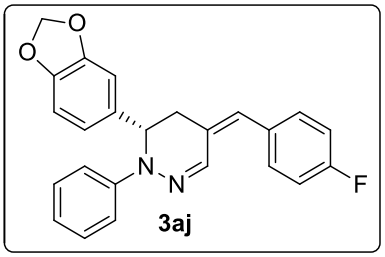

Reaction Time: 12 h; **1a** (0.050 g, 0.26 mmol); **2j** (0.055 g, 0.26 mmol); **3aj** (0.070 g, 0.18 mmol); **Purification:** Purified by silica gel column chromatography using 3% ethyl acetate in hexane as eluent; **Yield**: 70%; **Nature**: Yellow solid; **Melting point**: 132 °C; $[\alpha]_D^{25}$ = - 451.90 (c = 1.4, $CHCl_3$); **HPLC:** Chiralcel OD-H, *i*-PrOH/hexanes = 5/95, flow rate = 0.5 mL/min, I = 400 nm; t_R = 10.49 min (major), 21.57 min (minor); ***ee* = 85%**; **^{1}H-NMR (400 MHz)** : δ 7.46 (s, 1H), 7.30-7.24 (m, 6H), 7.05 (t, *J* = 17.4 Hz, 2H), 6.93 (t, *J* = 13.5 Hz, 1H), 6.75 (d, *J* = 7.8 Hz, 1H), 6.66 (m, 2H), 6.17 (bs, 1H), 5.93 (d, *J* = 7.3 Hz, 2H), 5.36 (d, *J* = 5.8 Hz, 1H), 3.2 (dd, *J* = 14.2, 5.5 Hz, 1H), 2.67 (d, *J* = 14.5Hz, 1H); **^{13}C-NMR (100 MHz)** : δ 163.3, 160.9, 148.1, 146.8, 146.1, 133.7, 132.3, 132.1, 131.0, 130.9, 129.1, 128.4, 123.3, 120.7, 119.2, 115.5, 115.3, 114.0, 108.6, 106.5, 101.2, 57.1, 34.8; **IR (Neat)**: 2923, 2853, 1598, 1501, 1338, 1233, 1131, 1039, 992, 935, 750 cm^{-1}; **HRMS (ESI, Q-TOF)** m/z: $[M+H]^+$ calculated for $C_{24}H_{20}FN_2O_2$ 387.1509, Found 387.1497

(*S*,*Z*)-6-(benzo[*d*][1,3]dioxol-5-yl)-4-(3-bromobenzylidene)-1-phenyl-1,4,5,6-tetrahydropyridazine (3ak)

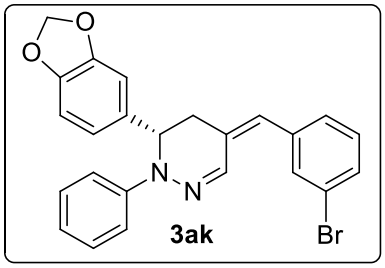

Reaction Time: 12 h; **1a** (0.050 g, 0.26 mmol); **2k** (0.071 g, 0.26 mmol); **3ak** (0.058 g, 0.13 mmol); **Purification:** Purified by silica gel column chromatography using 3% ethyl acetate in hexane as eluent; **Yield**: 50%; **Nature**: Yellow solid; **Melting point**: 78 °C; $[\alpha]_D^{25}$ = -319.27 (c = 0.2, $CHCl_3$); **HPLC:** Chiralcel OD-H, *i*-PrOH/hexanes = 10/90, flow rate = 0.5 mL/min, I = 372 nm; t_R = 10.22 min (major), 20.18 min (minor); ***ee* = 99%**; **^{1}H-NMR (400 MHz)** : δ 7.44 (s,1H), 7.40 (s, 1H), 7.38-7.35 (m, 1H), 7.27-7.18 (m, 6H), 6.90 (t, *J* = 13.7 Hz, 1H), 6.72 (d, *J* = 7.7 Hz, 1H), 6.63-6.60 (m, 2H), 6.08 (bs, 1H), 5.90 (d, *J* = 7.3 Hz, 2H), 5.32 (d, *J* = 5.5 Hz, 1H), 3.17 (dd, *J* = 14.6, 5.5 Hz, 1H), 2.65 (d, *J* = 14.5Hz, 1H); **^{13}C-NMR (100 MHz)**: δ 148.2, 146.8, 146.0, 134.9, 133.5, 132.0, 131.6, 130.9, 129.1, 128.2, 124.1, 121.5, 120.8, 119.2, 114.1, 108.6, 106.5, 101.1, 57.1, 34.8; **IR (Neat)**: 2923, 2854, 1596, 1494, 1442, 1338, 1294, 1253, 1130, 1039, 993, 936, 812, 750, 692 cm^{-1}; **HRMS (ESI, Q-TOF)** m/z: $[M+H]^+$ calculated for $C_{24}H_{20}BrN_2O_2$ 447.0708, Found 447.0694

(*S*,*Z*)-6-(benzo[*d*][1,3]dioxol-5-yl)-4-(3-methoxybenzylidene)-1-phenyl-1,4,5,6-tetrahydropyridazine (3al)

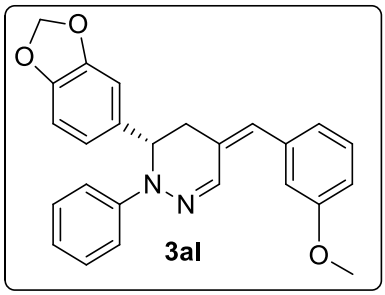

Reaction Time: 12 h; **1a** (0.050 g, 0.26 mmol); **2l** (0.058 g, 0.26 mmol); **3al** (0.055 g, 0.14 mmol); **Purification:** Purified by silica gel column chromatography using 8% ethyl acetate in hexane as eluent; **Yield**: 54%; **Nature**: Yellow solid; **Melting point**: 97 °C; $[\alpha]_D^{25}$ = -465.45 (c = 0.7, $CHCl_3$); **HPLC:** Chiralcel OD-H, *i*-PrOH/hexanes = 10/90, flow rate = 0.5 mL/min, I = 367 nm; t_R = 15.21 min (major), 27.33 min (minor); ***ee* = 93%**; **^{1}H-NMR (400 MHz)** : δ 7.51 (s, 1H), 7.26-7.20 (m, 5H), 6.90-6.87 (m,2H), 6.84-6.79 (m, 2H), 6.71 (d, *J* = 7.9 Hz, 1H), 6.64-6.61 (m, 2H), 6.15 (s, 1H), 5.89 (d, *J* = 7.2 Hz, 2H), 5.32 (d, *J* = 5.8 Hz, 1H), 3.79 (s, 3H), 3.17 (dd, *J* = 14.4, 5.8 Hz, 1H), 2.67 (d, *J* = 14.4 Hz, 1H); **^{13}C-NMR (100 MHz)** : δ 159.5, 148.1, 146.7, 146.2, 137.3, 133.7, 132.7, 129.6, 129.4, 129.1, 123.6, 122.0, 120.6,119.2, 114.7, 114.0, 113.1, 108.6, 106.5, 101.1, 57.2, 55.3, 34.9; **IR (Neat)**: 2921, 1593, 1490, 1249, 1127, 1039, 933, 751 cm^{-1}; **HRMS (ESI, Q-TOF)** m/z: $[M+H]^+$ calculated for $C_{25}H_{23}N_2O_3$ 399.1709, Found 399.1681

(*S*,*Z*)-6-(benzo[*d*][1,3]dioxol-5-yl)-4-(2-methylbenzylidene)-1-phenyl-1,4,5,6-tetrahydropyridazine (3am)

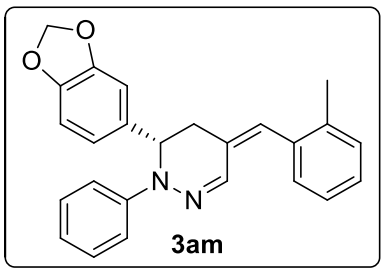

Reaction Time: 12 h; **1a** (0.050 g, 0.26 mmol); **2m** (0.054 g, 0.26 mmol); **3am** (0.052 g, 0.13 mmol); **Purification:** Purified by silica gel column chromatography using 5% ethyl acetate in hexane as eluent.; **Yield**: 52%; **Nature**: Yellow solid; **Melting point**: 118 °C; $[\alpha]_D^{25}$ = -395.28 (c = 1.0, $CHCl_3$); **HPLC:** Chiralcel OD-H, *i*-PrOH/hexanes = 10/90, flow rate = 0.5 mL/min, I = 359 nm; t_R = 8.07 min (major), 11.84 min (minor); ***ee* = 92%**; **^{1}H-NMR (400 MHz)** : δ 7.29 (s, 1H), 7.26-7.17 (m, 8H), 6.89 (t, *J* = 13.2 Hz, 1H), 6.74 (d, *J* = 8.0 Hz, 1H), 6.67-6.64 (m, 2H), 6.24 (s, 1H), 5.90 (d, *J* = 6.4 Hz, 2H), 5.35 (d, *J* = 5.6 Hz, 1H), 3.21 (dd, *J* = 14.2, 5.4 Hz, 1H), 2.71 (d, *J* = 14.3 Hz, 1H), 2.18 (s, 3H); **^{13}C-NMR (100 MHz)**: δ 148.1, 146.7, 146.2, 137.5, 133.9, 133.2, 133.0, 129.8, 129.3, 129.1, 129.0, 122.6, 120.5, 119.2, 114.0, 108.5, 106.6, 101.1, 57.2, 34.9, 21.4; **IR (Neat)**: 2923, 2854, 1597, 1489, 1337, 1294, 1235, 1130, 1038, 992, 936, 808, 748, 691 cm^{-1}; **HRMS (ESI, Q-TOF)** m/z: $[M+H]^+$ calculated for $C_{25}H_{23}N_2O_2$ 383.1760, Found 383.1733

(*S*,*Z*)-6-(benzo[*d*][1,3]dioxol-5-yl)-4-benzylidene-1-(*p*-tolyl)-1,4,5,6-tetrahydropyridazine (3an)

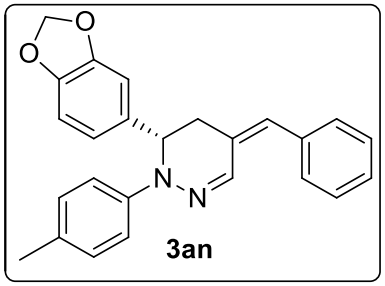

Reaction Time: 12 h; **1a** (0.050 g, 0.26 mmol); **2n** (0.054 g, 0.26 mmol); **3an** (0.040 g, 0.10 mmol); **Purification:** Purified by silica gel column chromatography using 4% ethyl acetate in hexane as eluent; **Yield**: 40%; **Nature**: Yellow solid; **Melting point**: 102 °C; $[\alpha]_D^{25}$ = -697.31 (c = 0.5, $CHCl_3$); **HPLC:** Chiralpak IC, *i*-PrOH/hexanes = 10/90, flow rate = 0.5 mL/min, I = 369 nm; t_R = 10.30 min (major), 13.29 min (minor); ***ee* = 91%**; **^{1}H-NMR (400 MHz)**: δ 7.47 (s, 1H), 7.32-7.24 (m, 5H), 7.09 (q, *J* = 27.0, 8.7 Hz, 4H), 6.71 (d, *J* = 7.9 Hz, 1H), 6.64-6.61 (m, 2H), 6.16 (bs, 1H), 5.89 (d, *J* = 7.3 Hz, 2H), 5.30 (d, *J* = 5.8 Hz, 1H), 3.17 (dd, *J* = 14.1, 5.4 Hz, 1H), 2.64 (d, *J* = 14.4 Hz, 1H), 2.26 (s, 3H); **^{13}C-NMR (100 MHz)**: δ 148.0, 146.7, 114.0, 138.6, 133.9, 132.2, 129.9, 129.6, 129.4, 128.4, 127.5, 123.4, 119.2, 114.1, 108.6, 106.6, 101.1, 57.3, 34.9, 20.6; **IR (Neat)**: 2919, 2854, 1454, 1254, 1032, 802 cm^{-1}; **HRMS (ESI, Q-TOF)** m/z: $[M+H]^+$ calculated for $C_{25}H_{23}N_2O_2$ 383.1760, Found 383.1726

(*S*,*Z*)-6-(benzo[*d*][1,3]dioxol-5-yl)-4-benzylidene-1-(4-fluorophenyl)-1,4,5,6-tetrahydropyridazine (3ao)

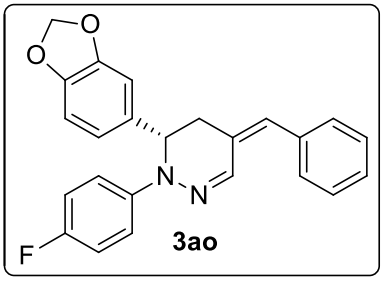

Reaction Time: 12 h; **1a** (0.050 g, 0.26 mmol); **2o** (0.055 g, 0.26 mmol); **3ao** (0.053 g, 0.14 mmol); **Purification:** Purified by silica gel column chromatography using 5% ethyl acetate in hexane as eluent; **Yield**: 53%; **Nature**: Yellow solid; **Melting point**: 65 °C; $[\alpha]_D^{25}$ = -320.10 (c = 0.8, $CHCl_3$); **HPLC:** Chiralpak IC, *i*-PrOH/hexanes = 10/90, flow rate = 0.5 mL/min, I = 378 nm; t_R = 16.43 min (major), 18.02 min (minor); ***ee* = 81.5%; ^{1}H-NMR (400 MHz)** : δ 7.47 (s, 1H), 7.35-7.23 (m, 5H), 7.16-7.12 (m, 2H), 6.93 (t, *J* = 17.4 Hz, 2H), 6.72 (d, *J* = 8.1 Hz, 1H), 6.63-6.59 (m, 2H), 6.19 (bs, 1H), 5.90 (d, *J* = 5.1 Hz, 2H), 5.25 (d, *J* = 5.6 Hz, 1H), 3.17 (dd, *J* = 14.4, 5.4 Hz, 1H), 2.65 (d, *J* = 14.5Hz, 1H); **^{13}C-NMR (100 MHz)** : 158.9, 156.5, 148.1, 146.8, 142.7, 139.1, 135.9, 133.6, 132.7, 130.8, 129.8, 129.4, 128.5, 127.6, 123.2, 119.8, 119.2, 116.1, 115.6, 115.4, 108.6, 106.5, 101.2, 57.6, 34.9; **IR (Neat)**: 2923, 2853, 1504, 1461, 1444, 1376, 1256, 1230, 1039, 937, 817, 749, 722, 703, 513 cm^{-1}; **HRMS (ESI, Q-TOF)** m/z: $[M+H]^+$ calculated for $C_{24}H_{20}FN_2O_2$ 387.1509, found 387.1498

(*S*,*Z*)-6-(benzo[*d*][1,3]dioxol-5-yl)-4-benzylidene-1-(4-chlorophenyl)-1,4,5,6-tetrahydropyridazine (3ap)

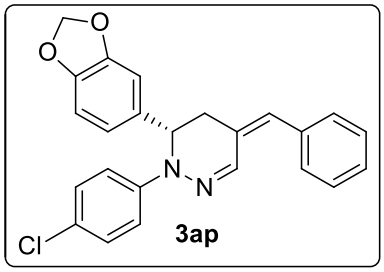

Reaction Time: 12 h**; 1a** (0.050 g, 0.26 mmol); **2p** (0.059 g, 0.26 mmol); **3ap** (0.054 g, 0.13 mmol)**; Purification:** Purified by silica gel column chromatography using 5% ethyl acetate in hexane as eluent; **Yield**: 51%**; Nature**: Yellow solid**; Melting point**: 126 °C**; $[\alpha]_D^{25}$ =** -392.74 (c = 1.0, $CHCl_3$)**; HPLC:** Chiralpak IC, *i*-PrOH/hexanes = 10/90, flow rate = 0.3 mL/min, I = 356 nm; t_R = 16.27 min (major), 18.43 min (minor); ***ee* = 81.5%; ^{1}H-NMR (400 MHz)** : δ 7.49 (s, 1H), 7.35-7.31 (m, 2H), 7.28-7.24 (m, 3H), 7.16 (q, *J* = 19.2, 9.2 Hz, 4H), 6.71 (d, *J* = 7.9 Hz, 1H), 6.61-6.58 (m, 2H), 6.22 (bs, 1H), 5.90 (d, *J* = 5.9 Hz, 2H), 5.27 (d, *J* = 5.6 Hz, 1H), 3.17 (dd, *J* = 14.3, 5.7 Hz, 1H), 2.65 (d, *J* = 14.4 Hz, 1H)**; ^{13}C-NMR (100 MHz)**: δ 148.2, 146.9, 114.8, 135.8, 133.3, 130.4, 129.4, 128.9, 128.4, 127.7, 125.4, 123.0, 119.2, 115.2, 108.6, 106.4, 101.2, 57.2, 34.8**; IR (Neat)**: 2899, 1591, 1489, 1338, 1240, 1128, 1039, 995, 931, 818, 742 cm^{-1}**; HRMS (ESI, Q-TOF)** m/z: $[M+H]^+$ calculated for $C_{24}H_{20}ClN_2O_2$ 403.1213, Found 403.1194

(*S*,*Z*)-4-benzylidene-6-(4-methoxyphenyl)-1-phenyl-1,4,5,6-tetrahydropyridazine (3ba)

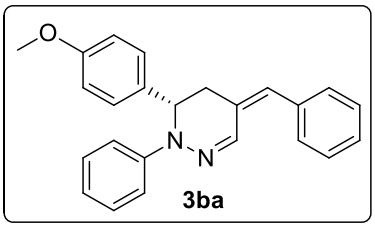

Reaction Time: 12 h; **1b** (0.050 g, 0.28 mmol); **2a** (0.056 g, 0.28 mmol); **3ba** (0.056 g, 0.16 mmol); **Purification:** Purified by silica gel column chromatography using 8% ethyl acetate in hexane as eluent; **Yield**: 56%; **Nature**: Yellow solid; **Melting point**: 101 °C; **$[\alpha]_D^{25}$ =** -669.26 (c = 0.8, $CHCl_3$); **HPLC:** Chiralcel OD-H, *i*-PrOH/hexanes = 10/90, flow rate = 0.5 mL/min, I = 397 nm; t_R = 7.67 min (major), 11.05 min (minor); ***ee* = 83%; ^{1}H-NMR (400 MHz)** : δ 7.53 (s, 1H), 7.37-7.24 (m, 10H), 7.12 (d, *J* = 8.7 Hz, 2H), 6.93-6.89 (m, 1H), 6.85 (d, *J* = 8.7 Hz, 2H), 6.20 (s, 1H), 5.41 (d, *J* = 5.6 Hz, 1H), 3.77 (s, 3H), 3.22 (dd, *J* = 14.2, 5.5 Hz, 1H), 2.71 (d, *J* = 14.2Hz, 1H); **^{13}C-NMR (100 MHz)**: δ 158.7, 146.3, 136.0, 132.7, 131.7, 129.6, 129.4, 129.1, 128.4, 127.5, 127.2, 123.5, 120.5, 114.2, 114.0, 56.9, 55.3, 34.8; **IR (Neat)**: 2924, 1597, 1499, 1306, 1249, 1175, 1128, 993, 843, 749, 694 cm^{-1}; **HRMS (ESI, Q-TOF)** m/z: $[M+H]^+$ calculated for $C_{24}H_{23}N_2O$ 355.1810, found 355.1801

(*S*,*Z*)-4-benzylidene-6-(3,4-dimethoxyphenyl)-1-phenyl-1,4,5,6-tetrahydropyridazine (3ca)

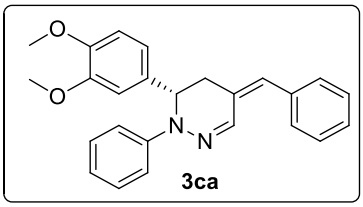

Reaction Time: 12 h; **1c** (0.050 g, 0.24 mmol); **2a** (0.047 g, 0.24 mmol); **3ca** (0.054 g, 0.14 mmol); **Purification:** Purified by silica gel column chromatography using 15% ethyl acetate in hexane as eluent; **Yield**: 58%; **Nature**: Yellow solid; **Melting point**: 116 °C; $[\alpha]_D^{25}$ = -354.91 (c = 0.95, $CHCl_3$); **HPLC:** Chiralcel OD-H, *i*-PrOH/hexanes = 10/90, flow rate = 1.0 mL/min, l = 358 nm) t_R = 5.36 min (major), 7.37 min (minor); ***ee* = 98%**; **^{1}H-NMR (400 MHz)** : δ 7.54 (s, 1H), 7.36-7.24 (m, 9H), 6.93-6.89 (m, 1H), 6.80 (d, *J* = 8.3 Hz, 1H), 6.76-6.74 (m, 1H), 6.70 (d, *J* = 2.2 Hz), 6.21 (s, 1H), 5.38 (d, *J* = 5.8 Hz, 1H), 3.84 (s, 6H), 3.23 (dd, *J* = 14.3, 5.5 Hz, 1H), 2.70 (d, *J* = 14.3Hz, 1H); **^{13}C-NMR (100 MHz)**: δ 149.2, 148.1, 146.3, 136.0, 132.6, 129.7, 129.3, 129.1, 128.4, 127.5, 123.5, 120.6, 118.3, 114.2, 111.3, 109.1, 57.3, 55.9, 34.9; **IR (Neat)**: 2927, 1595, 1501, 1256, 1135, 997, 929, 750 cm^{-1}; **HRMS (ESI, Q-TOF)** m/z: $[M+H]^+$ calculated for $C_{25}H_{25}N_2O_2$ 385.1916, found 385.1894

(*S*,*Z*)-4-benzylidene-1-phenyl-6-(*p*-tolyl)-1,4,5,6-tetrahydropyridazine (3da)

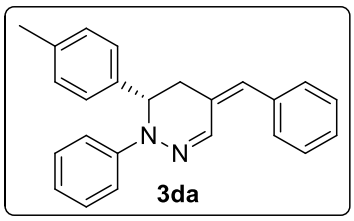

Reaction Time: 12 h; **1d** (0.050 g, 0.31 mmol); **2a** (0.061 g, 0.31 mmol); **3da** (0.040 g, 0.12 mmol); **Purification:** Purified by silica gel column chromatography using 5% ethyl acetate in hexane as eluent; **Yield**: 40%; **Nature**: Yellow solid; **Melting point**: 122 °C; $[\alpha]_D^{25}$ = -318.89 (c = 0.7, $CHCl_3$); **HPLC:** Chiralcel OD-H, *i*-PrOH/hexanes = 5/95, flow rate = 0.5 mL/min, I = 351 nm; t_R = 6.25 min (major), 9.10 min (minor); ***ee* = 76%**; **^{1}H-NMR (400 MHz)** : δ 7.49 (s, 1H), 7.33-7.29 (m, 2H), 7.26-7.21 (m, 7H), 7.07 (m, 4H), 6.89-6.84 (m, 1H), 6.16 (bs, 1H), 5.38 (d, *J* = 5.5 Hz, 1H), 3.20 (dd, *J* = 14.6, 5.8 Hz, 1H), 2.69 (d, *J* = 14.2Hz, 1H), 2.27 (s, 3H); **^{13}C-NMR (100 MHz)**: δ 146.3, 136.9, 136.8, 136.1, 132.7, 129.6, 129.4, 129.1, 128.4, 127.5, 125.9, 123.5, 120.5, 114.0, 57.3, 34.7, 21.2; **IR (Neat)**: 2922, 2853, 1597, 1495, 1361, 1130, 992, 923, 750, 693 cm^{-1}**; HRMS (ESI, Q-TOF)** m/z: $[M+H]^+$ calculated for $C_{24}H_{23}N_2$ 339.1861, found 339.1867

(*S*,*Z*)-4-benzylidene-1,6-diphenyl-1,4,5,6-tetrahydropyridazine (3ea)

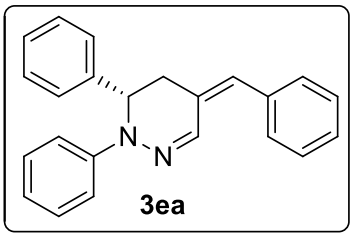

Reaction Time: 12 h; **1e** (0.050 g, 0.34 mmol); **2a** (0.067 g, 0.34 mmol); **3ea** (0.085 g, 0.26 mmol); **Purification:** Purified by silica gel column chromatography using 3% ethyl acetate in hexane as eluent; **Yield**: 77%; **Nature**: Yellow solid; **Melting point**: 140 °C; $[\alpha]_D^{25}$ = -352.53 (c = 1.0, $CHCl_3$); **HPLC:** Chiralcel OD-H, *i*-PrOH/hexanes = 5/95, flow rate = 0.5 mL/min, I = 365 nm; t_R =

7.12 min (major), 10.53 min (minor); ***ee* = 70%**; **^{1}H-NMR (400 MHz)**: δ 7.54 (s, 1H), 7.36-7.20 (m, 14H), 6.93-6.90 (m, 1H), 6.19 (s, 1H), 5.46 (d, *J* = 5.8 Hz, 1H), 3.26 (dd, *J* = 14.3, 5.7 Hz, 1H), 2.75 (d, *J* = 14.2Hz, 1H); **^{13}C-NMR (100 MHz)**: δ 146.3, 139.8, 136.0, 132.8, 129.7, 129.4, 129.1, 128.9, 128.4, 127.5, 127.3, 126.0, 123.4, 120.6, 114.0, 57.4, 34.7; **IR (Neat)**: 2923, 2853, 1597, 1539, 1495, 1452, 1362, 1259, 1130, 1076, 1031, 991, 932, 802, 749, 695, 626 cm^{-1}; **HRMS (ESI, Q-TOF)** m/z: $[M+H]^+$ calculated for $C_{23}H_{21}N_2$ 325.1705, found 325.1696

(*S*,*Z*)-4-benzylidene-6-(4-fluorophenyl)-1-phenyl-1,4,5,6-tetrahydropyridazine (3fa)

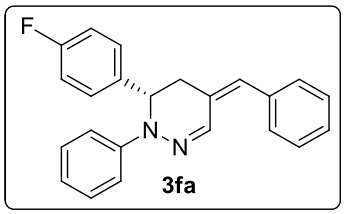

3fa

Reaction Time: 12 h; **1f** (0.050 g, 0.30 mmol); **2a** (0.059 g, 0.30mmol); **3fa** (0.082 g, 0.24 mmol); **Purification:** Purified by silica gel column chromatography using 8% ethyl acetate in hexane as eluent; **Yield**: 80%; **Nature**: Yellow solid; **Melting point**: 128 °C; **$[\alpha]_D^{25}$ = -**492.68 (c = 1.1, $CHCl_3$); **HPLC:** Chiralcel OD-H, *i*-PrOH/hexanes = 10/90, flow rate = 0.5 mL/min, I = 371 nm; t_R = 7.23 min (major), 10.93 min (minor); ***ee* = 94%**; **^{1}H-NMR (400 MHz)** : δ 7.50 (s, 1H), 7.34-7.30 (m, 2H), 7.26-7.18 (m, 7H), 7.157.12 (m, 2H), 6.97 (t, *J* = 13.8 Hz, 1H), 6.17 (s, 1H), 5.41 (d, *J* = 5.6 Hz, 1H), 3.21 (dd, *J* = 14.2, 5.5 Hz, 1H), 2.67 (d, *J* = 14.2Hz, 1H); **^{13}C-NMR (100 MHz)**: δ 146.1, 135.9, 135.5, 132.9, 130.0, 129.4, 129.1, 128.4, 127.8, 127.7, 127.6, 123.1, 120.7, 115.7, 114.0, 56.8, 34.8; **IR (Neat)**: 2924, 2854, 1597, 1495, 1229, 1129, 991, 922, 751, 693 cm^{-1}; **HRMS (ESI, Q-TOF)** m/z: $[M+H]^+$ calculated for $C_{23}H_{20}N_2F$ 343.1611, found 343.1613

(*S*,*Z*)-4-benzylidene-6-(4-bromophenyl)-1-phenyl-1,4,5,6-tetrahydropyridazine (3ga)

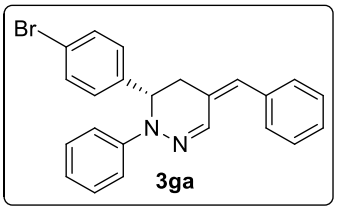

3ga

Reaction Time: 12 h; **1g** (0.060 g, 0.26 mmol); **2a** (0.052 g, 0.26 mmol); **3ga** (0.058 g, 0.14 mmol); **Purification:** Purified by silica gel column chromatography using 5% ethyl acetate in hexane as eluent; **Yield**: 55%; **Nature**: Yellow liquid; **$[\alpha]_D^{25}$ = -**325.80 (c = 0.9, $CHCl_3$); **HPLC:** Chiralpak IC, *i*-PrOH/hexanes = 10/90, flow rate = 0.3 mL/min, I = 379 nm; t_R = 14.40 min (major), 16.42 min (minor); ***ee* = 85%**; **^{1}H-NMR (400 MHz)** : δ 7.50 (s, 1H), 7.40 (d, *J* = 8.6 Hz, 2H), 7.31-7.17 (m, 9H), 7.04 (d, *J* = 8.7 Hz, 2H), 6.89 (t, *J* = 14.1 Hz, 1H), 6.17 (s, 1H), 5.36 (d, *J* = 5.9 Hz, 1H), 3.21 (dd, *J* = 14.6, 5.8 Hz, 1H), 2.66 (d, *J* = 14.5Hz, 1H); **^{13}C-NMR (100 MHz)**: δ 146.0, 138.9, 135.8, 133.0, 132.0, 130.11, 129.4, 129.1, 128.4, 127.9, 127.7, 126.0, 122.9, 121.2, 120.8, 114.0, 56.9, 34.5; **IR (Neat)**: 2920, 2853, 1594, 1490, 1356, 1126, 995, 923, 748, 693, 487 cm^{-1}; **HRMS (ESI, Q-TOF)** m/z: $[M+H]^+$ calculated for $C_{23}H_{20}N_2Br$ 403.0810, found 403.0787.

(*S*,*Z*)-4-benzylidene-6-mesityl-1-phenyl-1,4,5,6-tetrahydropyridazine (3ha)

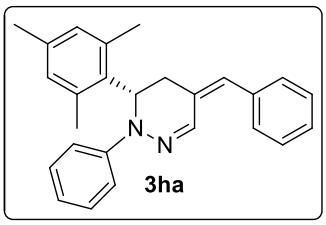

Reaction Time: 12 h; **1h** (0.050 g, 0.26 mmol); **2a** (0.052 g, 0.26 mmol); **3ha** (0.058 g, 0.16 mmol); **Purification:** Purified by silica gel column chromatography using 6% ethyl acetate in hexane as eluent; **Yield**: 60%; **Nature**: Yellow liquid; **$[\alpha]_D^{25}$ =** -60.34 (c = 0.6, $CHCl_3$); **HPLC:** Chiralpak IC, *i*-PrOH/hexanes = 10/90, flow rate = 0.5 mL/min, I = 344 nm; t_R = 8.49 min (major), 9.32 min (minor); ***ee* = 64.5%**; **^{1}H-NMR (400 MHz)** : δ 7.6 (s, 1H), 7.41-7.34 (m, 4H), 7.29-7.25 (m, 1H), 7.16 (t, *J* = 15.5 Hz, 2H), 7.06 (d, *J* = 8.1 Hz, 2H), 6.89-6.84 (m, H), 6.67 (bs, 1H), 6.27 (s, 1H), 5.39 (t, *J* = 13.2 Hz, 1H), 2.94 (dd, *J* = 14.6, 6.9 Hz, 1H), 2.81 (dd, *J* = 14.6, 6.4 Hz, 1H), 2.48 (s, 3H), 2.21 (s, 3H), 2.15 (s, 3H); **^{13}C-NMR (100 MHz)**: δ 146.8, 136.5, 136.1, 135.8, 135.5, 134.4, 131.9, 130.0, 129.3, 128.7, 128.5, 127.8, 127.5, 124.7, 121.2, 115.9, 55.3, 33.4, 20.8, 20.5; **IR (Neat)**: 2921, 2855, 1596, 1490, 1308, 1103, 1026, 802, 750, 694 cm^{-1}; **HRMS (ESI, Q-TOF)** m/z: $[M+H]^+$ calculated for $C_{26}H_{27}N_2$ 367.2174, found 367.2163

(*S*,*Z*)-4-benzylidene-6-(furan-2-yl)-1-phenyl-1,4,5,6-tetrahydropyridazine (3ia)

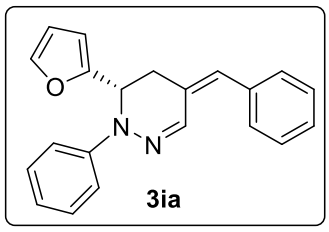

Reaction Time: 12 h; **1h** (0.035 g, 0.26 mmol); **2a** (0.051 g, 0.26 mmol); **3ha** (0.030 g, 0.09 mmol); **Purification:** Purified by silica gel column chromatography using 5% ethyl acetate in hexane as eluent; **Yield**: 36%; **Nature**: Yellow sticky liquid; **$[\alpha]_D^{25}$ =** -851.27 (c = 0.4, $CHCl_3$); **HPLC:** Chiralcel OD-H, *i*-PrOH/hexanes = 5/95, flow rate = 0.5 mL/min, I = 372 nm; t_R = 6.67 min (major), 8.59 min (minor); ***ee* = 91%**; **^{1}H-NMR (400 MHz)** : δ 7.52 (s, 1H), 7.37-7.27 (m, 10H), 6.95-6.91 (m, 1H), 6.35 (s, 1H), 6.25-6.23 (m,1H), 6.08 (d, *J* = 3.2 Hz, 1H), 5.48 (d, *J* = 5.4 Hz, 1H), 3.12 (dd, *J* = 14.9, 5.2 Hz, 1H), 2.95 (d, *J* = 14.6 Hz, 1H); **^{13}C-NMR (100 MHz)**: δ 151.4, 146.3, 142.1, 136.0, 133.0, 129.9, 129.4, 129.1, 128.5, 127.6, 123.8, 120.8, 114.4, 110.5, 107.9, 51.5, 31.8; **IR (Neat)**: 1595, 1493, 1342, 1296, 1259, 1129, 1073, 989, 928, 745, 692, 623, 596 cm^{-1}; **HRMS (ESI, Q-TOF)** m/z: $[M+H]^+$ calculated for $C_{21}H_{19}N_2O$ 315.1497, found 315.1501

(*S*,*Z*)-4-benzylidene-1-phenyl-6-(thiophen-2-yl)-1,4,5,6-tetrahydropyridazine (3ja)

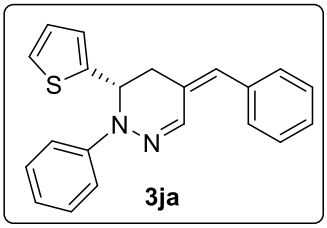

Reaction Time: 12 h; **1h** (0.040 g, 0.26 mmol); **2a** (0.051 g, 0.26 mmol); **3ha** (0.042 g, 0.12 mmol); **Purification:** Purified by silica gel column chromatography using 5% ethyl acetate in hexane as eluent; **Yield**: 49%; **Nature**: Yellow sticky liquid; **$[\alpha]_D^{25}$ =** -649.55 (c = 0.4, $CHCl_3$); **HPLC:** Chiralcel OD-H, *i*-PrOH/hexanes = 5/95, flow rate = 0.5 mL/min, I = 389 nm; t_R = 7.88 min (major), 11.20 min (minor); ***ee* = 94%**; **^{1}H-NMR**

(400 MHz) : δ 7.48 (s, 1H), 7.27-7.16 (m, 9H), 7.08-7.06 (m, 1H), 6.86-6.83 (m, 1H), 6.78 (d, *J* = 3.6 Hz, 2H), 6.25 (s, 1H), 5.61 (dd, *J* = 5.0, 2.2 Hz, 1H), 3.15 (dd, *J* = 14.6, 5.0 Hz, 1H), 2.69 (d, *J* = 14.6 Hz, 1H); **^{13}C-NMR (100 MHz)**: δ 146.1, 142.4, 136.0, 133.1, 130.6, 129.4, 129.1, 128.4, 127.6, 125.5, 125.0, 123.4, 120.9, 114.5, 53.4, 35.1; **IR (Neat)**: 2922, 1595, 1492, 1338, 1259, 1123, 988, 921, 801, 746, 691, 618, 510 cm^{-1}; **HRMS (ESI, Q-TOF)** m/z: $[M+H]^+$ calculated for $C_{21}H_{19}N_2S$ 331.1269, found 331.1273.

2.A.4.6. Chemical transformation of 3ba[5c]

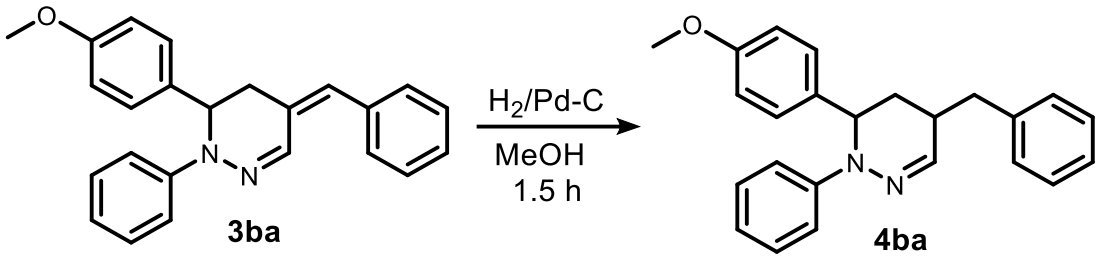

Procedure: Compound **3ba**, 10% Pd/C, and methanol were taken in a round bottom flask and stirred at 45 psi hydrogen pressure for 1.5 h. After completion of the reaction (monitored by TLC), the Pd/C was filtered off through a small pad of Celite, washed with methanol, and the solvent was removed under vacuum by a rotary evaporator. Then the crude product was purified by silica gel column chromatography (EtOAc/Hexane).

3ba (0.050 g, 0.14mmol); **4ba** (0.035 g, 0.098 mmol); **Yield**: 70%; **Nature**: oily yellowish liquid; **^{1}H-NMR (400 MHz)**: δ 7.26-7.17 (m, 5H), 7.09-7.06 (m, 4H), 6.93-6.91 (m, 2H), 6.87-6.85 (m, 2H), 6.83-6.81(m, 2H), 5.07 (t, *J* = 9.6 Hz, 1H), 3.79 (s, 3H), 2.53-2.47 (m, 2H), 2.31-2.24 (m, 1H), 2.15-2.11 (m, 1H), 2.05-1.98 (m, 1H); **^{13}C-NMR (100 MHz)**: δ 158.7, 146.9, 139.9, 139.1, 129.2, 128.6, 128.4, 127.9, 126.3, 120.0, 114.8, 114.3, 55.4, 54.5, 39.1, 33.5, 30.9; **IR (Neat)**: 2923, 2854, 1596, 1499, 1247, 1174, 1034, 948, 826, 746, 697 cm^{-1}; **HRMS (ESI, Q-TOF)** m/z: $[M+H]^+$ calculated for $C_{24}H_{25}N_2O$ 357.1967, found 357.1961.

2.A.5. References

(1) (a) Nicolaou, K. C.; Rigol, S. *Angew. Chem., Int. Ed*. **2019**, *58*, 11206-11241. (b) Nicolaou, K. C. *Angew. Chem., Int. Ed*., **2013**, *52*, 131-146.

(2) (a) Reissig, H. -U.; Zimmer, R. *Chem. Rev*. **2003**, *103*, 1151-1196.

(3) (a) Schneider, T. F.; Kaschel, J.; Werz, D. B. *Angew. Chem., Int. Ed*. **2014**, *53*, 5504-5523. (b) Cavitt, M. A.; Phun, L. H.; France, S. *Chem. Soc. Rev*. **2014**, *43*, 804-818. (c) Petzold, M.; Jones,

P. G.; Werz, D. B. *Angew. Chem. Int. Ed.* **2019,** *58*, 6225-6229. (d) Garve, L. K. B.; Petzold, M.; Jones, P. G.; Werz, D. B. *Org. Lett.* **2016**, *18*, 3, 564-567.

(4) (a) Pirenne, V.; Muriel, B. Waser, J. *Chem. Rev.* **2021**, *121*, 227-263.

(5) (a) Pohlhaus, P. D.; Sanders, S. D.; Parsons, A. T.; Li, W.; Johnson, J. S. *J. Am. Chem. Soc.* **2008**, *130*, 8642–8650. (b) Xia, Y.; Liu, X.; Feng, X. *Angew. Chem., Int. Ed*. **2021**, *60*, 9192-9204. (c) Verma, K.; Banerjee, P. *Adv. Synth. Catal*. **2016**, *358*, 2053-2058.

(6) (a) Ghosh, A.; Dey, R.; Banerjee, P. *Chem. Commun.* **2021**, *57*, 5359-5373. (b) Pandey, A. K.; Ghosh, A.; Banerjee, P. *Isr. J. Chem*, **2016**, *56*, 512-521.

(7) Singh, P.; Varshnaya, R. K.; Dey, R.; Banerjee, P. *Adv. Synth. Catal*. **2020**, *362*, 1447-1484.

(8) (a) Sparr, C.; Gilmour, R. *Angew. Chem. Int. Ed*. **2011**, *50*, 8391-8395. (b) Wallbaum, J.; Garve, L. K. B.; Jones, P. G.; Werz, D. B. *Chem. Eur. J.* **2016**, *22*, 18756-18759. (c) E.; Reyes, E.; Uria, U.; Carrillo, L.; Tejero, T.; Merino, P.; Vicario, J. L. *Chem. Eur. J*. **2018**, *24*, 8764–8768. (d) Li, L.; Li, Z.; Wang, Q. *Synlett.* **2009**, *11*, 1830–1834.

(9) Halskov, K. S.; Kniep, F.; Lauridsen, V. H.; Iversen, E. H.; Donslund, B. S.; Jørgensen, K. A. *J. Am. Chem. Soc.* **2015**, *137*, 1685-169.

(10) Diez, E. S.; Vesga, D. L.; Reyes, E.; Uria, U.; Carrillo, L.; Vicario, J. L. *Org. Lett*. **2016**, *18*, 1270-1273.

(11) (a) Hayashi, Y.; Gotoh, H.; Hayashi, T.; Shoji, M. *Angew. Chem. Int. Ed*. **2005**, *44*, 4212-4215. For reviews on diarylprolinol ethers as organocatalysts, see: (b) Donslund, B. S.; Johansen, T. K.; Poulsen, P. H.; Halskov, K. S.; Jørgensen, K. A. *Angew. Chem. Int. Ed*. **2015**, *54*, 13860-13874.

(12) Hong, L.; Sun, W.; Yang, D.; Li, G.; Wang, R. *Chem. Rev*. **2016**, *116*, 4006-4123.

(13) (a) Dey, R.; Banerjee, P. *Adv. Synth. Catal*. **2019**, *361*, 2849-2854. (b) Dey, R.; Rajput, S.; Banerjee, P. *Tetrahedron*. **2020**, *76(15)*, 131080.

(14) Arai, I., Mori, A., Yamamoto, H. *J. Am. Chem. Soc.* **1985**, *107*, 8254-8256.

(15) (a) Faber, K.; Griengl, H.; Steinreiber, J. *Chem. Eur. J.* **2008**, *14*, 8060–8072. (b) Faber, K. *Chem. Eur. J*. **2001**, *7*, 5004-5010.

(16) (a) Ito, H.; Kunii, S.; Sawamura, M. *Nat. Chem.* **2010**, *2*, 972–976. (b) Bartoszewicz, A.; Matier, C. D.; Fu, G. C. *J. Am. Chem. Soc.* **2019**, *141*, 14864-14869.

(17) (a) Blackmond, D. G. *Acc. Chem. Res*. **2000**, *33*, 402-411.

(18) (a) Huerta, F. F.; Minidis, A. B. E.; Bäckvall, J.-E. *Chem. Soc. Rev.* **2001**, *30*, 321–331; (b) Zhou, H.; Properzi, R.; Leutzsch, M.; Belanzoni, P.; Bistoni, G.; Tsuji, N.; Han, J. T.; Zhu, C.; List, B. *J. Am. Chem. Soc.* **2023**, *145*, 9, 4994–5000.

(19) (a) Smolobochkin, A. V.; Melyashova, A. S.; Voronina, J. K.; Strelnik, A. G.; Vatsadze, S. Z.; Burilov, A. R.; Pudovik, M. A.; Fedorova, O. A.; Sinyashina, O. G.; Gazizov, A. S. *RSC Adv*., **2017**, *7*, 50955–50960. (b) Wu, C.; Wan, J.; Song, C.; He, L.; Liu, H.; Li, X.; Li, J.; Hu, X.-G.; Xiao, H.-P.; Jiang, J. *Org. Biomol. Chem.* **2022**, *20*, 122–126.

(20) (a) P. Kumar, R. Dey, P. Banerjee, *Org. Lett*. **2018**, *20*, 5163; (b) R. Dey, P. Kumar, P. Banerjee, *J. Org. Chem*. **2018**, *83*, 5438.

(21) (a) Z. Tan, S. Zhang, Y. Zhang, Y. Li, M. Ni, B. Feng, J. Org. Chem. **2017**, 82, 9384; (b) M. Mishra, P. B. De, S. Pradhan, T. Punniyamurthy, *J. Org. Chem.* **2019**, *84*, 10901-10910; (c) D. Hong, X. Lin, Y. Zhu, M. Lei, Y. Wang, *Org. Lett.*, **2009**, *11*, *24*, 5678-5681; (d) A. K. Chakraborti, S. Bhagat, S. Rudrawar, *Tetrahedron Lett*., **2004**, *45*, 7641–7644; (e) X.-H. Zhang, H.-Q. Kang, Y.-Y. Tao, Y.-H. Li, J.-R. Zhao, Y.-Gao, L.-Y. Ma, H.-M. Liu; Eur. J. Med. Chem., **2021**, *218*, 113392; (f) A. Bamoniri, B. B. F. Mirjalili, N. Moshtael-Arani, *J. Mol. Catal. A Chem.*, **2014**, *393*, 272–278; (g) Z. Chen, H. Li, W. Dong, M. Miao, H. Ren, *Org. Lett.*, **2016**, *18*, 1334-1337; (h) G. Brahmachari, I. Karmakar, *Eur. J. Org. Chem.* **2019**, 5925–5933; (i) S. Xiaonan, T. Miaomiao, W. Muhua, Z. Xinying, F. Xuesen, *Chin. J. Org. Chem.* **2019**, *39*, 1630-1641; (j) M. Zhang, Z.-R. Shang, X.-T. Li, J.-N. Zhang, Y. Wang, K. Li, Y.-Y. Li, Z.-H. Zhang, *Synth. Commun.*, **2016**, *47*, 178-187.

2.A.6 NMR and FTIR spectra of compounds

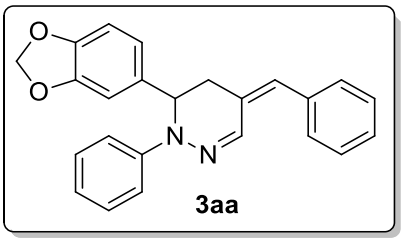

3aa

^{1}H-NMR ($CDCl_3$, 400MHz) of 3aa

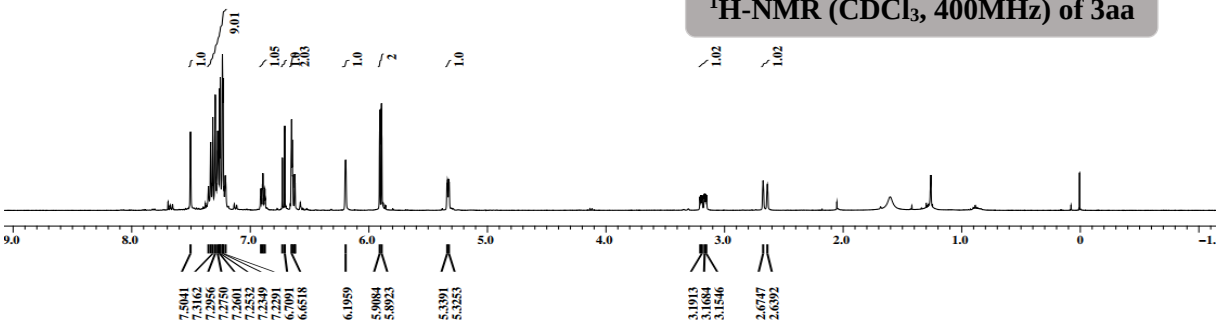

^{13}C-NMR ($CDCl_3$, 100MHz) of 3aa

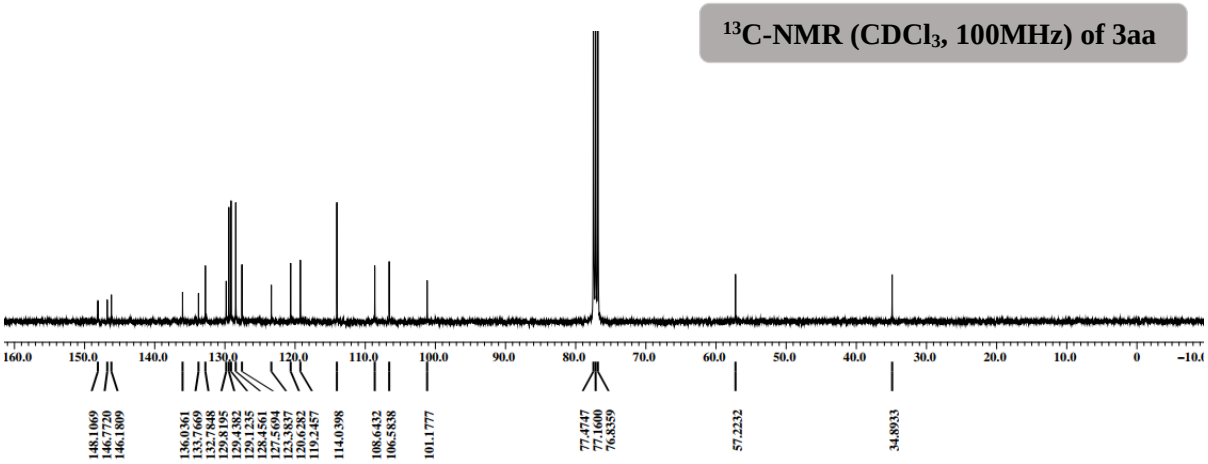

^{13}C DEPT ($CDCl_3$, 100MHz) of 3aa

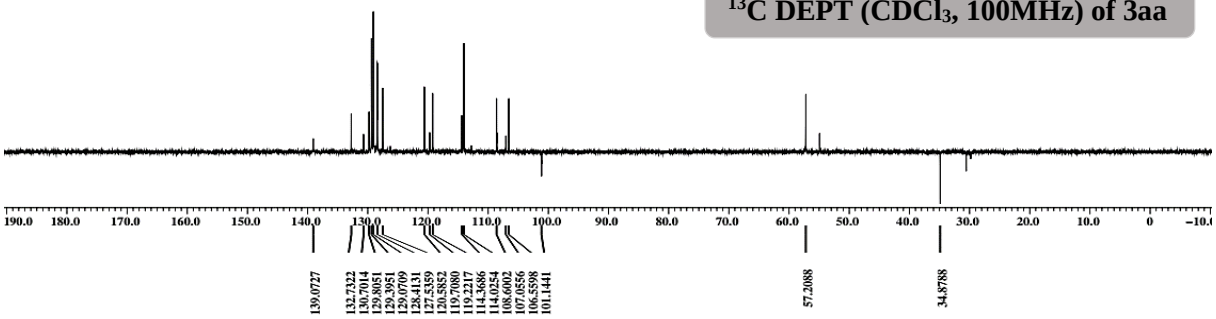

^{13}C DEPT, ^{1}H HETCOR NMR ($CDCl_3$, 100, 400 MHz) of 3aa

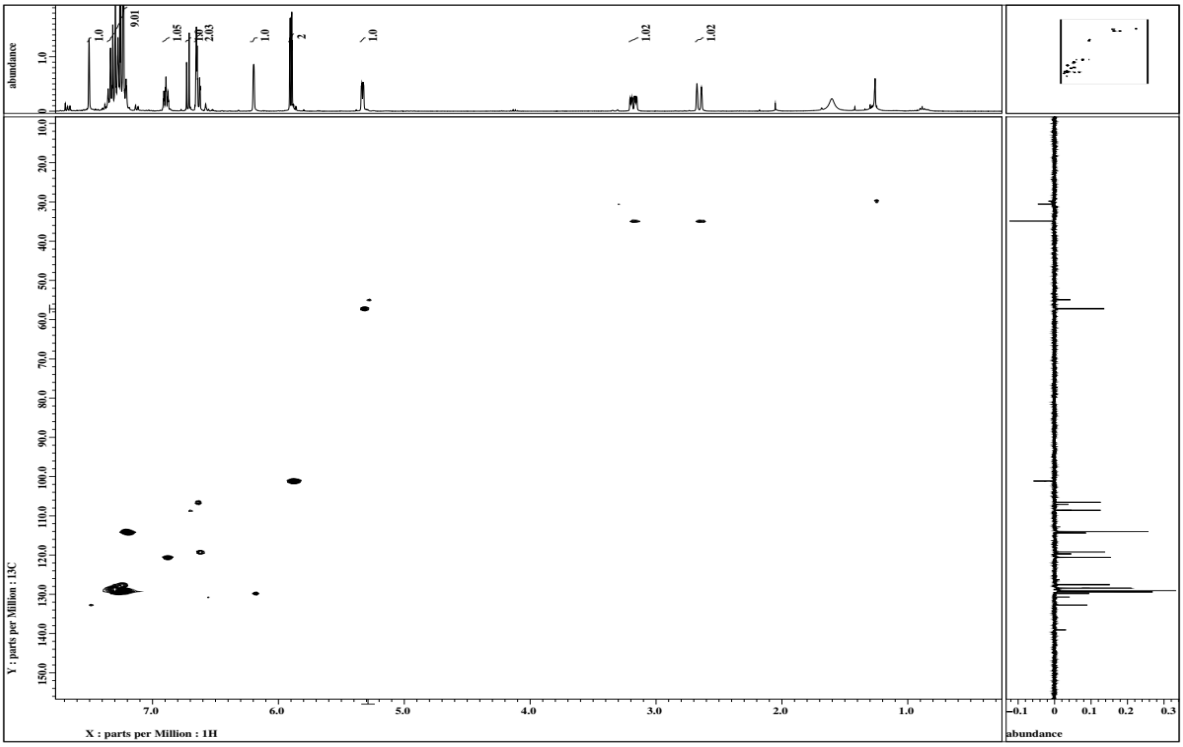

^{1}H COSY ($CDCl_3$, 400MHz) of 3aa

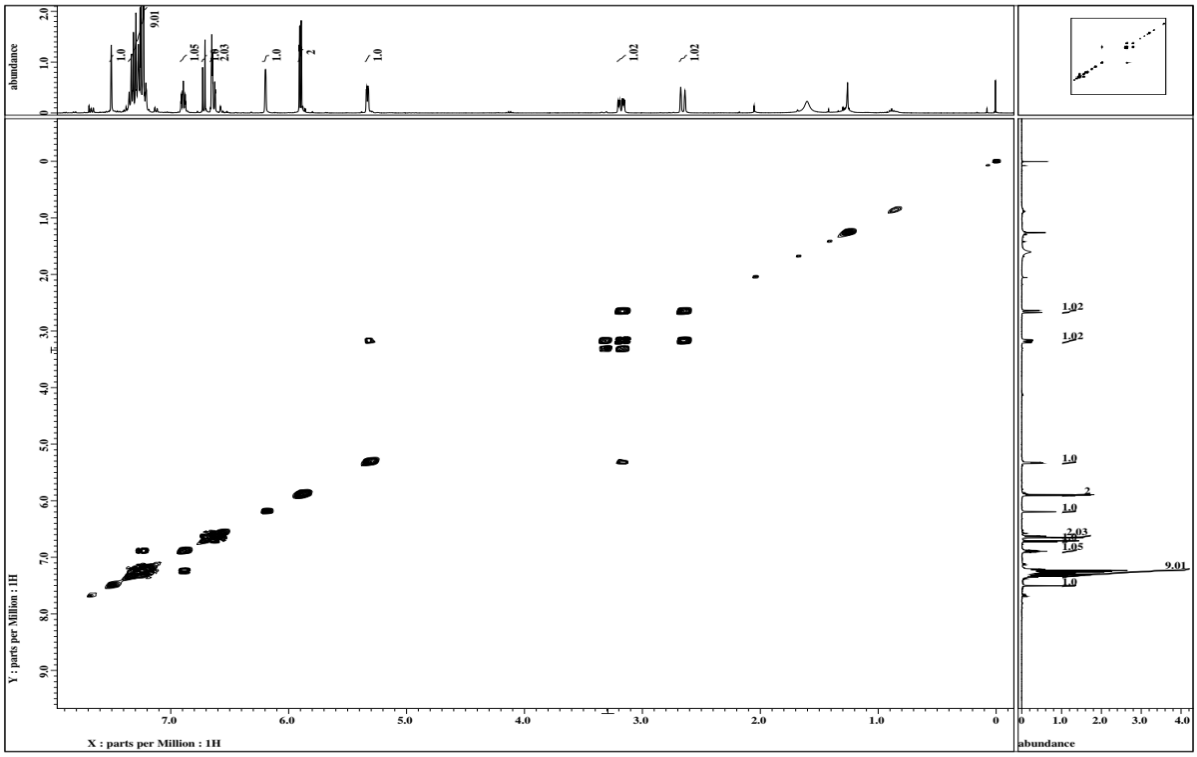

^{1}H-NOE ($CDCl_3$, 400MHz) of 3aa

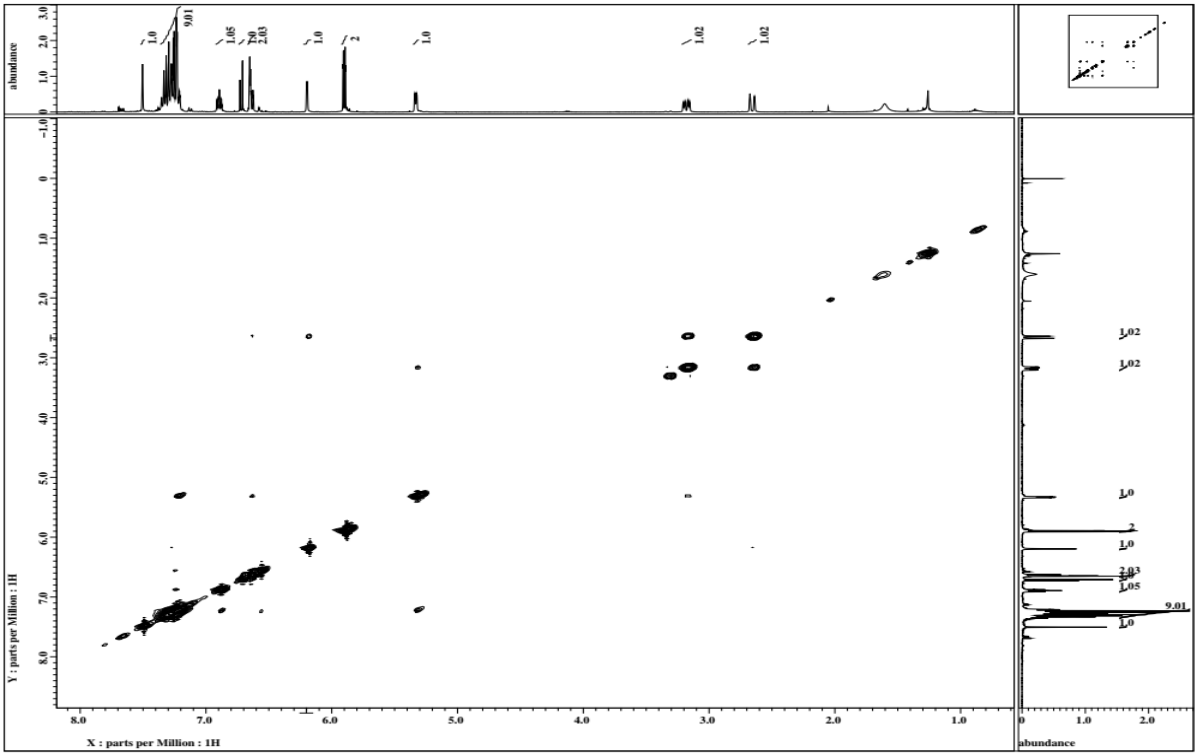

FTIR of 3aa

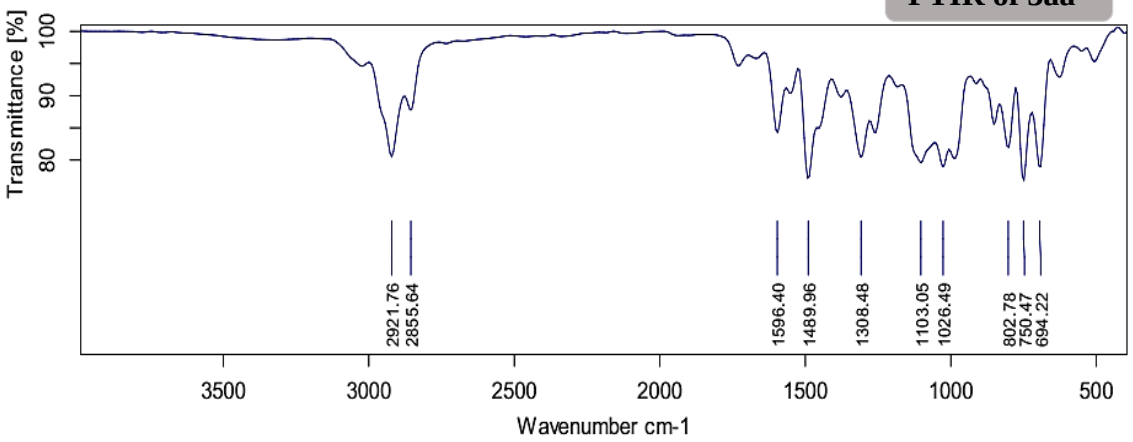

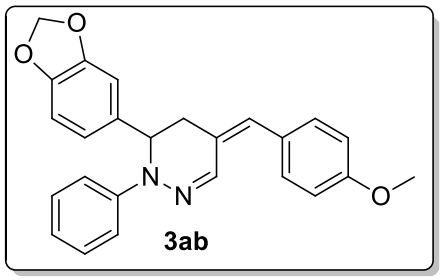

3ab

^{1}H-NMR ($CDCl_3$, 400MHz) of 3ab

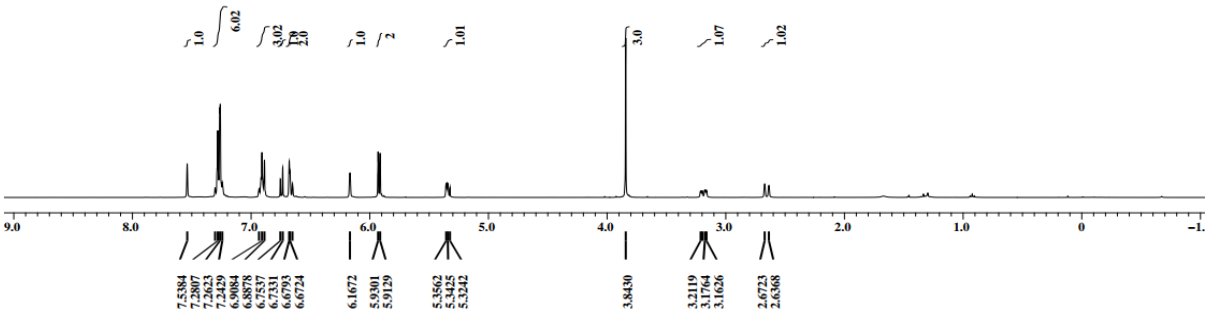

^{13}C-NMR ($CDCl_3$, 100MHz) of 3ab

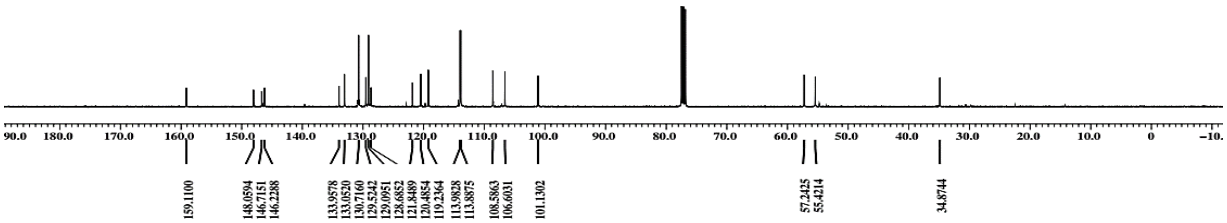

^{13}C DEPT ($CDCl_3$, 100MHz) of 3ab

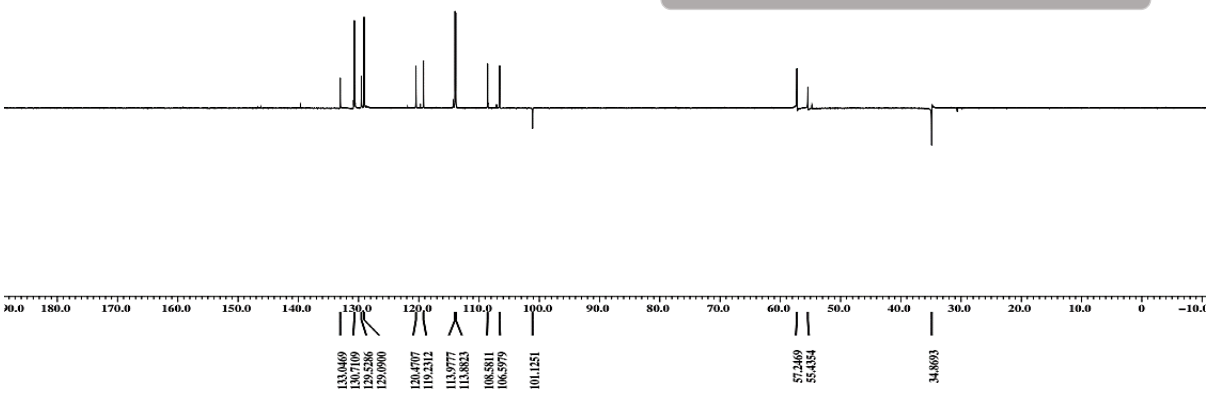

FTIR of 3ab

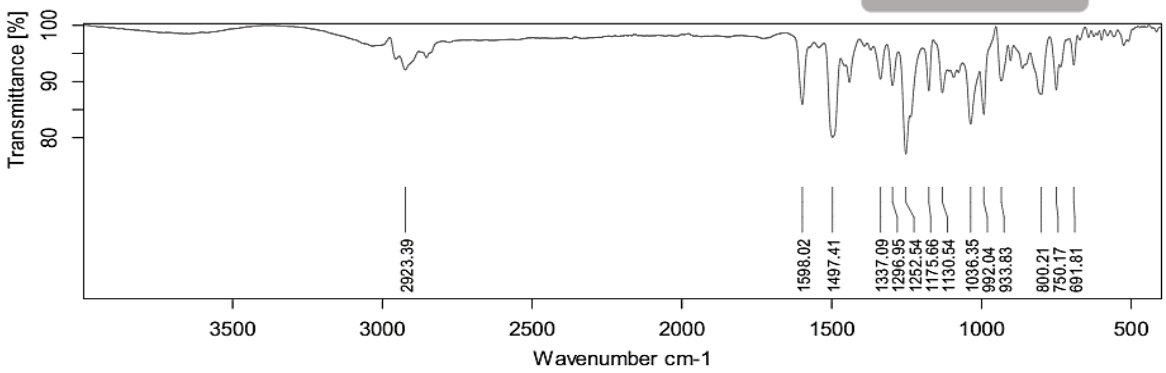

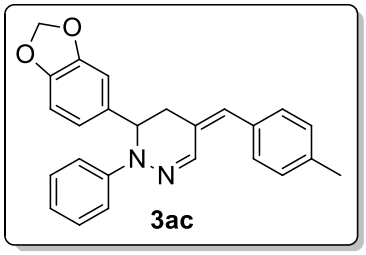

^{1}H-NMR ($CDCl_3$, 400MHz) of 3ac

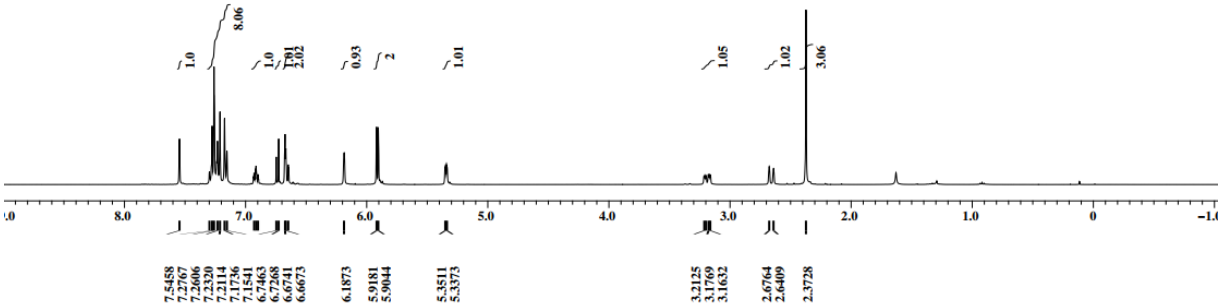

^{13}C-NMR ($CDCl_3$, 100MHz) of 3ac

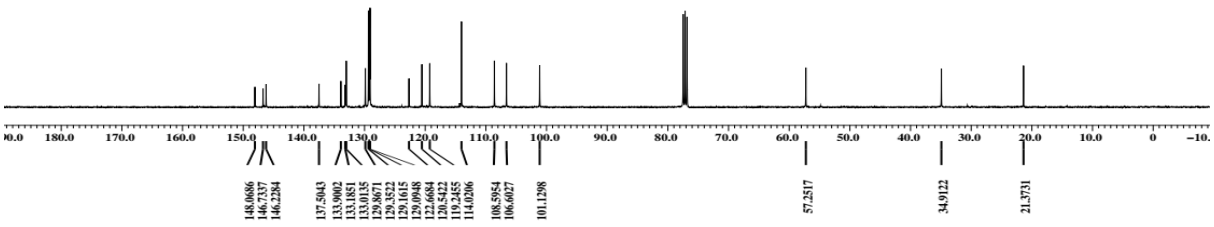

^{13}C DEPT ($CDCl_3$, 100MHz) of 3ac

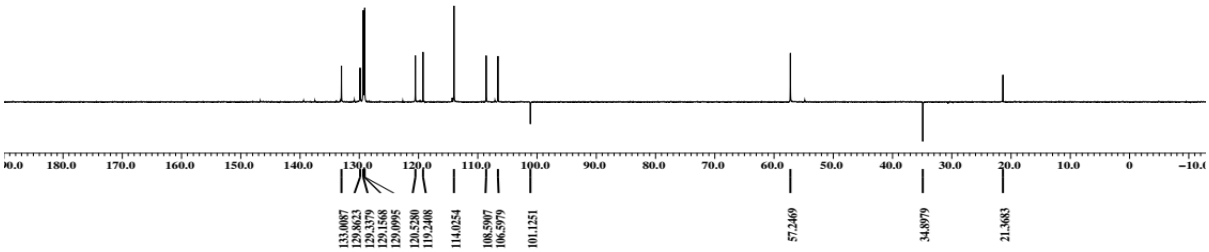

FTIR of 3ac

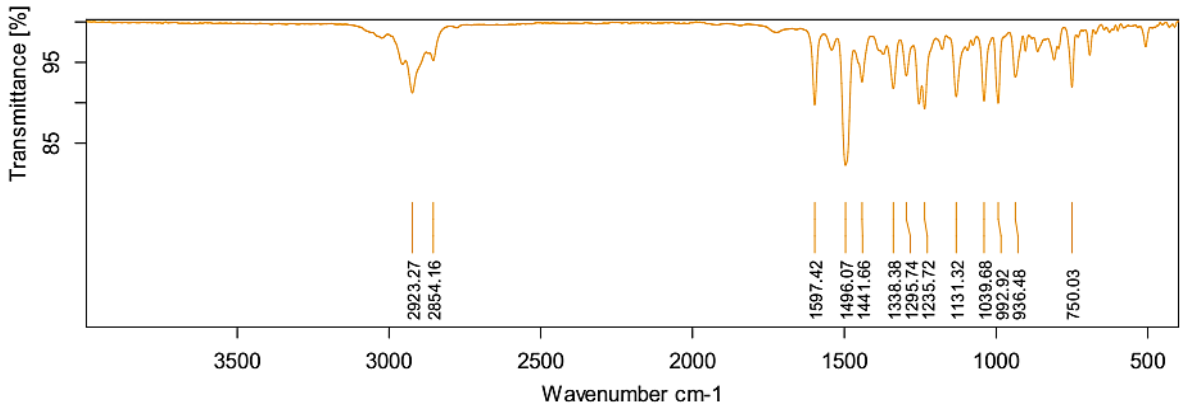

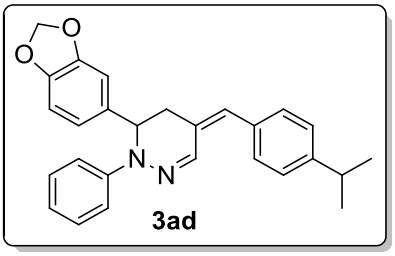

^{1}H-NMR ($CDCl_3$, 400MHz) of 3ad

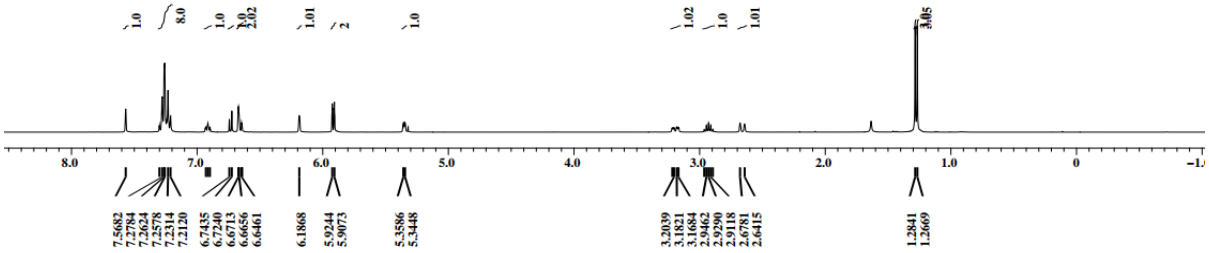

^{13}C-NMR ($CDCl_3$, 100MHz) of 3ad

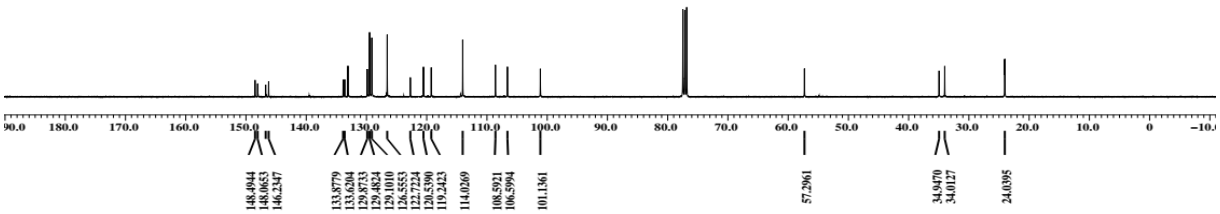

^{13}C DEPT ($CDCl_3$, 100MHz) of 3ad

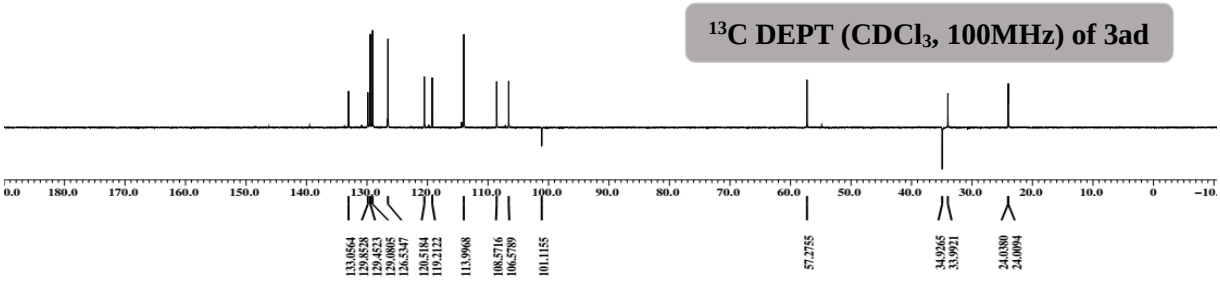

FTIR of 3ad

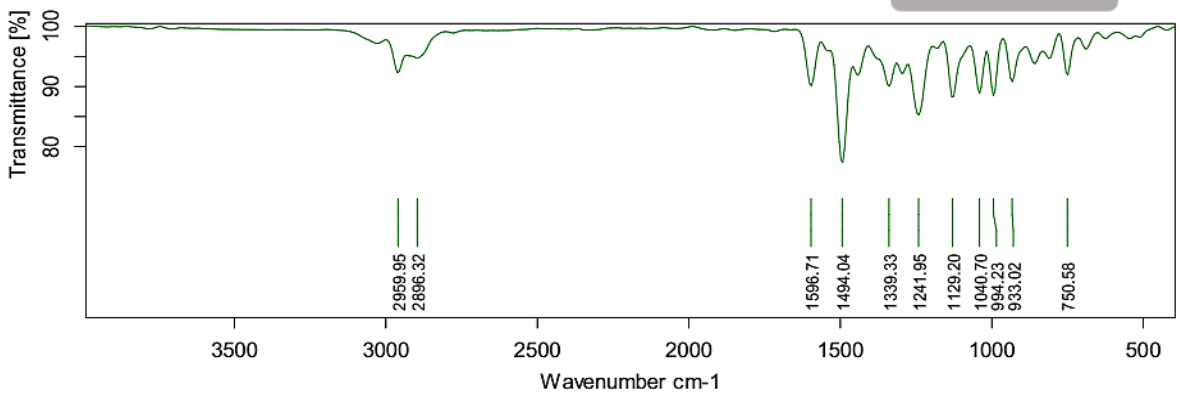

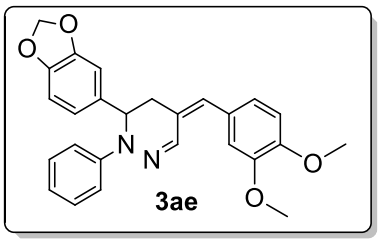

^{1}H-NMR ($CDCl_3$, 400MHz) of 3ae

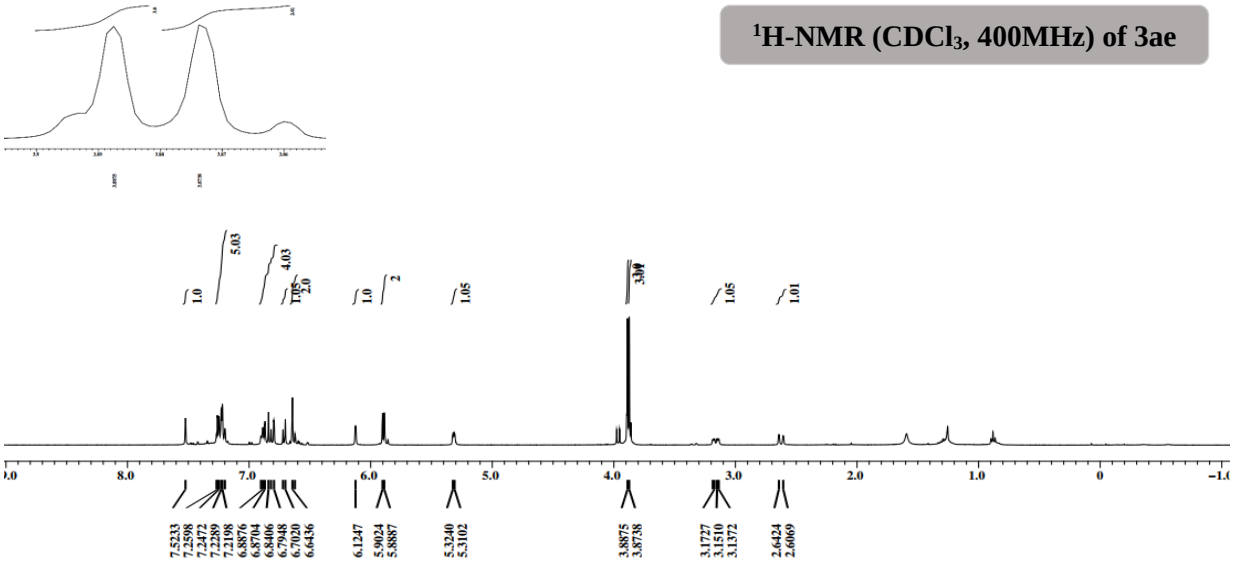

^{13}C-NMR ($CDCl_3$, 100MHz) of 3ae

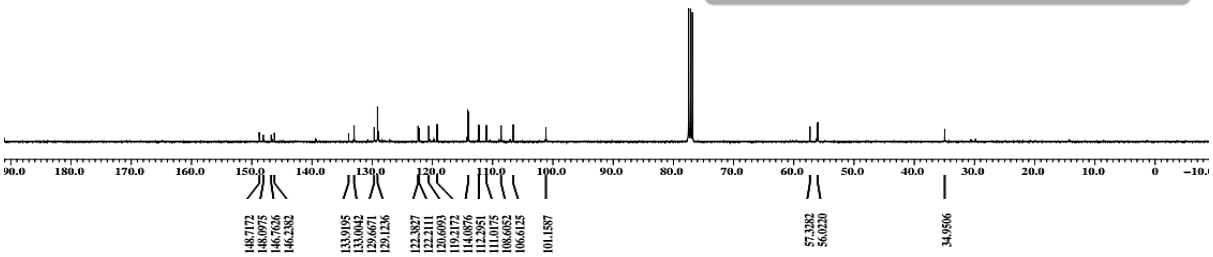

^{13}C DEPT ($CDCl_3$, 100MHz) of 3ae

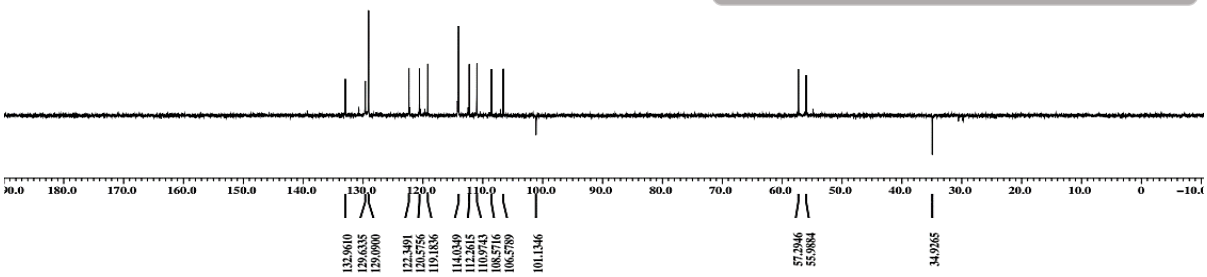

FTIR of 3ae

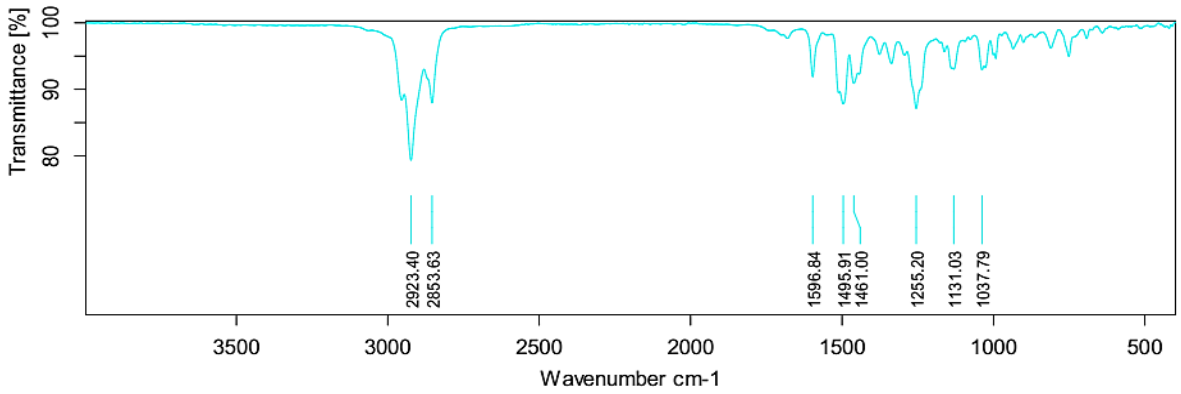

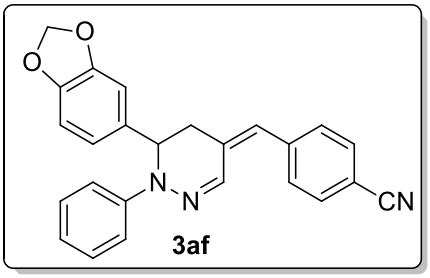

3af

^{1}H-NMR ($CDCl_3$, 400MHz) of 3af

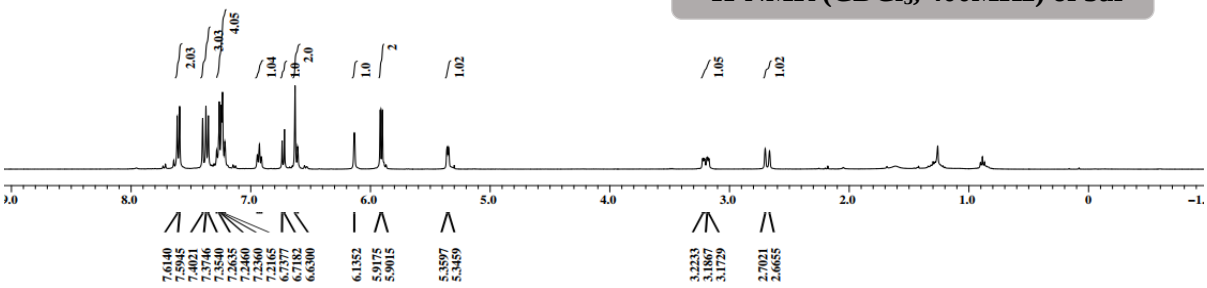

^{13}C-NMR ($CDCl_3$, 100MHz) of 3af

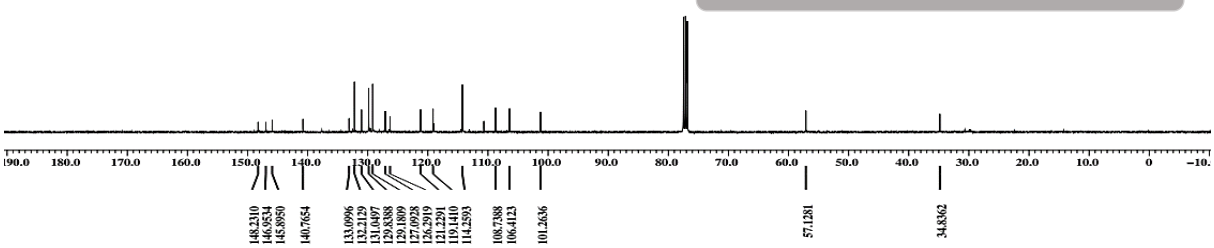

^{13}C DEPT ($CDCl_3$, 100MHz) of 3af

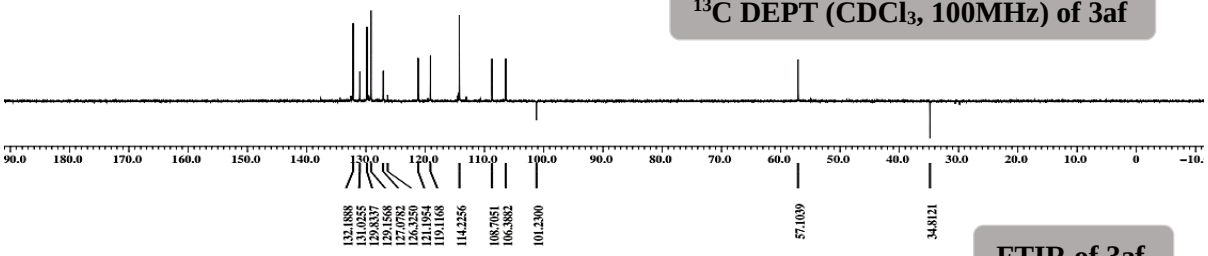

FTIR of 3af

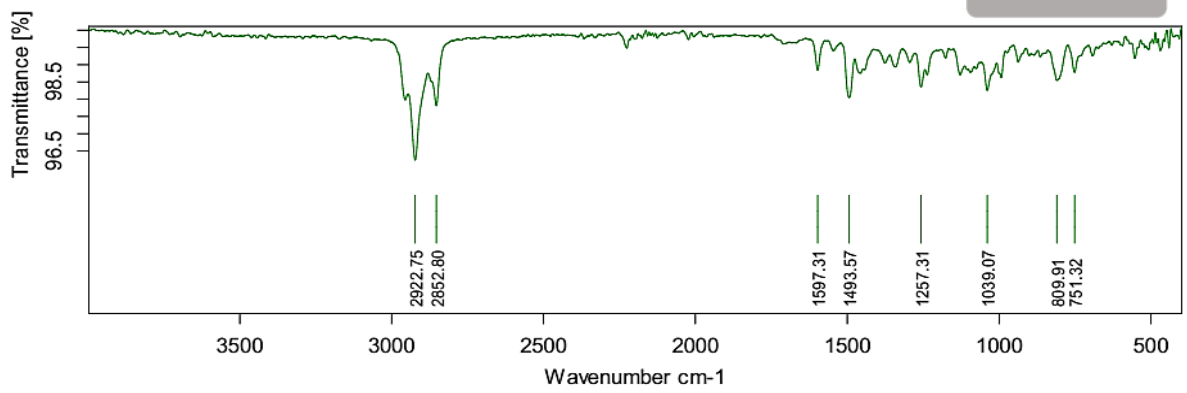

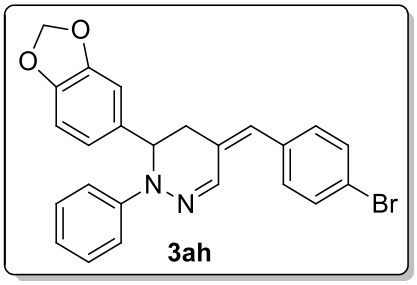

3ah

^{1}H-NMR ($CDCl_3$, 400MHz) of 3ah

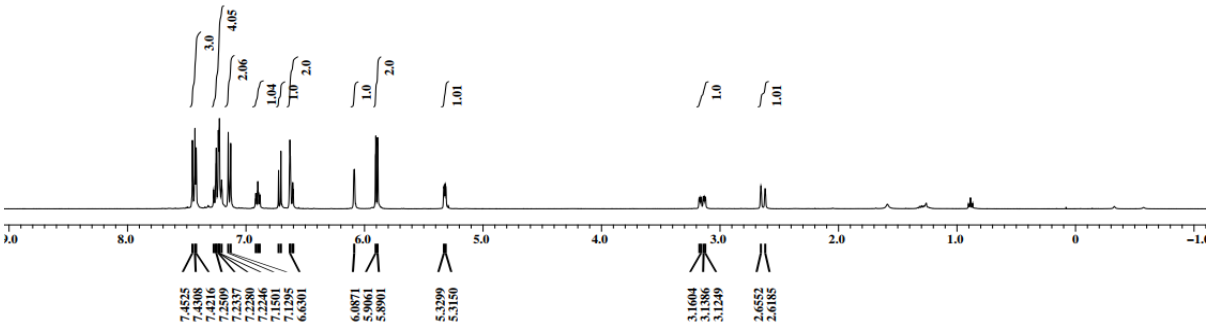

^{13}C-NMR ($CDCl_3$, 100MHz) of 3ah

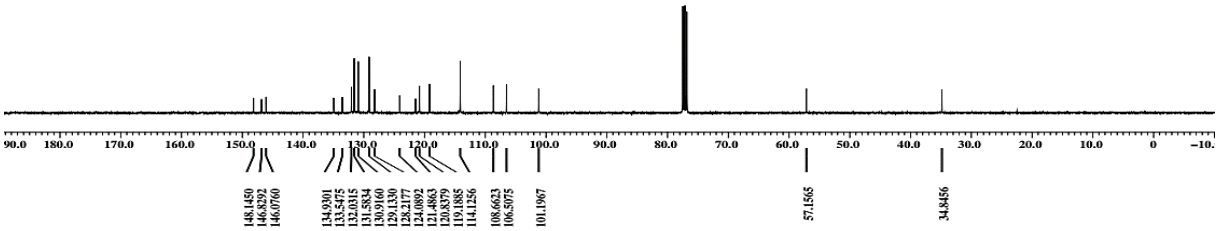

^{13}C DEPT ($CDCl_3$, 100MHz) of 3ah

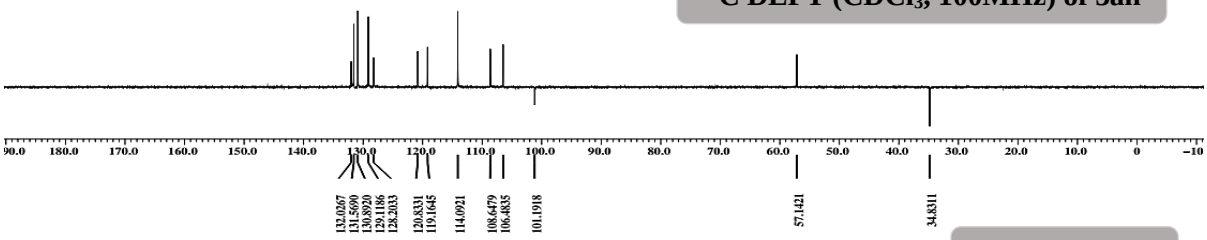

FTIR of 3ah

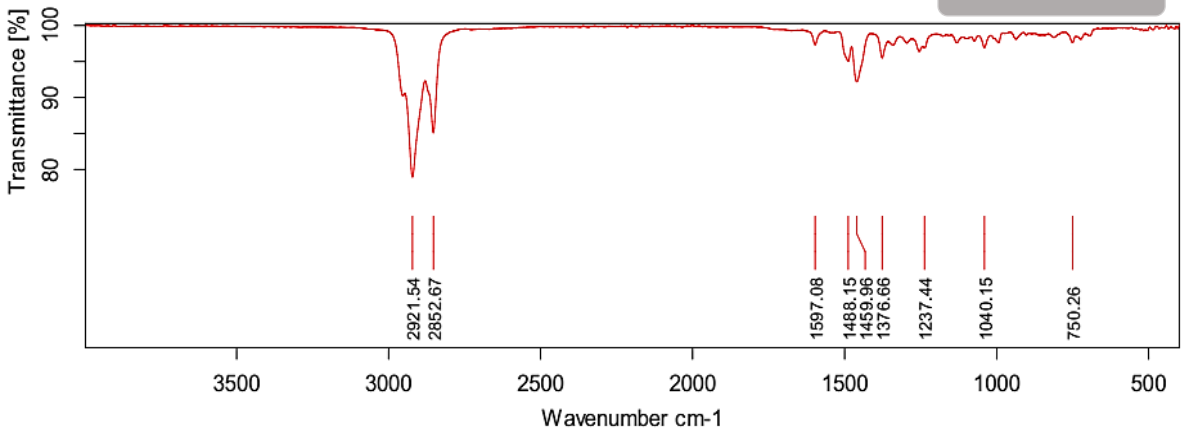

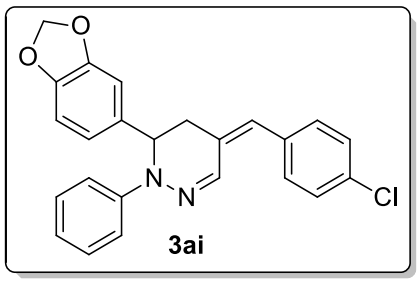

3ai

^{1}H-NMR ($CDCl_3$, 400MHz) of 3ai

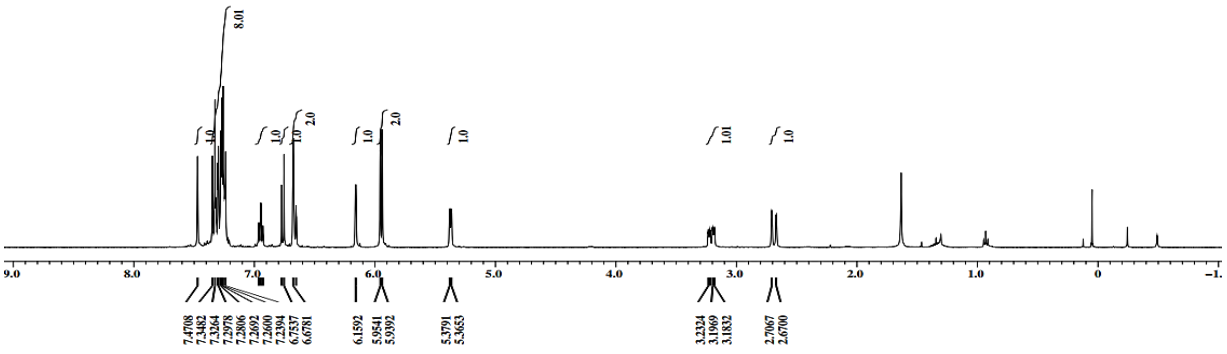

^{13}C-NMR ($CDCl_3$, 100MHz) of 3ai

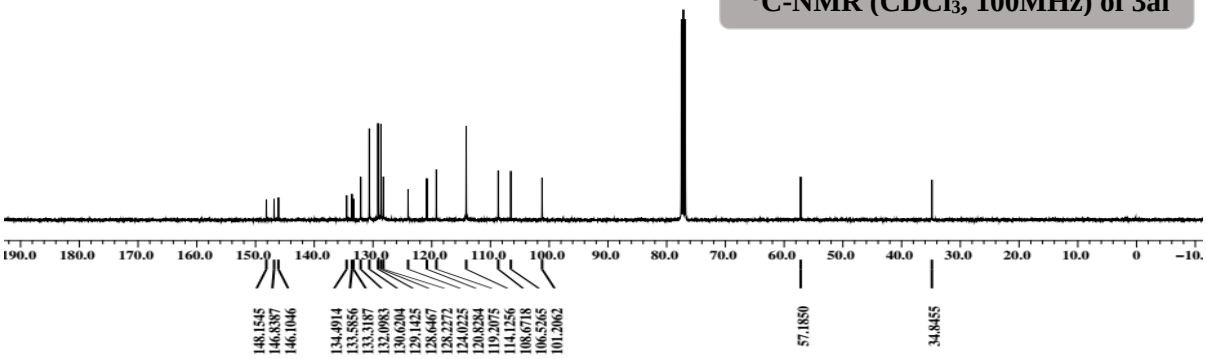

^{13}C DEPT ($CDCl_3$, 100MHz) of 3ai

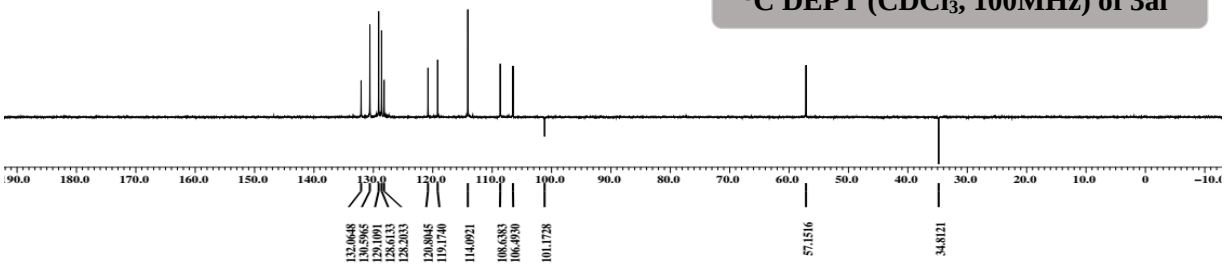

FTIR of 3ai

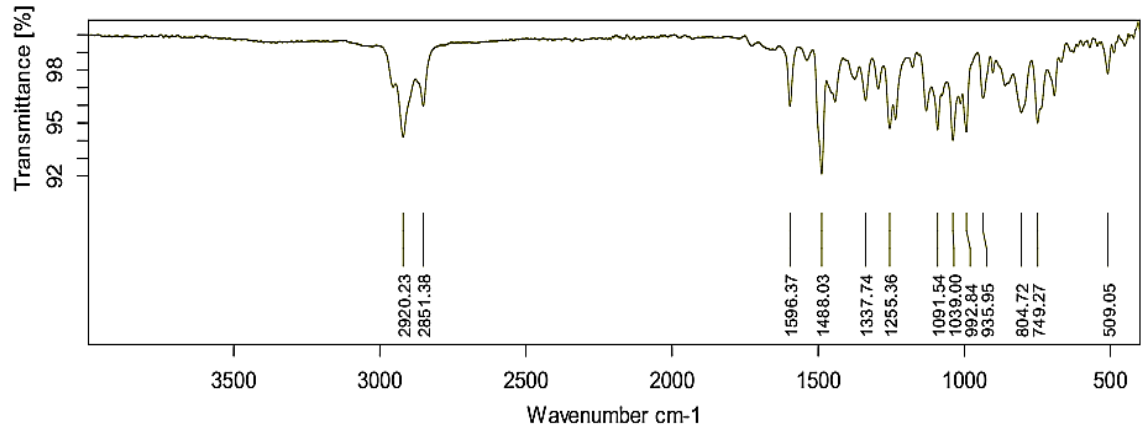

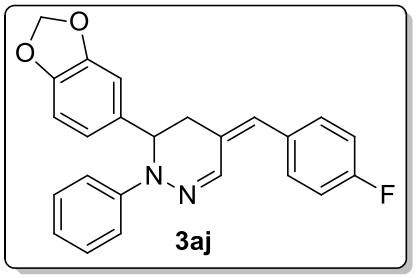

3aj

^{1}H-NMR ($CDCl_3$, 400MHz) of 3aj

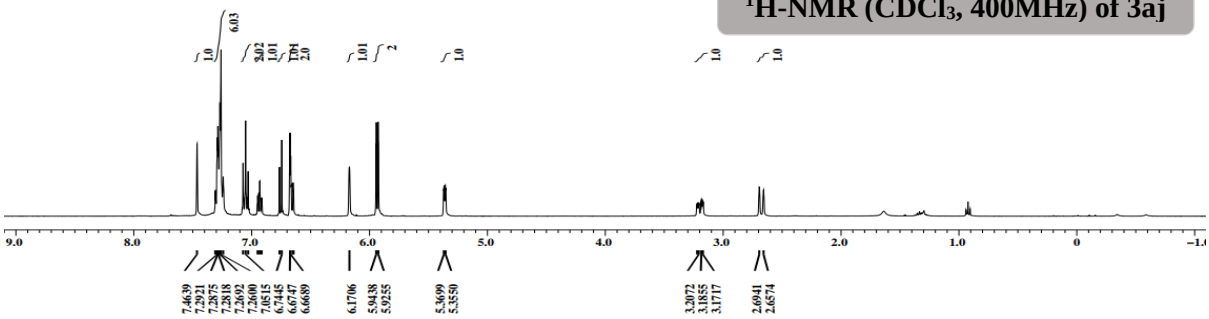

^{13}C-NMR ($CDCl_3$, 100MHz) of 3aj

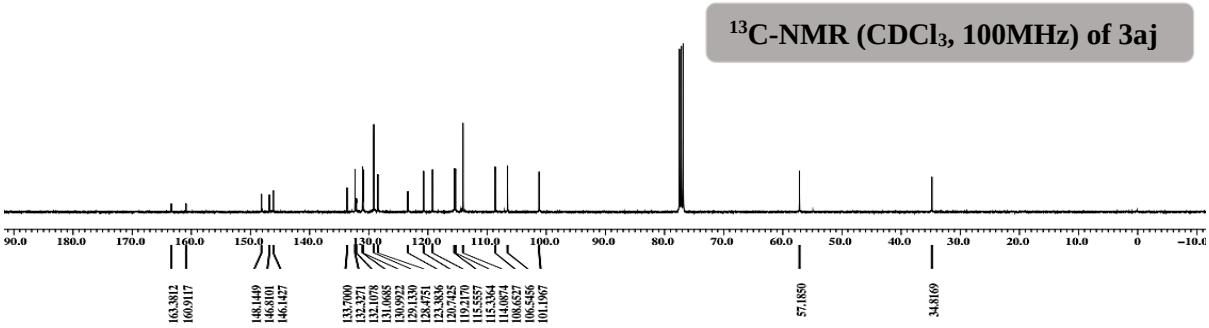

^{13}C DEPT ($CDCl_3$, 100MHz) of 3aj

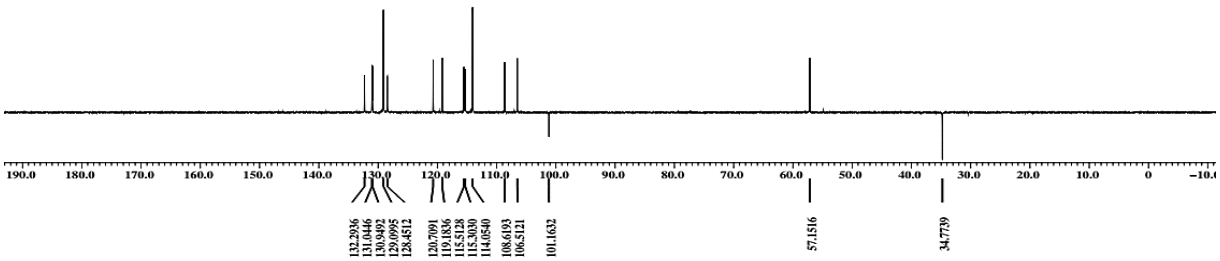

FTIR of 3aj

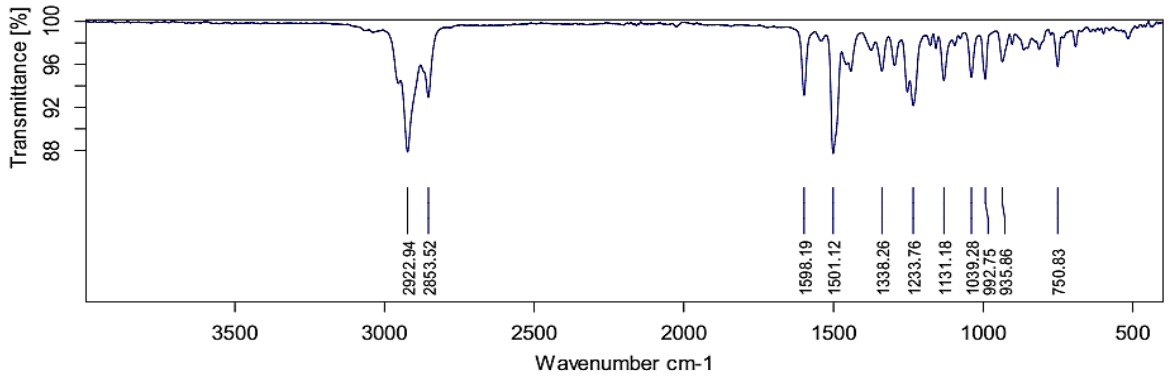

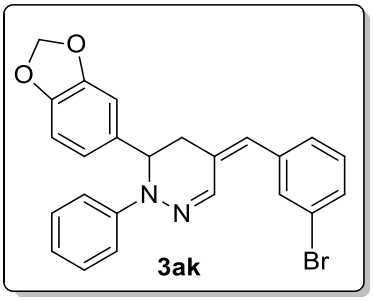

3ak

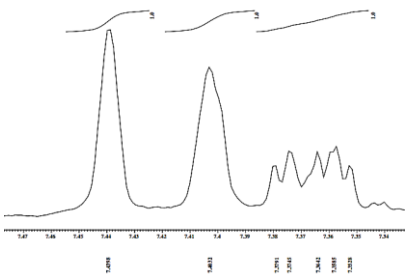

^{1}H-NMR ($CDCl_3$, 400MHz) of 3ak

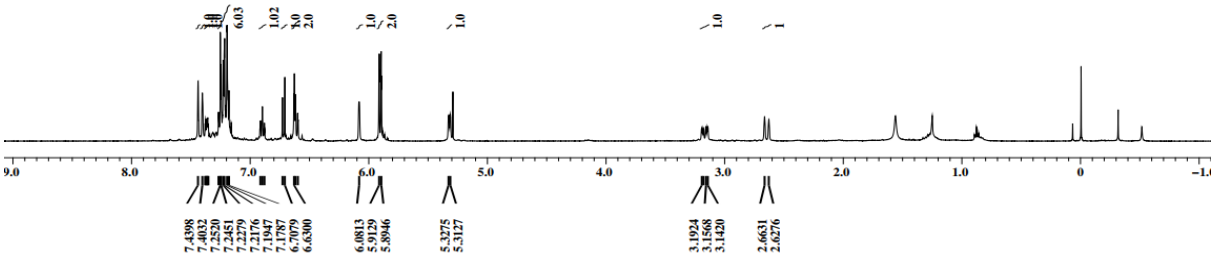

^{13}C-NMR ($CDCl_3$, 100MHz) of 3ak

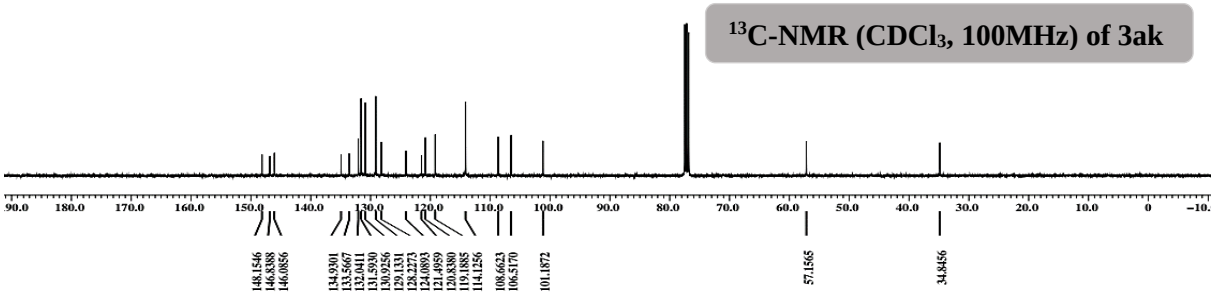

^{13}C DEPT ($CDCl_3$, 100MHz) of 3ak

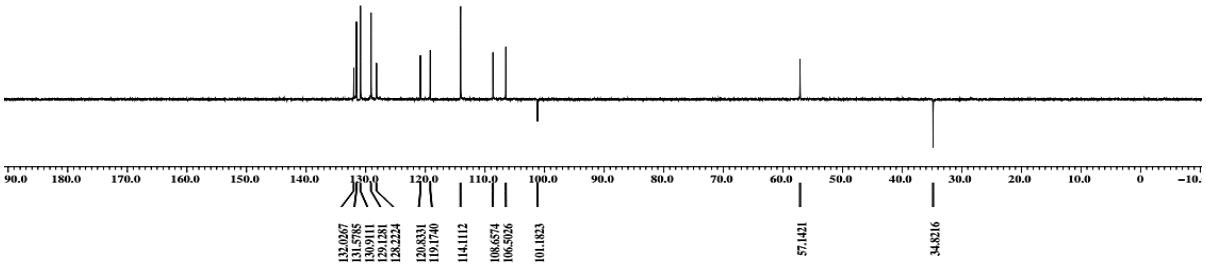

FTIR of 3ak

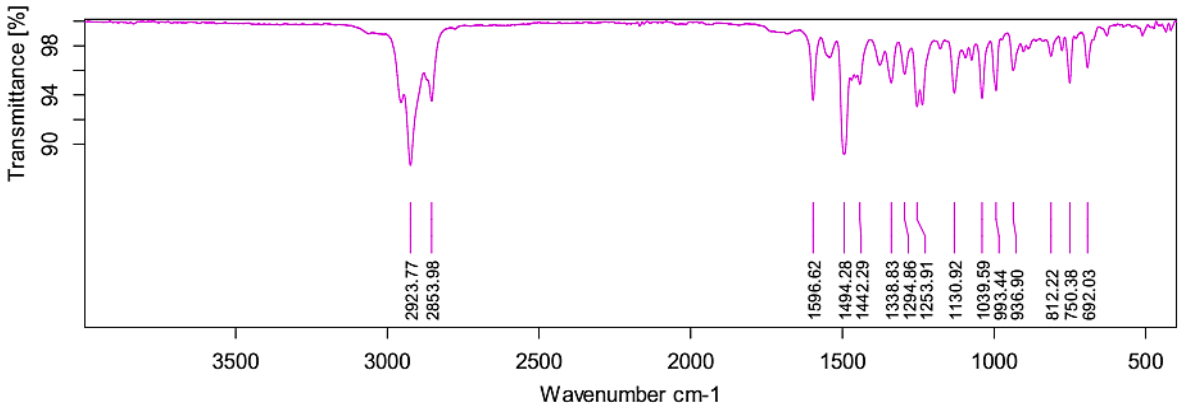

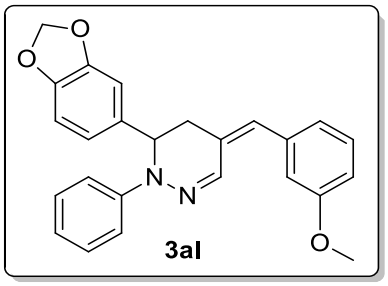

^{1}H-NMR ($CDCl_3$, 400MHz) of 3al

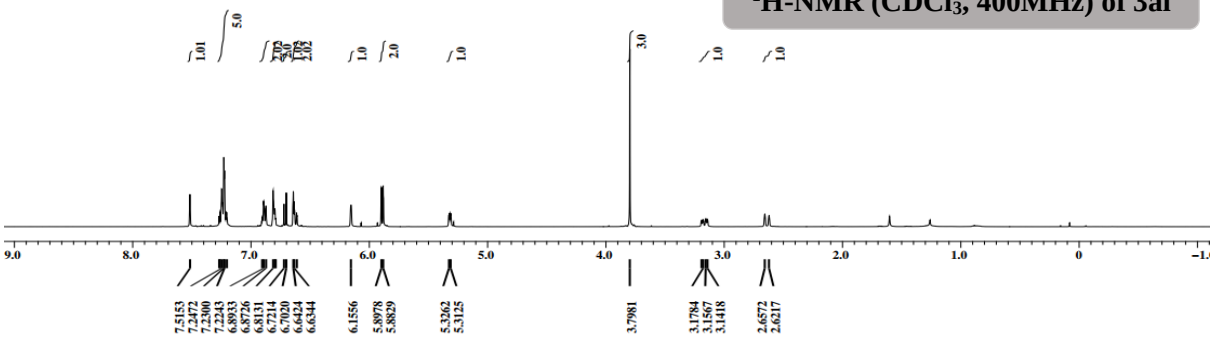

^{13}C-NMR ($CDCl_3$, 100MHz) of 3al

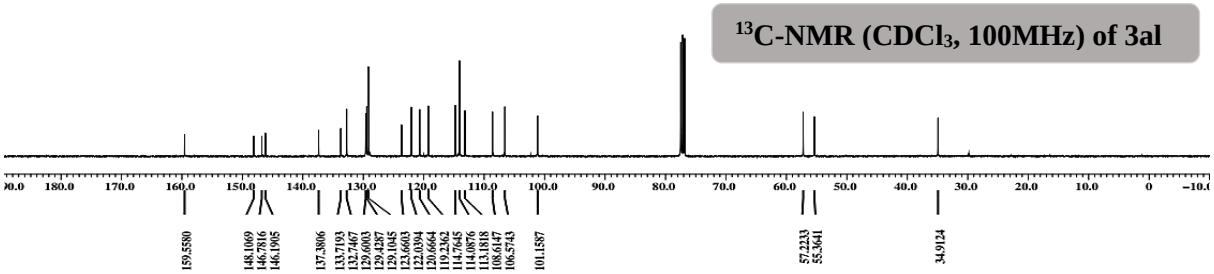

^{13}C DEPT ($CDCl_3$, 100MHz) of 3al

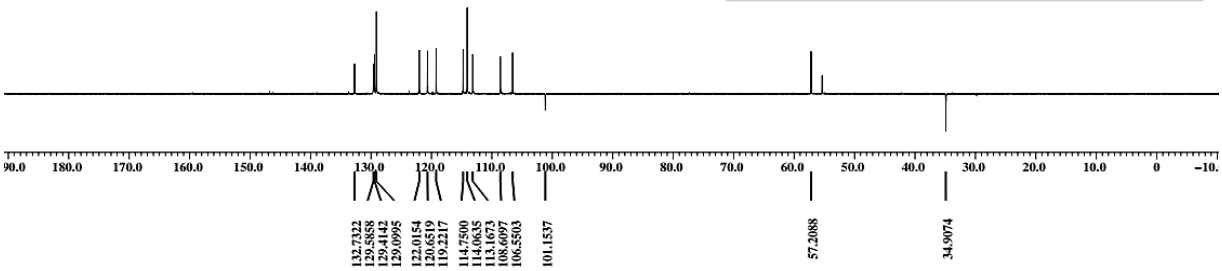

FTIR of 3al

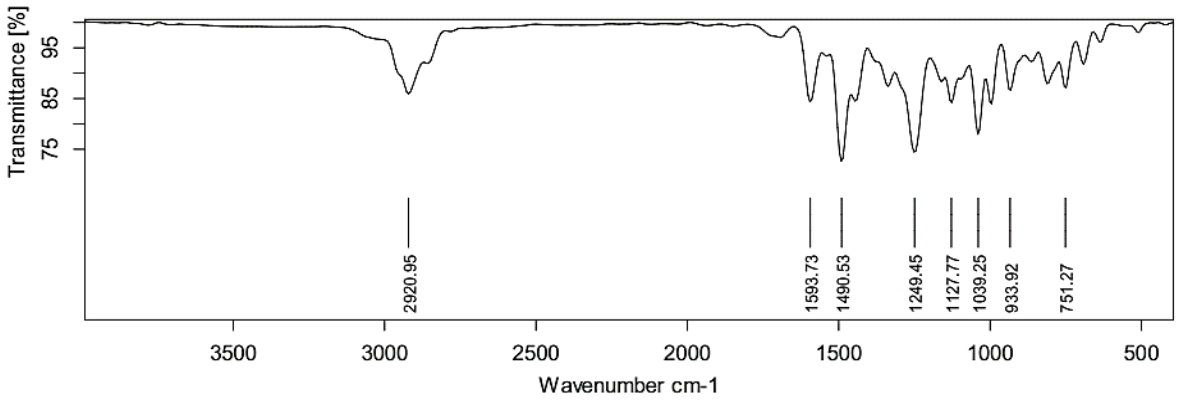

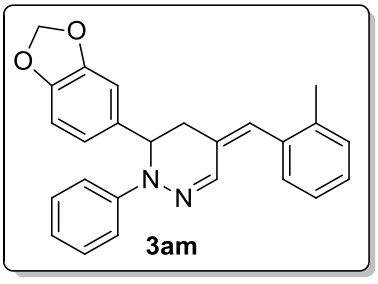

3am

^{1}H-NMR ($CDCl_3$, 400MHz) of 3am

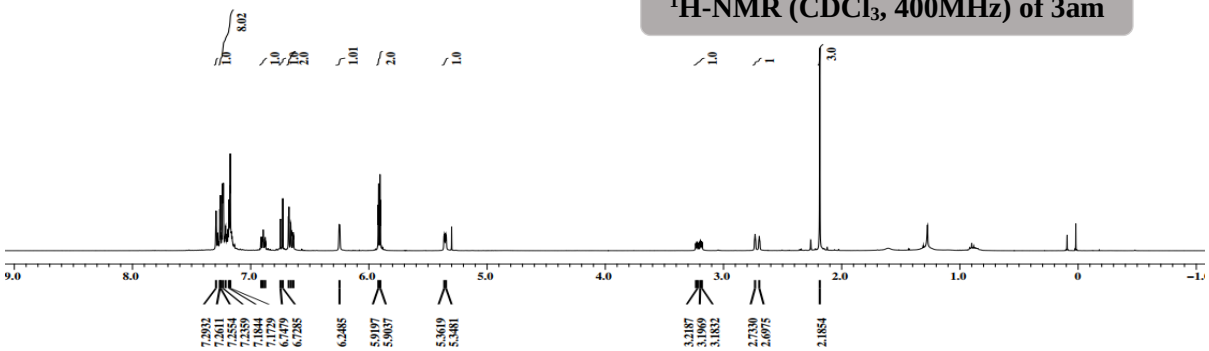

^{13}C-NMR ($CDCl_3$, 100MHz) of 3am

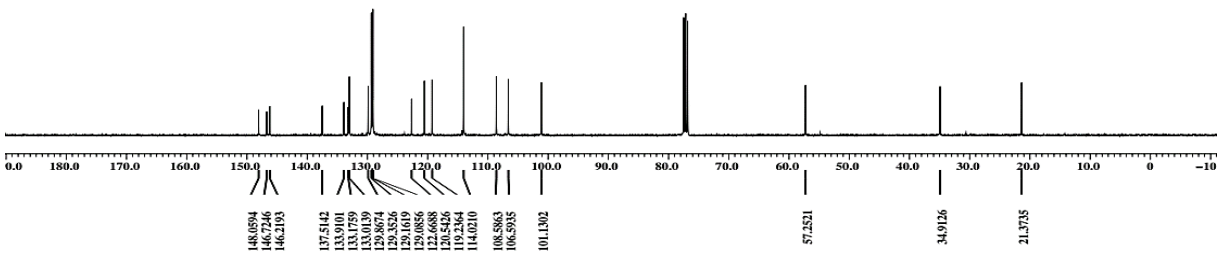

^{13}C DEPT ($CDCl_3$, 100MHz) of 3am

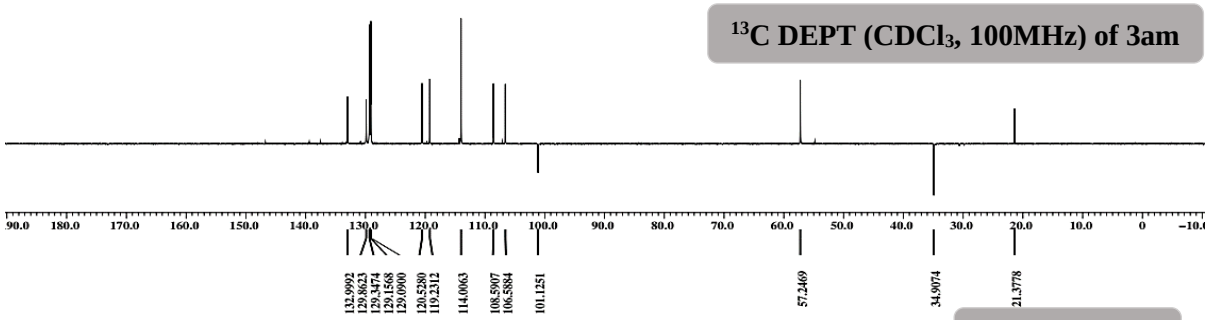

FTIR of 3am

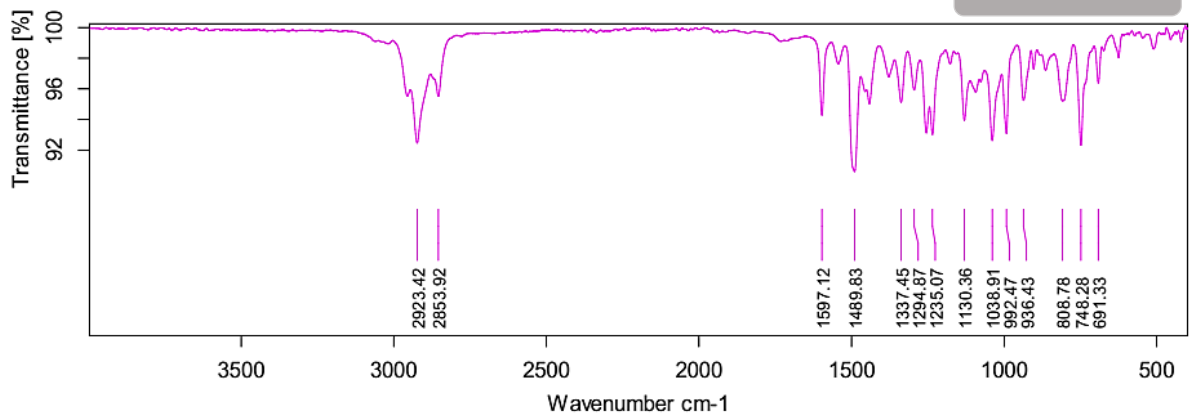

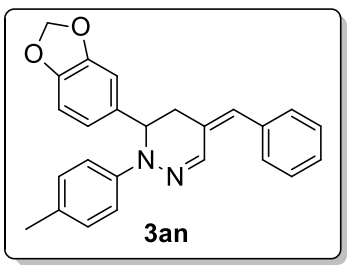

3an

^{1}H-NMR ($CDCl_3$, 400MHz) of 3an

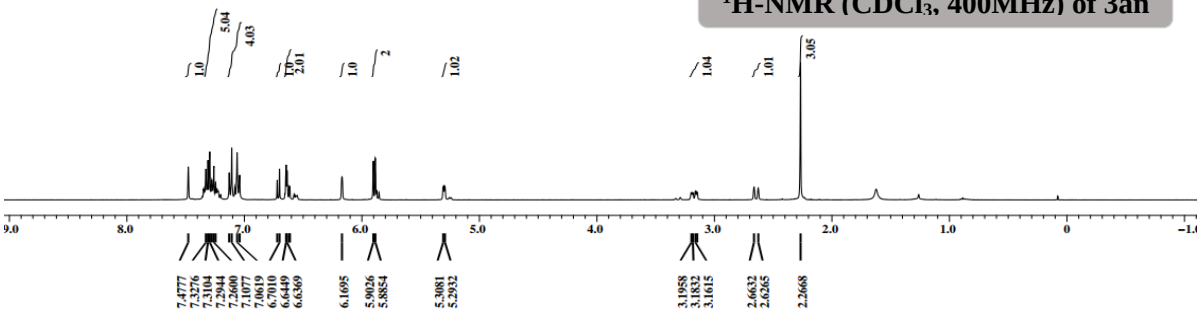

^{13}C-NMR ($CDCl_3$, 100MHz) of 3an

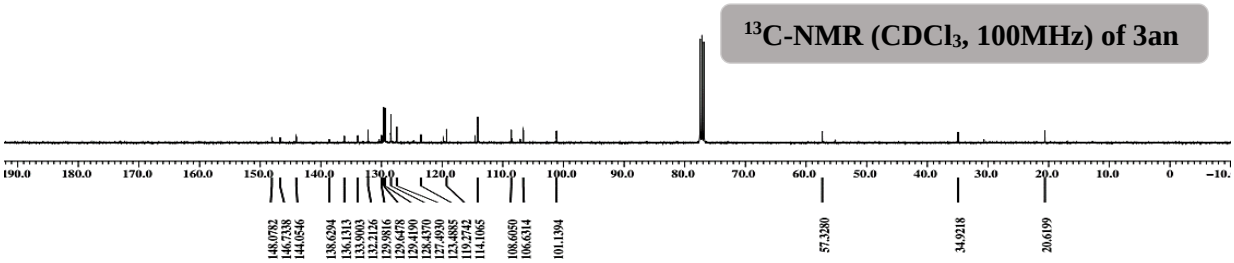

^{13}C DEPT ($CDCl_3$, 100MHz) of 3an

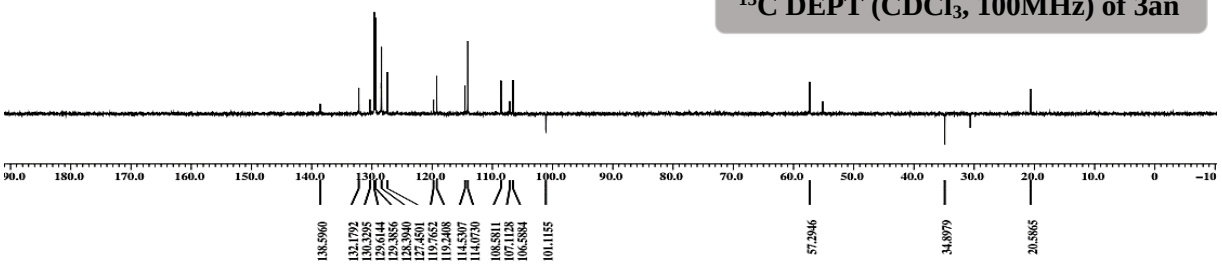

FTIR of 3an

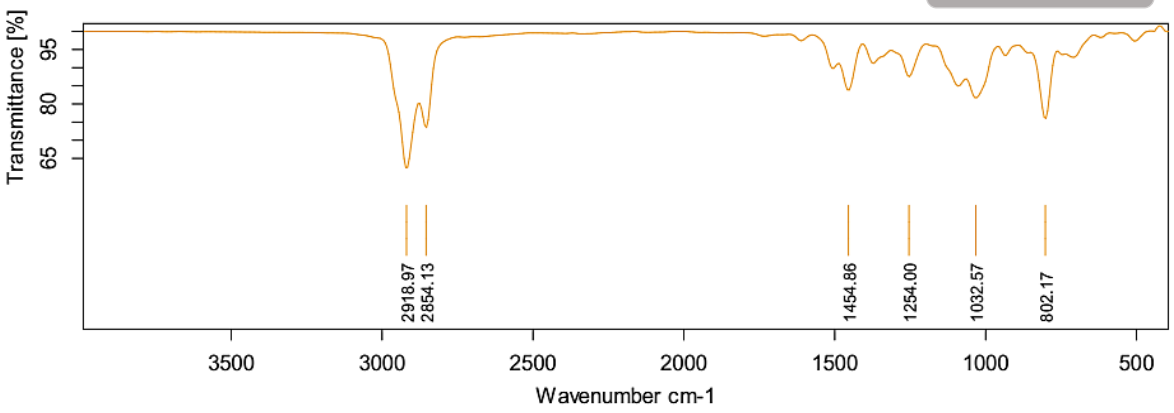

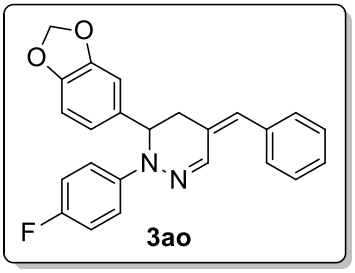

3ao

^{1}H-NMR ($CDCl_3$, 400MHz) of 3ao

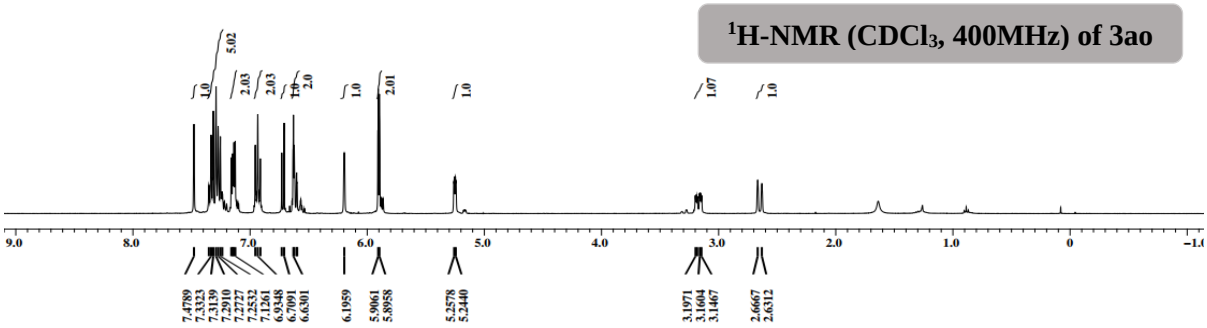

^{13}C-NMR ($CDCl_3$, 100MHz) of 3ao

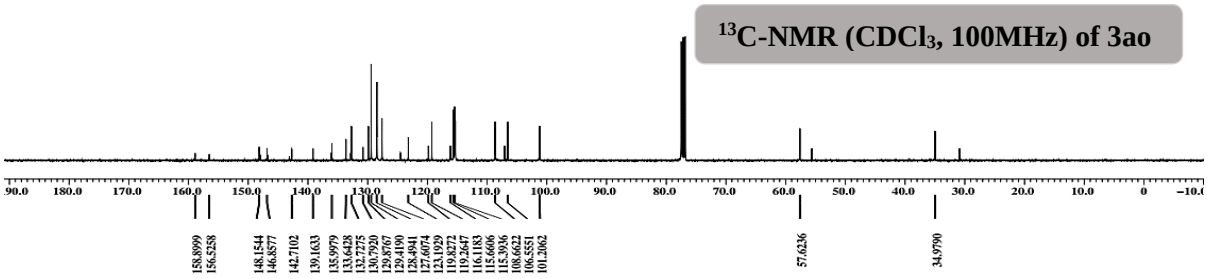

^{13}C DEPT ($CDCl_3$, 100MHz) of 3ao

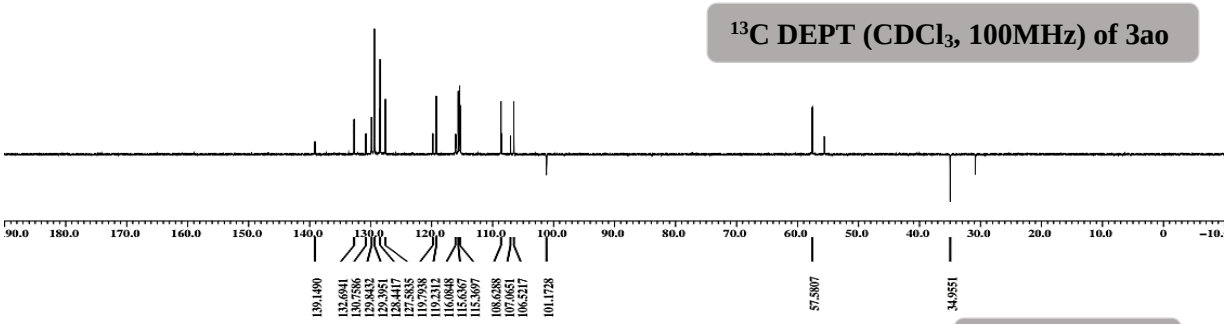

FTIR of 3ao

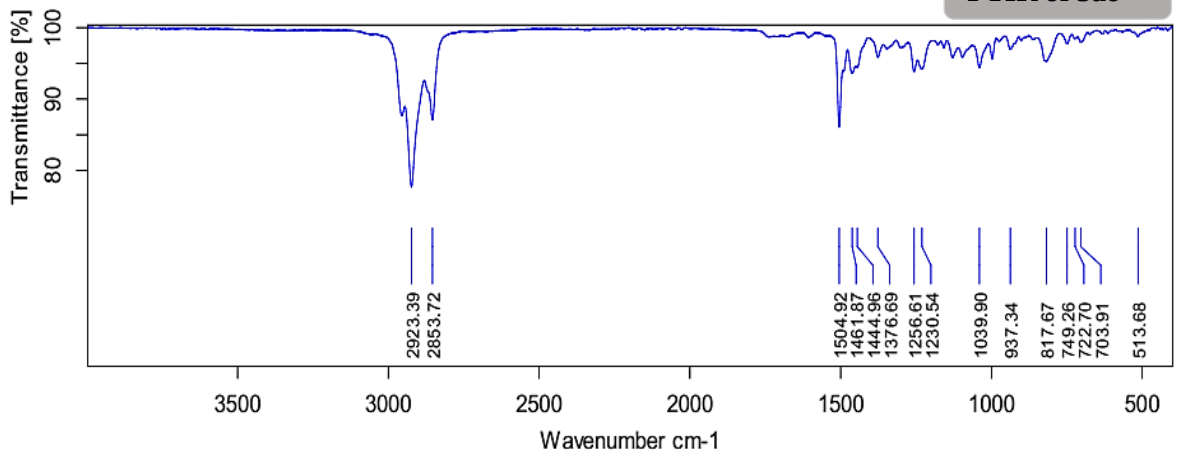

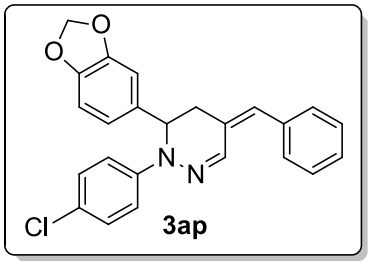

^{1}H-NMR ($CDCl_3$, 400MHz) of 3ap

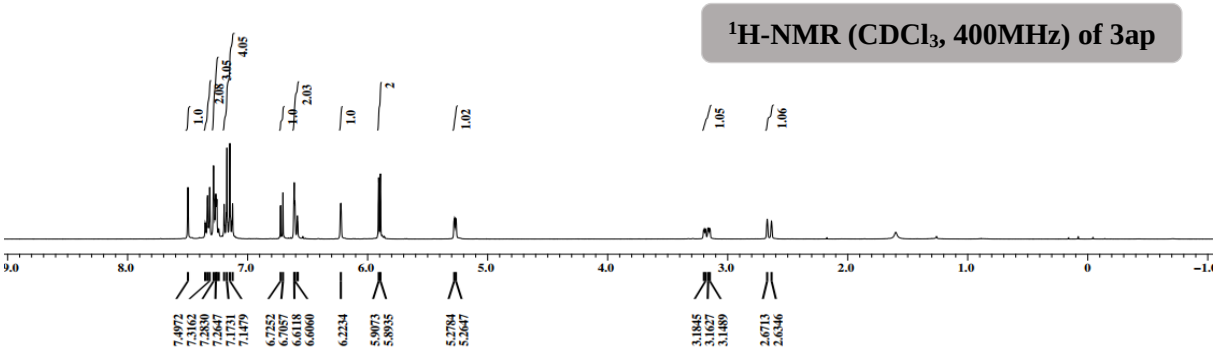

^{13}C-NMR ($CDCl_3$, 100MHz) of 3ap

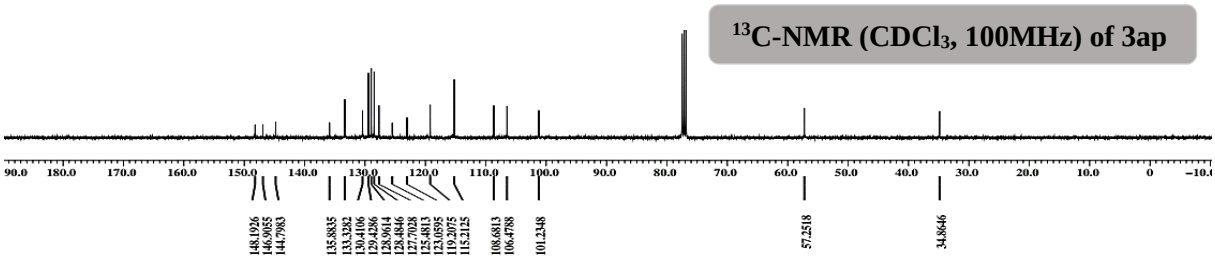

^{13}C DEPT ($CDCl_3$, 100MHz) of 3ap

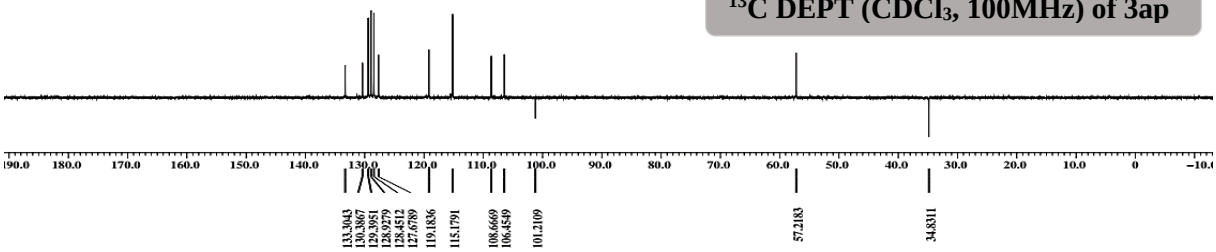

FTIR of 3ap

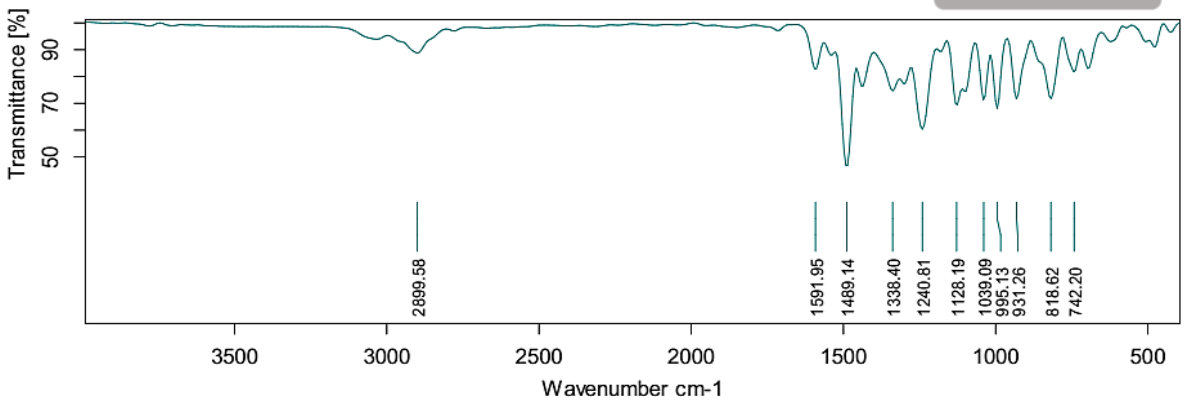

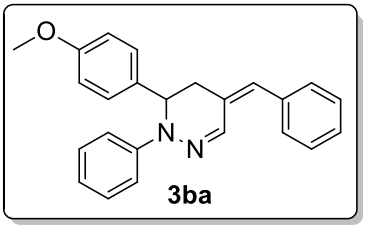

3ba

^{1}H-NMR ($CDCl_3$, 400MHz) of 3ba

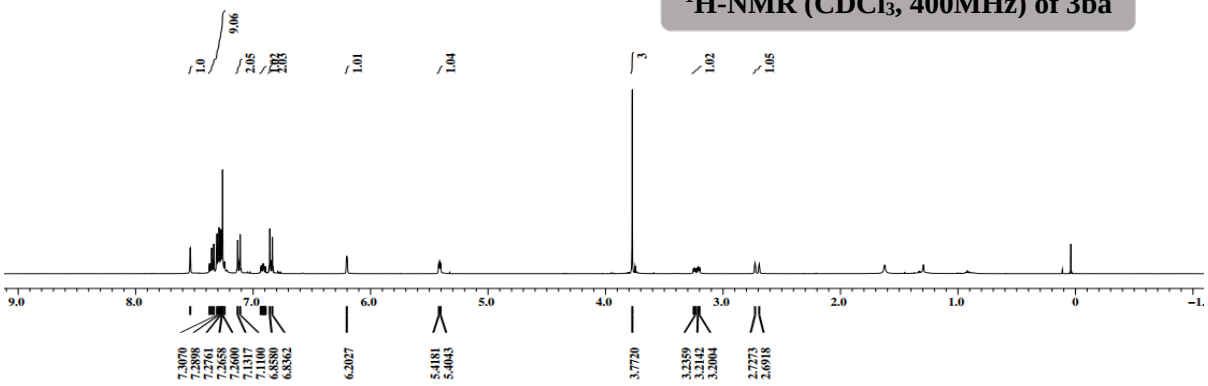

^{13}C-NMR ($CDCl_3$, 100MHz) of 3ba

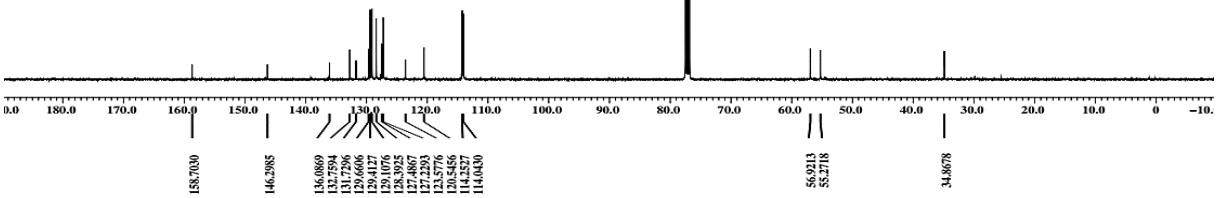

^{13}C DEPT ($CDCl_3$, 100MHz) of 3ba

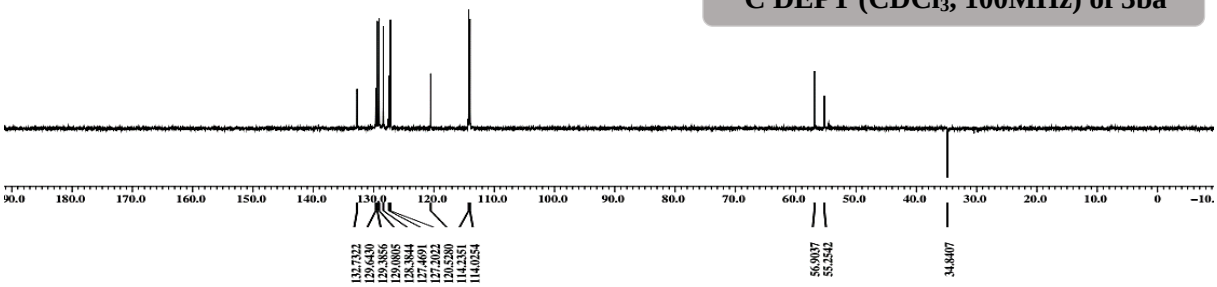

FTIR of 3ba

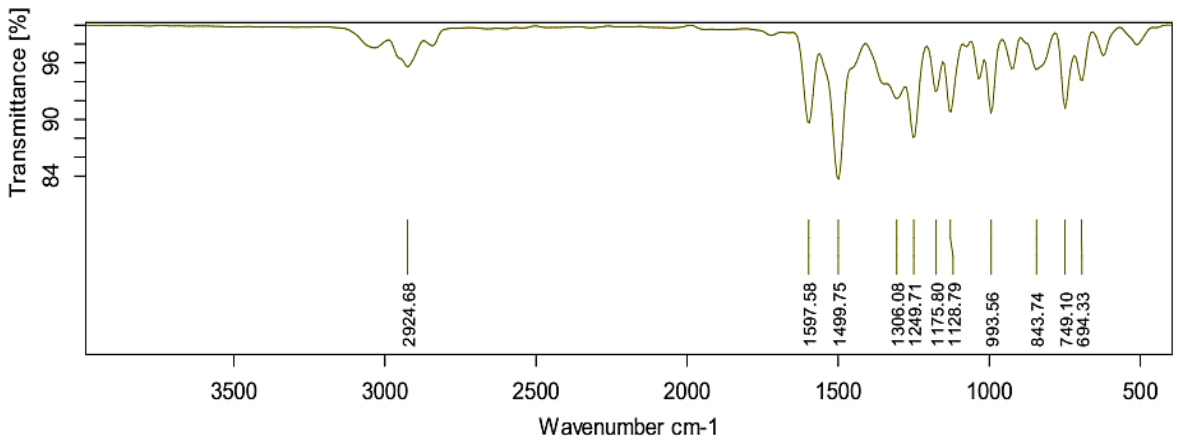

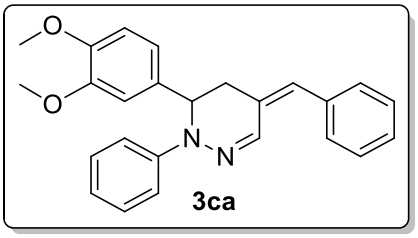

^{1}H-NMR ($CDCl_3$, 400MHz) of 3ca

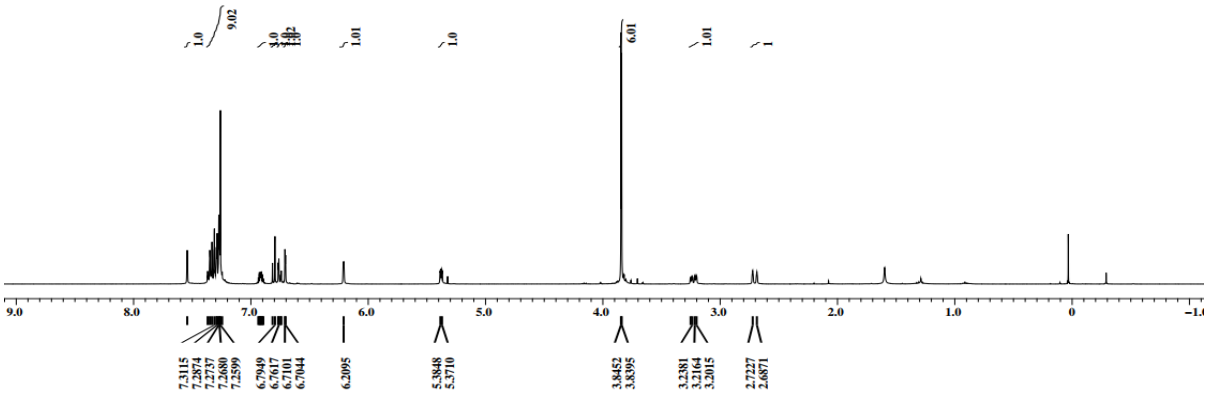

^{13}C-NMR ($CDCl_3$, 100MHz) of 3ca

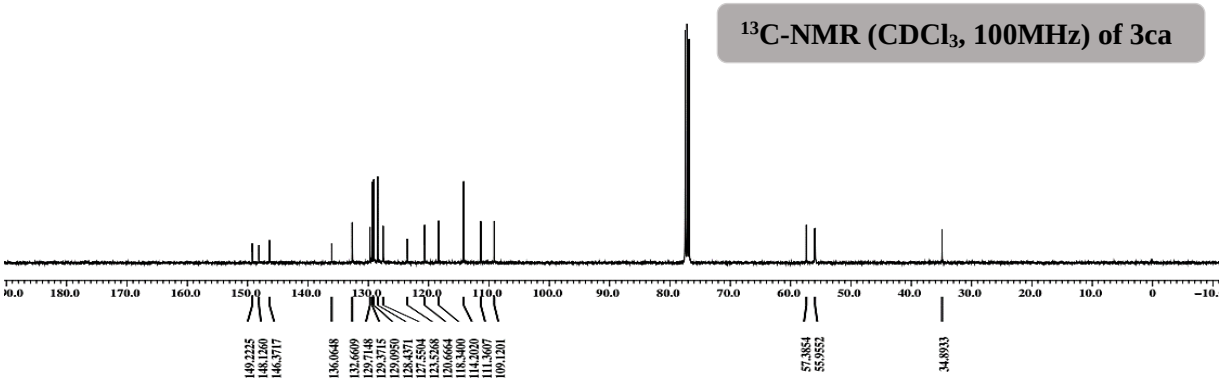

^{13}C DEPT ($CDCl_3$, 100MHz) of 3ca

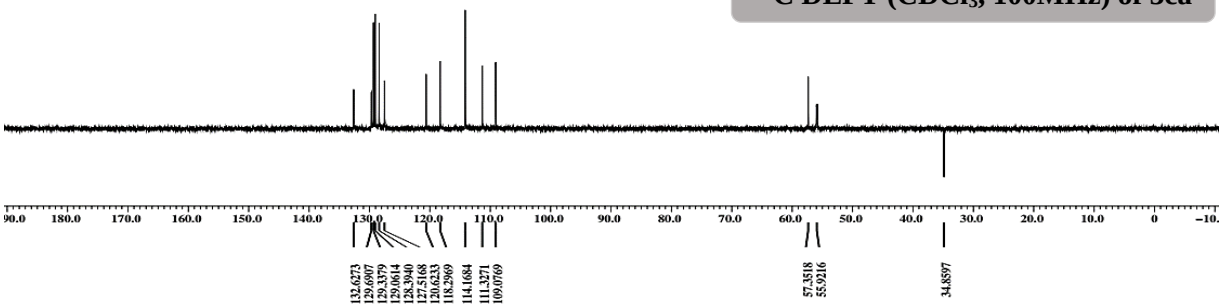

FTIR of 3ca

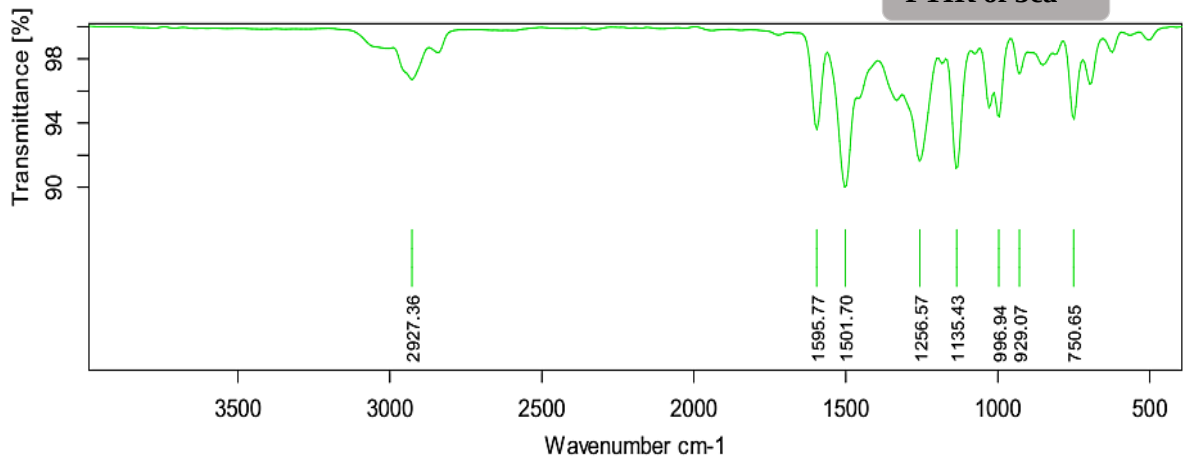

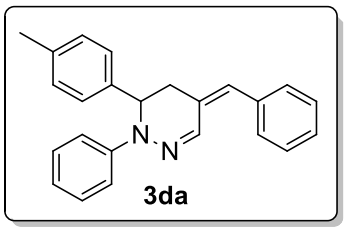

^{1}H-NMR ($CDCl_3$, 400MHz) of 3da

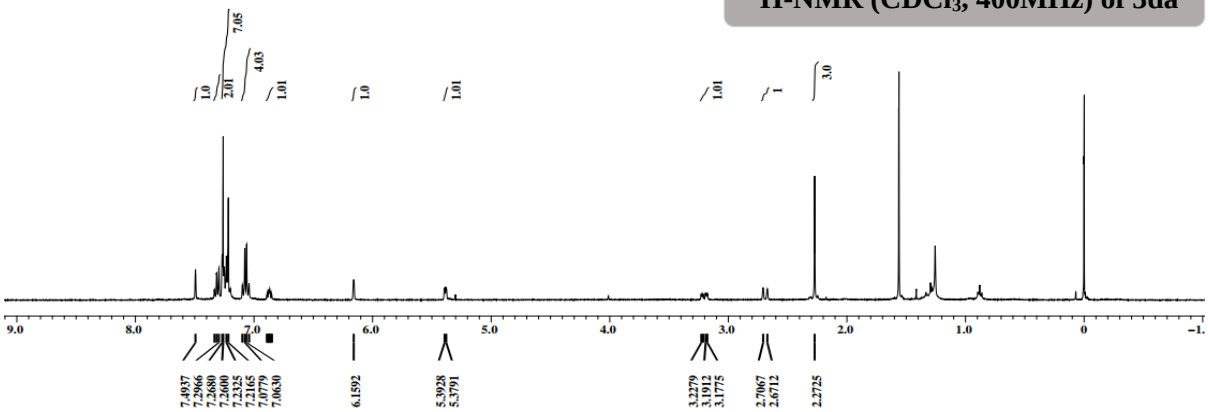

^{13}C-NMR ($CDCl_3$, 100MHz) of 3da

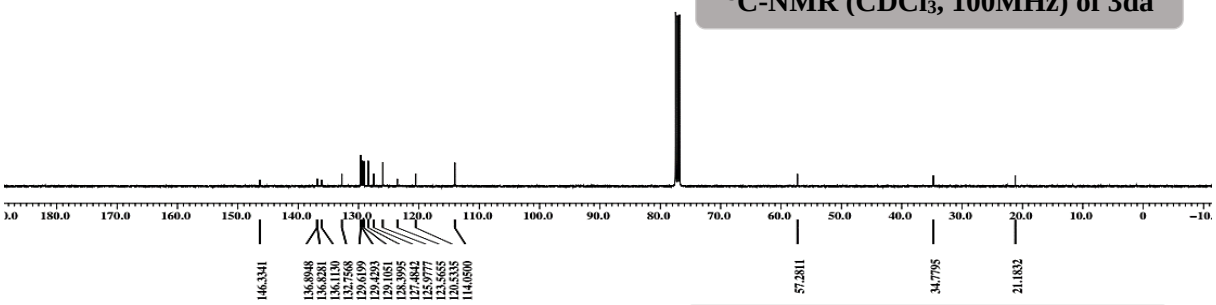

^{13}C DEPT ($CDCl_3$, 100MHz) of 3da

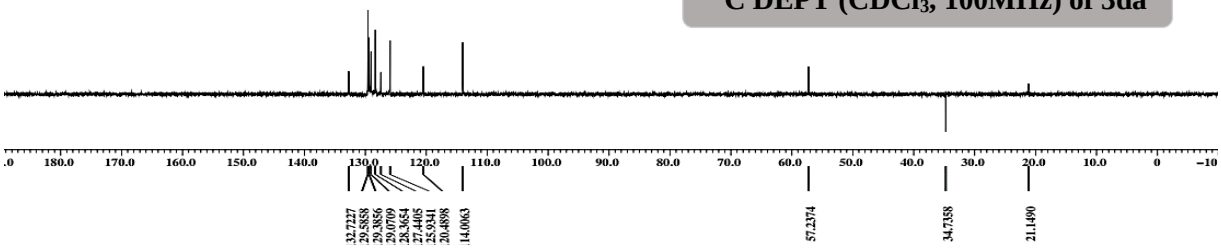

FTIR of 3da

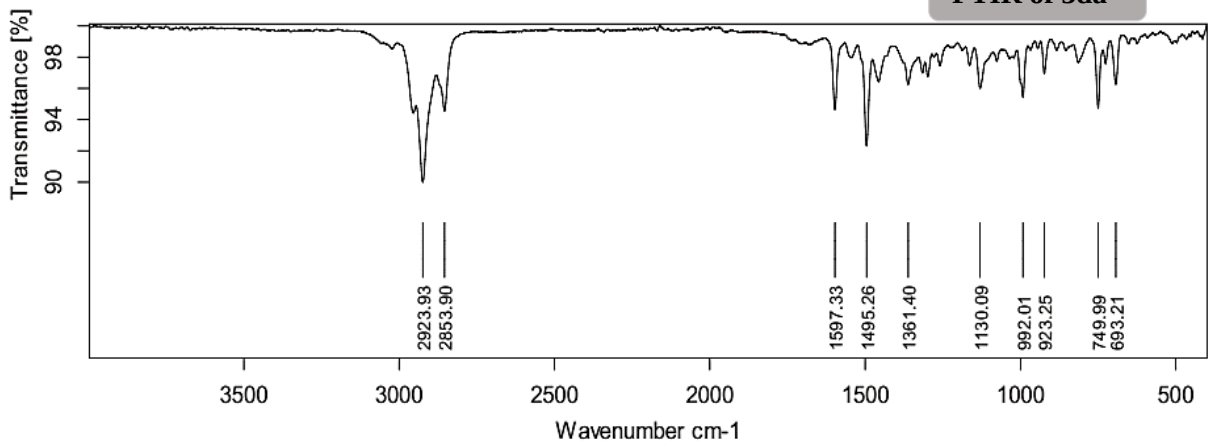

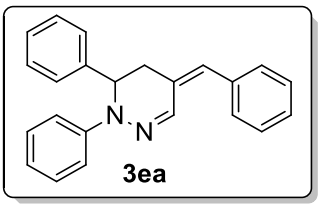

^{1}H-NMR ($CDCl_3$, 400MHz) of 3ea

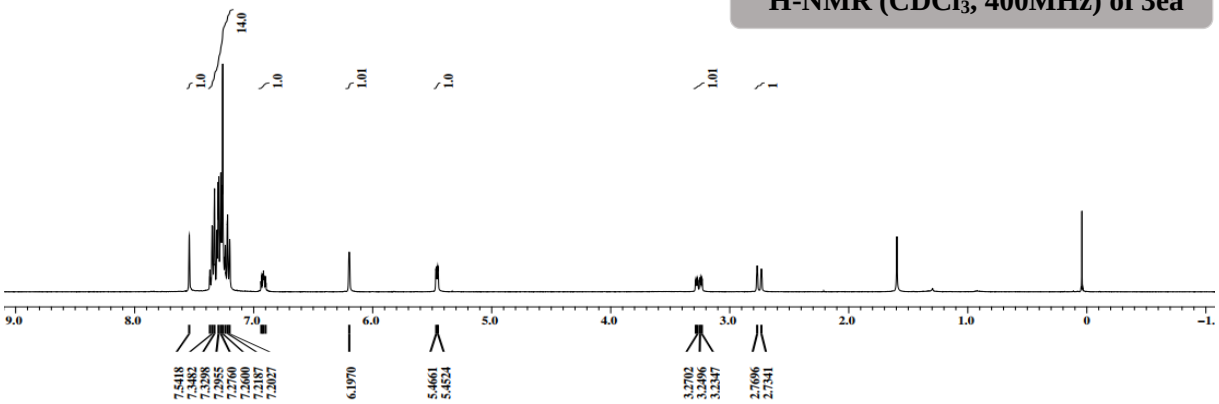

^{13}C-NMR ($CDCl_3$, 100MHz) of 3ea

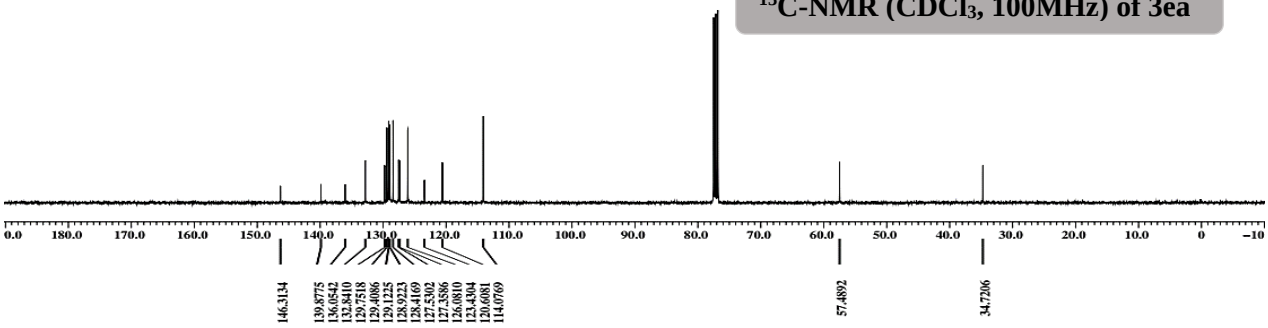

^{13}C DEPT ($CDCl_3$, 100MHz) of 3ea

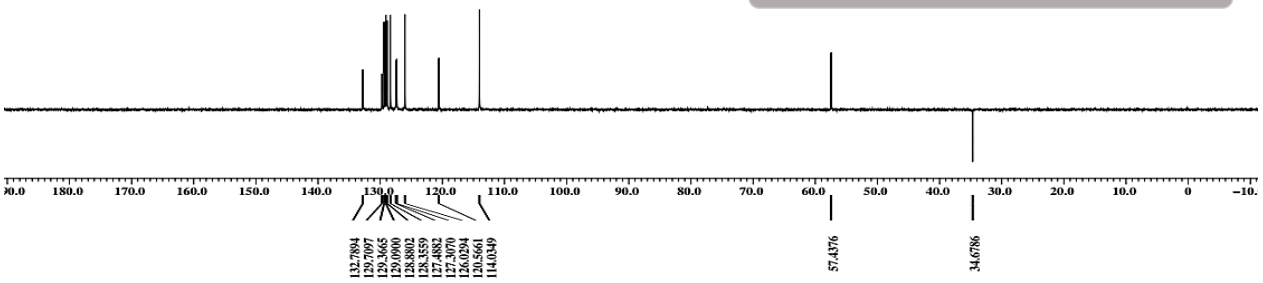

FTIR of 3ea

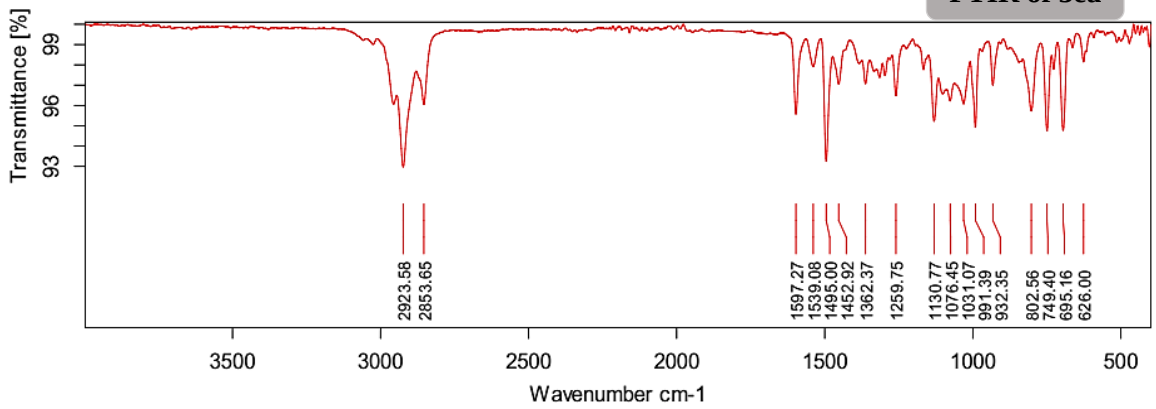

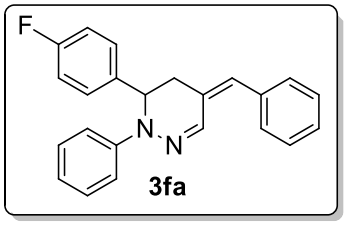

^{1}H-NMR ($CDCl_3$, 400MHz) of 3fa

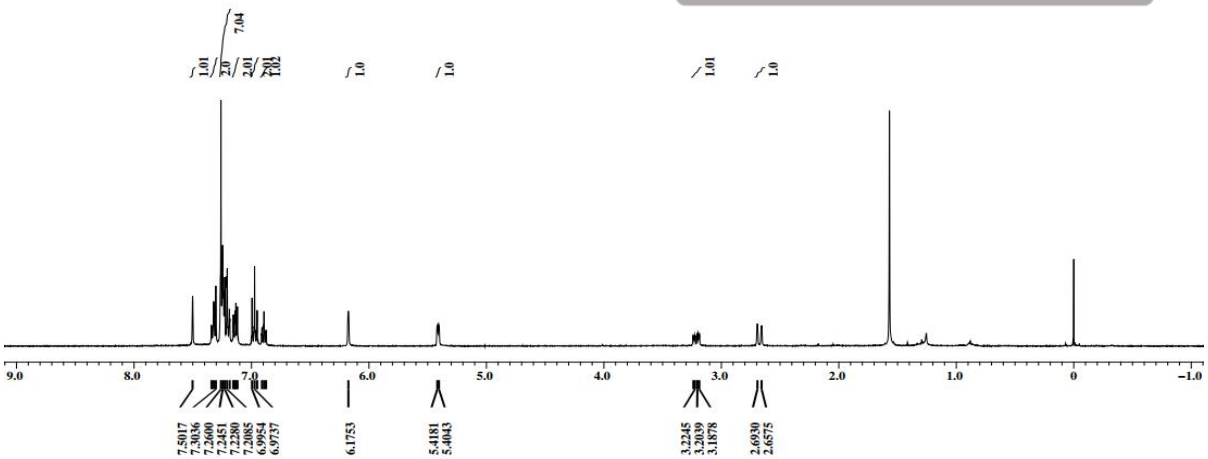

^{13}C-NMR ($CDCl_3$, 100MHz) of 3fa

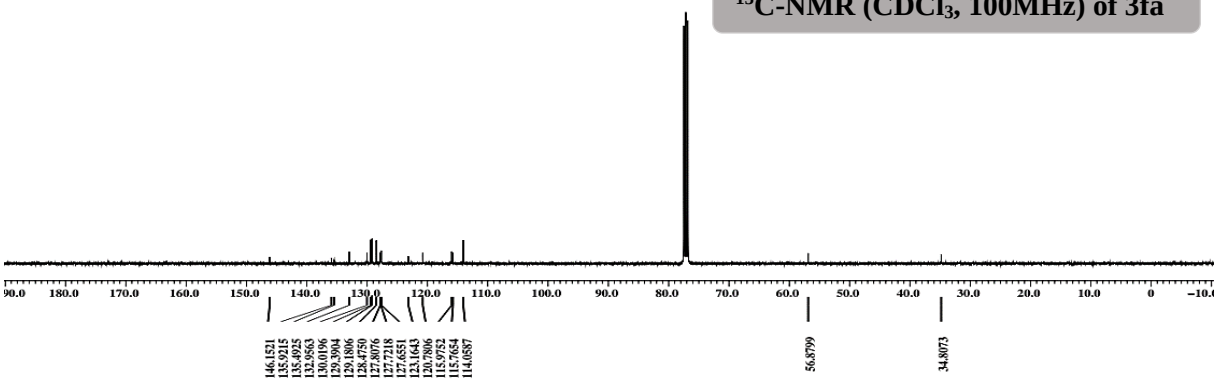

^{13}C DEPT ($CDCl_3$, 100MHz) of 3fa

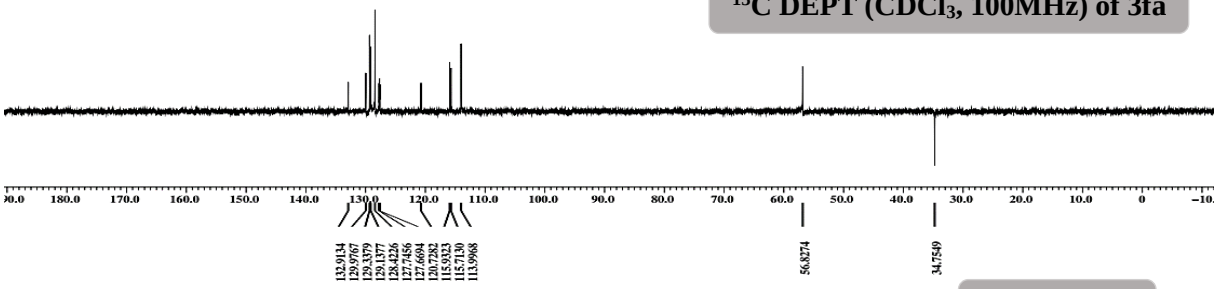

FTIR of 3fa

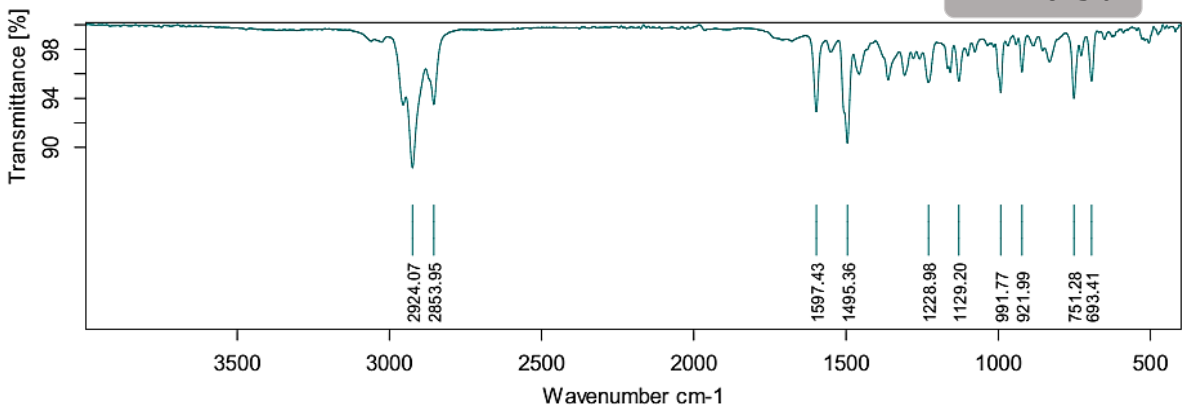

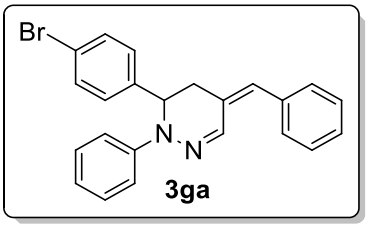

3ga

^{1}H-NMR ($CDCl_3$, 400MHz) of 3ga

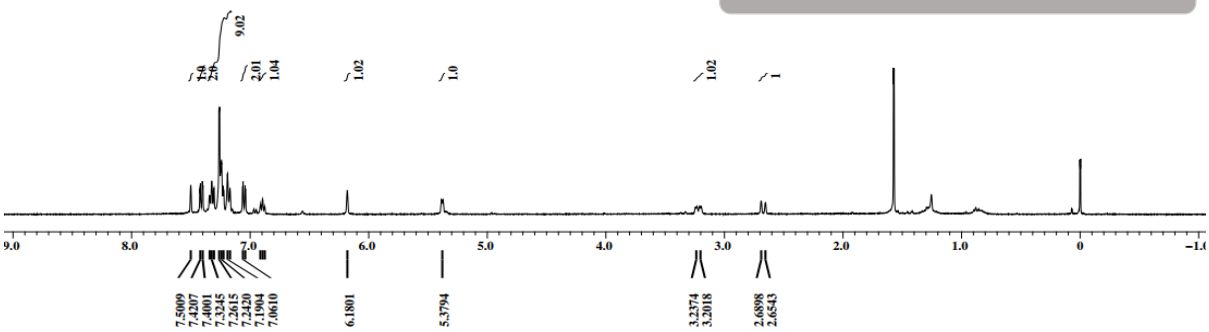

^{13}C-NMR ($CDCl_3$, 100MHz) of 3ga

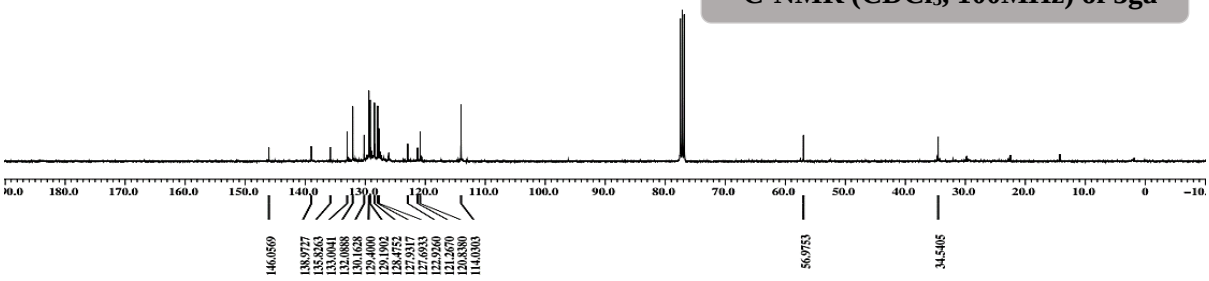

^{13}C DEPT ($CDCl_3$, 100MHz) of 3ga

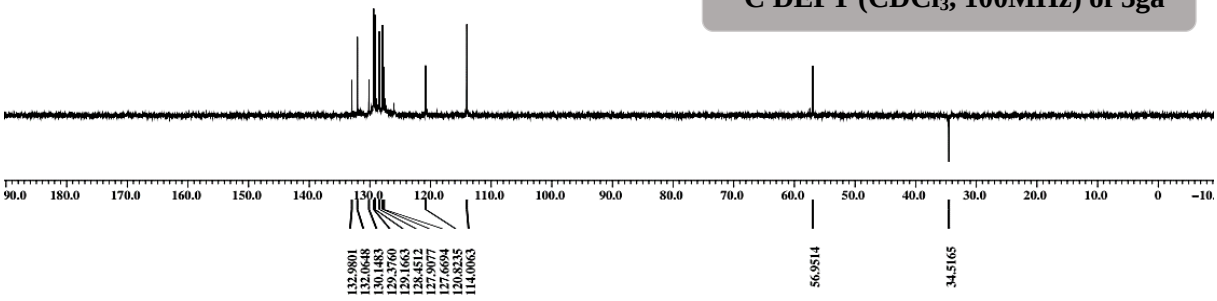

FTIR of 3ga

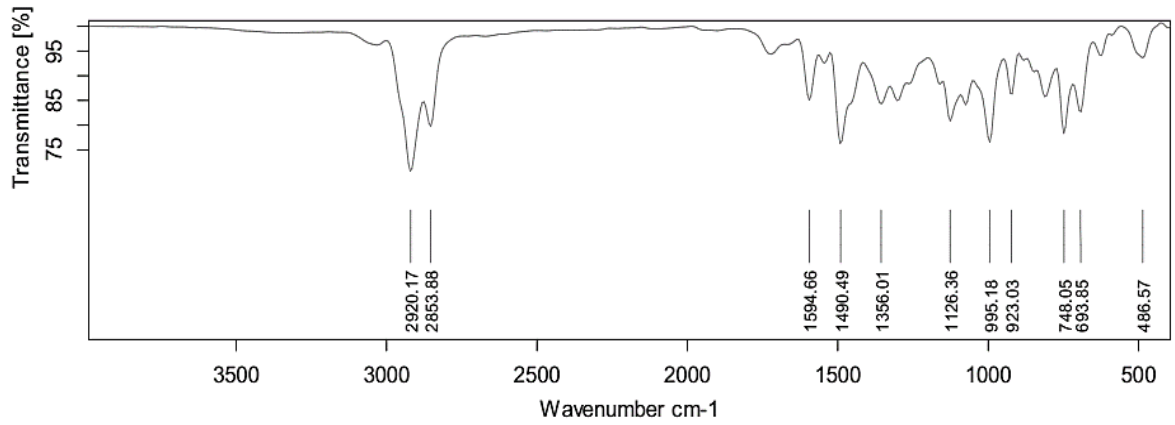

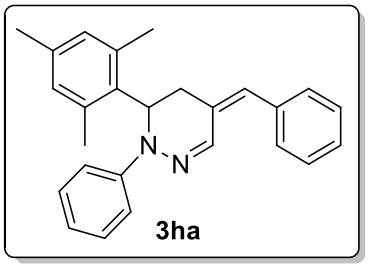

^{1}H-NMR ($CDCl_3$, 400MHz) of 3ha

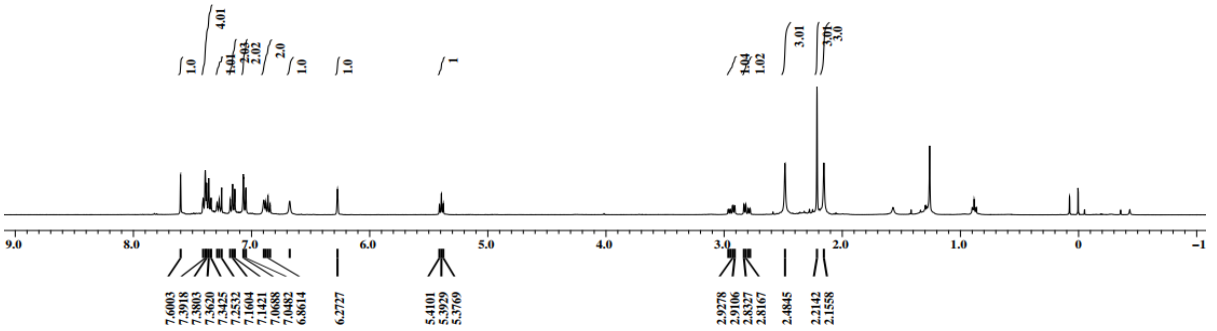

^{13}C-NMR ($CDCl_3$, 100MHz) of 3ha

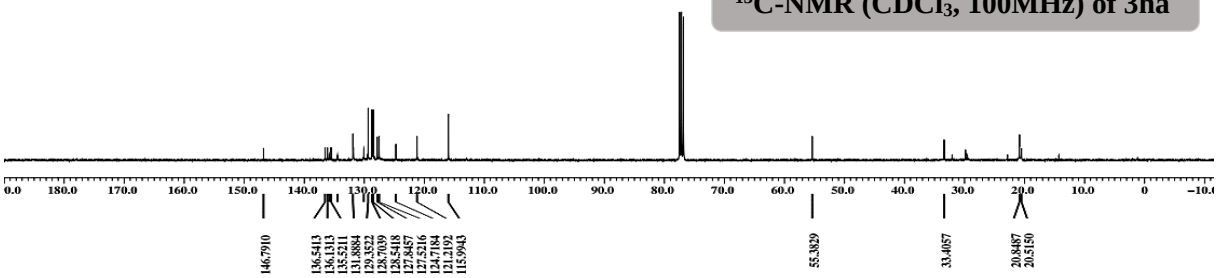

^{13}C DEPT ($CDCl_3$, 100MHz) of 3ha

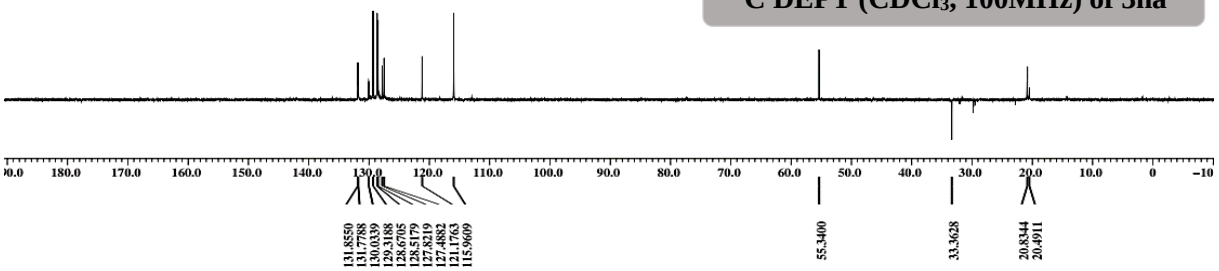

FTIR of 3ha

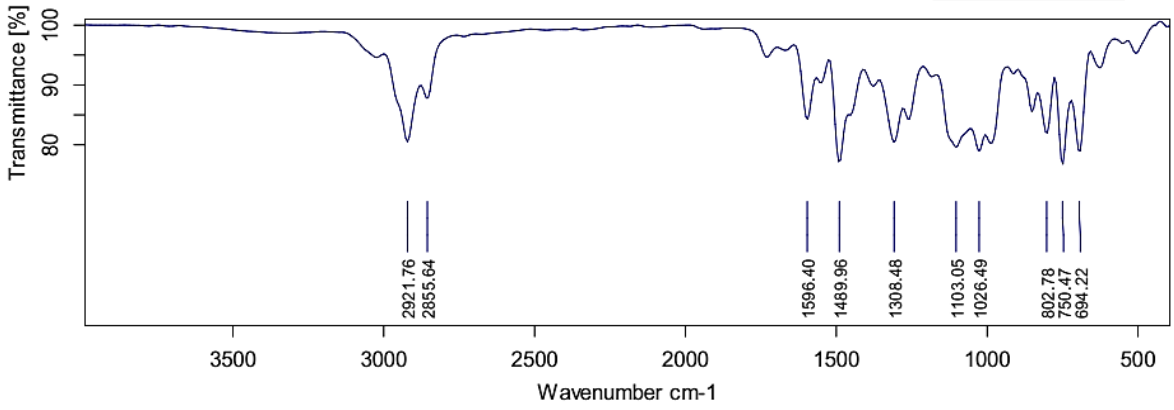

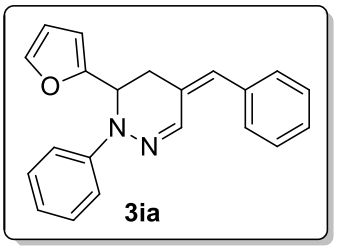

3ia

^{1}H-NMR ($CDCl_3$, 400MHz) of 3ia

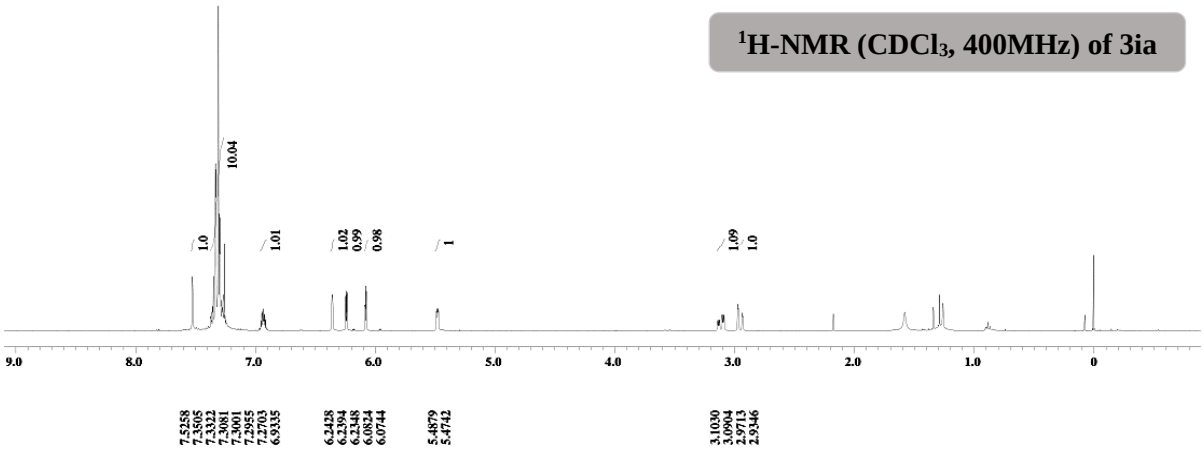

^{13}C-NMR ($CDCl_3$, 100MHz) of 3ia

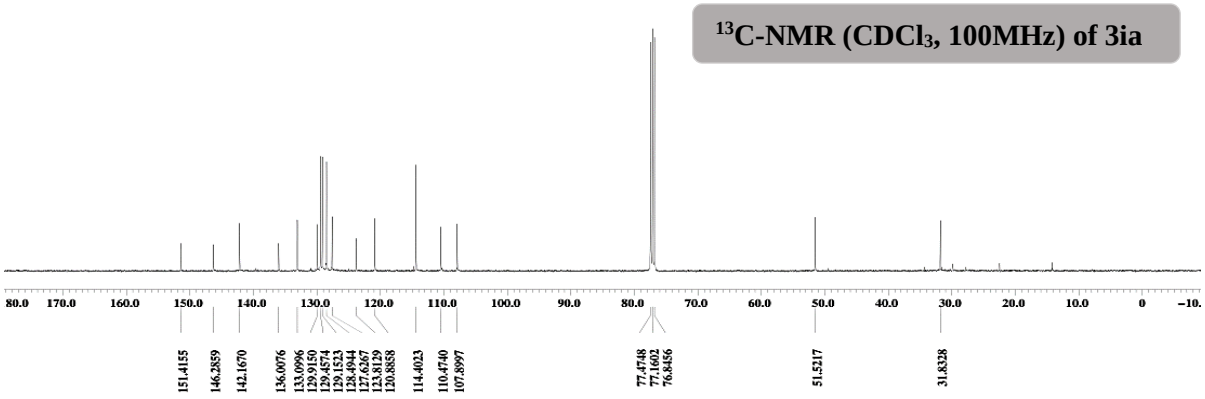

FTIR of 3ia

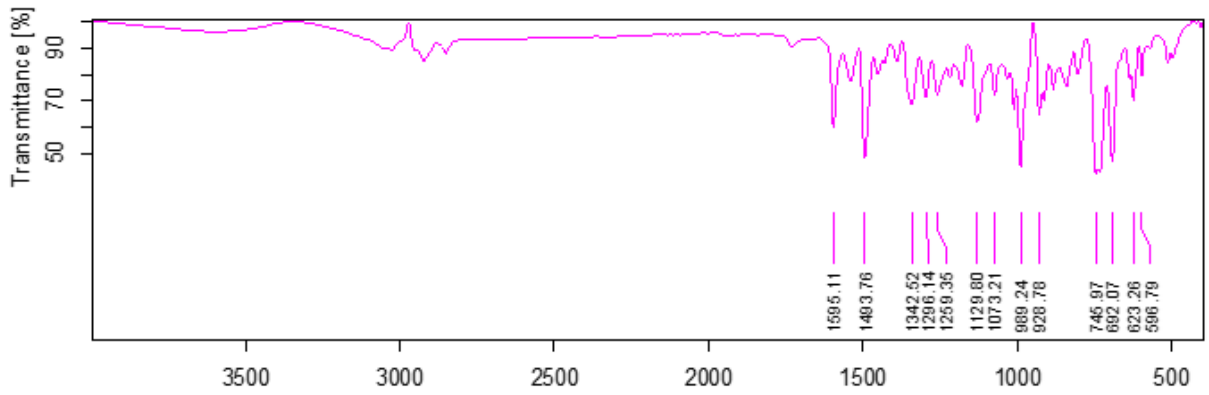

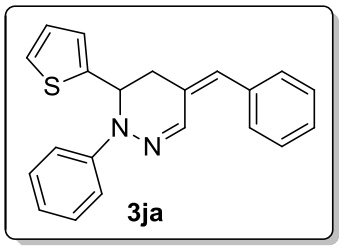

3ja

^{1}H-NMR ($CDCl_3$, 400MHz) of 3ja

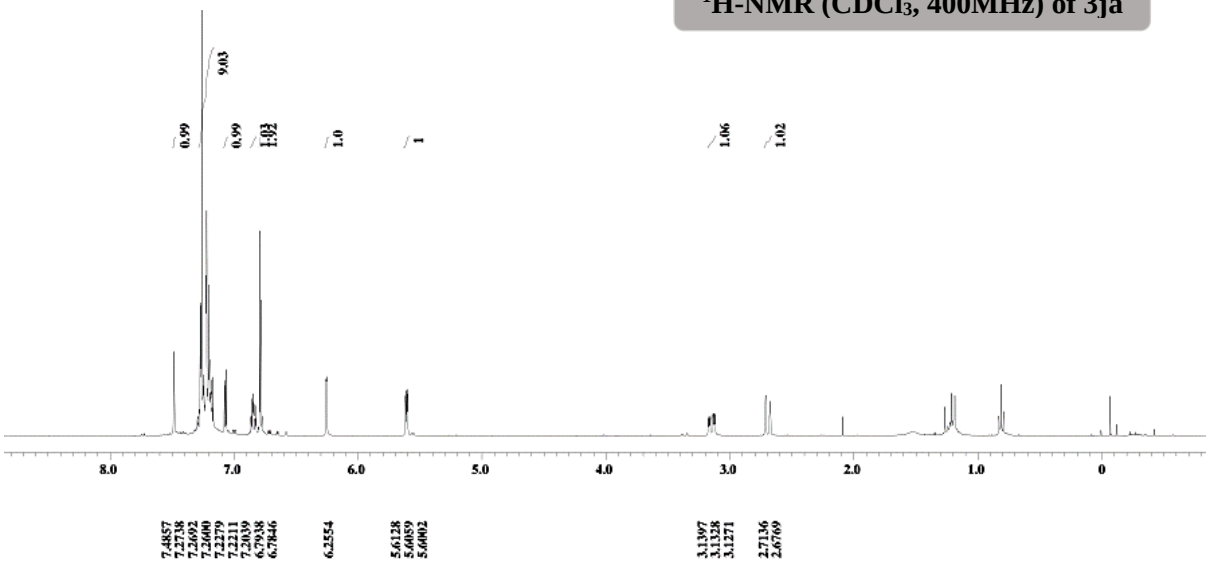

^{13}C-NMR ($CDCl_3$, 100MHz) of 3ja

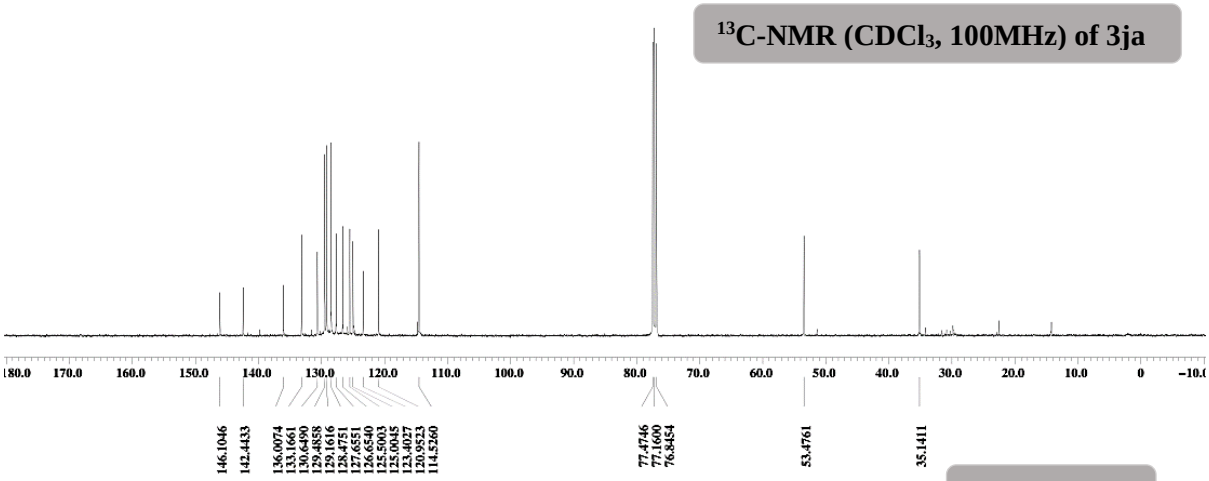

FTIR of 3ja

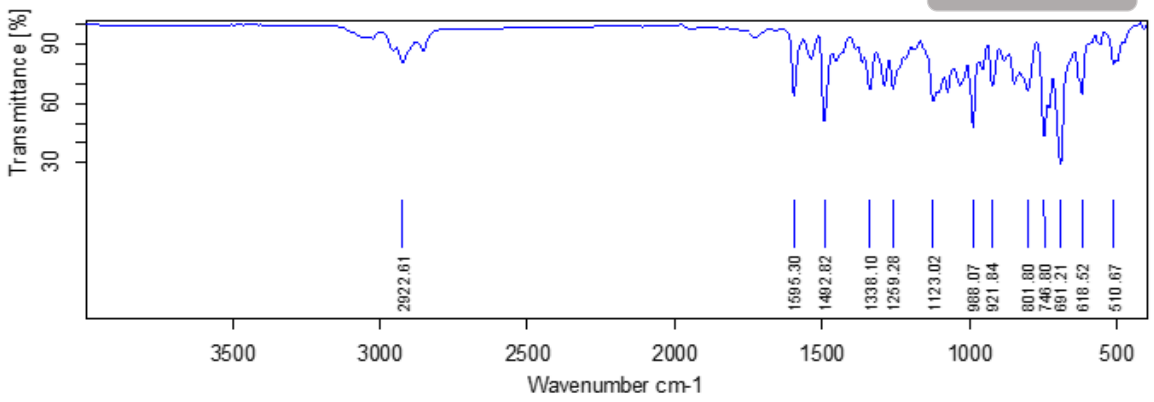

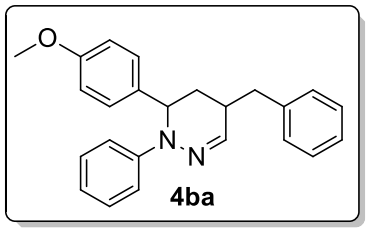

4ba

^{1}H-NMR ($CDCl_3$, 400MHz) of 4ba

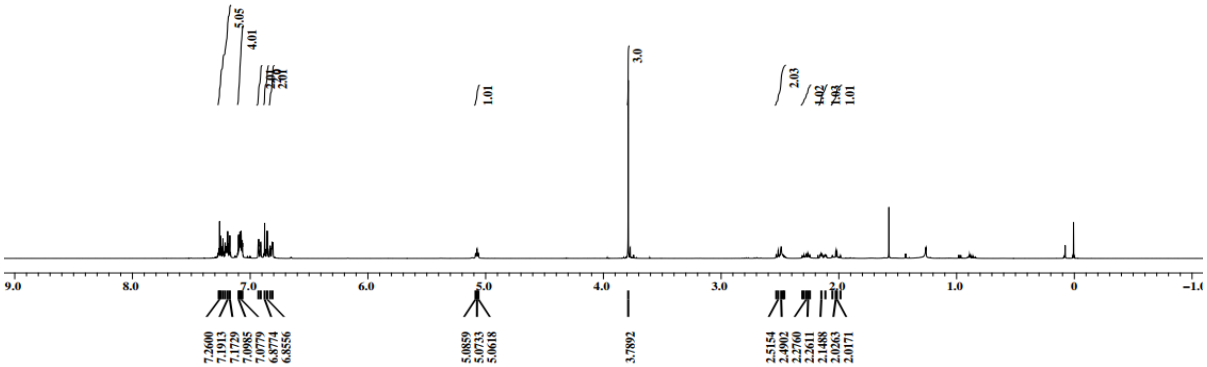

^{13}C NMR ($CDCl_3$, 100MHz) of 4ba

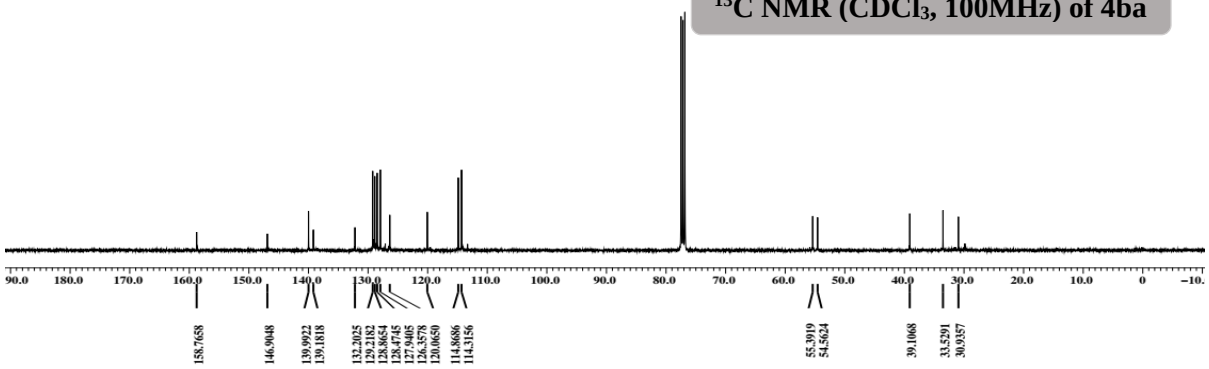

^{13}C DEPT ($CDCl_3$, 100MHz) of 4ba

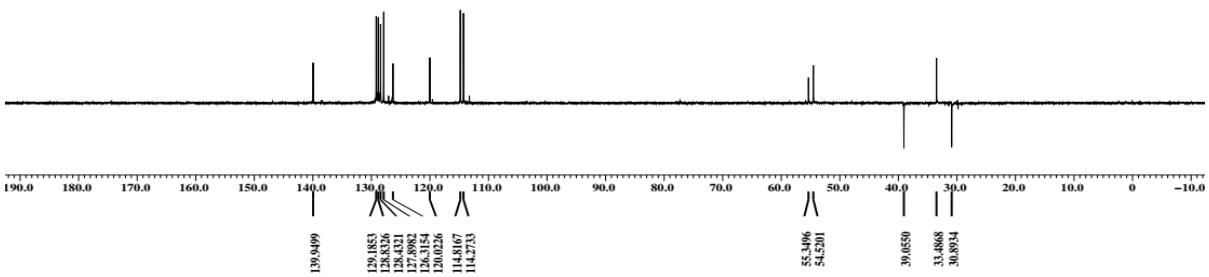

^{13}C DEPT, ^{1}H HETCOR NMR ($CDCl_3$, 100, 400 MHz) of 4ba

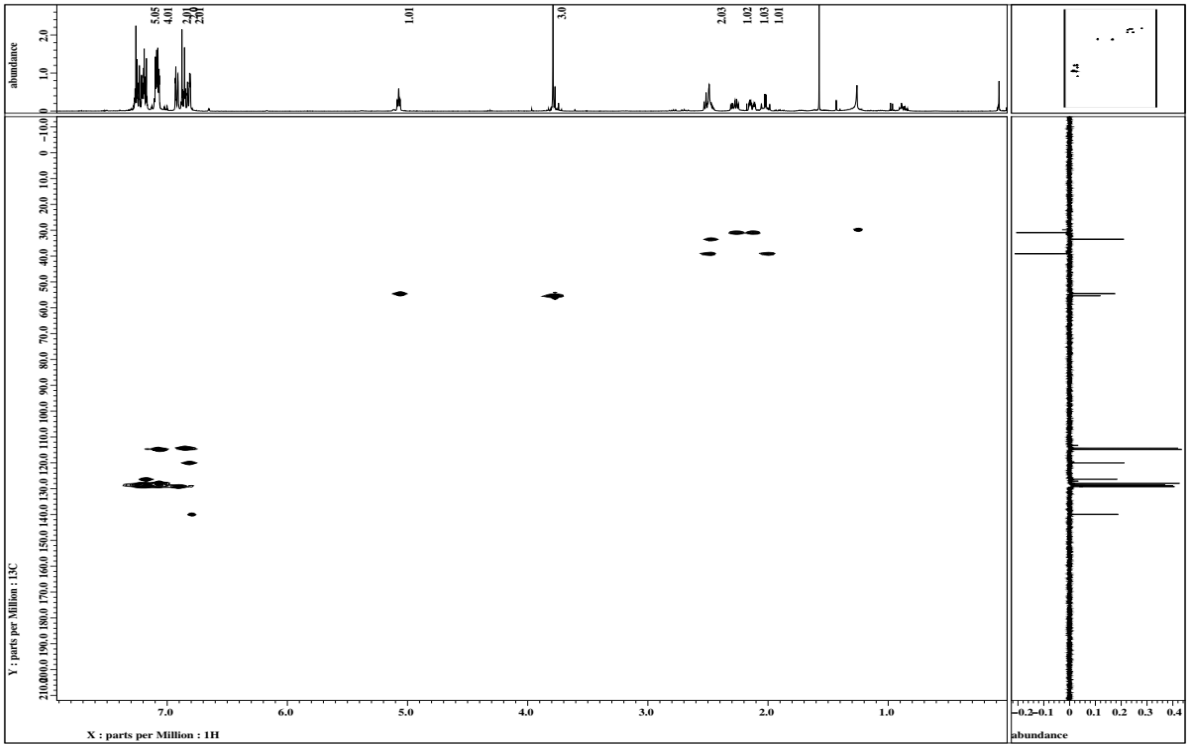

^{1}H COSY ($CDCl_3$, 400MHz) of 4ba

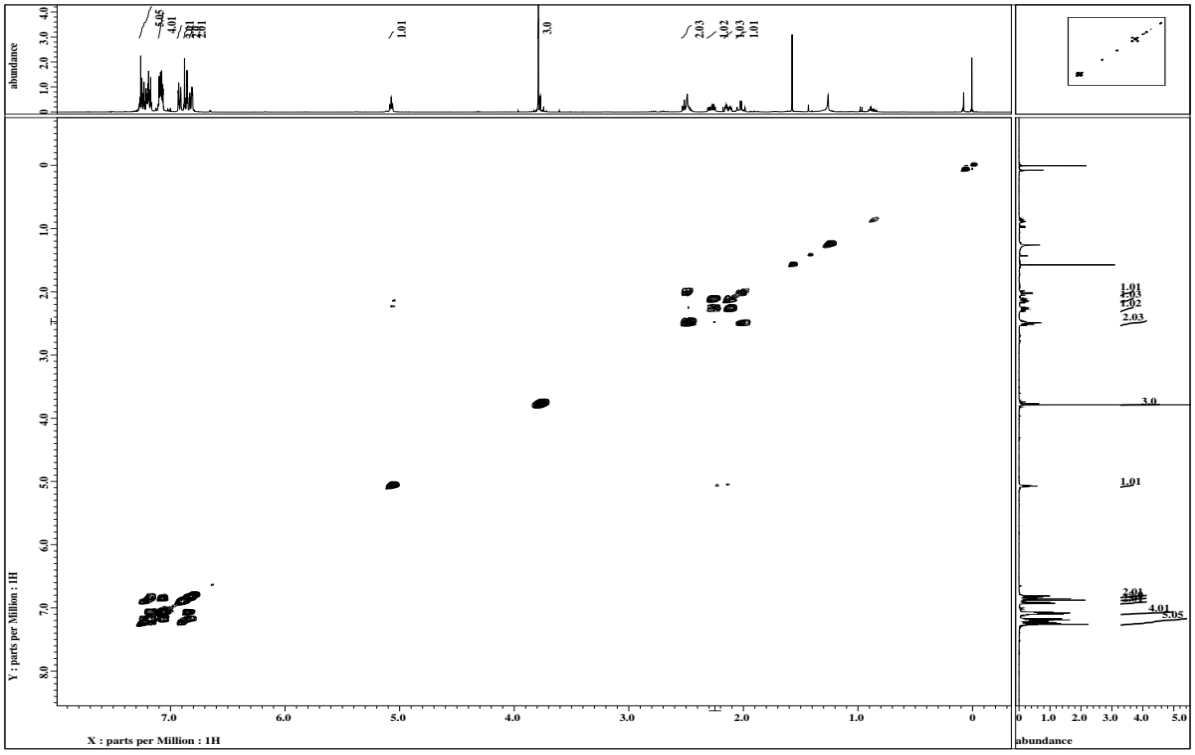

^{1}H-NOE ($CDCl_3$, 400MHz) of 4ba

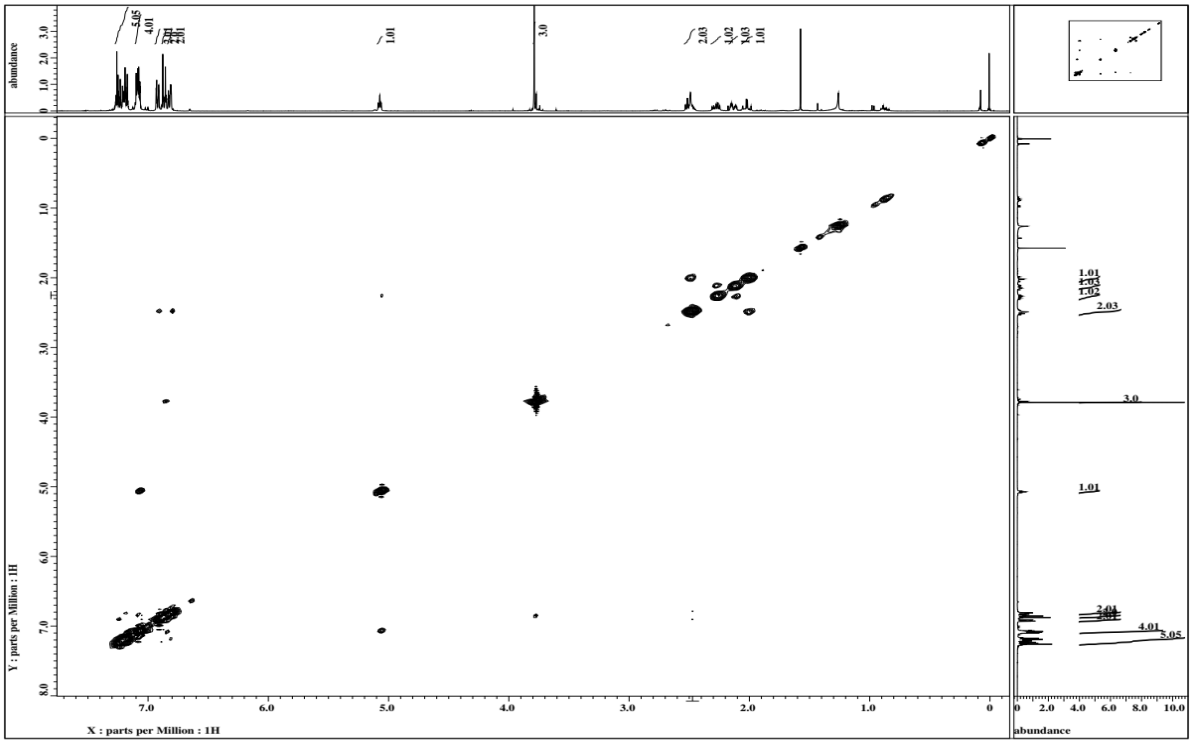

FTIR of 4ba

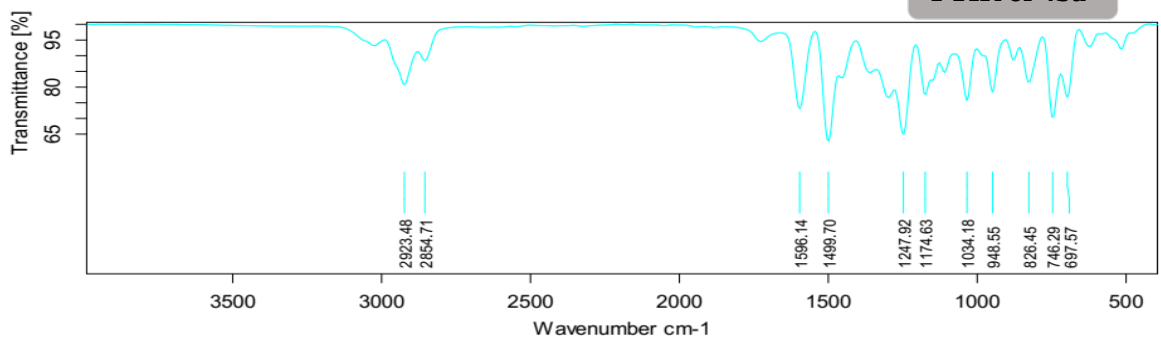

2.A.7. HPLC data of the compounds

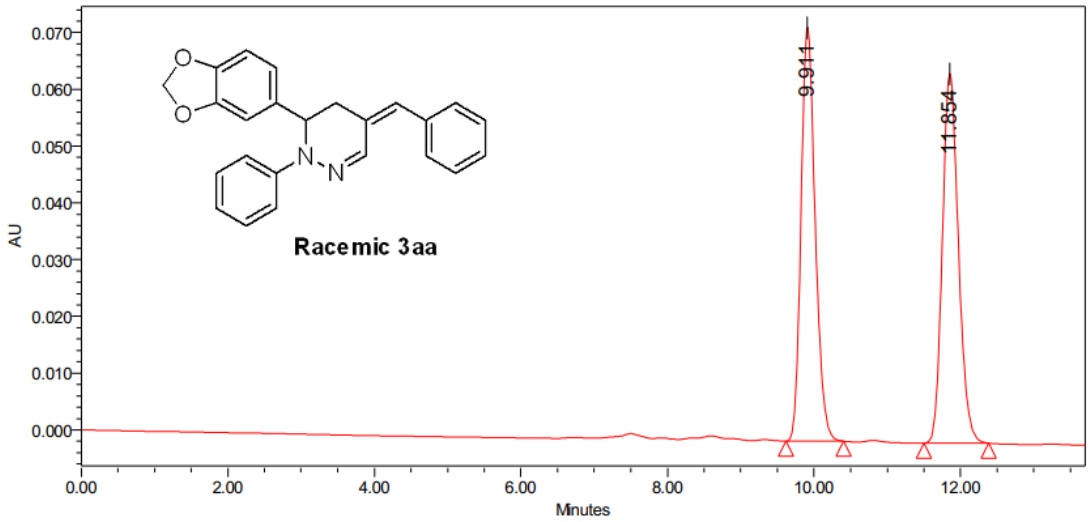

Peak Results

	Name	RT	Area	% Area
1		9.911	981632	49.79
2		11.854	989866	50.21

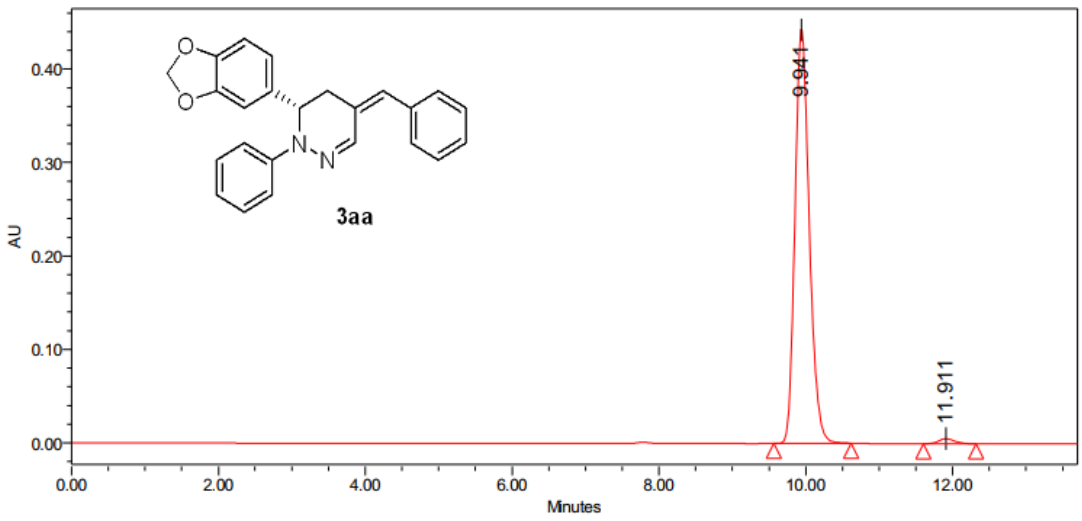

Peak Results

	Name	RT	Area	% Area
1		9.941	6000842	98.65
2		11.911	82099	1.35

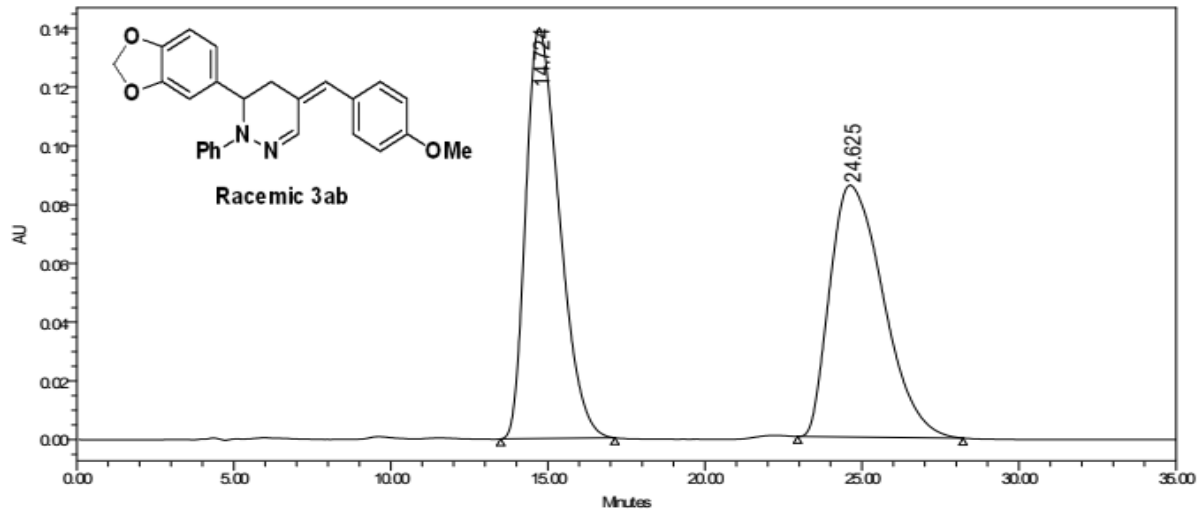

	RT	Area	%Area	Height
1	14.724	10380512	50.55	139727
2	24.625	10153849	49.45	85707

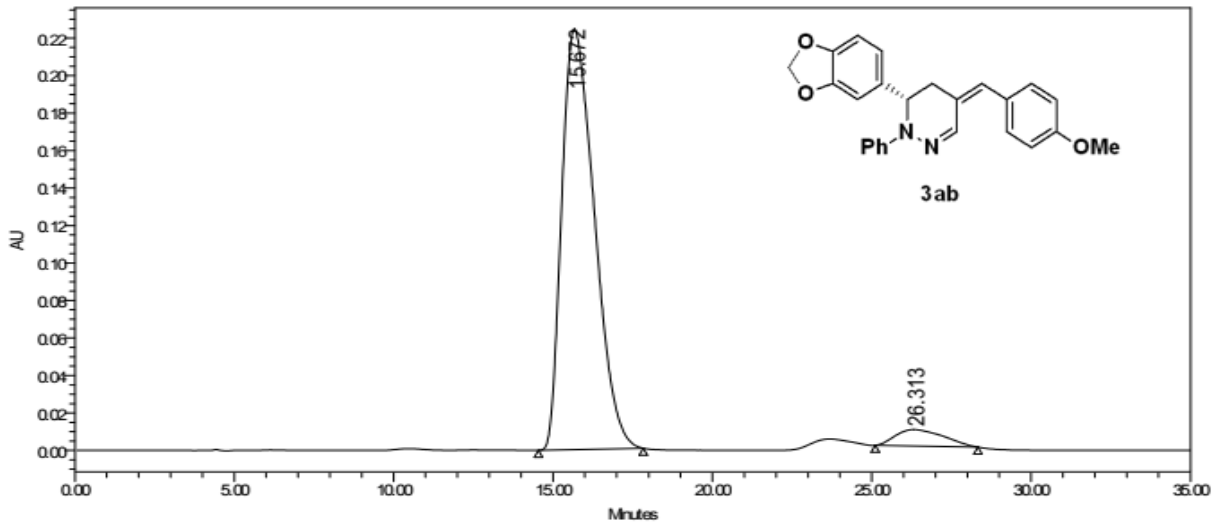

	RT	Area	%Area	Height
1	15.672	15975175	94.56	224430
2	26.313	918817	5.44	8761

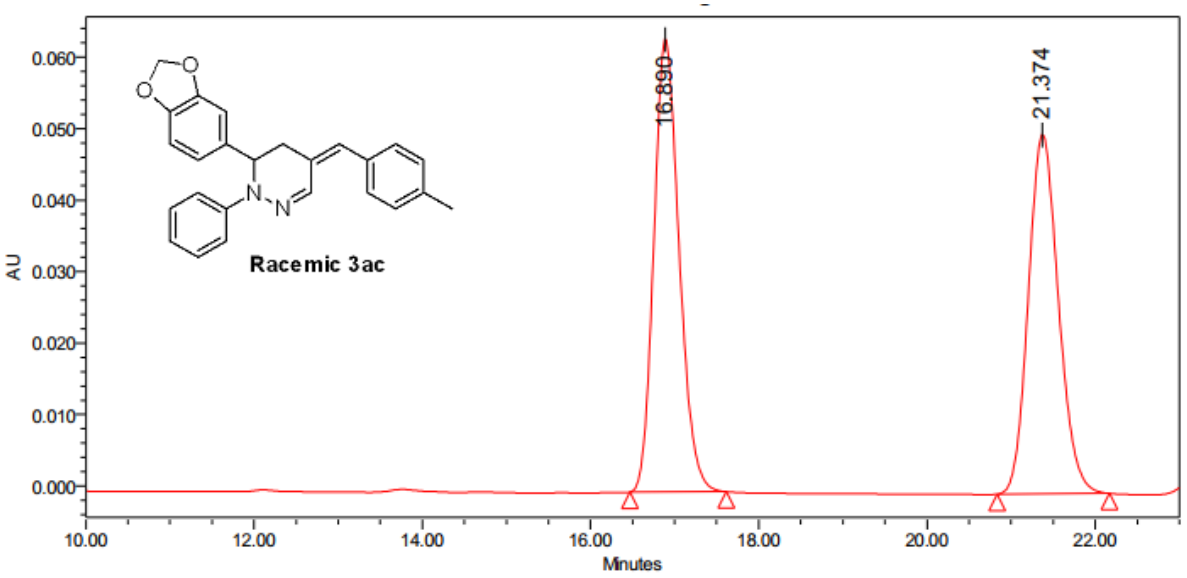

Peak Results

	Name	RT	Area	% Area
1		16.890	1322999	51.41
2		21.374	1250431	48.59

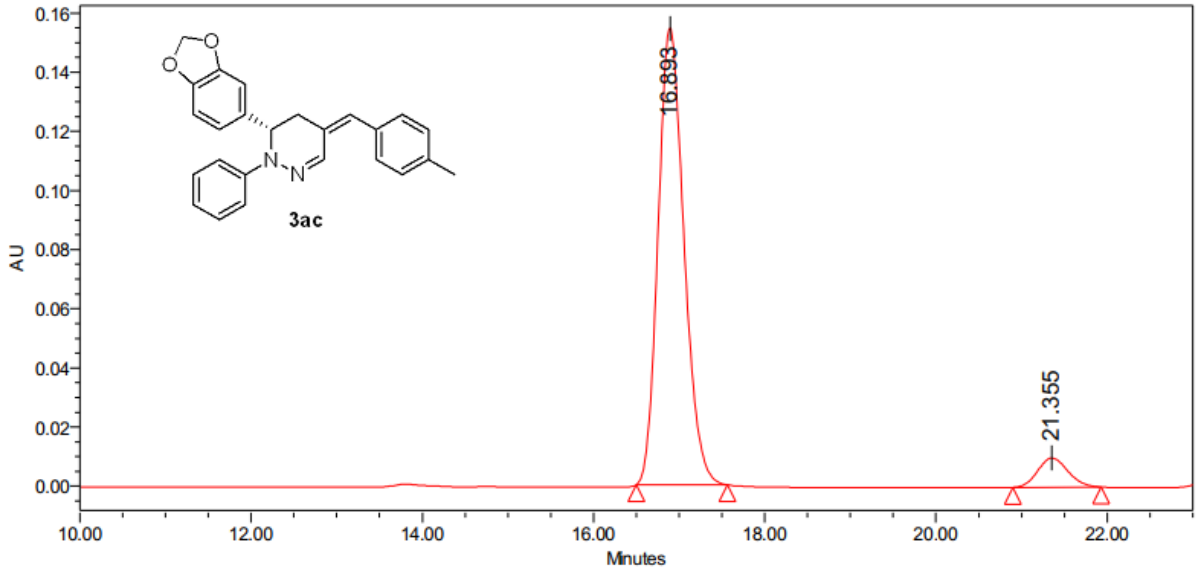

Peak Results

	Name	RT	Area	% Area
1		16.893	3235519	93.02
2		21.355	242658	6.98

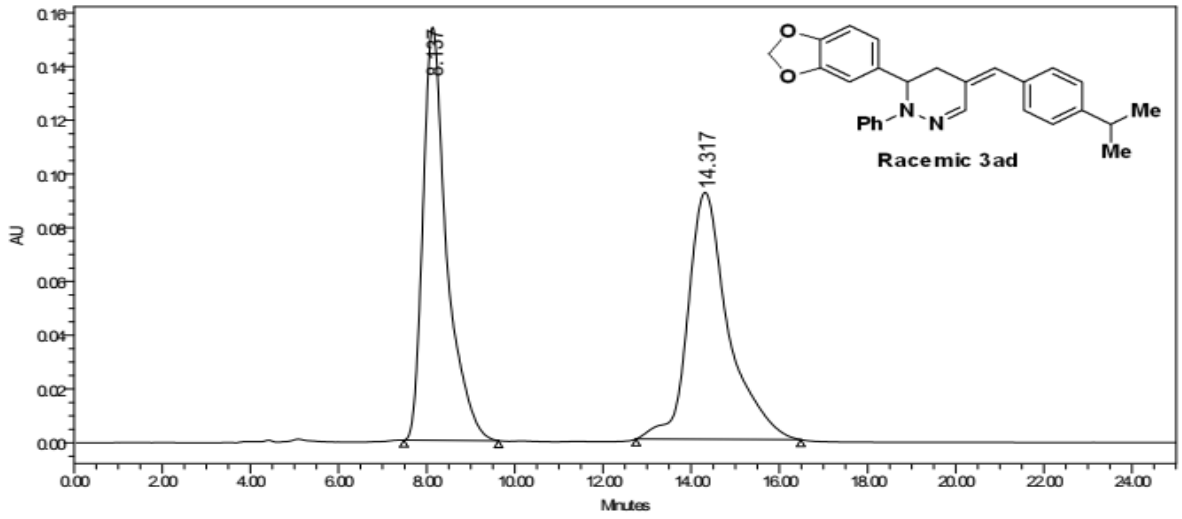

	RT	Area	%Area	Height
1	8.137	5753684	49.63	153608
2	14.317	5840484	50.37	91851

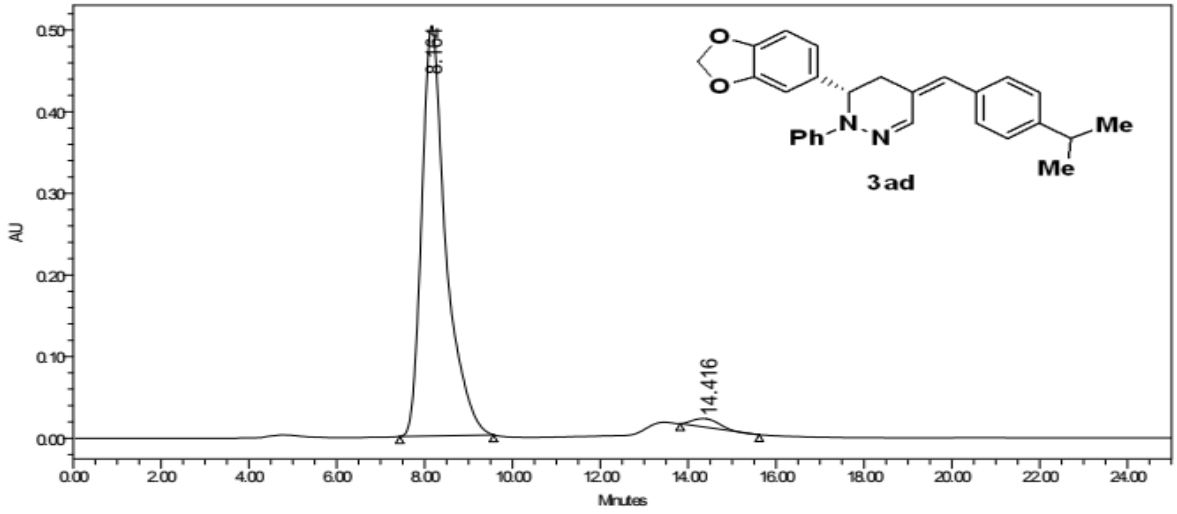

	RT	Area	%Area	Height
1	8.164	19167742	97.76	502367
2	14.416	439794	2.24	10471

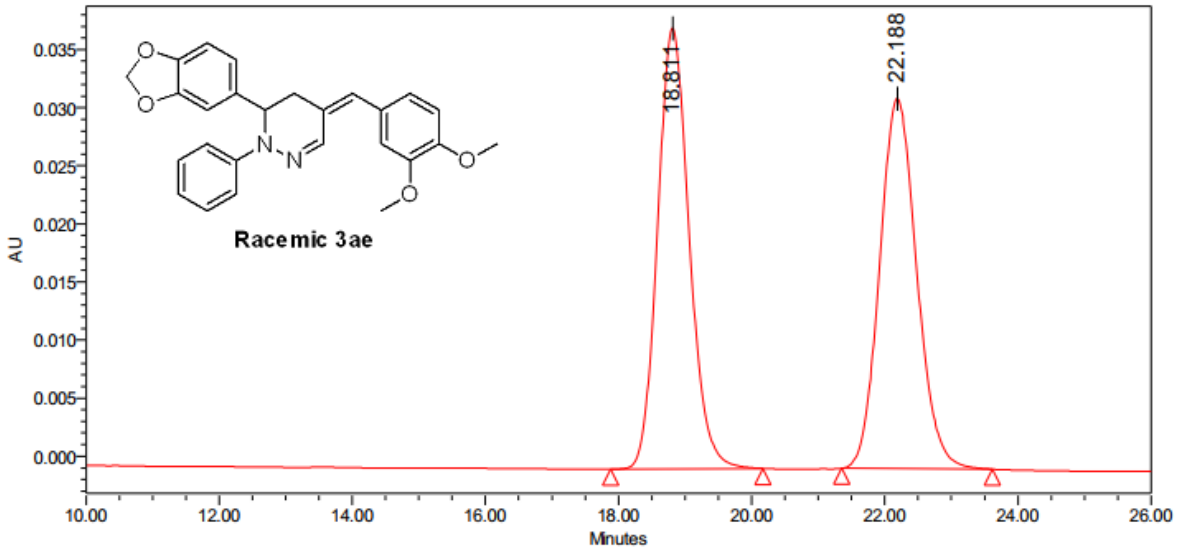

Peak Results

	Name	RT	Area	% Area
1		18.811	1248367	50.30
2		22.188	1233629	49.70

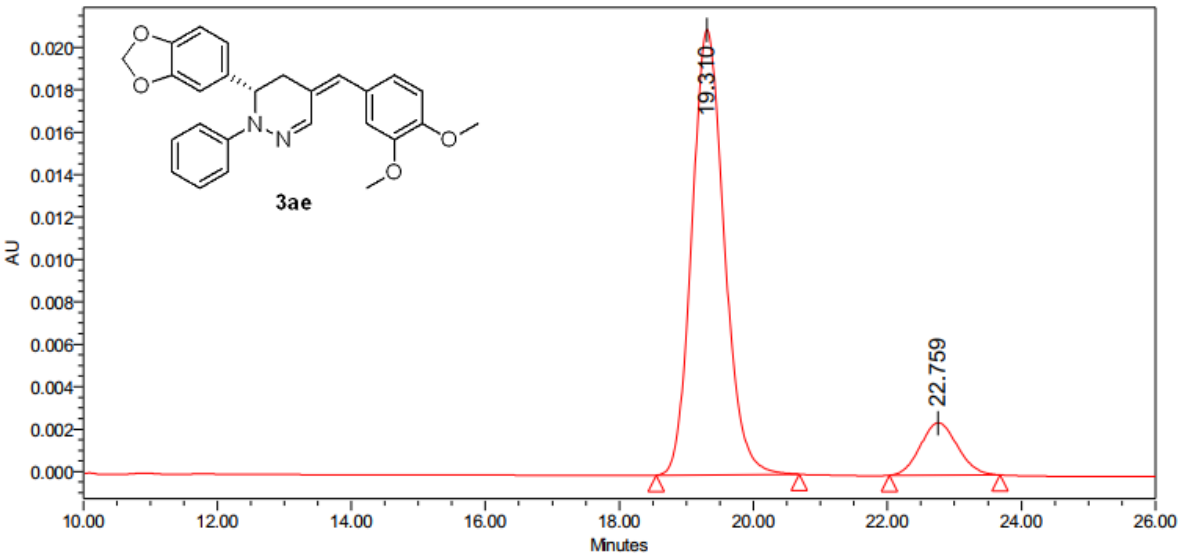

Peak Results

	Name	RT	Area	% Area
1		19.310	704241	88.11
2		22.759	95061	11.89

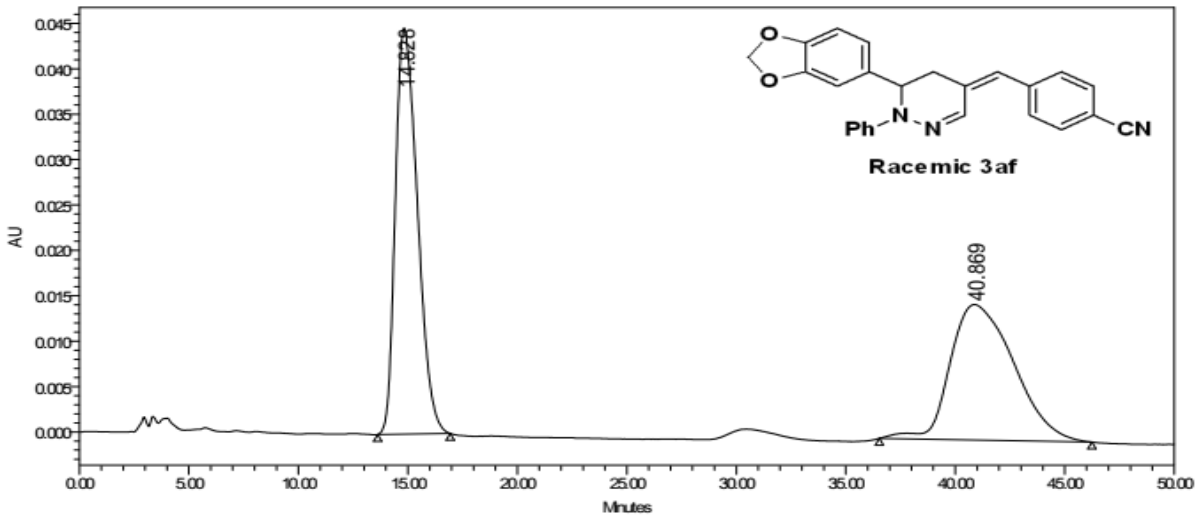

	RT	Area	%Area	Height
1	14.828	3140188	50.96	44692
2	40.869	3022468	49.04	14921

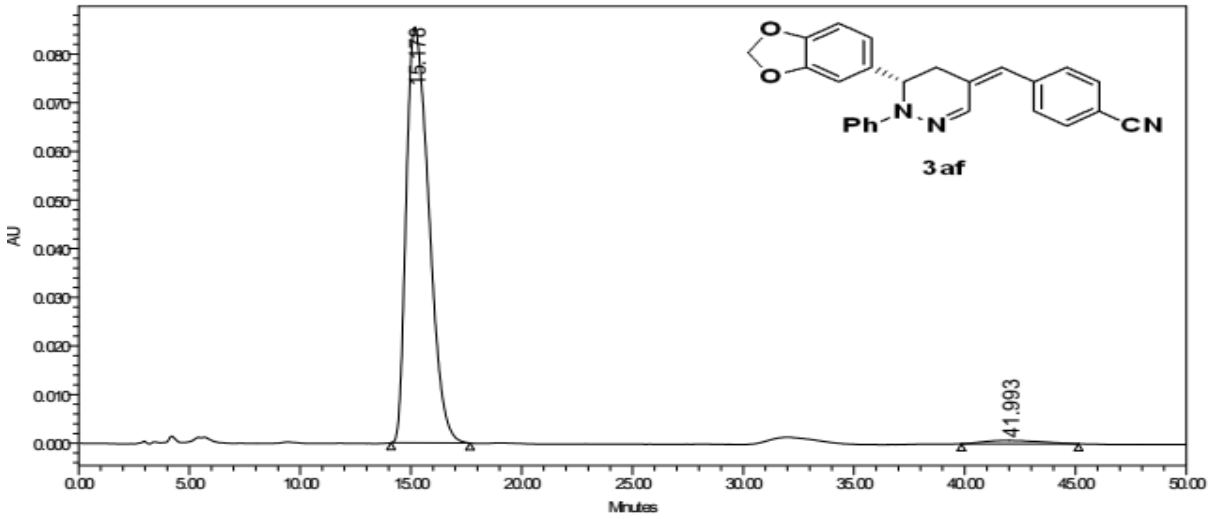

	RT	Area	%Area	Height
1	15.178	6060025	98.01	85493
2	41.993	122560	1.99	696

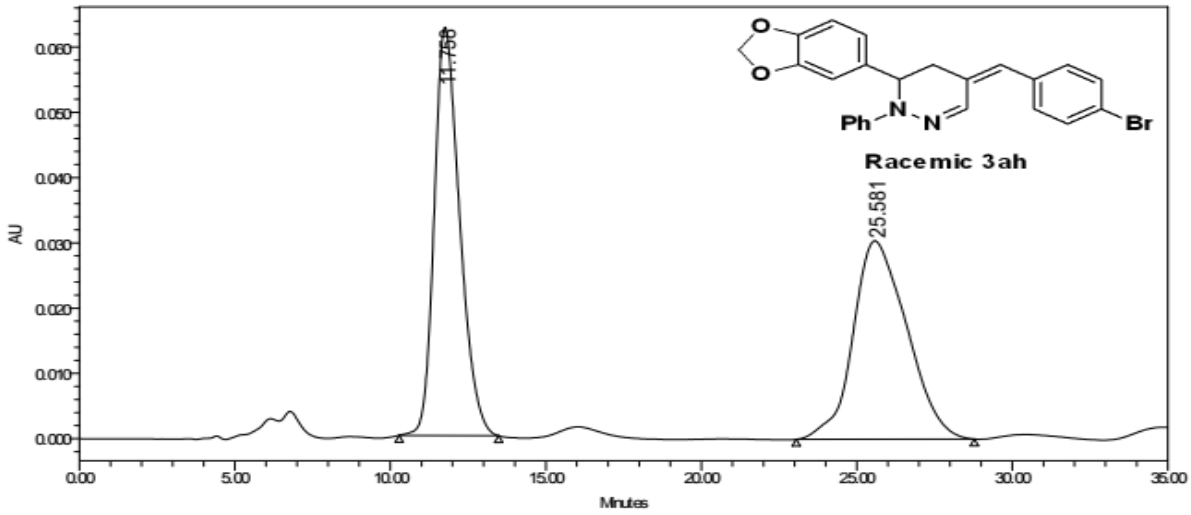

	RT	Area	%Area	Height
1	11.758	3663742	49.38	62561
2	25.581	3653114	50.62	30385

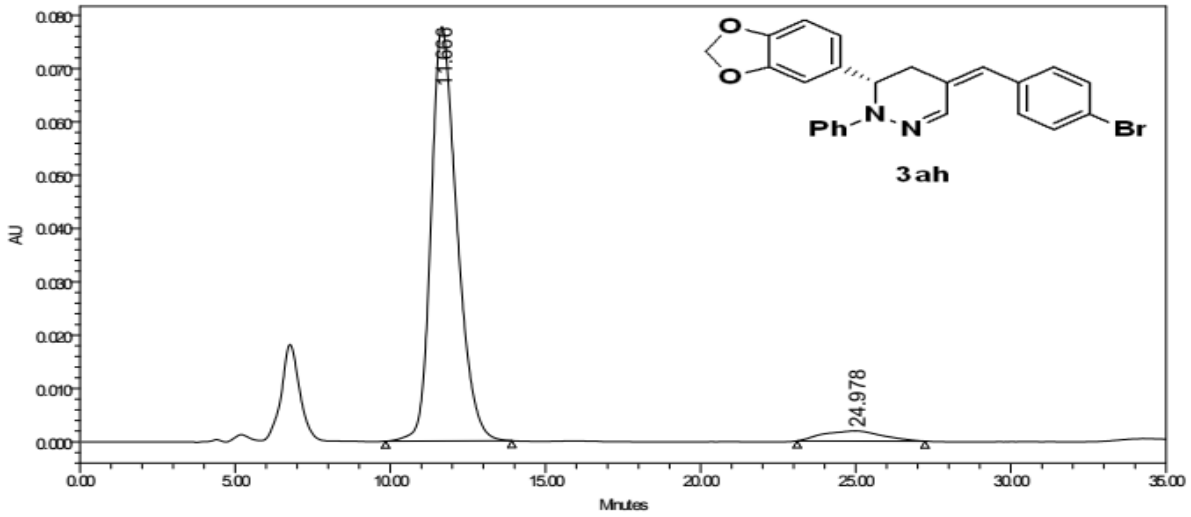

	RT	Area	%Area	Height
1	11.664	4507470	94.78	77649
2	24.978	248154	5.22	1884

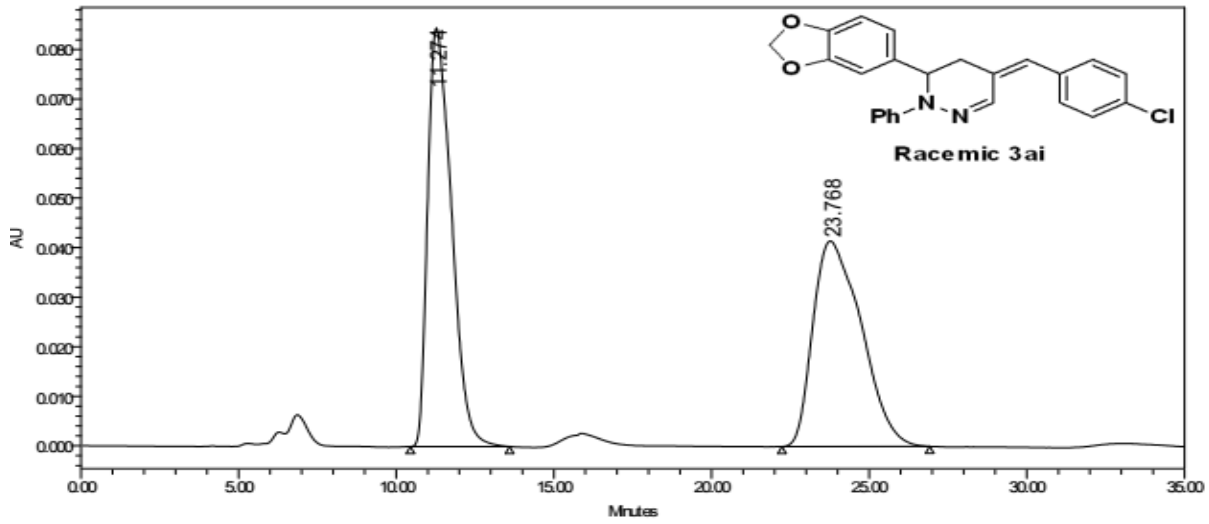

	RT	Area	%Area	Height
1	11.274	4440321	50.09	84459
2	23.768	4423564	49.91	41499

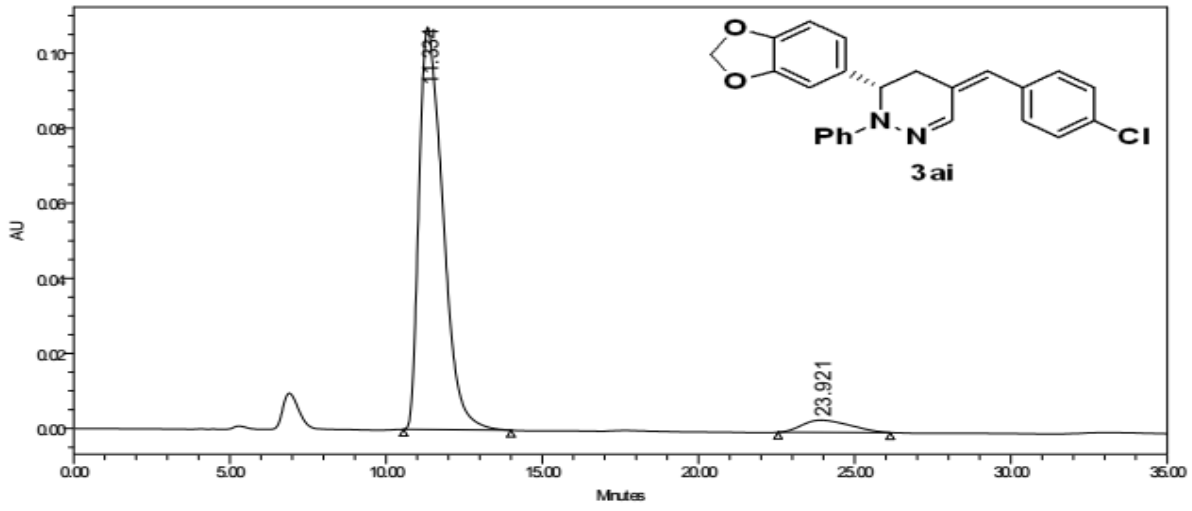

	RT	Area	%Area	Height
1	11.334	5883521	94.31	107140
2	23.921	342614	5.69	3249

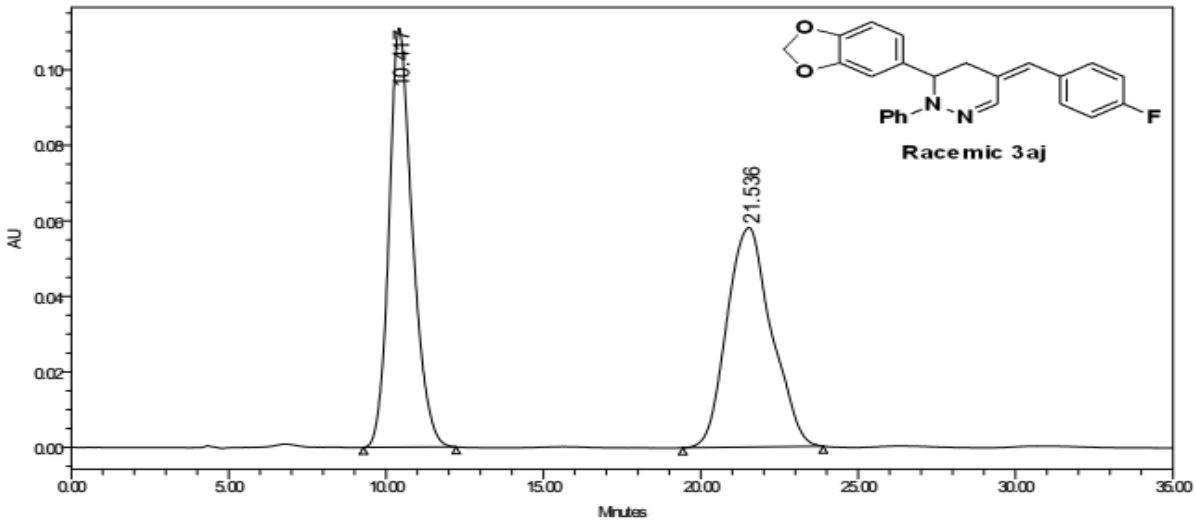

	RT	Area	%Area	Height
1	10.417	5743051	50.08	110960
2	21.536	5725392	49.92	58166

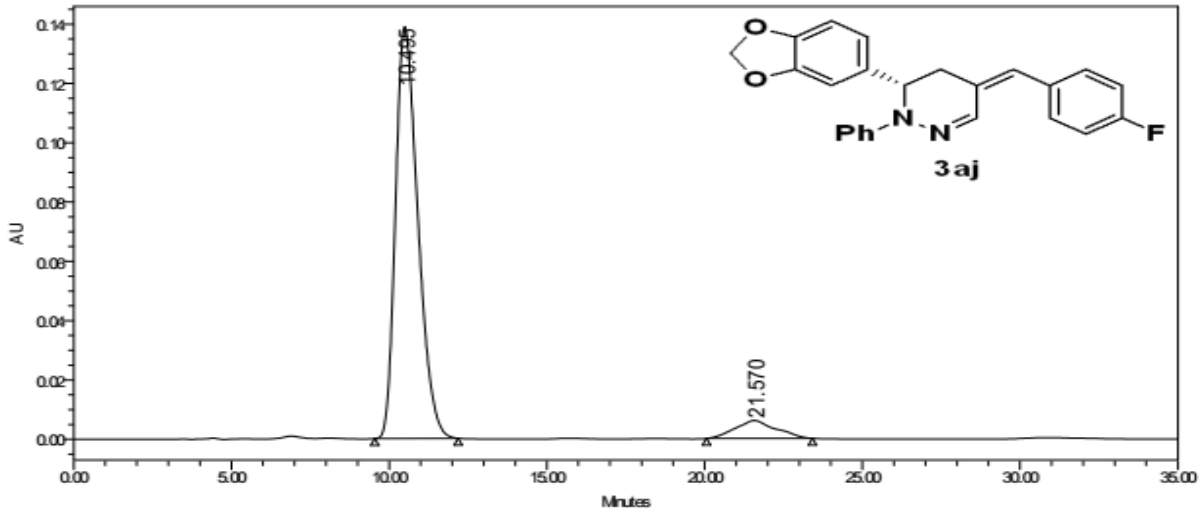

	RT	Area	%Area	Height
1	10.495	6832067	92.70	138774
2	21.570	538326	7.30	6009

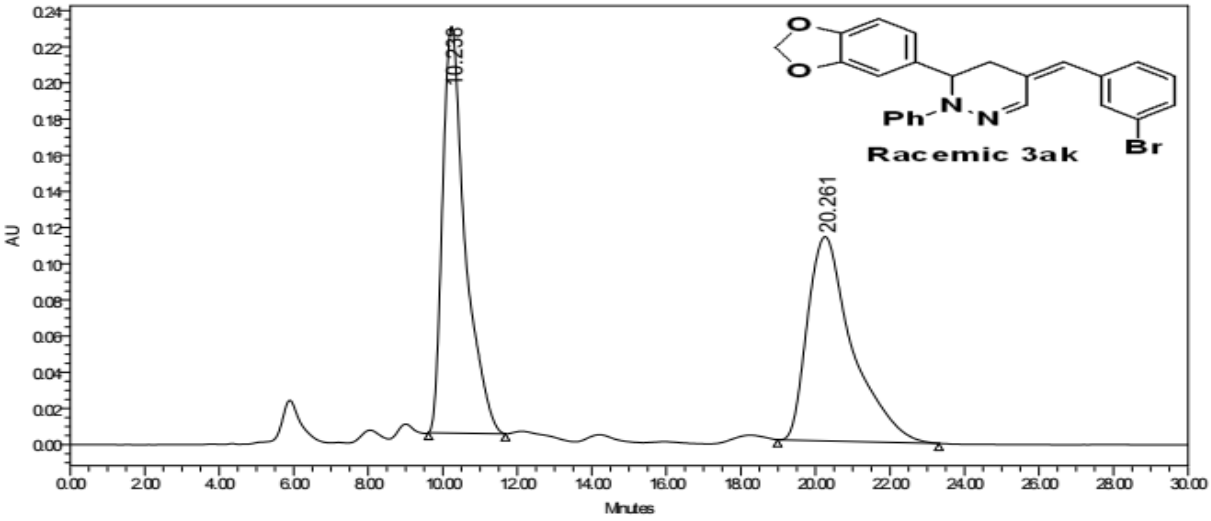

	RT	Area	%Area	Height
1	10.238	9490204	50.21	224675
2	20.261	9409422	49.79	112838

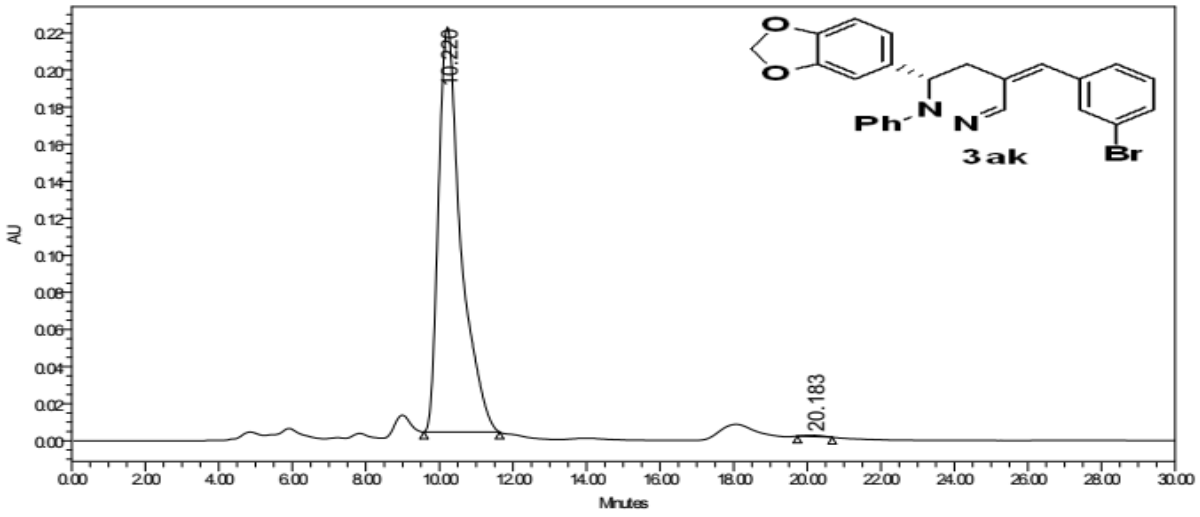

	RT	Area	%Area	Height
1	10.220	9256861	99.73	218429
2	20.183	25281	0.27	705

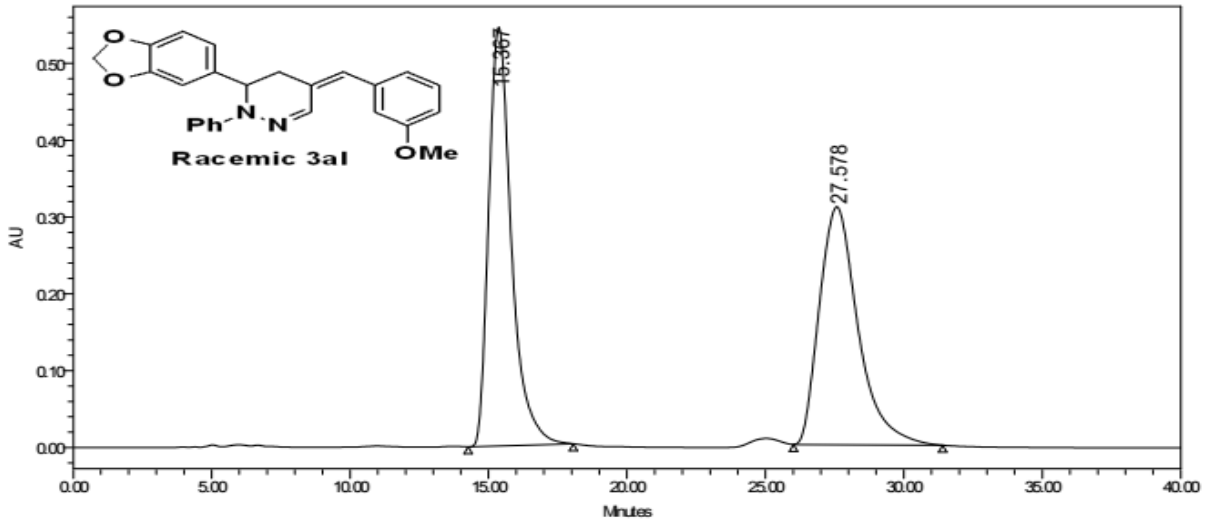

	RT	Area	%Area	Height
1	15.367	31026029	50.78	544699
2	27.578	30075809	49.22	309480

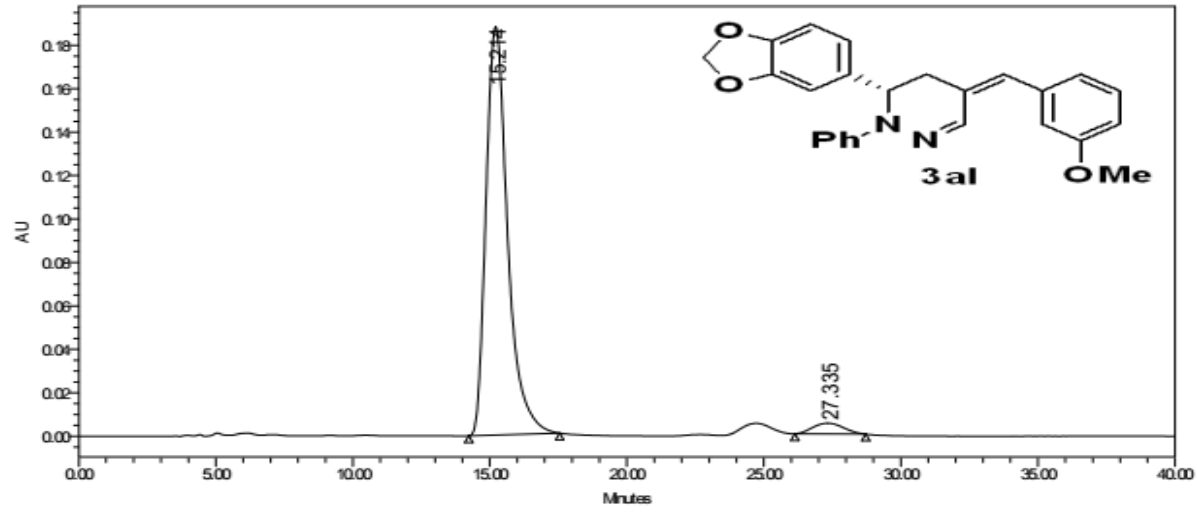

	RT	Area	%Area	Height
1	15.214	10317420	96.38	187926
2	27.335	387932	3.62	4949

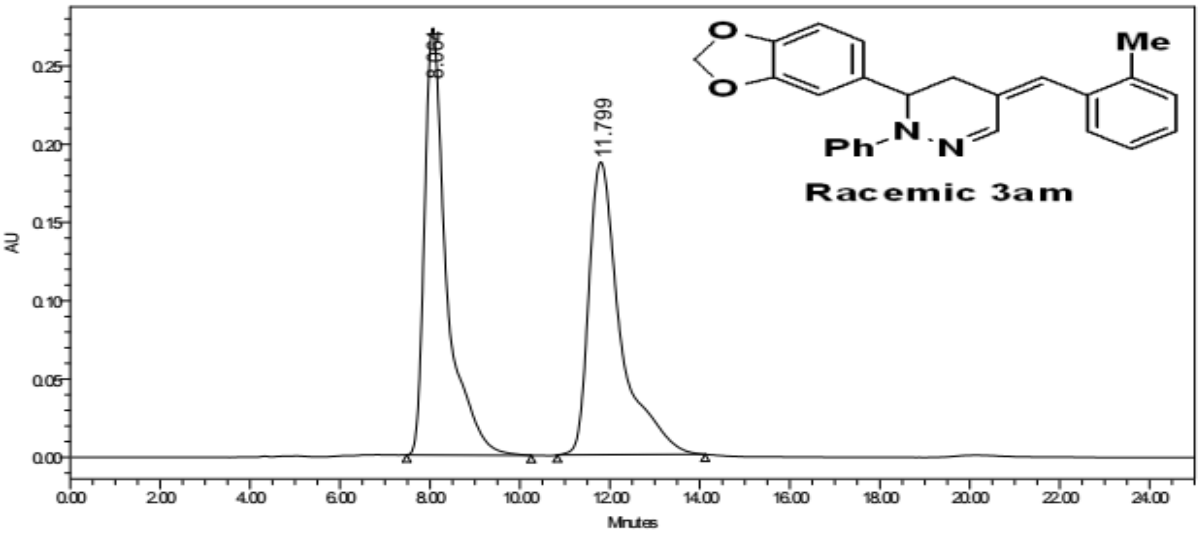

	RT	Area	%Area	Height
1	8.064	9369665	50.48	272518
2	11.79[illegible]	9181547	49.52	187148

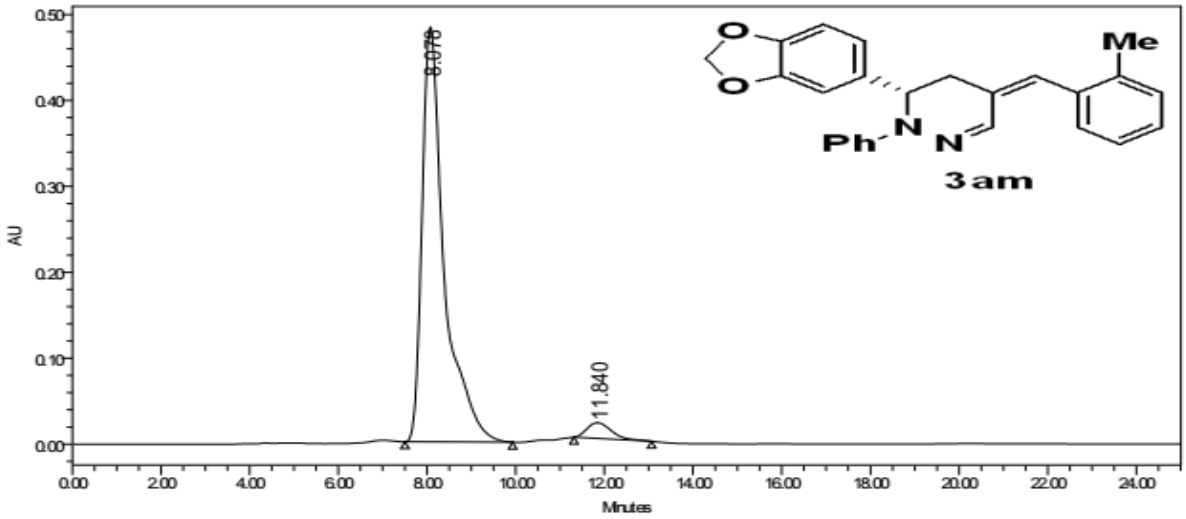

	RT	Area	%Area	Height
1	8.078	16779904	95.96	482877
2	11.84[illegible]	705953	4.04	18246

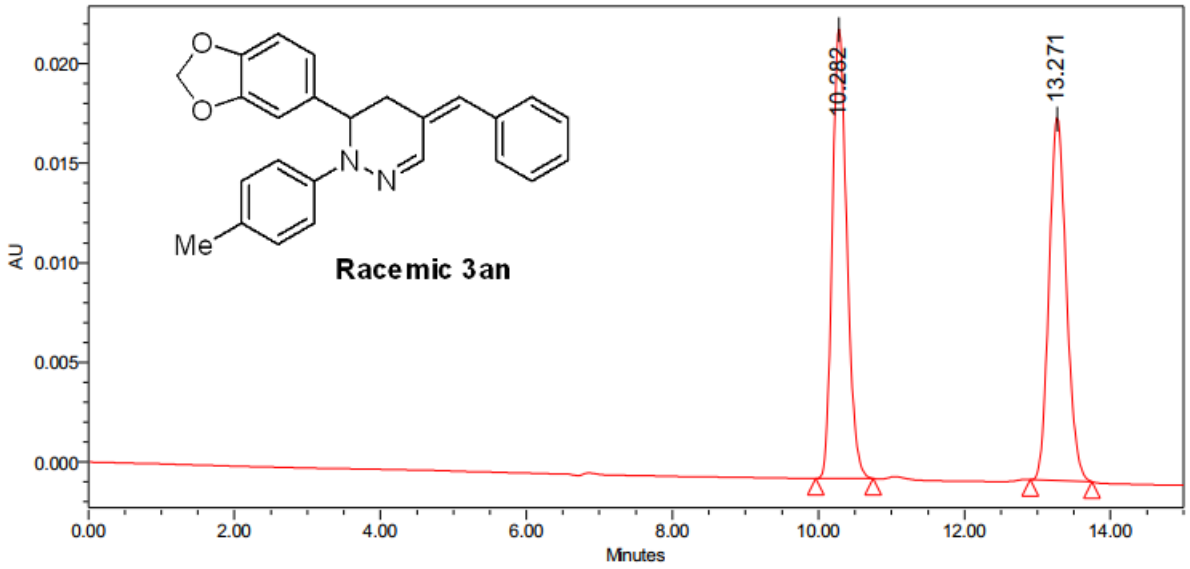

Peak Results

	Name	RT	Area	% Area
1		10.282	311050	50.91
2		13.271	299979	49.09

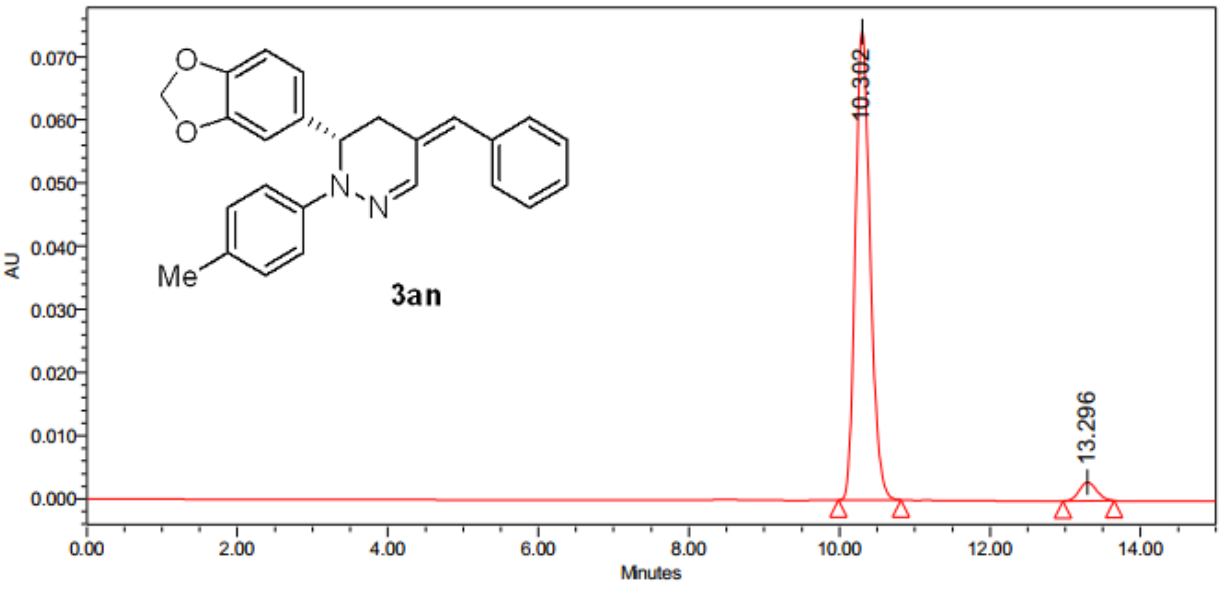

Peak Results

	Name	RT	Area	% Area
1		10.302	1017861	95.57
2		13.296	47214	4.43

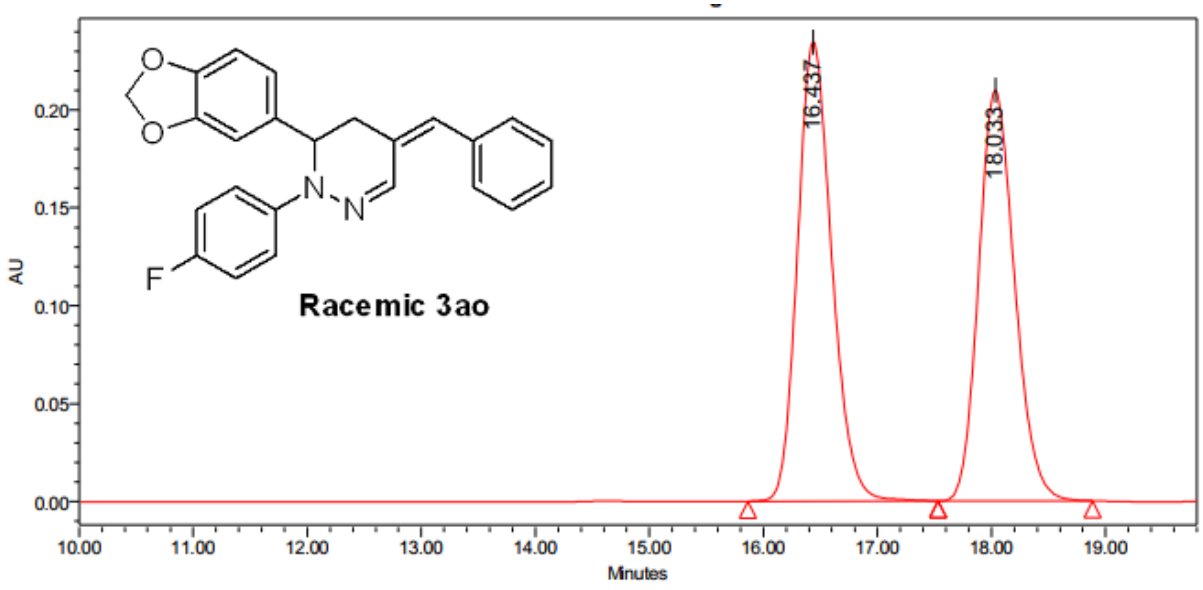

Peak Results

	Name	RT	Area	% Area
1		16.437	4894584	51.58
2		18.033	4594322	48.42

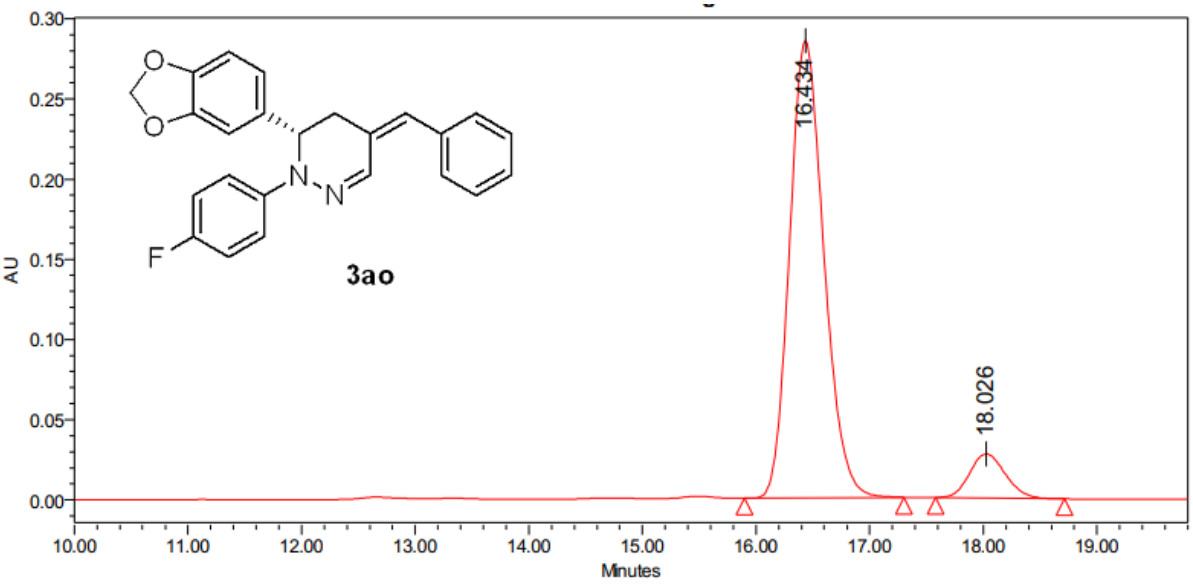

Peak Results

	Name	RT	Area	% Area
1		16.434	5980793	90.84
2		18.026	602795	9.16

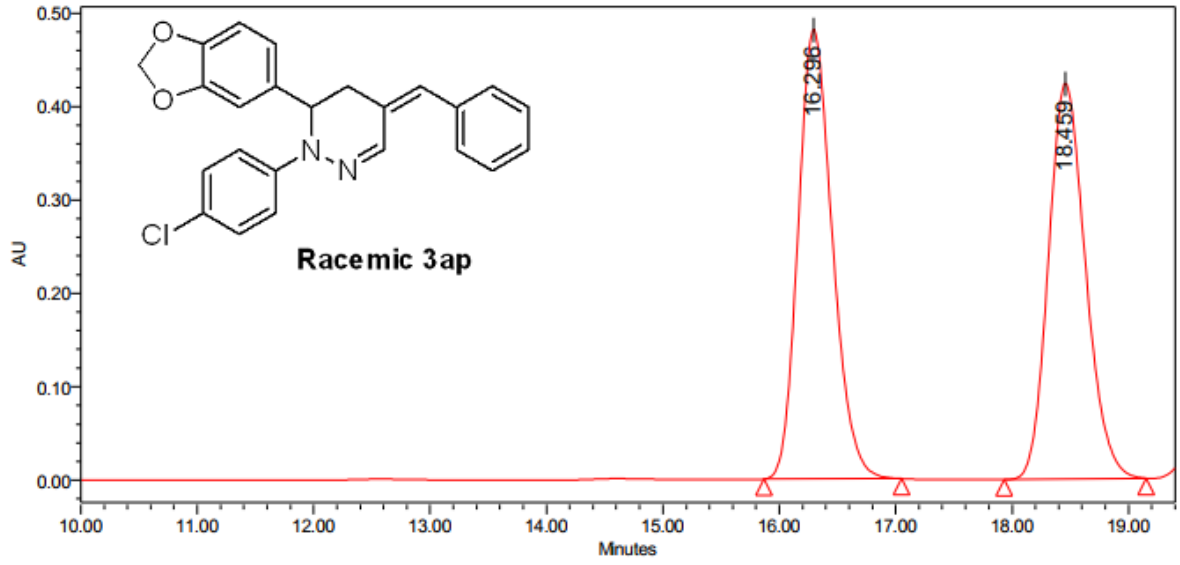

Peak Results

	Name	RT	Area	% Area
1		16.296	9852350	51.25
2		18.459	9373000	48.75

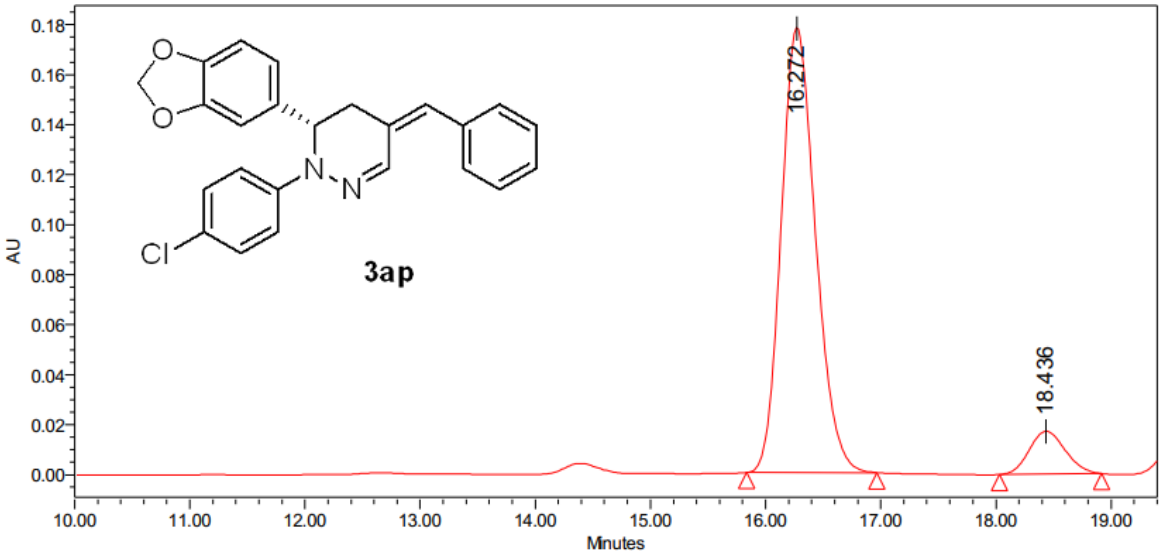

Peak Results

	Name	RT	Area	% Area
1		16.272	3680620	90.82
2		18.436	372009	9.18

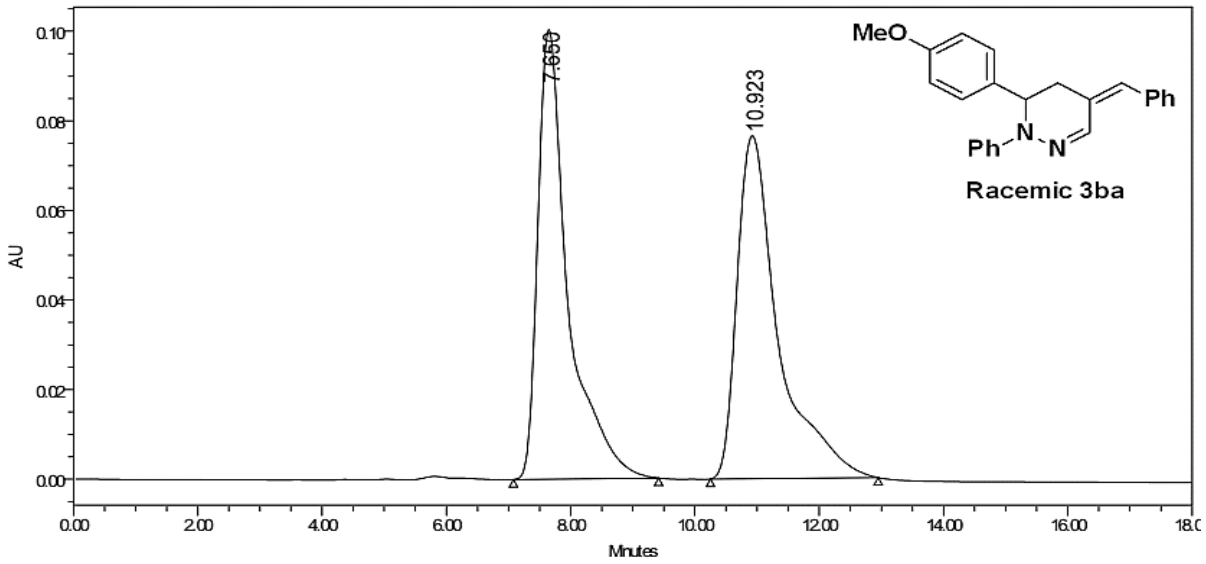

	RT	Area	%Area	Height
1	7.660	3387648	49.00	100328
2	10.923	3525973	51.00	76572

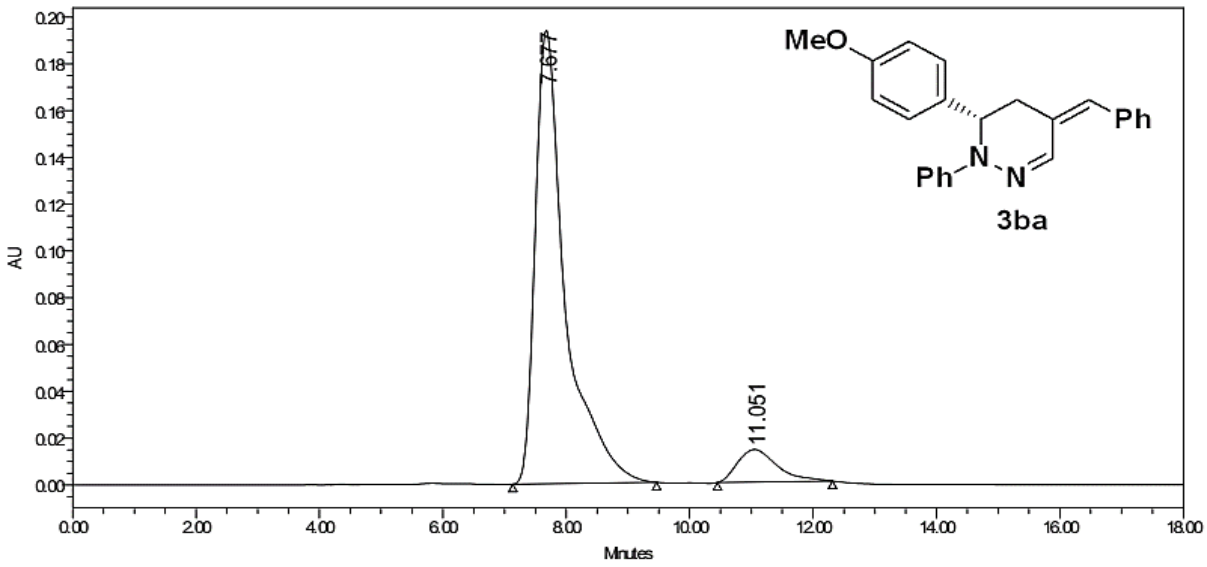

	RT	Area	%Area	Height
1	7.677	6568652	91.32	193792
2	11.051	623552	8.68	13934

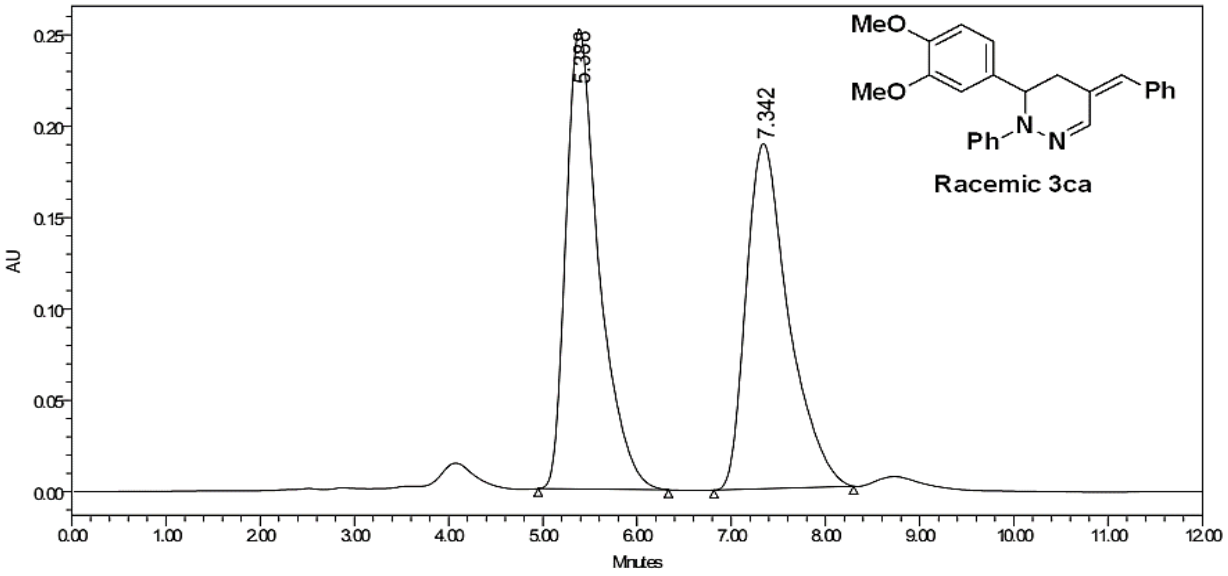

	RT	Area	%Area	Height
1	5.388	6129534	50.82	251772
2	7.342	5930722	49.18	189098

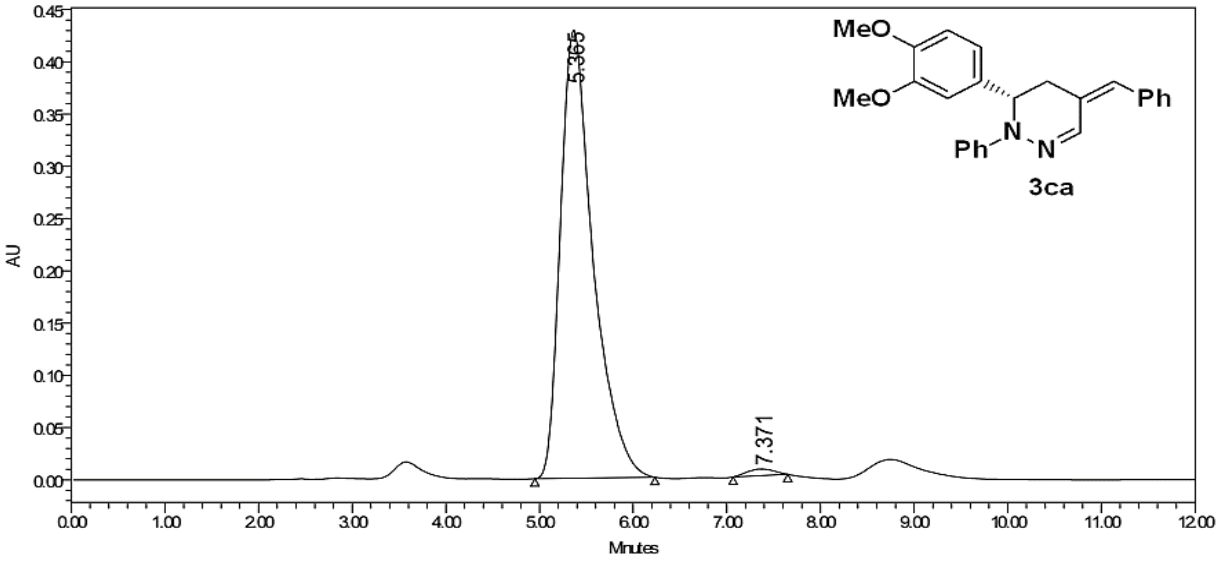

	RT	Area	%Area	Height
1	5.365	10403098	98.79	428760
2	7.371	127945	1.21	6320

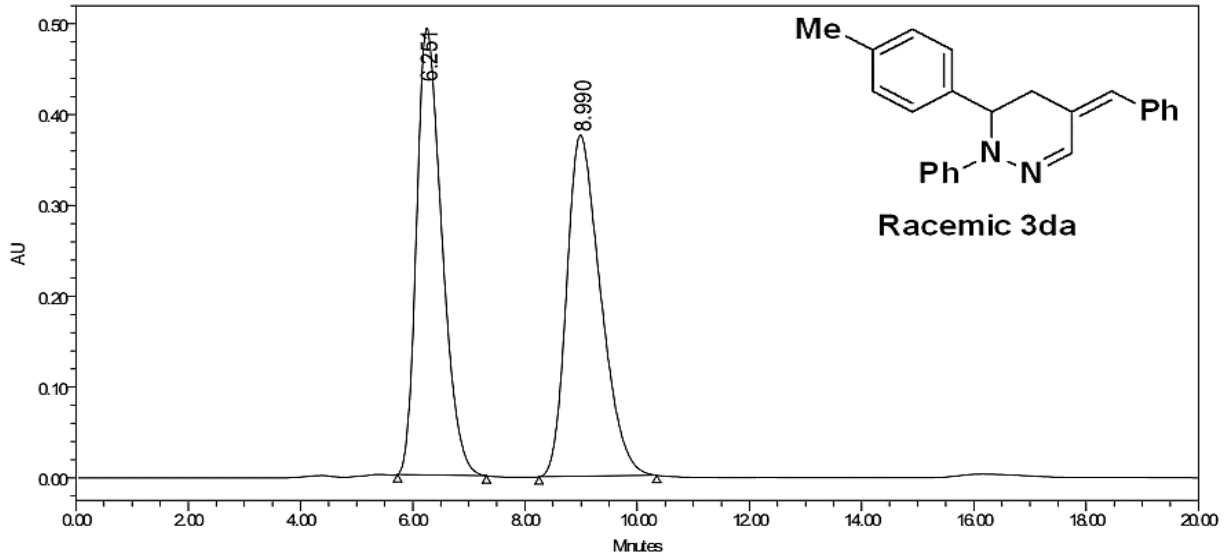

	RT	Area	%Area	Height
1	6.251	15430007	49.42	492010
2	8.990	15791892	50.58	375740

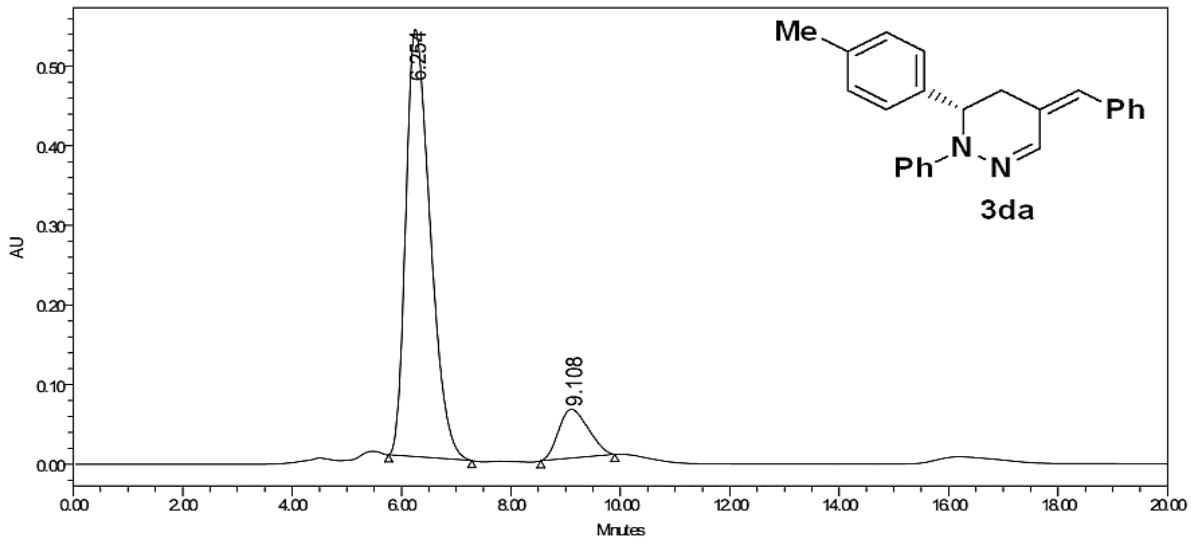

	RT	Area	%Area	Height
1	6.254	16644943	87.81	536838
2	9.108	2310729	12.19	61354

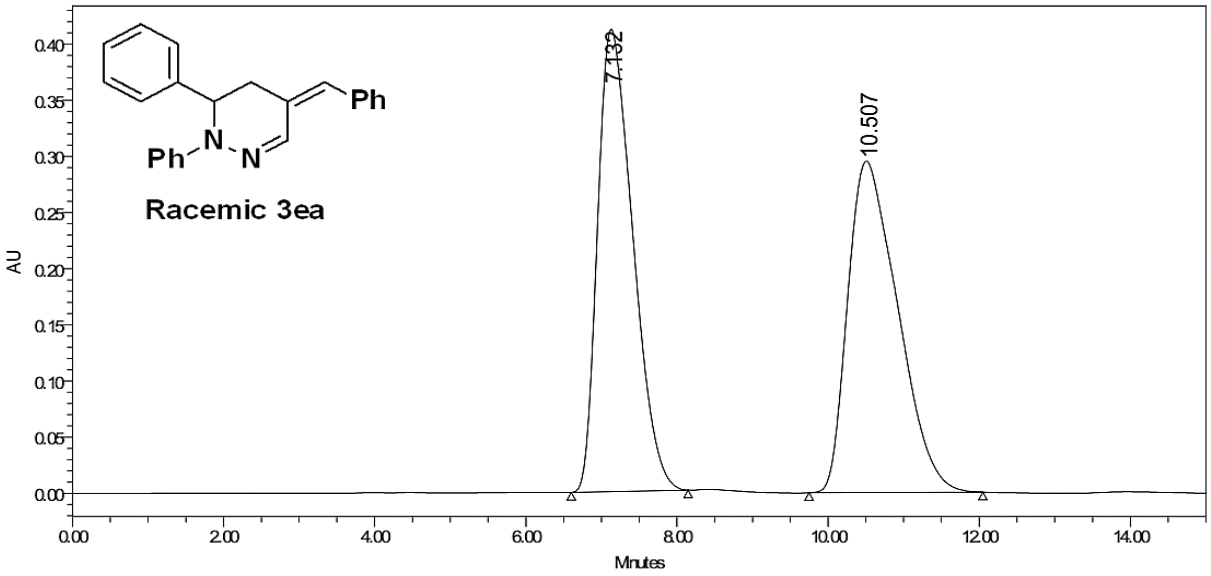

	RT	Area	%Area	Height
1	7.132	13374192	49.63	411743
2	10.507	13572044	50.37	295257

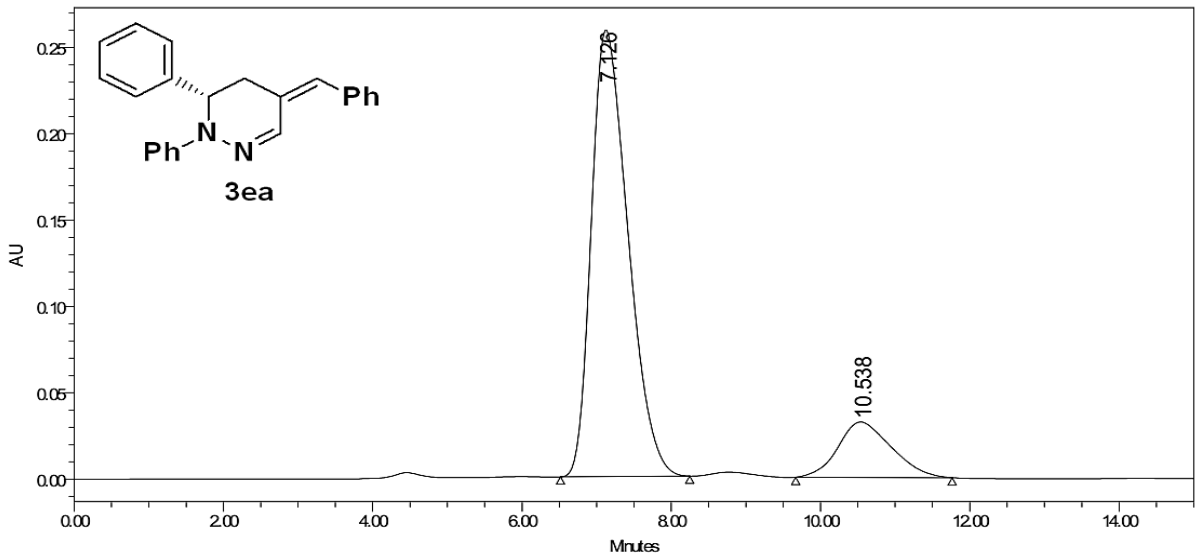

	RT	Area	%Area	Height
1	7.126	8846516	84.71	258620
2	10.538	1596606	15.29	32125

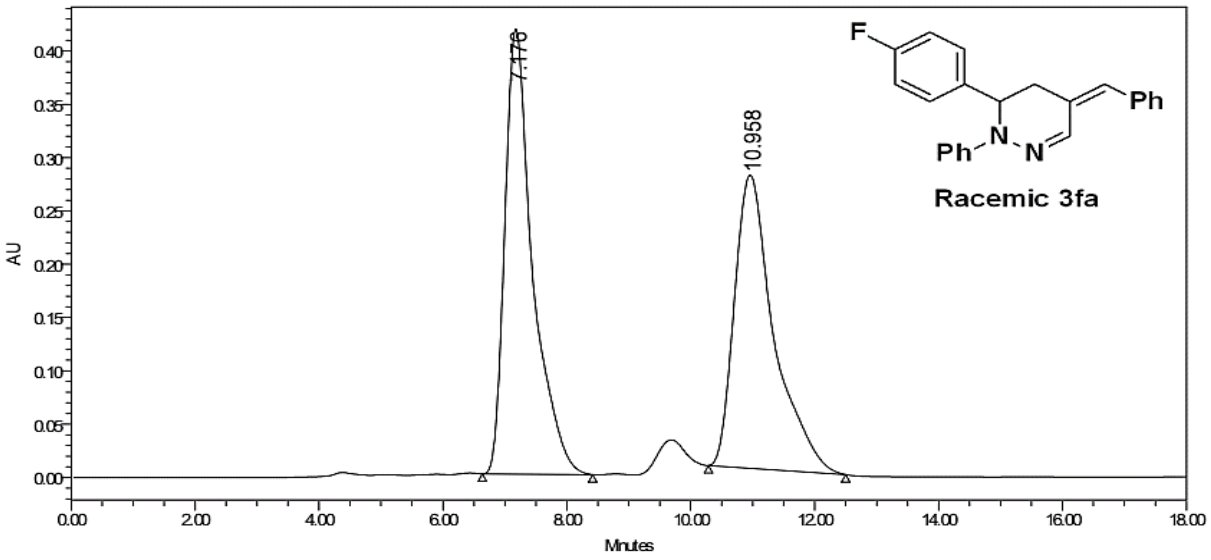

	RT	Area	%Area	Height
1	7.176	12979237	51.63	417383
2	10.958	12159321	48.37	275023

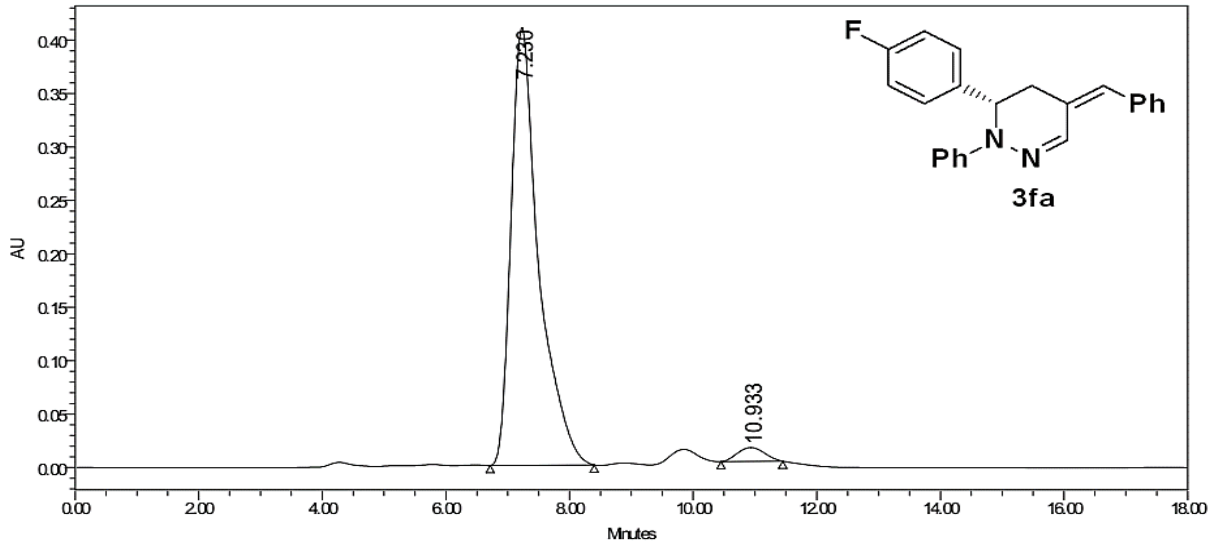

	RT	Area	%Area	Height
1	7.230	12799743	97.02	409519
2	10.933	392958	2.98	12865

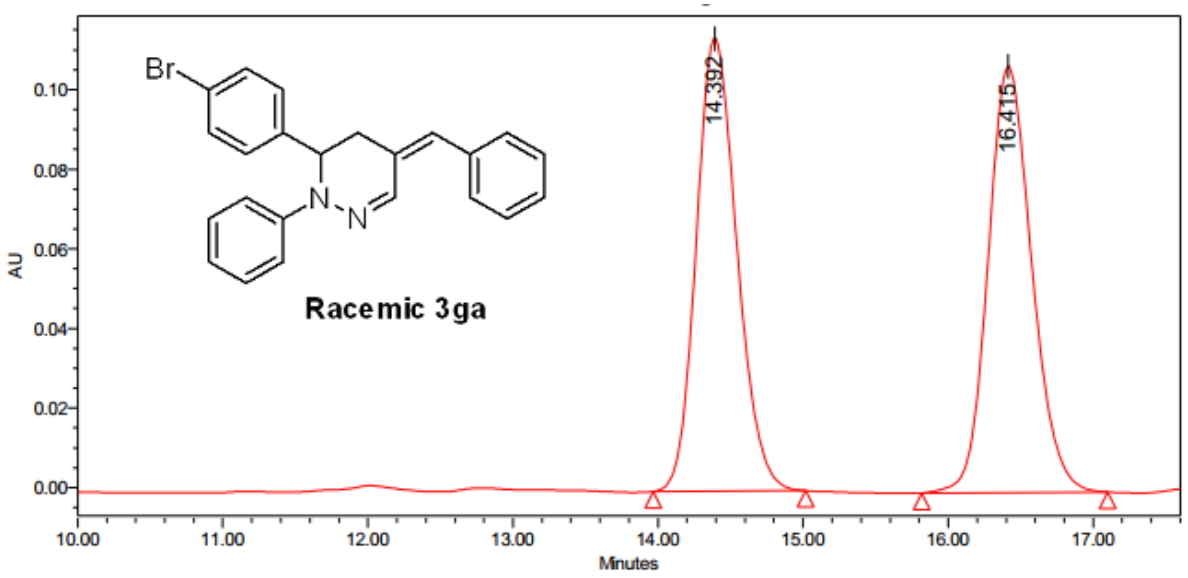

Peak Results

	Name	RT	Area	% Area
1		14.392	2214877	49.70
2		16.415	2241608	50.30

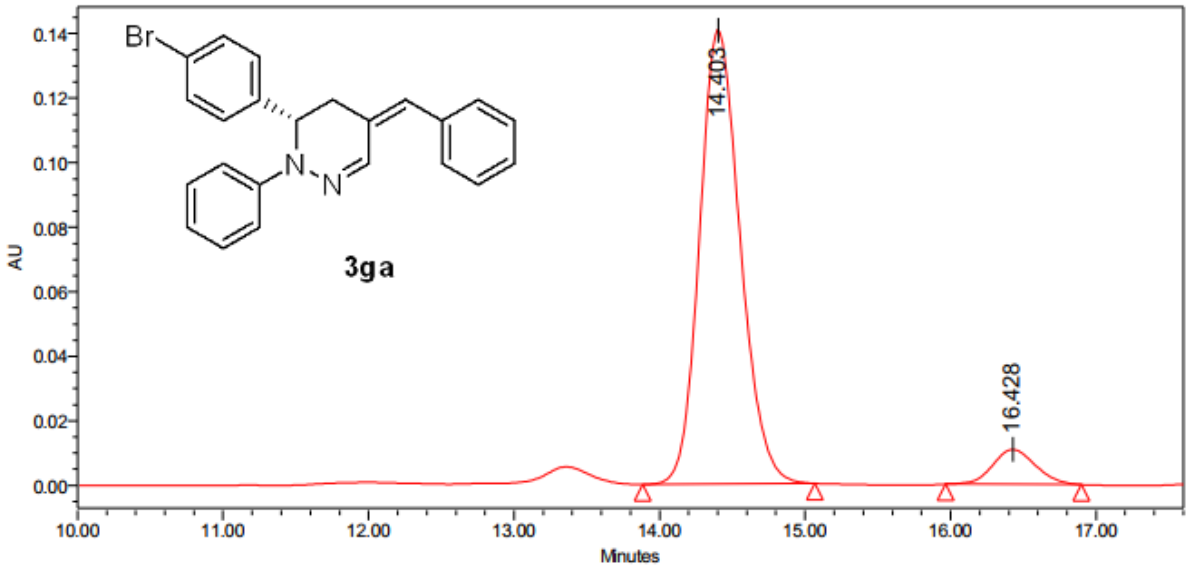

Peak Results

	Name	RT	Area	% Area
1		14.403	2730122	92.55
2		16.428	219797	7.45

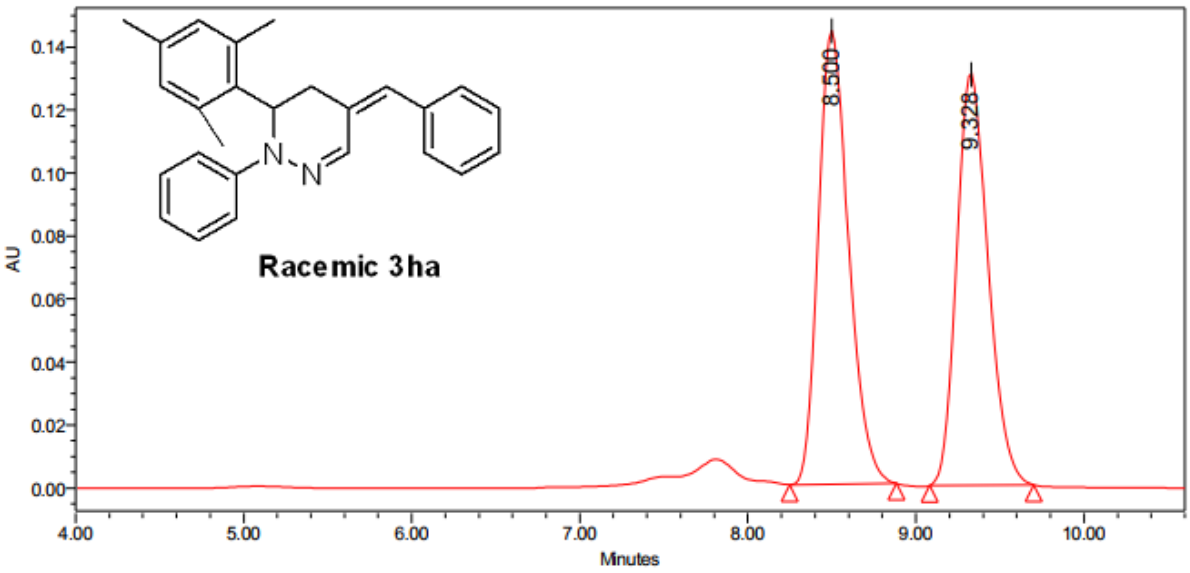

Peak Results

	Name	RT	Area	% Area
1		8.500	1805019	51.52
2		9.328	1698699	48.48

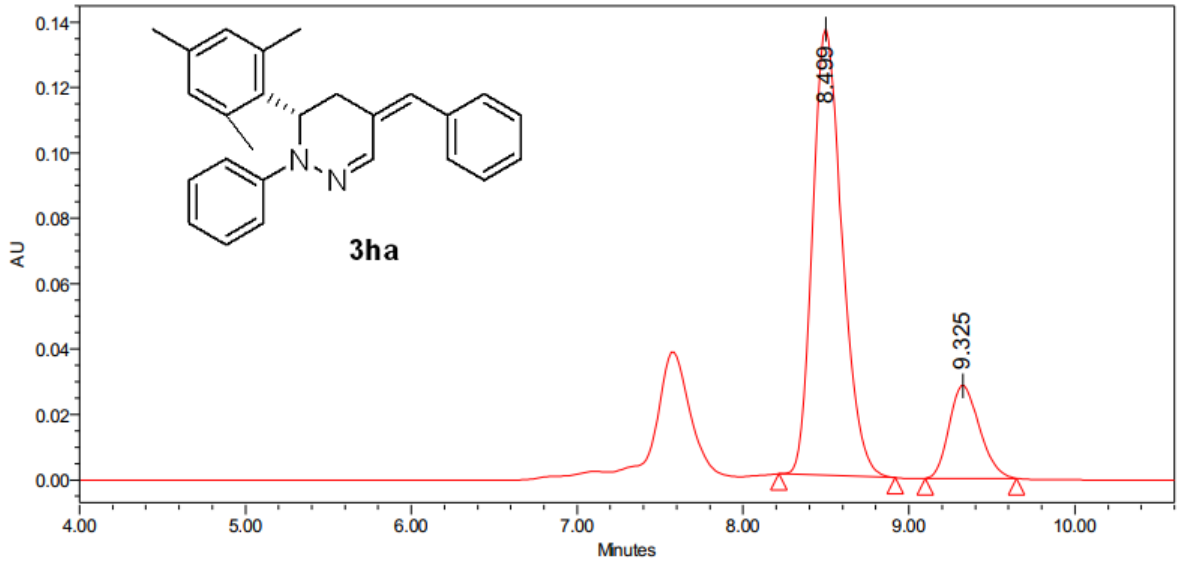

Peak Results

	Name	RT	Area	% Area
1		8.499	1687525	82.34
2		9.325	362023	17.66

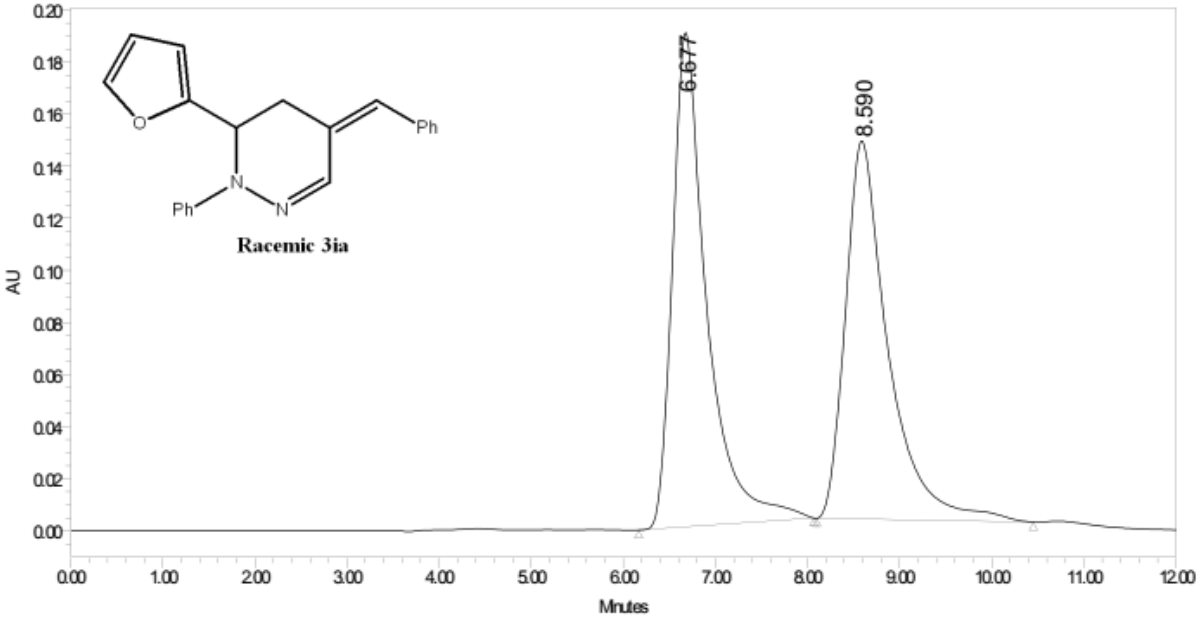

	RT	Area	%Area	Height
1	6.677	4888277	51.14	189846
2	8.590	4670529	48.86	145270

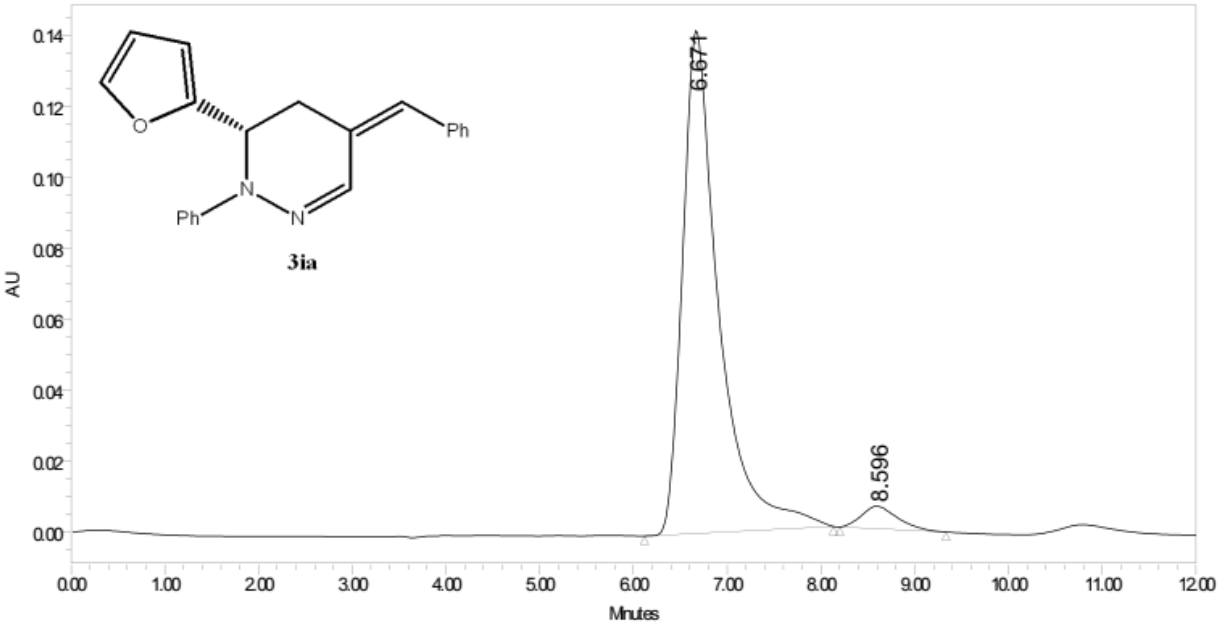

	RT	Area	%Area	Height
1	6.671	3800808	95.72	141552
2	8.596	169914	4.28	6349

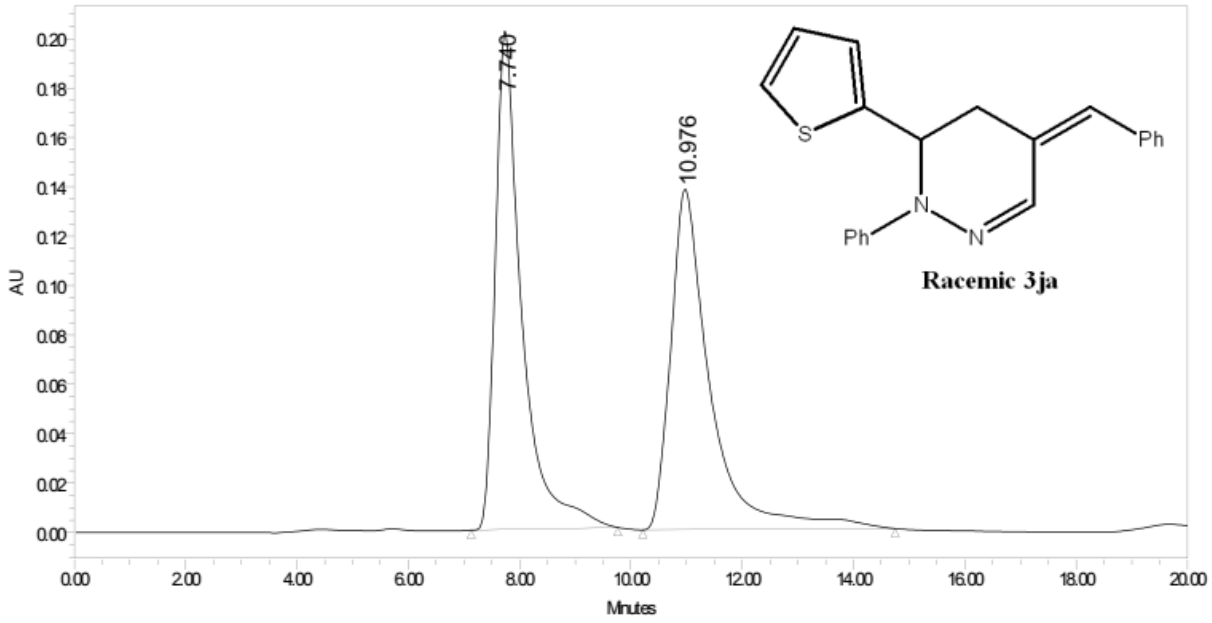

	RT	Area	%Area	Height
1	7.740	6658549	49.50	201875
2	10.976	6791792	50.50	137889

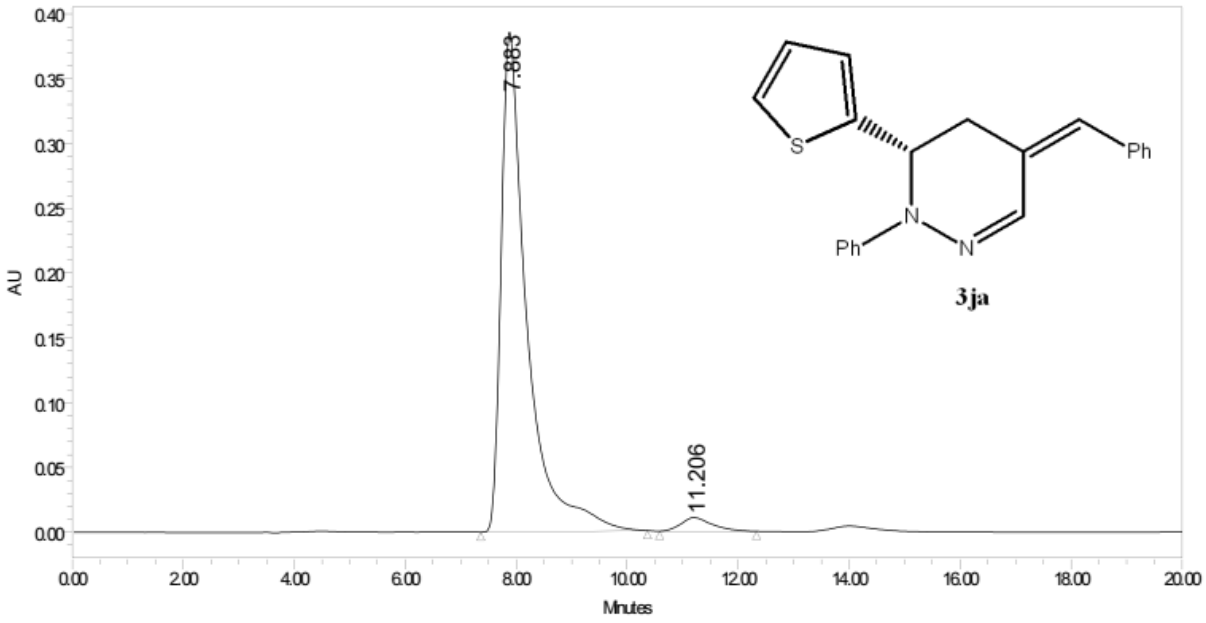

	RT	Area	%Area	Height
1	7.883	12408540	96.84	385517
2	11.206	404939	3.16	10454

Chapter 2B

Organocatalytic (3+3)-Cycloaddition of *Ortho*-Substituted Phenyl Nitrones with Aryl Cyclopropane Carbaldehydes: A Facile Access to Enantioenriched 1,2-Oxazinanes

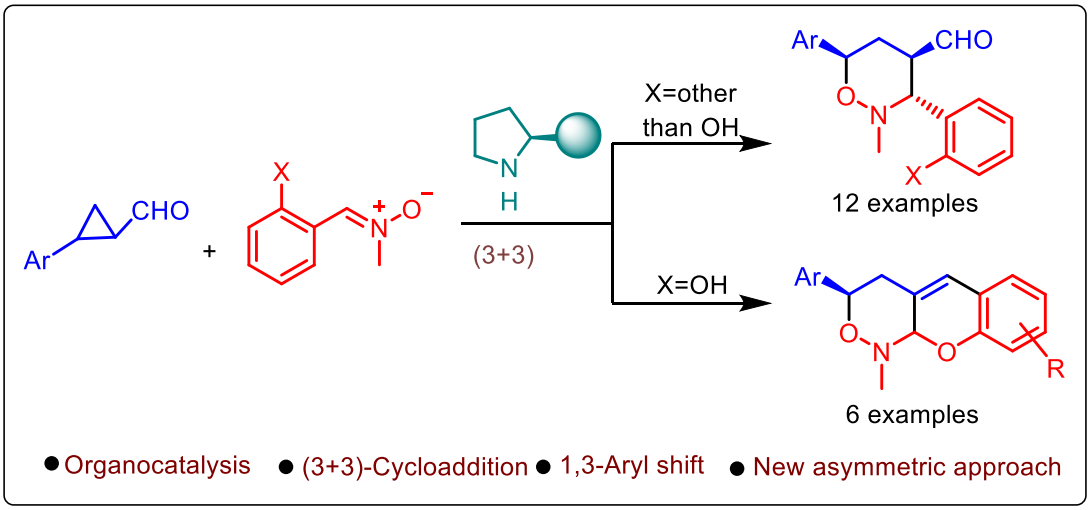

This work was published in *Chemical Communications* (A journal of *The Royal Society of Chemistry*). Please see the citation "Hazra, A.; Asit Ghosh, A.; Yadav, N.; Banerjee, P. *Chem. Commun.* **2023**, *59*, 11133–11136."

2.B.1. Introduction

Nitrogen-containing enantioenriched heterocycles are ubiquitous structural frameworks that are present in a diverse range of biologically active molecules.[1] Among them, chiral 1,2-oxazinanes gathered significant attention owing to their presence in several natural products which exhibit potent biological activities.[2] Therefore, a number of methodologies flourished over the decades for their enantioselective construction by various research groups; however, most of them involve nitrones as a main precursor.[3] Nitrones are one of the most useful and easily available starting materials for the construction of various biologically important nitrogen and oxygen-containing heterocycles.[3] Especially its ability to undergo the 1,3-dipolar cycloaddition has achieved remarkable attention from synthetic organic chemists for the past few decades.[3] In 2005, Sibi and coworkers reported the first enantioselective (3+3)-cycloaddition of nitrones with cyclopropane dicarboxylates in the presence of $Ni(ClO_4)_2$ and chiral ligand to obtain tetrahydro-1,2-oxazines with high enantiomeric excesses (Scheme 2.B.1.1.a).[4] Henceforth, several groups utilized this moiety for the asymmetric cycloaddition reaction to achieve enantioenriched heterocyclic frameworks.[3] A substantial development was made for the metal-catalyzed enantioselective cycloaddition reaction in the last two decades, but organocatalytic cycloaddition with nitrones is rarely reported.[5] At the very beginning of this century, the first organocatalytic 1,3-dipolar cycloaddition of nitrones with α,β-unsaturated aldehydes was reported by MacMillan's group via chiral imidazolidinone based secondary amine catalyst.[5a] Since this pioneering work, only a few asymmetric transformations were studied with nitrones; however, most of them are (3+2) type cycloaddition.[5] Evidently, organocatalytic enantioselective (3+3)-cycloaddition reactions with nitrones are still underexplored. Recently, in 2020 Shi *et al.* reported the first organocatalytic (3+3)-cycloaddition reaction of nitrones with 2-indolylmethanols in an asymmetric manner by utilizing the cooperative catalysis of hexafluoroisopropanol (HFIP) and chiral phosphoric acid (CPA) (Scheme 2.B.1.1.b).[6] In a different way, we sought to develop an enantioselective (3+3)-cycloaddition of nitrones by utilizing secondary amine-based organocatalysis with an appropriate three-carbon reacting partner.

In this context, donor-acceptor cyclopropanes are one of the most exploited three-membered synthons for their unique properties.[7] Over the years, this smallest carbocycle has achieved a remarkable evolution by engineering numerous cycloaddition reactions for the construction of various carbo- and heterocyclic frameworks of biological importance.[8] Our lab has been working in the field of donor-acceptor cyclopropane for the last decade and has established several notable transformations by Lewis and Brønsted acid catalysis.[9] We envisaged an organocatalytic approach to achieve asymmetric cycloaddition of donor-acceptor cyclopropane carbaldehydes (DACC) via iminium activation, which is rarely reported in the literature.[10] Though few enantioselective ring-opening reactions of *meso*-cyclopropane carbaldehydes were discussed earlier[11], the asymmetric

Scheme 2.B.1.1. Reports of enantioselective (3+3)-cycloaddition of Nitrones

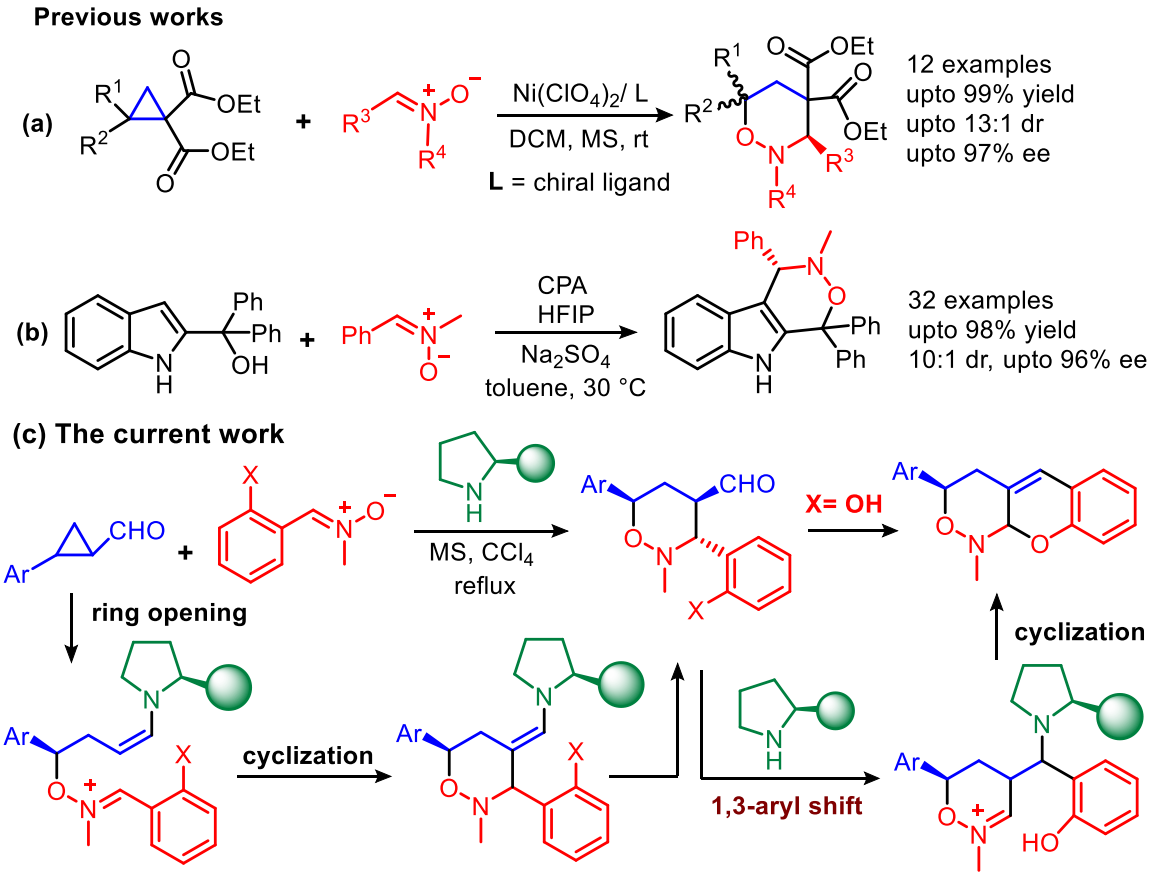

cycloaddition of *racemic*-DACCs still remains a challenge. In this endeavor, we envisioned that nitrones could undergo (3+3)-cycloaddition with the iminium-activated DACCs. Herein, we report an organocatalytic enantioselective (3+3)-cycloaddition of *trans racemic*-DACCs with *ortho*-substituted phenyl nitrones for the construction of enantioenriched 1,2-oxazinanes along with a novel class of compounds, i.e., tetrahydrochromeno[2,3-*c*][1,2]oxazines (Scheme 2.B.1.1.c).

2.B.2. Result and Discussion

We started to investigate our optimization studies with *para*-methoxyphenyl cyclopropane carbaldehyde **1a** and *ortho*-methyl phenyl nitrone **2a** as model substrates (Table 2.B.1.1). At first, the reaction was performed with 1 equivalent of **1a** and 1.5 equivalent of **2a** with 40 mol% of catalyst **I** in the presence of 4 Å molecular sieves in CCl_4 solvent at refluxing condition. Delightfully, our desired (3+3)-annulated product **4aa** was obtained after 10 hours in 44% yield with 75:25 enantiomeric ratio and 4:1 diastereomeric ratio (entry 1, Table 2.B.1.1). The stereochemistry of the major isomer of **4aa** was determined with the help of NOESY NMR and the crystal structure of **5aa** (*vide infra*). Here it is worth mentioning that, along with the desired product, the corresponding *para*-methoxy benzaldehyde **1a'** was also forming, which is believed to be a

Table 2.B.2.1. Optimization studies[a]

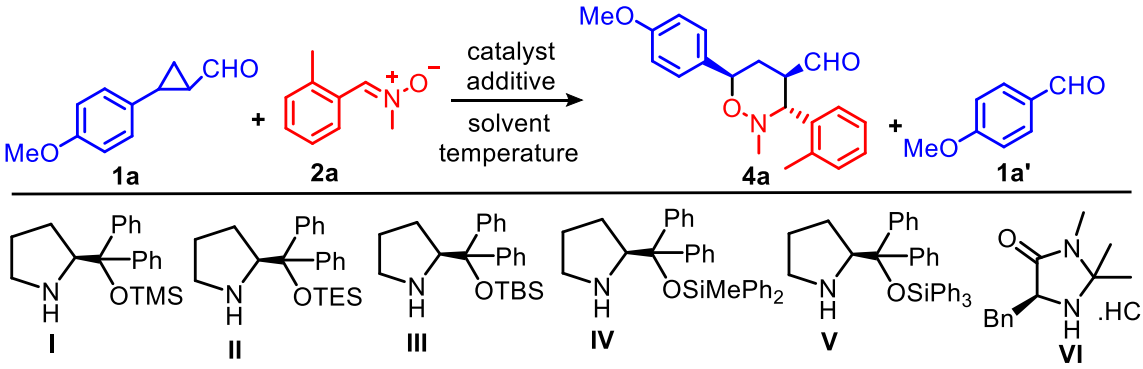

entry	catalyst	solvent	additive	yield[b] (%)	*er*[c]	dr[d]
1	I	CCl_4	-	45	75:25	4:1
2	I	DCM	-	n.r.[e]	-	-
3	I	DCE	-	n.r.[e]	-	-
4	I	$CHCl_3$	-	n.r.[e]	-	-
5	I	CH_3CN	-	n.r.[e]	-	-
6	I	Toluene	-	n.r.[e]	-	-
7	I	CCl_4	$PhCO_2H$	Cu(OTf)2[f]	-	-
8	I	CCl_4	TfOH	c.m.[f]	-	-
9	I	CCl_4	TFA	c.m.[f]	-	-
10	I	CCl_4	Et_3N	35	56:44	3:2
11	I	CCl_4	DABCO	36	57:43	3:1
12	I	CCl_4	DMAP	40	53:47	2.5:1
13	I	CCl_4	K_2CO_3	10	74:26	1.2:1
14	II	CCl_4	-	40	62:38	3:1
15	III	CCl_4	-	Trace	-	
16	IV	CCl_4	-	25	60:40	4:1
17	V	CCl_4	-	n.r.[e]	-	-
18	VI	CCl_4	-	n.r.[e]	-	-
19[g]	I	CCl_4	-	35	55:45	3:1
20[h]	I	CCl_4	-	35	75:25	4:1
21[i]	I	CCl_4	-	30	77:23	4:1
22[j]	I	CCl_4	-	35	55:45	1.1:1
23[k]	I	CCl_4	-	27	72:28	3:1
24[l]	I	CCl_4	-	22	54:46	2:1

[a]Unless otherwise all the reactions were carried out with 1 equiv. of **1a**, 1.5 equiv. of **2a**, 40 mol% of catalyst in the presence of 4 Å molecular sieves at refluxing condition for 10 h; [b]isolated yield by column chromatography; [c]determined by chiral HPLC analysis; [d]determined from crude nmr; [e]no reaction; [f]complex mixture; [g]reaction performed at room temperature for 6 d; [h]30 mol% catalyst taken; [i]50 mol% catalyst taken, [j]unsubstituted nitrone was used, [k]*para*-methyl nitrone was used, [l]*meta*-methoxy nitrone was used.

rearrangement product of **4a** (*vide infra*). Hereafter, various other reaction parameters were tested to increase both the yield and stereoselectivity of the product. At first, we checked the effect of solvents, but unfortunately, all other solvents, like DCM, $CHCl_3$, DCE, CH_3CN, and toluene failed to give the desired product (entries 2-6, Table 2.B.1.1). While complex reaction mixtures were

obtained with acid additives, possibly because of the substrate decomposition via Brønsted acid catalysis[12] (entries 7-9, Table 2.B.1.1), base additives like Et_3N, DABCO, DMAP, and K_2CO_3 failed to improve the stereoselectivity (entries 10-13, Table 2.B.1.1). Then we shifted our focus to other secondary amine-based prolinol catalysts to improve the enantioselectivity of the product. Whereas catalysts **II** and **IV** rendered the product with lower yield and stereoselectivity, catalyst **III** gave only a trace yield, and catalyst **V** could not catalyze the reaction (entries 14-17, Table 2.B.1.1). To our surprise, MacMillan's catalyst **VI** failed to catalyze this reaction (entry 18, Table 2.B.1.1). Finally, the effect of temperature was considered by performing the reaction at room temperature, which took a much longer time to give the product in a slightly decreased yield with almost no enantioselectivity (entry 19, Table 2.B.1.1). Similar stereoselectivity with no further improvement

Scheme 2.B.2.1. Substrate scope of cyclopropane carbaldehydes[a]

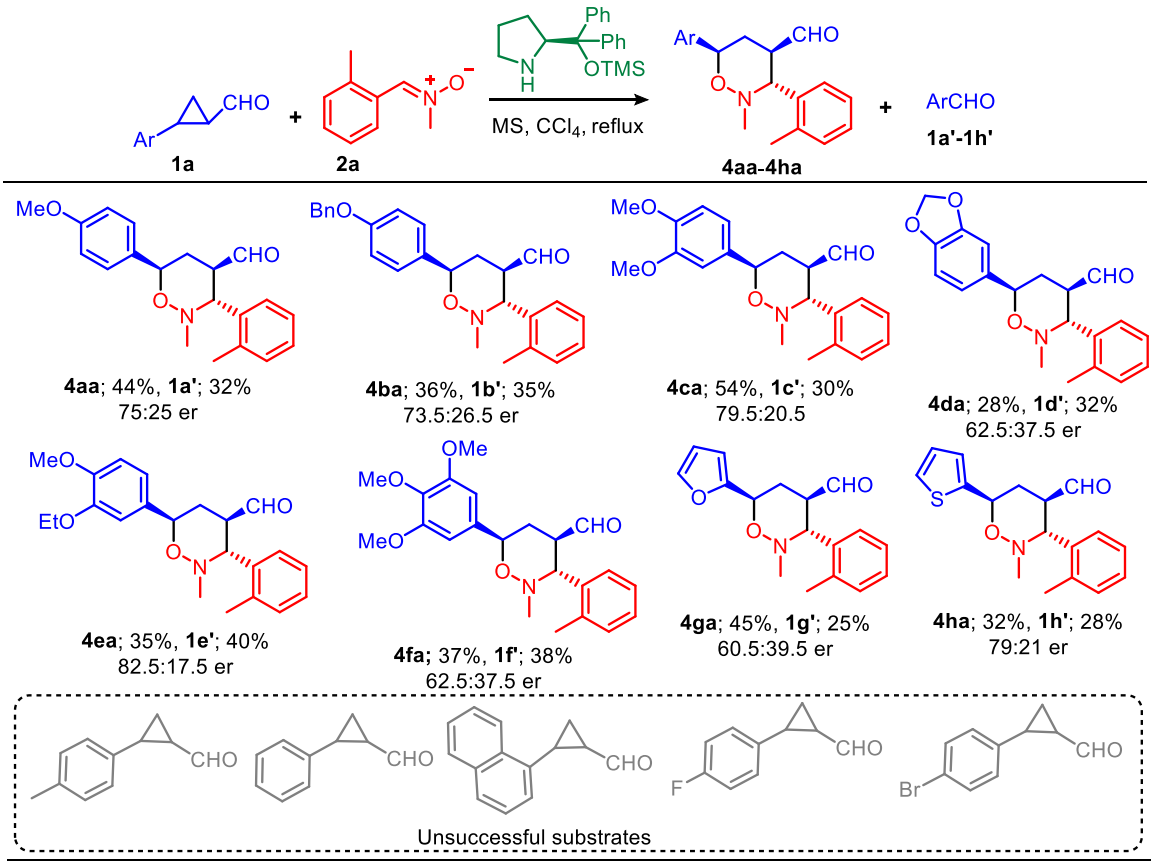

[a]Reaction conditions: **1** (0.28 mmol, 1 equiv.), **2a** (0.42 mmol, 1.5 equiv.), **I** (40 mol%), 2.5 mL of CCl_4, Molecular sieves (4 Å), reflux, 10 h, yields represent isolated products, *ee* values were determined by HPLC analysis, dr for all the compounds are 4:1.

in the yield was observed by increasing or decreasing the catalyst loading (entries 20-21, Table 2.B.1.1). Notably, when phenyl nitrone without *ortho*-substitution (**2a'**) was employed, the stereoselectivities were dramatically diminished (entry 22, Table 2.B.1.1). Eventually, the other substitution patterns were also tested and both the *para*-methyl and *meta*-methoxy substituted

nitrones gave lower yields with an inseparable diastereomeric mixture in low to poor enantiomeric ratios, respectively (entries 23-24, Table 2.B.1.1). So, entry 1 of Table 2.B.1.1 has been chosen as our optimized reaction conditions.

With the optimized condition in hand, at first, the generality and limitations of this designed methodology were investigated with respect to cyclopropane carbaldehydes (Scheme 2.B.2.1). All the electron-rich aryl cyclopropane carbaldehydes (**1a-1f**) participated in this transformation to give the corresponding products (**4aa-4fa**) in moderate yields with low to moderate stereoselectivities. Unfortunately, moderate electron-rich aryl groups like *para*-methyl, phenyl, and naphthyl-substituted cyclopropane carbaldehydes yielded only a trace amount of products that could be

Scheme 2.B.2.2. Substrate scope of 2-substituted nitrones[a]

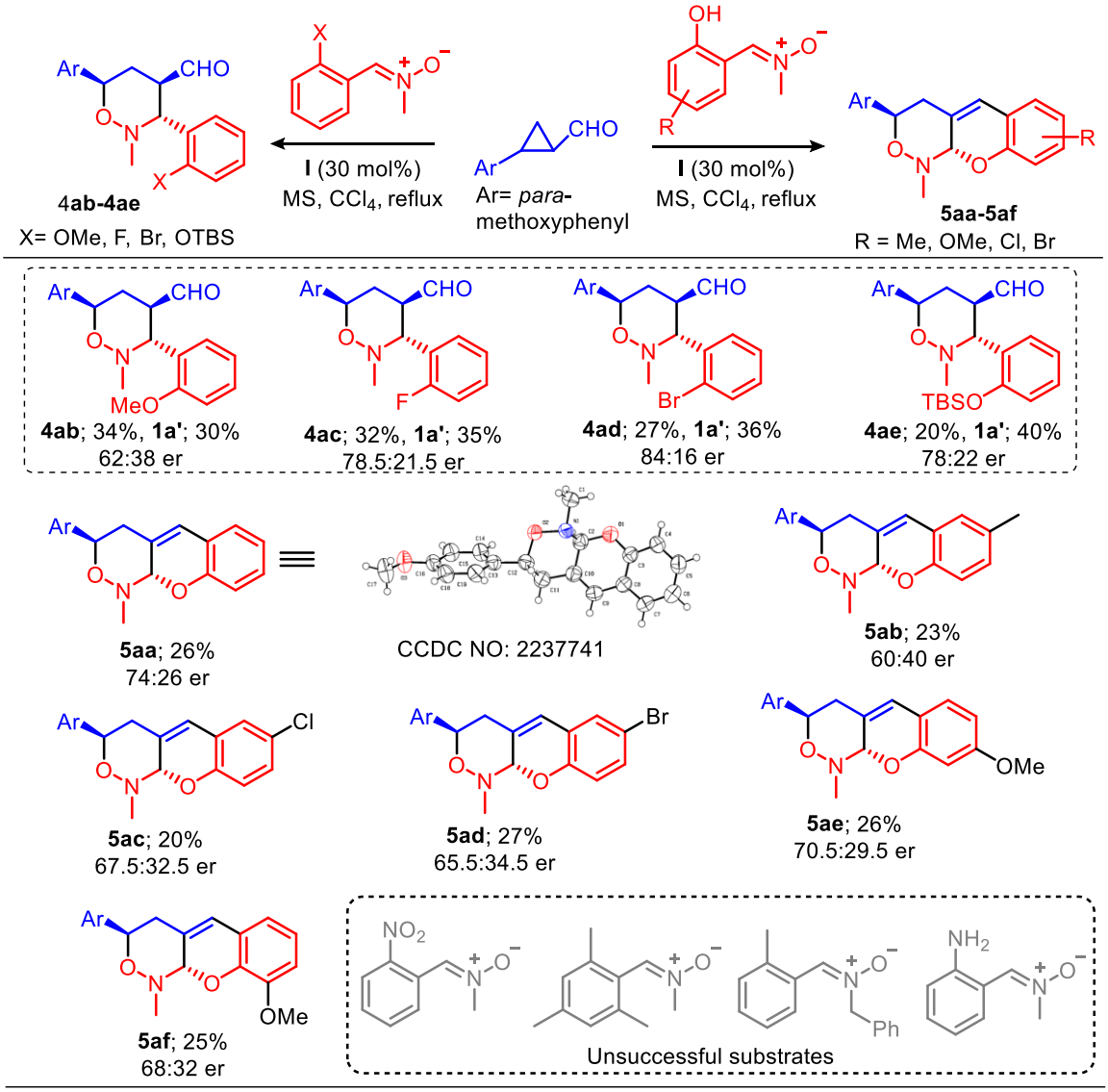

[a]Reaction conditions: **1** (0.28 mmol, 1 equiv.), **2** or **3** (0.42 mmol, 1.5 equiv.), **I** (40 mol%), 2.5 mL of CCl4, Molecular sieves (4 Å), reflux, 10 h, yields represent isolated products, ee values were determined by HPLC analysis, dr for **4ab-4ae** are 4:1, dr for **5aa-5af** are 9:1.

detected by HRMS only. On the other hand, halogen-containing aryl cyclopropane carbaldehydes failed to give the desired products. To our delight, heteroatom- containing aryl cyclopropane carbaldehydes (**1g**-**1h**) rendered the corresponding products (**4ga**-**4ha**) in low to moderate yields with low to moderate stereoselectivities. It is worth mentioning that in all these cases, the corresponding benzaldehydes (**1a'**-**1h'**) were also obtained as the side products by a rearrangement reaction[13] (Figure 2.B.4.6.1) with considerable yields in a range of 25-40% which attributed to the lower yield of the desired cycloadducts (**4aa**-**4ha**).

Next, the substrate scopes of the 2-substituted nitrones were explored for this (3+3)-annulation with *para*-methoxyphenyl cyclopropane carbaldehyde **1a** (Scheme 2.B.2.2). Electron-donating groups like methoxy and halogen-substituted nitrones (**2b**-**2d**) were delivered the products (**4ab**-**4ad**) in moderate yields with moderate stereoselectivities. However, electron-withdrawing nitro- and sterically hindered mesityl substituted nitrones failed to give the corresponding products. Unfortunately, benzyl substitution instead of methyl on the nitrogen center of nitrone could not deliver the desired product. Bulky groups like OTBS-substituted nitrone also tolerated the reaction but afforded the product in very low yield with moderate stereoselectivity. Surprisingly, nitrones with a hydroxyl group at the *ortho*-position (**3a**) rendered an unexpected product **5aa** with moderate enantioselectivity and excellent diastereomeric ratio, albeit of low overall yield. The structure of **5aa** was unambiguously confirmed by single crystal X-ray analysis. Then, we also checked the scope of these *ortho*-hydroxy nitrones with substitution at different positions of the phenyl group. Various methoxy, methyl, and halogen substitution at the different positions of phenyl (**3b**-**3f**) gave the products (**5ab**-**5af**) in almost similar yields with moderate stereoselectivities. However, when 2-hydroxy substituent was changed to the 2-amino one, it could not deliver the desired product.

Table 2.B.2.2. Time-dependent study of enantiomeric excess[a]

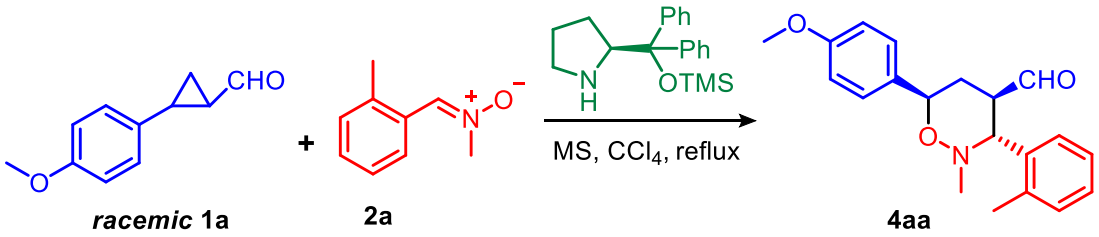

entry	time (h)	ee of the remaining cyclopropane[b]	ee of the final product[b]
1	4	35%	-40%
2	6	47%	5%
3	8	70%	52%
4	10	-	50%

[a]Reaction conditions: **1a** (0.28 mmol, 1 equiv.), **2a** (0.42 mmol, 1.5 equiv.), **I** (40 mol%), 2.5 mL of CCl_4, Molecular sieves (4 Å), reflux, [b]*ee* values were determined by HPLC analysis.

To gain insights into the mechanism of this transformation, we have performed a control experiment where the enantiomeric excess of the remaining cyclopropane carbaldehyde along with the furnished products was examined in particular time intervals, and a surprising outcome was encountered (Table 2.B.2.2). It was found that as the reaction progressed, the starting material, i.e., *racemic* cyclopropane carbaldehyde started to get enantioenriched, which indicates a simple kinetic resolution (KR).[14] As the overall enantioselectivity is not very high and no starting material remains after optimized reaction time, a simple kinetic resolution is not the case here. On the other hand, in the initial hours, the enantiomeric excess in favor of the opposite isomer (***ent*-4aa**) was obtained, which gradually inverted with time and as the reaction proceeded towards completion, the enantiomeric excess in favor of desired isomer (**4aa**) was observed. This experiment depicts that one enantiomer of the cyclopropane reacts faster to give the product (***ent*-4aa**) to some extent and eventually decomposes in the course of time, whereas the other enantiomer reacts slowly to give the desired product (**4aa**) in a comparatively efficient manner. So, this phenomenon illustrates that a matched/mismatched scenario[14a] is happening here, and the reaction possibly proceeds via a typical S_N2-KR pathway where one enantiomer of the substrate is producing one particular enantiomer of the product (**4aa**) while another one gives the opposite enantiomer (***ent*-4aa**) in less amount due to substrate decomposition and results in the decrement of the overall enantioselectivity of the product.

Scheme 2.B.2.3. Control experiments; (a) hydrolysis of **4ae**, (b) trapping of intermediates

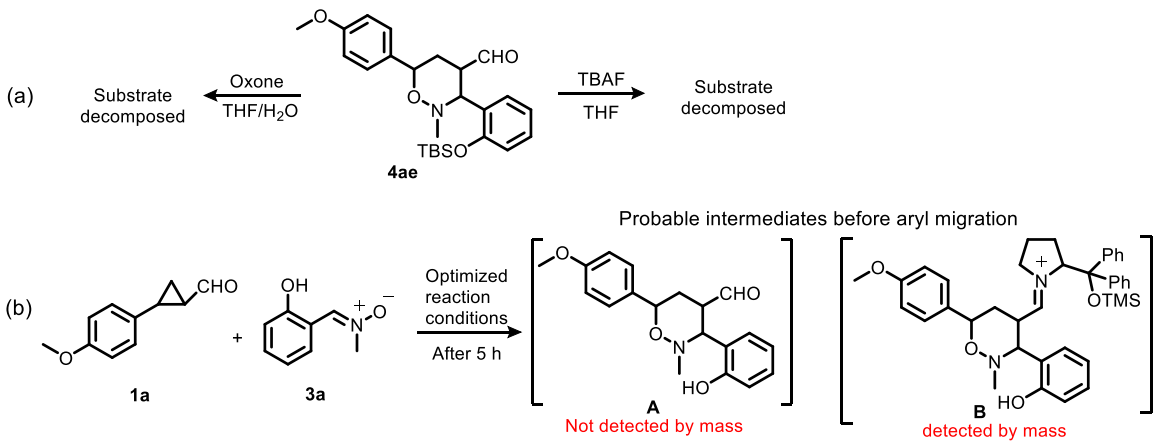

To check whether the aryl migration was occurring under catalytic or non-catalytic conditions, the product **4ae** was subjected to hydrolysis in both TBAF/THF condition and Oxone/water condition but the product got decomposed without forming either the free OH-containing product or the aryl migrated product (Scheme 2.B.2.3.a). Moreover, when a reaction was performed between **1a** and **3a** in the optimized condition, the *in situ* formed intermediate **B** was detected at half reaction completion time but no characteristic mass of the intermediate **A** was found (Scheme 2.B.2.3.b), which indicates that the aryl migration occurs under catalytic conditions only. However, a hydrogen

bonding between the H-atom of the hydroxyl group and the O-atom of nitrone moiety is believed to be the driving force for this intriguing 1,3-aryl shift which presumably follows an *ipso*-type pathway for the migration just before the second cyclization step (Scheme 2.B.1.1).

Finally, the synthetic utility of our designed methodology was demonstrated by executing some derivatization of our synthesized products (Scheme 2.B.2.4). At first, the $NaBH_4$ reduction was performed, which transformed the aldehyde group of **4aa** to corresponding alcohol **6a** in 67% yield. Next, Horner–Wadsworth–Emmons olefination of the aldehyde group was carried out with triethylphosphonoacetate in the presence of DBU and K_2CO_3 and successfully obtained the *trans*-alkene product **6b** in 74% yield. Moreover, when selective hydrogenation by hydrogen gas and palladium-charcoal was performed on **5aa**, the allylic bond was cleaved, and the double bond was reduced to give the product **7a** in 71% yield.

Scheme 2.B.2.4. Synthetic applications

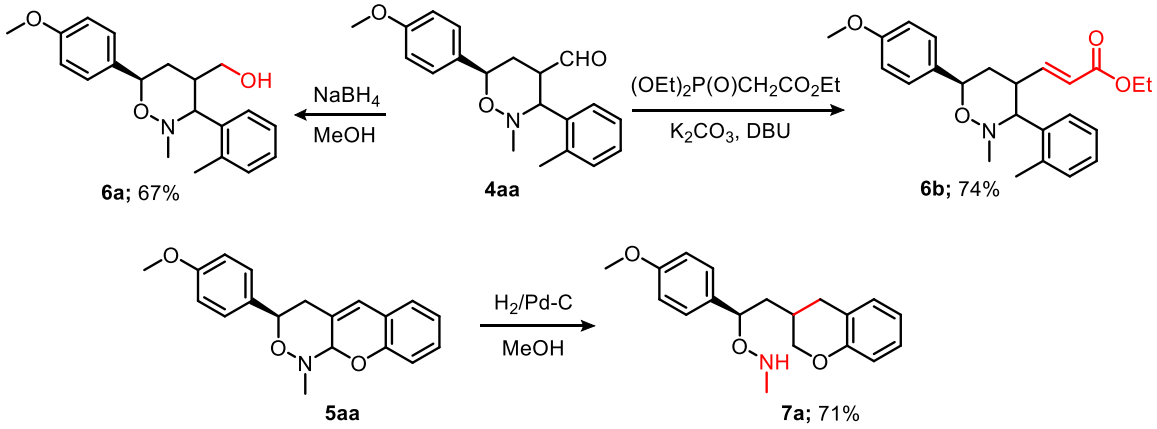

2.B.3. Conclusion

In conclusion, we have demonstrated an organocatalyzed enantioselective (3+3)-cycloaddition reaction of aryl cyclopropane carbaldehyde with *ortho*-substituted nitrones for the first time. A range of 1,2-oxazinanes and also a new type of scaffold tetrahydrochromeno[2,3-*c*][1,2]oxazines was synthesized in a newly diagnosed asymmetric technique by utilizing cheap and readily available prolinol-based Jørgensen-Hayashi catalyst.

2.B.4. Experimental Section

2.B.4.1. General Information

All reactions were carried out under inert atmosphere with oven-dried glasswares. All solvents and reagents were obtained from commercial sources and were purified following the standard procedure prior to use. Powdered molecular sieves (4Å MS) were dried at 200 °C under vacuum prior to use. Thin-layer chromatography was performed on Merck precoated silica gel 60 F254

aluminum sheets with detection under UV light at 254 nm and charring with *p*-anisaldehyde solution. Chromatographic purifications were performed with silica gel (230-400 mesh) and melting points were taken on Stuart digital melting point apparatus. Nuclear magnetic resonance (NMR) spectroscopy was performed using JEOL 400 MHz and HRMS was recorded on Waters Xevo G2-XS (Q-TOF). The ^{1}H NMR and ^{13}C NMR spectra were recorded in $CDCl_3$. Chemical shifts of ^{1}H and ^{13}C NMR spectra are expressed in parts per million (ppm). All coupling constants are absolute values and are expressed in Hertz. The description of the signals includes the following: s = singlet, d = doublet, dd = doublet of doublet, t = triplet, dt = doublet of triplet, q = quartet, dq = doublet of quartet, br = broad, and m = multiplet. Optical rotations were measured on a Anton Paar MCP 200, $[\alpha]^{D}$ values are given in $deg \cdot cm^{3} \cdot g^{-1} \cdot dm^{-1}$; concentration (c) in g $(100\ mL)^{-1}$. The enantiomeric excess (*ee*) values of the products were determined by High Performance Liquid Chromatography (Waters modular system) using Daicel Chiralpak IC, and ASH columns as chiral stationary phase.

2.B.4.2. General procedure for the preparation of *trans*-2-Arylcyclopropanecarbaldehydes (1)[1]

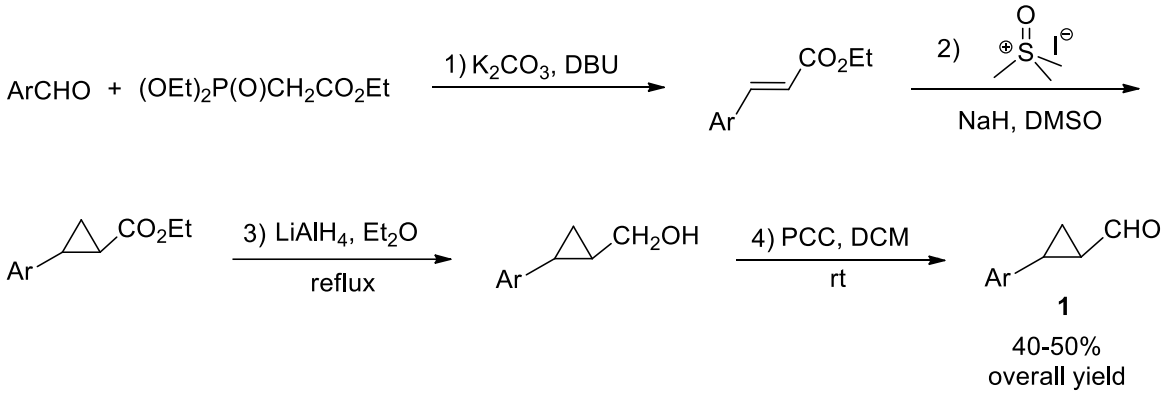

1) To a mixture of triethyl phosphonoacetate (1.1 equiv.), DBU (0.035 equiv.), and finely ground K_2CO_3 (2 equiv.) was added ArCHO (1 equiv.) and the resulting mixture was stirred using a magnetic stirrer for 4 h at room temperature under argon atmosphere. Ethyl acetate was added to the crude mixture and the solid was filtered off. The solid was rinsed with ethyl acetate and the combined filtrate was concentrated. The resulting oil was distilled under reduced pressure using a bulb-to-bulb apparatus (10 mm Hg/240 °C) to give corresponding alkene (yield 84%) (E:Z = 99:1).

2) A suspension of TMSOI (1.2 equiv.) and NaH (1.5 equiv.) in anhydrous DMSO (15 mL) was stirred for 1 h. A DMSO solution (14 mL) of alkene (14 mmol, 1 equiv) was added at 0 °C. The reaction mixture was stirred at 55 °C for 24 h. Another suspension of TMSOI (0.3 equiv.) and NaH (0.3 equiv.) in DMSO (10 mL) was added to the reaction mixture and reaction was stirred at 65 °C for 84 h. The solution was poured into a brine solution and extracted with ethyl acetate. Combined

organic layer was washed with water and dried over $MgSO_4$, concentrated and purified by silica gel column to afford corresponding cyclopropane derivative as a white solid (60-80% yield).

3) To a stirred solution of LAH (1.5 equiv.) in 7 mL diethyl ether was added dropwise a solution of cyclopropane ester (0.90 mmol, 1equiv.) in 3 mL diethyl ether under N_2 atmosphere. After addition was completed the reaction mixture was refluxed for another 6 h. The reaction mixture was then cooled to rt, and the excess LAH was destroyed by water. 15 mL of 10% H_2SO_4 and 8 mL of ether was added and the aqueous layer was extracted several times with diethyl ether. The combined organic layer was washed with water and 5% $NaHCO_3$, dried over $MgSO_4$ and concentrated in a rotary evaporator (90-95% yield). Without any further purification, the crude material (a colorless oil) was used for next step.

4) To a solution of cyclopropane alcohol (6.8 mmol, 1 equiv.) in dry DCM (14 mL), PCC (2 equiv.) was added in a portion-wise manner through a solid addition tube under N_2 atmosphere. After 3 h reaction mixture was filtered through a small plug of celite and concentrated in vacuo. The crude mixture was purified by silica gel column chromatography using ethyl acetate in hexane as an eluent. Starting from aryl aldehyde the 2-arylcyclopropanecarbaldehydes was obtained in 40-55% overall yield.

***trans*-2-(4-methoxyphenyl)cyclopropane-1-carbaldehyde (1a)**

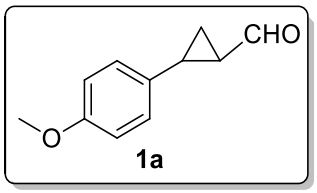

^{1}H NMR (400 MHz): δ 9.30 (d, J = 4.9 Hz, 1H), 7.05 (d, J = 8.7 Hz, 2H), 6.83 (d, J = 8.7 Hz, 2H), 3.79 (s, 3H) 2.63-2.56 (m, 1H), 2.13-2.06 (m, 1H), 1.73-1.67 (m, 1H), 1.51-1.45 (m, 1H)

***trans*-2-(4-(benzyloxy)phenyl)cyclopropanecarbaldehyde (1b)**

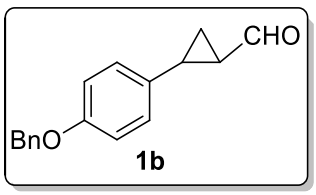

^{1}H NMR (400 MHz): δ 9.30 (d, J = 4.5 Hz, 1H), 7.44-7.31 (m, 5H), 7.04 (d, J = 8.5 Hz, 2H), 6.90 (d, J = 8.6 Hz, 2H), 5.04 (s, 2H), 2.62-2.55 (m, 1H), 2.13-2.06 (m, 1H), 1.72-1.67 (m, 1H), 1.51-1.45 (m, 1H)

***trans*-2-(3,4-dimethoxyphenyl)cyclopropanecarbaldehyde (1c)**

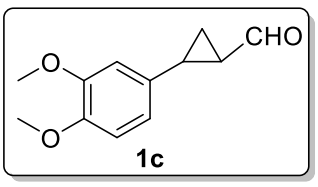

^{1}H NMR (400 MHz): δ 9.28 (d, J = 4.5 Hz, 1H), 6.77 (d, J = 8.3 Hz, 1H), 6.65 (d, J = 8.2 Hz, 2H), 3.85 (s, 3H), 3.83 (s, 3H), 2.62-2.55 (m, 1H), 2.13-2.06 (m, 1H), 1.71-1.65 (m, 1H), 1.51-1.46 (m, 1H)

***trans*-2-(3-ethoxy-4-methoxyphenyl)cyclopropanecarbaldehyde (1d)**

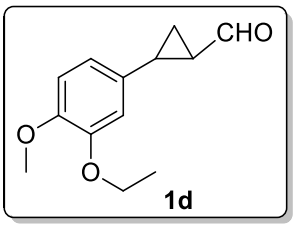

^{1}H NMR (400 MHz, CDCl3) δ 9.29 (d, J = 4.8 Hz, 1H), 6.78 (d, J = 8.8 Hz, 1H), 6.66−6.63 (m, 2H), 4.07 (q, J = 7.0 Hz, 2H), 3.84 (s, 3H), 2.61−2.54 (m, 1H), 2.12−2.05 (m, 1H), 1.72−1.65 (m, 1H), 1.50−1.46 (m, 1H), 1.45 (t, J = 7.0 Hz, 3H)

***trans*-2-(benzo[*d*][1,3]dioxol-5-yl)cyclopropanecarbaldehyde (1e)**

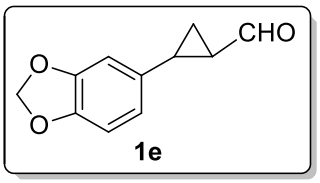

^{1}H NMR (400 MHz): *δ* 9.30 (d, *J* = 4.6 Hz, 1H), 6.73 (d, *J* = 8.2 Hz, 1H), 6.62 (d, *J* = 8.0 Hz, 1H), 6.57 (s, 1H), 5.93 (s, 2H), 2.60-2.55 (m, 1H), 2.12-2.04 (m, 1H), 1.71-1.66 (m, 1H), 1.49-1.43 (m, 1H)

***trans*-2-(3,4,5-trimethoxyphenyl)cyclopropanecarbaldehyde (1f)**

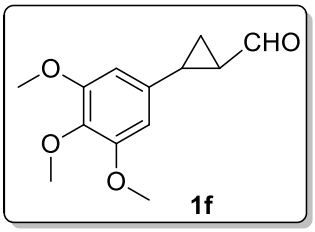

^{1}H NMR (400 MHz): *δ* 9.31 (d, J = 4.5 Hz, 1H), 6.33 (s, 2H), 3.84 (s, 6H), 3.81 (s, 3H), 2.62-2.56 (m, 1H), 2.18-2.11 (m, 1H), 1.73-1.67 (m, 1H), 1.53-1.47 (m, 1H)

***trans*-2-(furan-2-yl)cyclopropane-1-carbaldehyde (1g)**

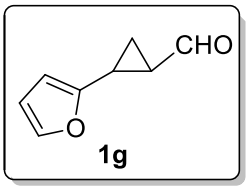

^{1}H NMR (400 MHz): *δ* 9.36 (d, J = 4.3 Hz, 1H), 7.27-7.25 (m, 1H), 6.30-6.28 (m, 1H), 6.10 (d, J = 3.3 Hz, 1H), 2.65-2.59 (m, 1H), 2.32-2.26 (m, 1H), 1.69-1.64 (m, 1H), 1.62-1.56 (m, 1H)

***trans*-2-(thiophen-2-yl)cyclopropane-1-carbaldehyde (1h)**

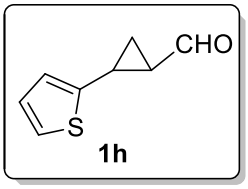

^{1}H NMR (400 MHz): *δ* 9.38 (d, J = 4.1 Hz, 1H), 7.13-7.11 (m, 1H), 6.92-6.90 (m, 1H), 6.85-6.84 (m, 1H), 2.84-2.78 (m, 1H), 2.25-2.20 (m, 1H), 1.79-1.74 (m, 1H), 1.55-1.50 (m, 1H)

2.B.4.3. General procedure for the preparation of 2-substituted nitrones (2)[16]

Aldehyde (1.0 equiv), *N*-methylhydroxylamine hydrochloride (2.0 equiv), Na_2CO_3 (2.2 equiv), and Na_2SO_4 (0.5 equiv) were added to a mortar and ground until completion. Et_2O was added, the mixture was filtered, and concentrated in vacuo.[16]

(*E*)-*N*-(2-methylbenzylidene)methanamine oxide (2a)

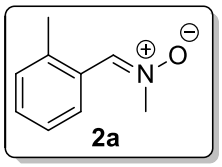

^{1}H NMR (400 MHz): δ 9.08-9.05 (m, 1H), 7.48 (s, 1H), 7.25-7.13 (m, 3H), 3.85 (s, 3H), 2.32 (s, 3H)

(E)-N-(2-methoxybenzylidene)methanamine oxide (2b)

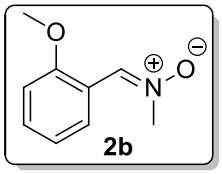

^{1}H NMR (400 MHz): δ 9.21-9.21 (m, 1H), 7.81 (s, 1H), 7.37-7.33 (m, 1H), 7.02-6.99 (m, 1H), 6.87-6.85 (m, 1H), 3.86 (s, 3H), 3.83 (s, 3H)

(*E*)-*N*-(2-fluorobenzylidne)methanamine oxide (2c)

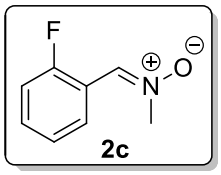

^{1}H NMR (400 MHz): δ 9.24-9.20 (m, 1H), 7.66 (s, 1H), 7.40-7.35 (m, 1H), 7.23-7.20 (m, 1H), 7.10-7.05 (m, 1H), 3.91 (s, 3H)

(*E*)-*N*-(2-bromobenzylidene)methanamine oxide (2d)

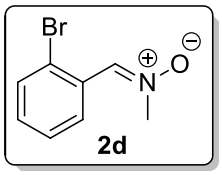

^{1}H NMR (400 MHz): δ 9.29-9.27 (m, 1H), 7.85 (s, 1H), 7.63-7.60 (m, 1H), 7.42-7.38 (m, 1H), 7.27-7.23 (m, 1H), 3.94 (s, 3H)

(*E*)-*N*-(2-((*tert*-butyldimethylsilyl)oxy)benzylidene)methanamine oxide (2e)

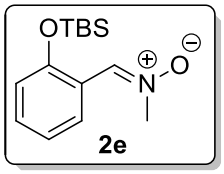

^{1}H NMR (400 MHz): δ 9.15-9.13 (m, 1H), 7.71 (s, 1H), 7.25-7.21 (m, 1H), 7.00-6.97 (m, 1H), 6.78 (d, *J*=8.2 Hz, 1H), 3.83 (s, 3H), 0.98 (s, 9H), 0.20 (s, 6H)

(*E*)-*N*-(2-hydroxybenzylidene)methanamine oxide (3a)

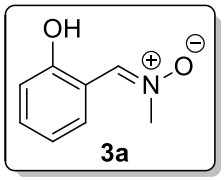

^{1}H NMR (400 MHz): δ 12.35 (s, 1H), 7.50 (S, 1H), 7.40-7.36 (m, 1H), 7.04 (dd, J=7.7 Hz, 1.8 Hz, 1H), 6.95 (d, J=8.6 Hz, 1H), 6.85-6.81 (m, 1H), 3.86 (s, 3H)

(*E*)-*N*-(2-hydroxy-5-methylbenzylidene)methanamine oxide (3b)

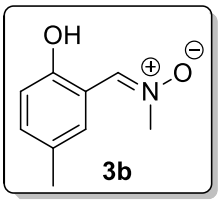

^{1}H NMR (400 MHz): δ 12.10 (s, 1H), 7.44 (S, 1H), 7.18 (dd, J=8.2 Hz, 2.2 Hz, 1H), 6.85 (d, J=8.2 Hz, 1H), 6.80-6.79 (m, 1H), 3.83 (s, 3H), 2.23 (s, 3H)

(*E*)-*N*-(5-chloro-2-hydroxybenzylidene)methanamine oxide (3c)

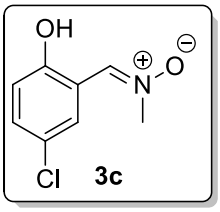

^{1}H NMR (400 MHz): δ 12.15 (s, 1H), 7.46 (S, 1H), 7.32 (dd, J=8.7 Hz, 2.3 Hz, 1H), 7.02 (d, J=2.4 Hz, 1H), 6.91 (d, J=8.8 Hz, 1H), 3.89 (s, 3H)

(*E*)-*N*-(5-bromo-2-hydroxybenzylidene)methanamine oxide (3d)

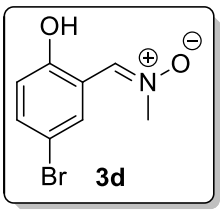

^{1}H NMR (400 MHz): δ 12.24 (s, 1H), 7.44-7.42 (m, 2H), 7.15 (d, J=2.7 Hz, 1H), 6.83 (d, J=8.7 Hz, 1H), 3.87 (s, 3H)

(*E*)-*N*-(2-hydroxy-4-methoxybenzylidene)methanamine oxide (3e)

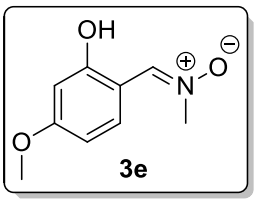

^{1}H NMR (400 MHz): δ 13.42 (s, 1H), 7.35 (s, 1H), 6.91 (d, J=8.5 Hz, 1H), 6.44-6.39 (m, 2H), 3.81 (s, 3H), 3.80 (s, 3H)

(*E*)-*N*-(2-hydroxy-3-methoxybenzylidene)methanamine oxide (3f)

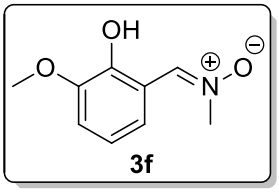

^{1}H NMR (400 MHz): δ 12.49 (s, 1H), 7.53 (s, 1H), 6.95 (d, J=7.9 Hz, 1H), 6.80-6.76 (m, 1H), 6.66 (d, J=8.0 Hz, 1H), 3.86 (s, 3H), 3.85 (s, 3H)

2.B.4.4. Representative procedure and substrate scope for the (3+3)-cycloaddition between cyclopropane carbaldehydes and 2-substituted nitrones

To a round-bottom flask equipped with a magnetic stir bar was charged with cyclopropane carbaldehyde (1 equiv.), 2-substituted nitrone (1.5 equiv.), activated 4 Å MS (200 mol%), and Jørgensen-Hayashi Catalyst I (0.4 equiv.) under nitrogen atmosphere. CCl_4 was added as a solvent to the reaction mixture and was stirred under reflux conditions for 10-12 hours. After the completion

of the reaction (as monitored by TLC), the reaction mixture was passed through a small pad of Celite, and the solvent was removed under reduced pressure by a rotary evaporator. Then the crude product was further purified by column chromatography on silica gel with EtOAc/hexane as eluent.

Racemic products were prepared according to the representative procedure 5 by using the racemic catalyst.

(6*R*)-6-(4-methoxyphenyl)-2-methyl-3-(*o*-tolyl)-1,2-oxazinane-4-carbaldehyde (4aa)

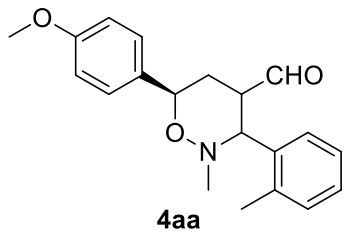

4aa

Prepared accoding to **GP 3**. **1a** (0.044 g, 0.25 mmol), **2a** (0.036 g, 0.37 mmol), **4aa** (0.036 g, 0.11 mmol); Yellowish sticky liquid, 44% overall yield; $[\alpha]_D^{25}$= -86.07 (c = 0.7, $CHCl_3$); 75:25 er of major diastereomer was determined by chiral HPLC analysis, [Chiralpak IC, hexane/i-PrOH = 90/10, 0.5 mL/min, t_R (minor) = 9.36 min, t_R (major) = 11.49 min]; **^{1}H NMR (400 MHz):** δ 9.40 (d, *J* = 1.8 Hz, 1H), 7.51 (d, *J* = 7.7 Hz, 1H), 7.37 (d, *J* = 8.6 Hz, 2H), 7.22-7.17 (m, 1H), 6.91 (d, *J* = 8.6 Hz, 2H), 5.00 (dd, *J* = 11.8, 1.8 Hz, 1H), 3.93 (d, *J* = 10.5 Hz, 1H), 3.81 (m, 1H), 3.34-3.28 (m, 1H), 2.43 (s, 3H), 2.41 (s, 3H), 2.18-2.15 (m, 1H), 1.99-1.89 (m, 1H); **^{13}C NMR (100 MHz):** δ 201.7, 159.6, 136.8, 136.6, 132.2, 130.8, 128.1, 128.0, 127.8, 127.3, 127.0, 114.0, 79.3, 65.7, 55.8, 55.4, 43.2, 31.9, 20.5; **HRMS (ESI, Q-TOF)** m/z: $[M+H]^+$ calculated for $C_{20}H_{24}NO_3$ 326.1756, Found 326.1751

(6*R*)-6-(4-(benzyloxy)phenyl)-2-methyl-3-(*o*-tolyl)-1,2-oxazinane-4-carbaldehyde (4ba)

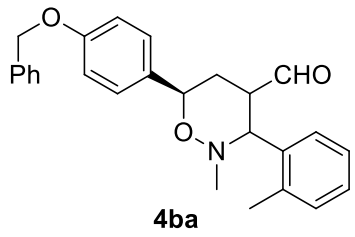

4ba

Prepared accoding to **GP 3**. **1a** (0.063 g, 0.25 mmol), **2a** (0.056 g, 0.37 mmol), **4ba** (0.036 g, 0.09 mmol); Yellowish sticky liquid, 36% overall yield; $[\alpha]_D^{25}$= -49.43 (c = 0.7, $CHCl_3$); 73.5:26.5 er of major diastereomer was determined by chiral HPLC analysis, [Chiralpak IC, hexane/i-PrOH = 90/10, 0.5 mL/min, t_R (minor) = 17.60 min, t_R (major) = 18.24 min]; **^{1}H NMR (400 MHz):** δ 9.39 (d, *J* = 1.8 Hz, 1H), 7.50-7.49 (m, 1H) 7.43-7.35 (m, 8H), 7.19-7.16 (m, 2H), 6.98 (d, *J* = 8.7 Hz, 2H), 5.07 (s, 2H), 4.99 (dd, *J* = 11.5, 1.8 Hz, 1H), 3.92 (d, *J* = 10.5 Hz, 1H), 3.33-3.27 (m, 1H), 2.42 (s, 3H), 2.40 (s, 3H), 2.18-2.13 (m, 1H), 1.98-1.89 (m, 1H); **^{13}C NMR (100 MHz):** δ 201.7, 158.8, 136.9, 136.8, 136.5, 132.4, 130.7, 128.7, 128.1, 128.0, 127.9, 127.5, 127.2, 127.0, 114.9, 79.3, 70.0, 65.7, 55.8, 43.1, 31.8, 20.5; **HRMS (ESI, Q-TOF)** m/z: $[M+H]^+$ calculated for $C_{26}H_{28}NO_3$ 402.2069, Found 402.2068

(6*R*)-6-(3,4-dimethoxyphenyl)-2-methyl-3-(*o*-tolyl)-1,2-oxazinane-4-carbaldehyde (4ca)

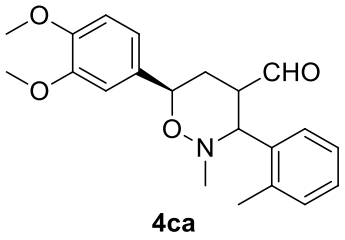

4ca

Prepared accoding to **GP 3**. **1c** (0.052 g, 0.25 mmol), **2a** (0.056 g, 0.37 mmol), **4ca** (0.048 g, 0.13 mmol); Yellowish sticky liquid, 54% overall yield; $[\alpha]_D^{25}$= -60.25 (c = 1.0, $CHCl_3$); 79.5:20.5 er of major diastereomer was determined by chiral HPLC analysis, [Chiralpak IC, hexane/i-PrOH = 80/20, 1.0 mL/min, t_R (major) = 28.98 min, t_R (minor) = 36.04 min]; **^{1}H NMR (400 MHz):** δ 9.41 (d, *J* = 1.4 Hz, 1H), 7.51 (d, *J* = 7.7 Hz, 1H), 7.28-7.17 (m, 4H), 6.99-6.97 (m, 2H), 6.88-6.86 (m, 1H), 4.99 (dd, *J* = 11.5, 1.9 Hz, 1H), 3.95 (s, 1H), 3.92 (s, 3H), 3.88 (s, 3H), 3.35-3.28 (m, 1H), 2.44 (s, 3H), 2.42 (s, 3H), 2.20-2.15 (m, 1H), 2.00-1.91 (m, 1H); **^{13}C NMR (100 MHz):** δ 201.8, 149.0, 136.8, 136.5, 132.4, 130.8, 128.0, 127.2, 127.0, 119.2, 111.0, 110.0, 79.6, 65.7, 56.0, 56.0, 55.8, 43.2, 31.8, 20.5; **HRMS (ESI, Q-TOF)** m/z: $[M+H]^+$ calculated for $C_{21}H_{26}NO_4$ 356.1862, Found 356.1858

(6*R*)-6-(benzo[*d*][1,3]dioxol-5-yl)-2-methyl-3-(*o*-tolyl)-1,2-oxazinane-4-carbaldehyde (4ea)

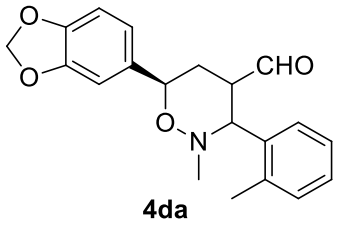

4da

Prepared accoding to **GP 3**. **1d** (0.048 g, 0.25 mmol), **2a** (0.056 g, 0.37 mmol), **4da** (0.024 g, 0.07 mmol); Yellowish sticky liquid, 28% overall yield; $[\alpha]_D^{25}$= -52.48 (c = 0.7, $CHCl_3$); 62.5:37.5 er of major diastereomer was determined by chiral HPLC analysis, [Chiralpak IC, hexane/i-PrOH = 90/10, 0.5 mL/min, t_R (minor) = 16.89 min, t_R (major) = 18.63 min]; **^{1}H NMR (400 MHz):** δ 9.39 (d, *J* = 1.4 Hz, 1H), 7.49 (d, *J* = 7.3 Hz, 1H), 7.23-7.16 (m, 3H), 6.94-6.93 (m, 1H), 6.90-6.88 (m, 1H), 6.81-6.79 (m, 1H), 5.96-5.93 (m, 2H), 4.95 (dd, *J* = 11.4, 2.1 Hz, 1H), 3.91 (d, *J* = 10.5 Hz, 1H), 3.32-3.26 (m, 1H), 2.42 (s, 3H), 2.40 (s, 3H), 2.17-2.12 (m, 1H), 1.94-1.84 (m, 1H); **^{13}C NMR (100 MHz):** δ 201.7, 147.9, 147.6, 136.7, 136.6, 133.9, 130.8, 128.0, 127.3, 127.0, 120.3, 108.3, 107.4, 101.2, 79.5, 65.7, 55.8, 43.2, 32.1, 20.5; **HRMS (ESI, Q-TOF)** m/z: $[M+H]^+$ calculated for $C_{20}H_{22}NO_4$ 340.1549, Found 340.1545

(6*R*)-6-(3-ethoxy-4-methoxyphenyl)-2-methyl-3-(*o*-tolyl)-1,2-oxazinane-4-carbaldehyde (4da)

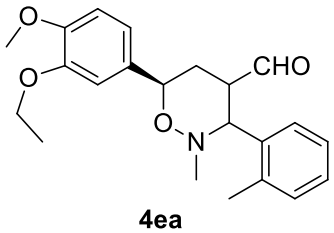

4ea

Prepared accoding to **GP 3**. **1e** (0.055 g, 0.25 mmol), **2a** (0.056 g, 0.37 mmol), **4ea** (0.032 g, 0.08 mmol); Yellowish sticky liquid, 35% overall yield; $[\alpha]_D^{25}$= -84.16 (c = 0.4, $CHCl_3$); 82.5:17.5 er of major diastereomer was determined by chiral HPLC analysis, [Chiralpak IC, hexane/i-PrOH = 80/20, 1.0 mL/min, t_R (major) = 17.88 min, t_R (minor) = 23.56 min]; **^{1}H NMR (400 MHz):** δ 9.40 (d, *J* = 1.5 Hz, 1H), 7.50 (d, *J* = 7.2 Hz, 1H), 7.23-7.16 (m, 3H), 6.98-6.96 (m, 2H), 6.87-6.85 (m, 1H), 4.97 (dd, *J* = 11.4, 2.0 Hz, 1H), 4.14 (q, *J* = 7.0 Hz, 2H), 3.93 (d, *J* = 10.0 Hz, 1H), 3.87 (s, 3H), 3.33-3.28 (m, 1H), 2.43 (s, 3H), 2.41 (s, 3H), 2.19-2.14 (m, 1H),

1.99-1.89 (m, 1H), 1.48 (t, *J* = 6.8 Hz, 3H); **^{13}C NMR (100 MHz):** δ 201.9, 149.3, 148.4, 136.8, 136.6, 132.4, 130.8, 128.0, 127.2, 127.0, 119.2, 111.4, 111.3, 79.6, 65.7, 64.4, 56.1, 55.8, 43.2, 31.8, 20.5, 14.9; **HRMS (ESI, Q-TOF)** m/z: $[M+H]^+$ calculated for $C_{22}H_{28}NO_4$ 370.2018, Found 370.2010

(6*R*)-2-methyl-3-(*o*-tolyl)-6-(3,4,5-trimethoxyphenyl)-1,2-oxazinane-4-carbaldehyde (4fa)

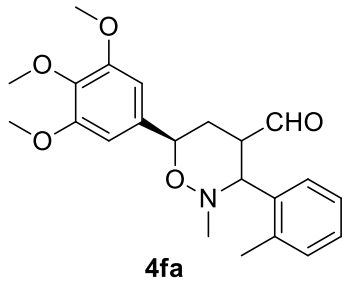

4fa

Prepared accoding to **GP 3**. **1f** (0.060 g, 0.25 mmol), **2a** (0.056 g, 0.37 mmol), **4fa** (0.036 g, 0.09 mmol);Yellowish sticky liquid, 37% overall yield; $[\alpha]_D^{25}$= -109.54 (c = 0.4, $CHCl_3$); 62.5:37.5 er of major diastereomer was determined by chiral HPLC analysis, [Chiralpak IC, hexane/i-PrOH = 60/40, 1.0 mL/min, t_R (minor) = 10.74 min, t_R (major) = 21.22 min]; **^{1}H NMR (400 MHz):** δ 9.40 (d, *J* = 1.3 Hz, 1H), 7.51 (d, *J* = 7.6 Hz, 1H), 7.28-7.18 (m, 3H), 6.65 (s, 2H), 4.98 (dd, *J* = 11.5, 2.2 Hz, 1H), 3.95 (d, *J* = 10.0 Hz, 1H), 3.90 (s, 6H), 3.84 (s, 3H), 3.35-3.28 (m, 1H), 2.45 (s, 3H), 2.42 (s, 3H), 2.20-2.16 (m, 1H), 1.99-1.89 (m, 1H); **^{13}C NMR (100 MHz):** δ 201.8, 153.4, 137.9, 136.7, 136.5, 135.5, 130.8, 128.0, 127.2, 127.0, 103.8, 80.0, 65.7, 60.9, 56.2, 55.7, 43.2, 32.0, 20.5; **HRMS (ESI, Q-TOF)** m/z: $[M+H]^+$ calculated for $C_{22}H_{28}NO_5$ 386.1967, Found 386.1964

(6*R*)-6-(furan-2-yl)-2-methyl-3-(*o*-tolyl)-1,2-oxazinane-4-carbaldehyde (4ka)

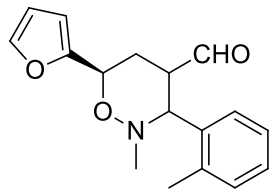

4ga

Prepared accoding to **GP 3**. **1g** (0.034 g, 0.25 mmol), **2a** (0.056 g, 0.37 mmol), **4ga** (0.036 g, 0.12 mmol);Yellowish sticky liquid, 45% overall yield; Yellowish sticky liquid, 45% overall yield; $[\alpha]_D^{25}$= -45.86 (c = 0.6, $CHCl_3$); 60.5:39.5 er of major diastereomer was determined by chiral HPLC analysis, [Chiracel ASH, hexane/i-PrOH = 90/10, 0.5 mL/min, t_R (major) = 6.93 min, t_R (minor) = 8.16 min]; **^{1}H NMR (400 MHz):** δ 9.37 (d, *J* = 1.3 Hz, 1H), 7.49 (d, *J* = 7.5 Hz, 1H), 7.44-7.43 (m, 1H), 7.24-7.16 (m, 3H), 6.43-6.42 (m, 1H), 6.38-6.37 (m, 1H), 5.12-5.09 (m, 1H), 3.92 (d, *J* = 10.5 Hz, 1H), 3.29-3.23 (m, 1H), 2.42 (s, 3H), 2.38 (s, 3H), 2.19-2.15 (m, 2H); **^{13}C NMR (100 MHz):** δ 201.5, 152.4, 142.9, 136.5, 130.8, 128.1, 127.2, 127.0, 110.4, 108.4, 73.0, 65.7, 55.4, 43.1, 28.7, 20.5; **HRMS (ESI, Q-TOF)** m/z: $[M+H]^+$ calculated for $C_{17}H_{20}NO_3$ 286.1443, Found 286.1437

(6*R*)-2-methyl-6-(thiophen-2-yl)-3-(*o*-tolyl)-1,2-oxazinane-4-carbaldehyde (4la)

Prepared accoding to **GP 3**. **1h** (0.038 g, 0.25 mmol), **2a** (0.056 g, 0.37 mmol), **4ha** (0.025 g, 0.08 mmol); Yellowish sticky liquid, 28% overall yield; $[\alpha]_D^{25}$= -46.49 (c = 0.5, $CHCl_3$); 79:21 er of major diastereomer was determined by chiral HPLC analysis, [Chiracel ASH, hexane/i-PrOH =

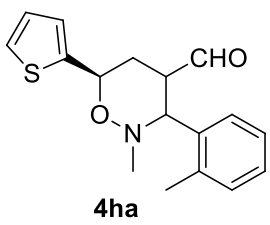

4ha

90/10, 0.5 mL/min, t_R (major) = 7.01 min, t_R (minor) = 8.07 min]; **^{1}H NMR (400 MHz):** δ 9.38 (d, J = 1.3 Hz, 1H), 7.49 (d, J = 7.6 Hz, 1H), 7.32-7.31 (m, 1H), 7.24-7.17 (m, 3H), 7.12-7.11 (m, 1H), 7.02-7.00 (m, 1H), 5.28 (dd, J = 11.6, 2.0 Hz, 1H), 3.94 (d, J = 10.6 Hz, 1H), 3.33-3.26 (m, 1H), 2.44 (s, 3H), 2.39 (s, 3H), 2.35-2.30 (m, 1H), 2.08-1.99 (m, 1H); **^{13}C NMR (100 MHz):** δ 201.5, 142.5, 136.6, 130.8, 128.1, 127.2, 127.0, 126.7, 125.7, 125.3, 75.3, 65.7, 55.6, 43.1, 32.4, 20.5; **HRMS (ESI, Q-TOF)** m/z: $[M+H]^+$ calculated for $C_{17}H_{20}NO_2S$ 302.1215, Found 302.1211

(6*R*)-3-(2-methoxyphenyl)-6-(4-methoxyphenyl)-2-methyl-1,2-oxazinane-4-carbaldehyde (4ab)

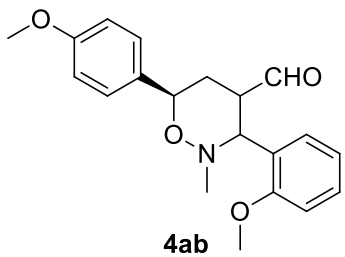

4ab

Prepared accoding to **GP 3**. **1a** (0.044 g, 0.25 mmol), **2b** (0.061 g, 0.37 mmol), **4ab** (0.029 g, 0.08 mmol); Yellowish sticky liquid, 34% overall yield; $[\alpha]_D^{25}$= -19.50 (c = 0.6, $CHCl_3$); 62:38 er of major diastereomer was determined by chiral HPLC analysis, [Chiralpak IC, hexane/i-PrOH = 95/5, 1.0 mL/min, t_R (minor) = 14.93 min, t_R (major) = 16.06 min]; **^{1}H NMR (400 MHz):** δ 9.37 (d, J = 1.4 Hz, 1H), 7.48-7.47 (m, 1H), 7.36 (d, J = 8.2 Hz, 2H), 7.30-7.27 (m, 1H), 7.03-6.99 (m, 1H), 6.92-6.89 (m, 3H), 4.96 (dd, J = 11.4, 2.3 Hz, 1H), 4.26 (d, J = 10.2 Hz, 1H), 3.84 (m, 3H), 3.81 (s, 3H), 3.09-3.04 (m, 1H), 2.47 (s, 3H), 2.12-2.07 (m, 1H), 2.01-1.92 (m, 1H); **^{13}C NMR (100 MHz):** δ 202.3, 159.6, 157.1, 132.3, 129.2, 128.1, 121.5, 114.0, 110.8, 79.2, 61.7, 55.6, 55.4, 43.6, 31.8; **HRMS (ESI, Q-TOF)** m/z: $[M+H]^+$ calculated for $C_{20}H_{24}NO_4$ 342.1705, Found 342.1705

(6*R*)-3-(2-fluorophenyl)-6-(4-methoxyphenyl)-2-methyl-1,2-oxazinane-4-carbaldehyde (4ac)

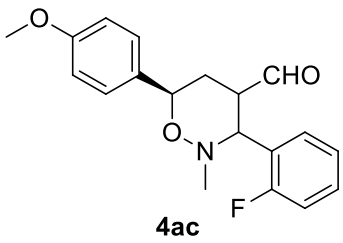

4ac

Prepared accoding to **GP 3**. **1a** (0.044 g, 0.25 mmol), **2c** (0.057 g, 0.37 mmol), **4ac** (0.027 g, 0.08 mmol); Yellowish sticky liquid, 32% overall yield; $[\alpha]_D^{25}$= -96.18 (c = 0.3, $CHCl_3$); 78.5:21.5 er of major diastereomer was determined by chiral HPLC analysis, [Chiralpak IC, hexane/i-PrOH = 90/10, 0.5 mL/min, t_R (minor) = 17.2 min, t_R (major) = 19.2 min]; **^{1}H NMR (400 MHz):** δ 9.46 (d, J = 1.3 Hz, 1H), 7.50-7.46 (m, 1H), 7.35 (d, J = 8.7 Hz, 2H), 7.32-7.28 (m, 1H), 7.21-7.17 (m, 1H), 7.11-7.06 (m, 1H), 6.91 (d, J = 8.8 Hz, 2H), 4.98 (dd, J = 11.4, 1.8 Hz, 1H), 4.05 (bs, 1H), 3.81 (s, 3H), 3.32-3.16 (m, 1H), 2.47 (s, 3H), 2.19-2.05 (m, 1H), 1.97-1.88 (m, 1H); **^{13}C NMR (100 MHz):** δ 201.1, 162.2, 159.7, 159.5, 132.0, 130.1, 130.0, 128.1, 125.0, 114.0, 55.4, 43.9, 31.9; **HRMS (ESI, Q-TOF)** m/z: $[M+H]^+$ calculated for $C_{19}H_{21}NO_3F$ 330.1505, Found 330.1500

(6*R*)-3-(2-bromophenyl)-6-(4-methoxyphenyl)-2-methyl-1,2-oxazinane-4-carbaldehyde (4ad)

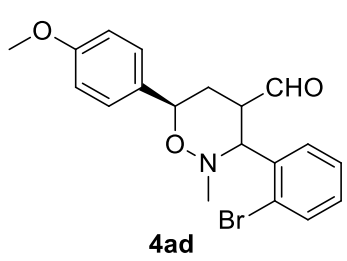

4ad

Prepared accoding to **GP 3**. **1a** (0.044 g, 0.25 mmol), **2d** (0.079 g, 0.37 mmol), **4ad** (0.027 g, 0.07 mmol); Yellowish sticky liquid, 27% overall yield; $[\alpha]_D^{25}$= -46.62 (c = 1.0, $CHCl_3$); 84:16 er of major diastereomer was determined by chiral HPLC analysis, [Chiralpak IC, hexane/i-PrOH = 90/10, 0.5 mL/min, t_R (minor) = 18.93 min, t_R (major) = 20.87 min]; **^{1}H NMR (400 MHz):** δ 9.47 (d, *J* = 1.8 Hz, 1H), 7.61 (dd, *J* = 8.2, 1.3 Hz, 1H), 7.55 (dd, *J* = 7.8, 1.8 Hz, 1H), 7.40-7.34 (m, 3H), 7.21-7.18 (m, 1H), 6.92 (d, *J* = 8.7 Hz, 2H), 4.97 (dd, *J* = 11.4, 2.2 Hz, 1H), 4.34 (d, *J* = 10.7 Hz, 1H), 3.81 (s, 3H), 3.15-3.08 (m, 1H), 2.47 (s, 3H), 2.16-2.11 (m, 1H), 2.04-1.95 (m, 1H); **^{13}C NMR (100 MHz):** δ 201.1, 159.7, 137.8, 133.3, 131.9, 129.8, 129.5, 128.5, 128.1, 125.1, 114.0, 79.3, 68.4, 56.1, 55.4, 43.4, 31.6; **HRMS (ESI, Q-TOF)** m/z: $[M+H]^+$ calculated for $C_{19}H_{21}NO_3Br$ 390.0705, Found 390.0700

(6*R*)-3-(2-((*tert*-butyldimethylsilyl)oxy)phenyl)-6-(4-methoxyphenyl)-2-methyl-1,2-oxazinane-4-carbaldehyde (4ae)

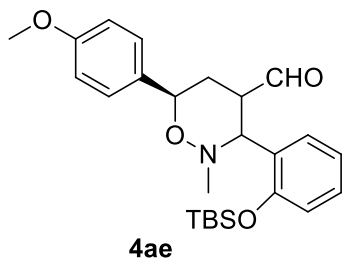

4ae

Prepared accoding to **GP 3**. **1a** (0.044 g, 0.25 mmol), **2e** (0.098 g, 0.37 mmol), **4ae** (0.022 g, 0.05 mmol); Yellowish sticky liquid, 20% overall yield; $[\alpha]_D^{25}$= 79.26 (c = 0.8, $CHCl_3$); 78:22 er of major diastereomer was determined by chiral HPLC analysis, [Chiracel ASH, hexane/i-PrOH = 90/10, 0.2 mL/min, t_R (minor) = 12.90 min, t_R (major) = 17.74 min]; **^{1}H NMR (400 MHz):** δ 9.38 (d, *J* = 1.6 Hz, 1H), 7.49-7.47 (m, 1H), 7.36 (d, *J* = 8.7 Hz, 2H), 7.19-7.15 (m, 1H), 7.02-6.98 (m, 1H), 6.91 (d, *J* = 8.6 Hz, 2H), 6.84-6.82 (m, 1H), 4.95 (dd, *J* = 11.5, 1.9 Hz, 1H), 4.19 (d, *J* = 10.8 Hz, 1H), 3.81 (s, 3H), 3.10-3.03 (m, 1H), 2.47 (s, 3H), 2.15-2.10 (m, 1H), 1.97-1.87 (m, 1H), 1.03 (s, 9H), 0.28 (s, 6H); **^{13}C NMR (100 MHz):** δ 202.2, 159.6, 153.6, 132.2, 128.9, 128.7, 128.5, 128.2, 121.9, 118.3, 114.0, 79.0, 62.6, 55.5, 55.4, 43.5, 31.6, 26.0, 18.4, -3.8; **HRMS (ESI, Q-TOF)** m/z: $[M+H]^+$ calculated for $C_{25}H_{36}NO_4Si$ 442.2414, Found 442.2411

(3*R*)-3-(4-methoxyphenyl)-1-methyl-1,3,4,10a-tetrahydrochromeno[2,3-*c*][1,2]oxazine (5aa)

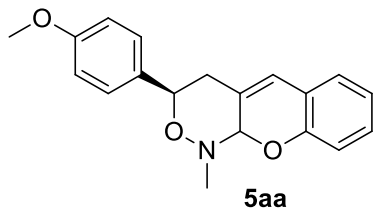

5aa

Prepared accoding to **GP 3**. **1a** (0.044 g, 0.25 mmol), **3a** (0.056 g, 0.37 mmol), **5aa** (0.020 g, 0.06 mmol); White solid; 26% overall yield; Melting point: 118-121 °C $[\alpha]_D^{25}$= 256.04 (c = 0.3 $CHCl_3$); 74:26 er of major diastereomer was determined by chiral HPLC analysis, [Chiralpak IC, hexane/i-PrOH = 90/10, 0.5 mL/min, t_R (major) = 14.61min, t_R (minor) = 15.47 min]; **^{1}H NMR (400 MHz):**

δ 7.33 (d, J = 8.3 Hz, 2H), 6.96-6.94 (m, 1H), 6.90 (d, J = 8.7 Hz, 2H), 6.88-6.86 (m, 1H), 6.80-6.78 (m, 1H), 6.30 (s, 1H), 5.18 (s, 1H), 4.92 (dd, J = 9.3, 4.3 Hz, 1H), 3.80 (s, 3H), 2.81 (s, 3H), 2.76-2.73 (m, 1H), 2.71-2.69 (m, 1H); **^{13}C NMR (100 MHz):** δ 159.7, 151.6, 131.8, 129.8, 128.9, 128.2, 127.9, 126.3, 121.7, 120.1, 119.3, 115.2, 114.0, 92.8, 80.9, 55.4, 41.7, 40.1; **HRMS (ESI, Q-TOF)** m/z: $[M+H]^+$ calculated for $C_{19}H_{20}NO_3$ 310.1443, Found 310.1434

(3*R*)-3-(4-methoxyphenyl)-1,7-dimethyl-1,3,4,10a-tetrahydrochromeno[2,3-*c*][1,2]oxazine (5ab)

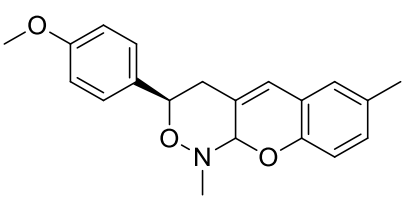

5ab

Prepared accoding to **GP 3**. **1a** (0.044 g, 0.25 mmol), **3b** (0.061 g, 0.37 mmol), **5ab** (0.019 g, 0.06 mmol); Colourless sticky liquid, 23% overall yield; $[\alpha]_D^{25}$= 75.25 (c = 0.9, $CHCl_3$); 60:40 er of major diastereomer was determined by chiral HPLC analysis, [Chiralpak IC, hexane/i-PrOH = 90/10, 0.5 mL/min, t_R (major) = 14.61min, t_R (minor) = 15.47 min]; **^{1}H NMR (400 MHz):** δ 7.33 (d, J = 8.7 Hz, 2H), 6.91-6.87 (m, 3H), 6.76 (d, J = 1.8 Hz, 1H), 6.70 (d, J = 8.2 Hz, 1H), 6.26 (s, 1H), 5.14 (s, 1H), 4.91 (dd, J = 9.8, 4.3 Hz, 1H), 3.80 (s, 3H), 2.81 (s, 3H), 2.76-2.72 (m, 1H), 2.70-2.69 (m, 1H); **^{13}C NMR (100 MHz):** δ 159.6, 149.5, 131.9, 130.8, 129.8, 129.3, 127.9, 126.7, 119.9, 119.4, 114.9, 92.8, 80.9, 55.4, 41.8, 40.1, 20.6; **HRMS (ESI, Q-TOF)** m/z: $[M+H]^+$ calculated for $C_{20}H_{22}NO_3$ 324.1600, Found 324.1617

(3*R*)-7-chloro-3-(4-methoxyphenyl)-1-methyl-1,3,4,10a-tetrahydrochromeno[2,3-*c*][1,2]oxazine (5ac)

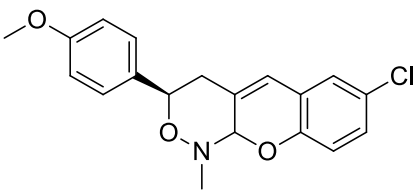

5ac

Prepared accoding to **GP 3**. **1a** (0.044 g, 0.25 mmol), **3c** (0.068 g, 0.37 mmol), **5ac** (0.018 g, 0.05 mmol); Colourless sticky liquid, 20% overall yield; $[\alpha]_D^{25}$= 80.98 (c = 0.8, $CHCl_3$); 67.5:32.5 er of major diastereomer was determined by chiral HPLC analysis, [Chiralpak IC, hexane/i-PrOH = 90/10, 0.5 mL/min, t_R (major) = 13.18 min, t_R (minor) = 14.45 min]; **^{1}H NMR (400 MHz):** δ 7.32 (d, J = 8.7 Hz, 2H), 7.04 (dd, J = 8.5, 2.7 Hz, 1H), 6.93 (d, J = 2.5 Hz, 1H), 6.90 (d, J = 8.9 Hz, 2H), 6.73 (d, J = 8.6 Hz, 1H), 6.24 (s, 1H), 5.17 (s, 1H), 4.91 (dd, J = 9.6, 4.5 Hz, 1H), 3.80 (s, 3H), 2.80 (s, 3H), 2.77-2.73 (m, 1H), 2.71-2.70 (m, 1H); **^{13}C NMR (100 MHz):** δ 159.7, 150.1, 131.5, 131.2, 128.4, 127.9, 126.3, 125.8, 121.5, 118.4, 116.5, 114.0, 92.8, 80.8, 55.4, 41.7, 40.0; **HRMS (ESI, Q-TOF)** m/z: $[M+H]^+$ calculated for $C_{19}H_{19}NO_3Cl$ 344.1053, Found 344.1080

(3*R*)-7-bromo-3-(4-methoxyphenyl)-1-methyl-1,3,4,10a-tetrahydrochromeno[2,3-*c*][1,2]oxazine (5ad)

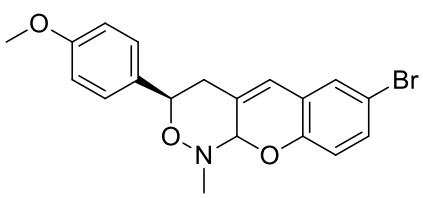

5ad

Prepared accoding to **GP 3**. **1a** (0.044 g, 0.25 mmol), **3d** (0.085 g, 0.37 mmol), **5ad** (0.026 g, 0.06 mmol); Colourless sticky liquid, 27% overall yield; $[\alpha]_D^{25}$= 102.64 (c = 0.6, $CHCl_3$); 65.5:34.5 er of major diastereomer was determined by chiral HPLC analysis, [Chiralpak IC, hexane/i-PrOH = 90/10, 0.5 mL/min, t_R (major) = 12.75 min, t_R (minor) = 13.74 min]; **^{1}H NMR (400 MHz):** δ 7.31 (d, *J* = 8.2 Hz, 2H), 7.17 (dd, *J* = 8.6, 2.2 Hz, 1H), 7.07 (d, *J* = 2.3 Hz, 1H), 6.90 (d, *J* = 8.7 Hz, 2H), 6.68 (d, *J* = 8.4 Hz, 1H), 6.23 (s, 1H), 5.17 (s, 1H), 4.90 (dd, *J* = 9.9, 4.1 Hz, 1H), 3.80 (s, 3H), 2.80 (s, 3H), 2.77-2.73 (m, 1H), 2.71-2.70 (m, 1H); **^{13}C NMR (100 MHz):** δ 159.5, 150.5, 131.2, 131.0, 128.5, 127.8, 121.9, 118.1, 116.8, 113.8, 113.4, 92.6, 80.7, 55.3, 41.6, 39.8; **HRMS (ESI, Q-TOF)** m/z: $[M+H]^+$ calculated for $C_{19}H_{19}NO_3Br$ 388.0548, Found 388.0563

(3*R*)-8-methoxy-3-(4-methoxyphenyl)-1-methyl-1,3,4,10a-tetrahydrochromeno[2,3-*c*][1,2]oxazine (5ae)

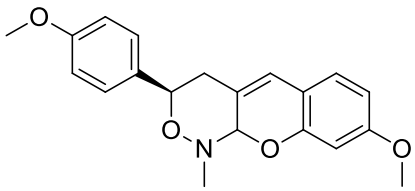

5ae

Prepared accoding to **GP 3**. **1a** (0.044 g, 0.25 mmol), **3e** (0.067 g, 0.37 mmol), **5ae** (0.022 g, 0.06 mmol); Colourless sticky liquid, 26% overall yield; $[\alpha]_D^{25}$= 59.82 (c = 0.9, $CHCl_3$); 70.5:29.5 er of major diastereomer was determined by chiral HPLC analysis, [Chiralpak IC, hexane/i-PrOH = 90/10, 0.5 mL/min, t_R (minor) = 22.29 min, t_R (major) = 22.29 min]; **^{1}H NMR (400 MHz):** δ 7.32 (d, *J* = 8.6 Hz, 2H), 6.90 (d, *J* = 8.7 Hz, 2H), 6.86 (d, *J* = 8.0 Hz, 1H), 6.43 (dd, *J* = 8.1, 2.2 Hz, 1H), 6.40 (d, *J* = 2.6 Hz, 1H), 6.25 (s, 1H), 5.15 (s, 1H), 4.90 (dd, *J* = 10.2, 3.9 Hz, 1H), 3.80 (s, 3H), 3.76 (s, 3H), 2.80 (s, 3H), 2.74-2.71 (m, 1H), 2.68-2.67 (m, 1H); **^{13}C NMR (100 MHz):** δ 160.4, 159.6, 152.7, 131.8, 128.2, 127.9, 126.8, 126.7, 118.9, 113.9, 113.3, 107.3, 101.3, 92.8, 80.0, 55.5, 53.4, 41.7, 39.9; **HRMS (ESI, Q-TOF)** m/z: $[M+H]^+$ calculated for $C_{20}H_{22}NO_4$ 340.1549, Found 340.1549

(3*R*)-9-methoxy-3-(4-methoxyphenyl)-1-methyl-1,3,4,10a-tetrahydrochromeno[2,3-*c*][1,2]oxazine (5af)

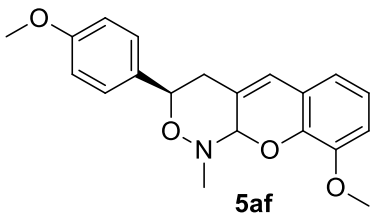

5af

Prepared accoding to **GP 3**. **1a** (0.044 g, 0.25 mmol), **3f** (0.067 g, 0.37 mmol), **5af** (0.021 g, 0.06 mmol); Colourless sticky liquid, 25% overall yield; $[\alpha]_D^{25}$= 125.24 (c = 0.4, $CHCl_3$); 68:32 er of major diastereomer was determined by chiral HPLC analysis, [Chiralpak IC, hexane/i-PrOH = 90/10, 0.5 mL/min, t_R (minor) = 22.29 min, t_R (major) = 22.29 min]; **^{1}H NMR (400 MHz):** δ 7.33 (d, *J* = 8.7 Hz, 1H), 6.91-6.87 (m, 3H), 6.76 (d, *J* = 1.8 Hz, 1H), 6.70 (d, *J* = 8.0 Hz, 1H), 6.26 (s, 1H), 5.14

(s, 1H), 4.92 (dd, *J* = 10.0, 4.0 Hz, 1H), 3.80 (s, 3H), 2.81 (s, 3H), 2.76-2.72 (m, 1H), 2.70-2.69 (m, 1H), 2.24 (s, 3H); **^{13}C NMR (100 MHz):** δ 159.6, 149.4, 131.8, 130.8, 129.8, 129.3, 127.9, 126.7, 119.8, 119.4, 114.9, 114.0, 92.8, 80.9, 55.4, 41.8, 40.0, 20.6; **HRMS (ESI, Q-TOF)** m/z: $[M+H]^+$ calculated for $C_{20}H_{22}NO_4$ 340.1549, Found 340.1552

2.B.4.5. Chemical transformations

((6*R*)-6-(4-methoxyphenyl)-2-methyl-3-(*o*-tolyl)-1,2-oxazinan-4-yl)methanol (6a)

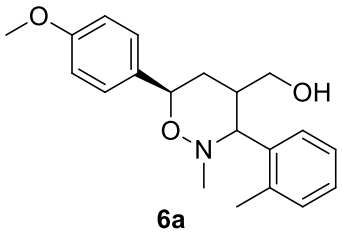

6a

Prepared accoding to the literature procedure.[17] **4aa** (0.022 g, 0.06 mmol), **NaBH$_4$** (0.005 g, 0.12 mmol), **6a** (0.015 g, 0.04 mmol); Colourless liquid, 67% yield; **^{1}H NMR (400 MHz):** δ 7.45 (d, *J* = 7.3 Hz, 1H), 7.38 (d, *J* = 8.7 Hz, 2H), 7.24-7.19 (m, 1H), 7.18-7.16 (m, 2H), 6.91 (d, *J* = 8.7 Hz, 2H), 5.01 (dd, *J* = 11.7, 2.0 Hz, 1H), 3.81 (s, 3H), 3.70 (d, *J* = 10.5 Hz, 1H), 3.44 (dd, *J* = 10.5, 3.6 Hz, 1H), 3.31 (dd, *J* = 10.7, 6.1 Hz, 1H), 2.41 (s, 3H), 2.40 (s, 3H), 2.38-2.32 (m, 1H), 2.16-2.12 (m, 1H), 1.86-1.77 (m, 1H); **^{13}C NMR (100 MHz):** δ 159.2, 138.1, 136.7, 132.8, 130.3, 128.0, 127.3, 127.0, 126.7, 113.7, 79.7, 67.8, 64.1, 55.2, 45.2, 43.6, 34.9, 29.6, 20.3; **HRMS (ESI, Q-TOF)** m/z: $[M+H]^+$ calculated for $C_{20}H_{26}NO_3$ 328.1913, Found 328.1911

(*E*)-ethyl 3-((6*R*)-6-(4-methoxyphenyl)-2-methyl-3-(*o*-tolyl)-1,2-oxazinan-4-yl)acrylate (6b)

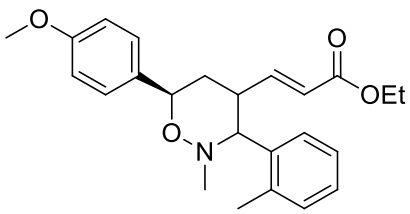

6b

Prepared according to the literature procedure.[18] **4aa** (0.020 g, 0.06 mmol); **6b** (0.018 g, 0.04 mmol), 74% yield; **^{1}H NMR (400 MHz):** δ 7.44 (d, *J* = 8.1 Hz, 1H), 7.37 (d, *J* = 8.7 Hz, 2H), 7.24-7.20 (m, 1H), 7.18-7.16 (m, 2H), 6.91 (d, *J* = 8.7 Hz, 2H), 6.64 (dd, *J* = 16.0, 7.7 Hz, 1H), 5.61 (dd, *J* = 16.0, 1.3 Hz, 1H), 5.02 (dd, *J* = 11.4, 1.8 Hz, 1H), 4.12-4.06 (m, 2H), 3.81 (s, 3H), 3.66 (d, *J* = 10.0 Hz, 1H), 3.03-2.95 (m, 1H), 2.42 (s, 3H), 2.32 (s, 3H), 2.09-2.04 (m, 1H), 1.93-1.84 (m, 1H), 1.21 (t, *J* = 6.9 Hz, 3H); **^{13}C NMR (100 MHz):** δ 166.3, 159.5, 147.8, 137.6, 136.5, 132.5, 130.5, 128.1, 127.5, 126.9, 126.7, 122.2, 114.0, 79.4, 69.4, 60.3, 55.4, 46.3, 43.9, 36.8, 20.4, 14.2; **HRMS (ESI, Q-TOF)** m/z: $[M+H]^+$ calculated for $C_{24}H_{30}NO_4$ 396.2175, Found 396.2179

***O*-((1*R*)-2-(chroman-3-yl)-1-(4-methoxyphenyl)ethyl)-N-methylhydroxylamine (7a)**

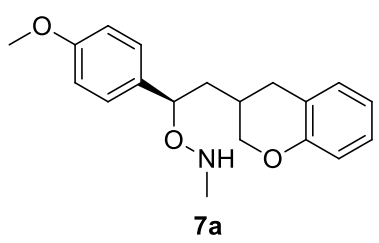

7a

Prepared according to the literature procedure.[19] **5aa** (0.025 g, 0.08 mmol), **7a** (0.018 g, 0.05 mmol), colourless liquid, 71% yield, **^{1}H NMR (400 MHz):** δ 8.32 (bs, 1H), 7.33 (d, J = 8.7 Hz, 2H), 7.17-7.10 (m, 2H), 6.94-6.85 (m, 4H), 5.29 (dd, J = 11.7, 2.0 Hz, 1H), 3.80 (s, 3H), 3.36-3.29 (m, 1H), 2.68 (dd, J = 13.8, 6.3 Hz, 1H), 2.62 (s, 3H), 2.58 (d, J = 2.3, Hz, 2H), 2.30-2.23 (m, 1H), 2.06-1.98 (m, 1H), 1.80-1.77 (m, 1H); **^{13}C NMR (100 MHz):** δ 159.6, 155.8, 132.5, 130.7, 128.2, 128.1, 126.6, 120.6, 117.4, 114.0, 76.5, 58.3, 55.4, 46.4, 35.9, 34.0, 31.4; **HRMS (ESI, Q-TOF)** m/z: $[M+H]^+$ calculated for $C_{19}H_{24}NO_3$ 314.1756, Found 314.1754

2.B.4.6. Rearrangement reaction

Figure 2.B.4.6.1. Rearrangement pathway for the production of aryl aldehydes

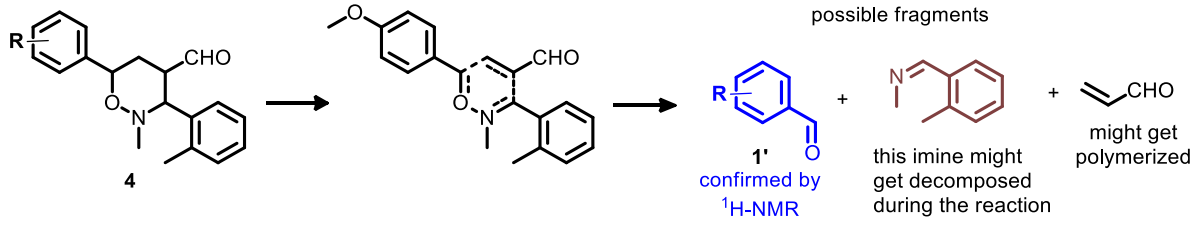

^{1}H-NMR ($CDCl_3$, 400MHz) of 1a'

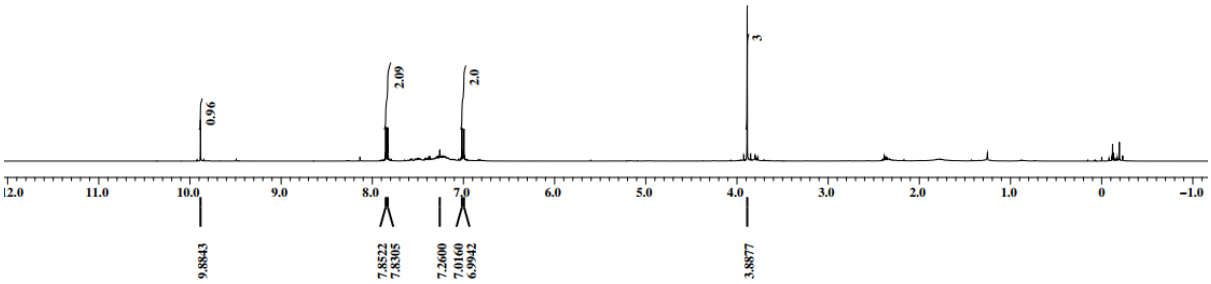

^{1}H-NMR ($CDCl_3$, 400MHz) of 1f'

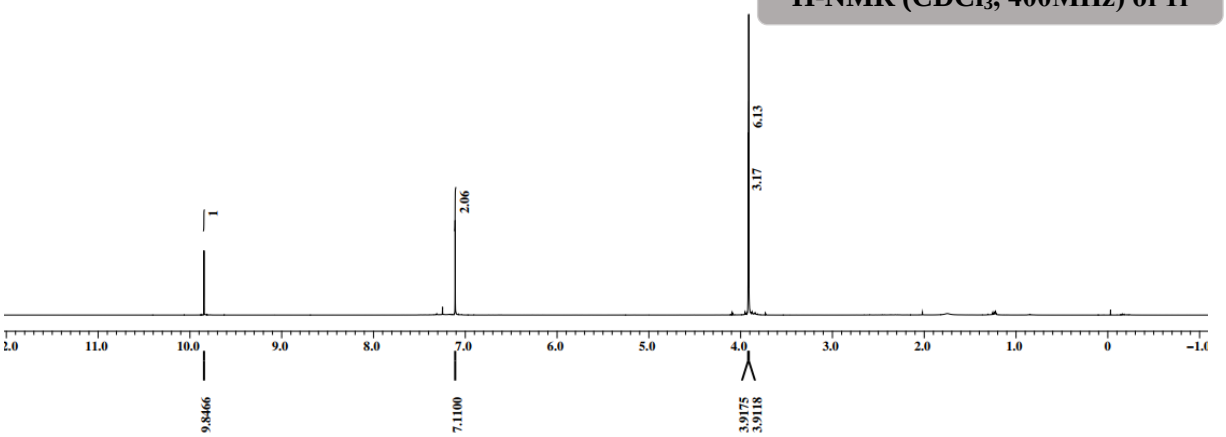

Mass data for Scheme 2.B.2.3.b

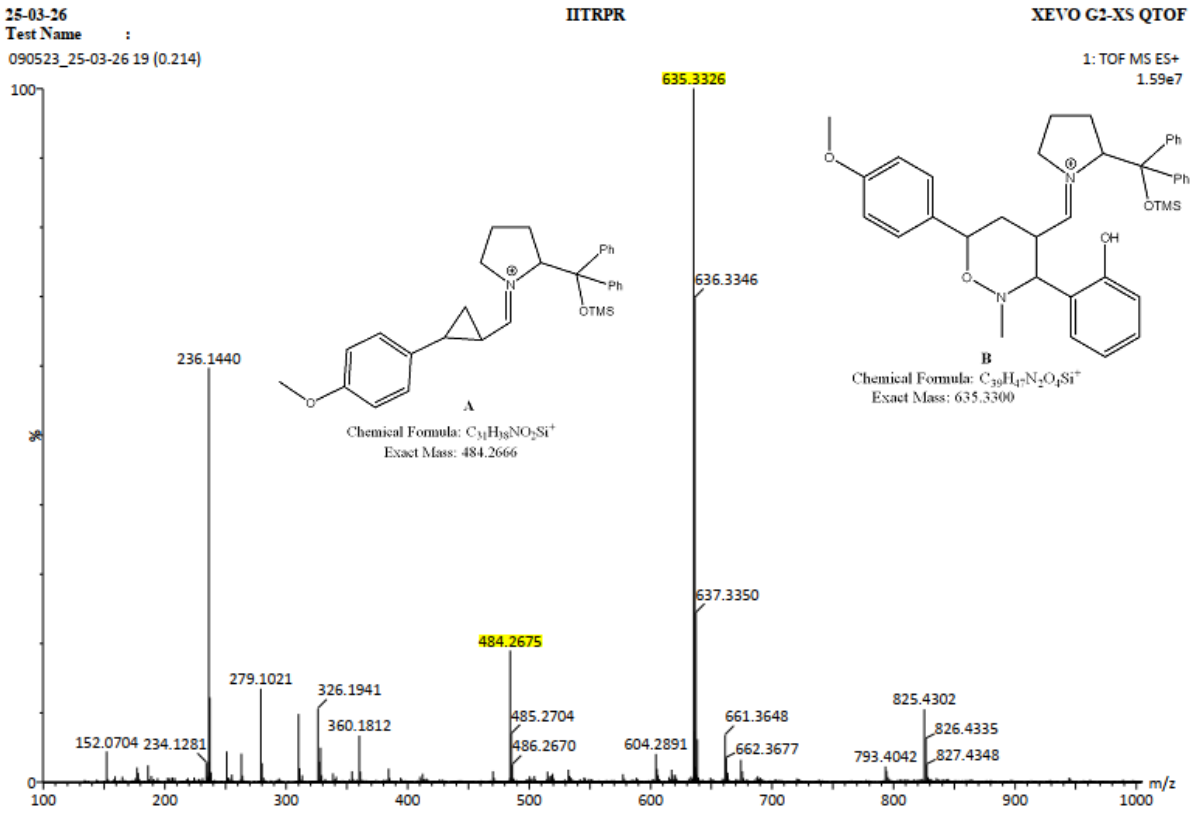

2.B.5. References

1. (a) Vitaku, E.; Smith, D. T.; Njardarson, J. T. *J. Med. Chem.* **2014**, *57*, 10257. (b) Kerru, N.; Gummidi, L.; Maddila, S.; Gangu, K. K.; Jonnalagadda, S. B. *Molecules.* **2020**, *25*, 1909. (c) Heravi, M. M.; Zadsirjan, V. *RSC Adv.* **2020**, *10*, 44247.

2. (a) Tsoungas, P. G. *Heterocycles.* **2002**, *57*, 1149; (b) Pfrengle, F.; Reissig, H.-U. *Chem. Soc. Rev.* **2010**, *39*, 549; (c) D. Yan, D.; Wang, K.; Bai, S.; Liu, B.; Bai, J.; Qi, X.; Hu, Y. *J. Am. Chem. Soc.* **2022**, *144*, 4269; (d) Zimmer, R.; Buchholz, M.; Collas, M.; Angermann, J.; Homann, K.; and Reissig, H.-U. *Eur. J. Org. Chem.* **2010**, 4111; (e) Cheng, S.; Yu, S. *Org. Biomol. Chem.* **2014**, *12*, 8607.

3. Murahashi, S.-I.; Imada, Y. *Chem. Rev.* **2019**, *119*, 4684.

4. Sibi, M. P.; Ma, Z.; Jasperse, C. P. *J. Am. Chem. Soc.* **2005**, *127*, 5764.

5. (a) Jen, W. S.; Wiener, J. J. M.; MacMillan, D. W. C. *J. Am. Chem. Soc.* **2000**, *122*, 9874; (b) Gioia, C.; Fini, F.; Mazzanti, A.; Bernardi, L.; Ricci, A. *J. Am. Chem. Soc.* **2009**, *131*, 9614; (c) Postikova, S.; Tite, T.; Levacher, V.; Brire, J.-F. *Adv. Synth. Catal*. **2013**, *355*, 2513; (d) Liu, Y.; Ao, J.; Paladhi, S.; Song, C. E.; Yan, H. *J. Am. Chem. Soc.* **2016**, *138*, 16486; (e) Tian, H.-Z.; Tang, Q.-G.; Lin, G.-Q.; Sun, X.-W. *RSC Adv.* **2022**, *12*, 15713.

6. Li, T.-Z.; Liu, S.-J.; Sun, Y-W.; Deng, S.; Tan, W.; Jiao, Y.; Zhang, Y.-C.; Shi, F. *Angew. Chem. Int. Ed.* **2020**, *59*, 2.

7. Reissig, H. -U.; Zimmer, R. *Chem. Rev*. **2003**, *103*, 1151.

8. (a) Schneider, T. F.; Kaschel, J.; Werz, D. B. *Angew. Chem., Int. Ed*., **2014**, *53*, 5504. (b) Cavitt, M. A.; Phun, L. H.; France, S. *Chem. Soc. Rev*. **2014**, *43*, 804. (c) Carson, C. A.; Kerr, M. A. *Chem. Soc. Rev.* **2009**, *38*, 3051. (d) Pirenne, V.; Muriel, B.; Waser, J. *Chem. Rev.* **2021**, *121*, 227. (e) Xia, Y.; Liu, X.; Feng, X. *Angew. Chem., Int. Ed*. **2021**, *60*, 9192.

9. (a) Ghosh, A.; Dey, R.; Banerjee, P. *Chem. Commun.* **2021**, *57*, 5359; (b) Pandey, A. K.; Ghosh, A.; Banerjee, P. *Isr. J. Chem*, **2016**, *56*, 512; (c) Singh, P.; Varshnaya, R. K.; Dey, R.; Banerjee, P. *Adv. Synth. Catal*. **2020**, *362*, 1447.

10. Li, L.; Li, Z.; and Wang, Q. *Synlett.*, **2009**, *11*, 1830.

11. (a) Sparr, C.; Gilmour, R. *Angew. Chem., Int. Ed*. **2011**, *50*, 8391. (b) Wallbaum, J.; Garve, L. K. B.; Jones, P. G.; Werz, D. B. *Chem. Eur. J.* **2016**, *22*, 18756 (c) Diaz, E.; Reyes, E.; Uria, U.; Carrillo, L.; Tejero, T.; Merino, P.; and Vicario, J. L. *Chem. Eur. J*. **2018**, *24*, 8764.

12. (a) Dey, R.; Banerjee, P. *Adv. Synth. Catal*. **2019**, *361*, 2849; (b) Dey, R.; Rajput, S.; and Banerjee, P. *Tetrahedron*. **2020**, *76*, 131080; (c) Singh, P.; Kaur, N.; Banerjee, P. *J. Org. Chem.* **2020**, *85*, 3393.

13. (a) Gygax, P; Gupta, T. K. D.; Eschenmoser, A. *Helv. Chim. Acta.* **1972**, *55*, 2205; (b) Kumar, P. S.; Rai, K. M. L. *E. -J. Chem*, **2012**, *9*, 131; (c) Erden, I.; Gärtner, C.; Ma, J.; Cabrera, G.; Markham, K.; Azimi, S.; Gronert, S. *Eur. J. Org. Chem.* **2017**, 5147.

14. (a) Faber, K.; Griengl, H.; Steinreiber, J. *Chem. Eur. J.* **2008**, *14*, 8060; (b) Faber, K. *Chem. Eur. J.* **2001**, *7*, 5004.

15. (a) Smolobochkin, A. V.; Melyashova, A. S.; Voronina, J. K.; Strelnik, A. G.; Vatsadze, S. Z.; Burilov, A. R.; Pudovik, M. A.; Fedorova, O. A.; Sinyashina, O. G.; Gazizov, A. S. *RSC Adv*. **2017**, *7*, 50955; (b) Chen, C.-H.; Yellol, G. S.; Lin, P.-T.; Sun, C.-M. O*rg. Lett.* **2011**, *13*, 5120.

16. Poulsen, P. H.; Vergura, S.; Monleon, A.; Jørgensen, D. K. B.; Jørgensen, K. A. *J. Am. Chem. Soc.* **2016**, *138*, 6412.

17. Blackburn, L.; Taylor, R. J. K. *Org. Lett*. **2001**, *3*, 1637.

18. Ando, K.; Yamada, K. *Green Chem*., **2011**, *13*, 1143

19. Verma, K.; Banerjee, P. *Adv. Synth. Catal.* **2016**, *358*, 2053.

2.B.6. NMR spectra and HPLC data of the compounds

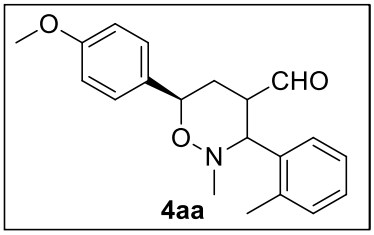

^{1}H-NMR ($CDCl_3$, 400MHz) of 4aa

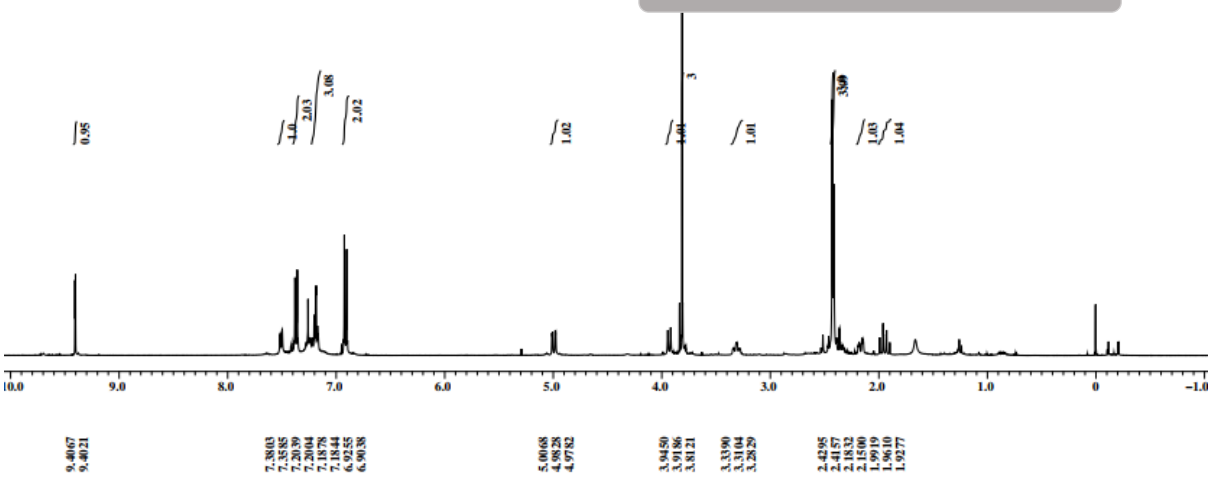

^{13}C-NMR ($CDCl_3$, 100MHz) of 4aa

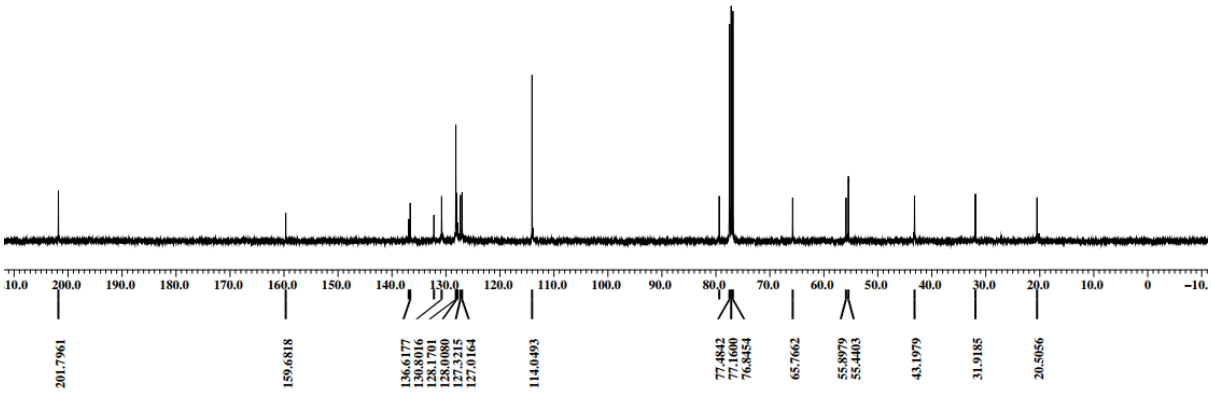

^{1}H-^{1}H COSY NMR ($CDCl_3$, 400MHz) of 4aa

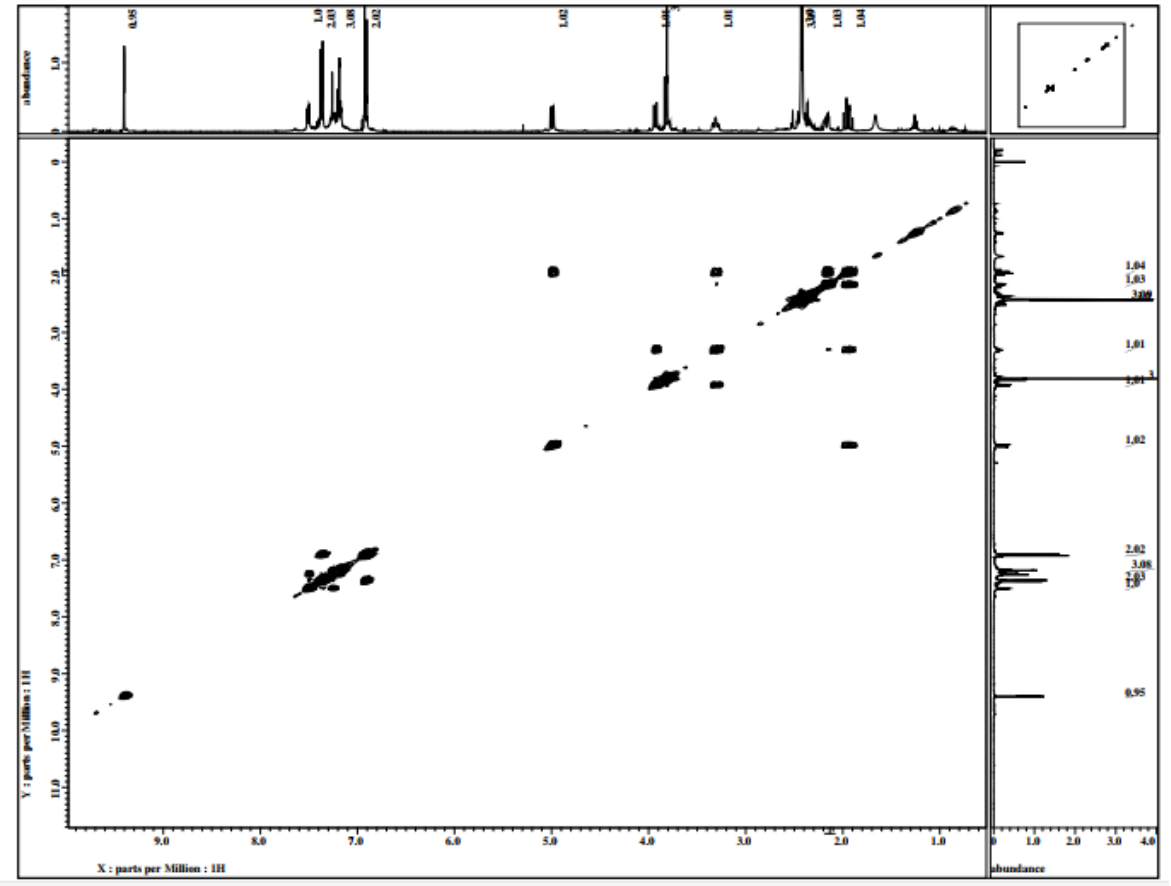

^{1}H-^{1}H NOESY NMR ($CDCl_3$, 400MHz) of 4aa

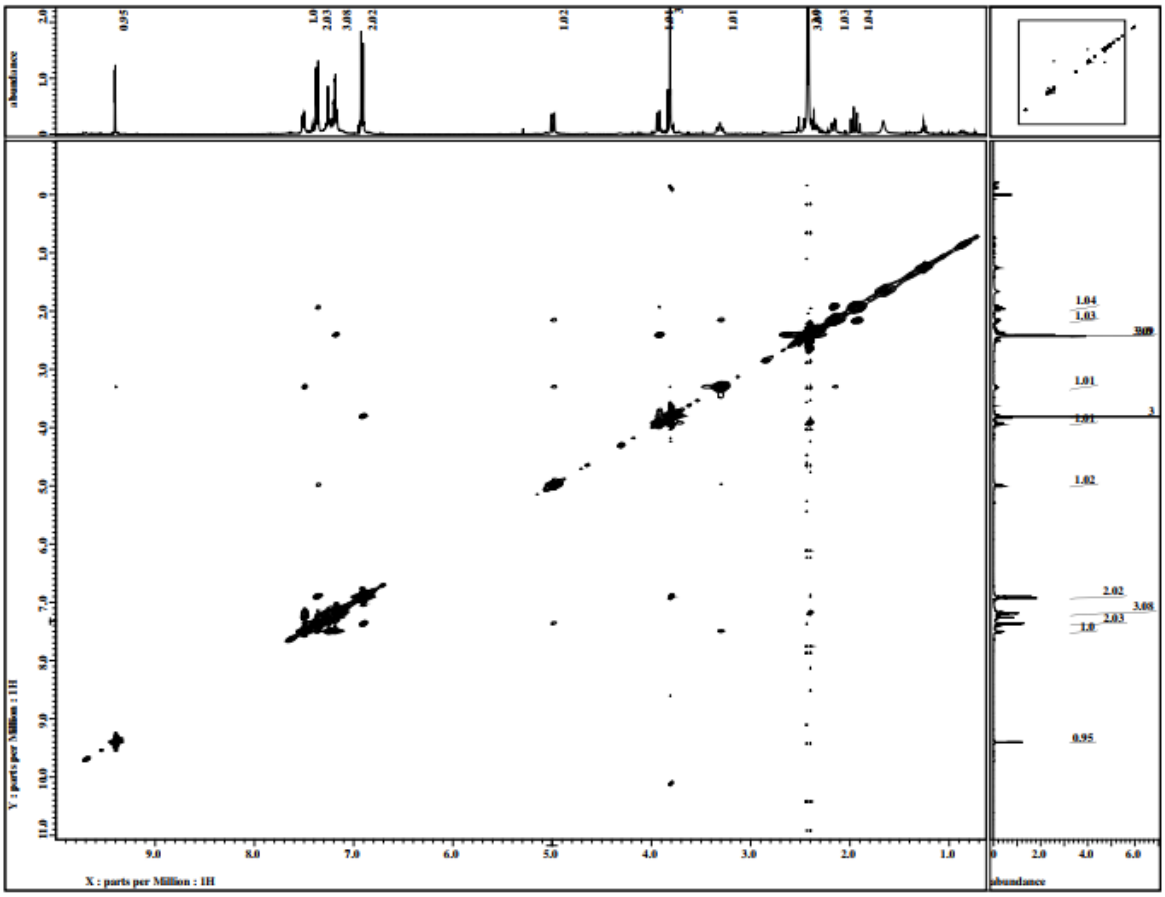

^{1}H-^{1}H NOESY NMR ($CDCl_3$, 400MHz) of 4aa ZOOM

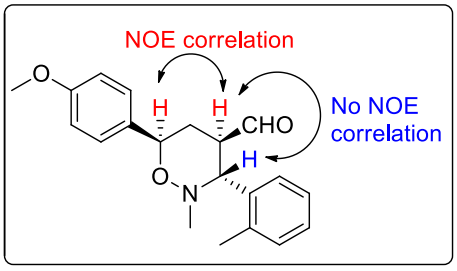

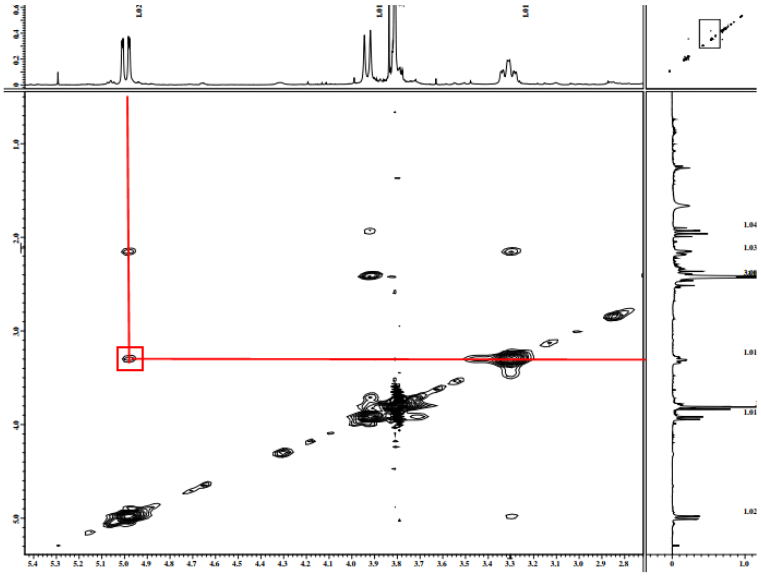

HPLC spectra of racemic 4aa

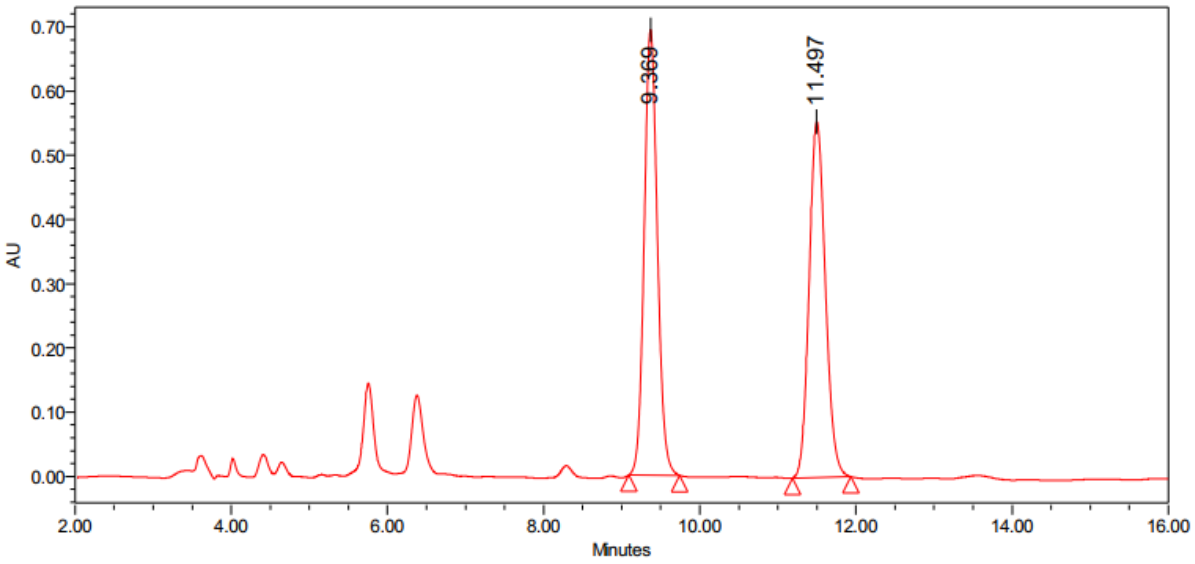

Peak Results

	Name	RT	Area	% Area
1		9.369	8137460	50.34
2		11.497	8026886	49.66

HPLC spectra of chiral 4aa

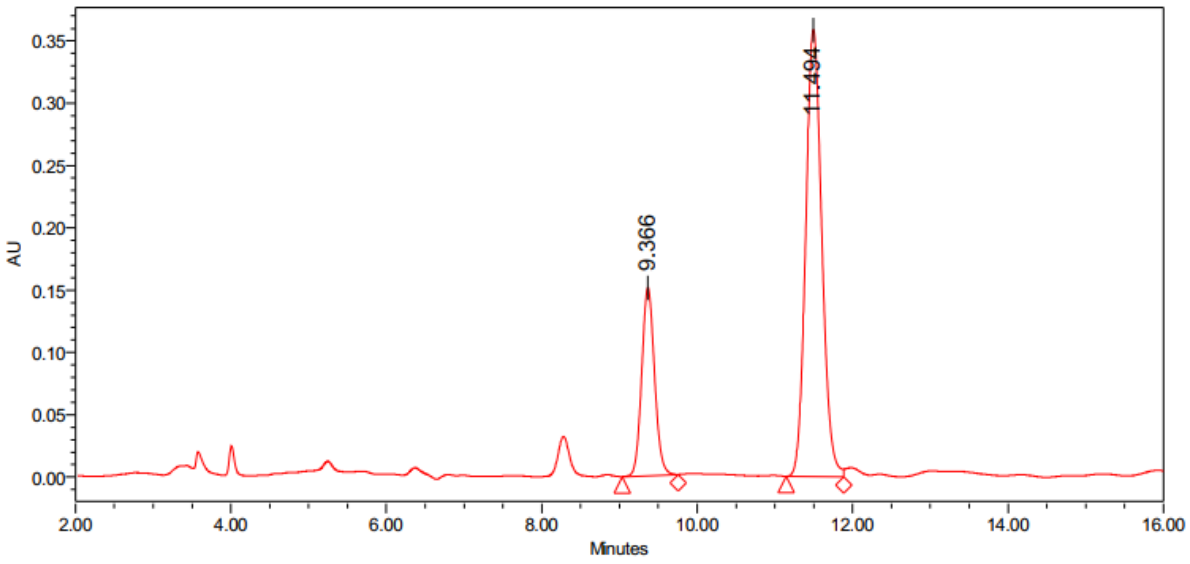

Peak Results

	Name	RT	Area	% Area
1		9.366	1744152	25.21
2		11.494	5174913	74.79

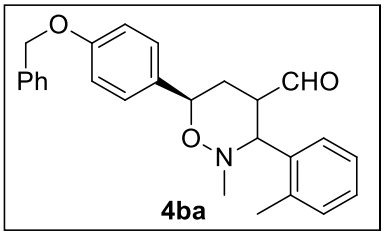

4ba

^{1}H-NMR ($CDCl_3$, 400MHz) of 4ba

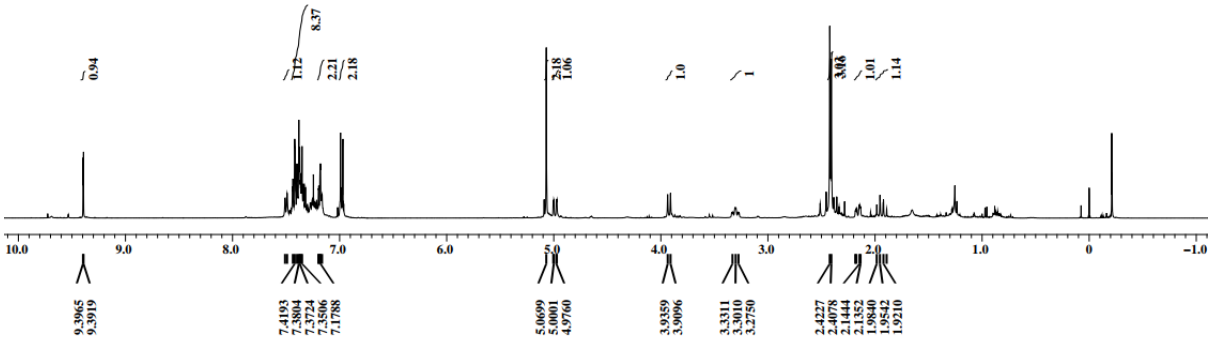

^{13}C-NMR ($CDCl_3$, 100MHz) of 4ba

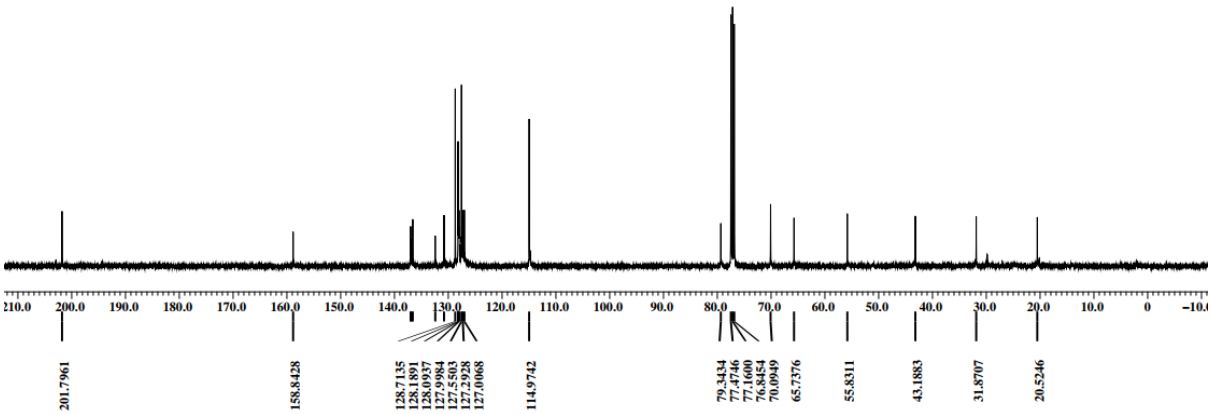

HPLC spectra of racemic 4ba

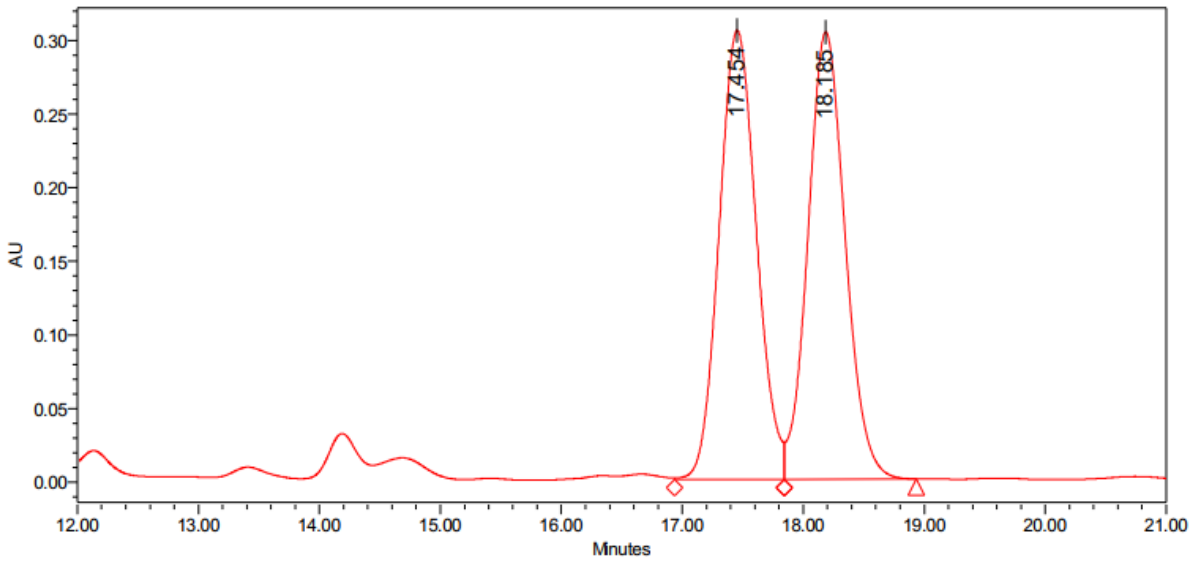

Peak Results

	Name	RT	Area	% Area
1		17.454	6537031	50.05
2		18.185	6523167	49.95

HPLC spectra of chiral 4ba

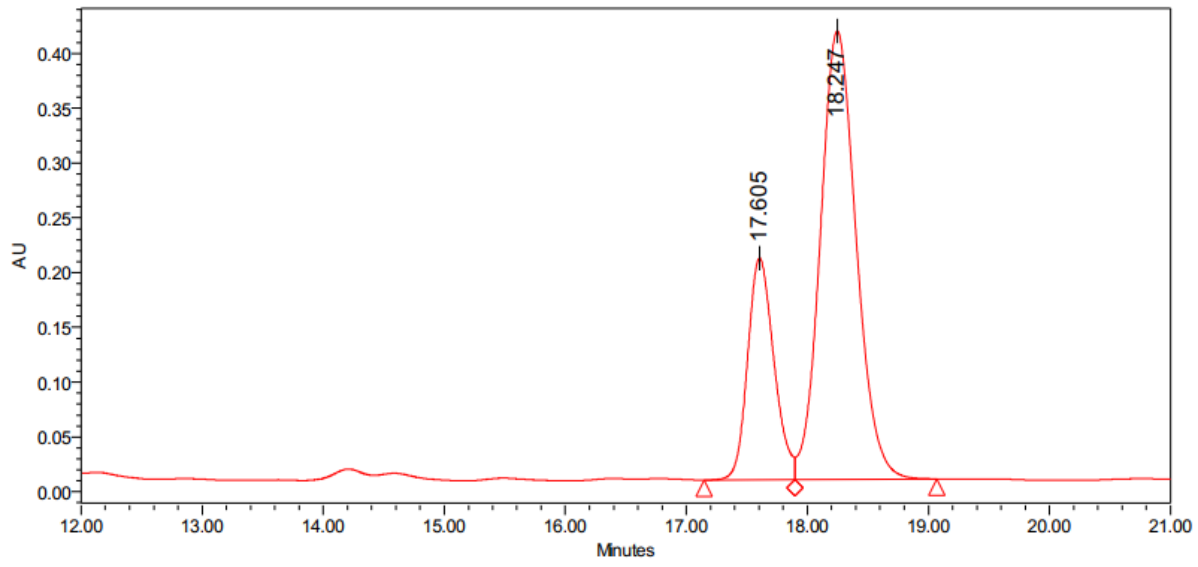

Peak Results

	Name	RT	Area	% Area
1		17.605	3052717	26.59
2		18.247	8429311	73.41

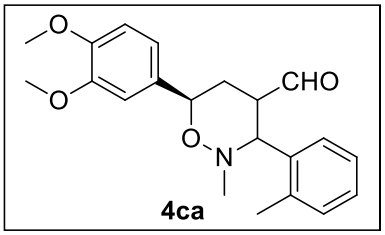

4ca

^{1}H-NMR ($CDCl_3$, 400MHz) of 4ca

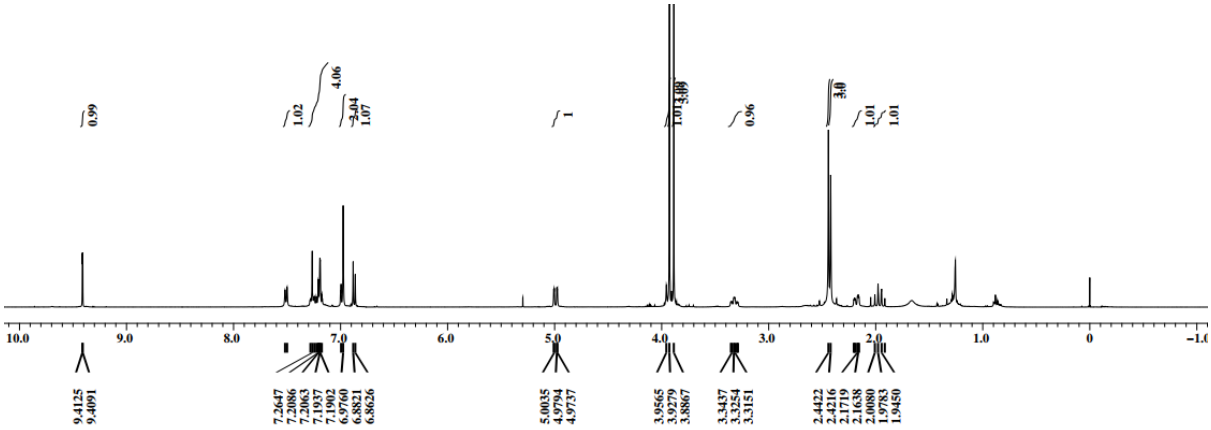

^{13}C-NMR ($CDCl_3$, 100MHz) of 4ca

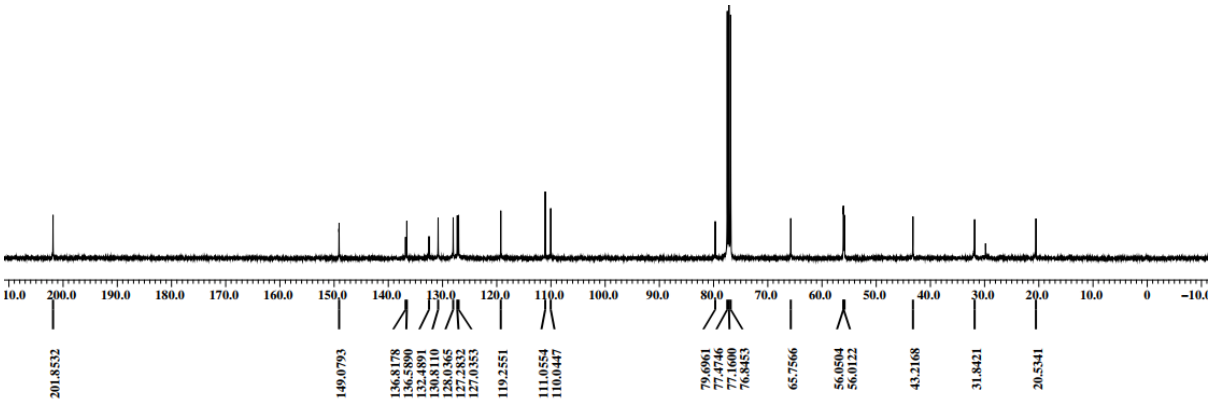

HPLC spectra of racemic 4ca

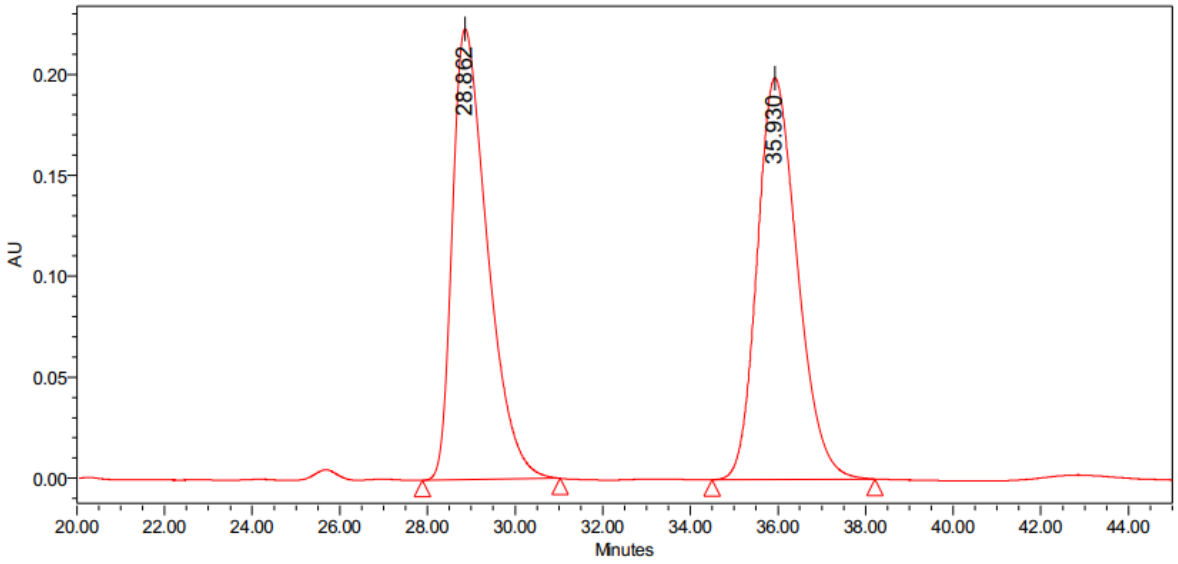

Peak Results

	Name	RT	Area	% Area
1		28.862	12434799	49.55
2		35.930	12660008	50.45

HPLC spectra of chiral 4ca

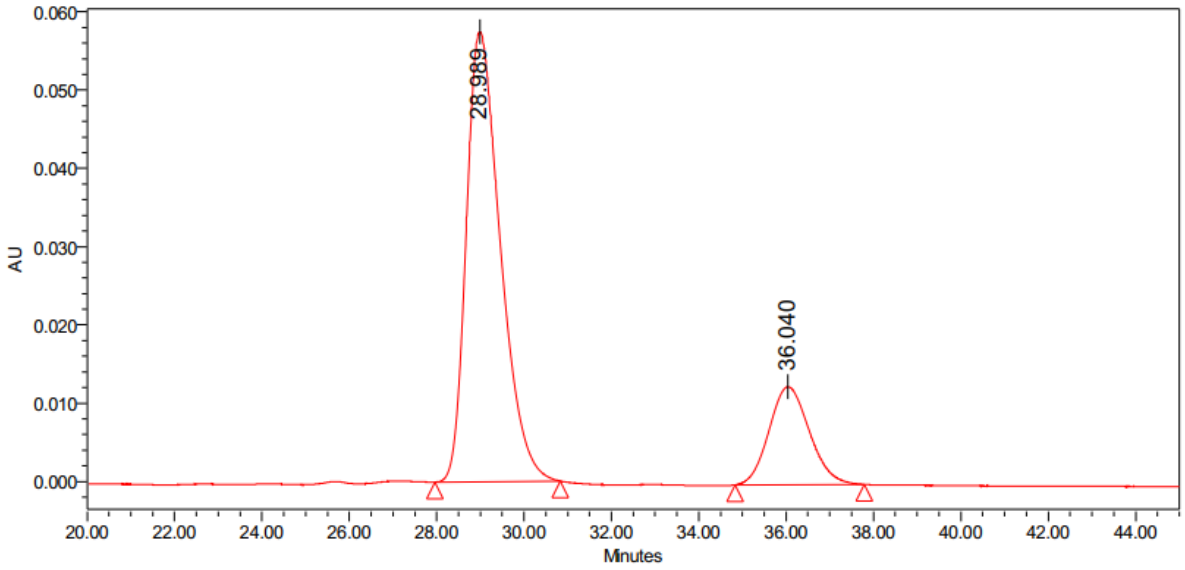

Peak Results

	Name	RT	Area	% Area
1		28.989	3129184	79.65
2		36.040	799360	20.35

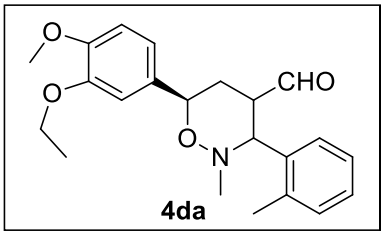

4da

^{1}H-NMR ($CDCl_3$, 400MHz) of 4da

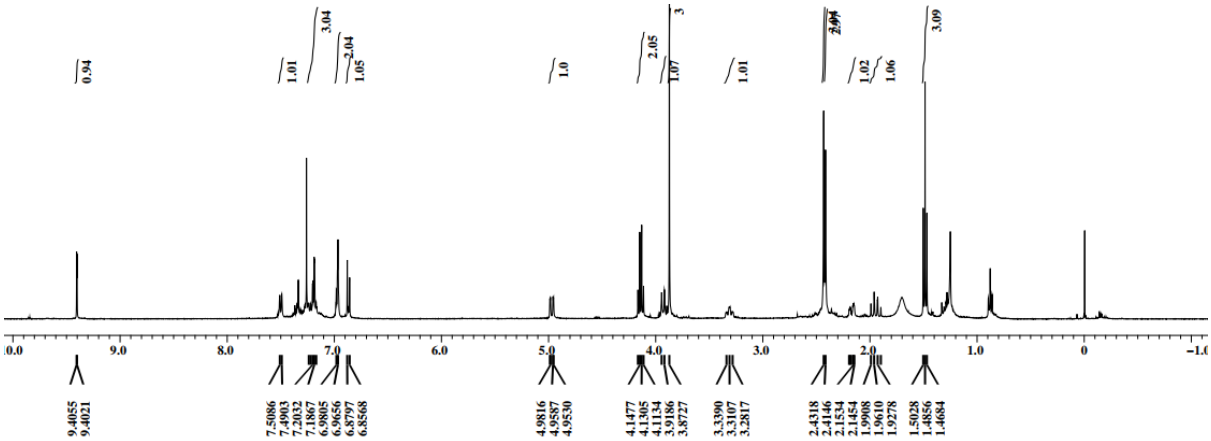

^{13}C-NMR ($CDCl_3$, 100MHz) of 4da

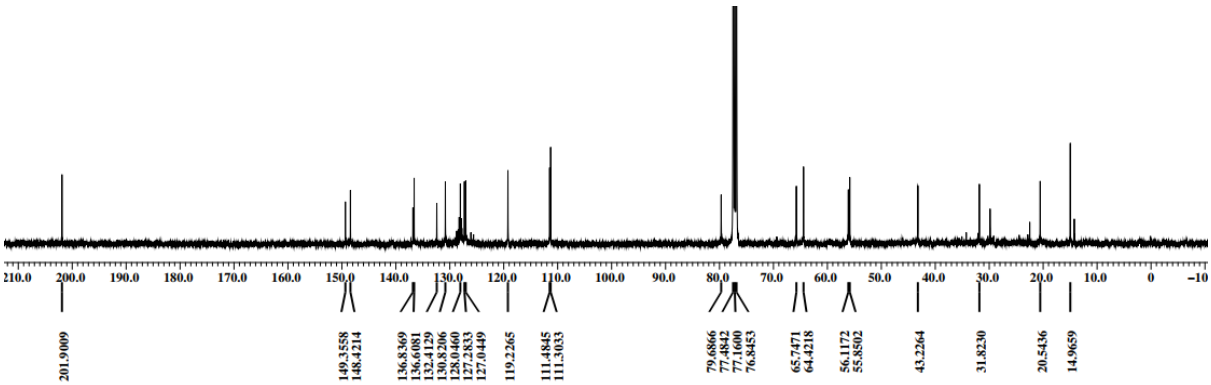

HPLC spectra of racemic 4da

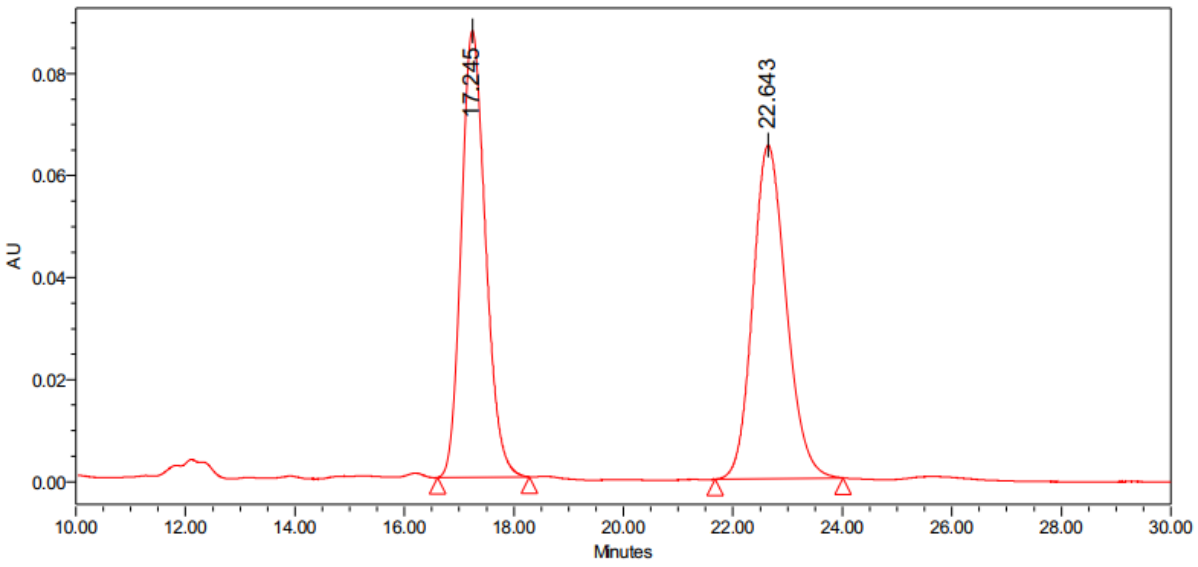

Peak Results

	Name	RT	Area	% Area
1		17.245	2688440	49.39
2		22.643	2754392	50.61

HPLC spectra of chiral 4da

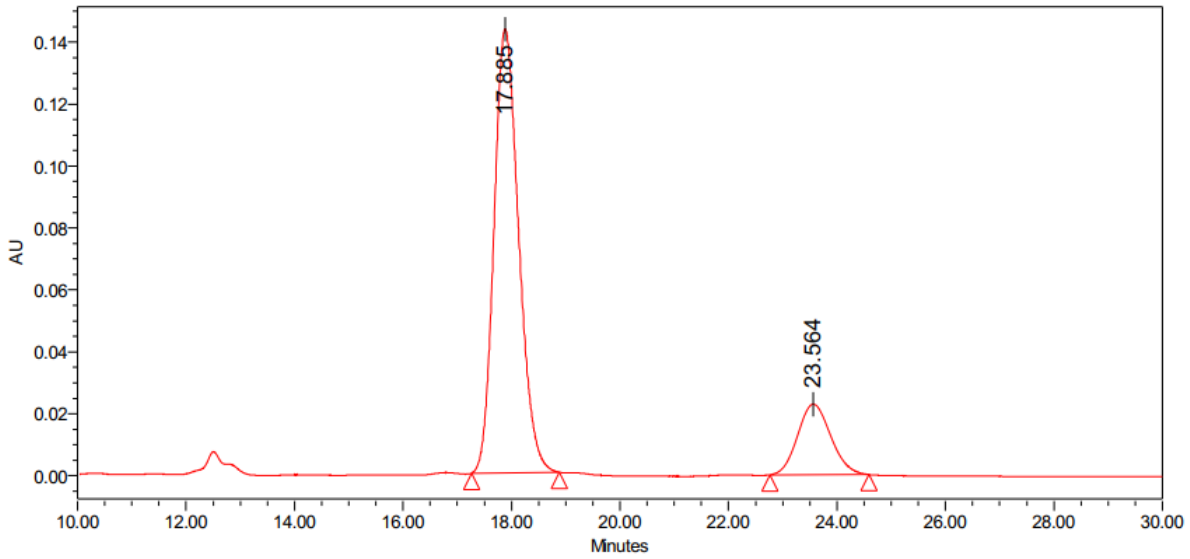

Peak Results

	Name	RT	Area	% Area
1		17.885	4516387	82.34
2		23.564	968732	17.66

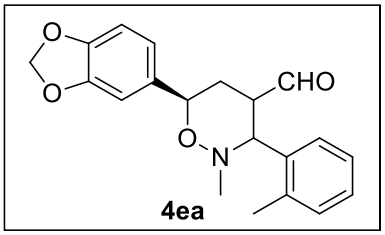

4ea

^{1}H-NMR ($CDCl_3$, 400MHz) of 4ea

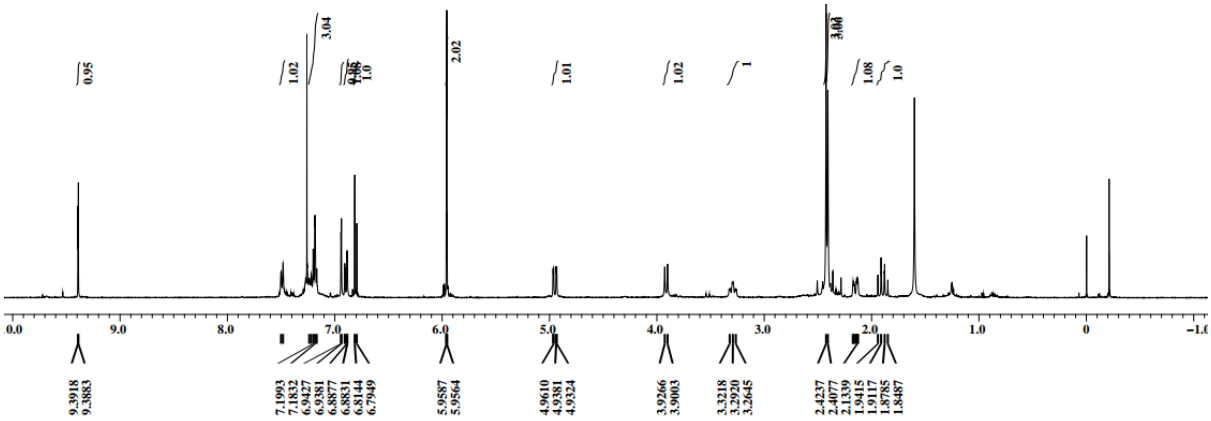

^{13}C-NMR ($CDCl_3$, 100MHz) of 4ea

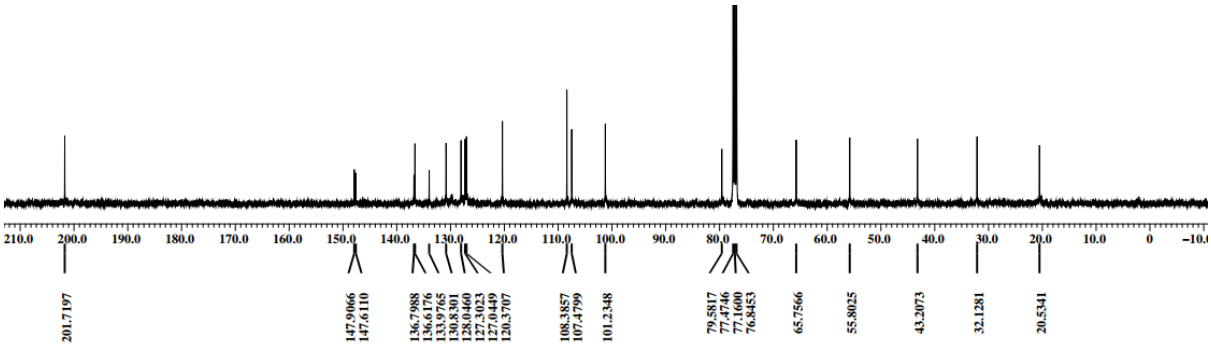

HPLC spectra of racemic 4ea

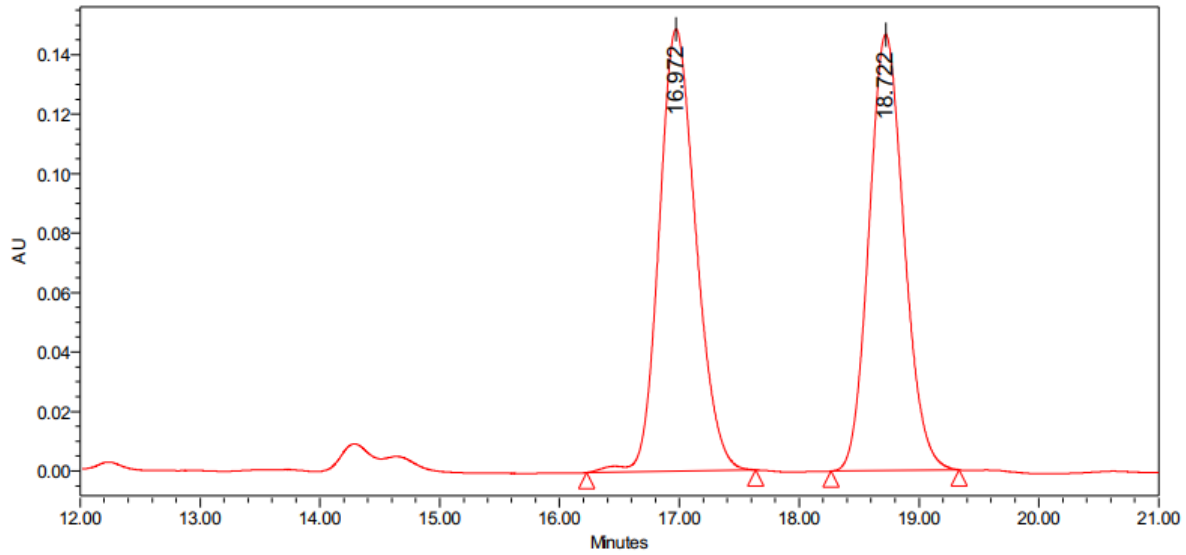

Peak Results

	Name	RT	Area	% Area
1		16.972	3172593	51.51
2		18.722	2987108	48.49

HPLC spectra of chiral 4ea

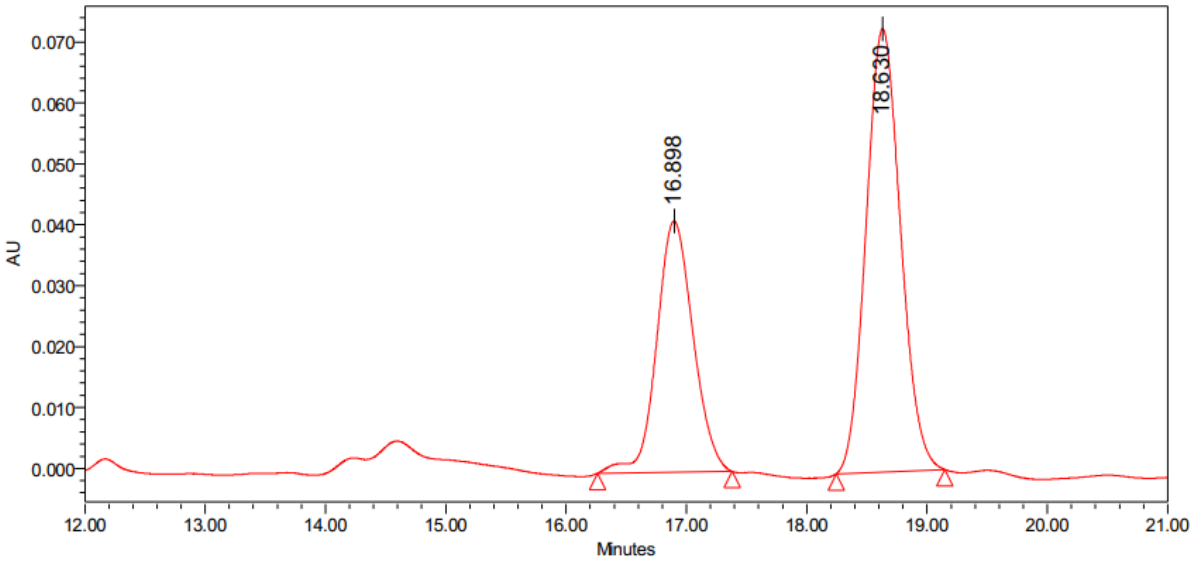

Peak Results

	Name	RT	Area	% Area
1		16.898	868034	37.44
2		18.630	1450514	62.56

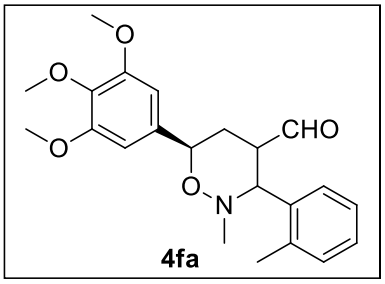

4fa

^{1}H-NMR ($CDCl_3$, 400MHz) of 4fa

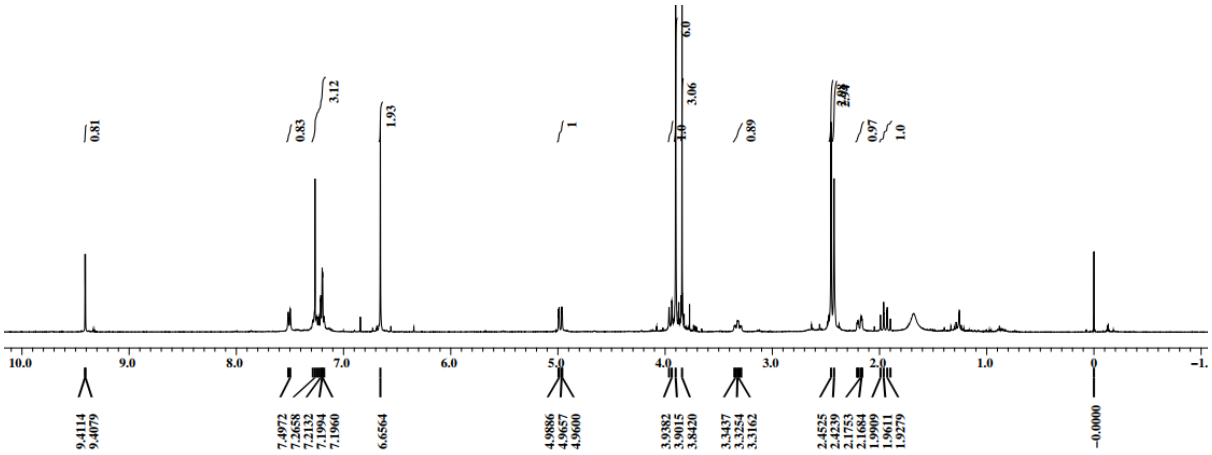

^{13}C-NMR ($CDCl_3$, 100MHz) of 4fa

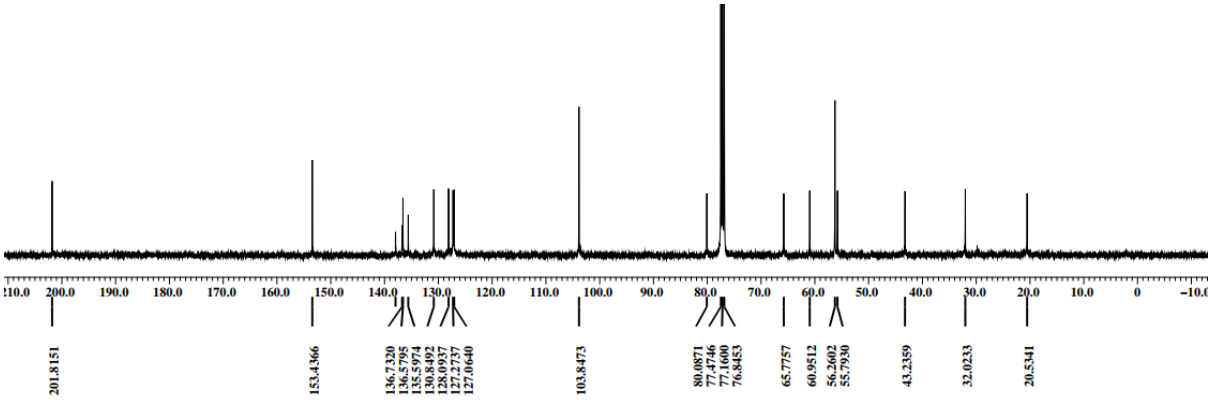

HPLC spectra of racemic 4fa

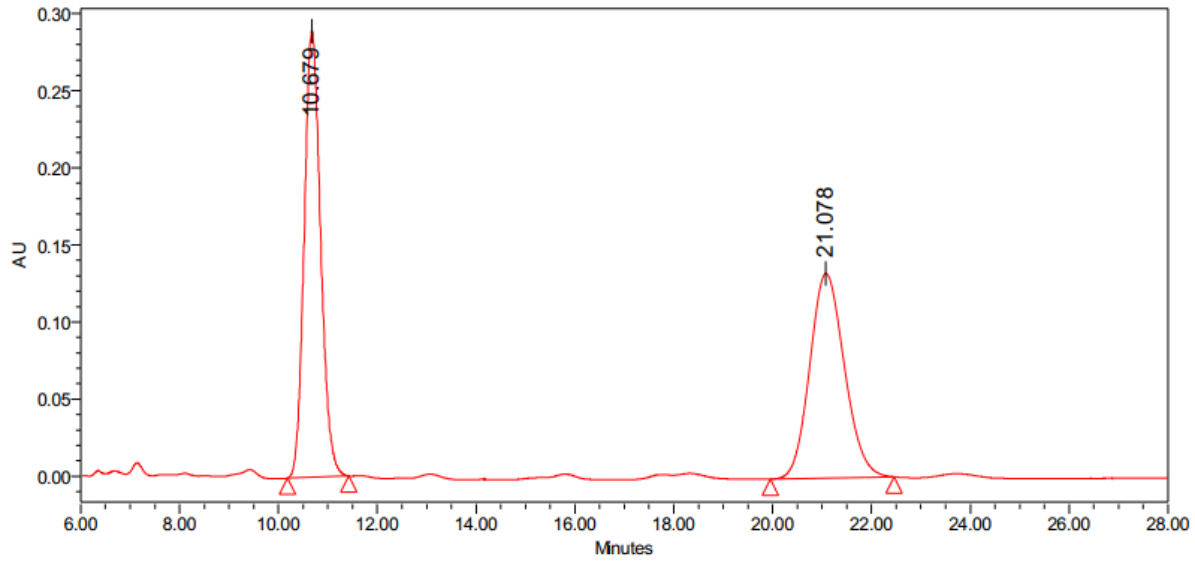

Peak Results

	Name	RT	Area	% Area
1		10.679	6637235	50.63
2		21.078	6471619	49.37

HPLC spectra of chiral 4fa

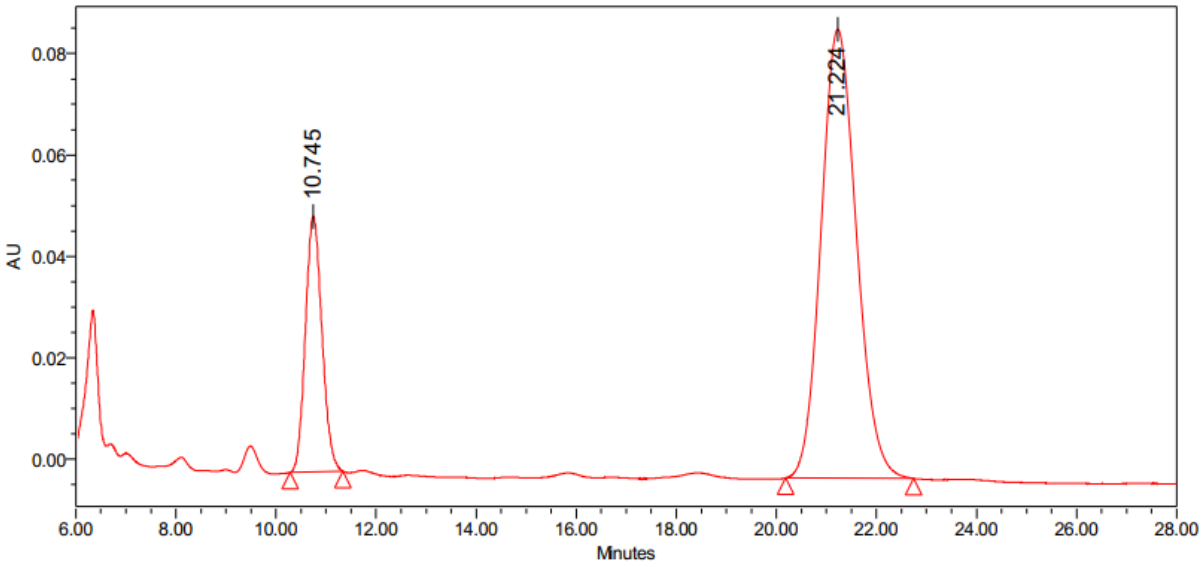

Peak Results

	Name	RT	Area	% Area
1		10.745	1151929	20.89
2		21.224	4362202	79.11

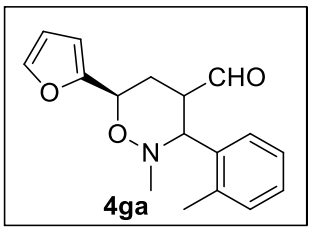

4ga

^{1}H-NMR ($CDCl_3$, 400MHz) of 4ga

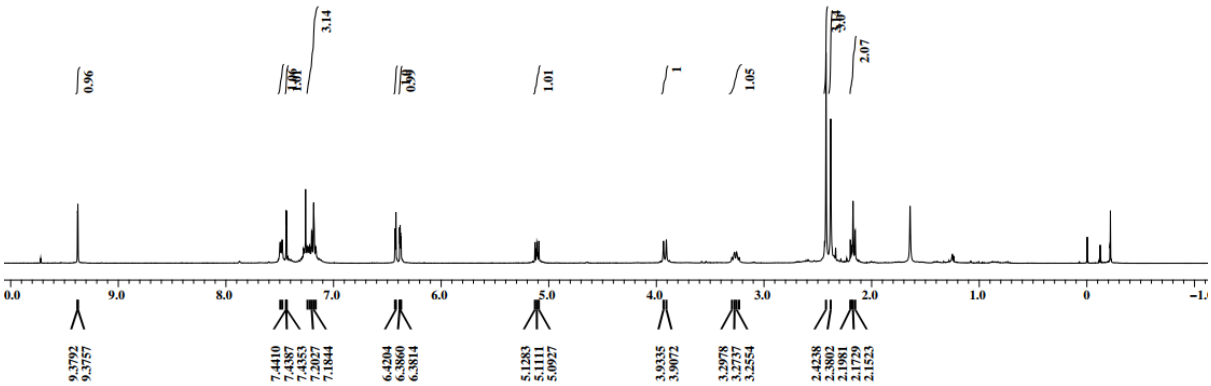

^{13}C-NMR ($CDCl_3$, 100MHz) of 4ga

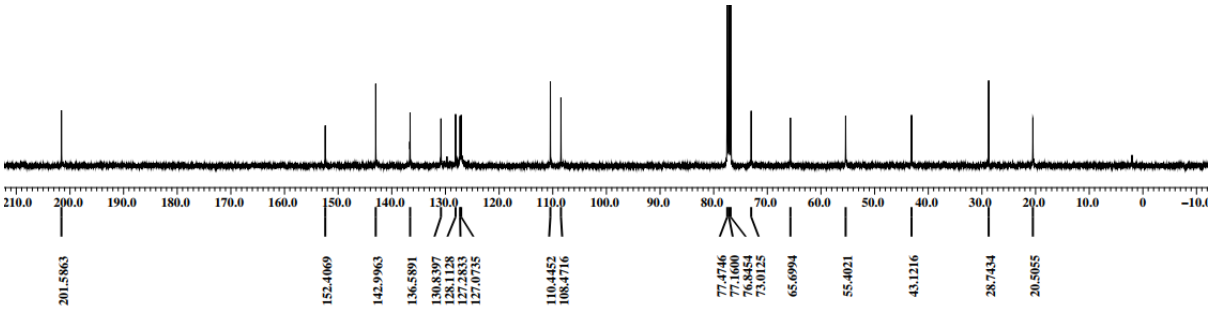

HPLC spectra of racemic 4ga

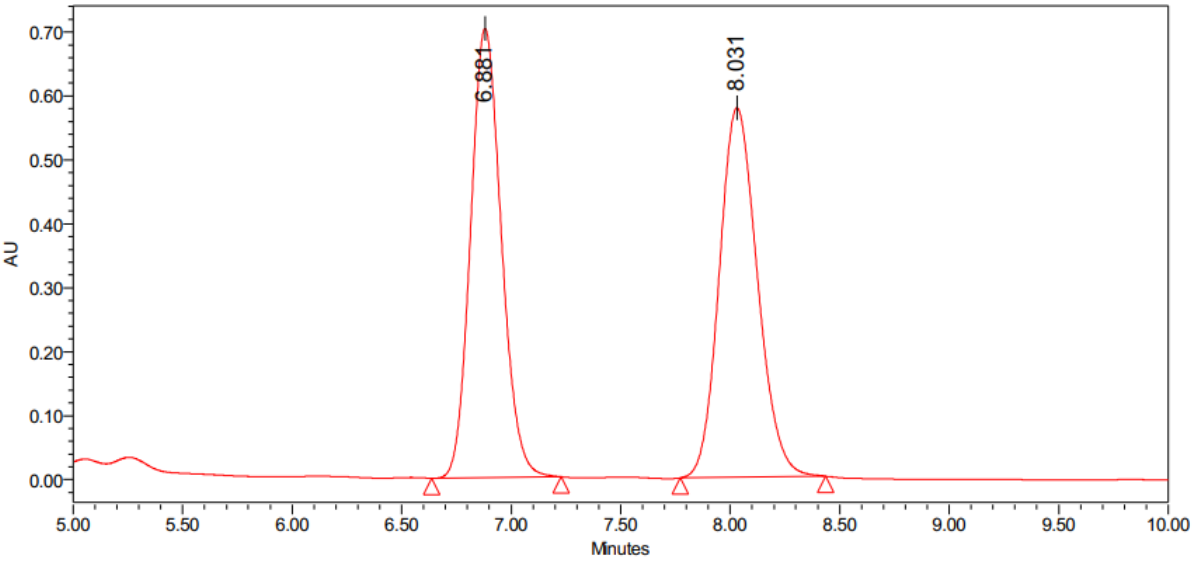

Peak Results

	Name	RT	Area	% Area
1		6.881	6863940	49.50
2		8.031	7003882	50.50

HPLC spectra of chiral 4ga

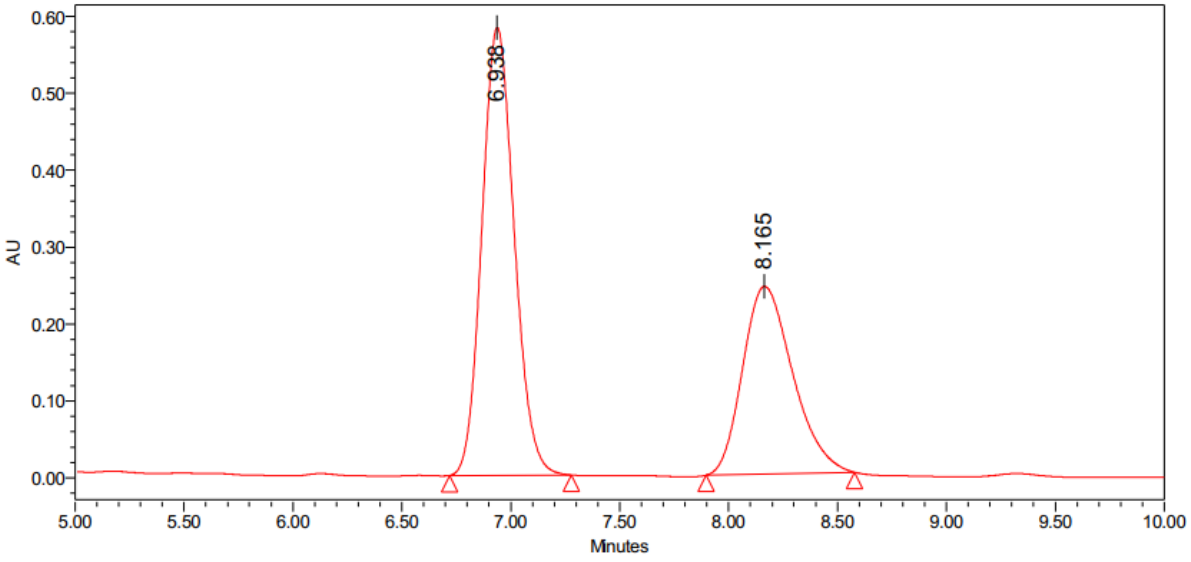

Peak Results

	Name	RT	Area	% Area
1		6.938	5999199	60.60
2		8.165	3899658	39.40

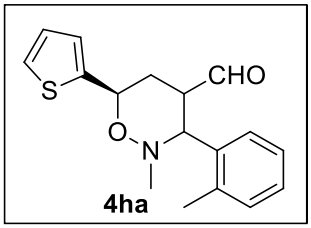

^{1}H-NMR ($CDCl_3$, 400MHz) of 4ha

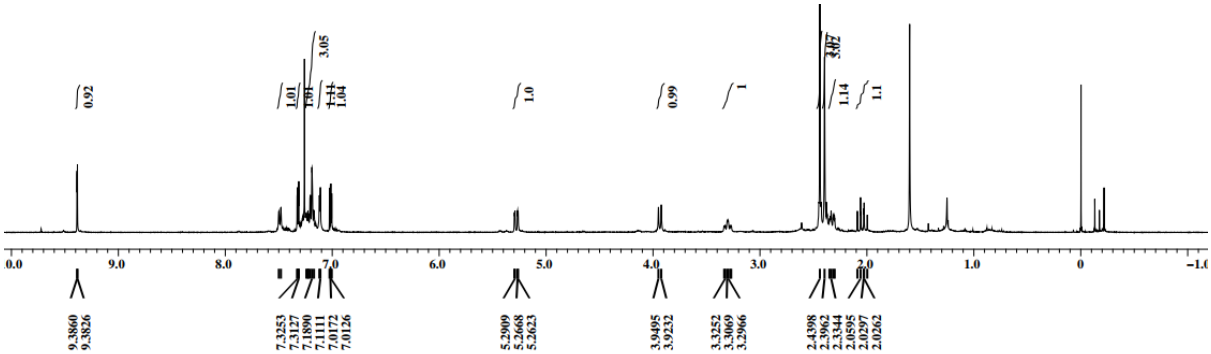

^{13}C-NMR ($CDCl_3$, 100MHz) of 4ha

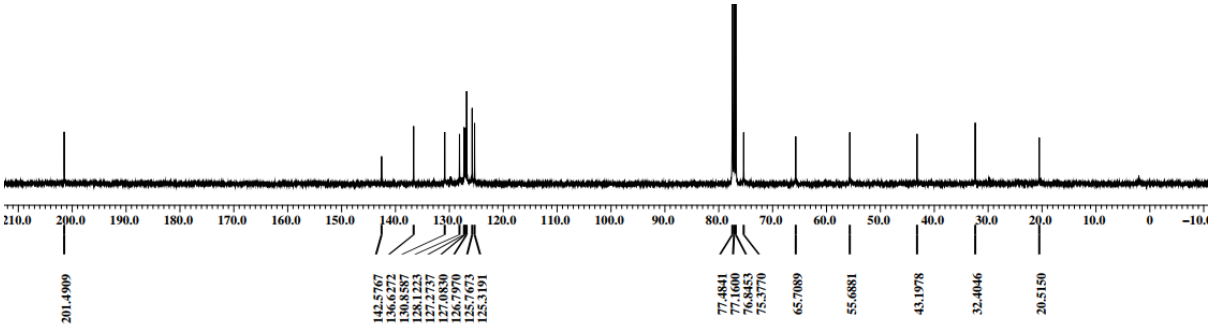

HPLC spectra of racemic 4ha

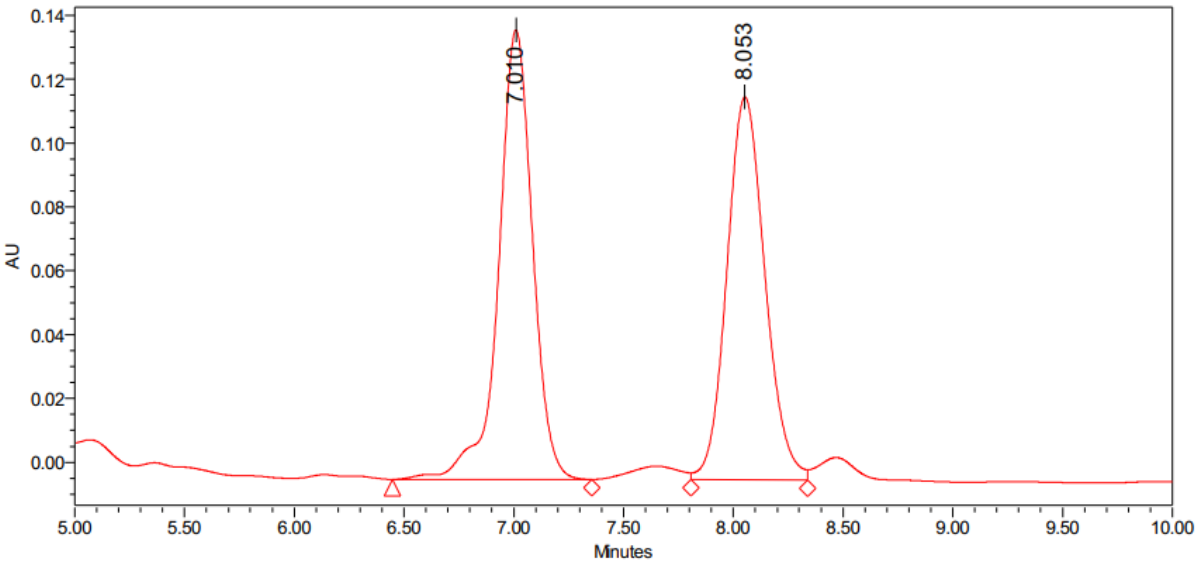

Peak Results

	Name	RT	Area	% Area
1		7.010	1519581	51.22
2		8.053	1447373	48.78

HPLC spectra of chiral 4ha

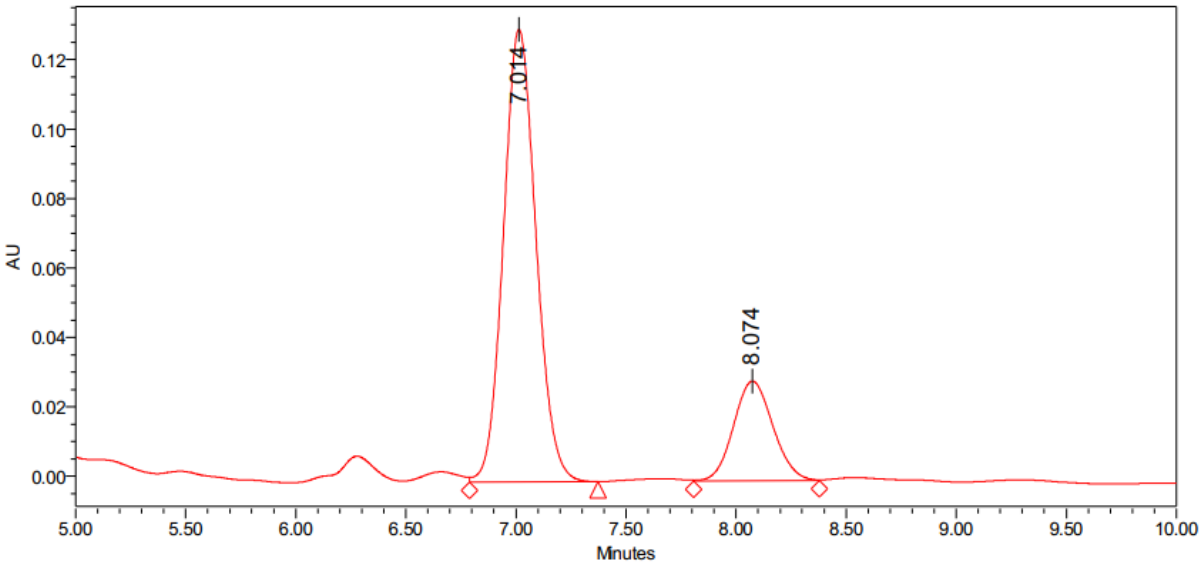

Peak Results

	Name	RT	Area	% Area
1		7.014	1344097	79.01
2		8.074	356979	20.99

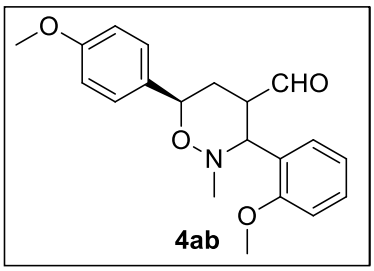

4ab

^{1}H-NMR ($CDCl_3$, 400MHz) of 4ab

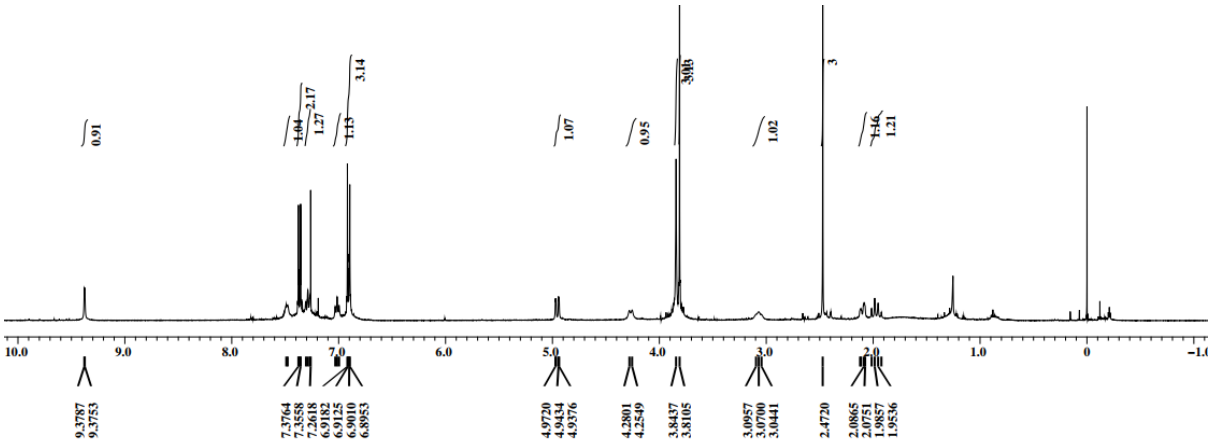

^{13}C-NMR ($CDCl_3$, 100MHz) of 4ab

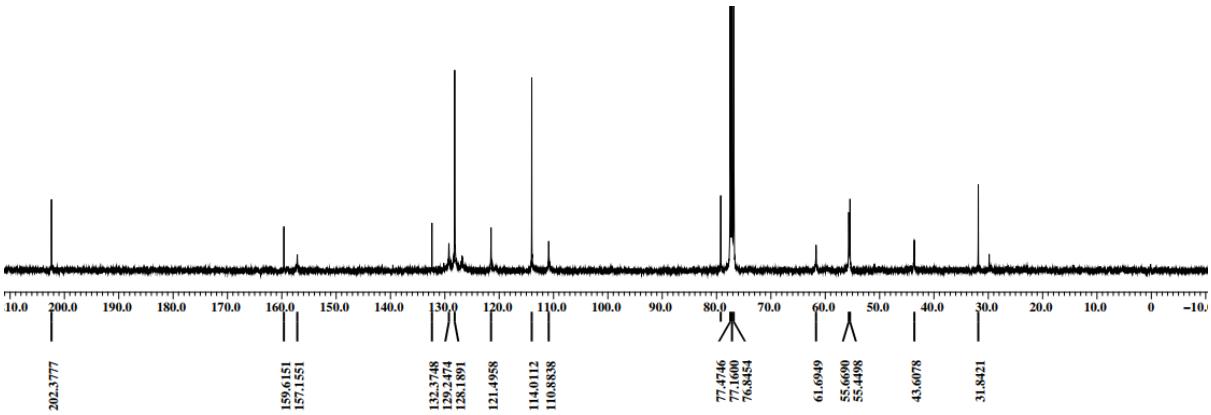

HPLC spectra of racemic 4ab

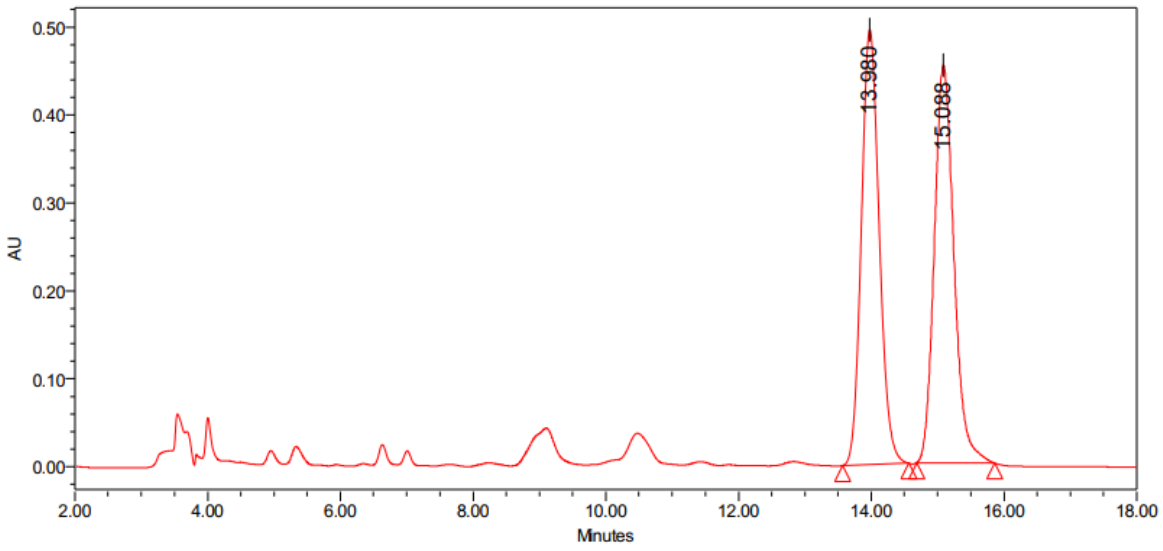

Peak Results

	Name	RT	Area	% Area
1		13.980	9249099	49.91
2		15.088	9281271	50.09

HPLC spectra of chiral 4ab

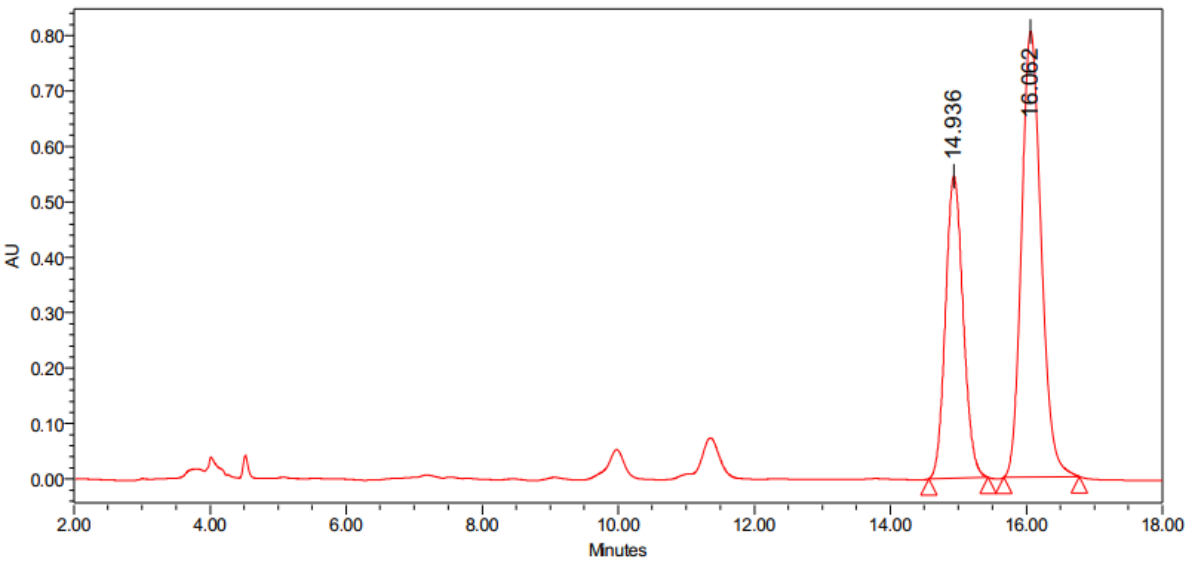

Peak Results

	Name	RT	Area	% Area
1		14.936	9810358	37.87
2		16.062	16093781	62.13

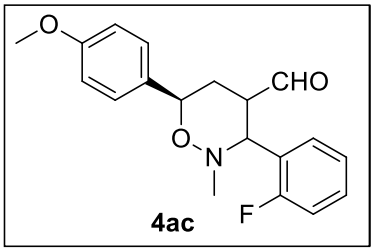

4ac

^{1}H-NMR ($CDCl_3$, 400MHz) of 4ac

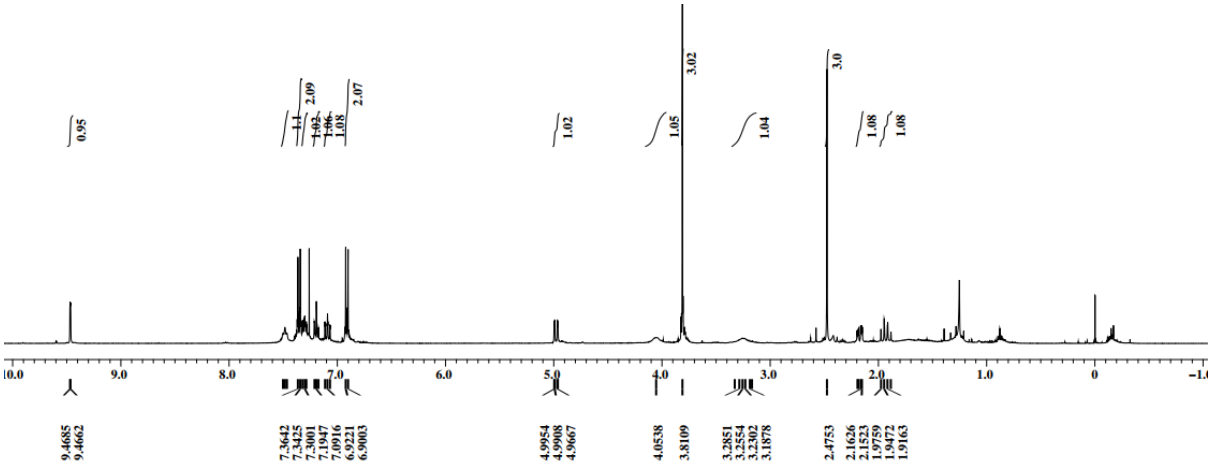

^{13}C-NMR ($CDCl_3$, 100MHz) of 4ac

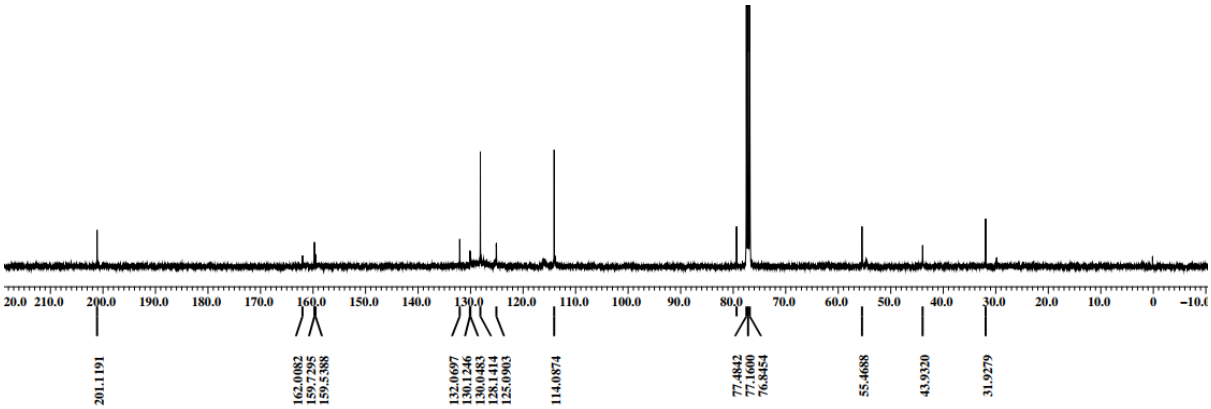

HPLC spectra of racemic 4ac

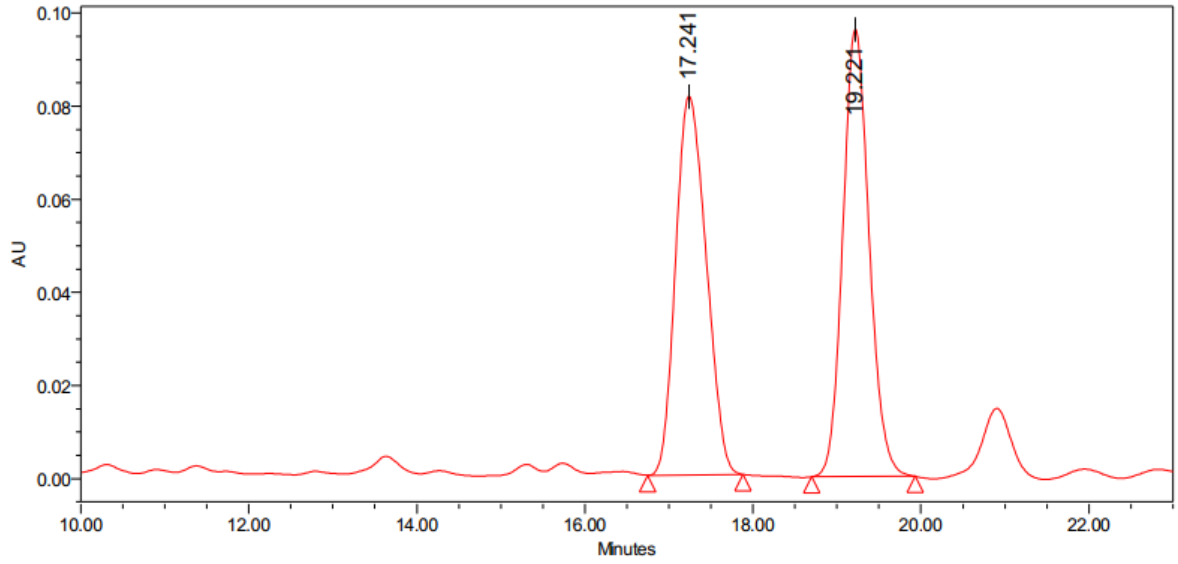

Peak Results

	Name	RT	Area	% Area
1		17.241	2054329	49.55
2		19.221	2091329	50.45

HPLC spectra of chiral 4ac

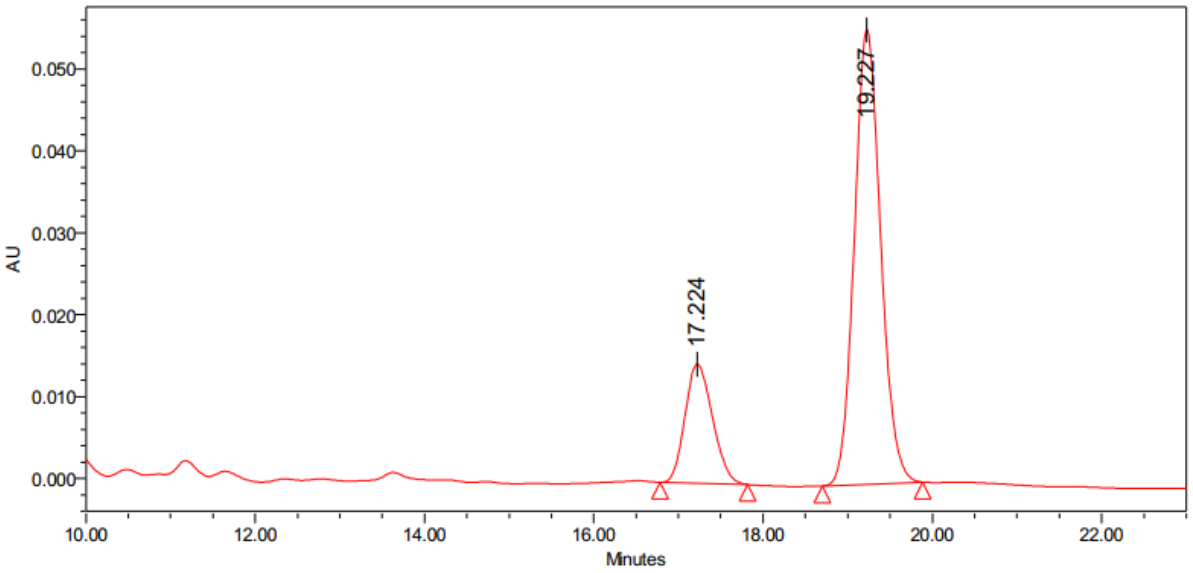

Peak Results

	Name	RT	Area	% Area
1		17.224	329205	21.52
2		19.227	1200389	78.48

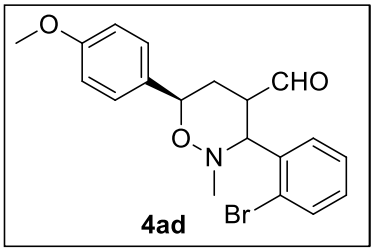

4ad

^{1}H-NMR ($CDCl_3$, 400MHz) of 4ad

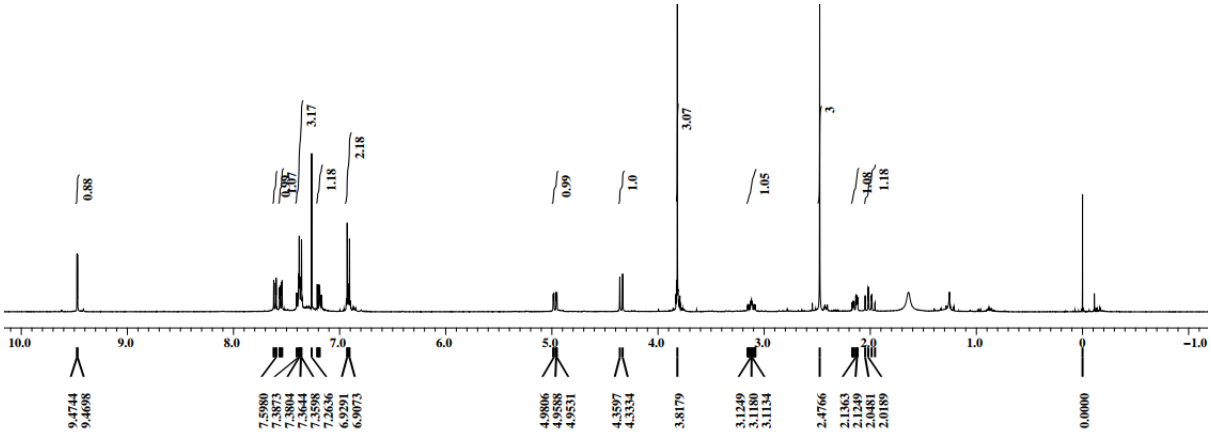

^{13}C-NMR ($CDCl_3$, 100MHz) of 4ad

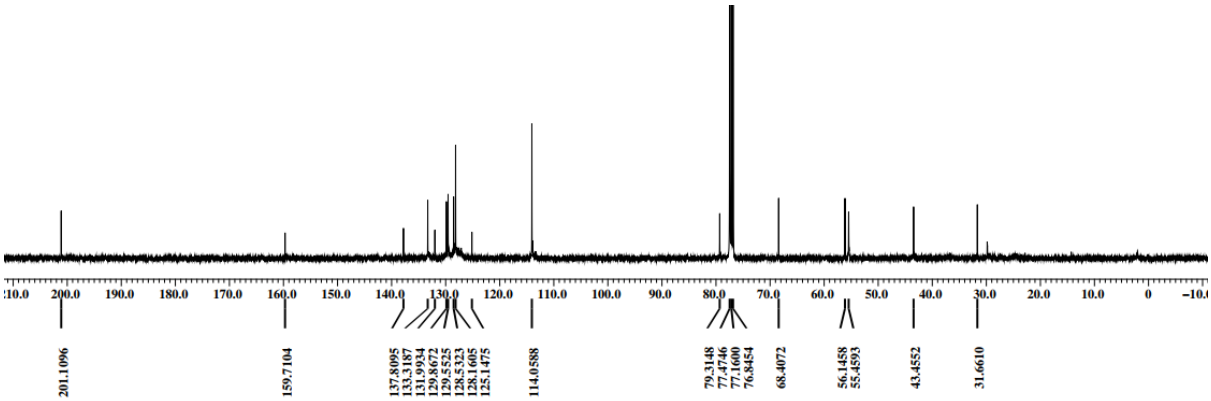

HPLC spectra of racemic 4ad

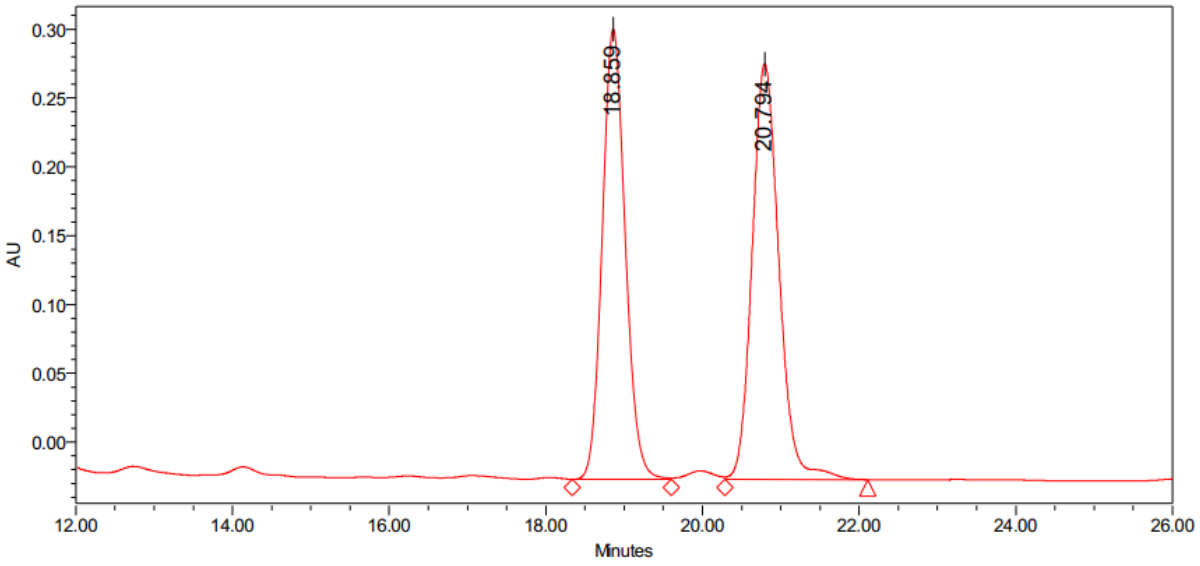

Peak Results

	Name	RT	Area	% Area
1		18.859	6668118	48.17
2		20.794	7174643	51.83

HPLC spectra of chiral 4ad

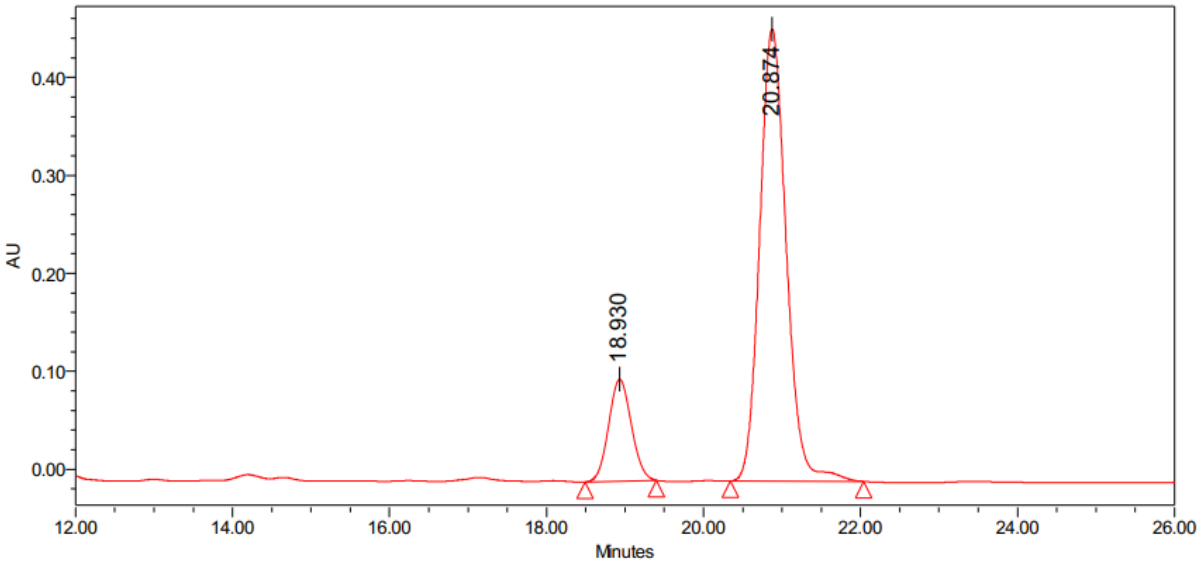

Peak Results

	Name	RT	Area	% Area
1		18.930	2091214	16.22
2		20.874	10801903	83.78

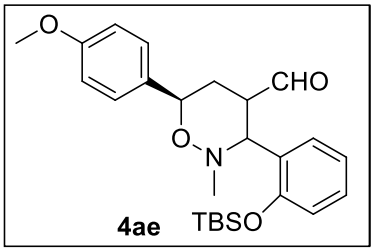

4ae

^{1}H-NMR ($CDCl_3$, 400MHz) of 4ae

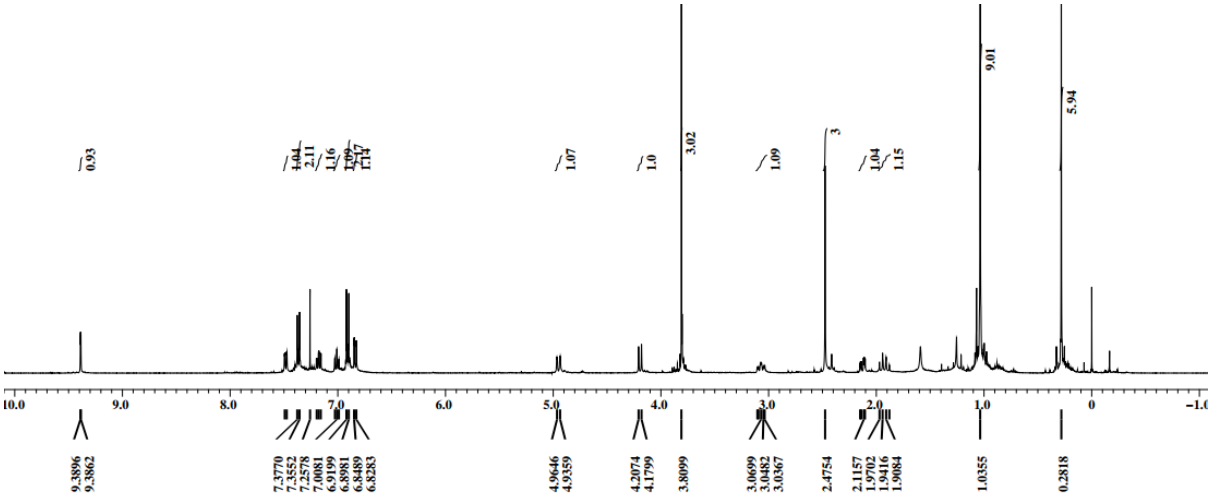

^{13}C-NMR ($CDCl_3$, 100MHz) of 4ae

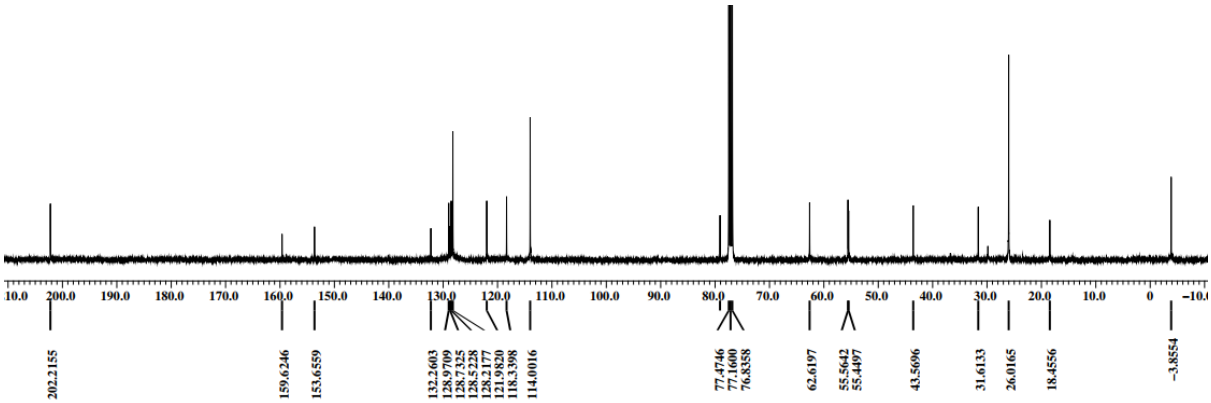

HPLC spectra of racemic 4ae

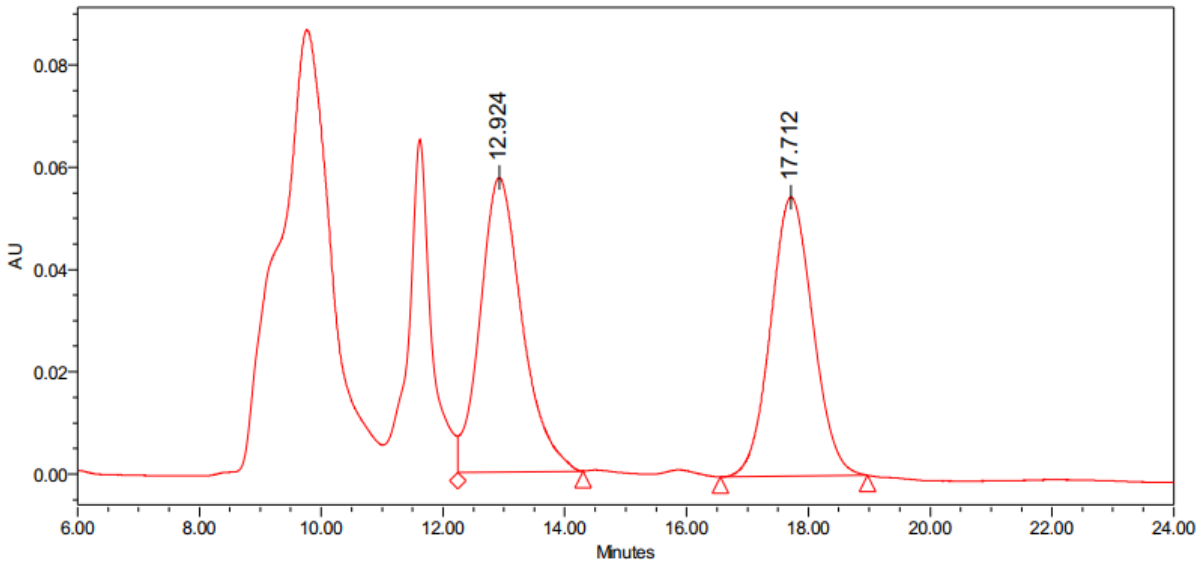

Peak Results

	Name	RT	Area	% Area
1		12.924	2758075	51.22
2		17.712	2626177	48.78

HPLC spectra of chiral 4ae

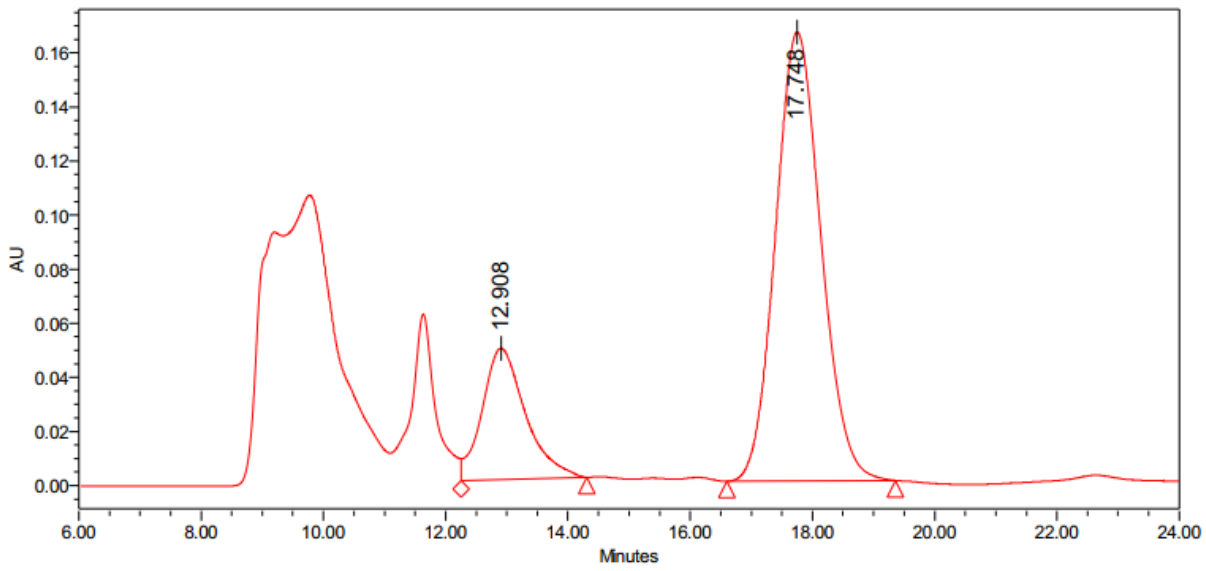

Peak Results

	Name	RT	Area	% Area
1		12.908	2385729	21.77
2		17.748	8575536	78.23

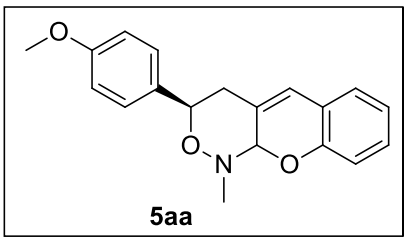

5aa

^{1}H-NMR ($CDCl_3$, 400MHz) of 5aa

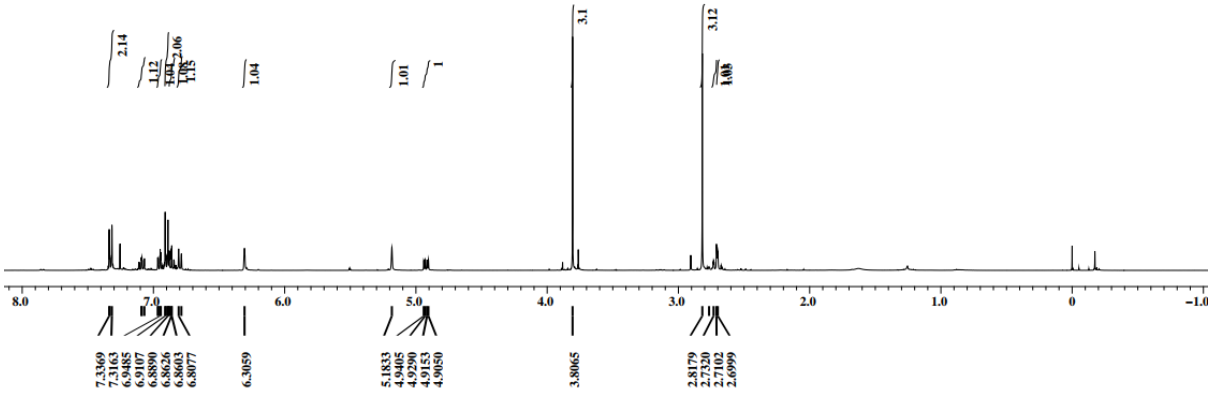

^{13}C-NMR ($CDCl_3$, 100MHz) of 5aa

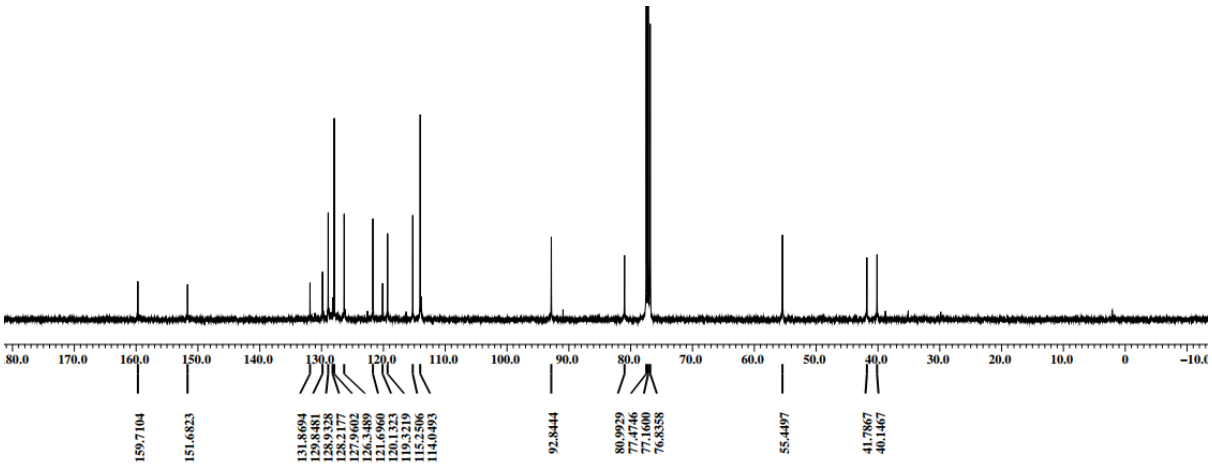

HPLC spectra of racemic 5aa

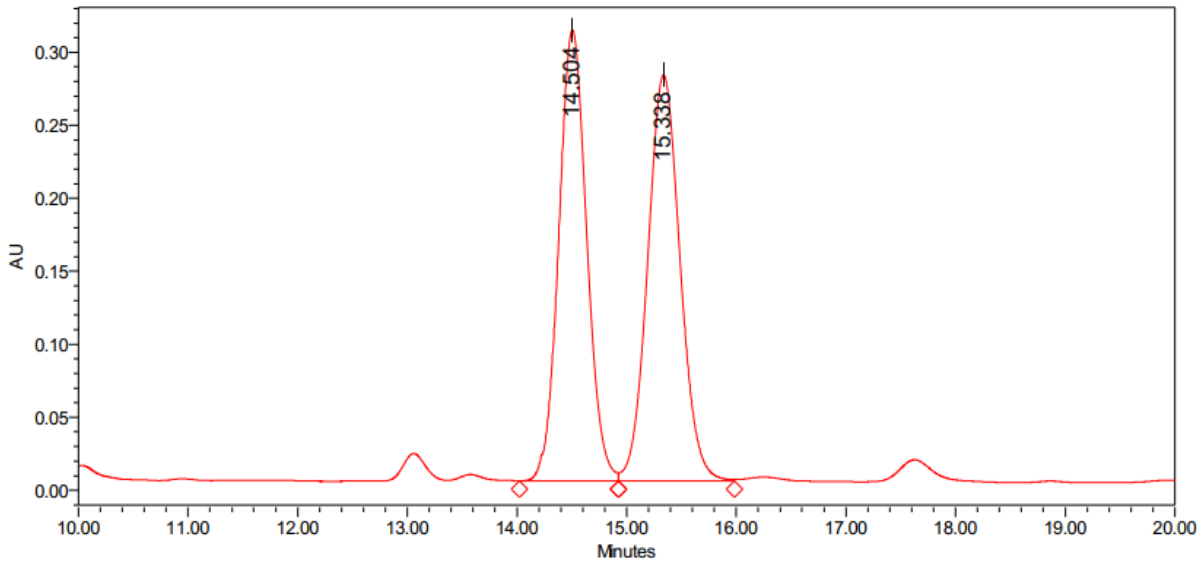

Peak Results

	Name	RT	Area	% Area
1		14.504	5478043	48.91
2		15.338	5722825	51.09

HPLC spectra of chiral 5aa

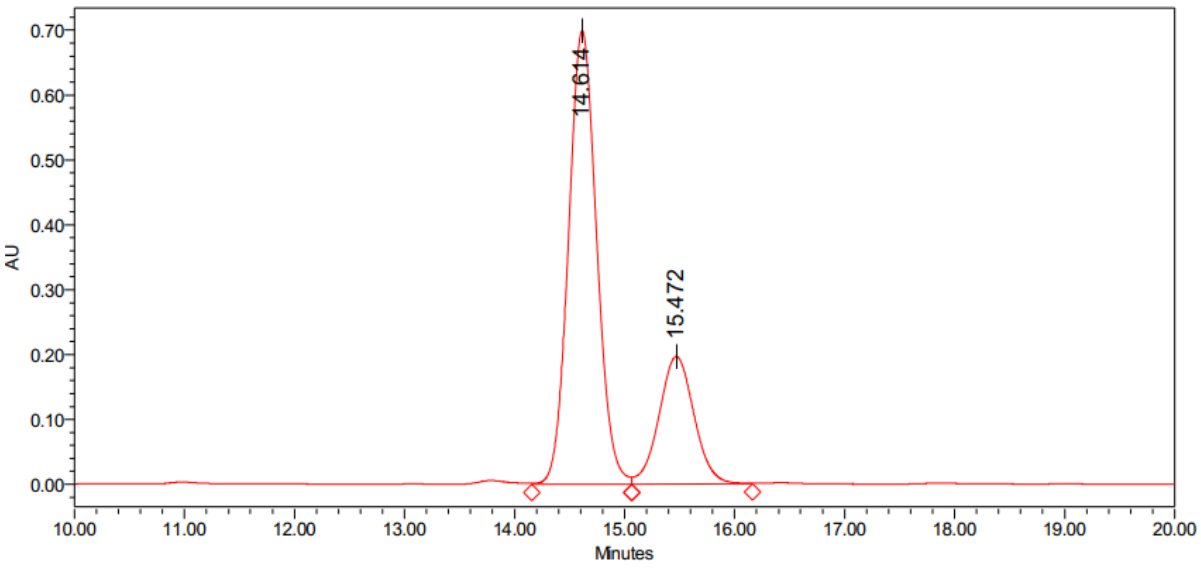

Peak Results

	Name	RT	Area	% Area
1		14.614	12404132	74.06
2		15.472	4345400	25.94

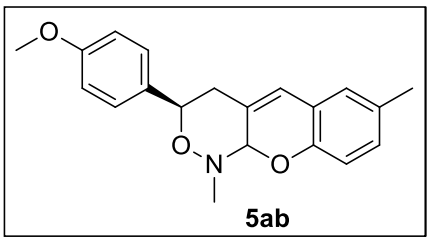

5ab

^{1}H-NMR ($CDCl_3$, 400MHz) of 5ab

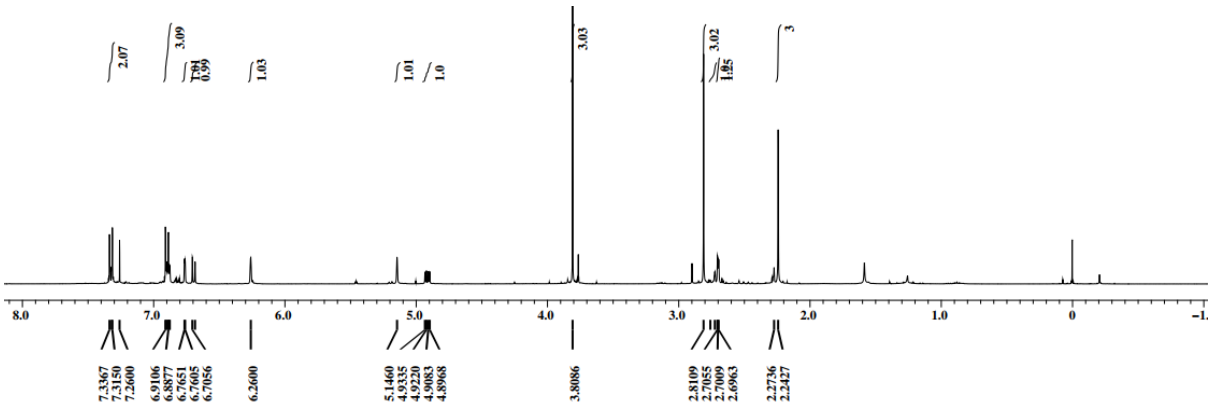

^{13}C-NMR ($CDCl_3$, 100MHz) of 5ab

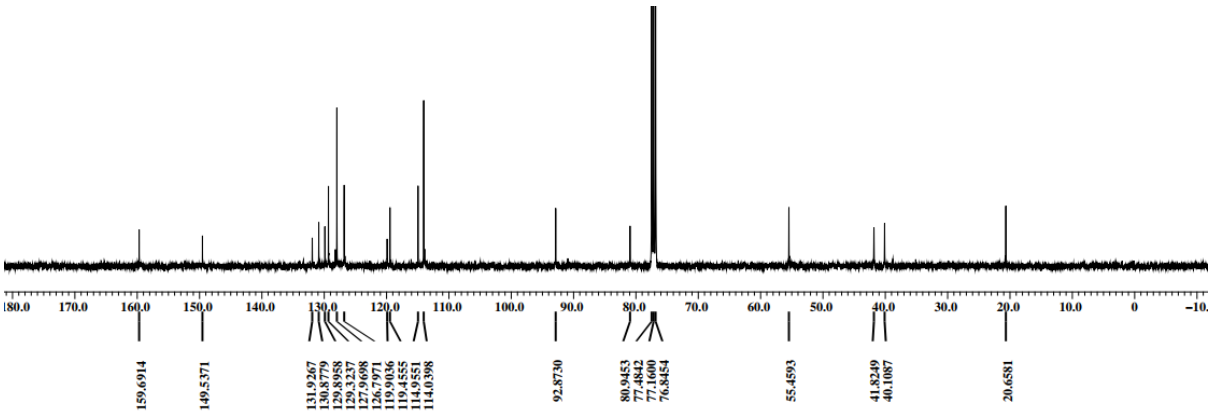

HPLC spectra of racemic 5ab

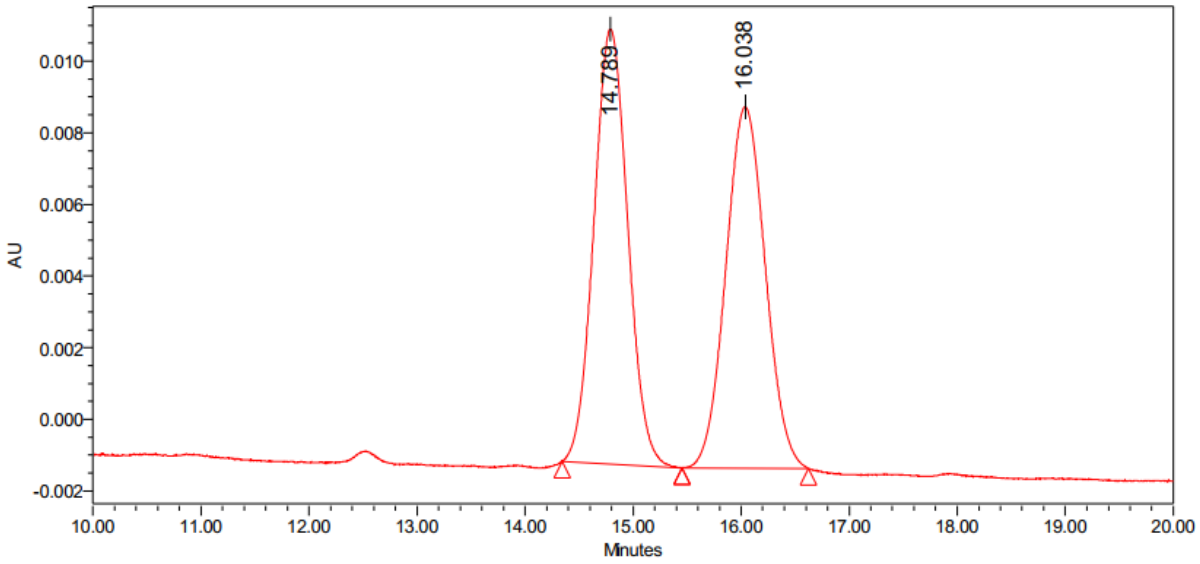

Peak Results

	Name	RT	Area	% Area
1		14.789	264946	50.77
2		16.038	256866	49.23

HPLC spectra of chiral 5ab

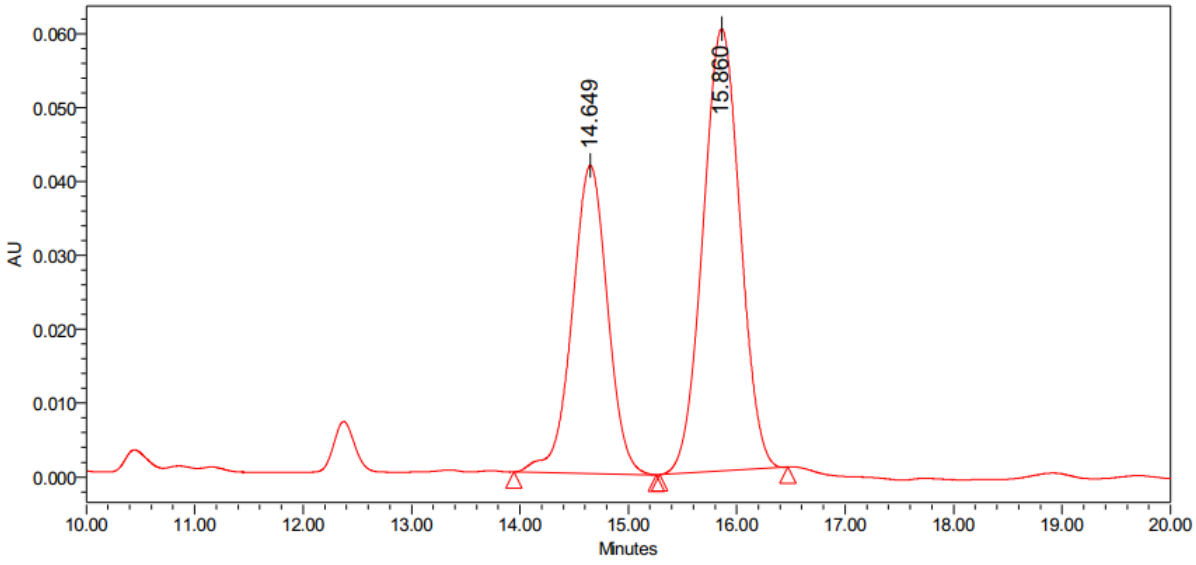

Peak Results

	Name	RT	Area	% Area
1		14.649	947804	39.88
2		15.860	1428604	60.12

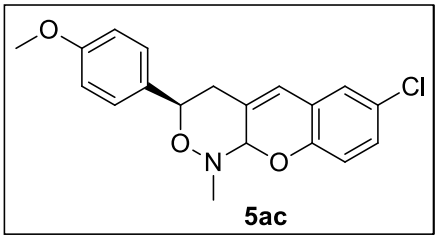

5ac

^{1}H-NMR ($CDCl_3$, 400MHz) of 5ac

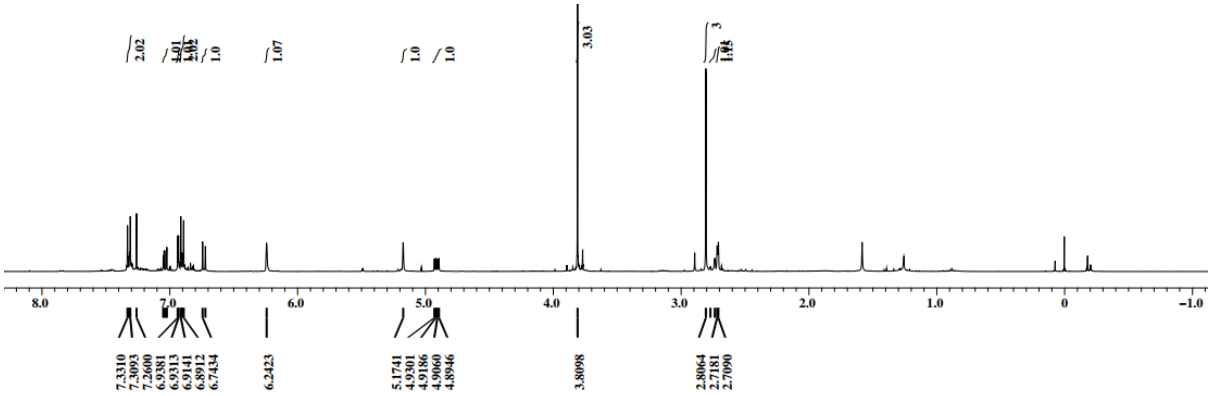

^{13}C-NMR ($CDCl_3$, 100MHz) of 5ac

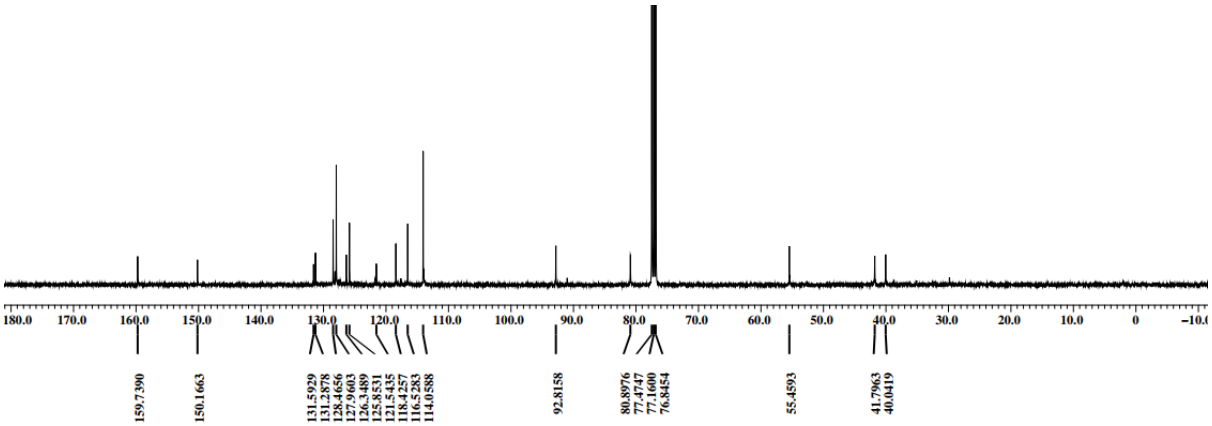

HPLC spectra of racemic 5ac

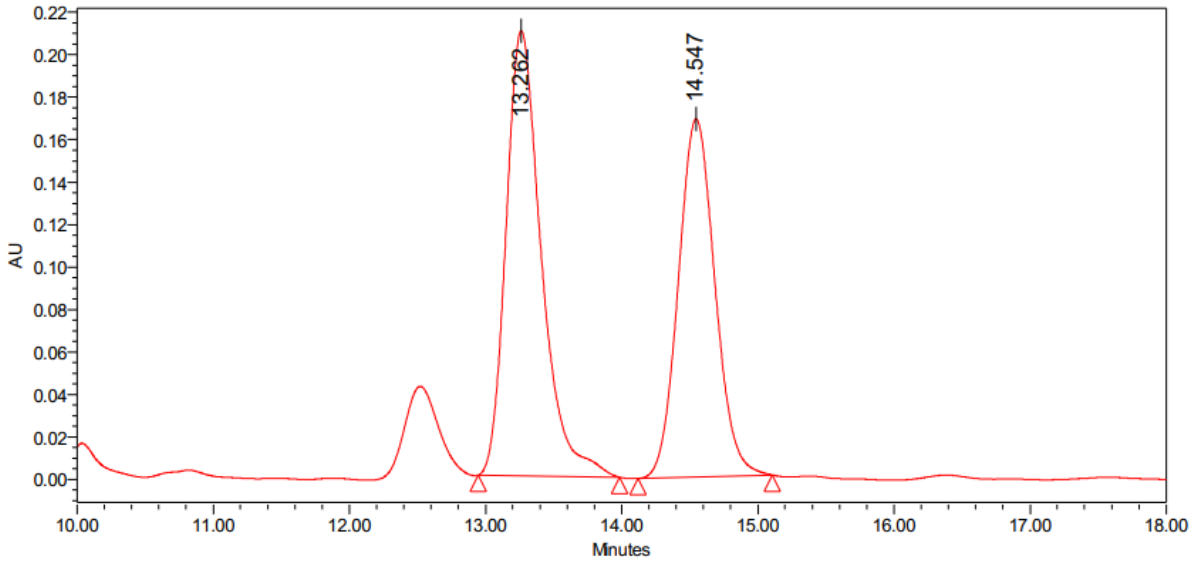

Peak Results

	Name	RT	Area	% Area
1		13.262	3769812	54.53
2		14.547	3144090	45.47

HPLC spectra of chiral 5ac

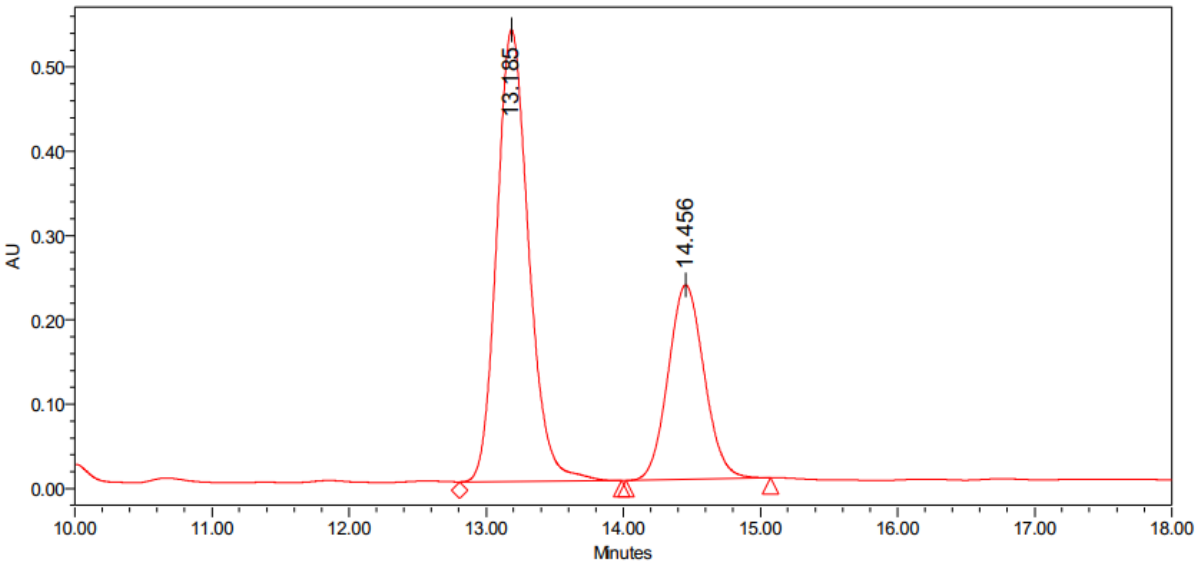

Peak Results

	Name	RT	Area	% Area
1		13.185	8662641	67.37
2		14.456	4196042	32.63

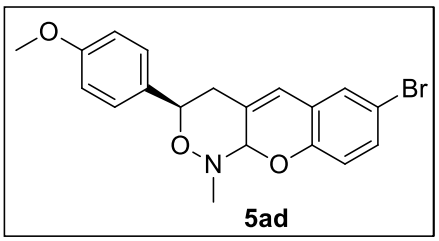

5ad

^{1}H-NMR ($CDCl_3$, 400MHz) of 5ad

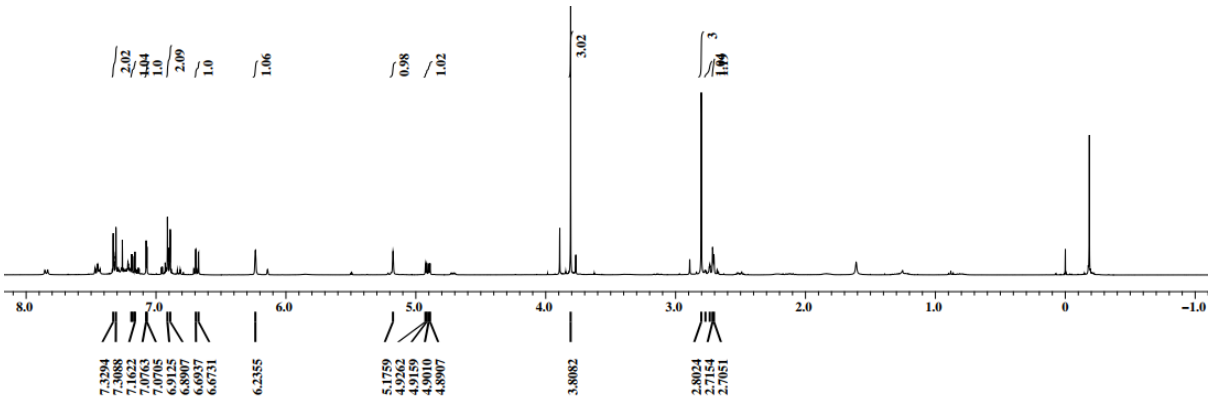

^{13}C-NMR ($CDCl_3$, 100MHz) of 5ad

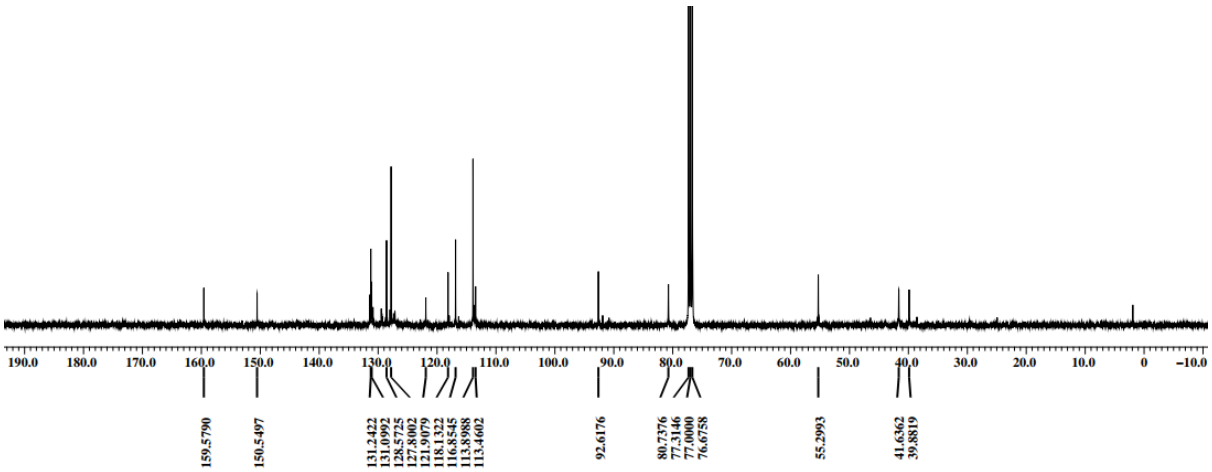

HPLC spectra of racemic 5ad

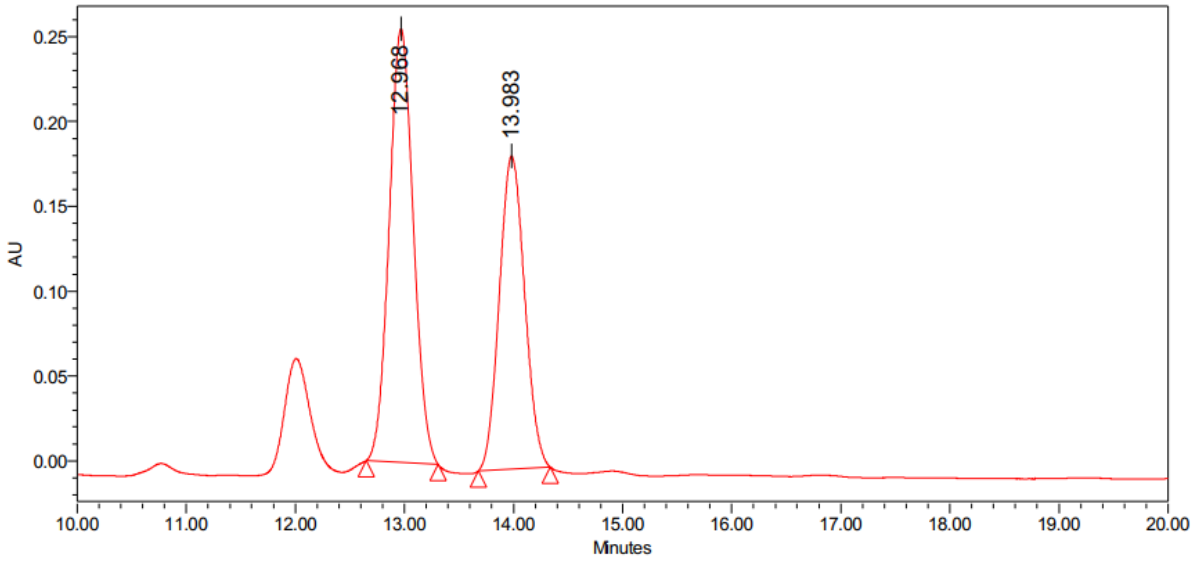

Peak Results

	Name	RT	Area	% Area
1		12.968	3921290	57.01
2		13.983	2956730	42.99

HPLC spectra of chiral 5ad

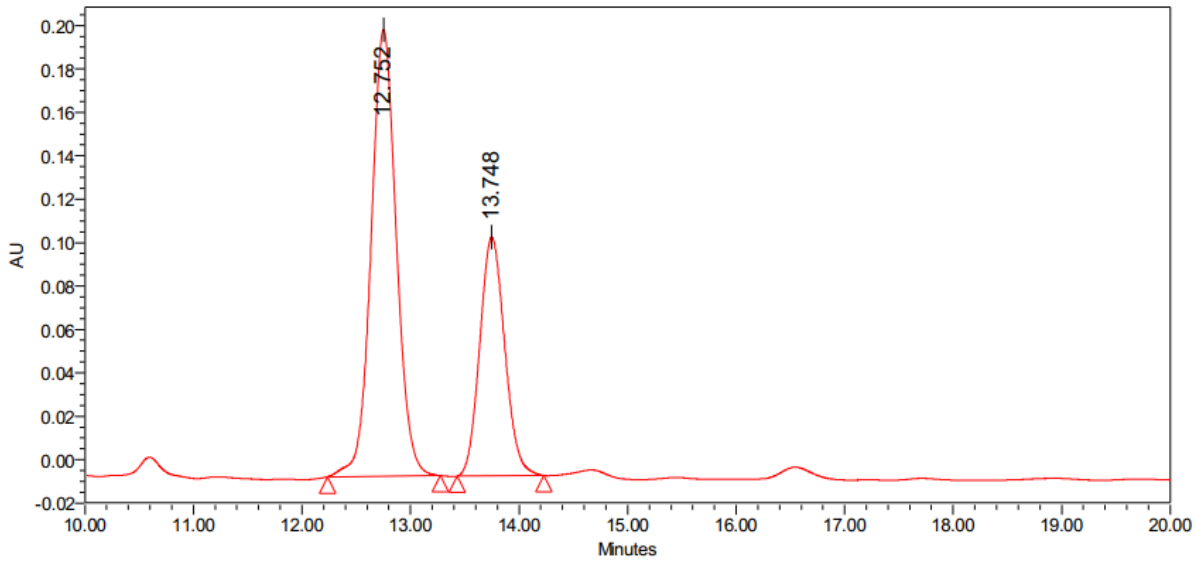

Peak Results

	Name	RT	Area	% Area
1		12.752	3314501	65.37
2		13.748	1755519	34.63

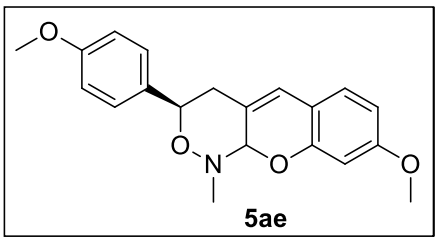

5ae

^{1}H-NMR ($CDCl_3$, 400MHz) of 5ae

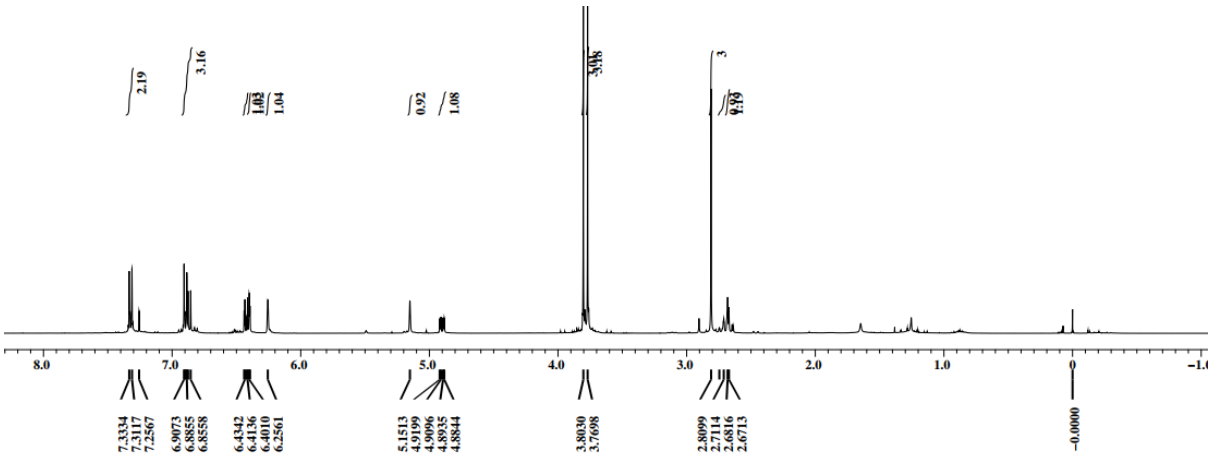

^{13}C-NMR ($CDCl_3$, 100MHz) of 5ae

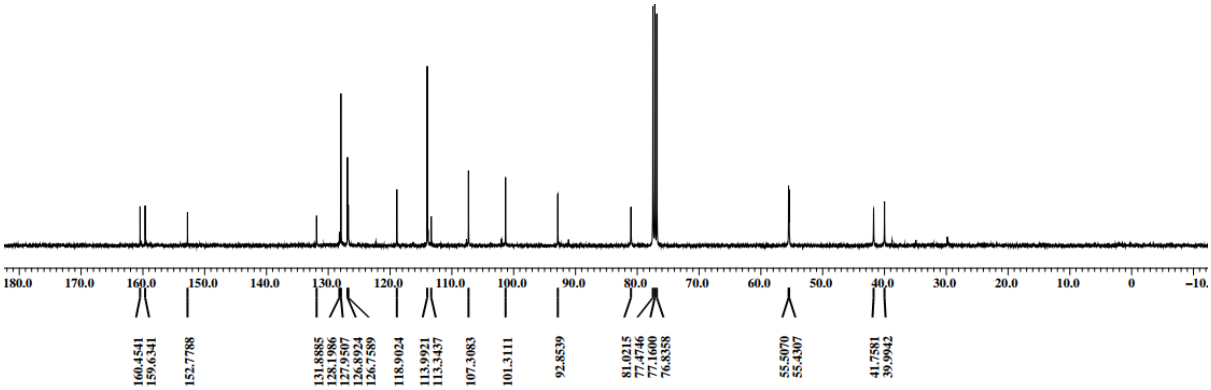

HPLC spectra of racemic 5ae

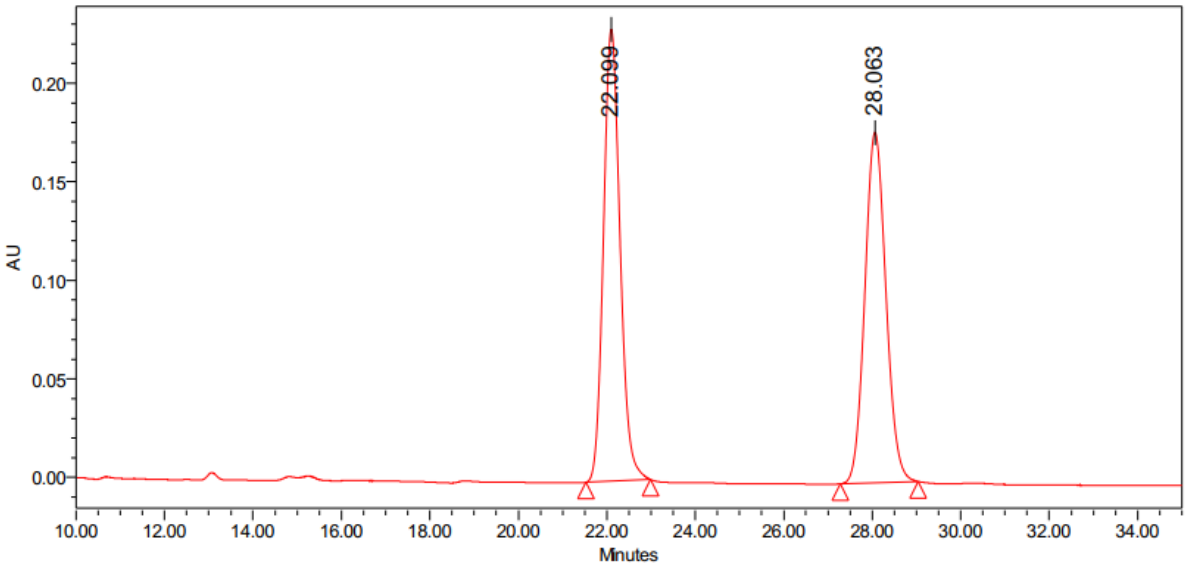

Peak Results

	Name	RT	Area	% Area
1		22.099	5972657	50.40
2		28.063	5876945	49.60

HPLC spectra of chiral 5ae

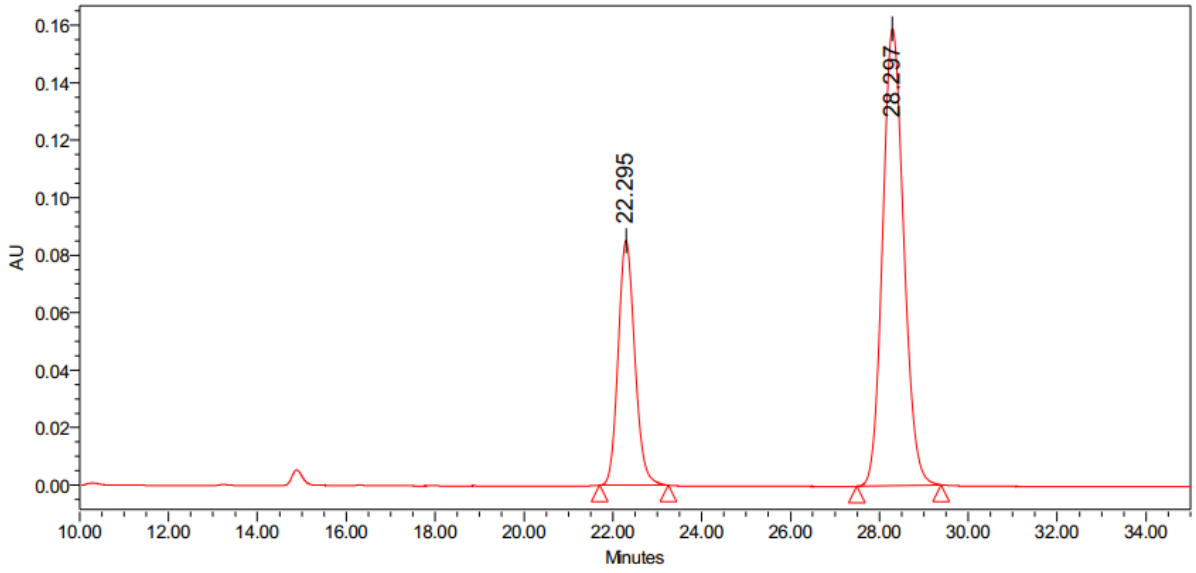

Peak Results

	Name	RT	Area	% Area
1		22.295	2215293	29.65
2		28.297	5255553	70.35

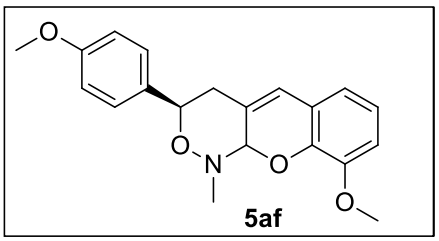

^{1}H-NMR ($CDCl_3$, 400MHz) of 5af

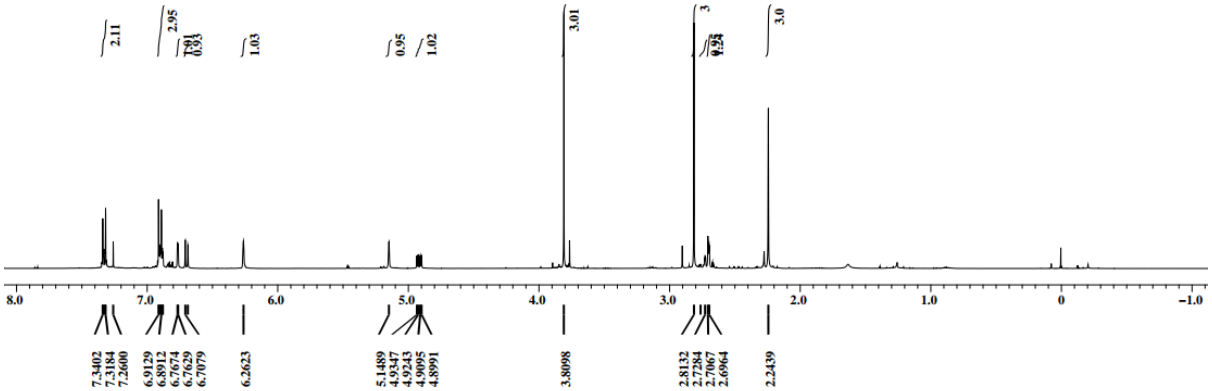

^{13}C-NMR ($CDCl_3$, 100MHz) of 5af

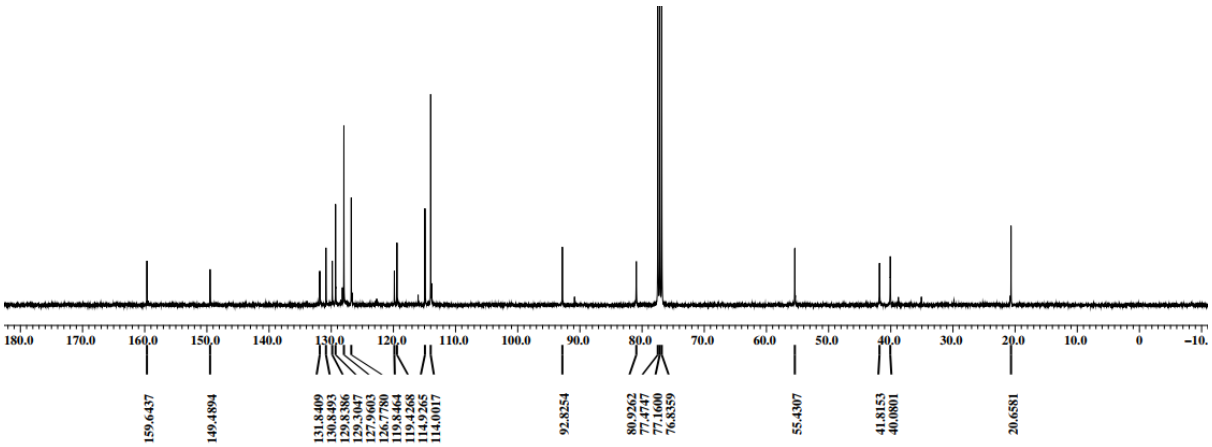

HPLC spectra of racemic 5af

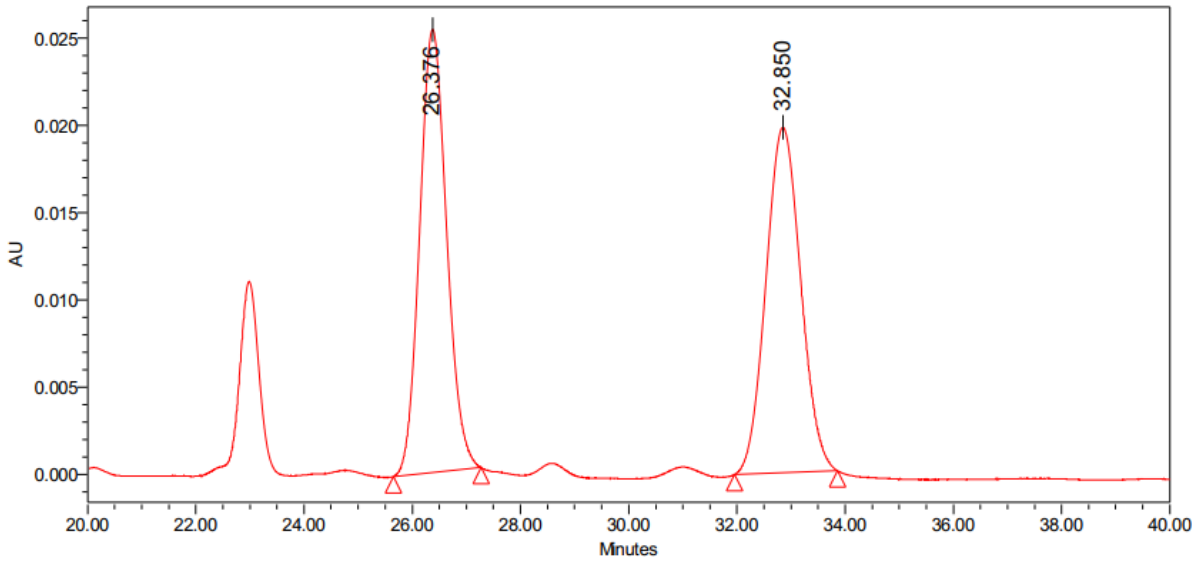

Peak Results

	Name	RT	Area	% Area
1		26.376	873597	49.82
2		32.850	879805	50.18

HPLC spectra of chiral 5af

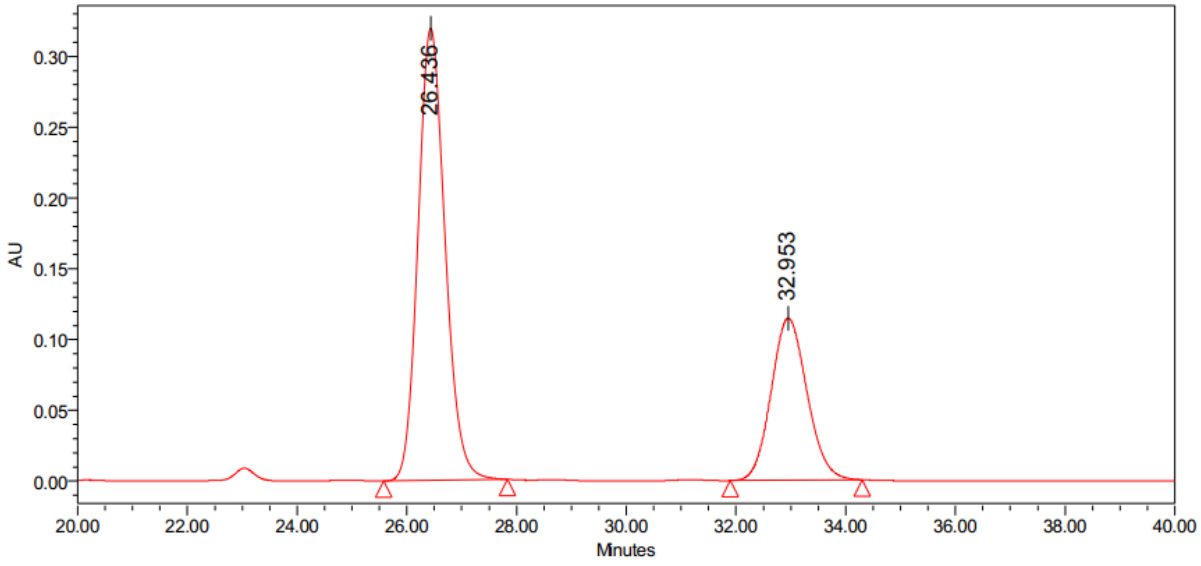

Peak Results

	Name	RT	Area	% Area
1		26.436	10929958	67.82
2		32.953	5186484	32.18

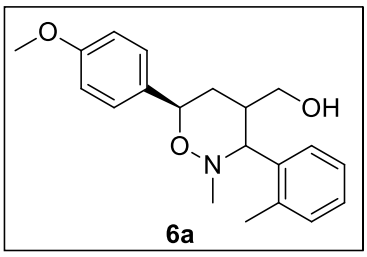

6a

^{1}H-NMR ($CDCl_3$, 400MHz) of 6a

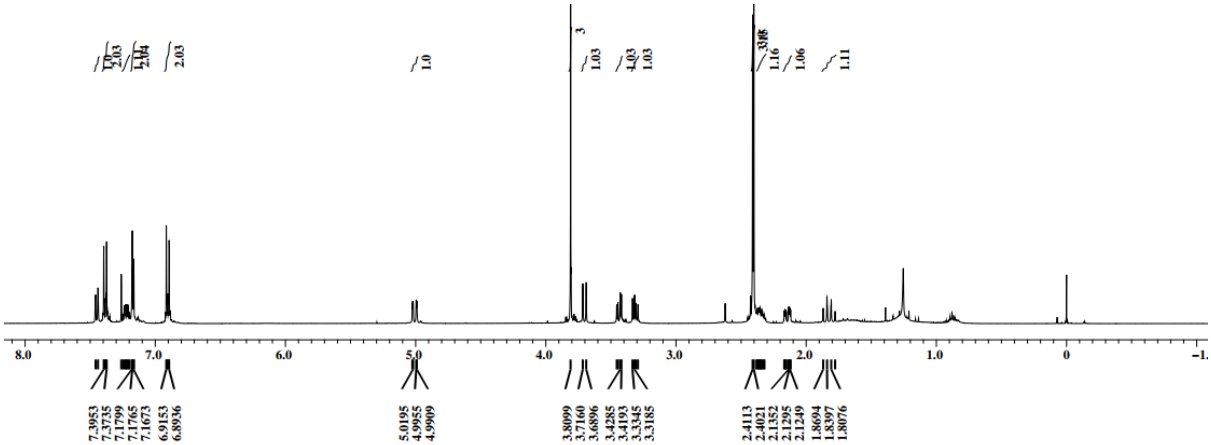

^{13}C-NMR ($CDCl_3$, 100MHz) of 6a

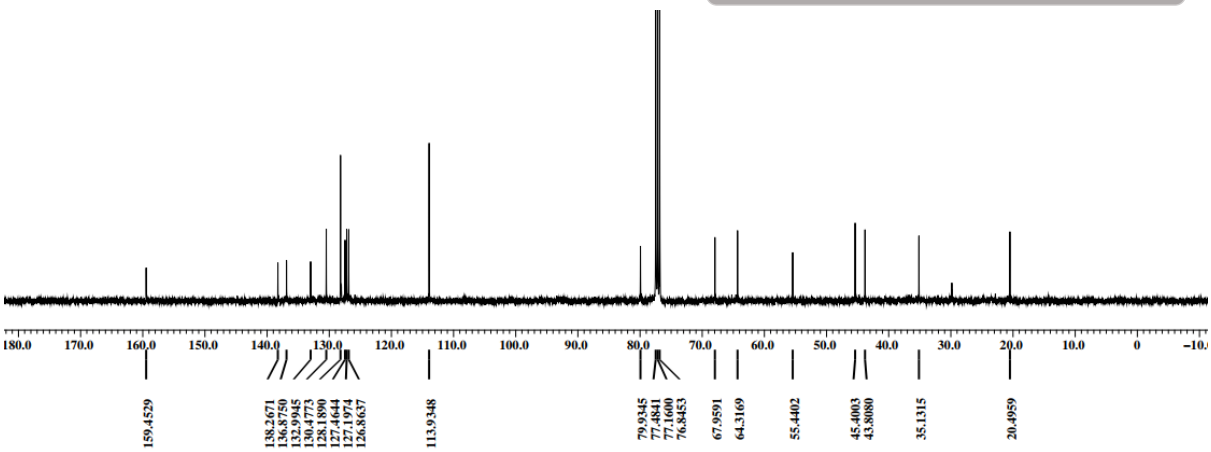

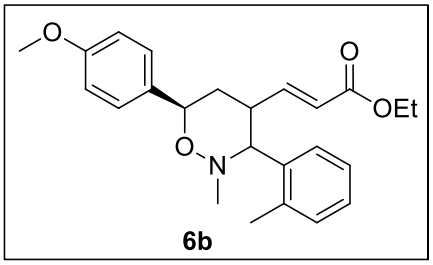

6b

^{1}H-NMR ($CDCl_3$, 400MHz) of 6b

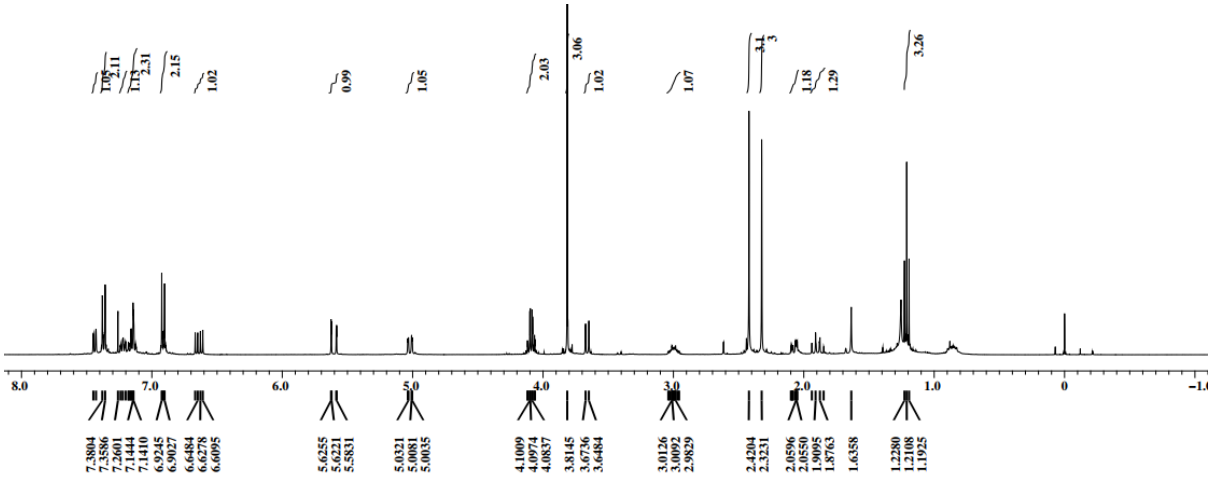

^{13}C-NMR ($CDCl_3$, 100MHz) of 6b

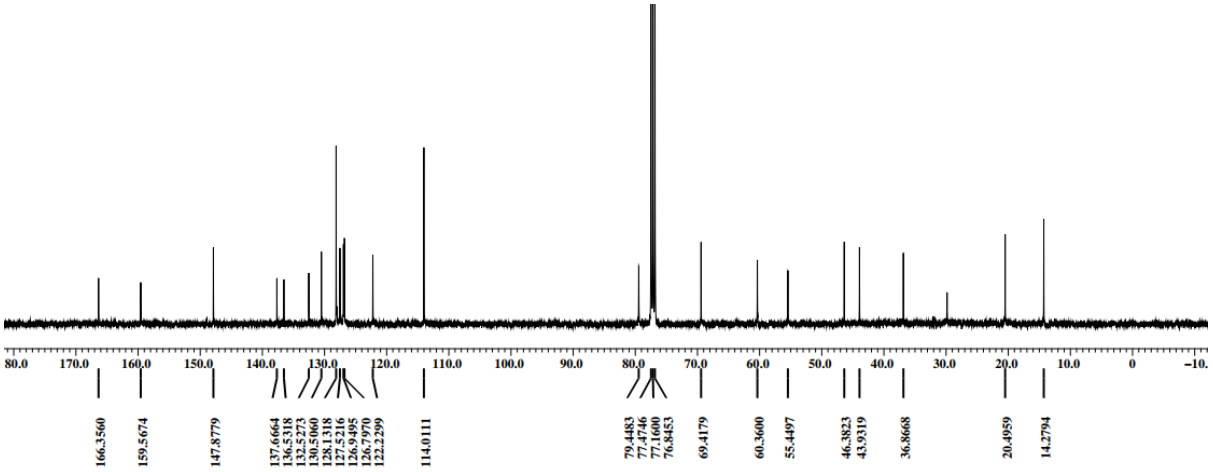

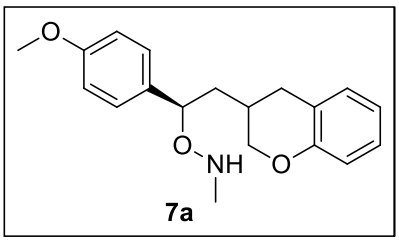

7a

^{1}H-NMR ($CDCl_3$, 400MHz) of 7a

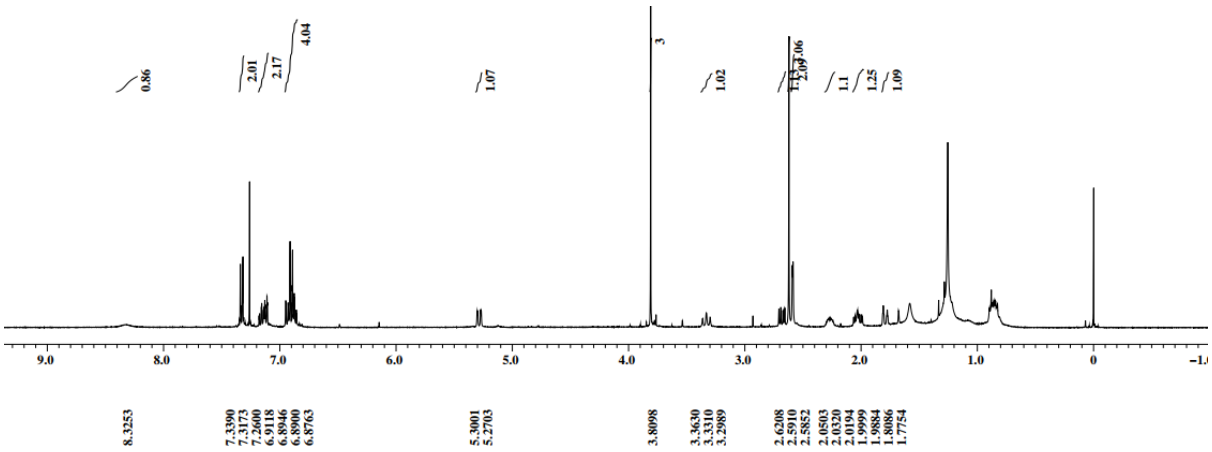

^{13}C-NMR ($CDCl_3$, 100MHz) of 7a

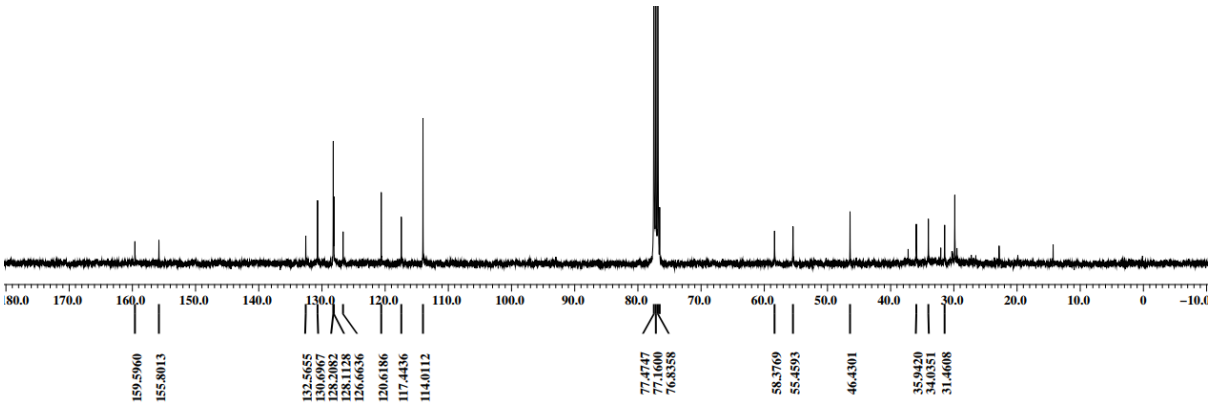

^{13}C, ^{1}H HSQC NMR ($CDCl_3$, 100, 400 MHz) of 7a

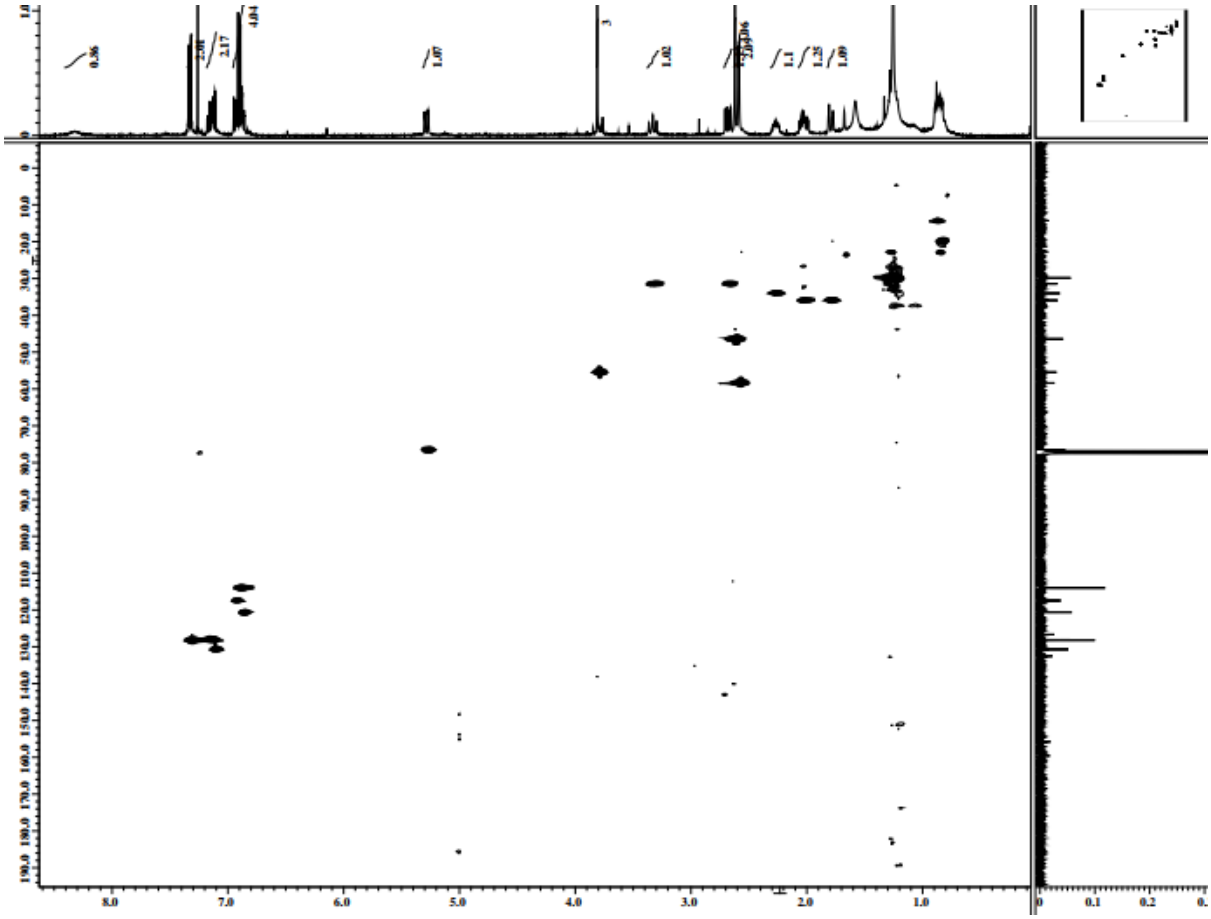

Chapter 3

Merging Two Strained Carbocycles: Lewis Acid Catalyzed Remote Site-Selective Friedel-Crafts Alkylation of *in situ* Generated *β*-Naphthol

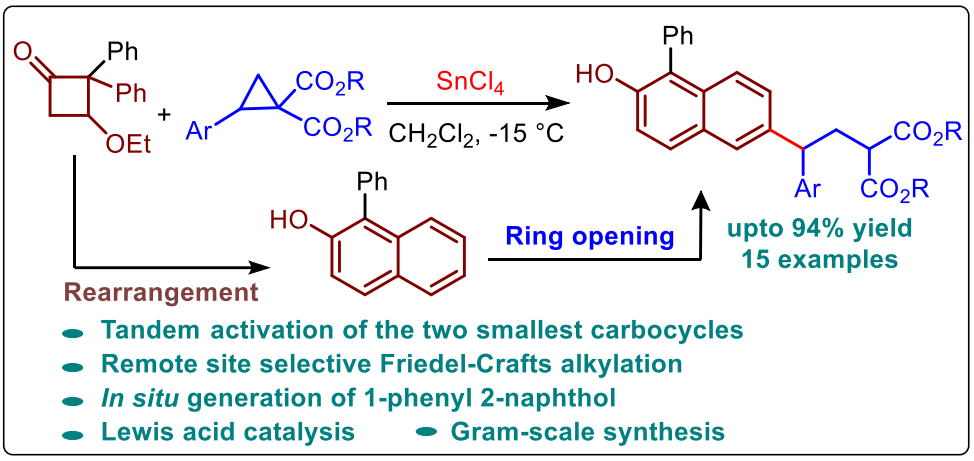

This work was published in *The Journal of Organic Chemistry* (A journal of the *American Chemical Society*). Please see the citation "Hazra, A.; Kanji, T.; Banerjee, P. *J. Org. Chem.* **2023**, *88*, 960−971."

3.1. Introduction

Small strained ring molecules are impressive building blocks in organic chemistry due to their unique reactivity. Over the years, various strained carbo- and heterocycles have been studied extensively to synthesize a myriad of biologically and pharmaceutically important molecular architectures.[1] However, methodologies exploiting a pair of different strained rings have remained underdeveloped.[2] 3-Donor cyclobutanones are one of the important classes of four-membered carbocycles which can generate 1,4-zwitterionic intermediate in the presence of Lewis acid by regioselective cleavage of the C2-C3 bond.[3] Several cycloaddition, rearrangement, and ring-opening reactions have been explored in the last few years using these four-membered synthons.[4] On the other hand, donor-acceptor cyclopropanes (DACs) are one of the most commonly exploited three-membered carbocycles owing to their ease of preparation and inimitable properties. The synergistic "push-pull" effect of vicinally installed donor and acceptor groups induces a C-C bond polarization which, upon activation with Lewis acid, can lead to the formation of a 1,3-zwitterionic intermediate. Utilizing this reactivity, an enormous number of ring opening, cycloaddition, and rearrangement reactions have been documented in the past few decades.[5] Our group has also contributed extensively in the field of DACs for the construction of various important carbocyclic and heterocyclic scaffolds.[6] However, reports of merging DACs with other strained ring molecules are still scarce (Scheme 3.1.1). In the last decade, our group has worked on the reactivity of two different strained rings in the presence of Lewis acids and successfully obtained different heterocyclic frameworks (Scheme 1 A). In 2015, our group disclosed a Lewis acid-catalyzed cycloaddition between DACs and epoxide for the synthesis of substituted tetrahydrofuran derivatives (Scheme 3.1.1.i).[7] Following this, other heteroatom-containing strained ring systems like aziridine and oxaziridine were also exploited by our group with DACs. While the former undergoes an annulation reaction to provide highly functionalized pyrroles[8], (Scheme 3.1.1.ii) the latter leads to the formation of an *N*-transferred product and the [3+2] cycloadduct in the presence

Scheme 3.1.1. Reactions of DACs with different small strained ring

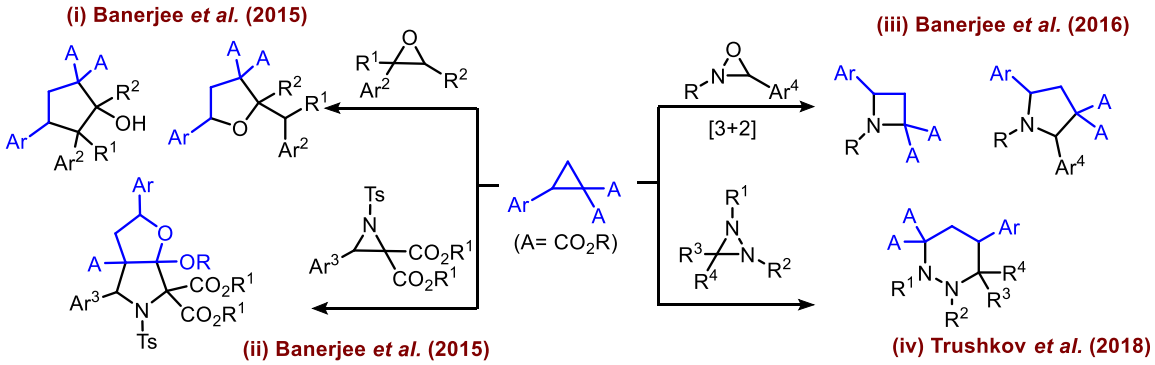

of the same Lewis acid (Scheme 3.1.1.iii).[9] In a similar endeavor, Trushkov *et al*. demonstrated a Lewis acid-mediated annulation between two different saturated small ring systems diaziridine and

cyclopropane (Scheme 3.1.1.iv).[10] Encouraged by these affirmative experiences, our group has made continuous efforts for further exploitation of other strained ring molecules with DACs. In this aspect, our aim is to utilize the reactivity of the two smallest carbocycles, i.e., 3-Donor cyclobutanones and donor-acceptor cyclopropanes, to construct valuable carbocyclic molecules. To the best of our knowledge, reactions between these two strained carbocycles have not yet been explored.

Scheme 3.1.2. Friedel-Crafts reaction of DACs with 2-naphthols; (a) Previous reports, (b) This work: Lewis acid catalyzed reaction between cyclobutanone and DACs

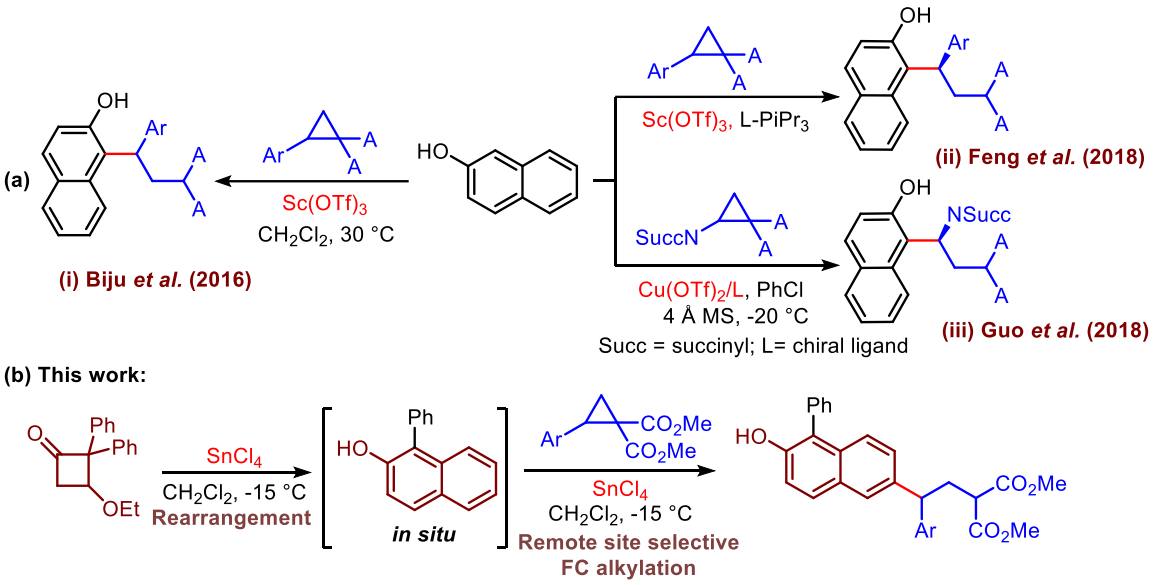

The Friedel-Crafts (FC) alkylation is one of the most powerful tools for the construction of carbon-carbon bonds onto an aromatic or heteroaromatic compound.[11] Since its invention by Charles Friedel and James Crafts in 1877, a diverse range of FC alkylation reactions have been developed to date with various types of arenes and heteroarenes.[12] In this regard, *β*-naphthol has achieved great interest as a notable precursor for its unique reactivity along with its low cost and easy handling. Several alkylating agents, such as olefins, imines, enamides, etc., have already been exploited with *β*-naphthol via metal, non-metal, and organocatalytic activation.[13] In this domain, DACs have become a great choice as an alkylating agent and successfully provided various *γ*-aryl butyric acid frameworks through ring opening with different electron-rich arenes and heteroarenes in the presence of various Lewis acids.[14] In 2016, Biju *et al.* reported the Friedel-Crafts reaction with *β*-naphthol and DAC in the presence of $Sc(OTf)_3$ for the construction of *γ*-naphthyl butyric acid skeletons (Scheme 3.1.2.a-i).[15] Later, in 2018, Feng *et al.*[16] discovered an asymmetric reaction of *β*-naphthol with cyclopropyl diketones via chiral *N, N'*-dioxide L-$PiPr_3$-Sc^{III} complex (Scheme 3.1.2.a-ii). In the same year, Guo et al.[17] developed an enantioselective FC alkylation of *β*-naphthol with donor-acceptor aminocyclopropane in the presence of $Cu(OTf)_2$ complexed with chiral bisoxazoline ligand (Scheme 3.1.2.a-iii). In this regard, it is worth mentioning that, in 2017, Werz

et al. demonstrated a ring opening of DACs by the *in situ* generated naphthoquinone dianions species by the combination of redox and Lewis acid catalysis.[18] Strikingly, in all these reactions, the alkylation took place by the nucleophilic attack from the 'α-position only, and methodologies for the selective alkylation from the other nucleophilic sites of β-naphthol are unexplored.[19] We envisioned that blocking the α-position of the β-naphthol could trigger the other nucleophilic sites for selective Friedel-Crafts alkylation. For this purpose, 3-ethoxy 2,2-diphenyl cyclobutanone is the best choice to generate 1-phenyl-2-naphthol via Lewis acid activation which was earlier reported by Huisgen *et. al*[20] in 1969. This 1-substituted 2-naphthol, has two typical sites for electrophilic attack those are C(1) and C(6). While the C(1) attack was accomplished by direct dearomative halogenation with NXS/water (X= Br, Cl) afforded 1,1-disubstituted 1,2-dihydronaphthalene-2-ones,[21] bromination with Br_2/AcOH leads to the formation of 6-bromo-1-phenylnaphthalen-2-ol.[22] Our aim was to utilize this 1-substituted 2-naphthol for the ring opening of DACs via FC alkylation from the remote nucleophilic site C(6). Herein, we report a 6-selective Friedel-Crafts alkylation of *in situ*-generated 2-naphthols from 3-ethoxy cyclobutanone with donor-acceptor cyclopropanes (Scheme 3.1.2.b).

3.2. Result and Discussion

To test our hypothesis, initially, cyclobutanone **1a** and DAC **2a** were chosen as the model substrates to find the optimization reaction condition (Table 3.2.1). From the literature precedences, it was evident that relatively strong Lewis acids were more suitable for the ring opening of this type of cyclobutanones.[4] So, we commenced our reaction with $BF_3{\cdot}Et_2O$ as Lewis acid in dichloromethane as solvent. Interestingly the Friedel-Crafts alkylated product was obtained in 33% yield along with the β-naphthol (obtained by the rearrangement of cyclobutanone) within 15 minutes at room temperature (Table 3.2.1, Entry 1). Hence we started screening several other strong Lewis acids to improve the efficiency of the reaction. Initially, in the presence of $TiCl_4$, a complex reaction mixture was obtained; presumably, this could be due to the decomposition of cyclopropane while the cyclobutanone remained unconsumed (Table 3.2.1, Entry 2). Delightfully the employment of $SnCl_4$ resulted in an improvement of the yield up to 51% (Table 3.2.1, Entry 3). Next, comparatively weaker Lewis acids like $Sc(OTf)_3$, $In(OTf)_3$, and $InCl_3$ were also tested, which afforded the desired product in poor to moderate yield (Table 3.2.1, Entries 4-6). However, in the presence of MgI_2, both the starting materials remain unreacted (Table 3.2.1, Entry 7) while $Bi(OTf)_3$ was unable to catalyze the Friedel-Crafts reaction giving only the rearrangement product (Table 3.2.1, Entry 8). Henceforth, $SnCl_4$ proved to be the best catalyst for this reaction. Subsequently, various other parameters like temperature, solvent, and catalyst loading were also screened to further improve the yield of the product. From the literature knowledge, it is noticeable that temperature plays a crucial role in the Lewis acid-catalyzed transformations. Therefore, the reaction was conducted at low temperatures. Pleasingly, the yield was enhanced to some extent (72%) when the reaction was

performed at 0 °C (Table 3.2.1, Entry 9). Further improvement was also achieved by lowering the temperature to -15 °C and obtaining the desired product in 84% yield (Table 3.2.1, Entry 10). However, a considerable decrease in the yield was observed when the temperature was further reduced (Table 3.2.1, Entry 11). To optimize the reaction further, we also checked the efficiency of

Table 3.2.1. Optimization of the reaction conditions

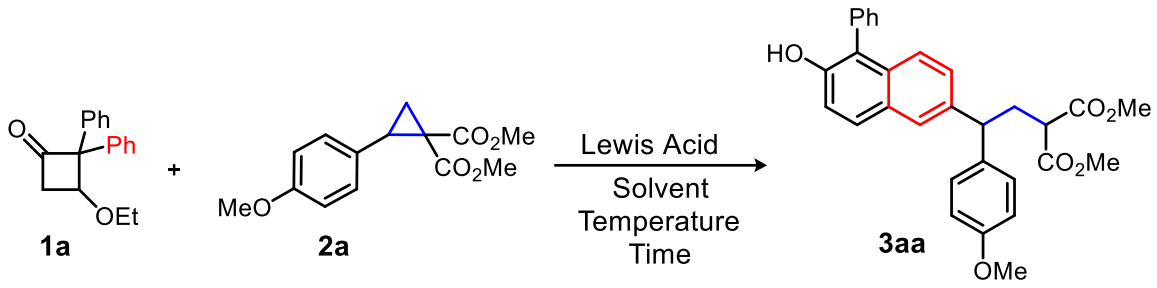

entry	LA	temp (°C)	solvent	yield
1	$BF_3{\cdot}Et_2O$	rt	DCM	33% [c]
2	$TiCl_4$	rt	DCM	c.m.[d]
3	$SnCl_4$	rt	DCM	51%
4	$Sc(OTf)_3$	rt	DCM	20%
5	$In(OTf)_3$	rt	DCM	29%
6	$InCl_3$	rt	DCM	42%
7	MgI_2	rt	DCM	n.r.[e]
8	$Bi(OTf)_3$	rt	DCM	n.r.[e]
9	$SnCl_4$	0	DCM	72%
10	**$SnCl_4$**	**-15**	**DCM**	**84%**
11	$SnCl_4$	-30	DCM	56%
12	$SnCl_4$	-15	DCB	65%
13	$SnCl_4$	-15	DCE	67%
14	$SnCl_4$	-15	MeCN	n.r.[d]
15	$SnCl_4$	-15	Toluene	n.r.[d]
16[f]	$SnCl_4$	-15	DCM	50%

[a]reaction was carried out under inert condition using **1a** (1 equiv.), **1b** (1 equiv.), Lewis acid (0.2 equiv.) and CH_2Cl_2 as a solvent for 15 minutes. [b]isolated yield after column chromatography; [c]$BF_3{\cdot}Et_2O$ was taken in 1 equivalent, [d]c.m.= no reaction, [e]n.r.= no reaction, [f]$SnCl_4$ was taken in 0.5 equivalent.

various solvents. Other halogenated solvents like DCE and DCB did not improve the yield as compared to DCM whereas MeCN and toluene were found fatal for this transformation (Table

3.2.1, Entry 12-15). Later, the higher catalyst loading was also examined and the desired product was obtained with reduced yield, possibly because of the substrate decomposition (Table 1, Entry 16). Therefore, the optimized conditions for this reaction were 1.0 equivalent of **1a**, 1.0 equivalent of **2a,** with 0.2 equivalent of $SnCl_4$ in DCM at -15 °C.

With the optimized conditions in hand, the generality of our protocol was evaluated with respect to DACs. Initially, the effect of substitutions on the aryl group of DACs was examined (Scheme 3.2.1). When the electron-rich *para*-methoxy substituted phenyl cyclopropane diester was employed for this reaction, it rendered the corresponding Friedel-Crafts alkylated product (**3aa**) with an excellent yield of 84%. However, 3,4-dimethoxy phenyl and piperonyl-containing DACs (**2b** and **2c**) rendered the products (**3ab** and **3ac**) with relatively lower yields (65% and 73%, respectively). In line with this result, other electron-rich substituents like benzofuran, *N*,*N*-dimethyl phenyl, and furan-derived cyclopropanes could not afford the desired products and yielded only the 1-phenylnaphthalen-2-ol (cyclobutanone rearrangement product). Possibly, due to the fact that, these highly reactive DACs undergo decomposition in the presence of strong Lewis acid $SnCl_4$ and became unavailable for the F.C. alkylation to render the desired products. Next, we focused on comparatively less activated *para*-methyl (**2d**) and *para*-isopropyl (**2e**) phenyl substituted DACs, which furnished the products (**3ad** and **3ae**) in good (82%) to satisfactory (70%) yields while much less activated phenyl cyclopropane diester (**2f**) afforded the product (**3af**) with slightly increased yield (86%). Apparently, electron withdrawing nitro substituted DACs could not furnish the desired product as the deficiency of electron on the donor group of cyclopropane made it too unactivated to undergo the reaction. Similarly, pyridine-containing cyclopropane also did not take part in this FC alkylation reaction. Noticeably, DACs containing *para*-halogen (F, Cl, Br) substituted phenyl rings (**2g, 2h, 2i**) were also tolerated well, but a longer reaction time was required. Whereas the fluoro-substituted DAC gave the product (**3ag**) with moderate yield (60%), the chloro- and bromo-substituted ones rendered the products (**3ah,** and **3ai**) with excellent yields (89% and 94%, respectively). Next, the *ortho*-substituted DAC (**2j**) also delivered the corresponding product (**3aj**) in good yield (82%). Furthermore, 1-naphthyl bearing DAC (**2k**) engendered the desired product (**3ak**) in compromised yield (47%). To our delight, indane fused DAC (**2l**) was also found compatible and provided the Friedel-Crafts alkylation product (**3al**) in good yield (81%). Moreover, styryl-substituted cyclopropane diester (**2m**) furnished the corresponding product (**3am**) with a similar yield (82%). In addition to that, an investigation regarding the variation of the acceptor group of the DACs was also carried out. Both ethyl and isopropyl esters containing cyclopropanes rendered the products (**3an** and **3ao**) in satisfactory yields (70% and 75%, respectively).

Then, some control experiments were conducted to gain insight into the mechanism of the discussed transformation. At first, only the cyclobutanone **1a** was subjected under the optimized condition,

Scheme 3.2.1. Substrate scopes[a,b]

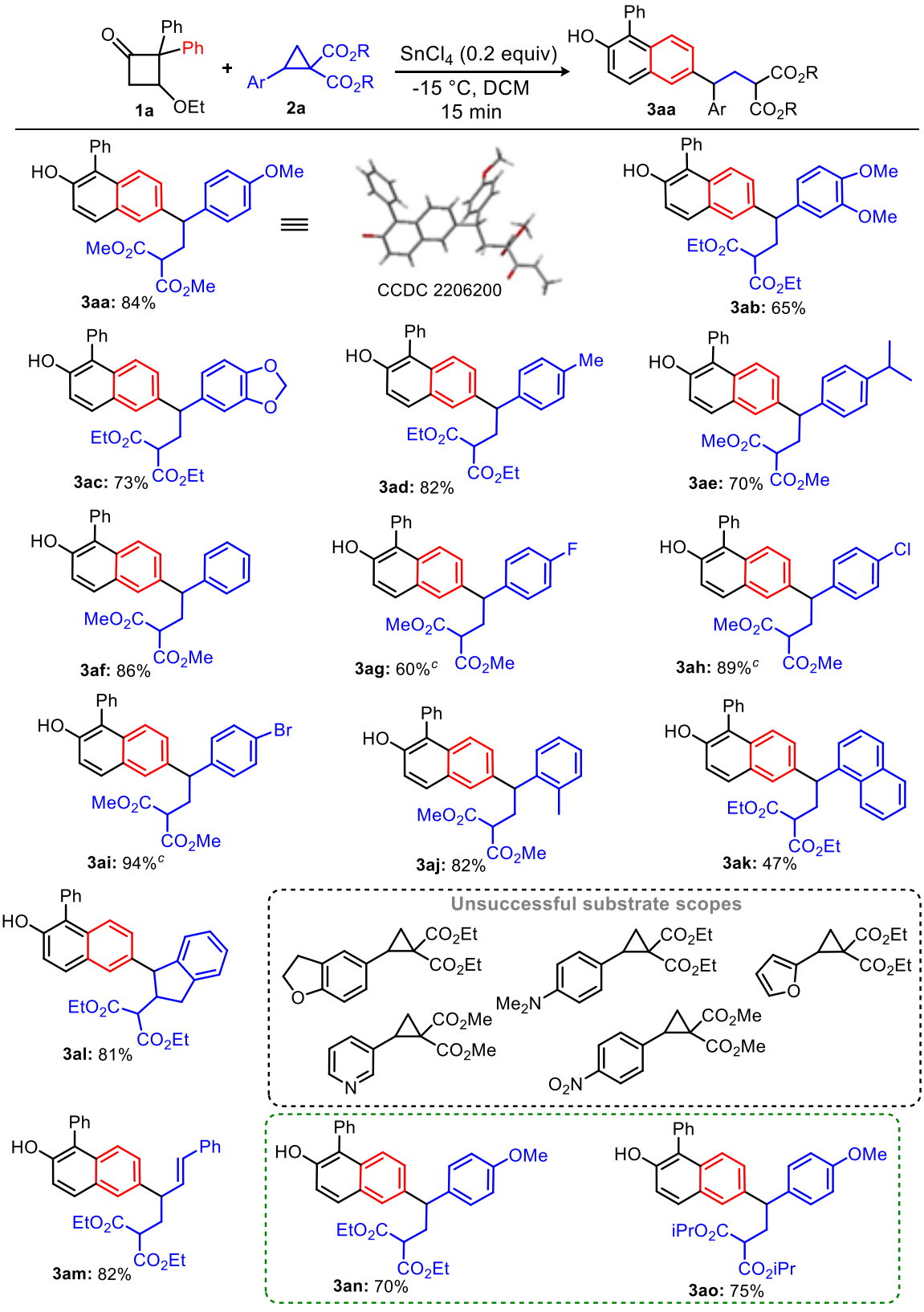

[a]Unless otherwise mentioned the reaction were carried out with 1 equiv of **1a**, 1 equiv of **2a**, and 0.2 equiv of $SnCl_4$ in dichloromethane at -15 °C for 15 min, [b]Isolated yield, [c]reaction performed for 2 h.

and as anticipated 1-phenyl *β*-naphthol (**IV**) was formed in quantitative yield (Scheme 3.2.2.A).

Further, this isolated *β*-naphthol (**IV**) derivative was treated with DAC **2a** under the optimized condition and successfully afforded the desired remote 6-selective FC alkylated product in good yield (Scheme 3.2.2.A). In addition to that, 3-ethoxy 2-phenyl cyclobutanone **1b** did not produce either the corresponding *β*-naphthol or the desired FC alkylated product under a similar condition. This experiment suggests that the presence of one phenyl group stabilizes the carbanion, which makes the intramolecular attack of other phenyl rings more feasible. Therefore, in the case of mono-phenyl-substituted species, the negative charge does not get stabilized enough in the intermediate (I') to happen the intramolecular FC reaction, which eventually leads to the decomposition of the substrate (Scheme 3.2.2.B). An alternative explanation for this experiment could be that in the presence of two phenyl group, one has always to be close to the activated carbonyl group to allow cyclization. Whereas the presence of only one phenyl group allows different conformation where the phenyl group could be far away from the activated carbonyl group (I'') to achieve lower steric hindrance which would be unfavorable for the cyclization and eventually lead to the complex reaction mixture (Scheme 3.2.2.B). Next, the fate of the reaction was examined when both the 1-

Scheme 3.2.2. Control experiment; (A) Sequential method and isolation of the *in situ* generated *β*-naphthol, (B) reaction with 2-phenyl 3-ethoxy cyclobutanone, (C) reaction with 6-substituted *β*-naphthol derivative.

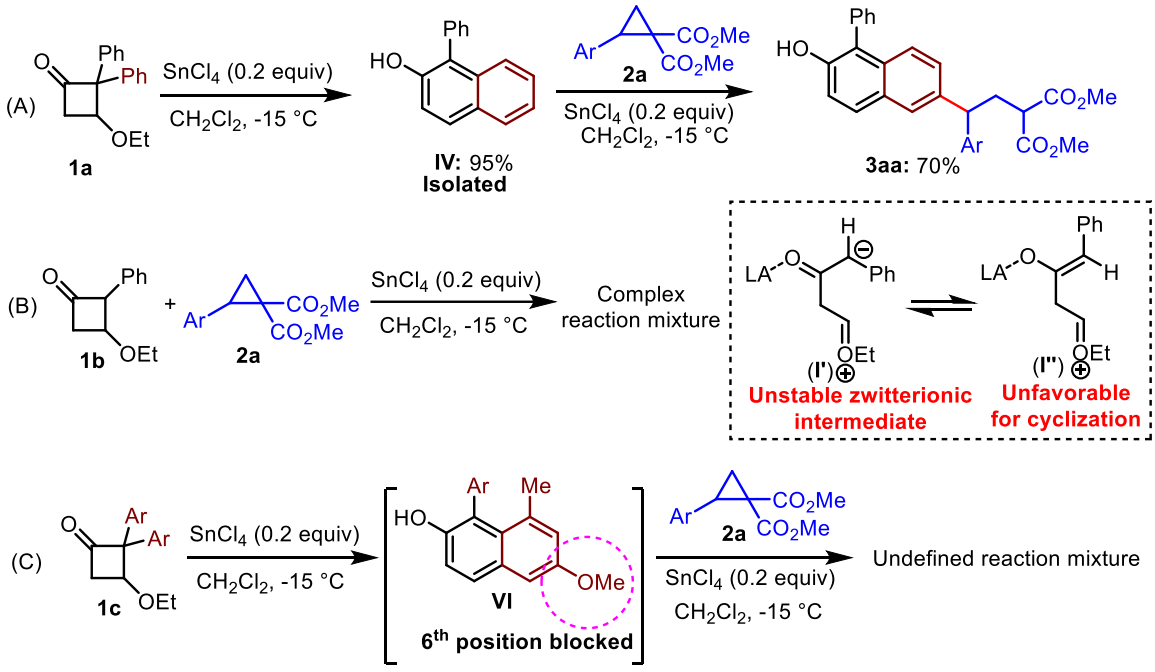

and 6-position of the *in situ* generated *β*-naphthol was blocked with phenyl and methoxy groups, respectively. For that purpose, 3-ethoxy-2,2-bis(4-methoxy-2-methylphenyl)cyclobutan-1-one (1c) was employed and a non-characterizable complex reaction mixture was obtained, establishing the site selectivity of this reaction (Scheme 3.2.2.C).

Scheme 3.2.3. Plausible mechanism

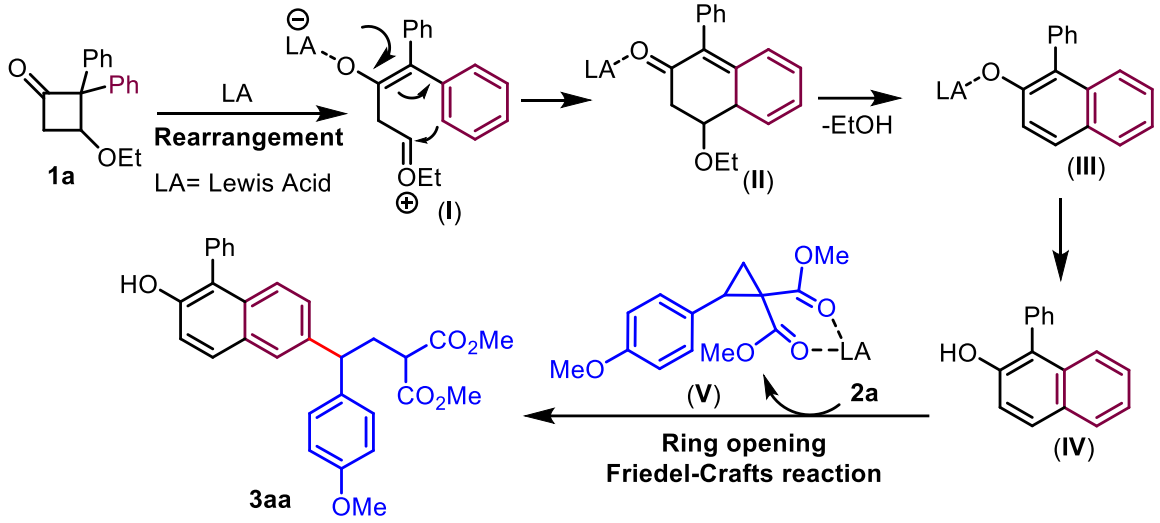

Scheme 3.2.4. Gram-Scale Experiment and Chemical Transformations

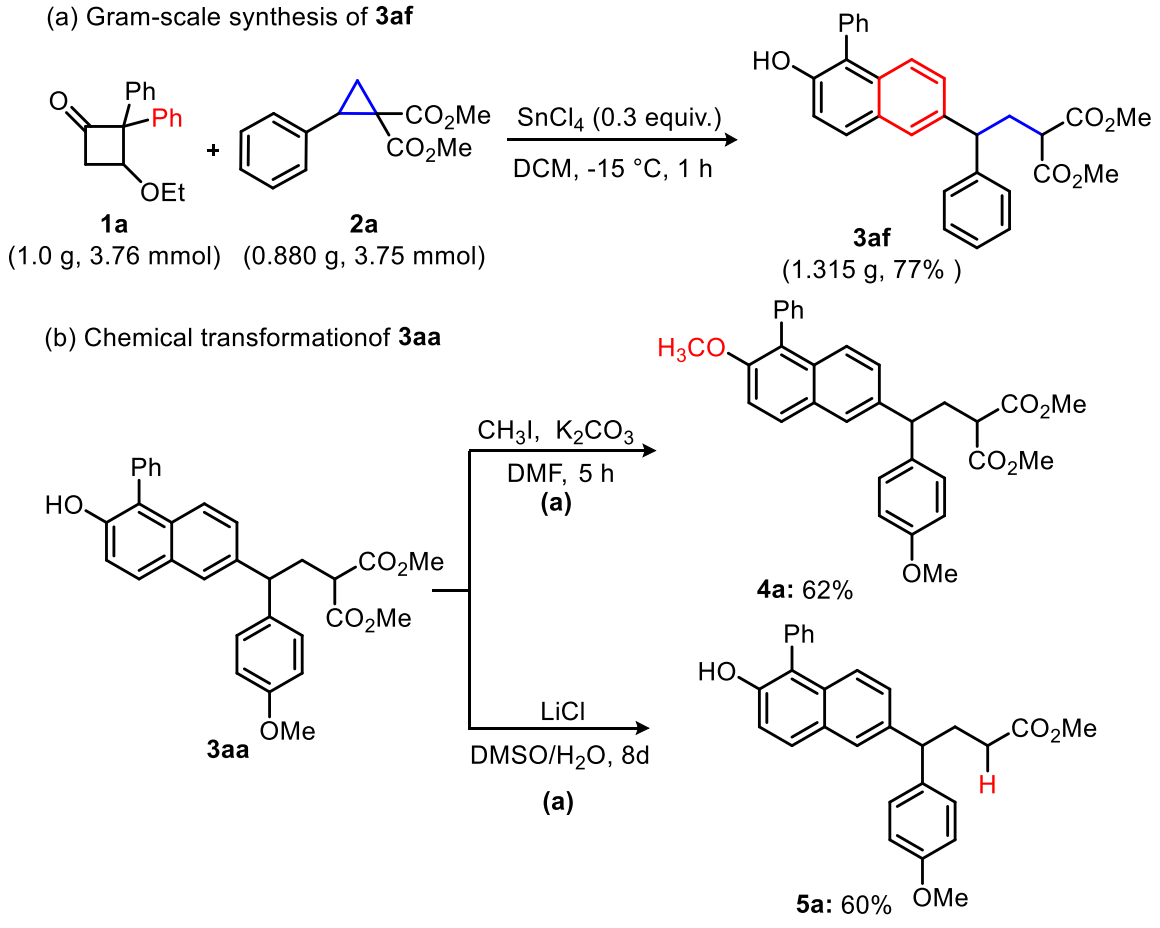

Based on the experimental results and the literature supports[20], a plausible mechanism of both *β*-naphthol formation and the selective Friedel-Crafts alkylation is proposed (Scheme 3.2.3). Initially, the cyclobutanone moiety generates the 1,4-zwitterionic intermediate (**I**) in the presence of Lewis acid ($SnCl_4$), which rearranges itself via intramolecular Friedel-Crafts reaction leading to the

formation of intermediate (**II**). Subsequent elimination of ethanol was followed to afford the 1-phenyl substituted 2-naphthol (**IV**) via intermediate (**III**). This *in situ* generated 2-naphthol (**IV**) further undergoes Friedel-Crafts reaction selectively from the 6th position via ring opening of Lewis acid ($SnCl_4$) coordinated cyclopropane diester (**V**), leading to the formation of desired product **3aa**.

To demonstrate the practical utility of our protocol, a gram-scale experiment was conducted and afforded the final product **3af** in 77% yield (Scheme 3.2.4.a). Furthermore, to check the synthetic utility of our designed methodology, a few post-functional modifications have been conducted (Scheme 3.2.4.b). Initially, methylation of the hydroxy group of the *β*-naphthol derivative **3aa** was achieved by reacting with one equivalent of methyl iodide, taking K_2CO_3 as a base.[23] Later, the Krapcho decarboxylation was also performed and successfully obtained the desired mono-decarboxylated product in moderate yield.[24]

3.3. Conclusion

In conclusion, tandem activation of the two smallest carbocycles has been demonstrated using Lewis acid catalysis. The diphenyl-substituted 3-ethoxy cyclobutanone led to the *in situ* formation of 1-phenyl 2-naphthol, which subsequently underwent the remote site-selective Friedel-Crafts alkylation with aryl cyclopropane diesters. A series of γ-naphthyl butyric acid derivatives were obtained via ring opening of the cyclopropane with good to excellent yields. Moreover, selective methylation and decarboxylation have been conducted smoothly for the synthetic transformation of the product.

3.4 Experimental Section

3.4.1. General Methods:

All reactions were carried out under an inert atmosphere with oven-dried glassware. All solvents and reagents were obtained from commercial sources and were purified following the standard procedure prior to use. The developed chromatogram was analyzed by UV lamp (254 nm) or *p*-anisaldehyde solution. Products were purified by flash chromatography on silica gel (mesh size 230−400). Melting points were determined using a Stuart SMP30 advanced digital melting point apparatus. Infrared (FTIR) spectra were recorded for the neat samples and reported in wavenumber (cm−1). Mass spectral data (HRMS) were obtained using the XEVO G2-XS QTOF instrument. Nuclear magnetic resonance (NMR) spectroscopy was performed using JEOL 400 MHz, JEOL 500 MHz, Bruker 400 MHz. Chemical shifts of ^{1}H, $^{13}C\{^{1}H\}$, ^{19}F, HMBC and HSQC NMR spectra are expressed in parts per million (ppm). All coupling constants are absolute values and are expressed in hertz (Hz). The description of the signals includes the following: s = singlet, d = doublet, dd = doublet of doublet, t = triplet, dt = doublet of triplet, q = quartet, dq = doublet of quartet, br = broad,

and m = multiplet. Structural assignments were made with additional information from gHSQC and gHMBC experiments.

3.4.2. General synthetic methods for the preparation of 3-ethoxy cyclobutanone[3b]: In inert atmosphere, to a solution of diphenylacetic acid (0.8 g, 3.77 mmol) in dry DCM (7 mL), oxayl chloride (0.387 mL, 4.52 mmol) was added dropwise at 0°C. After that, the mixture was stirred at room temperature for 3 hours, and the crude material was used for the next step without further purification. A solution of ethyl vinyl ether (0.54 g, 7.54 mmol) and triethylamine (0.63 mL, 4.52 mmol) in acetonitrile (2 mL) was added to the solution at room temperature for 1 h and the mixture was refluxed (on a silicone oil bath) for 4 h. After the filtration of precipitates, water was added to the filtrate, and the mixture was extracted with ether. The combined organic extracts were dried over anhydrous sodium sulfate and concentrated. The residue was purified by column chromatography on silica gel (hexane/ethyl acetate) gave **1a** 0.75 g (74.78%).

The same procedure was also followed for the preparation of **1b** and **1c** with commercially available phenylacetic acid and synthesized diaryl acetic acid[25] as the respective precursors and **1b** is known and characterization data were matched with the reported data[26].

3-ethoxy-2,2-diphenylcyclobutanone (1a). 2,2-diphenylacetyl chloride (1.0 g, 4.34mmol), **1a** (0.86 g, 3.36 mmol), Yield: 75%; Nature: crystalline solid; Color: white; The title compound was purified by column chromatography (Hexane/ethyl acetate = 9:1); R_f = 0.4; ^{1}H NMR (400 MHz, $CDCl_3$) δ 7.47 – 7.42 (m, 2H), 7.38-7.34 (m, 2H), 7.28-7.20 (m, 4H), 7.18 – 7.13 (m, 2H), 4.83 (dd, *J* = 7.5, 5.4 Hz, 1H), 3.53 (m, 1H), 3.44 – 3.32 (m, 2H), 3.19 (dd, *J* = 18.1, 5.3 Hz, 1H), 1.04 (t, *J* = 7.0 Hz, 3H); ^{13}C{^{1}H} NMR (100 MHz,$CDCl_3$): δ 207.8, 139.9, 138.1, 128.9, 128.8, 128.0, 127.6, 127.3, 127.1, 79.9, 73.7, 65.7, 51.9, 15.0; HRMS (ESI-TOF) m/z: $[M + H]^+$ Calculated for $C_{18}H_{19}O_2$ 267.1385; found 267.1372.

3-ethoxy-2-phenylcyclobutanone (1b). 2-phenylacetyl chloride (1.0 g, 6.5 mmol), **1b** (0.86 g, 4.54 mmol), Yield: 70%; Nature: oil; Color: light yellow; The title compound was purified by column chromatography (Hexane/ethyl acetate = 9:1); R_f = 0.5; ^{1}H NMR (400 MHz, $CDCl_3$) δ 7.35-7.30 (m, 2H), 7.27-7.22 (m, 3H), 4.53 – 4.42 (m, 1H), 4.37 (dd, *J* = 12.4, 6.1 Hz, 1H), 3.62 – 3.53 (m, 2H), 3.23 – 3.19 (m, 2H), 1.26 (d, *J* = 7.0 Hz, 3H).

3-ethoxy-2,2-bis(4-methoxy-2-methylphenyl)cyclobutan-1-one (1c). 2-(4-methoxy-2-methylphenyl)-2-(3-methoxy-5-methylphenyl)acetyl chloride (1.0 g, 3.14 mmol), **1c** (0.6 g,1.69 mmol), Yield: 54%; Nature: amorphous solid; Color: white; The title compound was purified by column chromatography (Hexane/ethyl acetate = 9:1); R_f = 0.3; ^{1}H NMR (400 MHz, $CDCl_3$) δ 7.20 (s, 1H), 7.10 (dd, *J* = 8.2, 2.2 Hz, 1H), 7.02 – 6.96 (m, 1H), 6.89 (d, *J* = 8.3 Hz, 1H), 6.83 (d, *J* = 8.2 Hz, 1H), 6.42 (s, 1H), 4.78 (dd, *J* = 7.9, 4.6 Hz, 1H), 3.78 (s, 3H), 3.75 (s, 3H), 3.49 – 3.29 (m, 3H), 3.21 (dd, *J* = 18.1, 4.6 Hz, 1H), 2.22 (s, 3H), 2.12 (s, 3H), 0.96 (t, *J* = 7.0 Hz, 3H); ^{13}C{^{1}H}

NMR (100 MHz,$CDCl_3$): δ 208.3, 156.5, 155.5, 130.8, 130.2, 129.8, 129.1, 128.9, 126.1, 125.9, 112.6, 111.5, 76.1, 74.1, 65.6, 56.3, 55.0, 51.2, 20.8, 20.7, 15.3; HRMS (ESI-TOF) m/z: $[M + H]^+$ Calculated for $C_{22}H_{26}O_4$ 355.1909; found 355.1899.

3.4.3. General synthetic methods for the preparation of Donor-Acceptor Cyclopropanes:[27] A round bottom flask equipped with a magnetic stir bar was charged with a Dean-Stark apparatus and condenser. Further, the reaction mixture was heated to reflux (on a silicone oil bath). Upon completion (monitored by TLC analysis), evaporation of solvent gave the crude product, which was purified by silica gel chromatography (230-400 mesh), and desired compound was eluted at 5-10% ethyl acetate in hexane. Appropriate aldehyde (1.0 equiv.), followed by benzene, dialkyl malonate (1.0 equiv.), piperidine (0.1 equiv.), and acetic acid (0.2 equiv.). The flask was equipped with a Dean-Stark apparatus and condenser. Further, the reaction mixture was heated to reflux (on a silicone oil bath). Upon completion (monitored by TLC analysis), evaporation of solvent gave the crude product, which was purified by silica gel chromatography (230-400 mesh), and desired compound was eluted at 5-10% ethyl acetate in hexane. Sodium hydride (2.5 equiv.) was taken in a two-neck, round-bottom flask and washed 3-4 times with dry hexane in order to remove the mineral oil. Further, the flask containing dry sodium hydride was added trimethylsulphoxonium iodide (2.0 equiv.), and dry DMSO under a nitrogen atmosphere. The mixture was cooled to 0 °C and stirred for 30 min. Next, a solution of appropriate benzylidene malonate (1.0 equiv.) in anhydrous DMSO was added, and the reaction mixture was allowed to stir at room temperature. Upon completion of the reaction (monitored by TLC analysis), the solution was poured into ice and extracted with ethyl acetate. The combined organic layers were washed once with brine solution, dried over sodium sulfate, filtered, and concentrated in vacuo to give the crude product, which was further purified by silica gel column chromatography (230-400 mesh), and the desired compound was eluted at 5-10% ethyl acetate in hexane. Using this procedure [**2a-2k**] and [**2m-2o**] were synthesized.[27a] **2l** was synthesized according to literature method[27b] and all these Cyclopropane derivatives are known and their characterization data were matched with the reported data.

Dimethyl 2-(4-methoxyphenyl)cyclopropane-1,1-dicarboxylate (2a). Dimethyl 2-(4-methoxybenzylidene)malonate (1.0 g, 4.0 mmol), **2a** (0.755 g, 2.8 mmol), 70% yield, Nature: liquid; Color: light yellow; The title compound was purified by column chromatography (Hexane/ethyl acetate = 9:1); R_f = 0.5; ^{1}H NMR (400 MHz, $CDCl_3$): δ 7.17-7.11 (m, 2H), 6.86-6.79 (m, 2H), 3.81 (s, 3H), 3.80 (s, 3H), 3.41 (s, 3H), 3.20 (t, J = 8.2 Hz, 1H), 2.18 (dd, J = 8.1, 5.2 Hz, 1H), 1.74 (dd, J = 9.3, 5.2 Hz, 1H).

Diethyl 2-(3,4-dimethoxyphenyl)cyclopropane-1,1-dicarboxylate (2b). Diethyl 2-(4-methoxybenzylidene)malonate (1.0 g, 3.6 mmol), **2b** (0.77 g, 2.6 mmol), Yield: 72%; Nature: amourphous solid; Color: white; The title compound was purified by column chromatography

(Hexane/ethyl acetate = 9:1); R_f = 0.5; ^{1}H NMR (400 MHz, $CDCl_3$): δ 6.77 – 6.69 (m, 3H), 4.27 – 4.14 (m, 2H), 3.91 – 3.84 (m, 2H), 3.84 (s, 3H), 3.83 (s, 3H), 3.16 (t, J = 8.6 Hz, 1H), 2.11 (dd, J = 7.9, 5.1 Hz, 1H), 1.66(dd, J = 9.2, 5.1 Hz, 1H), 1.28 (t, J = 7.1 Hz, 3H), 0.91 (t, J = 6.8 Hz, 3H).

Diethyl 2-(benzo[*d*][1,3]dioxol-5-yl)cyclopropane-1,1-dicarboxylate (2c). Diethyl 2-(benzo[d][1,3]dioxol-5-ylmethylene)malonate (1.0 g, 3.4 mmol), **2c** (0.82 g, 2.6 mmol), Yield: 76%; yield Nature: oil; Color: colorless; The title compound was purified by column chromatography (Hexane/ethyl acetate = 9:1); R_f = 0.4; ^{1}H NMR (400 MHz, $CDCl_3$): δ 6.70 – 6.65 (m, 3H), 5.90 (s, 2H), 4.27 – 4.14 (m, 2H), 3.95 –3.87 (m, 2H), 3.15 – 3.10 (m, 1H), 2.07 (dd, J = 7.9, 5.2 Hz, 1H), 1.65 (dd, J = 9.2, 5.1 Hz,1H), 1.27 (t, J = 7.1 Hz, 3H), 0.96 (t, J = 7.1 Hz, 3H).

Diethyl 2-(*p*-tolyl)cyclopropane-1,1-dicarboxylate (2d). Diethyl 2-(4-methylbenzylidene)malonate (1.0 g, 3.82 mmol), **2d** (0.67 g, 2.42 mmol), Yield: 65%; Nature: amorphous solid; Color: white; The title compound was purified by column chromatography (Hexane/ethyl acetate = 9:1); R_f = 0.5; ^{1}H NMR (400 MHz, $CDCl_3$): δ 7.10-7.16 (m, 4H), 4.02 (q, *J* = 7.1 Hz, 2H), 3.83 (q, *J* = 7.1 Hz, 2H), 3.34-3.38 (m, 1H), 2.36-2.38 (m, 1H), 2.32 (s, 3H), 2.24-2.27 (m, 1H), 1.12 (t, *J* = 7.1 Hz, 3H), 0.72 (t, *J* = 7.1 Hz, 3H).

Dimethyl 2-(4-isopropylphenyl)cyclopropane-1,1-dicarboxylate (2e). Dimethyl 2-(4-isopropylbenzylidene)malonate (1.0 g, 3.81 mmol), **2e** (0.70 g, 2.53 mmol), Yield: 67%; Nature: liquid; Color: yellow; The title compound was purified by column chromatography (Hexane/ethyl acetate = 9:1); R_f = 0.5; ^{1}H NMR (400 MHz, $CDCl_3$): δ 7.14-7.07 (m, 4H), 3.78 (s, 3H), 3.35 (s, 3H), 3.21-3.16 (m, 1H), 2.89-2.81 (m, 1H), 2.17 (dd, *J* = 8.0,5.2 Hz, 1H), 1.72 (dd, *J* = 9.3, 5.1 Hz, 1H), 1.21 (s, 1H), 1.19 (s, 1H).

Dimethyl 2-phenylcyclopropane-1,1-dicarboxylate (2f). Dimethyl 2-benzylidenemalonate (1.0 g, 4.54 mmol), **2f** (0.74 g, 3.16 mmol), Yield: 69%; Nature: crystalline solid; Color: white; The title compound was purified by column chromatography (Hexane/ethyl acetate = 9:1); R_f = 0.5; ^{1}H NMR (400 MHz, $CDCl_3$): δ 7.28-7.17 (m, 5H), 3.78 (s, 3H), 3.35 (s, 3H), 3.22 (t, J = 8.6 Hz, 1H), 2.19 (dd, J = 8.0, 5.2 Hz, 1H), 1.74 (dd, J = 9.2, 5.2 Hz, 1H).

Dimethyl 2-(4-fluorophenyl)cyclopropane-1,1-dicarboxylate (2g). Dimethyl 2-(4-fluorobenzylidene)malonate (1.0 g, 4.2 mmol), **2g** (0.6 g, 2.38 mmol), Yield: 56%; Nature: liquid; Color: light yellow; The title compound was purified by column chromatography (Hexane/ethyl acetate = 9:1); R_f = 0.5; ^{1}H NMR (400 MHz, $CDCl_3$): δ 7.19 – 7.10 (m, 2H), 6.98 – 6.89 (m, 2H), 3.77 (s, 3H), 3.37 (s, 3H), 3.18 (t, *J* = 8.6 Hz, 1H), 2.13 (dd, *J* = 8.0, 5.3 Hz, 1H), 1.72 (dd, *J* = 9.3, 5.3 Hz, 1H).

Dimethyl 2-(4-chlorophenyl)cyclopropane-1,1-dicarboxylate (2h). Dimethyl 2-(4-chlorobenzylidene)malonate (1.0 g, 3.93 mmol), **2h** (0.67 g, 2.5 mmol), Yield: 63%; Nature: liquid;

Color: light yellow; The title compound was purified by column chromatography (Hexane/ethyl acetate = 9:1); R_f = 0.5; ^{1}H NMR (400 MHz, $CDCl_3$): δ 7.26 – 7.20 (m, 2H), 7.14 – 7.06 (m, 2H), 3.77 (s, 3H), 3.39 (s, 3H), 3.21 – 3.12 (m, 1H), 2.14 (dd, *J* = 8.0, 5.3 Hz, 1H), 1.73 (dd, *J* = 9.3, 5.3 Hz, 1H).

Dimethyl 2-(4-bromophenyl)cyclopropane-1,1-dicarboxylate (2i). Dimethyl 2-(4-bromobenzylidene)malonate (1.0 g, 3.36 mmol), **2i** (0.71 g, 2.28 mmol), Yield: 67%; Nature: solid; Color: light yellow; The title compound was purified by column chromatography (Hexane/ethyl acetate = 9:1); R_f = 0.5; ^{1}H NMR (400 MHz, $CDCl_3$): δ 7.39 (d, *J* = 8.5 Hz, 2H), 7.06 (d, *J* = 8.4 Hz, 2H), 3.79 (s, 3H), 3.41 (s, 3H), 3.20 – 3.13 (m, 1H), 2.16 – 2.13 (m, 1H), 1.76 – 1.72 (m, 1H).

Dimethyl 2-(*o*-tolyl)cyclopropane-1,1-dicarboxylate (2j). Dimethyl 2-(2-methylbenzylidene)malonate (1.0 g, 4.27 mmol), **2j** (0.73 g, 2.94 mmol), Yield: 70%; Nature: amourphous solid; Color: white; The title compound was purified by column chromatography (Hexane/ethyl acetate = 9:1); R_f = 0.5; ^{1}H NMR (400 MHz, $CDCl_3$): δ 7.17 – 7.06 (m, 3H), 7.03 (d, J = 7.4 Hz, 1H), 3.80 (s, 3H), 3.28 (s, 3H), 3.18 (t, J = 8.7 Hz, 1H), 2.36 (s, 3H), 2.31 (dd, J = 8.3, 5.1 Hz,1H), 1.71(dd, J = 9.2, 5.1 Hz, 1H).

Diethyl 2-(naphthalen-1-yl)cyclopropane-1,1-dicarboxylate (2k). Diethyl 2-(naphthalen-1-ylmethylene)malonate (1.0 g, 3.35 mmol), **2k** (0.56 g, 1.8 mmol), Yield: 53%; Nature: amourphous solid; Color: pale yellow; The title compound was purified by column chromatography (Hexane/ethyl acetate = 9:1); R_f = 0.4; ^{1}H NMR (400 MHz, $CDCl_3$): δ 8.18 (d, *J* = 8.4 Hz, 1H), 7.80 (d, *J* = 7.9 Hz, 1H), 7.73 (d, *J* = 8.2 Hz, 1H), 7.55-7.51 (m, 1H), 7.49 – 7.44 (m, 1H), 7.39 – 7.34 (m, 1H), 7.28 (d, *J* = 8.0 Hz, 1H), 4.39 – 4.26 (m, 2H), 3.66 (t, *J* = 8.6 Hz, 1H), 3.53 (q, *J* = 7.2 Hz, 2H), 2.40 (dd, *J* = 8.1, 5.0 Hz, 1H), 1.80 (dd, *J* = 9.0, 5.0 Hz, 1H), 1.36 – 1.31 (m, 3H), 0.33 (t, *J* = 7.1 Hz, 3H).

Diethyl 6,6a-dihydrocyclopropa[*a*]indene-1,1(1a*H*)-dicarboxylate (2l). 1H-indene (1.0 g, 8.62 mmol), **2l** (1.88 g, 6.89 mmol), Yield: 80%; Nature: sticky liquid; Color: pale yellow; The title compound was purified by column chromatography (Hexane/ethyl acetate = 9:1); R_f = 0.5 ^{1}H NMR (400 MHz, $CDCl_3$): δ 7.38-7.36 (m, 1H), 7.16 – 7.09 (m, 3H), 4.23 – 4.15 (m, 2H), 3.73 (q, *J* = 6.9 Hz, 2H), 3.36 (d, *J* = 17.7 Hz, 1H), 3.30 – 3.23 (m, 2H), 2.66-2.63 (m, 1H), 1.26 (t, J = 7.1 Hz, 3H), 0.75 (t, J = 7.2 Hz, 3H).

(*E*)-diethyl 2-styrylcyclopropane-1,1-dicarboxylate (2m). (E)-diethyl 2-(3-phenylallylidene)malonate (1.0 g, 3.64 mmol), **2m** (0.28 g, 1.5 mmol), Yield: 42%; Nature: oil; Color: brown; The title compound was purified by column chromatography (Hexane/ethyl acetate = 9:1); R_f = 0.4; ^{1}H NMR (400 MHz, $CDCl_3$): δ 7.27 – 7.22 (m, 2H), 7.23 – 7.18 (m, 1H), 6.63 (d, *J* = 15.8 Hz, 1H), 5.80 (dd, *J* = 15.7, 8.8 Hz, 1H), 4.26 – 4.14 (m, 4H), 2.72 (dd, *J* = 16.7, 8.5 Hz,

1H), 1.80 (dd, *J* = 7.5, 4.9 Hz, 1H), 1.65 (dd, *J* = 9.0, 4.9 Hz, 1H), 1.27 (t, *J* = 7.1 Hz, 3H), 1.21 (t, *J* = 7.1 Hz, 3H).

Diethyl 2-(4-methoxyphenyl)cyclopropane-1,1-dicarboxylate (2n). Diethyl 2-(4-methoxybenzylidene)malonate (1.0 g, 3.6 mmol), **2n** (0.75 g, 2.58 mmol), Yield: 72%; Nature: oil; Color: colorless; The title compound was purified by column chromatography (Hexane/ethyl acetate = 9:1); R_f = 0.5; ^{1}H NMR (400 MHz, $CDCl_3$): δ 7.14 (d, *J* = 8.6 Hz, 2H), 6.79 (d, *J* = 8.64 Hz, 2H), 4.04 (q, *J* = 7.1 Hz, 2H), 3.87 (q, *J* = 7.1 Hz, 2H), 3.72 (s, 3H),3.33-3.37 (m, 1H), 2.29-2.32 (m, 1H), 2.24-2.27 (m, 1H), 1.11 (t, *J* = 7.1 Hz, 3H), 0.72 (t, *J* = 7.1 Hz,3H).

Diisopropyl 2-(4-methoxyphenyl)cyclopropane-1,1-dicarboxylate (2o). Diisopropyl 2-(4-methoxyphenyl)cyclopropane-1,1-dicarboxylate (1.0 g, 3.26 mmol), **2o** (0.73 g, 2.28 mmol), Yield: 70% Nature: oil; Color: colorless; The title compound was purified by column chromatography (Hexane/ethyl acetate = 9:1); R_f = 0.5; ^{1}H NMR (400 MHz, $CDCl_3$): δ 7.10 (d, *J* = 8.5 Hz, 2H), 6.77 (d, *J* = 8.7 Hz, 2H), 5.10-5.01 (m, 1H), 4.76-4.66 (m, 1H), 3.74 (s, 3H), 3.14 – 3.08 (m, 1H), 2.05 (dd, *J* = 7.9, 5.1 Hz, 1H), 1.59 (dd, *J* = 9.2, 5.1 Hz, 1H), 1.25 (d, *J* = 6.3 Hz, 3H), 1.23 (d, *J* = 6.3 Hz, 3H), 1.05 (d, *J* = 6.3 Hz, 3H), 0.72 (d, *J* = 6.3 Hz, 3H).

3.4.4. Representative procedure for synthesis 1,6-disubstituted *β*-naphthol: A round-bottom flask equipped with a magnetic stir bar was charged with 2,2-diphenyl 3-ethoxy cyclobutanone (0.2 mmol, 1 equiv.) and donor-acceptor cyclopropane (0.2 mmol, 1 equiv.) under inert atmosphere. Anhydrous dichloromethane (1 mL) was added to the reaction mixture and stirred at -15 °C. In another round-bottom flask, a stock solution of $SnCl_4$ (0.1 mL $SnCl_4$ and 4.9 mL of Anhydrous DCM) was prepared and 0.2 mL of stock solution (0.04 mmol, 0.2 equiv.) was added to the reaction mixture dropwise. The mixture was stirred at -15 °C until the completion of the reaction (as monitored by TLC). The solvent was evaporated on a rotary evaporator and further purified by silica gel column chromatography taking ethyl acetate/hexanes as eluent to afford products.

Dimethyl 2-(2-(6-hydroxy-5-phenylnaphthalen-2-yl)-2-(4-methoxyphenyl)ethyl)malonate (3aa). 1a (0.053 g, 0.2 mmol), **2a** (0.052 g, 0.2mmol), **3aa** (0.081g, .016 mmol); Reaction time: 15 min; Yield: 84%; Nature: white solid; Melting point: 137-140 ˚C; The title compound was purified by column chromatography (Hexane/ethyl acetate = 7:3) R_f = 0.5; ^{1}H NMR (400 MHz, $CDCl_3$): δ 7.74 (d, *J* = 8.9 Hz, 1H), 7.65 (d, *J* = 1.0 Hz, 1H), 7.59 – 7.51 (m, 2H), 7.51 – 7.44 (m, 1H), 7.37 (dd, *J* = 8.1, 1.3 Hz, 2H), 7.30 (d, *J* = 8.8 Hz, 1H), 7.23 (d, *J* = 9.0 Hz, 1H), 7.16 (d, *J* = 8.7 Hz, 2H), 7.15 (dd, *J* = 8.8, 1.8 Hz, 1H), 6.81 (d, *J* = 8.8 Hz, 2H), 5.16 (s, 1H), 4.00 (t, *J* = 8.0 Hz, 1H), 3.75 (s, 3H), 3.70 (s, 3H), 3.68 (s, 3H), 3.32 (t, *J* = 7.4 Hz, 1H), 2.77 – 2.66 (m, 2H); ^{13}C{^{1}H} NMR (100 MHz,$CDCl_3$): δ 169.92, 169.89, 158.3, 150.1, 138.6, 135.5, 134.2, 132.1, 131.2, 129.6, 129.4, 129.0, 128.7, 128.5, 127.1, 126.1, 125.2, 121.0, 117.6, 114.1, 56.3, 52.7, 50.1, 47.6, 34.5; **IR** (Neat): 3440 (br), 2953, 2925, 2852, 1733, 1601, 1510, 1439, 1381, 1302, 1277, 1248, 1150, 1032, 826,

761, 702, 553, 532 cm^{-1}; HRMS (ESI-TOF) m/z: $[M + Na]^+$ Calculated for $C_{30}H_{28}O_6Na$ 507.1784; found 507.1784.

Diethyl 2-(2-(3,4-dimethoxyphenyl)-2-(6-hydroxy-5-phenylnaphthalen-2-yl)ethyl)malonate (3ab). 1a (0.053 g, 0.264 mmol), **2b** (0.064 g, 0.2 mmol), **3ab** (0.070g, .013 mmol); Reaction time: 15 min; Yield: 65%; Nature: yellow sticky liquid; The title compound was purified by column chromatography (Hexane/ethyl acetate = 7:3) R_f = 0.3; ^1H NMR (400 MHz,$CDCl_3$): δ 7.74 (d, *J* = 8.9 Hz, 1H), 7.65 (d, *J* = 1.4 Hz, 1H), 7.54 (t, *J* = 7.5 Hz, 2H), 7.49 – 7.44 (m, 1H), 7.38 (d, *J* = 7.4 Hz, 2H), 7.31 (d, *J* = 8.8 Hz, 1H), 7.23 (d, *J* = 9.0 Hz, 1H), 7.17 (dd, *J* = 8.8, 1.8 Hz, 1H), 6.83 – 6.75 (m, 3H), 5.19 (s, 1H), 4.19 – 4.11 (m, 4H), 4.02 (t, *J* = 8.1 Hz, 1H), 3.82 (s, 3H), 3.81 (s, 3H), 3.28 (t, *J* = 7.3 Hz, 1H), 2.73 – 2.65 (m, 2H), 1.24 (t, *J* = 4.3 Hz, 3H), 1.21 (t, *J* = 4.3 Hz, 3H); $^{13}C\{^1H\}$ NMR (100 MHz,$CDCl_3$): δ 169.6, 169.5, 150.1, 149.0, 147.7, 138.5, 138.5, 136.0, 134.2, 132.1, 131.2, 129.6, 129.4, 128.9, 128.5, 127.1, 126.1, 125.2, 121.0, 119.9, 117.6, 111.4, 111.2, 61.5, 55.9, 50.4, 48.0, 34.4, 14.1; **IR** (Neat): 3436 (br), 3055, 2931, 2873, 1596, 1514, 1463, 1443, 1370, 1302, 1235, 1141, 1095, 1025, 951, 888, 855, 810, 760, 701, 557 cm^{-1}; HRMS (ESI-TOF) m/z: $[M + Na]^+$ Calculated for $C_{33}H_{34}O_7Na$ 565.2202; found 565.2202.

Diethyl 2-(2-(benzo[d][1,3]dioxol-5-yl)-2-(6-hydroxy-5-phenylnaphthalen-2-yl)ethyl)malonate (3ac). 1a (0.053 g, 0.2 mmol), **2c** (0.061 g, 0.2mmol), **3ac** (0.076 g, .014 mmol); Reaction time: 15 min; Yield: 73%; Nature: yellow sticky liquid; The title compound was purified by column chromatography (Hexane/ethyl acetate = 7:3) R_f = 0.4; ^1H NMR (400 MHz,$CDCl_3$): δ 7.74 (d, *J* = 8.9 Hz, 1H), 7.65 (d, *J* = 1.5 Hz, 1H), 7.57 – 7.53 (m, 2H), 7.50 – 7.45 (m, 1H), 7.40 – 7.35 (m, 2H), 7.30 (d, *J* = 8.8 Hz, 1H), 7.25 – 7.22 (m, 1H), 7.15 (dd, *J* = 8.8, 1.8 Hz, 1H), 6.75 – 6.69 (m, 3H), 5.88 (dd, *J* = 2.7, 1.3 Hz, 2H), 5.17 (s, 1H), 4.20 – 4.11 (m, 4H), 3.99 (t, *J* = 8.0 Hz, 1H), 3.26 (t, *J* = 7.4 Hz, 1H), 2.73 – 2.59 (m, 2H), 1.25 (d, *J* = 7.2 Hz, 3H), 1.22 (t, *J* = 4.9 Hz, 3H); $^{13}C\{^1H\}$ NMR (100 MHz, $CDCl_3$): δ 169.5, 169.4, 150.1, 147.9, 146.2, 138.4, 137.4, 134.1, 132.2, 131.2, 129.7, 129.4, 128.9, 128.6, 127.1, 126.1, 125.3, 121.1, 121.0, 117.7, 108.4, 108.3, 101.0, 61.6, 50.3, 48.0, 34.4, 14.2; **IR** (Neat): 3445 (br), 2980, 2930, 1726, 1599, 1503, 1486, 1441, 1370, 1302, 1226, 1149, 1097, 1036, 934, 859, 812, 760, 735, 702, 628, 556 cm^{-1}; HRMS (ESI-TOF) m/z: $[M + Na]^+$ Calculated for $C_{32}H_{30}O_7Na$ 549.1889; found 549.1884.

Diethyl 2-(2-(6-hydroxy-5-phenylnaphthalen-2-yl)-2-(p-tolyl)ethyl)malonate (3ad). 1a (0.053 g, 0.2 mmol), **2d** (0.0552 g, 0.2mmol), **3ad** (0.082 g, .016 mmol); Reaction time: 15 min; Yield: 82%; Nature: yellow sticky liquid; The title compound was purified by column chromatography (Hexane/ethyl acetate = 7:3) R_f = 0.5; ^1H NMR(400 MHz, $CDCl_3$): δ 7.75 (d, *J*= 8.69 Hz, 1H), 7.68 (s, 1H), 7.57-7.53 (m, 2H), 7.50-7.46 (m, 1H), 7.39-7.37 (m, 2H), 7.32-7.30 (m, 1H), 7.25-7.23 (m, 1H), 7.19-7.15 (m, 3H), 7.09 (d, *J*=8.23 Hz, 2H), 5.19 (s, 1H), 4.20-4.11 (m, 4H), 4.05 (t, *J*= 8.06, 1H), 3.28 (t, *J*=7.36 Hz, 1H), 2.74-2.69 (m, 2H), 2.29 (s, 3H), 1.26 (t, *J*= 2.3 Hz, 3H), 1.23

(t, *J*=2.3 Hz, 3H); $^{13}C\{^{1}H\}$ NMR (100 MHz,$CDCl_3$): 169.57, 169.55, 150.1, 140.4, 138.5, 136.2, 134.2, 132.1, 131.2, 129.6, 129.4, 128.9, 128.5, 127.9, 127.1, 126.2, 125.2, 121.0, 117.6, 61.5, 50.4, 48.0, 34.3, 21.0, 14.19, 14.16; **IR** (Neat): 3445 (br), 2980, 2925, 1727, 1599, 1510, 1444, 13701, 1275, 1222, 1148, 1095, 1024, 950, 859, 818, 760, 736, 701, 630, 553, 520 cm^{-1}; HRMS (ESI-TOF) m/z: $[M + Na]^+$ Calculated for $C_{32}H_{32}O_5Na$ 519.2147; found 519.2147.

Dimethyl 2-(2-(6-hydroxy-5-phenylnaphthalen-2-yl)-2-(4-isopropylphenyl)ethyl)malonate (3ae). 1a (0.053 g, 0.2 mmol), **2e** (0.055 g, 0.2mmol), **3ae** (0.072g, .014 mmol); Reaction time: 15 min; Yield: 70%; Nature: yellow sticky liquid; The title compound was purified by column chromatography (Hexane/ethyl acetate = 7:3) R_f = 0.5; ^{1}H NMR (400 MHz, $CDCl_3$): δ 7.75 (d, *J* = 8.9 Hz, 1H), 7.66 (d, *J* = 1.4 Hz, 1H), 7.57 – 7.51 (m, 1H), 7.50 – 7.43 (m, 1H), 7.39 – 7.35 (m, 2H), 7.29 (d, *J* = 8.6 Hz, 1H), 7.22 (d, *J* = 8.9 Hz, 1H), 7.18 – 7.10 (m, 5H), 5.08 (s, 1H), 4.01 (t, *J* = 8.0 Hz, 1H), 3.69 (s, 3H), 3.67 (s, 3H), 3.31 (t, *J* = 7.4 Hz, 1H), 2.83 (m, 1H), 2.71 (t, *J* = 7.7 Hz, 2H), 1.19 (s, 3H), 1.18 (s, 3H); $^{13}C\{^{1}H\}$ NMR (100 MHz, $CDCl_3$): 169.9, 150.0, 147.1, 138.4, 134.1, 132.1, 131.2, 129.7, 129.4, 128.9, 128.6, 127.8, 127.1, 126.7, 126.3, 125.2, 121.0, 117.6, 52.7, 50.1, 48.1, 34.4, 33.7, 24.1; **IR** (Neat): 3444 (br), 2957, 2925, 1733, 1649, 1599, 1541, 1509, 1435, 1382, 1277, 1225, 1151, 1052, 1018, 825, 760, 702, 590, 518 cm^{-1}; HRMS (ESI-TOF) m/z: $[M + Na]^+$ Calculated for $C_{32}H_{32}O_5Na$ 519.2147; found 519.2147.

Dimethyl 2-(2-(6-hydroxy-5-phenylnaphthalen-2-yl)-2-phenylethyl)malonate (3af). 1a (0.053 g, 0.2 mmol), **2f** (0.046 g, 0.2mmol), **3af** (0.078g, 0.17 mmol); Reaction time: 15 min; Yield: 86%; Nature: yellow solid; Melting point: 50-53 °C; The title compound was purified by column chromatography (Hexane/ethyl acetate = 7:3) R_f = 0.5; ^{1}H NMR (400 MHz, HSQC, HMBC, $CDCl_3$): δ 7.79 (d, *J* = 8.9 Hz, 1H), 7.70 (d, *J* = 1.6 Hz, 1H), 7.62 – 7.55 (m, 2H), 7.54 – 7.48 (m, 1H), 7.45 – 7.38 (m, 2H), 7.35 – 7.26 (m, 7H), 7.24 – 7.19 (m, 2H), 5.15 (s, 1H), 4.09 (t, *J* = 8.0 Hz, 1H), 3.72 (d, *J* = 9.7 Hz, 6H), 3.35 (t, *J* = 7.4 Hz, 1H), 2.82 – 2.72 (m, 2H); $^{13}C\{^{1}H\}$ NMR (100 MHz, HSQC, HMBC, $CDCl_3$): δ 169.8, 150.1, 143.4, 138.1, 134.2, 132.2, 131.2, 129.6, 129.4, 128.9, 128.7, 128.5, 128.0, 127.1, 126.7, 126.3, 125.3, 117.7, 52.7, 50.1, 48.4, 34.3; **IR** (Neat): 3445 (br), 2952, 1731, 1598, 1493, 1436, 1381, 1276, 1224, 1149, 1073, 1048, 1029, 951, 890, 823, 757, 736, 701, 592, 554, 517 cm^{-1}; HRMS (ESI-TOF) m/z: $[M + Na]^+$ Calculated for $C_{29}H_{26}O_5Na$ 477.1678; found 477.1678.

Dimethyl 2-(2-(4-fluorophenyl)-2-(6-hydroxy-5-phenylnaphthalen-2-yl)ethyl)malonate (3ag). 1a (0.053 g, 0.2 mmol), **2g** (0.050 g, 0.2 mmol), **3ag** (0.056 g, 0.012 mmol); Reaction time: 120 min; Yield: (60%). Nature: white solid Melting Point: 139-141 °C; The title compound was purified by column chromatography (Hexane/ethyl acetate = 7:3) R_f = 0.5; ^{1}H NMR (400 MHz, $CDCl_3$): δ 7.75 (d, J = 8.9 Hz, 1H), 7.64 (d, *J* = 1.6 Hz, 1H), 7.55 (t, *J* = 7.4 Hz, 2H), 7.50 – 7.45 (m, 1H), 7.40 – 7.35 (m, 2H), 7.31 (d, J = 8.7 Hz, 1H), 7.25 (d, J = 2.5 Hz, 1H), 7.23 – 7.18 (m, 2H), 7.12 (dd, J

= 8.8, 1.9 Hz, 1H), 6.99 – 6.90 (m, 2H), 5.13 (s, 1H), 4.04 (t, J = 8.0 Hz, 1H), 3.71 (s, 3H), 3.68 (s, 3H), 3.29 (t, *J* = 7.4 Hz, 1H), 2.82 – 2.61 (m, 2H). $^{13}C\{^1H\}$ NMR (100 MHz, $CDCl_3$): δ 169.7, 161.7 (d, *J* = 245.0 Hz), 150.2, 139.2, 139.1, 137.8, 133.2 (d, *J* = 183.4 Hz), 131.1, 129.6, 129.5, 129.4, 128.9, 128.6, 126.9, 126.2, 125.4, 121.0, 117.7, 115.5 (d, *J* = 21.0 Hz), 52.7, 50.0, 47.6, 34.4; ^{19}F NMR (376 MHz, $CDCl_3$): δ −116.38; **IR** (Neat): 3445 (br), 2953, 1731, 1600, 1507, 1475, 1436, 1381, 1277, 1223, 1156, 1050, 1014, 951, 890, 826, 761, 736, 703, 555, 526 cm^{-1}; HRMS (ESI-TOF) m/z: $[M + Na]^+$ Calculated for $C_{29}H_{25}O_5FNa$ 495.1584; found 495.1586.

Dimethyl 2-(2-(4-Cholorophenyl)-2-(6-hydroxy-5-phenylnaphthalen-2-yl)ethyl)malonate (3ah). 1a (0.053 g, 0.2 mmol), **2h** (0.053 g, 0.2 mmol), **3ah** (0.086 g, 0.18 mmol); Reaction time: 120 min. Yield: 89%; Nature: white Solid. Melting Point: 148-151 °C; The title compound was purified by column chromatography (Hexane/ethyl acetate = 7:3) R_f = 0.5; ^1H NMR (400 MHz, $CDCl_3$) δ 7.75 (d, *J* = 8.9 Hz, 1H), 7.64 (d, *J* = 1.5 Hz, 1H), 7.55 (t, *J* = 7.4 Hz, 2H), 7.50 – 7.45 (m, 1H), 7.37 (dd, *J* = 8.0, 1.2 Hz, 2H), 7.31 (d, *J* = 8.8 Hz, 1H), 7.26 – 7.17 (m, 3H), 7.13 (dd, *J* = 8.8, 1.8 Hz, 1H), 7.01 – 6.91 (m, 2H), 5.18 (s, 1H), 4.04 (t, *J* = 8.0 Hz, 1H), 3.71 (s, 3H), 3.68 (s, 3H), 3.29 (t, *J* = 7.4 Hz, 1H), 2.76 – 2.65 (m, 2H); $^{13}C\{^1H\}$ NMR (100 MHz, $CDCl_3$) δ 169.7, 162.8, 160.4, 150.2, 139.2, 139.1, 137.8, 134.0, 132.2, 131.1, 129.6, 129.5, 129.4, 128.9, 128.6, 126.9, 126.2, 125.4, 121.0, 117.7, 115.6, 115.4, 52.7, 50.0, 47.6, 34.4; **IR** (Neat): 3724 (br), 1733, 1695, 1649, 1598, 1575, 1552, 1541, 1522, 1494, 1433, 1380, 1339, 1275, 1225, 1149, 1090, 1013, 864, 822, 760, 729, 702, 610, 548, 527, 516 cm^{-1}; HRMS (ESI-TOF) m/z: $[M + Na]^+$ Calculated for $C_{29}H_{25}O_5ClNa$ 511.1288; found 511.1288.

Dimethyl 2-(2-(4-bromophenyl)-2-(6-hydroxy-5-phenylnaphthalen-2-yl)ethyl)malonate (3ai). 1a (0.053 g, 0.2 mmol), **2i** (0.062 g, 0.2 mmol), **3ai** (0.1 g, 0.19 mmol); Reaction time: 120 min; Yield: 94%; Nature: Colorless sticky liquid; The title compound was purified by column chromatography (Hexane/ethyl acetate = 7:3) R_f = 0.4; ^1H NMR (400 MHz,$CDCl_3$): δ 7.75 (d, *J* = 8.9 Hz, 1H), 7.64 (d, *J* = 1.6 Hz, 1H), 7.57 – 7.53 (m, 2H), 7.50 – 7.45 (m, 1H), 7.41 – 7.35 (m, 4H), 7.31 (d, *J* = 8.8 Hz, 1H), 7.27 – 7.23 (m, 1H), 7.15 – 7.09 (m, 3H), 5.20 (s, 1H), 4.02 (t, *J* = 8.0 Hz, 1H), 3.71 (s, 3H), 3.68 (s, 3H), 3.29 (t, *J* = 7.4 Hz, 1H), 2.74 – 2.66 (m, 2H); $^{13}C\{^1H\}$ NMR (100 MHz, $CDCl_3$): δ 169.7, 150.2, 142.5, 137.4, 134.0, 132.2, 132.1, 131.7, 131.1, 129.7, 129.7, 129.4, 128.9, 128.6, 127.5, 126.9, 126.3, 125.4, 121.0, 120.5, 117.8, 52.7, 49.9, 47.8, 34.1; **IR** (Neat): 3464 (br), 2952, 1782, 1733, 1598, 1488, 1436, 1276, 1225, 1153, 1073, 1009, 949, 823, 760, 703, 555 cm^{-1}; HRMS (ESI-TOF) m/z: $[M + Na]^+$ Calculated for $C_{29}H_{25}O_5BrNa$ 555.0783; found 555.0783.

Dimethyl 2-(2-(6-hydroxy-5-phenylnaphthalen-2-yl)-2-(o-tolyl)ethyl)malonate (3aj). 1a (0.053 g, 0.2 mmol), **2j** (0.049 g, 0.2mmol), **3aj** (0.076g, 0.16 mmol); Reaction time: 15 min. Yield: 82%; Nature: yellow sticky liquid; The title compound was purified by column chromatography

(Hexane/ethyl acetate = 7:3) R_f = 0.4; ^{1}H NMR (400 MHz,$CDCl_3$): δ 7.72 (d, *J* = 8.9 Hz, 1H), 7.60 (d, *J* = 1.6 Hz, 1H), 7.57 – 7.52 (m, 2H), 7.50 – 7.45 (m, 1H), 7.39 – 7.33 (m, 3H), 7.29 (d, *J* = 8.7 Hz, 1H), 7.25 – 7.20 (m, 2H), 7.16 (dd, *J* = 8.8, 1.8 Hz, 1H), 7.11 (d, *J* = 4.0 Hz, 2H), 5.15 (s, 1H), 4.27 (t, *J* = 7.9 Hz, 1H), 3.72 (s, 3H), 3.66 (s, 3H), 3.38 (t, *J* = 7.4 Hz, 1H), 2.74 – 2.64 (m, 2H), 2.26 (s, 3H); ^{13}C{^{1}H} NMR (100 MHz,$CDCl_3$): δ 169.9, 150.1, 141.1, 137.7, 136.6, 134.1, 132.1, 131.2, 131.2, 130.9, 129.7, 129.4, 128.9, 128.6, 127.3, 126.8, 126.7, 126.6, 126.3, 125.2, 120.9, 117.6, 52.7, 50.0, 44.0, 34.7, 19.9; **IR** (Neat): 3445 (br), 2952, 1732, 1599, 1490, 1436, 1381, 1276, 1224, 1150, 1073, 1045, 951, 891, 827, 757, 735, 702, 559 cm^{-1}; HRMS (ESI-TOF) m/z: [M + Na]$^+$ Calculated for $C_{30}H_{28}O_5Na$ 491.1834; found 491.1835.

Diethyl 2-(2-(6-hydroxy-5-phenylnaphthalen-2-yl)-2-(naphthalen-1-yl)ethyl)malonate (3ak). 1a (0.053 g, 0.2 mmol), **2k** (0.06 g, 0.2 mmol), **3ak** (0.050g, 0.094 mmol) Reaction time: 15 min; Yield: 47%; Nature: colorless sticky liquid; The title compound was purified by column chromatography (Hexane/ethyl acetate = 7:3) R_f = 0.4; ^{1}H NMR (400 MHz, $CDCl_3$): δ 8.17 (d, *J* = 7.7 Hz, 1H), 7.81 (dd, *J* = 7.0, 2.4 Hz, 1H), 7.73 (dd, *J* = 5.0, 3.7 Hz, 3H), 7.57 – 7.50 (m, 2H), 7.51 – 7.39 (m, 6H), 7.36 (t, *J* = 8.1 Hz, 2H), 7.29 (d, *J* = 8.8 Hz, 1H), 7.22 (d, *J* = 8.9 Hz, 1H), 5.14 (s, 1H), 4.94 (t, *J* = 7.9 Hz, 1H), 4.21 (q, *J* = 7.2 Hz, 2H), 4.09 (m, 2H), 3.42 (t, *J* = 7.4 Hz, 1H), 2.90 – 2.76 (m, 2H), 1.26 (d, *J* = 7.2 Hz, 3H), 1.16 (t, *J* = 7.1 Hz, 3H); ^{13}C{^{1}H} NMR (100 MHz, $CDCl_3$): δ 169.6, 169.5, 150.0, 139.0, 138.0, 134.1, 134.1, 132.1, 131.9, 131.2, 131.1, 129.6, 129.4, 128.9, 128.9, 128.5, 127.5, 127.3, 126.8, 126.2, 125.5, 125.4, 125.2, 124.5, 123.6, 120.9, 117.6, 77.4, 77.1, 76.8, 61.6, 61.5, 50.3, 43.5, 34.7, 14.2, 14.0; **IR** (Neat): 3444 (br), 2926, 1728, 1598, 1508, 1473, 1443, 1370, 1301, 1275, 1224, 1150, 1095, 1027, 950, 859, 829, 780, 761, 702, 559 cm^{-1}; HRMS (ESI-TOF) m/z: [M + Na]$^+$ Calculated for $C_{35}H_{32}O_5Na$ 555.2147; found 555.2147.

Diethyl 2-(1-(6-hydroxy-5-phenylnaphthalen-2-yl)-2,3-dihydro-1H-inden-2-yl)malonate (3al). 1a (0.053 g, 0.2 mmol), **2l** (0.054 g, 0.2 mmol), **3al** (0.080 g, 0.16 mmol); Reaction time: 15 min. Yield: 81%; Nature: yellow sticky liquid; The title compound was purified by column chromatography (Hexane/ethyl acetate = 7:3) R_f = 0.5; ^{1}H NMR (400 MHz, $CDCl_3$): δ 7.74 (d, *J* = 8.9 Hz, 1H), 7.62 (d, *J* = 1.7 Hz, 1H), 7.59 – 7.54 (m, 2H), 7.51 – 7.46 (m, 1H), 7.42 – 7.38 (m, 2H), 7.34 (d, *J* = 8.7 Hz, 1H), 7.27 – 7.23 (m, 2H), 7.21 – 7.13 (m, 2H), 7.09 (t, *J* = 7.4 Hz, 1H), 6.81 (d, *J* = 7.5 Hz, 1H), 5.17 (s, 1H), 4.34 (d, *J* = 9.1 Hz, 1H), 4.21 – 4.13 (m, 2H), 3.92 – 3.70 (m, 2H), 3.59 (d, *J* = 7.3 Hz, 1H), 3.38 (dd, *J* = 15.7, 7.8 Hz, 1H), 3.21 – 3.13 (m, 1H), 2.96 (dd, *J* = 15.6, 9.1 Hz, 1H), 1.26 (d, *J* = 7.2 Hz, 3H), 1.03 (t, *J* = 7.1 Hz, 3H); ^{13}C{^{1}H} NMR (100 MHz,$CDCl_3$): δ 168.6, 168.6, 150.1, 145.7, 142.1, 137.8, 134.2, 132.4, 131.2, 131.2, 129.7, 129.3, 128.9, 128.6, 127.9, 127.4, 127.1, 126.8, 125.2, 125.1, 124.4, 121.1, 117.6, 61.5, 54.6, 48.8, 35.8, 14.2, 13.8; **IR** (Neat): 3445 (br), 2979, 2932, 1725, 1598, 1474, 1443, 1370, 1352, 1303, 1274, 1221, 1147, 1026, 955, 909, 860, 826, 749, 702, 649, 592, 558 cm^{-1}; HRMS (ESI-TOF) m/z: [M + Na]$^+$ Calculated for $C_{32}H_{30}O_5Na$ 517.1991; found 517.1986.

(*E*)-diethyl 2-(2-(6-hydroxy-5-phenylnaphthalen-2-yl)-4-phenylbut-3-en-1-yl)malonate (3am). 1a (0.053 g, 0.2 mmol), **2m** (0.057 g, 0.2 mmol), **3am** (0.083 g, 0.16 mmol); Reaction time: 15 min. Yield: 82%; Nature: yellow sticky liquid; The title compound was purified by column chromatography (Hexane/ethyl acetate = 7:3) R_f = 0.4; ^{1}H NMR (400 MHz,$CDCl_3$): δ 7.76 (d, *J* = 8.9 Hz, 1H), 7.65 (d, *J* = 1.5 Hz, 1H), 7.57 (t, *J* = 7.3 Hz, 2H), 7.52 – 7.47 (m, 1H), 7.42 – 7.39 (m, 2H), 7.36 (d, *J* = 8.7 Hz, 1H), 7.32 (d, *J* = 7.1 Hz, 2H), 7.30 – 7.25 (m, 3H), 7.24 (d, *J* = 4.3 Hz, 2H), 6.45 (d, *J* = 15.9 Hz, 1H), 6.33 (dd, *J* = 15.8, 7.8 Hz, 1H), 5.17 (s, 1H), 4.22 – 4.07 (m, 4H), 3.60 (q, *J* = 7.8 Hz, 1H), 3.36 (t, *J* = 7.4 Hz, 1H), 2.53 – 2.43 (m, 2H), 1.23 (t, *J* = 3.9 Hz, 3H), 1.20 (t, *J* = 3.2 Hz, 3H); ^{13}C{^{1}H} NMR (100 MHz,$CDCl_3$): δ 172.1, 151.9, 139.4, 124.2, 123.6, 116.0, 114.2, 83.6, 65.1, 33.9, 32.0, 31.7, 31.6, 31.5, 30.3, 30.2, 29.8, 29.8, 29.7, 29.6, 29.5, 29.4, 29.3, 29.1, 28.7, 27.1, 26.0, 25.1, 22.8, 14.2; **IR** (Neat): 3445 (br), 2980, 2929, 1727, 1599, 1493, 1473, 1444, 1370, 1301, 1272, 1222, 1149, 1096, 1071, 1027, 967, 887, 860, 827, 756, 697, 557 cm^{-1}; HRMS (ESI-TOF) m/z: $[M + Na]^+$ Calculated for $C_{33}H_{32}O_5Na$ 531.2147; found 531.2156.

Diethyl 2-(2-(6-hydroxy-5-phenylnaphthalen-2-yl)-2-(4-methoxyphenyl)ethyl)malonate (3an). 1a (0.053 g, 0.2 mmol), **2n** (0.058 g, 0.2 mmol), **3an** (0.071 g, 0.14 mmol); Reaction time: 15 min; Yield: 70%; Nature: colorless sticky liquid; The title compound was purified by column chromatography (Hexane/ethyl acetate = 7:3) R_f = 0.5; ^{1}H NMR (400 MHz,$CDCl_3$): δ 7.75 (d, *J* = 8.9 Hz, 1H), 7.66 (d, *J* = 1.5 Hz, 1H), 7.56-7.50 (m, 2H), 7.51 – 7.46 (m, 1H), 7.38-7.35 (m, 2H), 7.30 (d, *J* = 8.7 Hz, 1H), 7.24 (d, *J* = 8.8 Hz, 1H), 7.19 – 7.15 (m, 3H), 6.82 (d, *J* = 8.7 Hz, 2H), 5.15 (s, 1H), 4.21 – 4.12 (m, 4H), 4.02 (t, *J* = 8.0 Hz, 1H), 3.76 (s, 3H), 3.26 (t, *J* = 7.4 Hz, 1H), 2.74 – 2.65 (m, 2H), 1.26 (d, *J* = 7.0 Hz, 3H), 1.22 (t, *J* = 4.8 Hz, 3H); ^{13}C{^{1}H} NMR (100 MHz,$CDCl_3$): δ 169.6, 169.5, 158.2, 150.0, 138.7, 135.6, 134.1, 132.1, 131.2, 129.7, 129.4, 129.0, 128.9, 128.6, 127.2, 126.2, 125.2, 121.0, 117.6, 114.0, 61.5, 55.3, 50.4, 47.6, 34.4, 14.1; **IR** (Neat): 3445 (br), 2928, 1726, 1600, 1509, 1443, 1370, 1301, 1246, 1224, 1175, 1147, 1114, 1095, 1029, 951, 893, 826, 760, 736, 702, 556, 553 cm^{-1}; HRMS (ESI-TOF) m/z: $[M + Na]^+$ Calculated for $C_{35}H_{32}O_5Na$ 535.2097; found 535.2098.

Diisopropyl 2-(2-(6-hydroxy-5-phenylnaphthalen-2-yl)-2-(4-methoxyphenyl)ethyl)malonate (3ao). 1a (0.053 g, 0.2 mmol), **2o** (0.064 g, 0.2 mmol), **3ao** (0.08 g, 0.15 mmol); Reaction time: 15 min; Yield: 75%; Nature: colorless sticky liquid; The title compound was purified by column chromatography (Hexane/ethyl acetate = 7:3) R_f = 0.4; ^{1}H NMR (400 MHz,$CDCl_3$): δ 7.74 (d, *J* = 8.9 Hz, 1H), 7.65 (d, *J* = 1.3 Hz, 1H), 7.57 – 7.52 (m, 2H), 7.49 – 7.46 (m, 1H), 7.39 – 7.36 (m, 2H), 7.30 (d, *J* = 8.8 Hz, 1H), 7.25 – 7.22 (m, 1H), 7.19 – 7.15 (m, 3H), 6.81 (d, *J* = 8.7 Hz, 2H), 5.18 (s, 1H), 5.08 – 4.98 (m, 2H), 4.02 (t, *J* = 8.1 Hz, 1H), 3.75 (s, 3H), 3.18 (t, *J* = 7.5 Hz, 1H), 2.70 – 2.63 (m, 2H), 1.24 – 1.19 (m, 12H); ^{13}C{^{1}H} NMR (100 MHz, $CDCl_3$): δ 169.1, 158.4, 150.0, 138.7, 135.6, 134.2, 132.1, 131.2, 129.6, 129.4, 129.0, 128.9, 128.5, 127.2, 126.2, 125.2, 121.1, 121.0, 117.6, 114.0, 68.9, 55.3, 50.7, 47.5, 34.3, 21.8, 21.7, 21.7; **IR** (Neat): 3445 (br), 2980, 2934,

1721, 1600, 1509, 1466, 1374, 1246, 1176, 1148, 1100, 1034, 988, 951, 903, 824, 760, 736, 702, 556, 532 cm^{-1}; HRMS (ESI-TOF) m/z: $[M + Na]^+$ Calculated for $C_{34}H_{36}O_6Na$ 563.2401; found 563.2407.

3.4.5. Procedure for the gram-scale synthesis of 3af: A round-bottom flask equipped with a magnetic stir bar was charged with 2,2-diphenyl 3-ethoxy cyclobutanone (3.76 mmol, 1 equiv.) and donor-acceptor cyclopropane (3.76 mmol, 1 equiv.) under inert atmosphere. Anhydrous dichloromethane (5 mL) was added to the reaction mixture and stirred at -15 °C and then 0.1 mL of $SnCl_4$ was added dropwise. The reaction mixture was stirred at -15 °C until the completion of the reaction (as monitored by TLC). The solvent was evaporated on a rotary evaporator and purified by silica gel column chromatography with ethyl acetate/hexanes as eluent to afford products **3af** 1.315 g in 77% yield.

3.4.6. General procedure for the methylation of 3aa[21]: A round-bottom flask equipped with a magnetic stir bar was charged **3aa** (0.030 g, 0.06 mmol), K_2CO_3 (0.008 g, 0.06 mmol) and MeI (0.012 g, 0.09mmol) in DMF. On completion (as monitored by TLC), the reaction was quenched with water. The organic layer was washed with water and the aqueous layer was extracted with DCM. The combined layer was dried and the solvent was removed in vacuo. The crude mixture was further purified by column chromatography on silica gel with ethyl acetate/hexane as eluent to afford **4a** with 62% yield.

Dimethyl 2-(2-(6-methoxy-5-phenylnaphthalen-2-yl)-2-(4-methoxyphenyl)ethyl)malonate (4a). 3aa (0.030 g, 0.06 mmol), MeI (0.012 g, 0.09mmol), K_2CO_3 (0.008 g, 0.06 mmol), **4a** (0.018 g, 0.0372 mmol); Reaction time: 5 h; Yield: 62%; Nature: Yellow oil; The title compound was purified by column chromatography (Hexane/ethyl acetate = 7:3) R_f = 0.6; ^1H NMR (400 MHz, $CDCl_3$): δ 7.82 (d, *J* = 9.0 Hz, 1H), 7.65 (d, *J* = 1.6 Hz, 1H), 7.45 (m, 2H), 7.40 – 7.30 (m, 5H), 7.18 – 7.11 (m, 3H), 6.80 (d, *J* = 8.7 Hz, 2H), 3.99 (t, *J* = 8.0 Hz, 1H), 3.81 (s, 3H), 3.75 (s, 3H), 3.70 (s, 3H), 3.68 (s, 3H), 3.31 (t, *J* = 7.4 Hz, 1H), 2.77 – 2.57(m, 2H); $^{13}C\{^1H\}$ NMR (100 MHz, $CDCl_3$): δ 169.9, 169.8, 158.2, 153.6, 138.7, 136.3, 135.4, 132.4, 130.9, 129.0, 128.2, 127.1, 127.0, 125.8, 125.7, 125.3, 114.0, 56.8, 55.3, 52.6, 50.1, 47.6, 34.4, 29.7; **IR** (Neat): 2922, 2850, 2567, 1733, 1602, 1512, 1437, 1259, 1221, 1174, 1057, 828 cm^{-1}; HRMS (ESI-TOF) m/z: $[M + Na]^+$ Calculated for $C_{31}H_{30}O_6Na$ 521.1940; found 521.1940.

3.4.7. General procedure for the decarboxylation of 3aa[22]: To the solution of adduct **3aa** (0.030 g, 0.06 mmol) in DMSO (4 mL) were added LiCl (0.012 g, 0.36 mmol) and H_2O (1 drop), and the reaction mixture was heated at 160 °C (on a silicone oil bath) until consumption of starting material (as monitored by TLC). Three milliliters of water was added to the mixture, and the mixture was extracted with diethyl ether, dried over Na_2SO_4, and purified by flash column chromatography using a 10–20% acetone/hexane solvent system and obtained the desired product **5a** with 60% yield.

Methyl 4-(6-hydroxy-5-phenylnaphthalen-2-yl)-4-(4-methoxyphenyl)butanoate (5a). 3aa (0.030 g, 0.06 mmol), LiCl (0.012 g, 0.36 mmol) **5a** (0.015 g, 0.036 mmol); Reaction time: 8 d; Yield: 60%; Nature: Yellow oil; The title compound was purified by column chromatography (Hexane/ethyl acetate = 7:3) R_f = 0.6; ^{1}H NMR (400 MHz, $CDCl_3$): δ 7.74 (d, *J* = 8.9 Hz, 1H), 7.64 (d, *J* = 1.1 Hz, 1H), 7.58 – 7.51 (m, 2H), 7.50 – 7.45 (m, 1H), 7.37 (d, *J* = 6.7 Hz, 2H), 7.29 (d, *J* = 8.7 Hz, 1H), 7.22 (d, *J* = 8.9 Hz, 1H), 7.16 (d, *J* = 8.4 Hz, 3H), 6.80 (d, *J* = 8.7 Hz, 2H), 5.12 (s, 1H), 3.98 (t, *J* = 7.7 Hz, 1H), 3.74 (s, 3H), 3.62 (s, 3H), 2.41 (m, 2H), 2.29 (t, *J* = 7.3 Hz, 2H); ^{13}C{^{1}H} NMR (100 MHz, $CDCl_3$): δ 174.0, 158.1, 149.9, 139.4, 136.3, 134.2, 132.0, 131.2, 129.6, 129.3, 128.9, 128.9, 128.5, 127.2, 126.0, 125.1, 120.9, 117.5, 113.9, 55.3, 51.6, 49.4, 32.6, 30.6, 29.8; **IR** (Neat): 3401 (br), 3034, 2929, 1732, 1599, 1510, 1441, 1303, 1247, 1224, 1176, 1145, 1033, 951, 886, 823, 761, 702, 555, 533 cm^{-1}; HRMS (ESI-TOF) m/z: $[M + H]^+$ Calculated for $C_{28}H_{27}O_4$ 427.1909; found 427.1937.

3.4.8. Procedure for the control Experiment: A round-bottom flask equipped with a magnetic stir bar was charged with 2,2-diphenyl 3-ethoxy cyclobutanone (0.2 mmol, 1 equiv.) under inert atmosphere. Anhydrous dichloromethane (1 mL) was added to the reaction mixture and stirred at -15 °C. In another round-bottom flask, a stock solution of $SnCl_4$ (0.1 mL $SnCl_4$ and 4.9 mL of Anhydrous DCM) was prepared and 0.2 mL of stock solution (0.04 mmol, 0.2 equiv.) was added to the reaction mixture dropwise. The mixture was stirred at -15 °C until the completion of the reaction (as monitored by TLC). The solvent was evaporated on a rotary evaporator and further purified by silica gel column chromatography taking ethyl acetate/hexanes as eluent to afford product **IV** and this molecule is known and their characterization data were matched with the reported data[20,28].

1-phenylnaphthalen-2-ol (IV). 1a (0.053 g, 0.2 mmol), **IV** (0.042g, 0.19 mmol); Reaction time: 5 min; Yield: 95%; Nature: white solid; The title compound was purified by column chromatography (Hexane/ethyl acetate = 7:3); R_f = 0.7; ^{1}H NMR (400 MHz, $CDCl_3$): δ 7.82 – 7.77 (m, 2H), 7.61 – 7.56 (m, 2H), 7.53 – 7.47 (m, 1H), 7.44 – 7.38 (m, 3H), 7.35 – 7.30 (m, 2H), 7.26 (d, *J* = 9.3 Hz, 1H), 5.15 (s, 1H).

3.5. References

(1) (a) Pirenne, V.; Muriel, B.; Waser, J. *Chem. Rev.* **2021**, *121*, 227-263. (b) Robiette, R.; Caillé, J. *Org. Biomol. Chem.* **2021**, *19*, 5702–5724. (c) Thirumalaikumar, M. *Org. Prep. Proced. Int.* **2022**, *54*, 1-39. (d) Moschona, F.; Savvopoulou, I.; Tsitopoulou, M.; Tataraki, D.; Rassias, G. *Catalysts.* **2020**, *10*, 1117. (e) Watson, I. D. G.; YU, L.; Yudin, A. K. *Acc. Chem. Res.* **2006,** *39*, 194-206. (f) Williamson, K. S.; Michaelis, D. J.; Yoon, T. P. *Chem. Rev.* **2014**, *114*, 8016-8036. (g) Ren, Q.; Yang, W.; Lan, Y.; Qin, X. He, Y.; Yuan, L. *Molecules.* **2018**, *23*, 2656. (h) Tachrim, Z. P.; Wang, L.; Murai, Y.; Hashimoto, M. *Molecules.* **2021**, *26*, 4496.

(2) Ghosh, A.; Dey, R.; Banerjee, P. *Chem. Commun.*, **2021**, *57*, 5359–5373.

(3) Matsuo, J. *Tetrahedron Lett*. **2014,** *55*, 2589–2595.

(4) (a) Ishida, N. Murakami, M. *Chem. Rev.* **2021**, *121*, 264-299. (b) Sasaki, S.; Tanaka, H.; Ishibashi, H.; Matsuo, J. *J. Am. Chem. Soc*. **2008**, *130*, 11600–11601. (c) Lin, Y.; Yang, X.; Pan, W.; Rao, Y. *Org. Lett*. **2016**, *18*, 2304-2307. (d) Okado, R. Ishibashi, H.; Matsuo, J. *Org. Lett.* **2010**, *12*, 3266-3268. (e) Shan, G.; Liu, P.; Rao, Y. *Org. Lett.* **2011**, *13*, 1746–1749. (f) Shan, G.; Sun, X.; Xia, Q.; Rao, Y. *Org. Lett.*, **2011**, *13*, 5770–5773. (g) Kawano, M.; Kiuchi, T.; Negishi, S.; Tanaka, H.; Hoshikawa, T.; Ishibashi, H.; Matsuo, J. *Angew. Chem. Int. Ed*. **2013**, *52*, 906–910. (h) Zhou, Y.; Tang, Z.; Song, Q. *Adv. Synth. Catal*. **2017,** *359*, 952–958. (i) Shima, Y.; Matsuo, J. *Tetrahedron Lett.* **2016**, *57*, 4066–4069. (j) Kanie, M.; Ikawa, Y.; Yoshimura, T.; Matsuo, J. *Tetrahedron Lett.* **2019**, *60*, 150910.

(5) (a) Reissig, H. -U.; Zimmer, R. *Chem. Rev*. **2003**, *103*, 1151-1196. (b) Schneider, T. F.; Kaschel, J.; Werz, D. B. *Angew. Chem., Int. Ed*. **2014**, *53*, 5504-5523. (c) Cavitt, M. A.; Phun, L. H.; France, S. *Chem. Soc. Rev*. **2014**, *43*, 804-818. (d) Carson, C. A.; Kerr, M. A. *Chem. Soc. Rev.* **2009**, *38*, 3051–3060. (e) Augustin, A. U.; Werz, D. B. *Acc. Chem. Res.* **2021**, *54*, 1528-1541. (f) Liu, J.; Liu, R.; Wei, Y.; Shi, M. *Trends in Chemistry*. **2019,** *1*, 779-793. (g) Budynina, E. M.; Ivanov, K. L.; Sorokin, I. D.; Melnikov, M. Y. *Synthesis*. **2017**, *49*, 3035-3068. (h) Ivanova, O. A.; Andronov, V. A.; Vasin, V. S.; Shumsky, A. N.; Rybakov, V. B.; Voskressensky, L. G.; Trushkov, I. V. *Org. Lett.* **2018**, *20*, 7947-7952. (i) Xiao, J.-A.; Li, J.; Xia, P.-J.; Zhou, Z.-F.; Deng, Z. X.; Xiang, H.-Y.; Chen, X.-Q.; Yang, H.; *J. Org. Chem*. **2016**, *81*, 11185-11194.

(6) For selected reviews, see (a) Pandey, A. K.; Ghosh, A.; Banerjee, P. *Isr. J. Chem*, **2016**, *56*, 512-521. (b) Singh, P.; Varshnaya, R. K.; Dey, R.; Banerjee, P. *Adv. Synth. Catal*. **2020**, *362*, 1447-1484. For selected papers, see (c) Dey, R.; Banerjee, P. *Org. Lett*. **2017**, *19*, 304-307. (d) Dey, R.; Kumar, P. Banerjee, P. *J. Org. Chem*. **2018**, *83*, 5438-5449. (e) Kumar, P.; Kumar, R.; Banerjee, P. *J. Org. Chem*. **2020**, *85*, 6535-6550. (f) Taily, I. M.; Saha, D. Banerjee, P. *Eur. J. Org. Chem*. **2019**, 7804–7813. (g) Varshnaya, R. K.; Banerjee, P. *J. Org. Chem.* **2019**, *84*, 1614−1623. (h) Vermaa, K. Banerjee, P. *Adv. Synth. Catal*. **2016**, *358*, 2053–2058. (i) Saha, D.; Taily, I. M.; Banerjee, P. *Eur. J. Org. Chem.* **2021**, 5053–5057.

(7) Pandey, A. K.; Ghosh, A.; Banerjee, P. *Eur. J. Org. Chem.* **2015**, 2517–2523.

(8) Ghosh, A.; Pandey, A. K.; Banerjee, P. *J. Org. Chem.* **2015**, *80*, 7235-7242.

(9) Ghosh, A.; Mandal, S.; Chattaraj, P. K.; Banerjee, P. *Org. Lett.* **2016**, *18*, 4940-4943.

(10) Chagarovskiy, A. O.; Vasin, V. S.; Kuznetsov, V. V.; Ivanova, O. A.; Rybakov, V. B.; Shumsky, A. N.; Makhova, N. N.; Trushkov, I. V. *Angew. Chem. Int. Ed*. **2018**, *57*, 10338–10342.

(11) Calloway, N. O. *Chem. Rev*. **1935**, *17*, 327–392.

(12) (a) Rueping, M.; Nachtsheim, B. J. *Beilstein J. Org. Chem.* **2010,** *6*, 6. (b) Zadsirjan, V.; Saedi, P.; Momeni, T.; Heravi, M. M. *RSC Adv.*, **2018**, *8*, 40061–40163.

(13) (a) Reddy, C. R.; Sindhu, C.; Sudhakar, C.; Nagendra, S.; Das, B. *Synthesis.* **2010**, *21*, 3731–3735. (b) Niu, L. F.; Xin, Y. C.; Wang, R. L.; Jiang, F.; Xu, P. F.; Hui, X. P. *Synlett*. **2010**, *5*, 765–768. (c) Kang, L.; Xu, X.; Jia, X.; Wang, X.; Yuan, Y.; Xie, H.; Huo, C. *Tetrahedron.* **2014**, *70*, 1055-1059. (d) Li, C. Y.; Xiang, M.; Zhang, J.; Li, W. S.; Zou, Y.; Tiana, F.; Wang, L. X. *Org. Biomol. Chem.*, **2021**, *19*, 7690–7694.

(14) (a) Wales, S. M.; Walker, M. M.; Johnson, J. S. *Org. Lett.*, **2013**, *15*, 2558–2561. (b) Talukdar, R.; Saha, A.; Tiwari, D. P.; Ghorai, M. K. *Tetrahedron.* **2016**, *72*, 613-624.

(15) Kaicharla, T.; Roy, T.; Thangaraj, M.; Gonnade, R. G.; Biju, A. T. *Angew. Chem. Int. Ed.* **2016**, *55*, 10061–10064.

(16) (a) Xia, Y.; Chang, F.; Lin, L.; Xu, Y.; Liu, X.; Feng, X. *Org. Chem. Front.*, **2018**, *5*, 1293–1296.

(17) Zhu, M.; Wang, D. C.; Xie, M. S.; Qu, G. R.; Guo, H. M. *Chem. Eur. J.* **2018**, *24*, 15512–15516.

(18) (a) Lucht, A.; Patalag, L. J.; Augustin, A. U.; Jones, P. G.; Werz, D. B. *Angew. Chem. Int. Ed.* **2017**, *56*, 10587 –10591. (b) Lucht, A.; Sobottka, S.; Patalag, L. J. Jones, P. G. Reissig, H. -U.; Sarkar, B.; Werz, D. B. *Chem. Eur. J.* **2019**, *25*, 10359–10365.

(19) Chaudhary, A. *Mol. Divers.* **2021**, *25*, 1211–1245.

(20) Feiler, L. A.; Otto, P.; Huisgen, R. *Chem. Ber*. **1969**, *102*, 3405-3427.

(21) Zhang, Z.; Sun, Q.; Xu, D.; Xia, C.; Sun. W. *Green Chem.*, **2016**, *18*, 5485–5492.

(22) Chen, T.; Chen, S.; Fu, S.; Qin, S.; Liu, B. *Synlett.* **2019**, *30*, 903–909.

(23) Sun, C.; Ren, C.; Wei, Y.; Qin, B.; Zeng, H. *Chem. Commun.* **2013**, *49*, 5307-5309.

(24) Varshnaya, R. K.; Banerjee, P. *J. Org. Chem.* **2019**, *84*, 1614−1623.

(25) Moore, D. L.; Denton, A. E.; Kohinke, R. M.; Craig, B. R.; Brenzovich, W. E. *Synth. Commun.* **2016**, *46*, 604-612.

(26) Matsuo, J.; Okuno, R.; Takeuchi, K.; Kawano M.; Ishibashi, H. *Tetrahedron Lett*. **2010**, *51*, 3736-3737.

(27) (a) Corey, E. J.; Chaykovsky, M. *J. Am. Chem. Soc.* **1965**, *87*, 1353–1364. (b) Gonzalez-Bobes, F.; Fenster, M. D. B.; Kiau, S.; Kolla, L.; Kolotuchin, S.; Soumeillant, M. *Adv. Synth. Catal.* **2008**, *350*, 813-816.

(28) Huang, C.; Gevorgyan, V. *J. Am. Chem. Soc.* **2009**, *131*, 10844–10845.

3.6. NMR spectra of the compounds

^{1}H (400MHz, $CDCl_3$) NMR of **3aa**

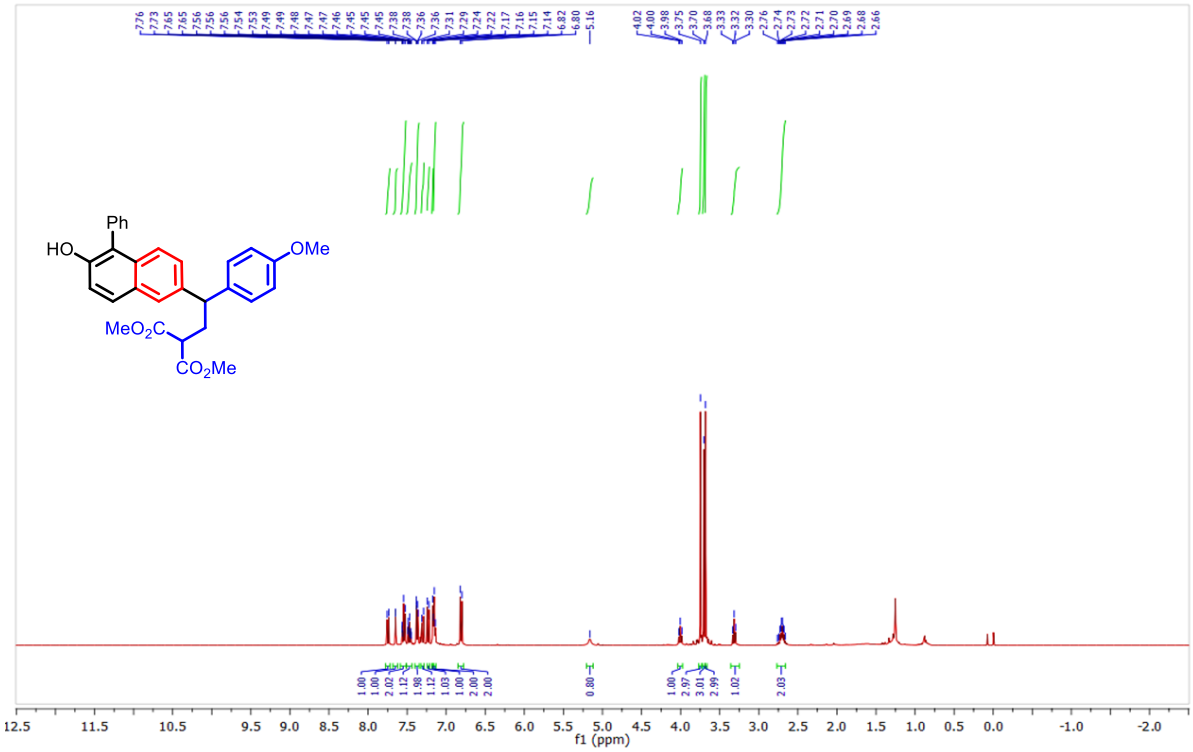

^{13}C {^{1}H} (100MHz, $CDCl_3$) NMR of **3aa**

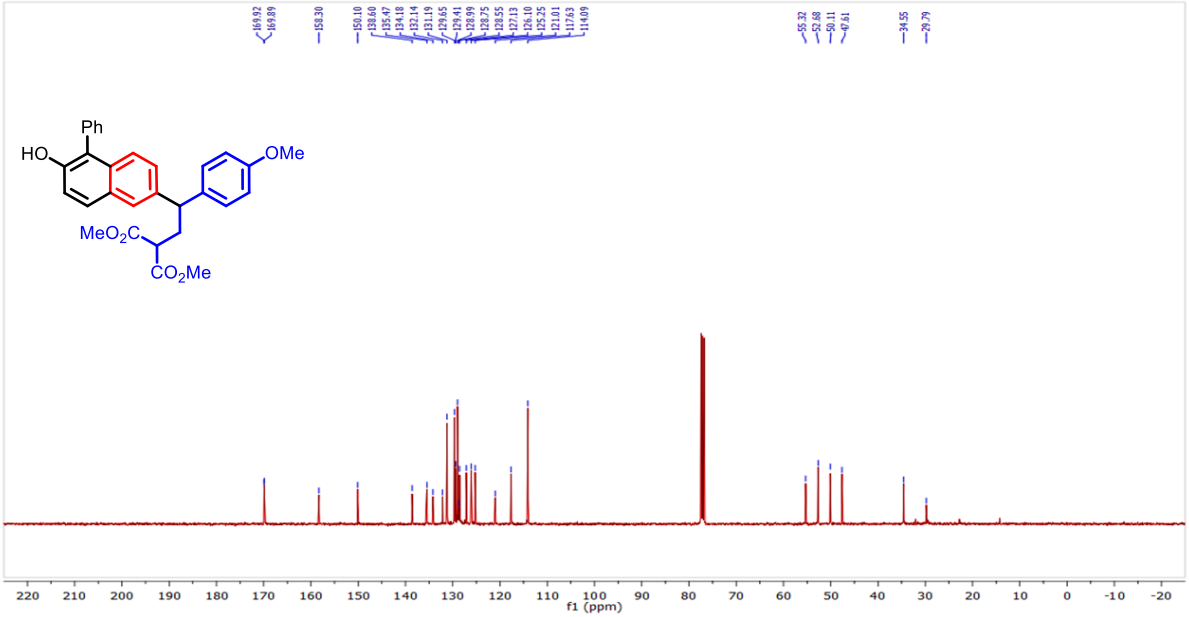

^{1}H (400MHz, $CDCl_3$) NMR of **3ab**

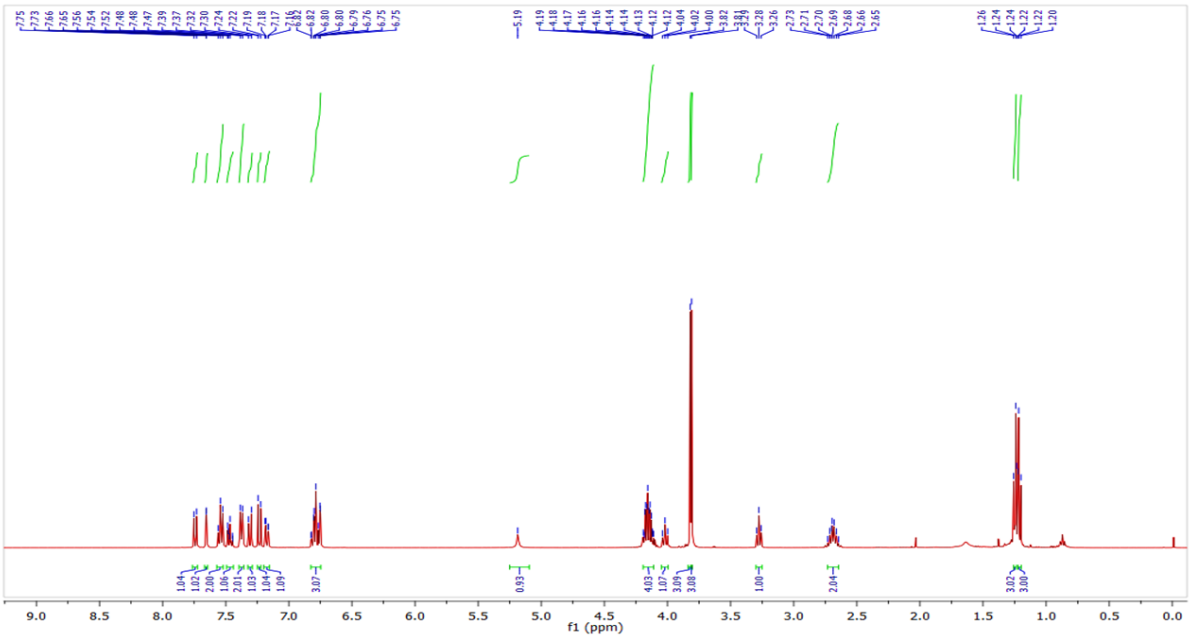

^{13}C {^{1}H} (100MHz, $CDCl_3$) NMR of **3ab**

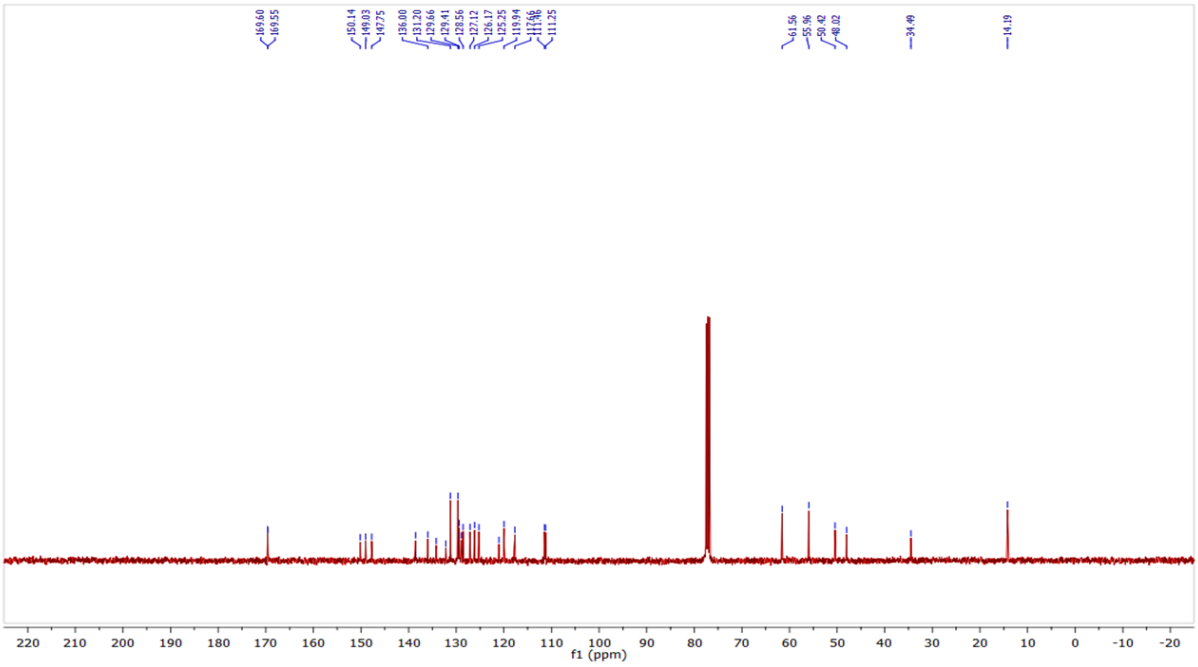

^{1}H (400MHz, $CDCl_3$) NMR of **3ac**

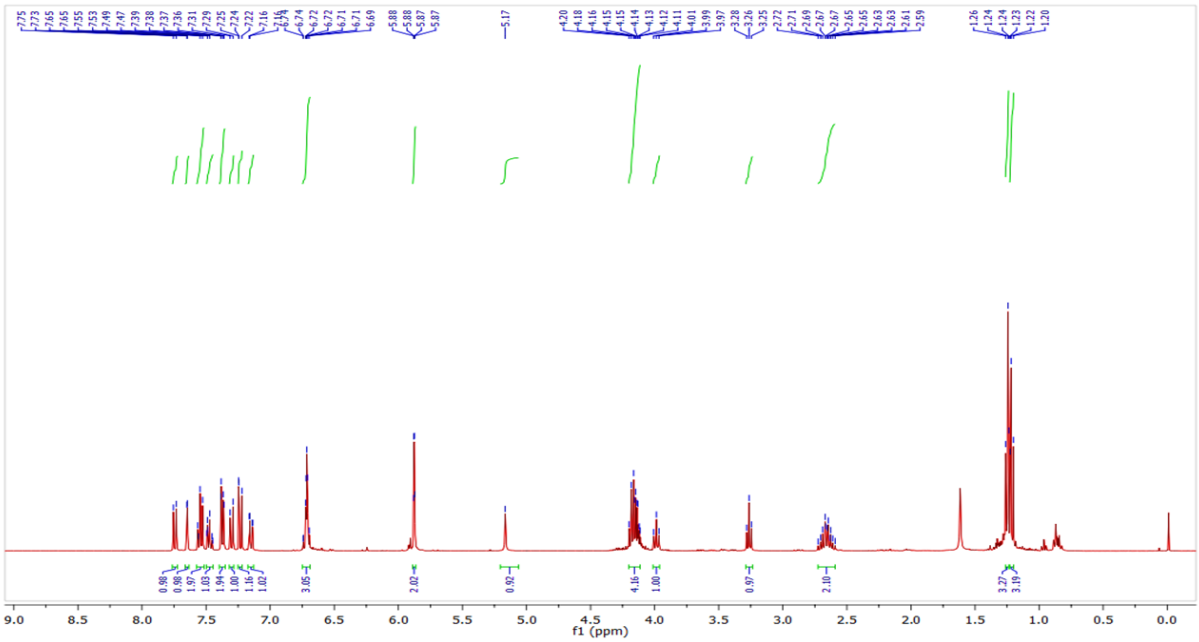

^{13}C {^{1}H} (100MHz, $CDCl_3$) NMR of **3ac**

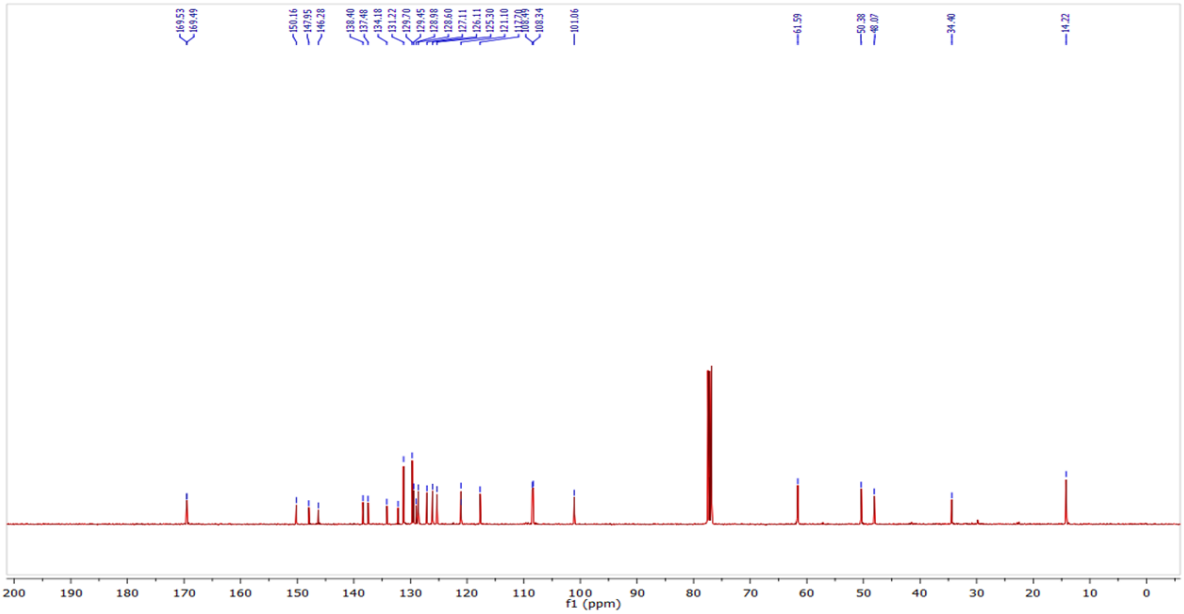

^{1}H (400MHz, $CDCl_3$) NMR of **3ad**

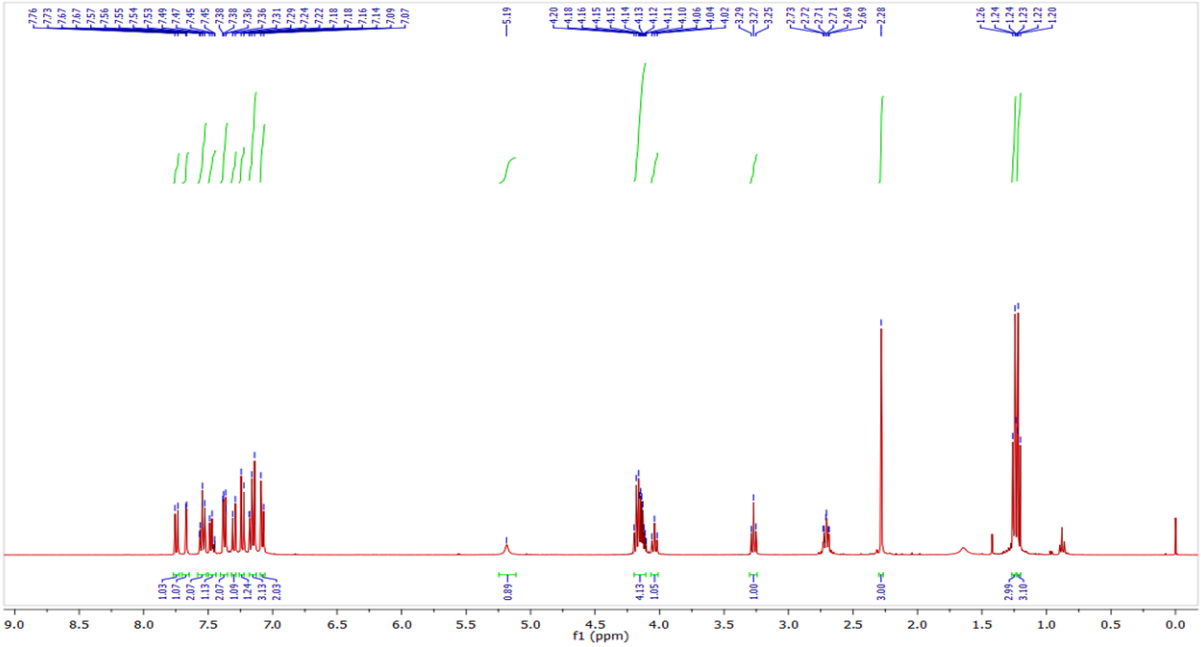

^{13}C {^{1}H} (100MHz, $CDCl_3$) NMR of **3ad**

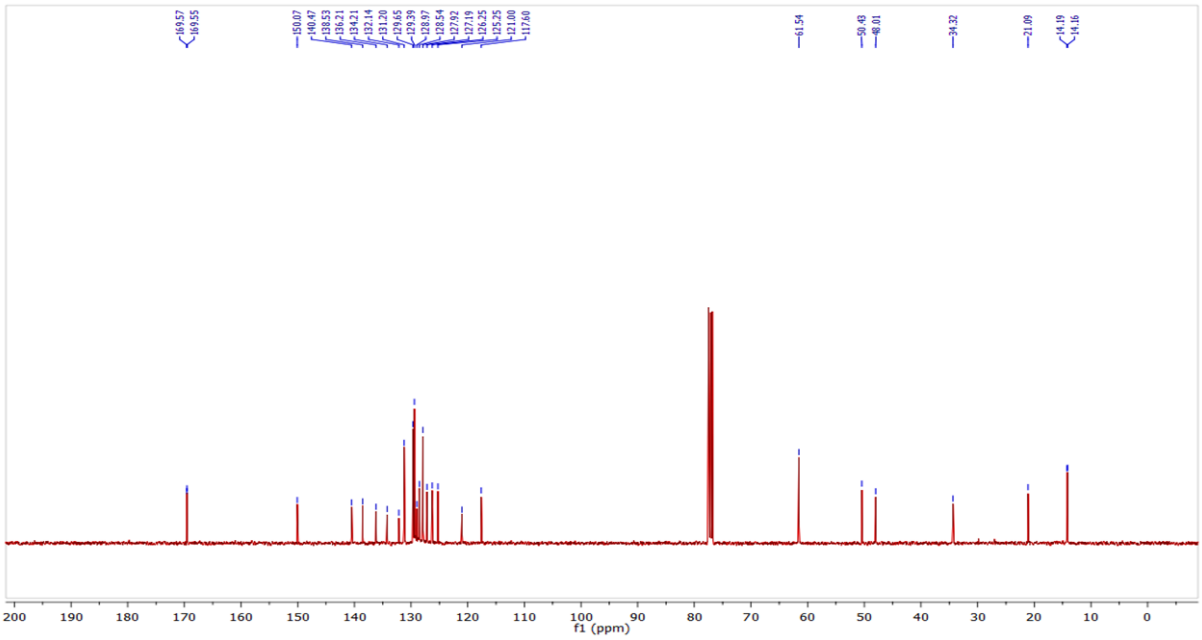

^{1}H (400MHz, $CDCl_3$) NMR of **3ae**

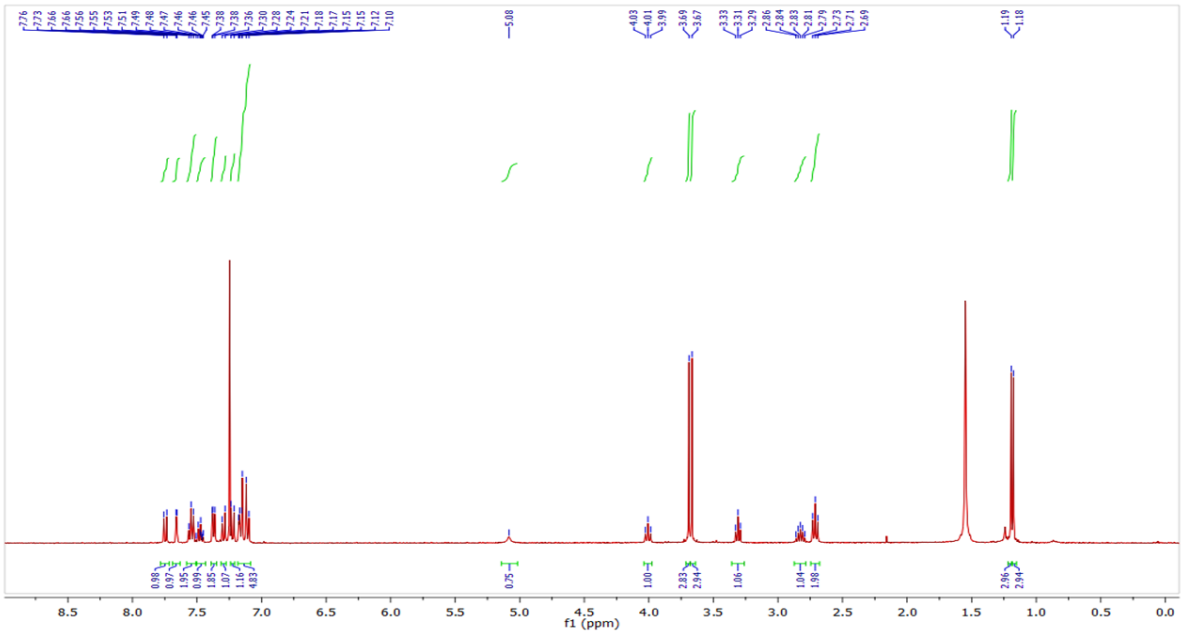

^{13}C {^{1}H} (100MHz, $CDCl_3$) NMR of **3ae**

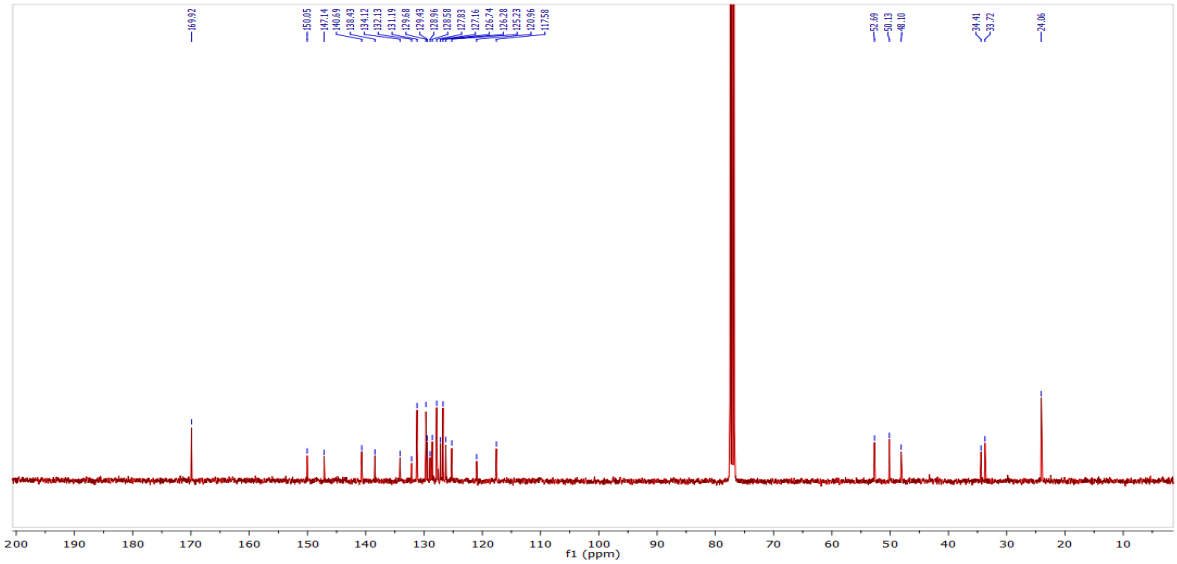

^{1}H (400MHz, $CDCl_3$) NMR of **3af**

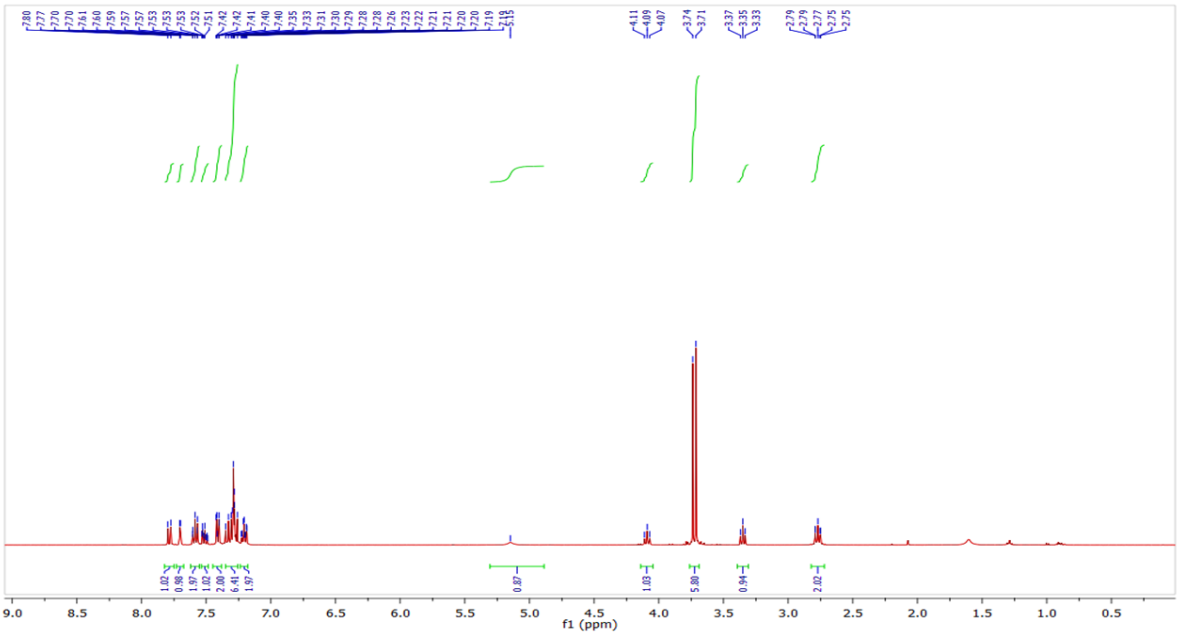

^{13}C {^{1}H} (100MHz, $CDCl_3$) NMR of **3af**

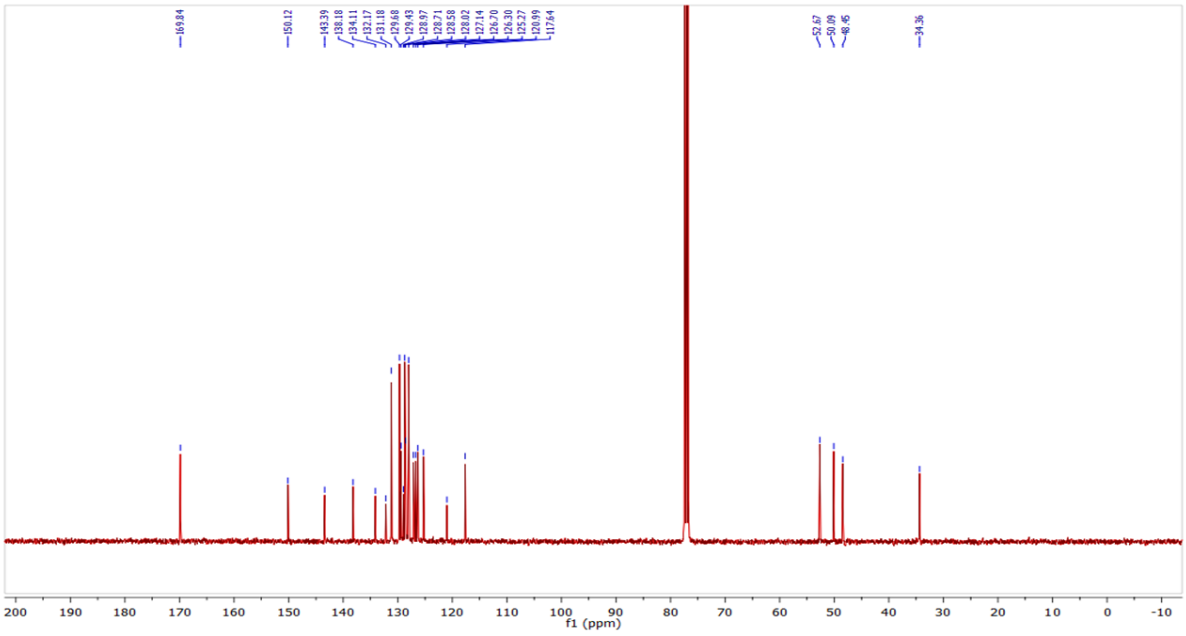

HSQC of **3af**

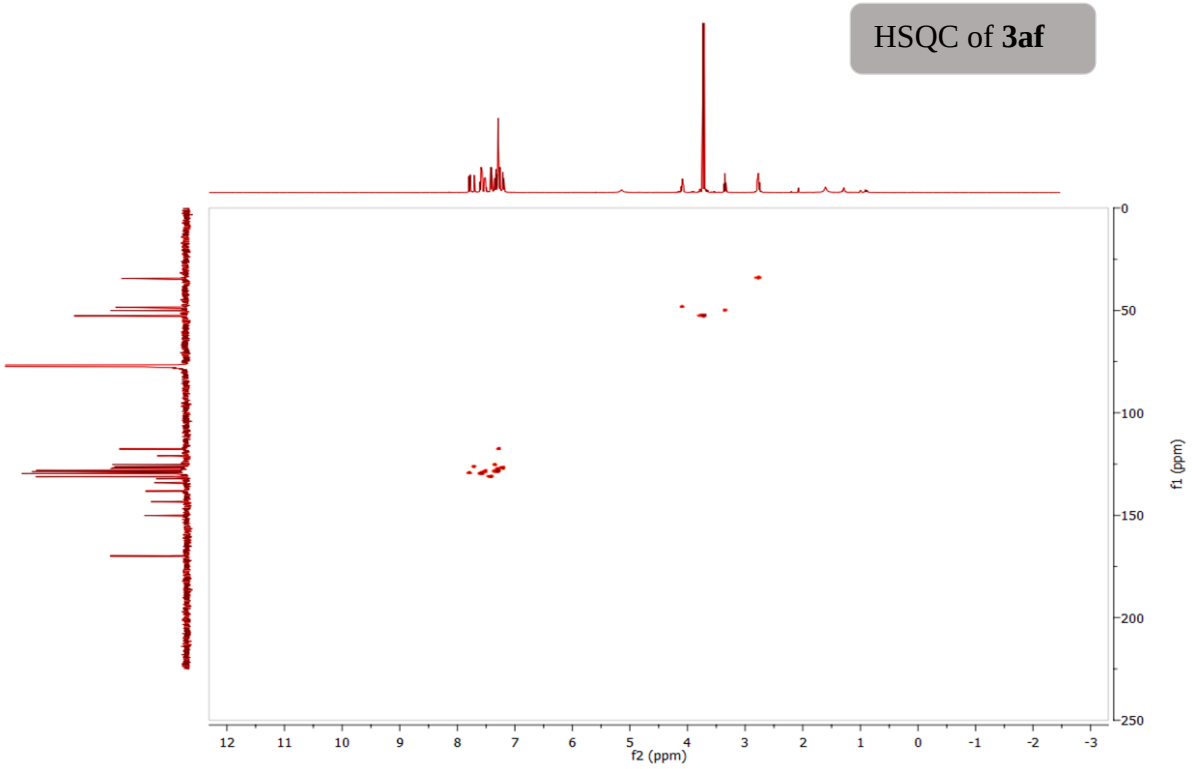

HSQC of **3af** (zoom)

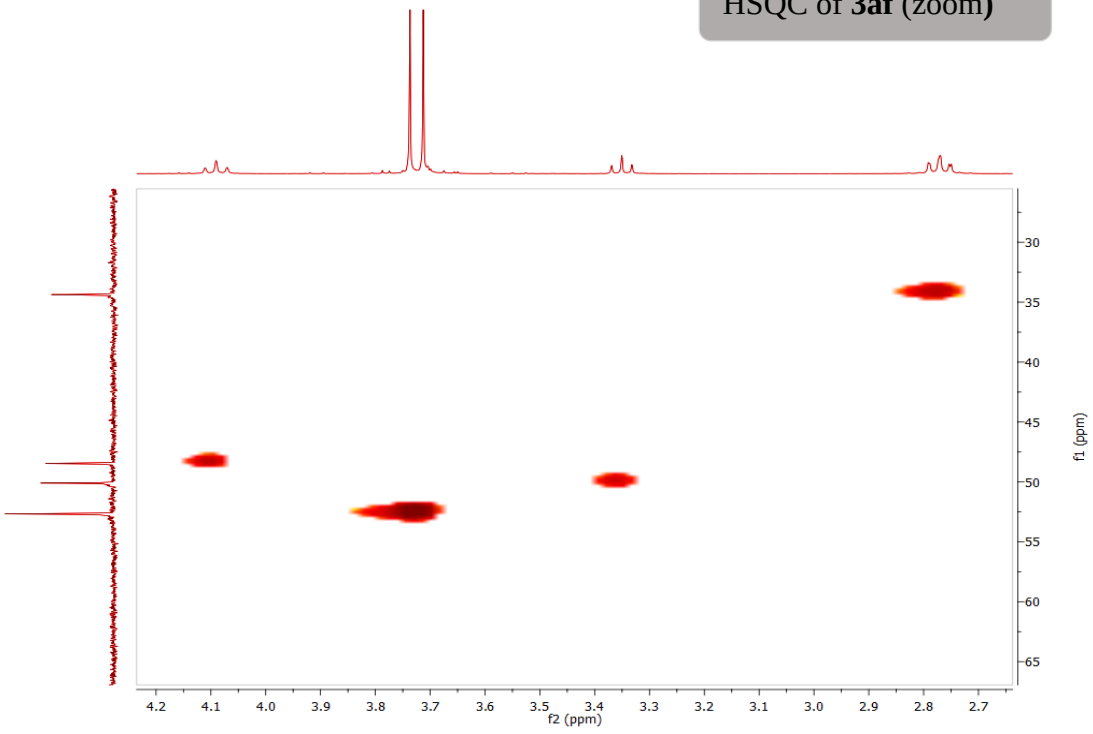

HMBC of **3af**

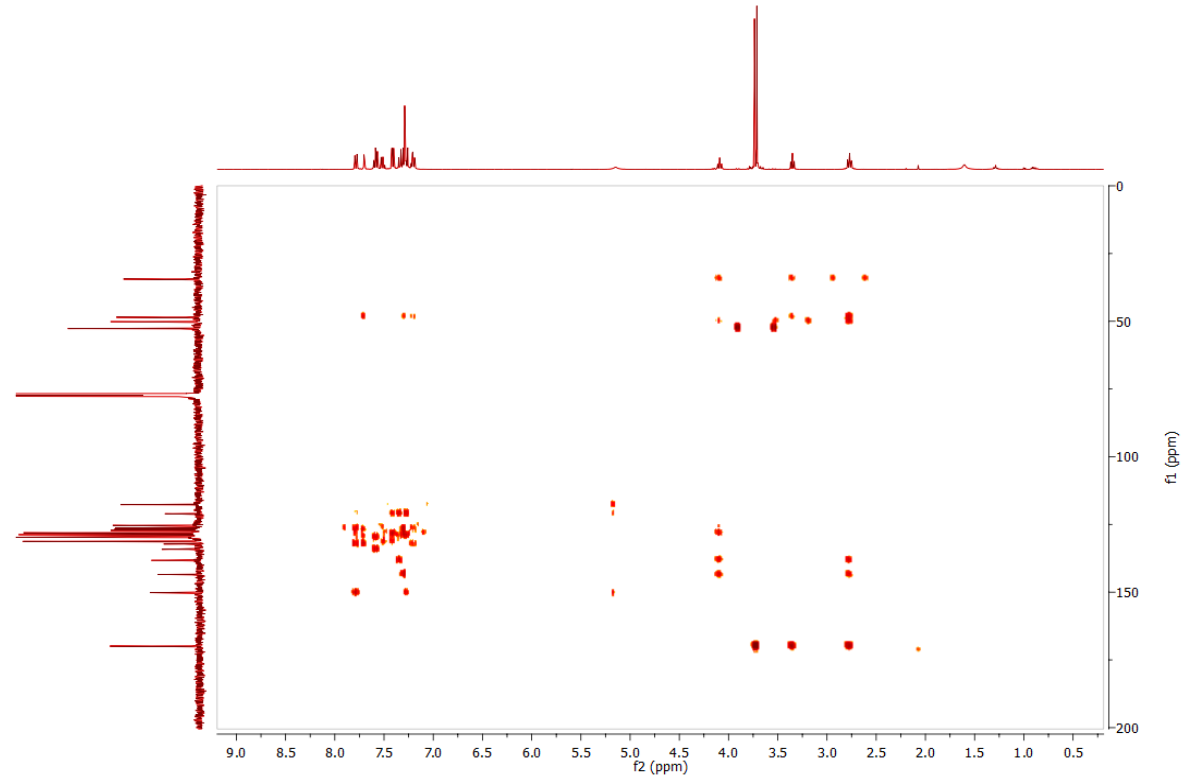

HMBC of **3af** (zoom)

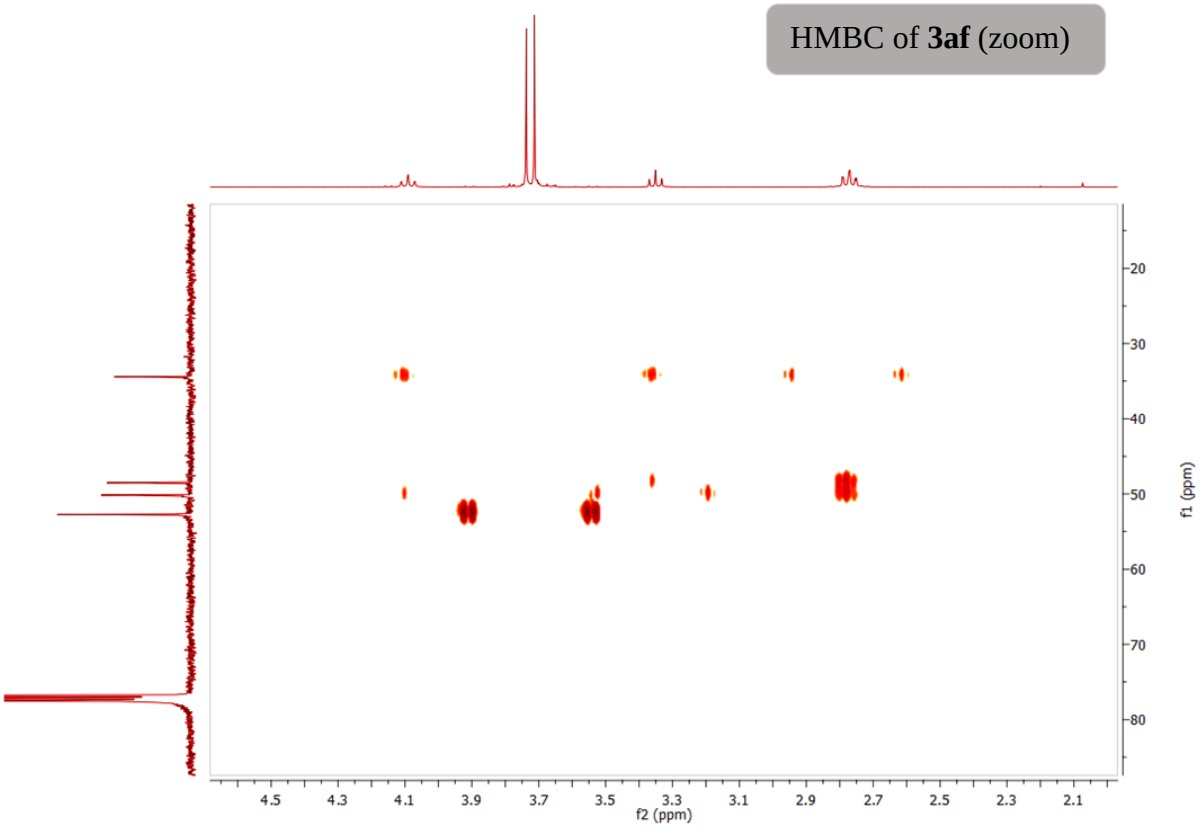

HMBC of **3af** (zoom)

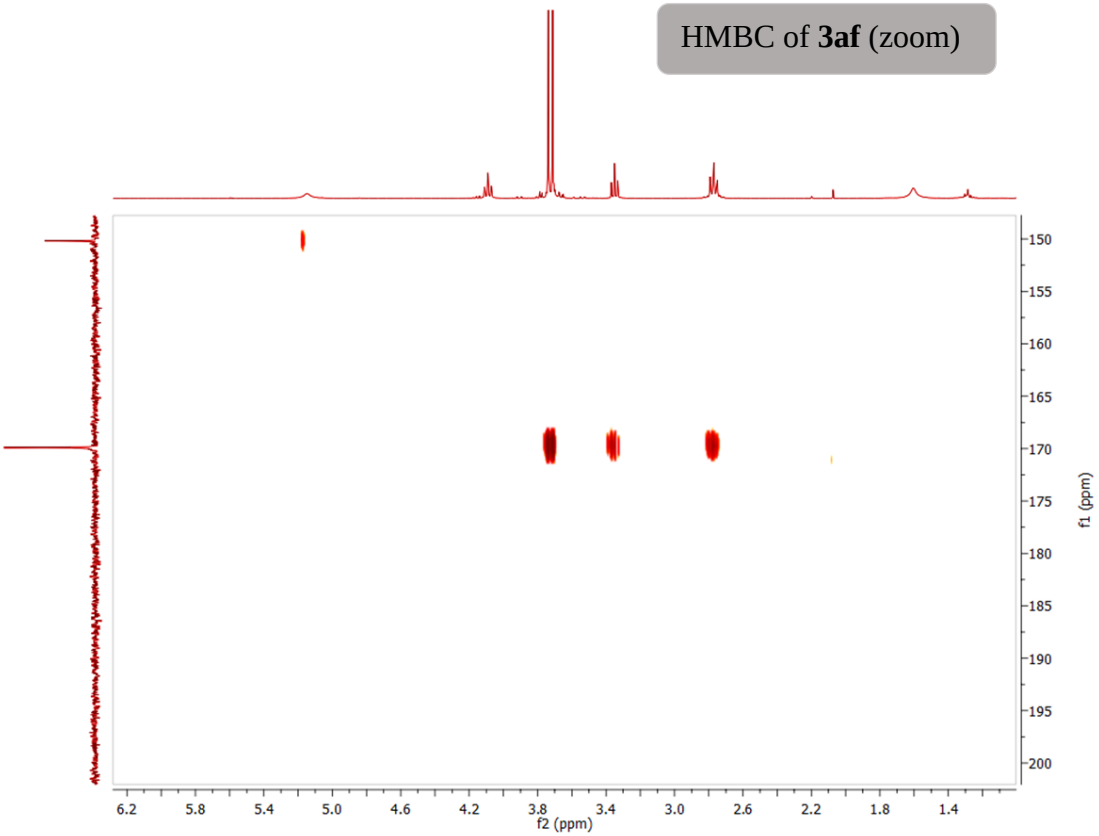

^{1}H (400MHz, $CDCl_3$) NMR of **3ag**

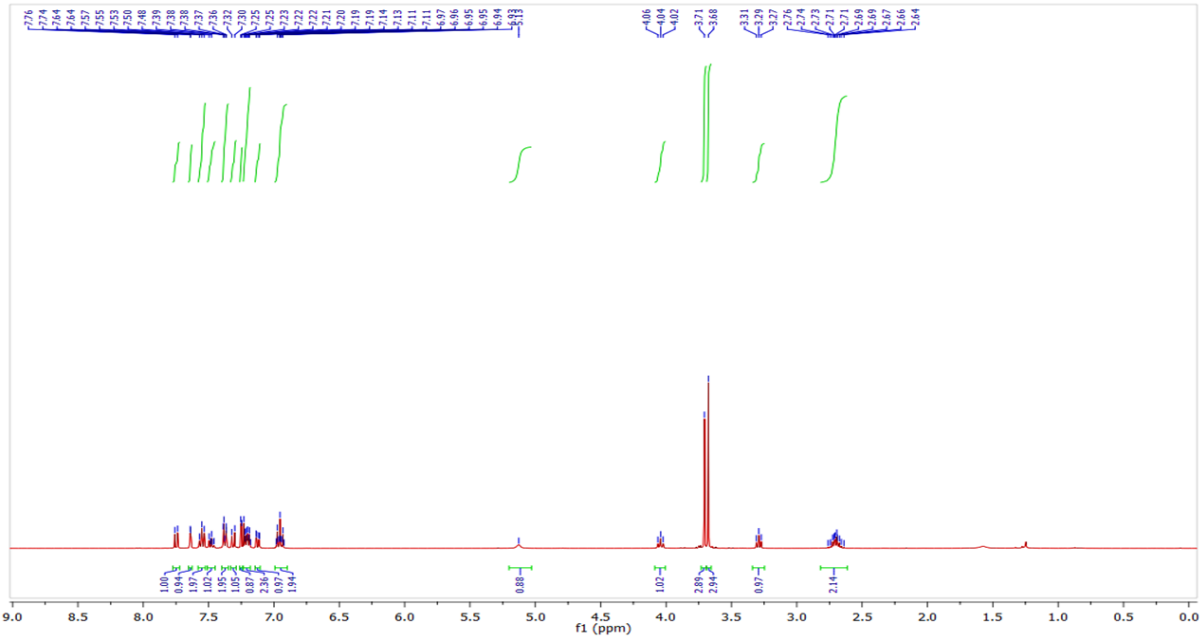

^{13}C {^{1}H} (100MHz, $CDCl_3$) NMR of **3ag**

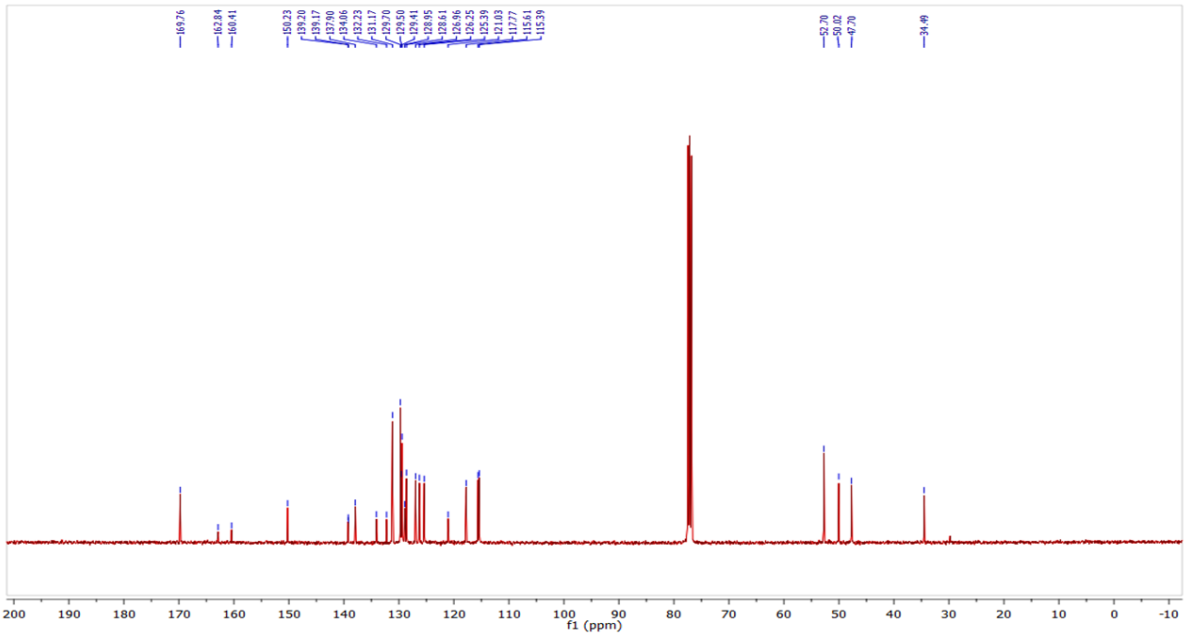

^{19}F (376MHz, $CDCl_3$) NMR of **3ag**

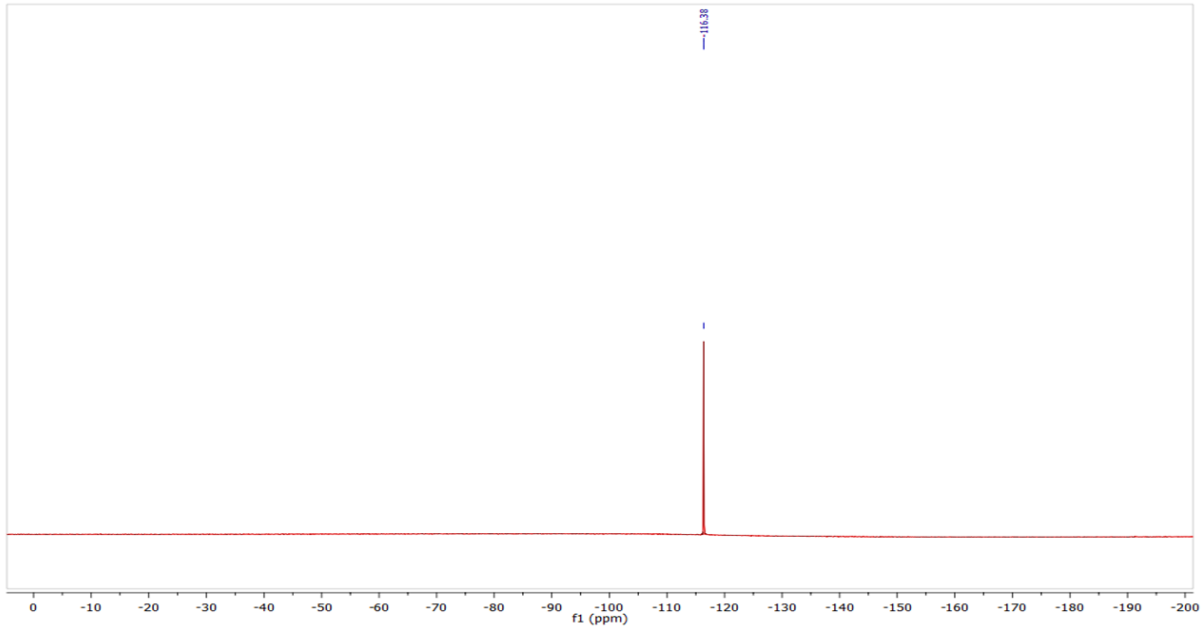

^{1}H (400MHz, $CDCl_3$) NMR of **3ah**

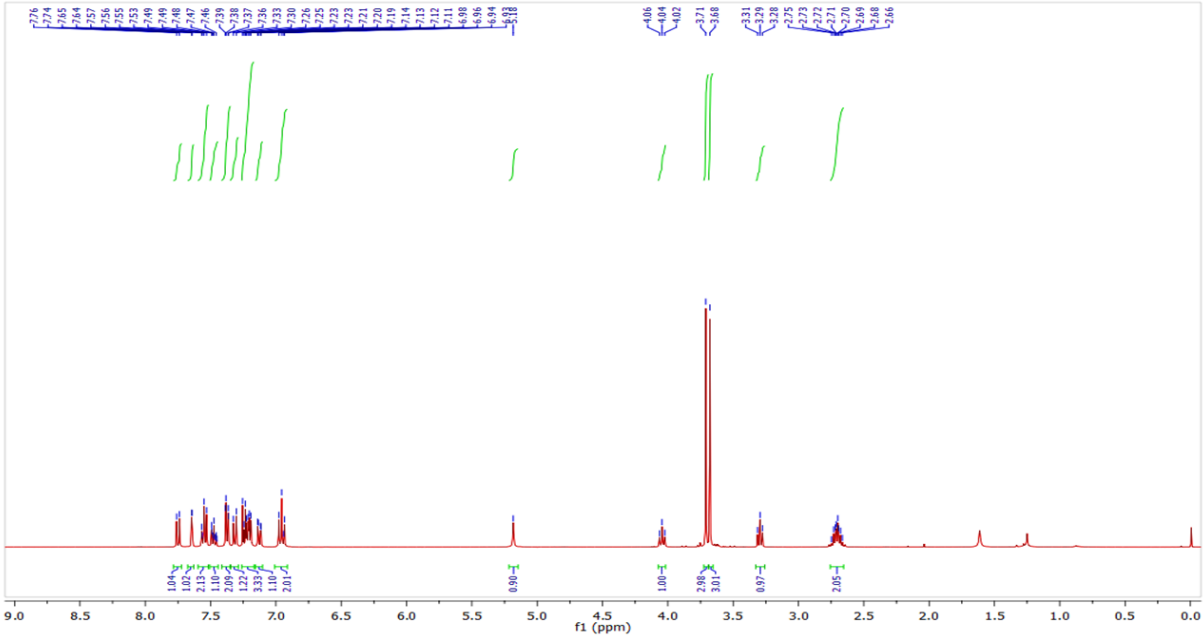

^{13}C {^{1}H} (100MHz, $CDCl_3$) NMR of **3ah**

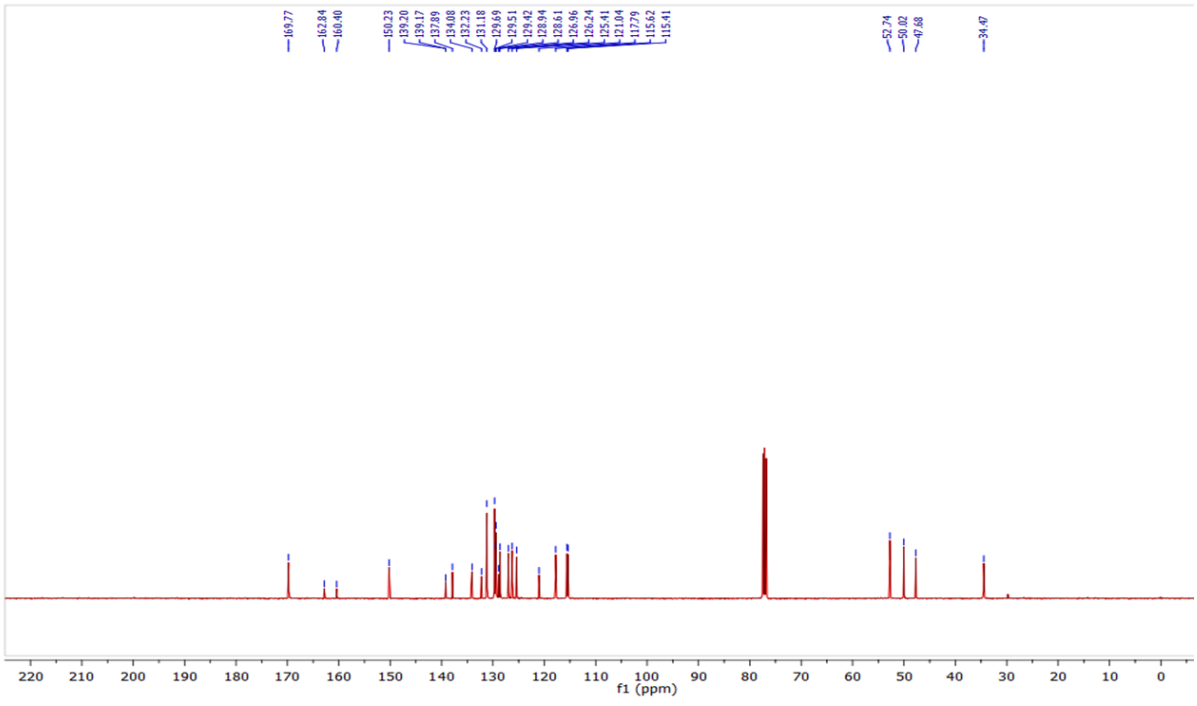

^{1}H (400MHz, $CDCl_3$) NMR of **3ai**

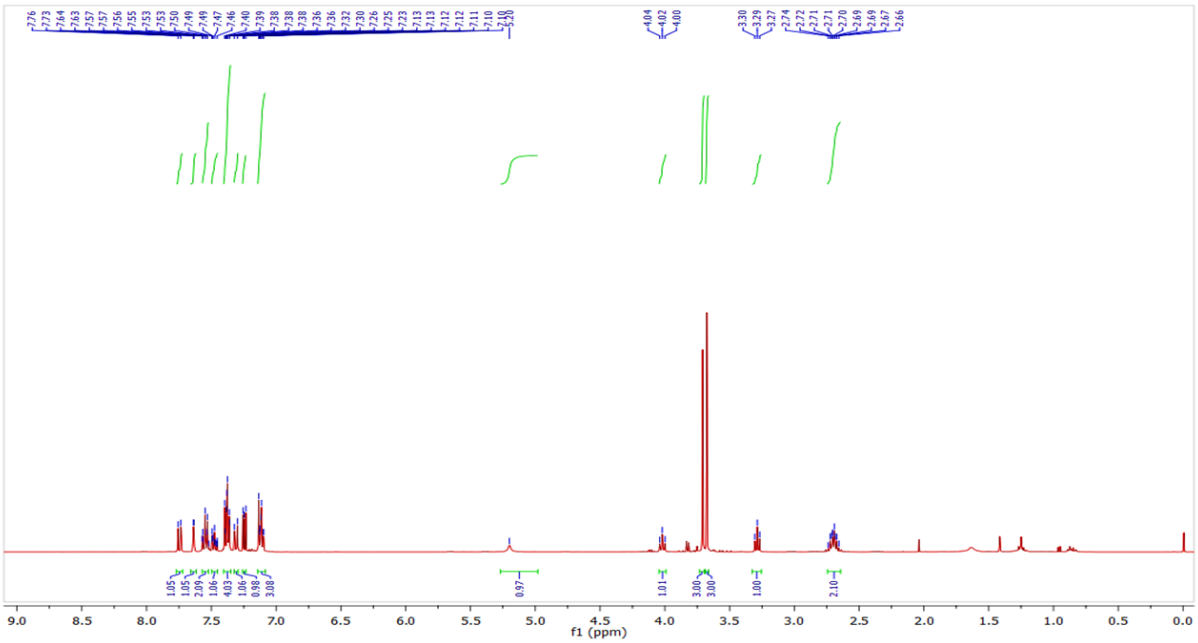

^{13}C {^{1}H} (100MHz, $CDCl_3$) NMR of **3ai**

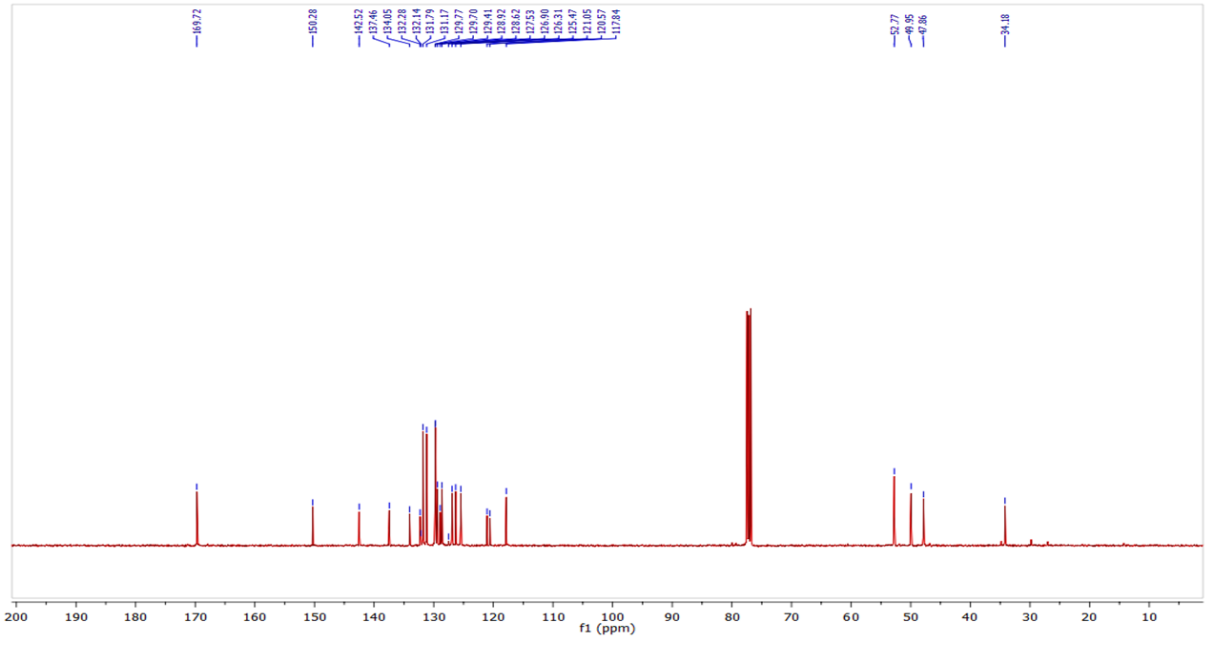

^{1}H (400MHz, $CDCl_3$) NMR of **3aj**

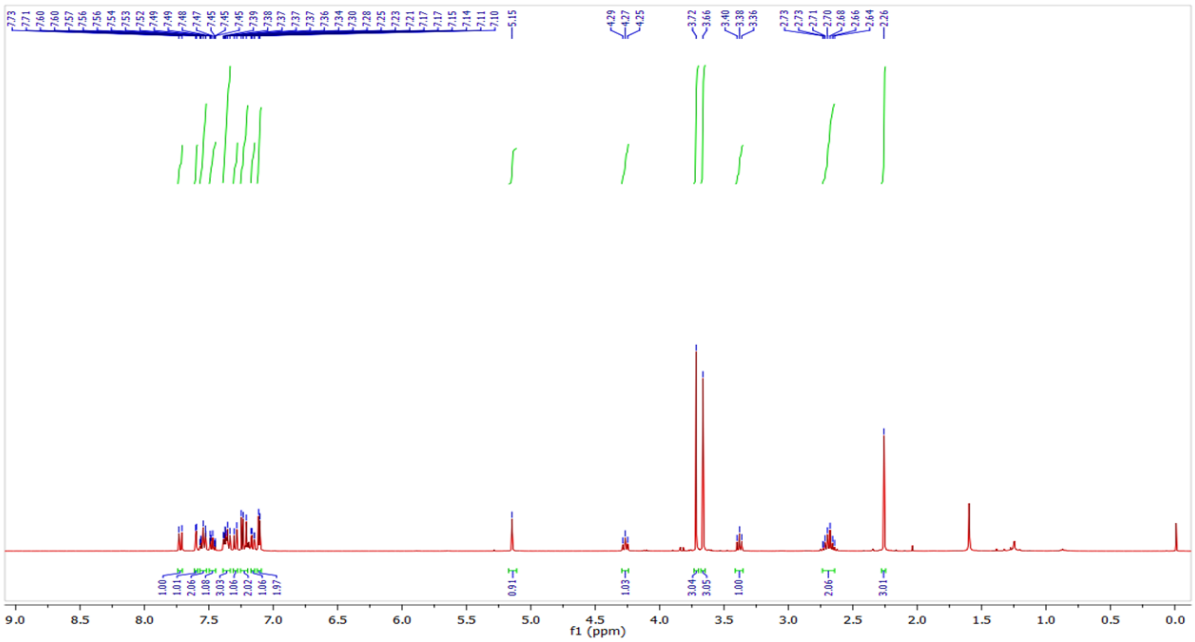

^{13}C {^{1}H} (100MHz, $CDCl_3$) NMR of **3aj**

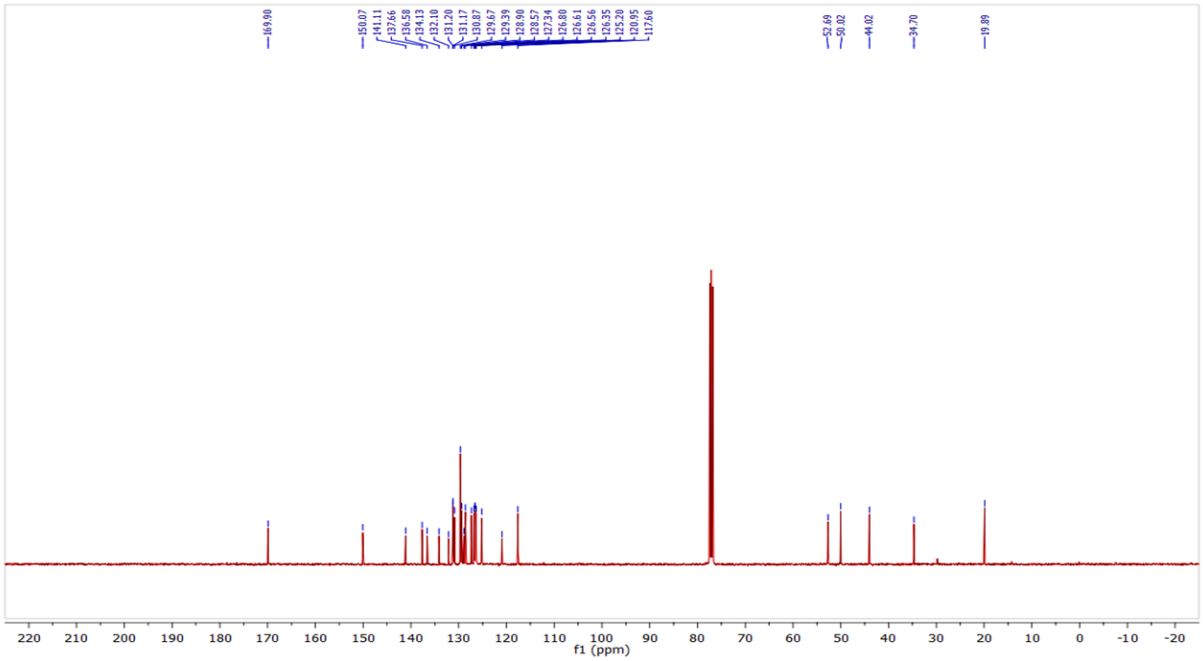

^{1}H (400MHz, $CDCl_3$) NMR of **3ak**

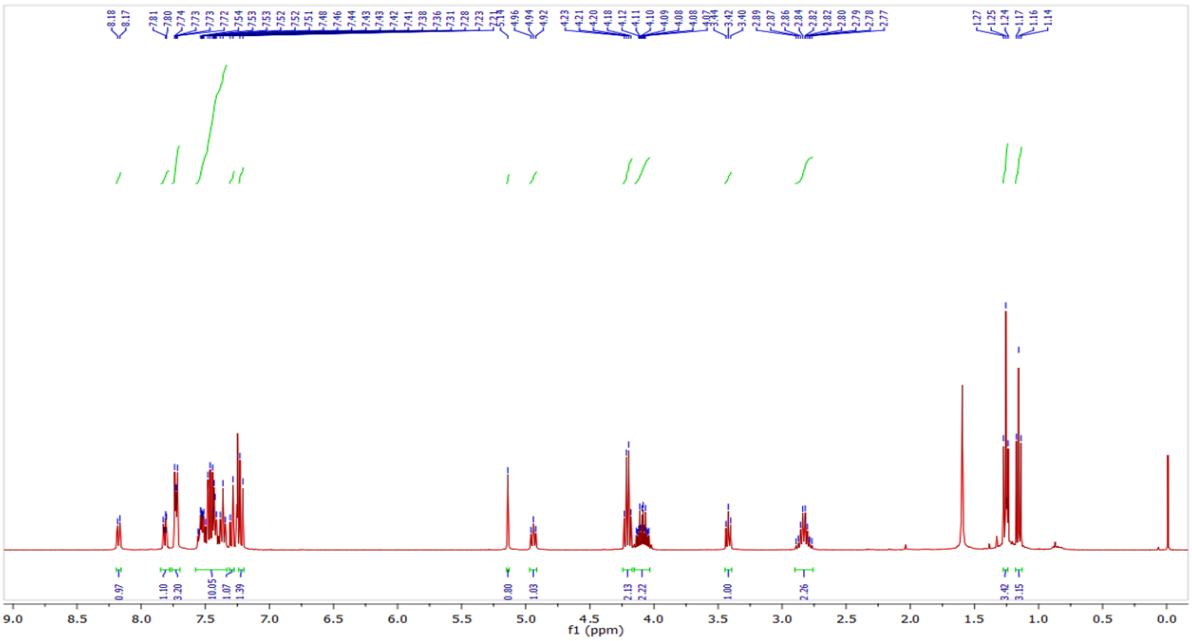

^{13}C {^{1}H} (100MHz, $CDCl_3$) NMR of **3ak**

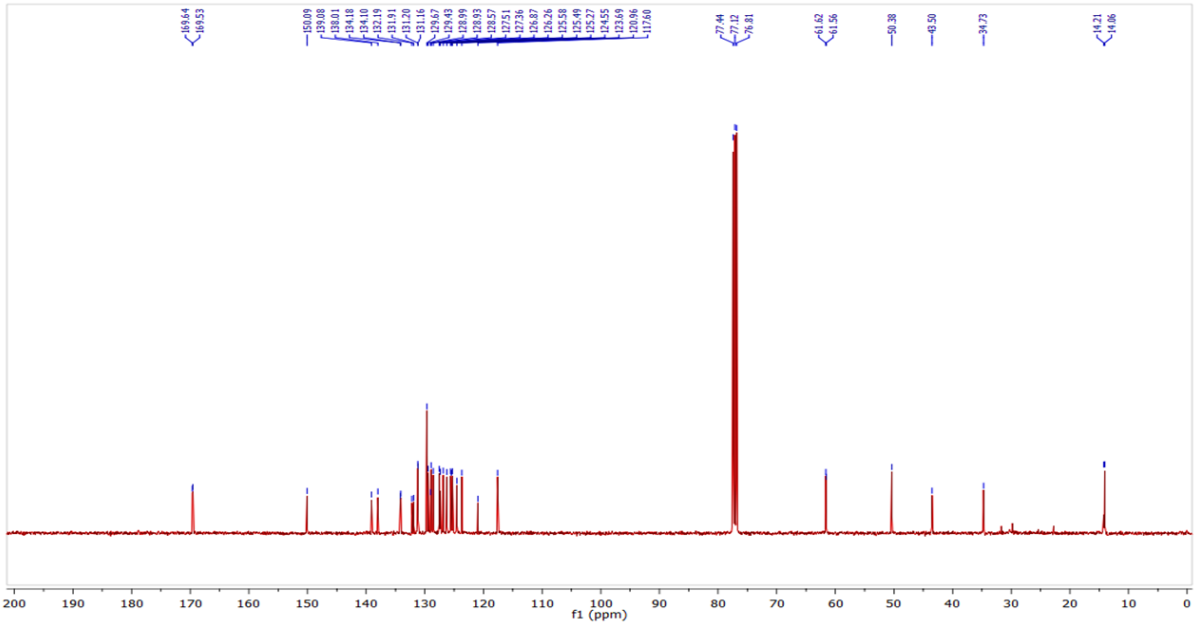

^{1}H (400MHz, $CDCl_3$) NMR of **3al**

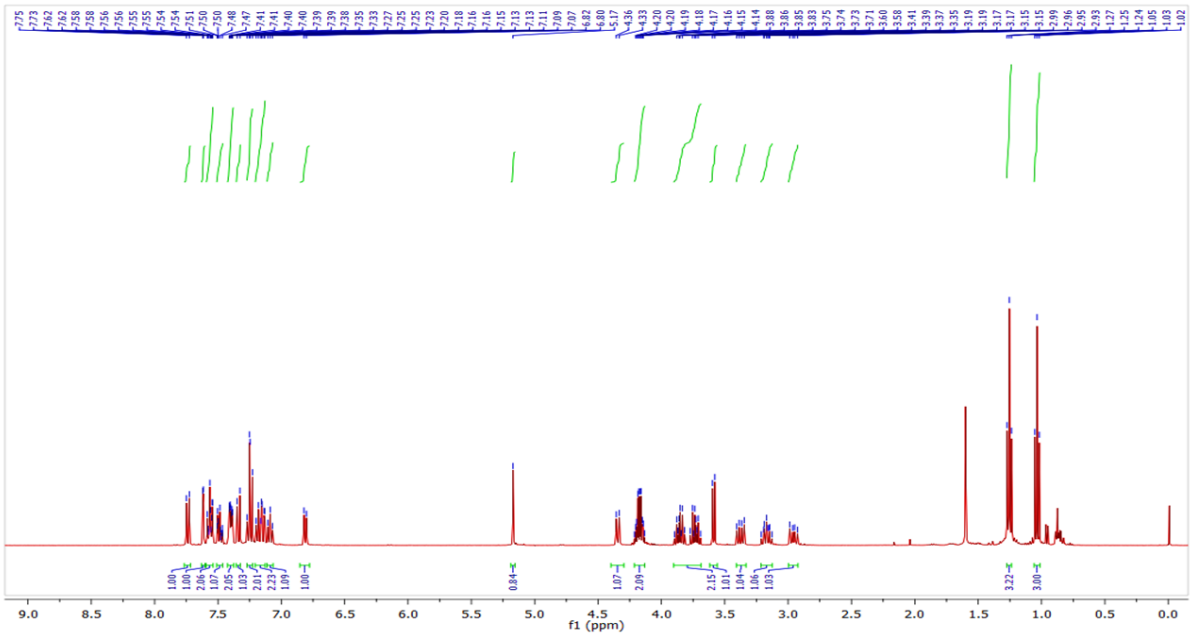

^{13}C {^{1}H} (100MHz, $CDCl_3$) NMR of **3al**

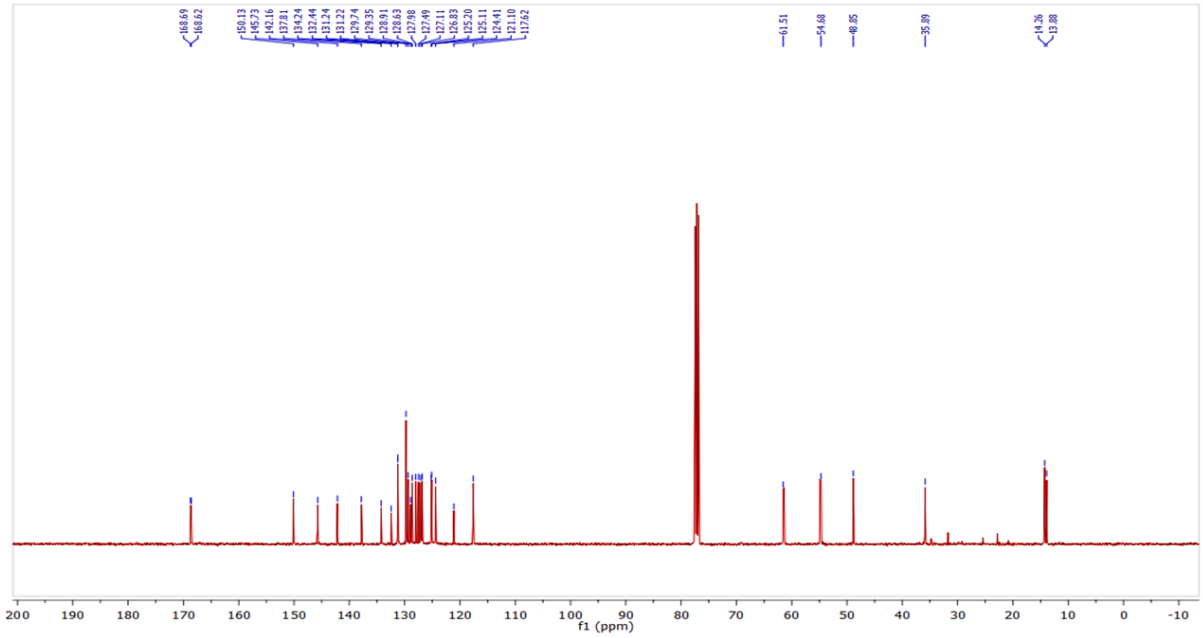

^{1}H (400MHz, $CDCl_3$) NMR of **3am**

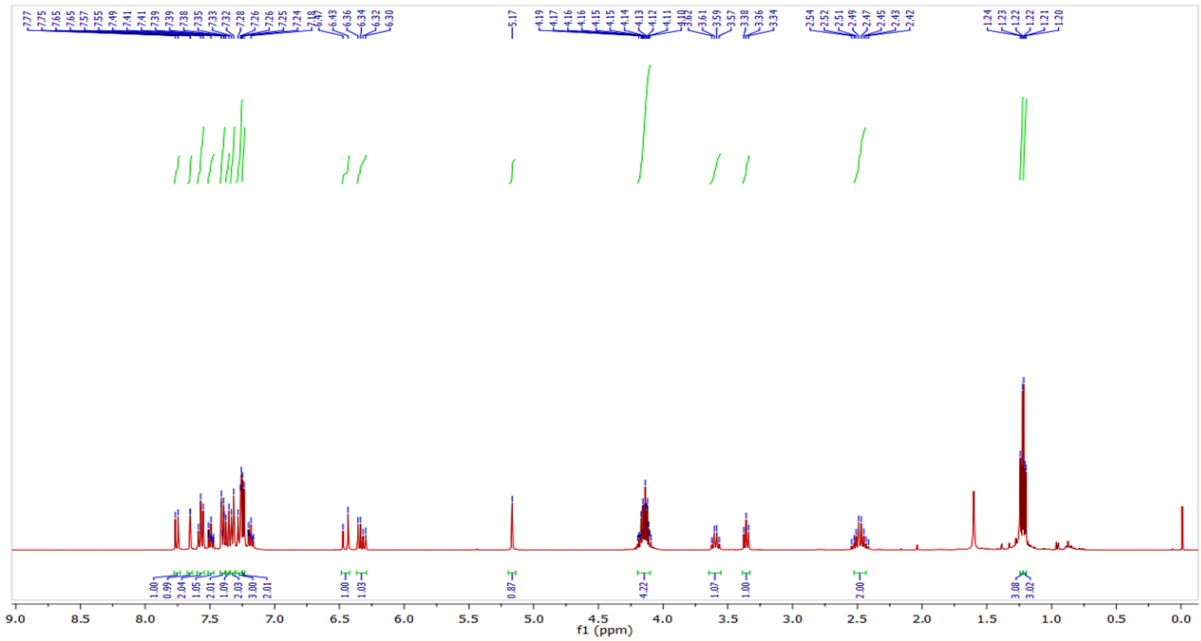

^{13}C {^{1}H} (100MHz, $CDCl_3$) NMR of **3am**

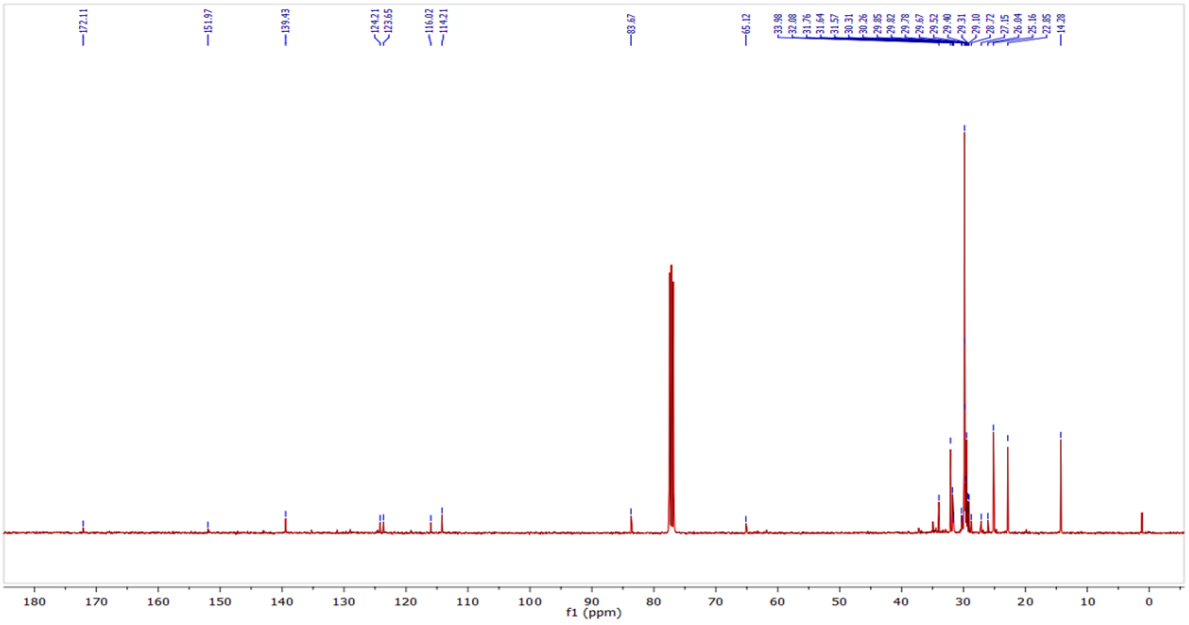

^{1}H (400MHz, $CDCl_3$) NMR of **3an**

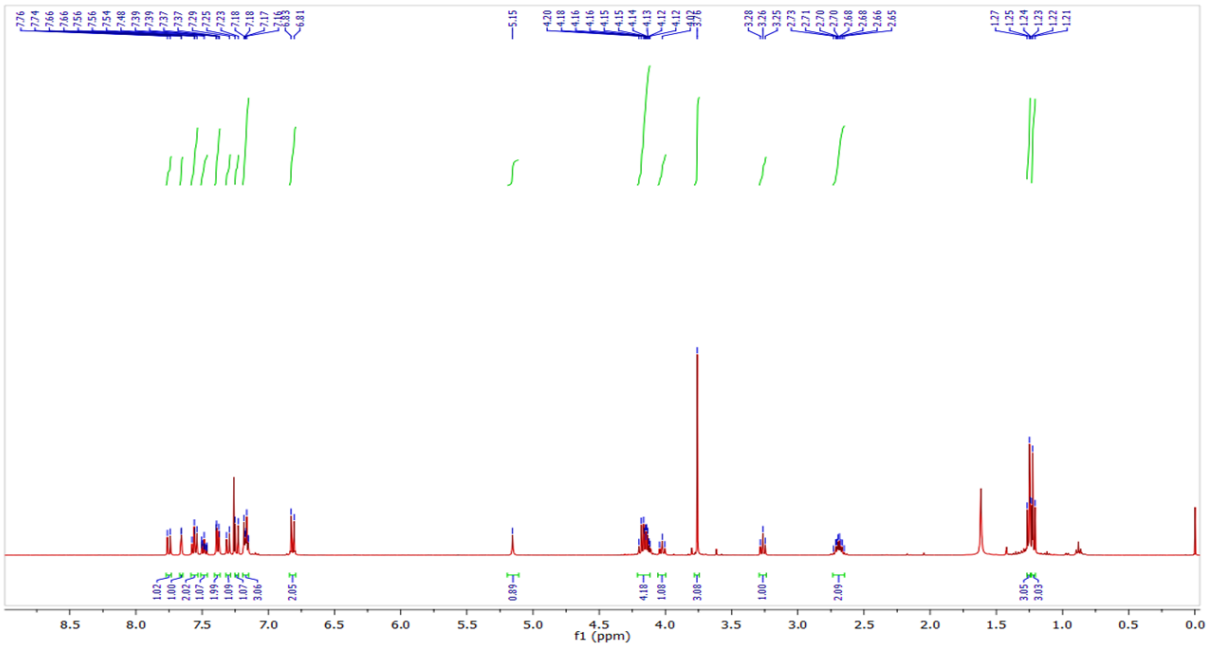

^{13}C {^{1}H} (100MHz, $CDCl_3$) NMR of **3an**

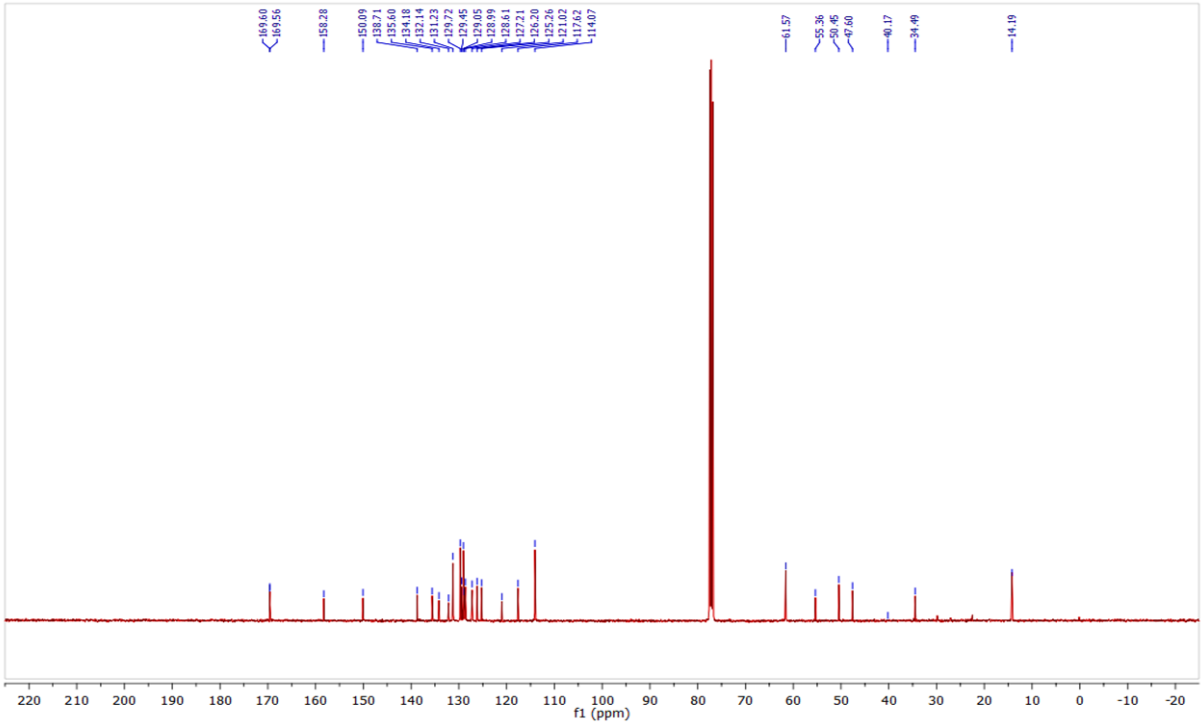

^{1}H (400MHz, $CDCl_3$) NMR of **3ao**

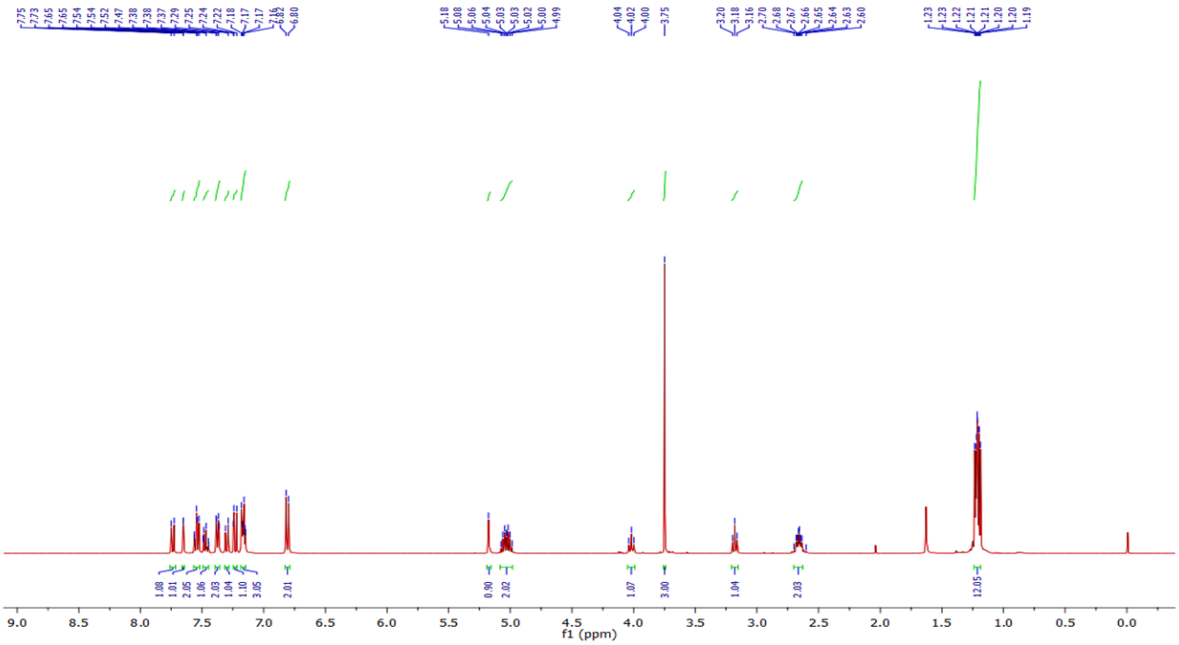

^{13}C {^{1}H} (100MHz, $CDCl_3$) NMR of **3ao**

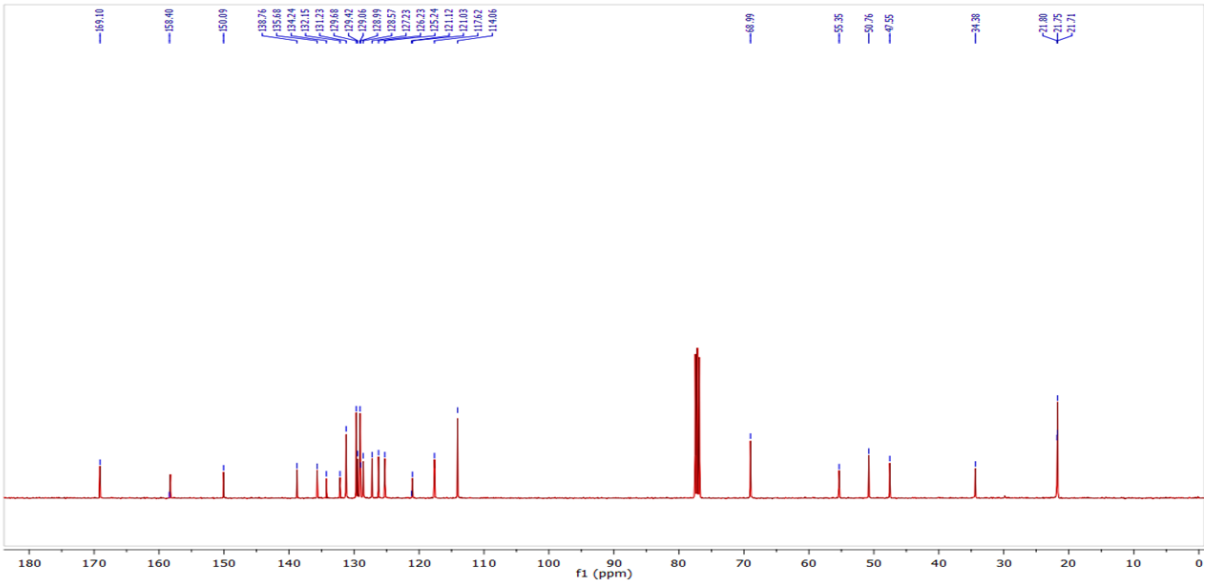

^{1}H (400MHz, $CDCl_3$) NMR of **4a**

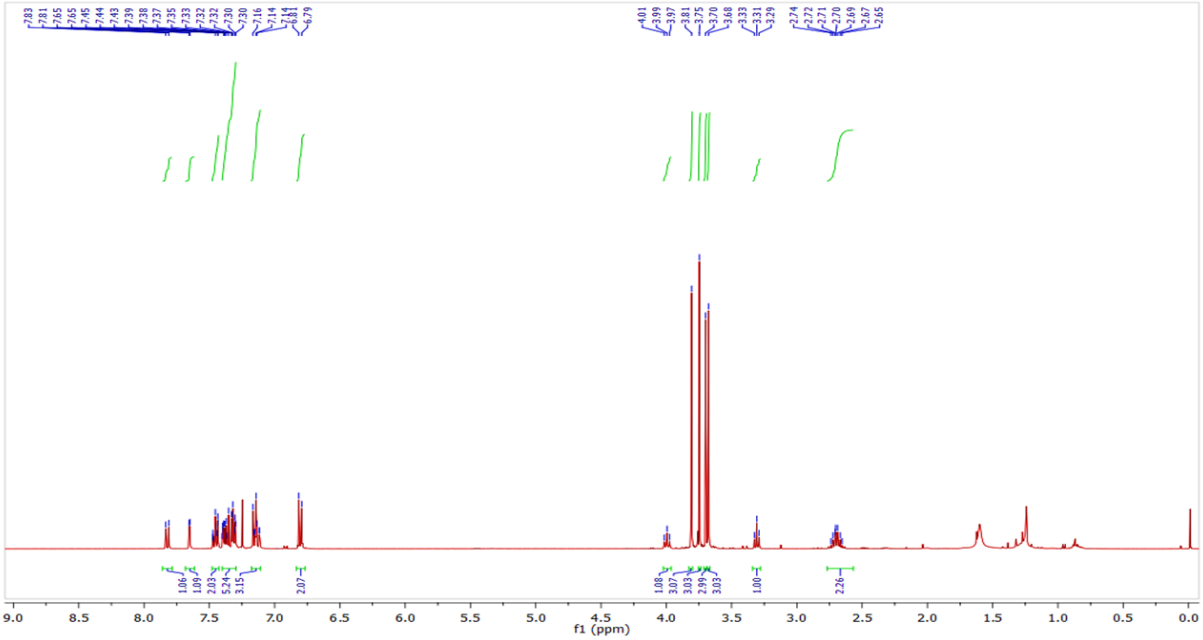

^{13}C {^{1}H} (100MHz, $CDCl_3$) NMR of **4a**

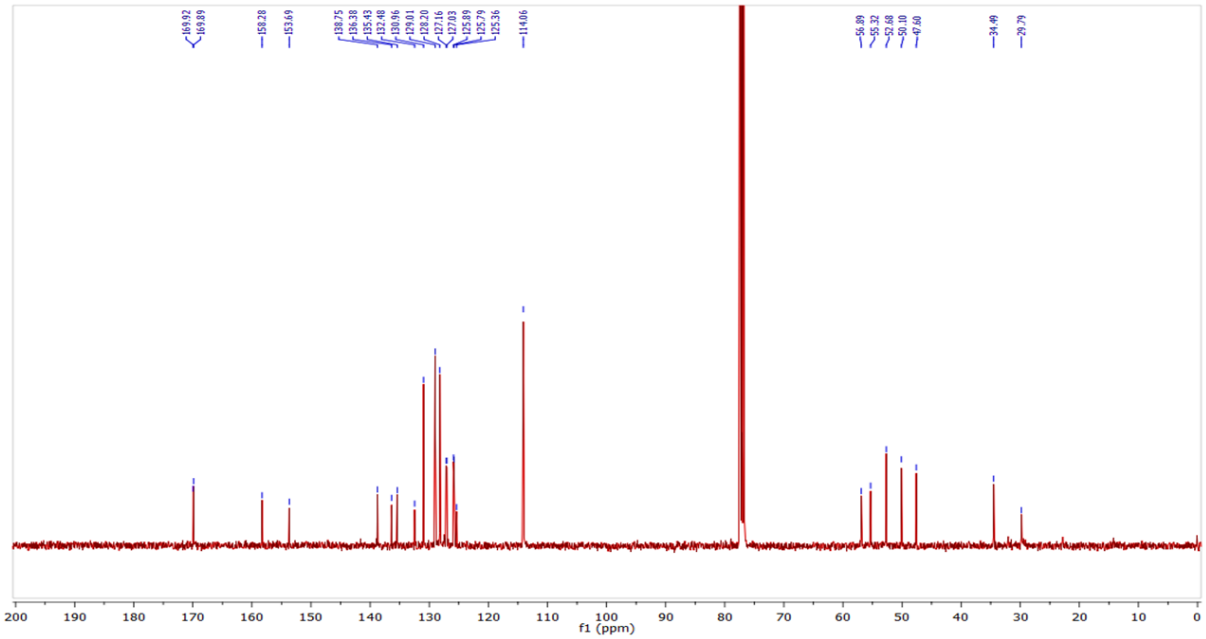

^{1}H (400MHz, $CDCl_3$) NMR of **5a**

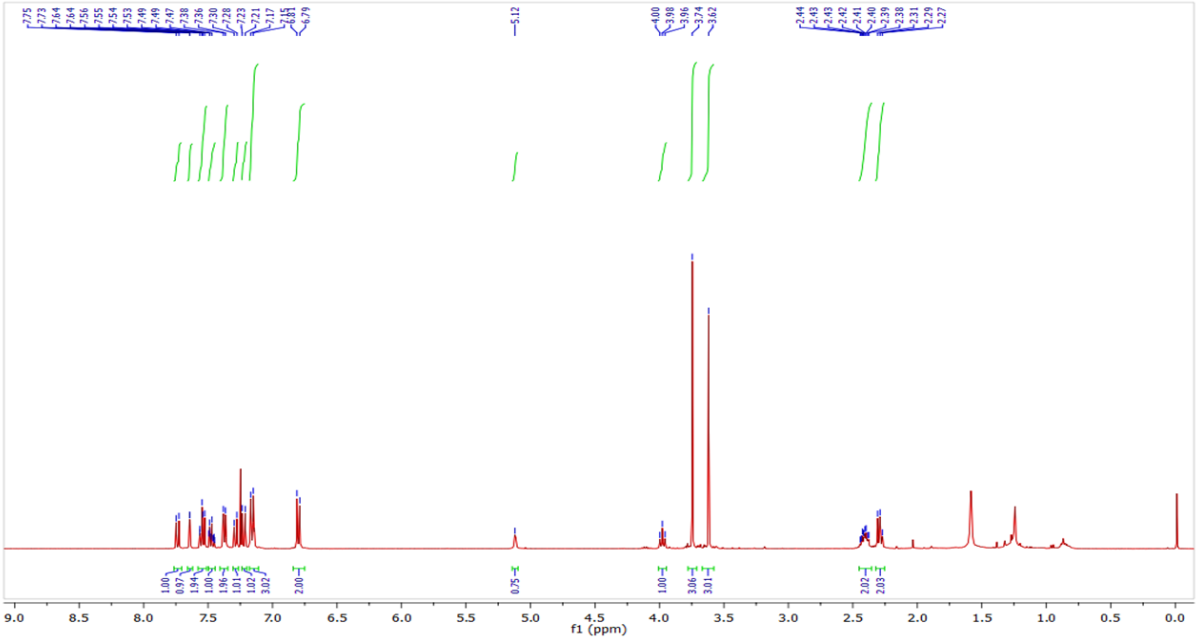

^{13}C {^{1}H} (100MHz, $CDCl_3$) NMR of **5a**

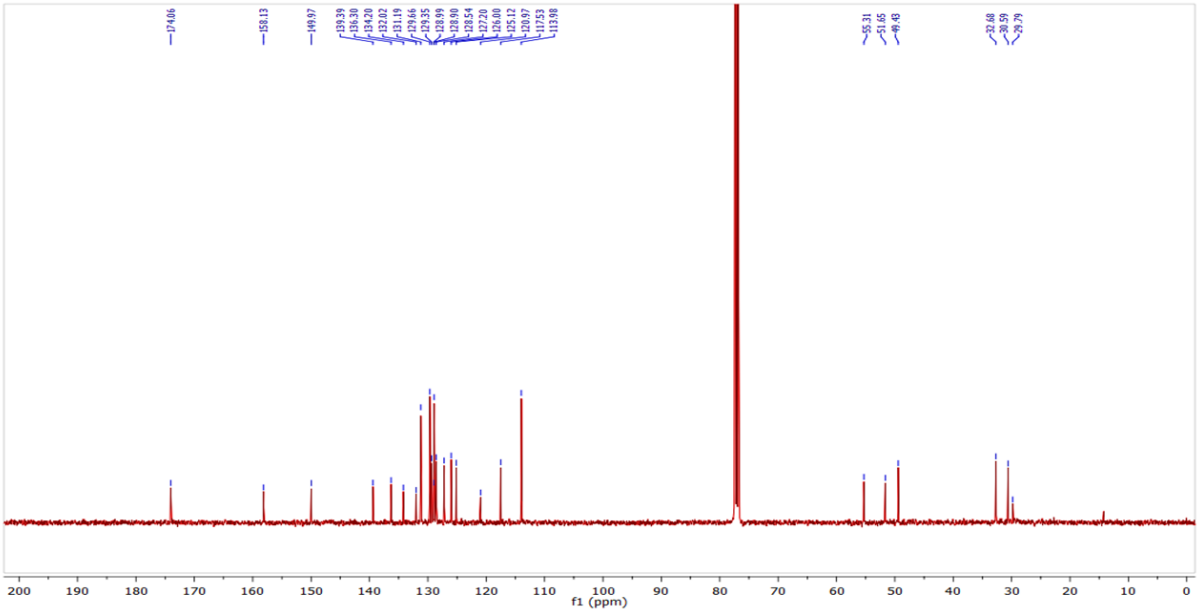

^{1}H (400MHz, $CDCl_3$) NMR of **IV**

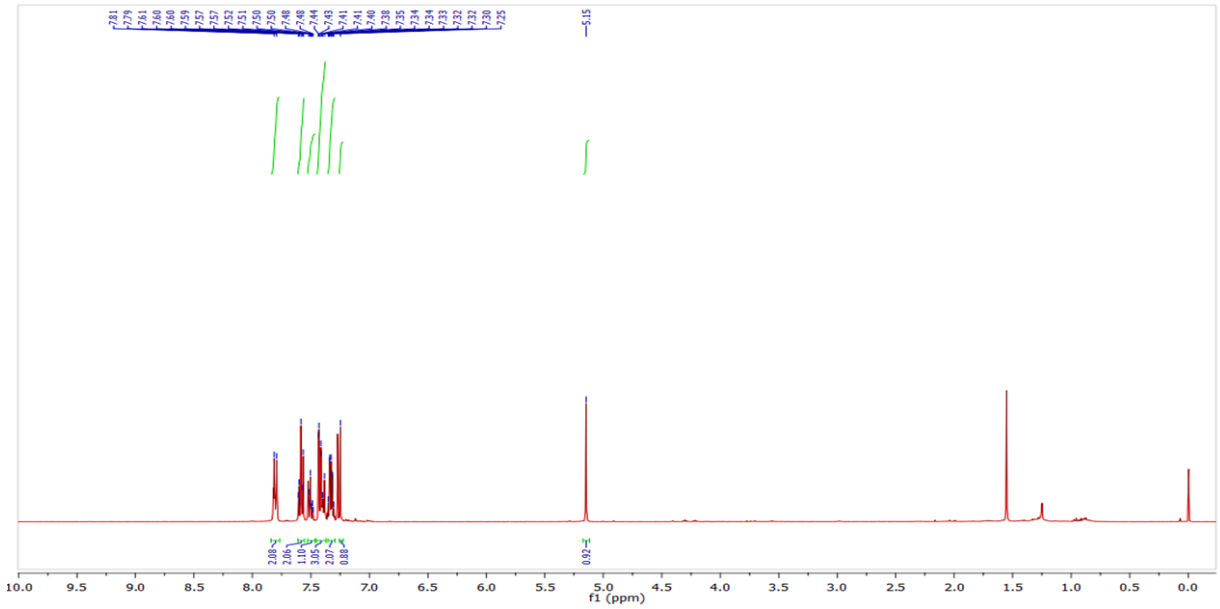

Chapter 4

Brønsted Acid Catalyzed Cascade Ring-Opening/Cyclization of 3-Ethoxy Cyclobutanones to Access 2,8-Dioxabicyclo[3.3.1]nonane Derivatives

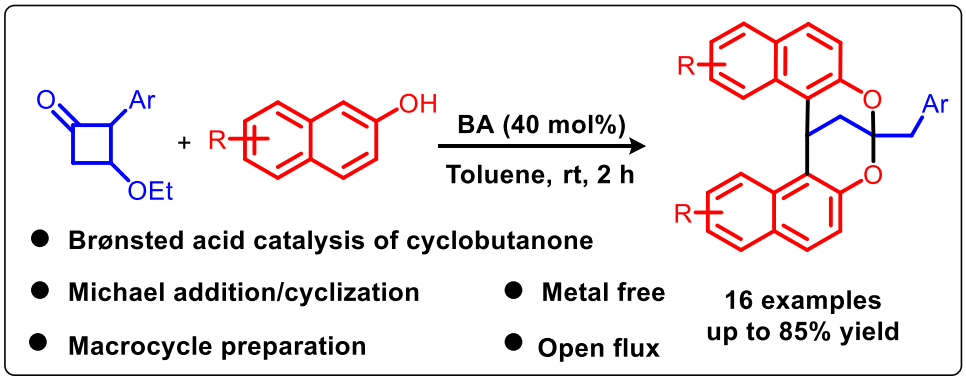

This work was published in *The Journal of Organic Chemistry* (A journal of the *American Chemical Society*). Please see the citation "Hazra, A.; Kanji, T.; Ghosh, A.; Yadav, N.; Banerjee, P. *J. Org. Chem.* **2024**, *89*, 8458−8467."

4.1. Introduction

The development of new methodologies to architect complex heterocyclic frameworks through small molecule activation has always fascinated the synthetic community.[1] Out of numerous heterocycles embedded with two oxygen atoms, 2,8-dioxabicyclo[3.3.1]nonanes gathered significant attraction as these types of bicyclic moieties constitute several flavonoid compounds that serve as important drugs like procyanidin A1, dracoflavan C, dracoflavan D, ephedrannin B, and diinsinin which shows crucial biological activities like antiviral, anti-inflammatory, antioxidant, enzyme inhibition, and anticancer, etc.[2] Moreover, these bicyclic cores are analogs to Tröger's base, which has a rigid V-shaped structure.[3] Various strategies have been engineered in the past few decades for the construction of this rigid diaryl substituted bicyclic ketals. In 1982, Whitesides *et al*. reported the synthesis of dioxabicyclo[3.3.1]-nonene by reacting *β*-naphthol with malonaldehyde tetramethyl acetal in the presence of trifluoroacetic acid (Scheme 4.1.1.a, left).[4] After that, earlier in this century, Mashraqui *et al*. developed a Lewis acid-catalyzed three-component reaction for the formation of [3.3.1]-bicyclic ketal derivatives (Scheme 4.1.1.a, right).[5] Another method of preparing this type of skeleton involves the annulation of flavylium ion with phloroglucinol which was discovered by Jurd *et al*. in the biomimetic synthetic study in 1965[6] (Scheme 4.1.1.b) and further exploited by various other groups[7] also. Other than these, the rest of

Scheme 4.1.1. Previous reports for the synthesis of dioxabicyclo[3.3.1]nonanes

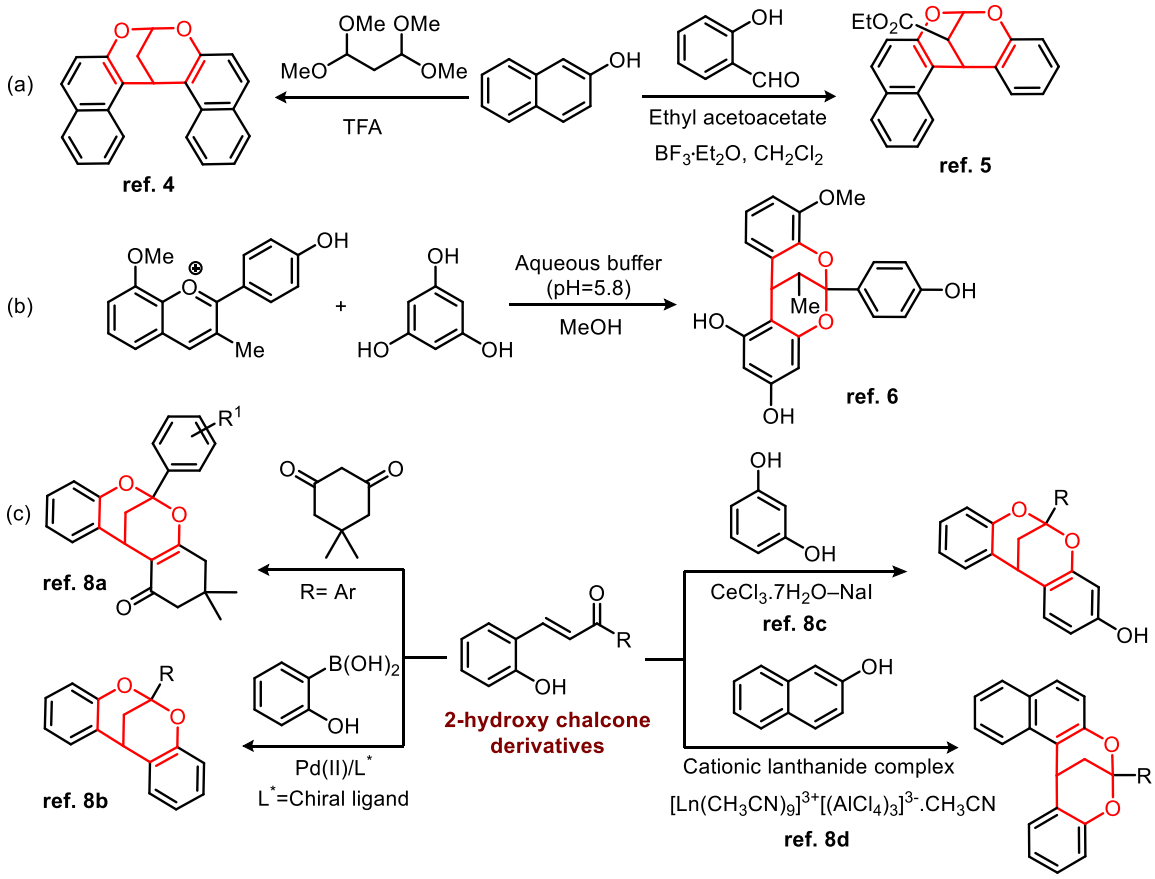

the emethods mostly evolved around a similar precursor, i.e., 2-hydroxy chalcones with different other reacting partners (Scheme 4.1.1.c).[8] So, developing new methodologies for constructing these diaryl substituted 2,8-dioxabicyclo[3.3.1]nonanes remains highly desirable.

Scheme 4.1.2. Brønsted acid-catalyzed reactions of 3-donor cyclobutanones

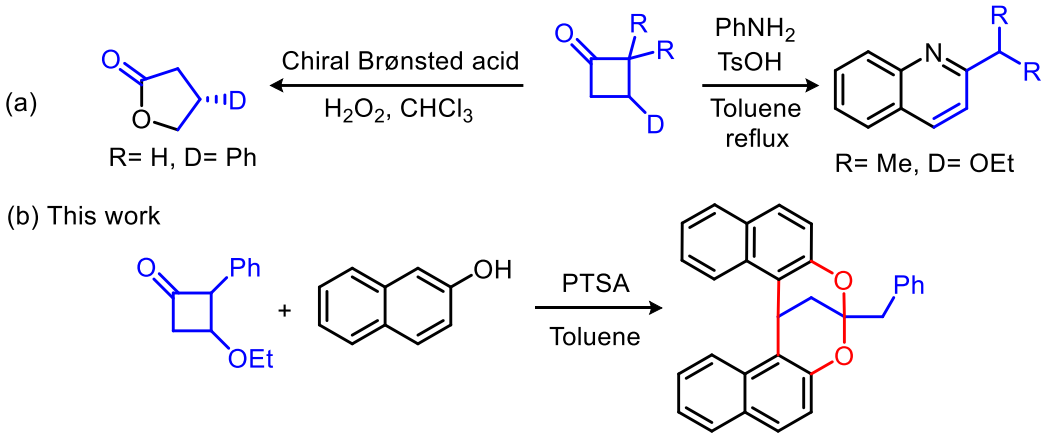

Over the years, small carbocycles have captured considerable recognition for their unique reactivity to undergo various organic transformations via strain release and have been utilized to construct numerous biologically important frameworks.[1a, 1b] 3-Donor cyclobutanones remain distinguished among the four-membered carbocycles for their unique reactivity.[1b,9] This particular cyclobutanone can undergo a regioselective cleavage of C2-C3 bond in the presence of Lewis acid to generate a 1,4-zwitterionic intermediate[9] which lead to a variety of ring-opening, rearrangement, and cycloaddition reactions.[10] Though most of these reactions were performed under Lewis acid catalysis,[10] activation of these four-membered synthons via Brønsted acid (BA) catalysis is still scarce. In 1965, Meen *et al*. reported a reaction of 3-ethoxy-2,2-dimethylcyclobutanone with aniline, which transformed into the corresponding N-phenyl imine at first, followed by the rearrangement to form 2- isopropylisoquioline in the presence of a catalytic amount of *p*-TsOH (Scheme 4.1.2.a, right).[11] Later, in 2008, Ding *et al*. demonstrated a chiral BA-catalyzed enantioselective Baeyer-Villiger oxidation of 3-substituted cyclobutanones to furnish γ-lactones with excellent enantioselectivities (Scheme 4.1.2.a, left).[12] However, to the best of our knowledge, no reports were found on BA-catalyzed direct ring-opening or cyclization with these types of 3-ethoxy cyclobutanones. So, we envisioned that Brønsted acid could effectively activate the 3-ethoxy cyclobutanones to undergo a ring-opening followed by a cyclization reaction with naphthol derivatives to furnish oxygen-containing heterocyclic scaffolds. Herein, we report a Brønsted acid-catalyzed cascade ring-opening/cyclization of 3-ethoxy 2-substituted cyclobutanones with naphthols for the formation of 2,8-dioxabicyclo[3.3.1]nonane derivatives (Scheme 4.1.2.b).

4.2. Result and Discussion

We commenced our reaction by taking 3-ethoxy 2-phenyl cyclobutanone **1a** and 2-naphthol **2a** as model substrates to achieve the optimization conditions (Table 4.2.1). The present study started with 1 equivalent of **1a**, 1 equivalent of **2a,** and 20 mol% of *p*-toluene sulphonic acid (PTSA) and stirred in DCM at room temperature. Delightfully, the desired product **3aa** was obtained with only 32% yield within 2 hours (Entry 1, Table 4.2.1), and the corresponding structure was unambiguously confirmed by single crystal x-ray analysis. Afterward, various other Brønsted acids were screened to improve the yield of the product. While camphorsulphonic acid (CSA) furnished

Table 4.2.1. Optimization of reaction conditions[a]

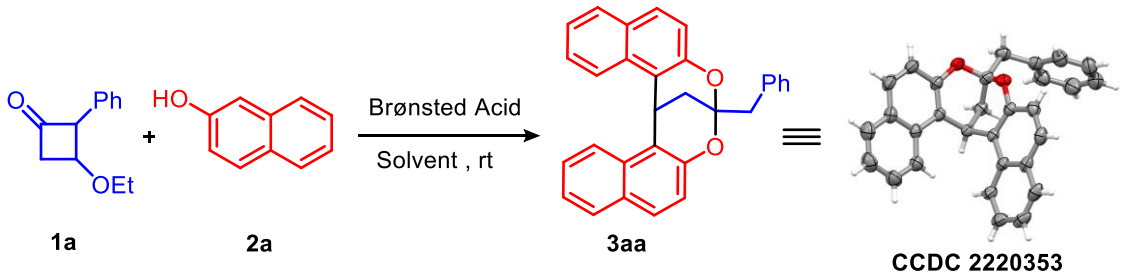

Entry	Brønsted acid	Solvent	Yield (%)[b]
1	PTSA	DCM	32
2	CSA	DCM	28
3	TfOH	DCM	Trace
4	TFA	DCM	N.R.
5	HFIP	DCM	N.R.
6	AcOH	DCM	N.R.
7	BzOH	DCM	N.R.
8[c]	PTSA	DCM	48
9[c]	PTSA	Acetone	51
10[c]	PTSA	Isopropanol	52
11[c]	PTSA	MeCN	10
12[c]	PTSA	THF	Trace
13[c]	PTSA	Toluene	58
14[c]	PTSA	HFIP	N.R.
15[c]	PTSA	EtOH	N.R.
16[c]	PTSA	Toluene:Dioxane (1:1)	N.R.
17[c,d]	**PTSA**	**Toluene**	**72**
18[c,e]	PTSA	Toluene	65

[a]Reaction conditions **1a** (0.15 mmol), **2a** (0.15 mmol), PTSA (0.03 mmol), 1 mL toluene, at room temperature for 2 h, [b]isolated yield, [c]0.30 mmol of **2a** used, [d]0.4 equiv. of PTSA, [e]0.5 equiv. of PTSA.

the product with a similar yield (Entry 2, Table 4.2.1), triflic acid (TfOH) gave only a trace amount of product (Entry 3, Table 4.2.1). However, trifluoroacetic acid (TFA), acetic acid (AcOH), benzoic acid (BzOH), and hexafluoroisopropanol (HFIP) failed to render the desired product (Entries 4-7, Table 4.2.1). As two mole of 2-naphthol were reacting with only one mole of 3-ethoxy cyclobutanone, the reaction was performed with 2 equivalent of 2-naphthol, and expectedly, an

enhancement in the yield was observed (Entry 8, Table 4.2.1). Next, other parameters, like the effect of solvent and catalyst loading, were also checked for this methodology. While slight improvement in the yields was observed with acetone and isopropanol (Entries 9-10, Table 4.2.1), solvents like MeCN and THF provided poor to trace amounts of yield (Entries 11-12, Table 4.2.1). Afterward, when toluene was employed (Entry 13, Table 4.2.1), it rendered the desired product with a satisfactory yield (58%). Noticeably, solvents like ethanol, HFIP, and the mixture of solvent toluene: dioxane (1:1) failed to produce the desired product (Entries 14-16, Table 4.2.1). To our delight, increasing the catalyst loading to 0.4 equivalent furnished the desired product with 72% yield (Entry 17, Table 4.2.1) whereas further increasing the catalyst loading reduces the yield (Entry 18, Table 4.2.1). So, 1 equivalent of **1a** and 2 equivalent of **2a** with 40 mol% of PTSA in toluene at room temperature were chosen as the optimized reaction conditions for this proposed methodology.

Scheme 4.2.1. Substrate scope of 3-ethoxy cyclobutanone[a,b]

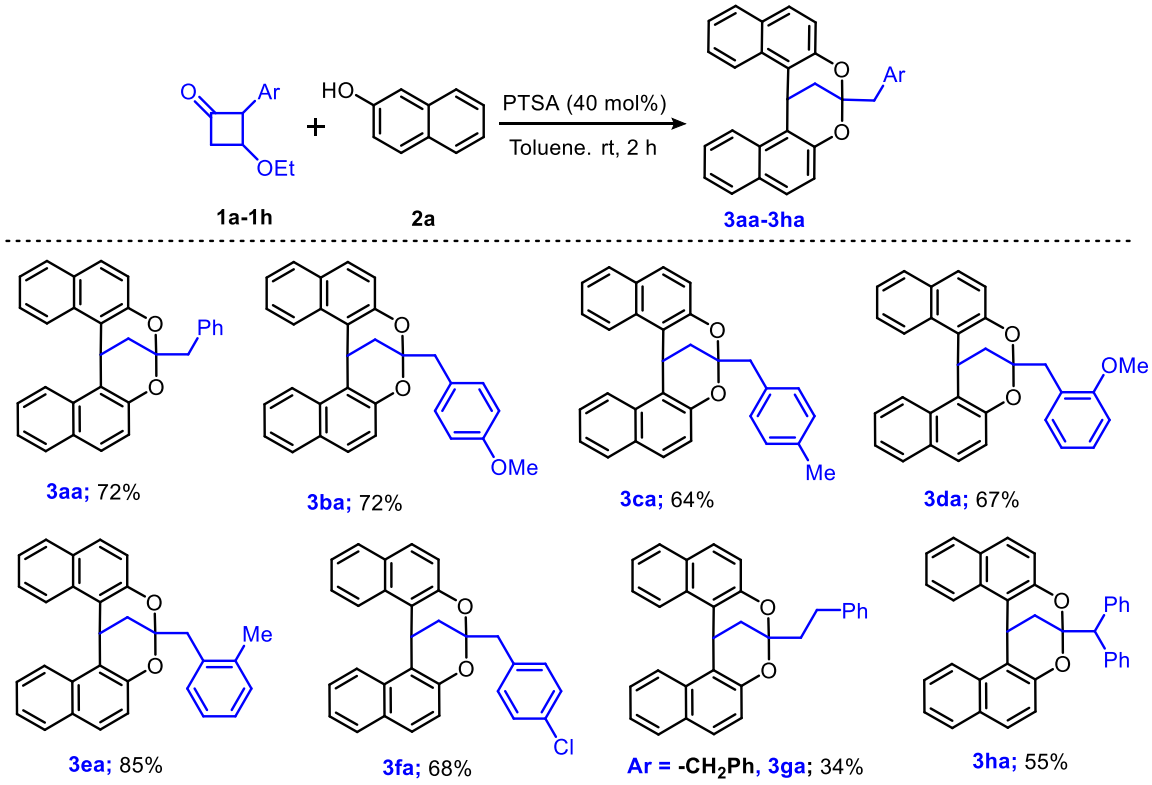

[a]Reaction conditions: **1a** (0.15 mmol), **2a** (0.30 mmol), PTSA (0.06 mmol), 1 mL toluene, at room temperature for 2 h, [b]isolated yield.

After getting the optimized condition in hand, we first started to explore the substrate scope variation of different aryl-substituted 3-ethoxy cyclobutanones (Scheme 4.2.1). Cyclobutanones with electron-rich substituents (methyl, methoxy) at both the *para* and *ortho*-positions of the aryl group (**2b-2e**) rendered the corresponding products (**3ba-3ea**) in good yields. Then, halogen-substituted (*para* chloro) cyclobutanone **1f** was also screened which furnished the desired product

3fa in 68% yield. However, benzyl-substituted cyclobutanone delivered the product **3ga** with a compromising yield, whereas diphenyl-substituted cyclobutanones **1h** tolerated the reaction well to give the corresponding product **3ha** a satisfactory yield.

Scheme 4.2.2. Substrate scope of naphthols[a,b]

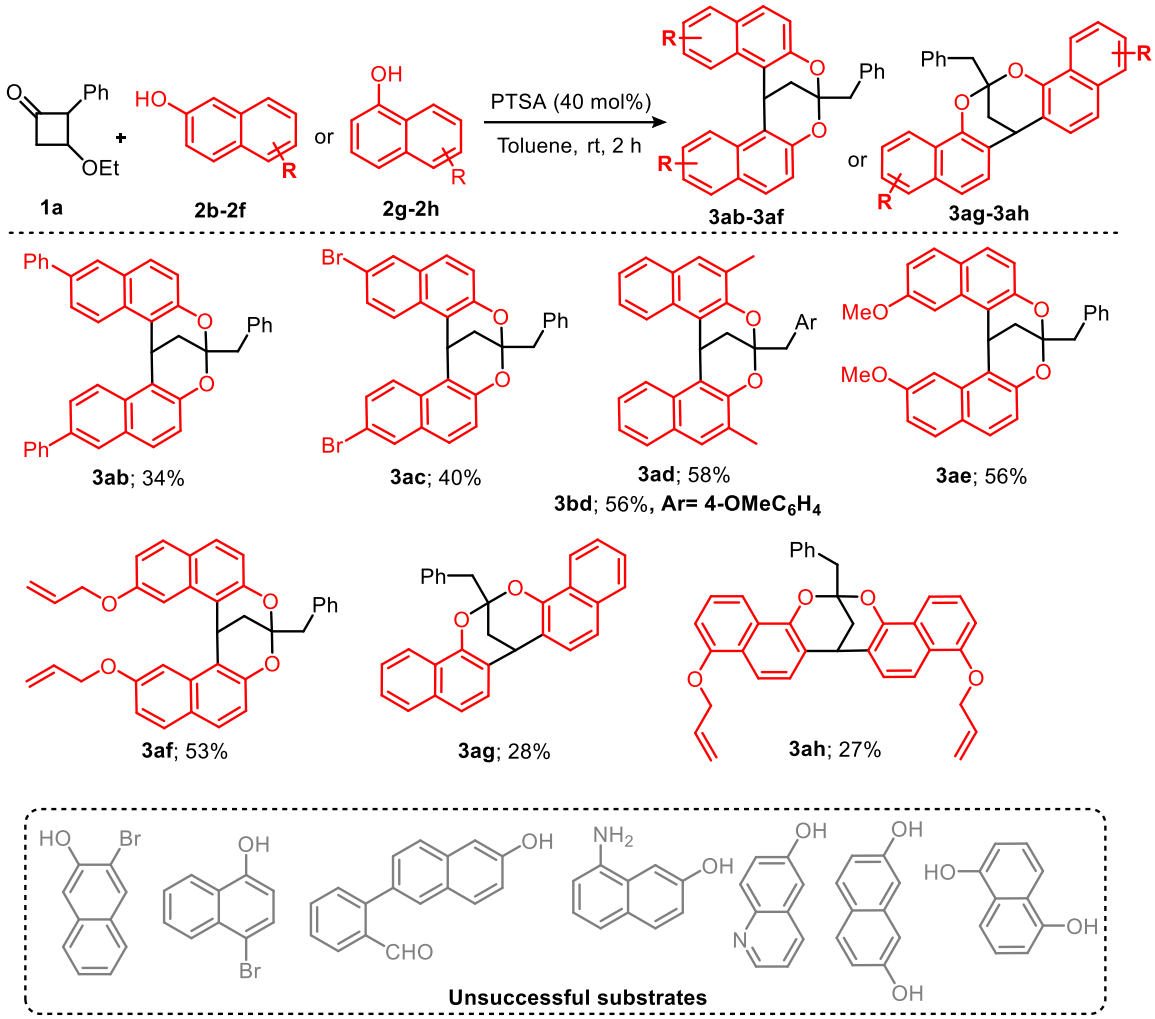

[a]Reaction conditions: **1a** (0.15 mmol), **2a** (0.30 mmol), PTSA (0.06 mmol), 1 mL toluene, at room temperature for 2 h, [b]isolated yield.

Next, we also investigated the scope and limitations of naphthol derivatives (Scheme 4.2.2). Both phenyl and bromo substitution at the 6-position of the 2-naphthol (**2b** and **2c**) furnished the corresponding products **3ab** and **3ac,** respectively, in low to moderate yields. Unfortunately, benzaldehyde substitution at the 6-position of 2-naphthol did not deliver the desired product. Next, 3-substituted naphthols were also tested for this methodology, where the 3-methyl 2-naphthol **2d** tolerated the reaction well with both phenyl and *para*-methoxy phenyl substituted cyclobutanones to give the products **3ad** and **3bd** with 58% and 56% yields respectively but 3-bromo substituted one failed to give the corresponding product. Subsequently, 7-substituted 2-naphthols were also employed for this reaction, and it was found that 2,7-dihydroxy naphthalene did not undergo the

reaction while 7-methoxy 2-naphthol rendered the product **3ae** with satisfactory yield. Delightfully, 7-(allyloxy)naphthalen-2-ol (**2f**) was also converted to the corresponding product **3af** in moderate yield. However, 8-amino 2-naphthol and 6-hydroxyquinoline failed to give the desired products. Interestingly, when 1-naphthol **2g** was employed, it also delivered the product **3ag,** though the yield was considerably low possibly due to the lower nucleophilicity of the carbon center on the 2-position of 1-naphthol. Hereafter, few other 1-naphthol derivatives were tested, however, only 5-(allyloxy)naphthalen-1-ol **2h** was able to provide the desired product **3ah** while 4-bromo 1-naphthol and 1,5-dihydroxy naphthalene failed to yield the corresponding products.

After the successful substrate scope evaluation, we conducted some control experiments to gain insights into the reaction mechanism. At first, 3-ethoxy cyclobutanone **1a** was reacted with 1,3,5-trimethoxy benzene and 4-methoxy phenol separately in the optimized reaction condition, but no such double addition products[13] or even simple Friedel-Crafts arylated products[14] were obtained (Scheme 4.2.3.a). Further, when trimethoxy benzene was employed along with 2-naphthol **2a** and cyclobutanone **1a** only the naphthol-containing product **3aa** was attained. These experiments denote that only the naphthol derivatives could undergo this reaction in the presence of Brønsted

Scheme 4.2.3. Control experiments

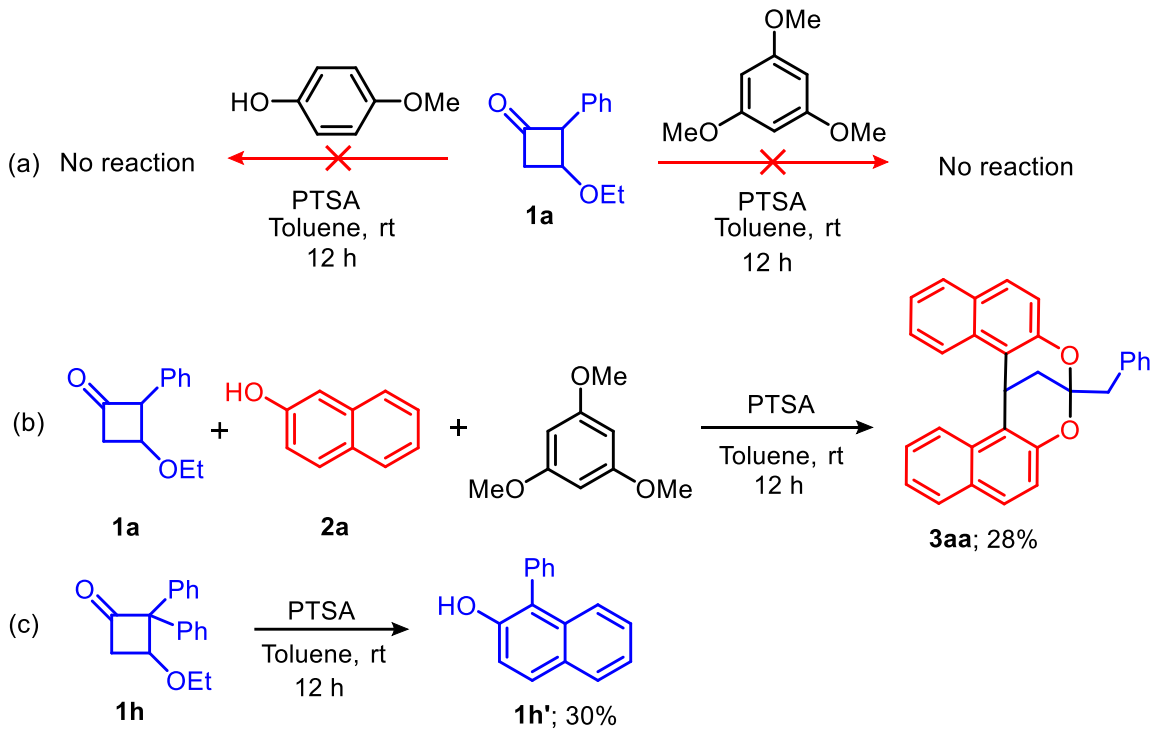

acid while other electron-rich aryl groups failed to deliver a similar kind of reactivity (Scheme 4.2.3.b). Moreover, to check the Brønsted acid activation of cyclobutanone, we performed a reaction with 2,2-diphenyl 3-ethoxy cyclobutanone **1h** in the presence of only PTSA and obtained the desired rearrangement product **1h'** (Scheme 4.2.3.c) which previously established to be formed

by the activation of Lewis acids only.[10h, 15] This experiment confirmed that the ring opening of the 3-ethoxy cyclobutanones could also be possible by the influence of Brønsted acids.

Based on the previous literature reports[10,11] and aforementioned control experiments, the plausible mechanism of this ring-opening/cyclization is outlined in Scheme 4.2.4. At first, the carbonyl group of cyclobutanone **1a** gets protonated, which could polarize the C2-C3 bond, and eventually, the ring-opening of cyclobutanone could happen via the nucleophilic attack of 2-naphthol at the C3 center leading to the formation of intermediate **I**. Later, the enolization and removal of ethanol generated the intermediate **II**. This intermediate could now undergo two possible pathways. In path A, another naphthol could facilitate the Michael addition to render the intermediate **III**, which later on, by double cyclization from the two oxygen atoms of naphthols engendered the desired product **3aa**. Whereas, in path B, cyclization from the hydroxyl group of intermediate **II** could furnish a dihydropyrylium-type intermediate **IV**. Subsequently, a (3+3)-annulation[16] with another molecule of 2-naphthol could lead to the formation of the desired product **3aa**.

Scheme 4.2.4. Plausible mechanism

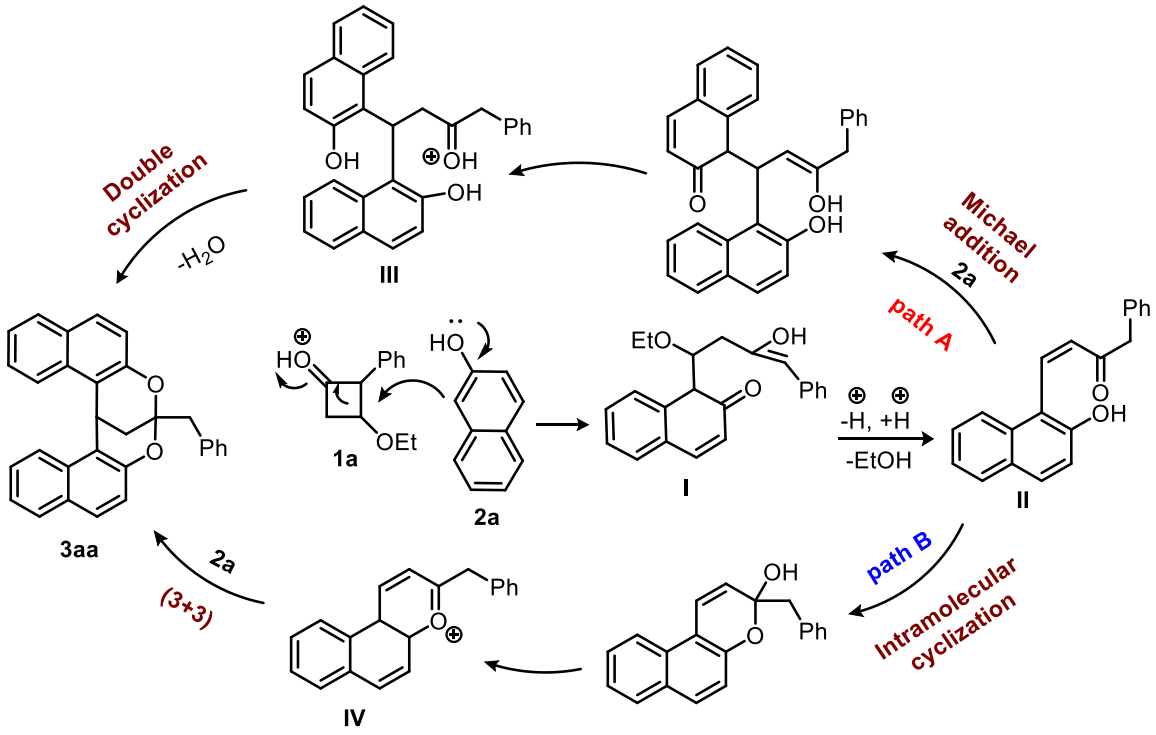

Finally, for the practical utility of our protocol, a gram-scale experiment was conducted where the final product **3aa** was obtained in 41% yield (Scheme 4.2.5.a). Additionally, to check the synthetic utility of our designed methodology, we have executed a ring closing metathesis[17] (RCM) where the synthesized product **3af** was transformed into a 15-membered macrocyclic scaffold **3afa** in the presence of Grubb's second-generation catalyst (Scheme 4.2.5.b). These types of heteroatom-containing complex 15-membered macrocycles can be found in biologically important molecules,[18]

can be utilized as metal-ion recognition and complexing agents, and often can also show antitumor and inhibitory activities.[19] Here, it is worth noticing that only the intramolecular cyclization happened where **3afa** were obtained with a 3:2 ratio of *trans:cis* isomers, and no intermolecular cyclization product was detected. A similar type of transformation was also tried with the product **3ah**, but unfortunately, it could not deliver the expected intermolecular cyclization product.

Scheme 4.2.5. Gram-scale experiment and synthetic transformation

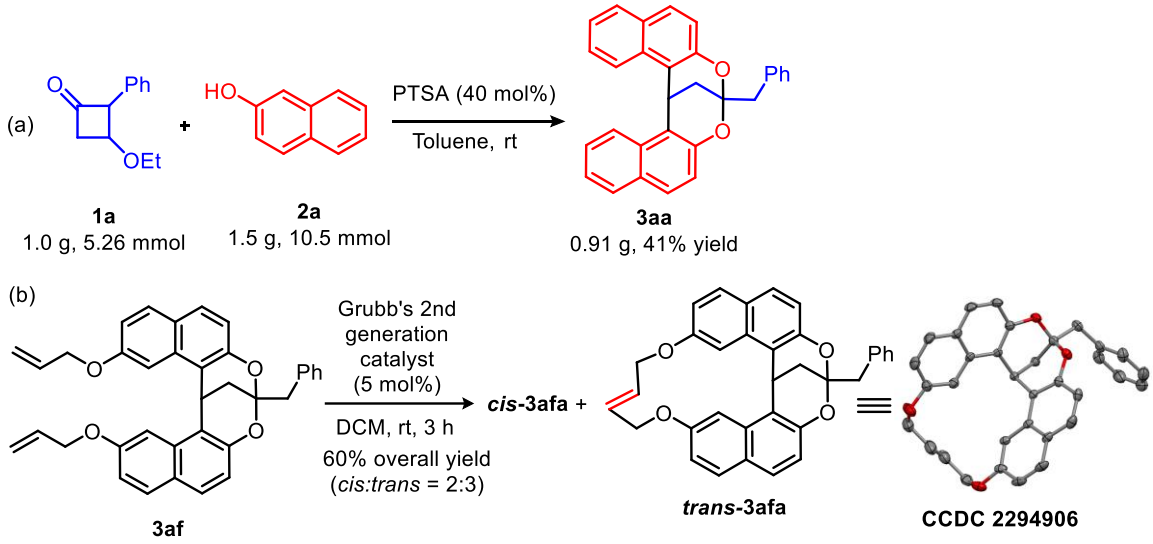

4.3. Conclusion

In conclusion, a new methodology for the construction of 2,8-dioxabicyclo[3.3.1]nonanes has been demonstrated by Brønsted acid activation of 3-ethoxy cyclobutanone. Various naphthol derivatives rendered the desired bicyclic ketals in poor to good yields via ring-opening of cyclobutanone followed by Michael addition/cyclization or (3+3)-annulation. Moreover, a 15-membered macrocyclic framework was also synthesized by ring-closing metathesis. Further studies to obtain unsymmetrical bicyclo[3.3.1]nonane derivatives and to utilize this protocol for constructing more complex molecular structures are still in progress in our laboratory.

4.4. Experimental Section

4.4.1. General Information

All reactions were carried out under an inert atmosphere with oven-dried glassware. All solvents and reagents were obtained from commercial sources and were purified following the standard procedure prior to use. All the naphthol derivatives except **2b**, **2f**, and **2h** are purchased from commercially available sources. The developed chromatogram was analyzed by UV lamp (254 nm) or *p*-anisaldehyde solution. Products were purified by flash chromatography on silica gel (mesh size 230-400). Melting points were determined using a Stuart SMP30 advanced digital melting

point apparatus. Mass spectral data (HRMS) were obtained using the XEVO G2-XS QTOF instrument. Nuclear magnetic resonance (NMR) spectroscopy was performed using JEOL 400 MHz. Chemical shifts of 1H, 13C{1H}, and HSQC NMR spectra are expressed in parts per million (ppm). All coupling constants are absolute values and are expressed in hertz (Hz). The description of the signals includes the following: s = singlet, d = doublet, dd = doublet of doublet, t = triplet, ddt = doublet of doublet of triplet, dq = doublet of quartet, br = broad, and m = multiplet.

4.4.2. General synthetic methods for the preparation of 3-ethoxy cyclobutanone[10a,10h]. In an inert atmosphere, to a solution of phenylacetic acid derivatives (3.7 mmol, 1 equiv.) in dry DCM (10 mL), oxalyl chloride (4.52 mmol, 1.5 equiv.) was added dropwise at 0 °C. After that, the mixture was stirred at room temperature for 3 h, and the crude material was used for the next step without further purification. A solution of ethyl vinyl ether (7.54 mmol, 2 equiv.) and triethylamine (4.52 mmol, 1.5 equiv.) in acetonitrile (2 mL) was added to the solution at room temperature for 1 h, and the mixture was refluxed (in a silicone oil bath) for 4 h. After the filtration of precipitates, water was added to the filtrate, and the mixture was extracted with ether. The combined organic extracts were dried over anhydrous sodium sulfate and concentrated. The residue was purified by silica gel column chromatography (hexane/ethyl acetate) and obtained the products **1a-1f** in 40-70% yields. For the preparation of **1g,** the same procedure was followed where the corresponding diphenylacetic acid was taken instead of phenylacetic acid.

3-ethoxy-2-phenylcyclobutanone (1a). 2-phenylacetyl chloride (1.0 g, 6.5 mmol), **1a** (0.86 g, 4.54 mmol), Yield: 70%; Nature: oil; Color: light yellow; The title compound was purified by column chromatography (Hexane/ethyl acetate = 9:1); R_f = 0.5; ^{1}H NMR (400 MHz, $CDCl_3$) δ 7.36 – 7.30 (m, 2H), 7.27 – 7.21 (m, 3H), 4.46-4.43 (m, 1H), 4.40 – 4.35 (m, 1H), 3.62 – 3.53 (m, 2H), 3.23 – 3.20 (m, 2H), 1.25 (t, *J* = 7.1 Hz, 3H).

3-ethoxy-2-(4-methoxyphenyl)cyclobutanone (1b). 2-(4-methoxyphenyl)acetyl chloride (0.5 g, 2.7 mmol), **1b** (0.35 g, 1.58 mmol), Yield: 58%; Nature: oil; Color: yellow; The title compound was purified by column chromatography (Hexane/ethyl acetate = 8:2); ^{1}H NMR (400 MHz, $CDCl_3$): δ 7.15 (d, *J* = 8.8 Hz, 2H), 6.87 (d, *J* = 8.7 Hz, 2H), 4.40-4.38 (m, 1H), 4.34-4.29 (m, 1H), 3.79 (s, 3H), 3.64 – 3.52 (m, 2H), 3.24 – 3.18 (m, 2H), 1.26 (t, *J* = 7.0 Hz, 3H).

3-ethoxy-2-(*p*-tolyl)cyclobutanone (1c). 2-(p-tolyl)acetyl chloride (0.5 g, 2.96 mmol), **1c** (0.15 g, 0.73 mmol), Yield: 25%; Nature: oil; Color: light yellow; The title compound was purified by column chromatography (Hexane/ethyl acetate = 9:1); ^{1}H NMR (400 MHz, $CDCl_3$): δ 7.16 – 7.11(m, 4H), 4.42-4.40 (m, 1H), 4.38-4.33 (m, 1H), 3.63 – 3.54 (m, 2H), 3.22 – 3.20 (m, 2H), 2.33 (s, 3H), 1.26 (t, *J* = 7.0 Hz, 3H).

3-ethoxy-2-(2-methoxyphenyl)cyclobutanone (1d). 2-(2-methoxyphenyl)acetyl chloride (0.2 g, 1.08 mmol), **1d** (0.15 g, 0.68 mmol), Yield: 63%; Nature: oil; Color: yellow; The title compound was purified by column chromatography (Hexane/ethyl acetate = 8:2); ^{1}H NMR (400 MHz, $CDCl_3$): δ 7.27 – 7.23 (m, 1H), 7.08 (dd, *J* = 7.4, 1.7 Hz, 1H), 6.91 (td, *J* = 7.4, 1.0 Hz, 1H), 6.87 (d, *J* = 8.2 Hz, 1H), 4.48 (m, 1H), 4.29 – 4.27 (m, 1H), 3.78 (s, 3H), 3.57-3.34 (m, 3H), 3.15 – 3.08 (m, 1H), 1.21 (t, *J* = 7.0 Hz, 3H).

3-ethoxy-2-(*o*-tolyl)cyclobutanone (1e). 2-(o-tolyl)acetyl chloride (0.2 g, 1.18 mmol), **1e** (0.12 g, 0.58 mmol), Yield: 50%; Nature: oil; Color: light yellow; The title compound was purified by column chromatography (Hexane/ethyl acetate = 9:1); ^{1}H NMR (400 MHz, $CDCl_3$): δ 7.18 – 7.15 (m, 4H), 4.64-4.62 (m, 1H), 4.45-4.40 (m, 1H), 3.58 – 3.51 (m, 2H), 3.24-3.21 (m, 2H), 2.35 (s, 3H), 1.24 (t, *J* = 7.0 Hz, 3H).

2-(4-chlorophenyl)-3-ethoxycyclobutanone (1f). 2-(4-chlorophenyl)acetic acid (0.5 g, 2.93 mmol), **1f** (0.2 g, 0.93 mmol), Yield: 32%; Nature: oil; Color: yellow; The title compound was purified by column chromatography (Hexane/ethyl acetate = 9:1); ^{1}H NMR (400 MHz, $CDCl_3$): δ 7.31 – 7.27 (m, 2H), 7.18 – 7.14 (m, 2H), 4.41 (dd, *J* = 5.8, 2.2 Hz, 1H), 4.34 – 4.29 (m, 1H), 3.61 – 3.51 (m, 2H), 3.24 – 3.19 (m, 2H), 1.25 (t, *J* = 7.0 Hz, 3H).

2-benzyl-3-ethoxycyclobutanone (1g). 3-phenylpropanoyl chloride (0.5 g, 2.96 mmol), **1g** (0.2 g, 0.99 mmol), Yield: 33%; Nature: oil; Color: yellow; The title compound was purified by column chromatography (Hexane/ethyl acetate = 9:1); ^{1}H NMR (400 MHz, $CDCl_3$): δ 7.28 – 7.19 (m, 5H), 4.31 – 4.24 (m, 1H), 3.58 – 3.50 (m, 2H), 3.40 (dq, *J* = 14.1, 7.0 Hz, 1H), 3.23 – 3.13 (m, 1H), 3.11 – 3.05 (m, 1H), 2.95 – 2.86 (m, 2H), 1.23 (t, *J* = 7.0 Hz, 3H).

3-ethoxy-2,2-diphenylcyclobutanone (1h). 2,2-diphenylacetyl chloride (1.0 g, 4.34 mmol), **1h** (0.86 g, 3.36 mmol), Yield: 75%; Nature: crystalline solid; Color: white; The title compound was purified by column chromatography (Hexane/ethyl acetate = 9:1); ^{1}H NMR (400 MHz, $CDCl_3$) δ 7.47 – 7.42 (m, 2H), 7.38-7.34 (m, 2H), 7.28-7.20 (m, 4H), 7.18 – 7.13 (m, 2H), 4.83 (dd, *J* = 7.5, 5.4 Hz, 1H), 3.53 (m, 1H), 3.44 – 3.32 (m, 2H), 3.19 (dd, *J* = 18.1, 5.3 Hz, 1H), 1.04 (t, *J* = 7.0 Hz, 3H).

6-phenylnaphthalen-2-ol (2b). Prepared According to the reported literature method.[20] 6-bromonaphthalen-2-ol (0.11 g, 0.50 mmol), 2b (0.052 g, 0.23 mmol), Yield: 47%; Nature: solid; Color: white; The title compound was purified by column chromatography (Hexane/ethyl acetate = 7:3); ^{1}H NMR (400 MHz, $CDCl_3$): δ 7.98 (s, 1H), 7.81 (d, *J* = 8.8 Hz, 1H), 7.77-7.75 (m, 1H), 7.73 – 7.68 (m, 3H), 7.50-7.46 (m, 2H), 7.38-7.34 (m, 1H), 7.18 (d, *J* = 2.4 Hz, 1H), 7.13 (dd, *J* = 8.8, 2.5 Hz, 1H), 5.06 (s, 1H).

7-(allyloxy)naphthalen-2-ol (2f). Prepared according to the reported literature method.[21] naphthalene-2,7-diol (0.5 g, 3.12 mmol), 2f (0.2 g, 0.99 mmol), Yield: 32%; Nature: solid; Color: brown; The title compound was purified by column chromatography (Hexane/ethyl acetate = 9:1); ^{1}H NMR (400 MHz, $CDCl_3$): δ 7.65 (dd, *J* = 8.8, 3.8 Hz, 2H), 7.08 – 6.91 (m, 4H), 6.36 (s, 1H), 6.11 (ddt, *J* = 16.8, 10.6, 5.4 Hz, 1H), 5.54 – 5.40 (m, 1H), 5.34-5.30 (m, 1H), 4.66 – 4.50 (m, 2H).

5-(allyloxy)naphthalen-1-ol (2h). Prepared according to the reported literature method.[22] naphthalene-1,5-diol (0.5 g, 3.12 mmol), 2h (0.19 g, 0.95 mmol), Yield: 30%; Nature: solid; Color: brown; The title compound was purified by column chromatography (Hexane/ethyl acetate = 9:1); ^{1}H NMR (400 MHz, $CDCl_3$): δ 7.97 – 7.84 (m, 1H), 7.81 – 7.70 (m, 1H), 7.47 – 7.20 (m, 2H), 6.85-6.83 (m, 2H), 6.17 (ddt, *J* = 17.3, 10.5, 5.1 Hz, 1H), 5.83 (s, 1H), 5.55-5.49 (m, 1H), 5.36 – 5.31 (m, 1H), 4.76 – 4.65 (m, 2H).

4.4.3. Representative procedure for the synthesis of diaryl substituted 2,8-dioxabicyclo[3.3.1]nonanes: To a round-bottom flask equipped with a magnetic stir bar was charged with 3-ethoxy 2-phenyl cyclobutanone (1 equiv.), 2-naphthol (2 equiv.), and PTSA (40 mol%). Toluene was added as a solvent to the reaction mixture and was stirred under an open atmosphere for 2 hours. After the completion of the reaction (as monitored by TLC), the solvent was removed under reduced pressure by a rotary evaporator. Then, the crude product was further purified by column chromatography on silica gel with EtOAc/hexane as eluent to afford the products **3aa-3ga** and **3ab-3ah**.

8-benzyl-16*H*-8,16-methanodinaphtho[2,1-*d*:1',2'-*g*][1,3]dioxocine (3aa). 1a (0.030 g, 0.15 mmol), **2a** (0.044 g, 0.30 mmol), **3aa** (0.047 g, 0.11 mmol), white crystalline solid, Melting point 189-192 °C; 72% yield, The title compound was purified by column chromatography (hexane/ethyl acetate = 19.5:0.5); ^{1}H NMR (400 MHz, $CDCl_3$): δ 8.54 (d, *J* = 8.6 Hz, 2H), 7.70 (d, *J* = 7.2 Hz, 2H), 7.60 (d, *J* = 8.9 Hz, 2H), 7.53 (m, 2H), 7.45 – 7.41 (m, 2H), 7.32 – 7.27 (m, 4H), 7.23 (m, 1H), 7.19 (d, *J* = 8.9 Hz, 2H), 5.33 (t, *J* = 3.1 Hz, 1H), 3.56 (s, 2H), 2.26 (d, *J* = 3.2 Hz, 2H). ^{13}C{^{1}H} NMR (101 MHz, $CDCl_3$): δ 151.1, 135.2, 131.2, 130.8, 129.7, 128.8, 128.5, 128.3, 127.1, 126.3, 123.4, 122.9, 118.6, 118.5, 98.9, 45.6, 30.1, 24.7. HRMS (ESI, Q-TOF) m/z: $[M+H]^+$ calculated for $C_{30}H_{23}O_2$ 415.1698, Found 415.1698.

8-(4-methoxybenzyl)-16*H*-8,16-methanodinaphtho[2,1-*d*:1',2'-*g*][1,3]dioxocine (3ba). 1b (0.034 g, 0.15 mmol), **2a** (0.044 g, 0.30 mmol), **3ba** (0.050 g, 0.11 mmol), white amorphous solid, Melting point 186-189 °C; 72% yield; The title compound was purified by column chromatography (hexane/ethyl acetate = 19:1); ^{1}H NMR (400 MHz, $CDCl_3$): δ 8.54 (d, *J* = 8.6 Hz, 2H), 7.70 (d, *J* = 8.2 Hz, 2H), 7.59 (d, *J* = 8.8 Hz, 2H), 7.55 – 7.49 (m, 2H), 7.34 (d, *J* = 8.7 Hz, 2H), 7.31 – 7.27 (m, 2H), 7.17 (d, *J* = 8.8 Hz, 2H), 6.82 (d, *J* = 8.7 Hz, 2H), 5.33 (t, *J* = 3.1 Hz, 1H), 3.75 (s, 3H), 3.49 (s, 2H), 2.25 (d, *J* = 3.2 Hz, 2H). ^{13}C{^{1}H} NMR (101 MHz, $CDCl_3$): δ 158.7, 151.1, 131.7, 131.2,

129.7, 128.8, 128.5, 127.2, 126.3, 123.4, 122.8, 118.6, 118.5, 113.7, 99.0, 55.2, 44.7, 30.1, 24.7. HRMS (ESI, Q-TOF) m/z: $[M+H]^+$ calculated for $C_{31}H_{25}O_3$ 445.1804, Found 445.1806**.**

8-(4-methylbenzyl)-16*H*-8,16-methanodinaphtho[2,1-*d*:1',2'-*g*][1,3]dioxocine (3ca). 1c (0.032 g, 0.15 mmol), **2a** (0.044 g, 0.30 mmol), **3ca** (0.042 g, 0.09 mmol), white amorphous solid, Melting point 161-163 °C; 64% yield; The title compound was purified by column chromatography (hexane/ethyl acetate = 19:1); ^{1}H NMR (400 MHz, $CDCl_3$): δ 8.54 (d, *J* = 8.6 Hz, 2H), 7.70 (d, *J* = 7.8 Hz, 2H), 7.60 (d, *J* = 8.8 Hz, 2H), 7.54-7.51 (m, 2H), 7.33 – 7.28 (m, 4H), 7.19 (d, *J* = 8.8 Hz, 2H), 7.09 (d, *J* = 7.9 Hz, 2H), 5.33 (t, *J* = 3.0 Hz, 1H), 3.52 (s, 2H), 2.29 (s, 3H), 2.26 (d, *J* = 3.1 Hz, 2H). ^{13}C{^{1}H} NMR (101 MHz, $CDCl_3$): δ 151.2, 136.6, 132.0, 131.2, 130.6, 129.7, 129.0, 128.8, 128.5, 126.3, 123.4, 122.8, 118.6, 118.5, 99.0, 45.2, 30.1, 24.7, 21.1. HRMS (ESI, Q-TOF) m/z: $[M+H]^+$ calculated for $C_{31}H_{25}O_2$ 429.1855, Found 429.1854.

8-(2-methoxybenzyl)-16*H*-8,16-methanodinaphtho[2,1-*d*:1',2'-*g*][1,3]dioxocine (3da). 1d (0.034 g, 0.15 mmol), **2a** (0.044 g, 0.30 mmol), **3da** (0.047 g, 0.10 mmol), yellow amorphous solid, Melting point 212-215 °C; 67% yield; The title compound was purified by column chromatography (hexane/ethyl acetate = 19.5:0.5); ^{1}H NMR (400 MHz, $CDCl_3$): δ 8.54 (d, *J* = 8.6 Hz, 2H), 7.70 (d, *J* = 8.2 Hz, 2H), 7.58 (d, *J* = 8.8 Hz, 2H), 7.55 – 7.49 (m, 3H), 7.31 – 7.26 (m, 2H), 7.22 – 7.15 (m, 3H), 6.92 – 6.87 (m, 1H), 6.84 (d, *J* = 8.2 Hz, 1H), 5.31 (t, *J* = 3.1 Hz, 1H), 3.82 (s, 3H), 3.65 (s, 2H), 2.31 (d, *J* = 3.2 Hz, 2H). ^{13}C{^{1}H} NMR (101 MHz, $CDCl_3$): δ 158.0, 151.3, 132.9, 131.2, 129.6, 128.8, 128.4, 128.3, 126.2, 123.6, 123.3, 122.8, 120.4, 118.6, 118.6, 110.4, 99.6, 77.4, 77.1, 76.8, 55.3, 38.4, 29.7, 24.7. HRMS (ESI, Q-TOF) m/z: $[M+H]^+$ calculated for $C_{31}H_{25}O_3$ 445.1804, Found 445.1790.

8-(2-methylbenzyl)-16*H*-8,16-methanodinaphtho[2,1-*d*:1',2'-*g*][1,3]dioxocine (3ea). 1e (0.032 g, 0.15 mmol), **2a** (0.044 g, 0.30 mmol), **3ea** (0.054 g, 0.12 mmol), yellowish sticky liquid, 85% yield; The title compound was purified by column chromatography (hexane/ethyl acetate = 19.5:0.5); ^{1}H NMR (400 MHz, $CDCl_3$): δ 8.54 (d, *J* = 8.6 Hz, 2H), 7.69 (d, *J* = 7.8 Hz, 2H), 7.58 (d, *J* = 8.9 Hz, 2H), 7.56 – 7.49 (m, 2H), 7.43-7.41 (m, 1H), 7.31-7.27 (m, 2H), 7.19 – 7.10 (m, 5H), 5.35 (t, *J* = 3.1 Hz, 1H), 3.61 (s, 2H), 2.54 (s, 3H), 2.35 (d, *J* = 3.1 Hz, 2H). ^{13}C{^{1}H} NMR (101 MHz, $CDCl_3$): δ 151.1, 137.8, 133.5, 131.9, 131.1, 130.5, 129.7, 128.8, 128.5, 127.2, 126.3, 125.7, 123.4, 122.8, 118.5, 118.4, 99.6, 77.4, 77.1, 76.8, 42.1, 30.3, 24.7, 20.6. HRMS (ESI, Q-TOF) m/z: $[M+H]^+$ calculated for $C_{31}H_{25}O_2$ 429.1855, Found 429.1858.

8-(4-chlorobenzyl)-16*H*-8,16-methanodinaphtho[2,1-*d*:1',2'-*g*][1,3]dioxocine (3fa). 1f (0.035 g, 0.15 mmol), **2a** (0.044 g, 0.30 mmol), **3fa** (0.048 g, 0.10 mmol), yellow amorphous solid, Melting point 224-227 °C; yield 68%; The title compound was purified by column chromatography (hexane/ethyl acetate = 19.5:0.5); ^{1}H NMR (400 MHz, $CDCl_3$): δ 8.53 (d, *J* = 8.6 Hz, 2H), 7.69 (d, *J* = 8.2 Hz, 2H), 7.58 (d, *J* = 8.8 Hz, 2H), 7.55 – 7.49 (m, 2H), 7.37 – 7.33 (m, 2H), 7.32 – 7.23 (m,

4H), 7.15 (d, *J* = 8.9 Hz, 2H), 5.32 (t, *J* = 3.1 Hz, 1H), 3.50 (s, 2H), 2.22 (d, *J* = 3.2 Hz, 2H**).** $^{13}C\{^1H\}$ NMR (101 MHz, $CDCl_3$): δ 150.9, 133.6, 133.1, 132.1, 131.1, 129.7, 128.8, 128.6, 128.4, 126.4, 123.5, 122.8, 118.4, 98.6, 77.4, 77.1, 76.8, 44.9, 30.2, 24.7. HRMS (ESI, Q-TOF) m/z: $[M+H]^+$ calculated for $C_{30}H_{21}ClO_2$ 449.1308, Found 449.1313.

8-phenethyl-16*H*-8,16-methanodinaphtho[2,1-*d*:1',2'-*g*][1,3]dioxocine (3ga). 1g (0.032 g, 0.15 mmol), **2a** (0.044 g, 0.30 mmol), **3ga** (0.023 g, 0.05 mmol), white amorphous solid, Melting point 208-212 °C; 34% yield; The title compound was purified by column chromatography (hexane/ethyl acetate = 19.5:0.5); ^1H NMR (400 MHz, $CDCl_3$): δ 8.60 (d, *J* = 8.6 Hz, 2H), 7.73 (d, *J* = 7.9 Hz, 2H), 7.61 (d, *J* = 8.8 Hz, 2H), 7.58-7.54 (m, 2H), 7.34 – 7.30 (m, 6H), 7.25 – 7.21 (m, 1H), 7.16 (d, *J* = 8.8 Hz, 2H), 5.42 (t, *J* = 3.1 Hz, 1H), 3.07 – 3.03 (m, 2H), 2.587– 2.53 (m, 2H), 2.44 (d, *J* = 3.2 Hz, 2H). $^{13}C\{^1H\}$ NMR (101 MHz, $CDCl_3$): δ 151.2, 141.6, 131.2, 129.7, 128.9, 128.6, 128.5, 126.4, 126.1, 123.4, 122.9, 118.6, 118.6, 98.7, 66.0, 41.3, 31.1, 29.7, 24.9, 15.4. HRMS (ESI, Q-TOF) m/z: $[M+H]^+$ calculated for $C_{31}H_{25}O_2$ 429.1855, Found 429.1857.

8-benzhydryl-16*H*-8,16-methanodinaphtho[2,1-*d*:1',2'-*g*][1,3]dioxocine (3ha). 1h (0.041 g, 0.15 mmol), **2a** (0.044 g, 0.30 mmol), **3ha** (0.042 g, 0.08 mmol), Yellowish sticky liquid, 55% yield; The title compound was purified by column chromatography (hexane/ethyl acetate = 19.5:0.5); ^1H NMR (400 MHz, $CDCl_3$): δ 8.55 (d, *J* = 8.6 Hz, 2H), 7.74 – 7.64 (m, 6H), 7.60 (d, *J* = 8.9 Hz, 2H), 7.55-7.51 (m, 2H), 7.35 – 7.27 (m, 7H), 7.25 – 7.23 (m, 1H), 7.18 (d, *J* = 8.9 Hz, 2H), 5.34 (t, *J* = 3.1 Hz, 1H), 4.65 (s, 1H), 2.38 (d, *J* = 3.2 Hz, 2H). $^{13}C\{^1H\}$ NMR (101 MHz, $CDCl_3$): δ 151.0, 139.8, 131.2, 130.2, 129.8, 128.8, 128.5, 128.4, 127.0, 126.3, 123.5, 122.9, 118.7, 118.6, 99.8, 60.5, 31.4, 24.9. HRMS (ESI, Q-TOF) m/z: $[M+H]^+$ calculated for $C_{36}H_{27}O_2$ 491.2011, Found 491.2008.

8-benzyl-3,13-diphenyl-16*H*-8,16-methanodinaphtho[2,1-*d*:1',2'-*g*][1,3]dioxocine (3ab). 1a (0.030 g, 0.15 mmol), **2b** (0.066 g, 0.30 mmol), **3ab** (0.031 g, 0.05 mmol), colorless sticky liquid, 34% yield; The title compound was purified by column chromatography (hexane/ethyl acetate = 19.5:0.5); ^1H NMR (400 MHz, $CDCl_3$): δ 8.61 (d, *J* = 8.9 Hz, 2H), 7.90 (d, *J* = 1.9 Hz, 2H), 7.81 (dd, *J* = 8.8, 1.9 Hz, 2H), 7.68 – 7.62 (m, 6H), 7.47 – 7.40 (m, 6H), 7.35 – 7.26 (m, 4H), 7.24 – 7.18 (m, 3H), 5.36 (t, *J* = 3.0 Hz, 1H), 3.57 (s, 2H), 2.29 (d, *J* = 3.1 Hz, 2H). $^{13}C\{^1H\}$ NMR (101 MHz, $CDCl_3$): δ 151.2, 140.8, 136.1, 135.1, 130.8, 130.3, 130.0, 128.9, 128.3, 127.2, 127.1, 126.7, 125.9, 123.4, 119.0, 118.4, 99.0, 77.4, 77.1, 76.8, 45.7, 30.1, 24.8. HRMS (ESI, Q-TOF) m/z: $[M+H]^+$ calculated for $C_{42}H_{31}O_2$ 567.2324, Found 567.2316.

8-benzyl-3,13-dibromo-16*H*-8,16-methanodinaphtho[2,1-*d*:1',2'-*g*][1,3]dioxocine (3ac). 1a (0.030 g, 0.15 mmol), **2c** (0.067 g, 0.30 mmol), **3ac** (0.036 g, 0.06 mmol), white amorphous solid, Melting point 188-191 °C; 40% yield; The title compound was purified by column chromatography (hexane/ethyl acetate = 19.5:0.5); ^1H NMR (400 MHz, $CDCl_3$): δ 8.28 (d, *J* = 9.1 Hz, 2H), 7.84 (d,

J = 2.0 Hz, 2H), 7.57 (dd, *J* = 9.1, 2.1 Hz, 2H), 7.49 (d, *J* = 8.9 Hz, 2H), 7.43 – 7.39 (m, 2H), 7.32 – 7.27 (m, 2H), 7.25 – 7.20 (m, 1H), 7.18 (d, *J* = 8.9 Hz, 2H), 5.19 (t, *J* = 3.1 Hz, 1H), 3.54 (s, 2H), 2.25 (d, *J* = 3.1 Hz, 2H). $^{13}C\{^{1}H\}$ NMR (101 MHz, $CDCl_3$): δ 151.4, 134.9, 130.9, 130.8, 129.6, 128.4, 127.8, 127.2, 124.3, 119.7, 118.4, 117.2, 99.0, 45.6, 29.9, 24.7. HRMS (ESI, Q-TOF) m/z: $[M+H]^+$ calculated for $C_{30}H_{21}Br_2O_2$ 570.9908, Found 570.9902.

8-benzyl-6,10-dimethyl-16*H*-8,16-methanodinaphtho[2,1-*d*:1',2'-*g*][1,3]dioxocine (3ad). 1a (0.030 g, 0.15 mmol), **2d** (0.047 g, 0.30 mmol), **3ad** (0.041 g, 0.09 mmol), white amorphous solid, Melting point 190-192 °C; 58% yield; The title compound was purified by column chromatography (hexane/ethyl acetate = 19.5:0.5); ^{1}H NMR (400 MHz, $CDCl_3$): δ 8.50 (d, *J* = 8.5 Hz, 2H), 7.61 (d, *J* = 8.2 Hz, 2H), 7.48 – 7.44 (m, 3H), 7.42 (s, 2H), 7.34 – 7.29 (m, 2H), 7.28 – 7.22 (m, 4H), 5.33 (t, *J* = 3.2 Hz, 1H), 3.55 (s, 2H), 2.43 (s, 6H), 2.28 (d, *J* = 3.2 Hz, 2H).

$^{13}C\{^{1}H\}$ NMR (101 MHz, $CDCl_3$): δ 150.2, 135.4, 130.9, 130.0, 129.4, 128.1, 128.0, 127.9, 127.5, 127.0, 125.2, 123.2, 122.6, 117.9, 98.4, 46.2, 30.3, 24.9, 17.2. HRMS (ESI, Q-TOF) m/z: $[M+H]^+$ calculated for $C_{32}H_{27}O_2$ 443.2011, Found 443.1999.

8-(4-methoxybenzyl)-6,10-dimethyl-16*H*-8,16-methanodinaphtho[2,1-*d*:1',2'-*g*][1,3]dioxocine (3bd). 1b (0.030 g, 0.13 mmol), **2d** (0.043 mg, 0.27 mmol), **3bd** (0.037 mg, 0.07 mmol), white amorphous solid, Melting point 198-201 °C; 56% yield; The title compound was purified by column chromatography (hexane/ethyl acetate = 19.5:0.5); ^{1}H NMR (400 MHz, $CDCl_3$): δ 8.50 (d, *J* = 8.6 Hz, 2H), 7.62 (d, *J* = 8.2 Hz, 2H), 7.49 – 7.41 (m, 4H), 7.37 (d, *J* = 8.6 Hz, 2H), 7.27-7.24 (m, 2H), 6.86 (d, *J* = 8.6 Hz, 2H), 5.33 (t, *J* = 3.1 Hz, 1H), 3.78 (s, 3H), 3.49 (s, 2H), 2.43 (s, 6H), 2.26 (d, *J* = 3.1 Hz, 2H). $^{13}C\{^{1}H\}$ NMR (101 MHz, $CDCl_3$): δ 158.7, 150.3, 131.9, 130.1, 129.4, 128.1, 127.9, 127.6, 125.3, 123.3, 122.7, 118.0, 113.6, 98.6, 55.3, 45.3, 30.3, 25.0, 17.3. HRMS (ESI, Q-TOF) m/z: $[M+H]^+$ calculated for $C_{33}H_{29}O_3$ 473.2117, Found 473.2123.

8-benzyl-2,14-dimethoxy-16*H*-8,16-methanodinaphtho[2,1-*d*:1',2'-*g*][1,3]dioxocine (3ae). 1a (0.030 g, 0.15 mmol), **2e** (0.052 g, 0.30 mmol), **3ae** (0.042 g, 0.08 mmol), white amorphous solid, Melting point 200-203 °C; 56% yield; The title compound was purified by column chromatography (hexane/ethyl acetate = 19:1); ^{1}H NMR (400 MHz, $CDCl_3$): δ 7.85 (d, *J* = 2.3 Hz, 2H), 7.63 (d, *J* = 8.9 Hz, 2H), 7.53 (d, *J* = 8.8 Hz, 2H), 7.44-7.42 (m, 2H), 7.31 – 7.26 (m, 2H), 7.24 – 7.20 (m, 1H), 7.05 (d, *J* = 8.8 Hz, 2H), 6.99 (dd, *J* = 8.9, 2.4 Hz, 2H), 5.13 (t, *J* = 3.1 Hz, 1H), 3.95 (s, 6H), 3.55 (s, 2H), 2.23 (d, *J* = 3.2 Hz, 2H). $^{13}C\{^{1}H\}$ NMR (101 MHz, $CDCl_3$): δ 158.2, 151.7, 135.2, 132.6, 130.8, 130.4, 128.3, 127.0, 125.0, 117.5, 116.2, 114.1, 104.3, 99.0, 55.8, 45.6, 30.5, 25.1. HRMS (ESI, Q-TOF) m/z: $[M+H]^+$ calculated for $C_{32}H_{27}O_4$ 475.1909, Found 475.1904.

2,14-bis(allyloxy)-8-benzyl-16*H*-8,16-methanodinaphtho[2,1-*d*:1',2'-*g*][1,3]dioxocine (3af). 1a (0.030 g, 0.15 mmol), **2f** (0.060 g, 0.30 mmol), **3af** (0.044 g, 0.08 mmol), light yellow amorphous

solid, Melting point 150-152 °C; 53% yield; The title compound was purified by column chromatography (hexane/ethyl acetate = 19:1); ^{1}H NMR (400 MHz, $CDCl_3$): δ 7.87 (d, *J* = 2.2 Hz, 2H), 7.63 (d, *J* = 9.0 Hz, 2H), 7.53 (d, *J* = 8.8 Hz, 2H), 7.45-7.42 (m, 2H), 7.32 – 7.28 (m, 2H), 7.25 – 7.20 (m, 1H), 7.06 (d, *J* = 8.8 Hz, 2H), 7.02 (dd, *J* = 9.0, 2.3 Hz, 2H), 6.13 (m, 2H), 5.51-5.45(m, 2H), 5.35-5.31 (m, 2H), 5.11 (t, *J* = 3.0 Hz, 1H), 4.76-4.71 (m, 2H), 4.67 – 4.62 (m, 2H), 3.56 (s, 2H), 2.23 (d, *J* = 3.1 Hz, 2H). ^{13}C{^{1}H} NMR (101 MHz, $CDCl_3$): δ 157.3, 151.7, 135.2, 133.4, 132.6, 130.8, 130.4, 128.3, 127.0, 125.1, 117.8, 117.5, 116.3, 114.6, 105.1, 99.0, 69.3, 45.6, 30.4, 25.1. HRMS (ESI, Q-TOF) m/z: $[M+H]^+$ calculated for $C_{36}H_{31}O_4$ 527.2222, Found 527.2218.

15-benzyl-7*H*-7,15-methanodinaphtho[1,2-*d*:2',1'-*g*][1,3]dioxocine (3ag). 1a (0.030 g, 0.15 mmol), **2g** (0.044 g, 0.30 mmol), **3ag** (0.020 g, 0.04 mmol), light brown amorphous solid, Melting point 232-235 °C; 28% yield; The title compound was purified by column chromatography (hexane/ethyl acetate = 19.5:0.5); ^{1}H NMR (400 MHz, $CDCl_3$): δ 8.31-8.29 (m, 2H), 7.70 (d, *J* = 8.0 Hz, 2H), 7.60 – 7.56 (m, 2H), 7.50 – 7.43 (m, 2H), 7.42 – 7.37 (m, 2H), 7.36 – 7.30 (m, 6H), 7.28 – 7.22 (m, 1H), 4.15 (t, *J* = 3.0 Hz, 1H), 3.76 (s, 2H), 2.30 (d, *J* = 3.1 Hz, 2H). ^{13}C{^{1}H} NMR (101 MHz, $CDCl_3$): δ 147.0, 135.4, 133.5, 130.9, 128.3, 127.5, 127.0, 125.9, 125.5, 125.2, 124.5, 121.8, 120.8, 120.7, 99.7, 46.5, 33.8, 29.2. HRMS (ESI, Q-TOF) m/z: $[M+H]^+$ calculated for $C_{30}H_{23}O_2$ 415.1698, Found 415.1694.

4,10-bis(allyloxy)-15-benzyl-7*H*-7,15-methanodinaphtho[1,2-*d*:2',1'-*g*][1,3]dioxocine (3ah). 1a (0.030 g, 0.15 mmol), **2h** (0.060 g, 0.30 mmol), **3ah** (0.023 g, 0.04 mmol), yellowish amorphous solid, Melting point 180-184 °C; 27% yield; The title compound was purified by column chromatography (hexane/ethyl acetate = 19:1); ^{1}H NMR (400 MHz, $CDCl_3$): δ 7.88 (d, *J* = 8.4 Hz, 2H), 7.79 (d, *J* = 8.8 Hz, 2H), 7.56 (d, *J* = 7.1 Hz, 2H), 7.38 – 7.28 (m, 6H), 7.26 – 7.21 (m, 1H), 6.75 (d, *J* = 7.7 Hz, 2H), 6.17 – 6.06 (m, 2H), 5.49 – 5.43 (m, 2H), 5.32 – 5.26 (m, 2H), 4.67 – 4.63 (m, 4H), 4.15 (t, *J* = 2.9 Hz, 1H), 3.73 (s, 2H), 2.27 (d, *J* = 2.9 Hz, 2H). ^{13}C{^{1}H} NMR (101 MHz, $CDCl_3$): δ 154.2, 146.9, 135.5, 133.4, 131.0, 130.8, 128.3, 127.0, 125.8, 125.6, 125.5, 124.4, 121.4, 117.3, 115.0, 114.3, 105.4, 99.8, 69.0, 46.5, 33.8, 29.2. HRMS (ESI, Q-TOF) m/z: $[M+H]^+$ calculated for $C_{36}H_{31}O_4$ 527.2222, Found 527.2225.

4.4.4. General procedure for the ring-closing metathesis of 3af[23]: Compound **3af** (1 equiv.) was dissolved in dry CH_2Cl_2, and Grubbs second generation catalyst (0.05 equiv.) was added to the mixture and stirred for 3 hours at room temperature. After completion monitored by TLC, the solvent was evaporated under reduced pressure, and the crude residue was purified by silica gel column chromatography (EtOAc/hexane) to obtain the product 3afa with 3: 2 ratio of trans: cis mixture with an overall yield of 64%; The title compound was purified by column chromatography (hexane/ethyl acetate = 19.5:0.5 to 19:1); **3af** (0.030 g, 0.05 mmol), **3afa** (0.017 g, 0.03 mmol), 60% overall yield (*trans: cis = 3:2*).

***cis*-3afa:** white amorphous solid, Melting point 170-172 °C; ^{1}H NMR (400 MHz, $CDCl_3$): δ 7.79 (s, 2H), 7.58 (dd, *J* = 8.8, 3.8 Hz, 2H), 7.49 (dd, *J* = 8.8, 3.6 Hz, 2H), 7.43-7.41 (m, 2H), 7.31 – 7.20 (m, 3H), 7.02 (dd, *J* = 8.8, 3.9 Hz, 2H), 6.94-6.92 (m, 2H), 5.76 (s, 2H), 5.03-4.98 (m, 3H), 4.85 – 4.81 (m, 2H), 3.55 (d, *J* = 3.4 Hz, 2H), 2.27 (s, 2H). ^{13}C{^{1}H} NMR (101 MHz, $CDCl_3$): δ 157.7, 151.7, 135.2, 132.5, 130.8, 130.3, 128.3, 128.2, 128.1, 127.1, 125.1, 117.7, 116.6, 116.2, 103.7, 99.2, 68.1, 45.6, 30.2, 25.2. HRMS of *cis*-3afa (ESI, Q-TOF) m/z: $[M+H]^+$ calculated for $C_{34}H_{27}O_4$ 499.1909, Found 499.1913.

***trans*-3afa:** white amorphous solid, Melting point 257-260 °C; ^{1}H NMR (400 MHz, $CDCl_3$): δ 7.74 (d, *J* = 2.2 Hz, 2H), 7.56 (d, *J* = 8.8 Hz, 2H), 7.48 (d, *J* = 8.8 Hz, 2H), 7.42-7.41 (m, 2H), 7.30 – 7.25 (m, 2H), 7.23 – 7.18 (m, 1H), 7.03 (d, *J* = 8.8 Hz, 2H), 6.98 (dd, *J* = 8.8, 2.3 Hz, 2H), 6.23 – 6.20 (m, 2H), 5.10 (t, *J* = 3.1 Hz, 1H), 5.00 (d, *J* = 13.9 Hz, 2H), 4.68 – 4.60 (m, 2H), 3.53 (s, 2H), 2.28 (d, *J* = 3.2 Hz, 2H). ^{13}C{^{1}H} NMR (101 MHz, $CDCl_3$): δ 158.5, 151.9, 135.2, 132.4, 130.8, 130.1, 128.7, 128.3, 128.2, 127.1, 125.4, 117.7, 116.5, 105.5, 98.4, 70.1, 45.7, 30.1, 24.7. HRMS (ESI, Q-TOF) m/z: $[M+H]^+$ calculated for $C_{34}H_{27}O_4$ 499.1909, Found 499.1910.

4.4.5. Procedure for the gram-scale synthesis of 3aa. A round bottom flask equipped with a magnetic stir bar was charged with 3-ethoxy 2-phenyl cyclobutanone (5.26 mmol, 1 equiv.,), 2-naphthol (10.5 mmol, 2 equiv.), and PTSA (2.08 mmol, 0.40 equiv.). Toluene (45 mL) was added as a solvent to the reaction mixture and was stirred under an open atmosphere until the completion of the reaction (as monitored by TLC). The solvent was removed under reduced pressure by a rotary evaporator. Then, the crude product was further purified by column chromatography on silica gel with EtOAc/hexane as eluent to afford the product 3aa (0.91 g, 2.19 mmol) in 41% yield.

4.5. References

(1) (a) Reissig, H.-U.; Zimmer, R. *Chem. Rev.* **2003**, *103*, 1151-1196. (b) Ishida, N.; Murakami, M. *Chem. Rev.* **2021**, *121*, 264-299. (c) Watson, I. D. G.; YU, L.; Yudin, A. K. *Acc. Chem. Res.* **2006**, *39*, 194-206. (d) Williamson, K. S.; Michaelis, D. J.; Yoon, T. P. *Chem. Rev.* **2014**, *114*, 8016-8036. (e) Ghosh, A.; Dey, R.; Banerjee, P. *Chem. Commun.* **2021**, *57*, 5359-5373.

(2) (a) Arnone, A.; Nasini, G.; de Pava, O. V.; Merlini, L. *J. Nat. Prod.* **1997**, *60*, 971-975. (b) Dumontet, V.; van Hung, N.; Adeline, M. T.; Riche, C.; Chiaroni, A.; Sevenet T.; Gue´ritte, F. *J. Nat. Prod.* **2004**, *67*, 858-862. (c) Xu, M. F.; Shen, L. Q.; Wang, K. W. *Fitoterapia.* **2009**, *80*, 461-464. (d) Nakashima, K. I.; Abe, N.; Kamiya, F.; Ito, T.; Oyama, M.; Iinuma, M. *Helv. Chim. Acta.* **2009**, *92*, 1999-2008.

(3) Yin, G.; Ren, T.; Rao, Y.; Zhou, Y.; Li, Z.; Shu, W.; Wu, A. *J. Org. Chem.* **2013,** *78*, 3132-3141.

(4) Allan, J. A. V.; Giannini, D. D.; Whitesides, T. H. *J. Org. Chem.* **1982**, *47*, 820-823.

(5) Mashraqui, S. H.; Patil, M. B.; Mistry, H. D.; Ghadigaonkar, S.; Meetsma, A. *Chem. Lett*, **2004**, *33*, 1058-1059.

(6) Jurd, L.; Waiss, A. C. Jr.; *Tetrahedron.* **1965**, *21*, 1471-1483.

(7) (a) Selenski, C.; Pettus, T. R. R. *Tetrahedron*. **2006**, *62(22)*, 5298-5307. (b) Yang, Z. Y.; He, Y.; Toste, F. *J. Am. Chem. Soc.* **2016**, *138*, 9775-9778.

(8) (a) Wang, S.; Lin, J.-J.; Cui, X.; Li, J.-P.; Huang, C. *J. Org. Chem.* **2021**, *86*, 16396-16408. (b) Wang, F.; Chen, F.; Qu, M.; Li, T.; Liu, Y.; Shi, M. *Chem. Commun.*, **2013**, *49*, 3360-3362. (c) Ganguly, N. C.; Roy, S.; Mondal, P. *RSC Adv.*, **2014**, *4*, 42078-42086. (d) Zhu, Y.; Yao, Z.; Xu, F. *Tetrahedron*. **2018**, *74*, 4211-4219. (e) Srinivas, V.; Koketsu, M. *J. Org. Chem*. **2013**, *78*, 11612-11617. (f) Li, J.; Wang, S.; Xu, G.; Cui, X.; Zi, B.; Liu, T.; Huang, C. *Asian J. Org. Chem.* **2022**, *11*, e202100797.

(9) Matsuo, J. *Tetrahedron Lett.* **2014**, *55*, 2589.

(10) (a) Sasaki, S.; Tanaka, H.; Ishibashi, H.; Matsuo, J. *J. Am. Chem. Soc.* **2008**, *130*, 11600-11601. (b) Lin, Y.; Yang, X.; Pan, W.; Rao, Y. *Org. Lett.* **2016**, *18*, 2304-2307. (c) Okado, R.; Ishibashi, H.; Matsuo, J. *Org. Lett.* **2010**, *12*, 3266-3268. (d) Shan, G.; Liu, P.; Rao, Y. *Org. Lett.* **2011**, *13*, 1746-1749. (e) Shan, G.; Sun, X.; Xia, Q.; Rao, Y. *Org. Lett.* **2011**, *13*, 5770-5773. (f) Kawano, M.; Kiuchi, T.; Negishi, S.; Tanaka, H.; Hoshikawa, T.; Ishibashi, H.; Matsuo, J. *Angew. Chem., Int. Ed.* **2013**, *52*, 906-910. (g) Zhou, Y.; Tang, Z.; Song, Q. *Adv. Synth. Catal.* **2017**, *359*, 952-958. (h) Hazra, A.; Kanji, T.; Banerjee, P. *J. Org. Chem.* **2023**, *88*, 960-971.

(11) Martin, J. C.; Meen, R. *J. Org. Chem*. **1965**, *30*, 4311-4313.

(12) Xu, S.; Wang, Z.; Zhang, X.; Zhang, X.; Ding, K. *Angew. Chem. Int. Ed.* **2008**, *47*, 2840-2843.

(13) Rahmatpour, A.; Sajjadinezhad, S. M.; Mirkani, A.; Notash, B. *Tetrahedron.* **2021**, *95*, 132341.

(14) Kanie, M.; Yoshimura, T.; Matsuo, J. *Synthesis*. **2018**, *50*, 548-554.

(15) Feiler, L. A.; Otto, P.; Huisgen, R. *Chem. Ber.* **1969,** *102*, 3405-3427.

(16) Liu, H.; Wang, Y.; Guo, X.; Huo, L.; Xu, Z.; Zhang, W.; Qiu, S.; Yang, B.; Tan, H. *Org. Lett.* **2018**, *20*, 546-549.

(17) Gradillas, A.; Castells, J. P. *Angew. Chem. Int. Ed.* **2006**, *45*, 6086-6101.

(18) (a) Boisnard, S.; Carbonnelle, A.-C.; Zhu, J. *Org. Lett*. **2001**, *3*, 2061-2064. (b) Bonazzi, S.; Cheng, B.; Wzorek, J. S.; Evans, D. A. *J. Am. Chem. Soc.* **2013**, *135*, 9338-9341.

(19) (a) Lindoy, L. F.; Lip, H. C.; Rea, J. H.; Smith, R. J.; Henrick, K.; Mcpartlin, M.; Tasker, P. A. *Inorg. Chem.* **1980**, *19*, 3360-3365. (b) Pota, K.; Molnar, E.; Kalman, F. K.; Freire, D. M.; Tircsó, G.; Green, K. N. *Inorg. Chem.* **2020**, *59*, 11366-11376. (c) Boraey, H. A. E.; Gammal, O. A. E. *Spectrochim. Acta - A: Mol. Biomol. Spectrosc*. **2015**, *138*, 553-562. (d) Shimizu, T.; Takahashi, N.; Huber, V. J.; Asawa, Y.; Ueda, H.; Yoshimori, A.; Muramatsu, Y.; Seimiya, H.; Kouji, H.; Nakamura, H.; Oguri, H. *Bioorg. Med. Chem.* **2021**, *30*, 115949.

(20) Frotscher, M.; Ziegler, E.; Oberwinkler, S. M.; Kruchten, P.; Neugebauer, A.; Fetzer, L.; Scherer, C.; Vieira, U. M.; Messinger, J.; Thole, H.; Hartmann, R. W. *J. Med. Chem.* **2008**, *51*, *7*, 2158–2169.

(21) Kamble, S. B.; Maliekal, P. J.; Dharpure, P. D.; Badani, P. M.; Karnik, A. V. *J. Org. Chem.* **2020**, *85*, 7739-7747.

(22) Svestka, D.; Otevrel, J.; Bobal, P. *Adv. Synth. Catal.* **2022**, *364*, 2174–2183.

(23) (a) Chatterjee, A. K.; Choi, T.-L.; Sanders, D. P.; Grubbs, R. H. (b) Bunrit, A.; Sawadjoon, S.; Tšupova, S.; Sjöberg, P. J. R.; J. Samec, S. M. *J. Org. Chem.* **2016**, *81*, 4, 1450–1460.

4.6. NMR Spectra of the Compounds

^{1}H-NMR ($CDCl_3$, 400MHz) of 3aa

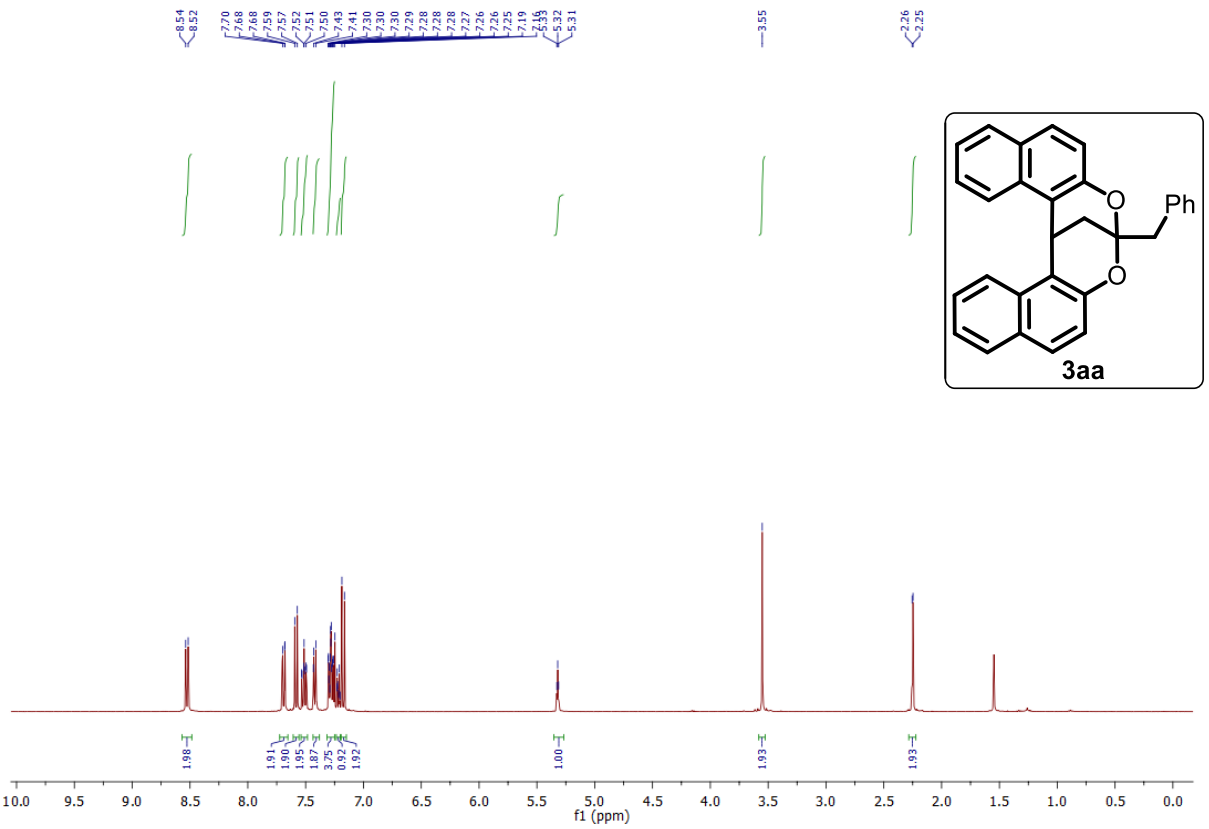

$^{13}C\{^{1}H\}$ -NMR ($CDCl_3$, 101MHz) of 3aa

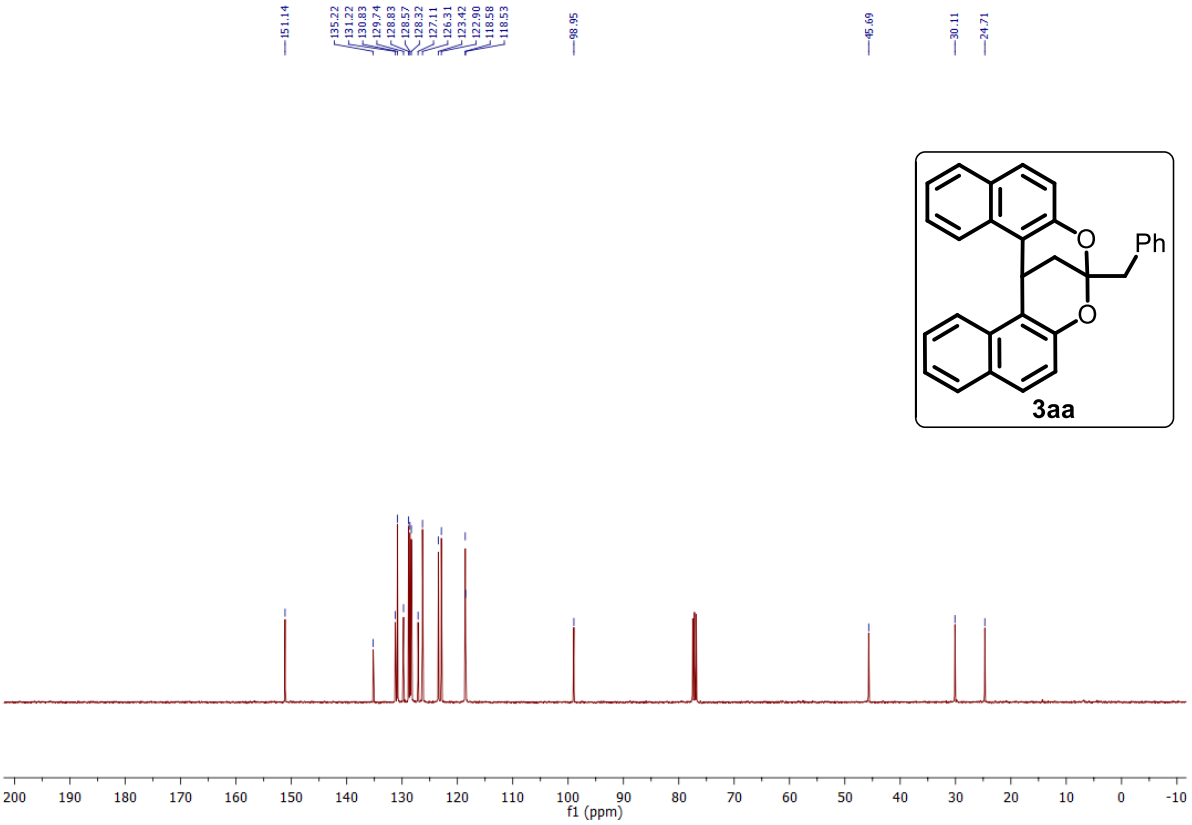

^{1}H-NMR ($CDCl_3$, 400MHz) of 3ba

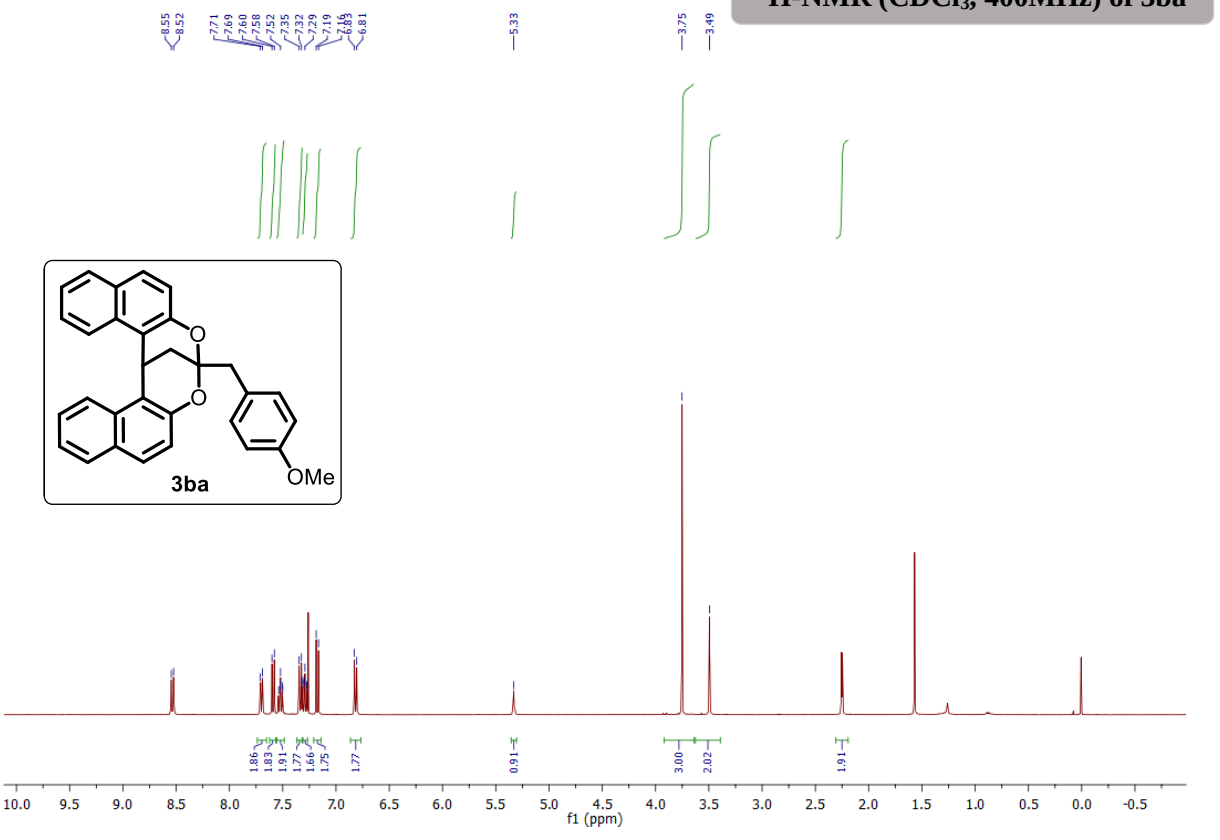

$^{13}C\{^{1}H\}$ -NMR ($CDCl_3$, 101MHz) of 3ba

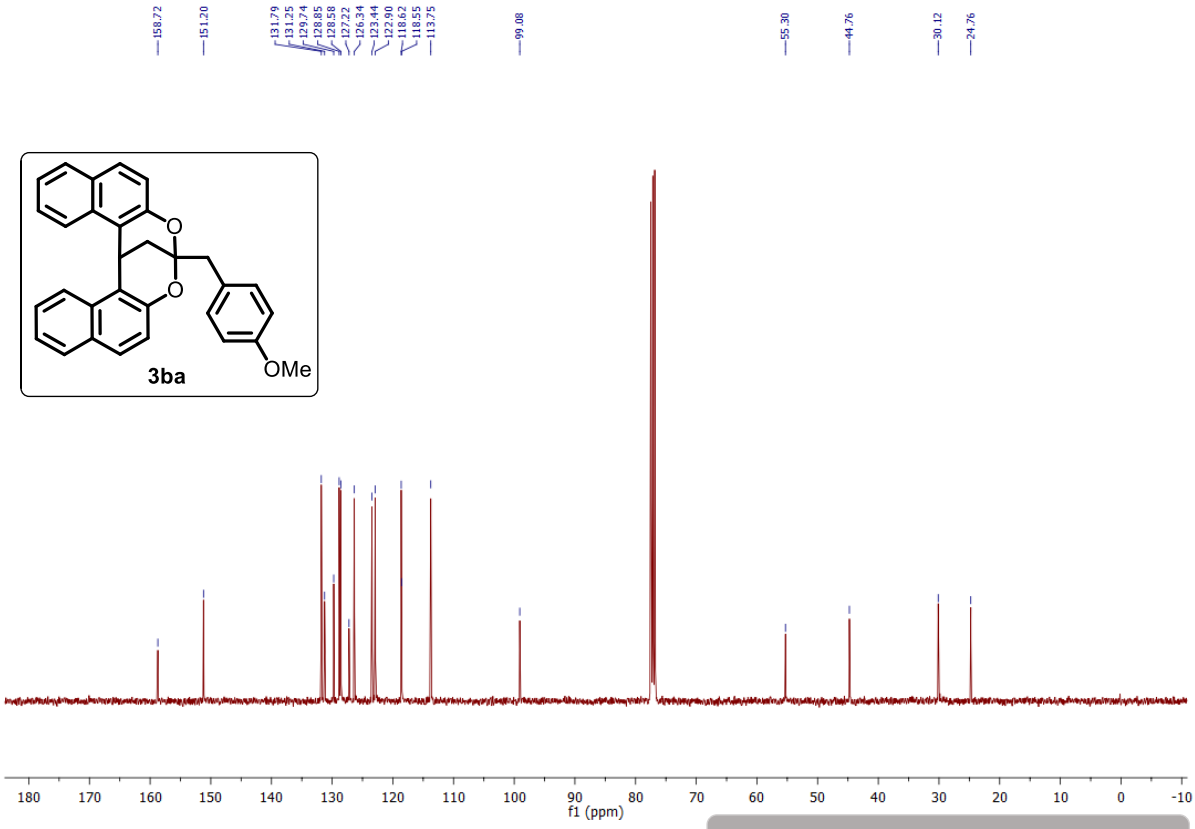

^{1}H-NMR ($CDCl_3$, 400MHz) of 3ca

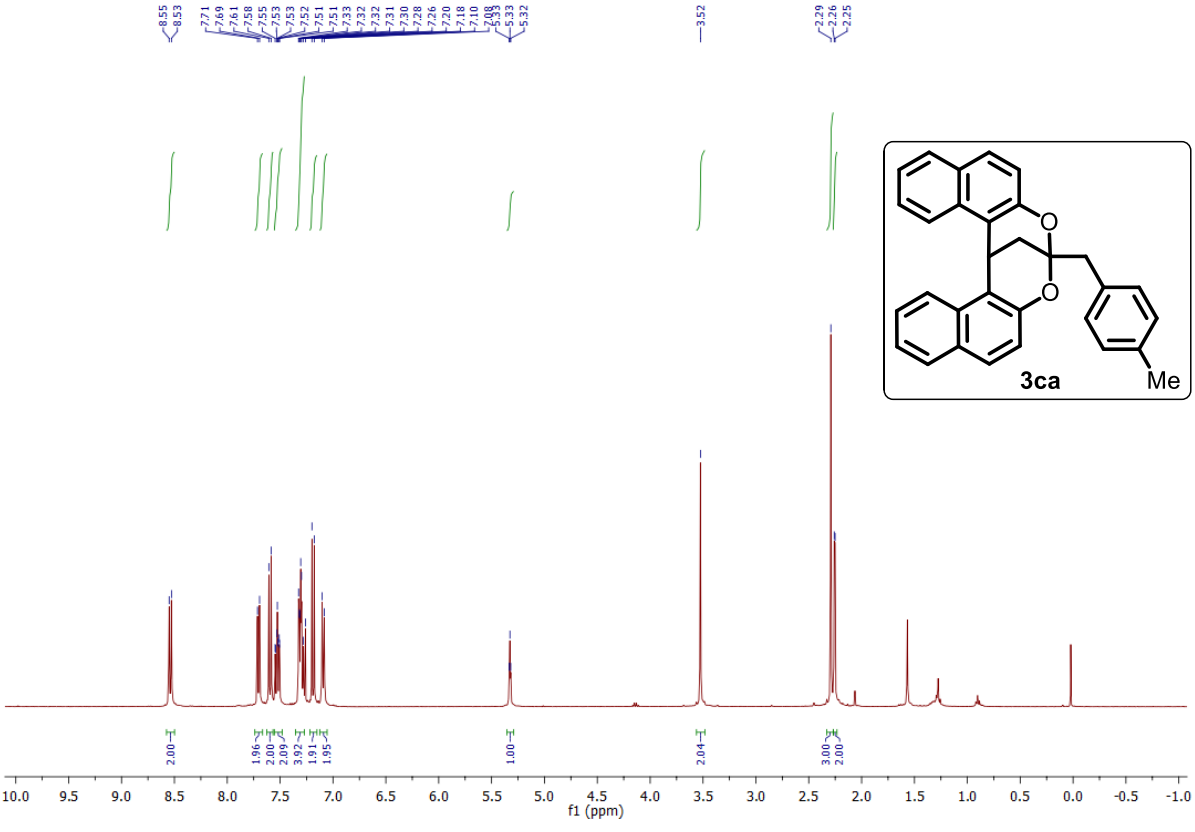

$^{13}C\{^{1}H\}$ -NMR ($CDCl_3$, 101MHz) of 3ca

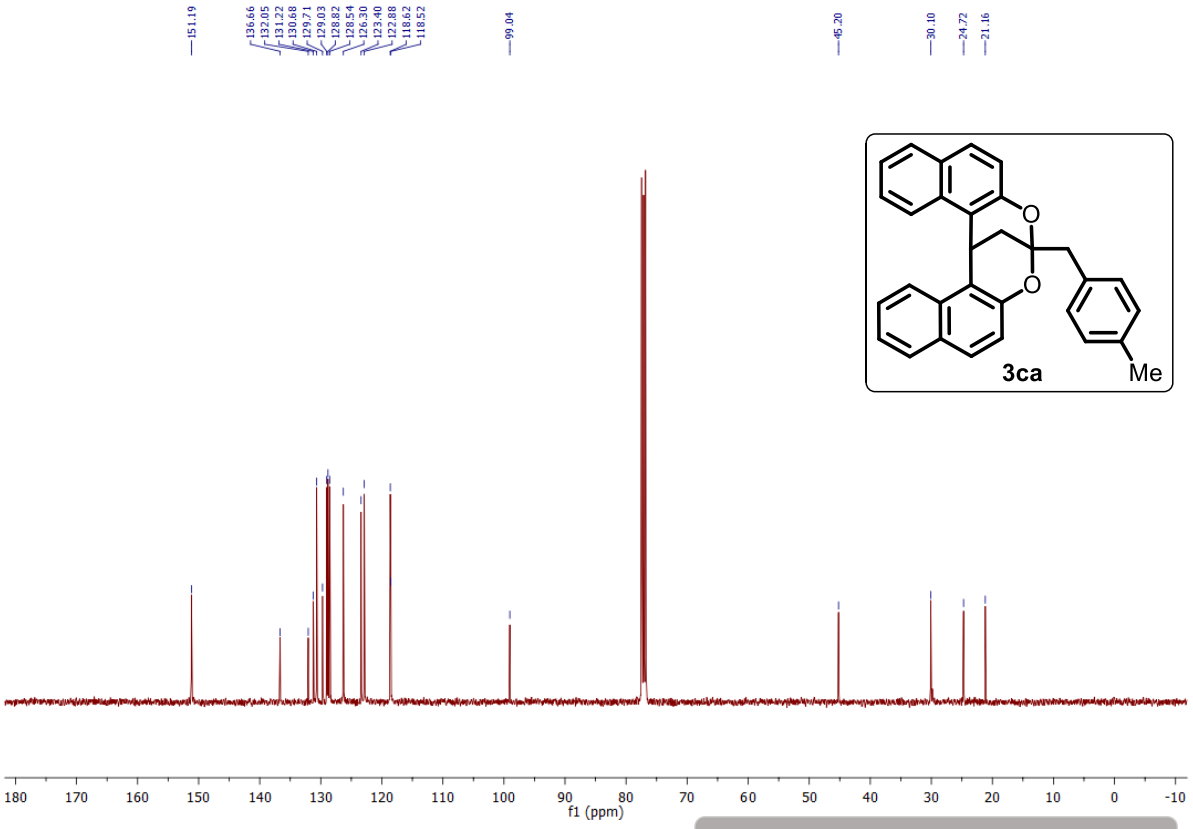

^{1}H-NMR ($CDCl_3$, 400MHz) of 3da

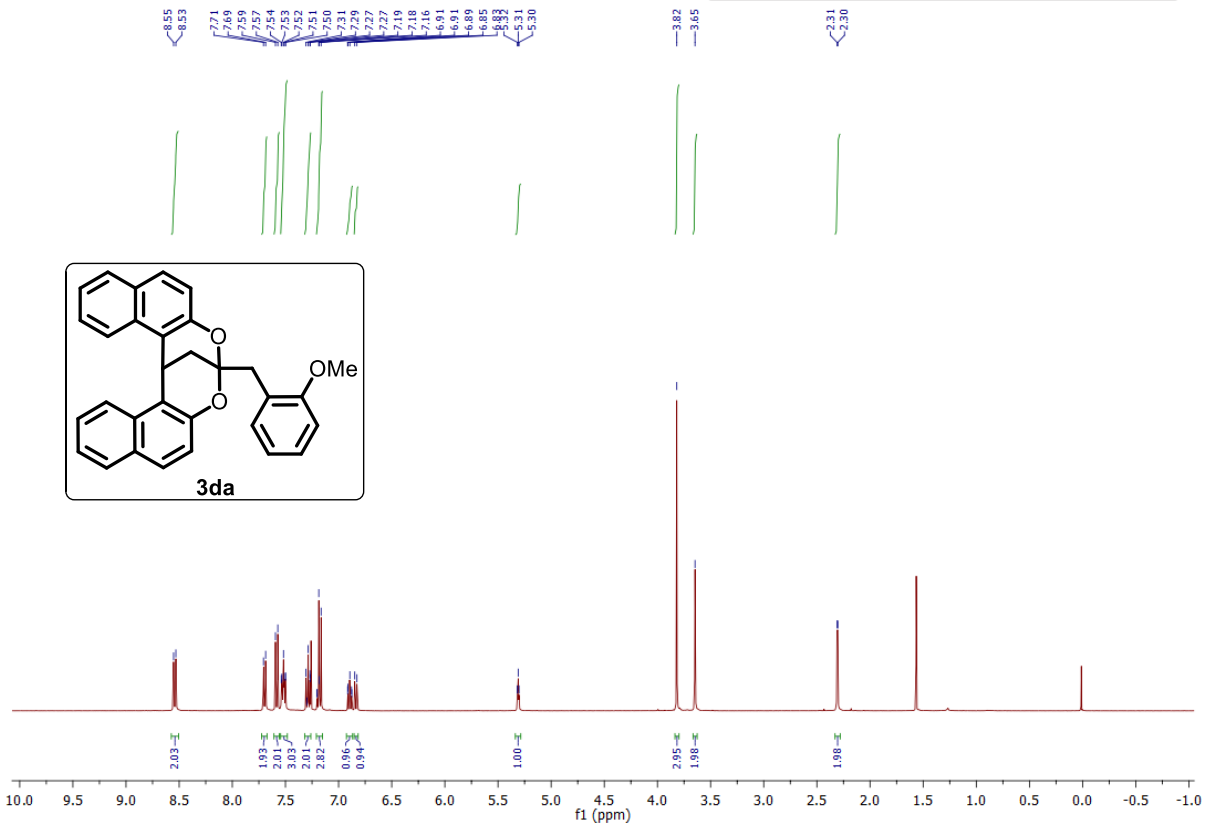

$^{13}C\{^{1}H\}$ -NMR ($CDCl_3$, 101MHz) of 3da

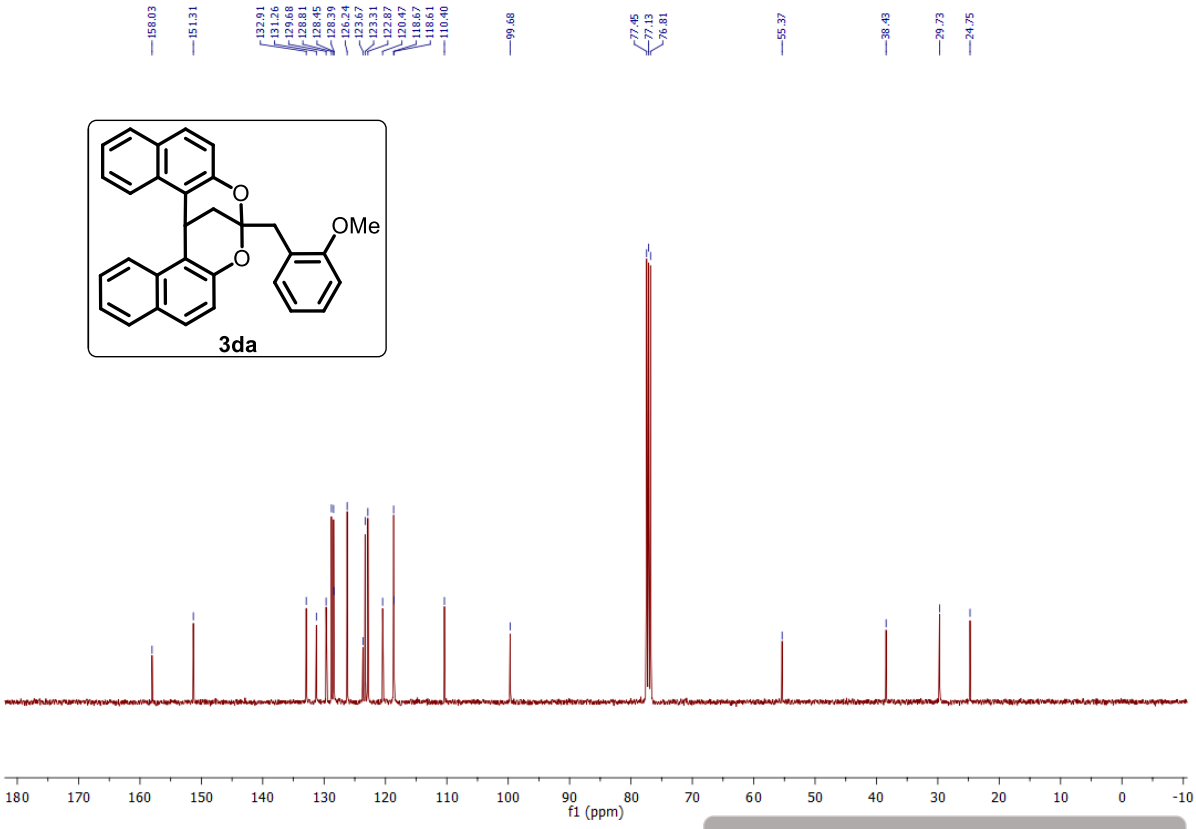

^{1}H-NMR ($CDCl_3$, 400MHz) of 3ea

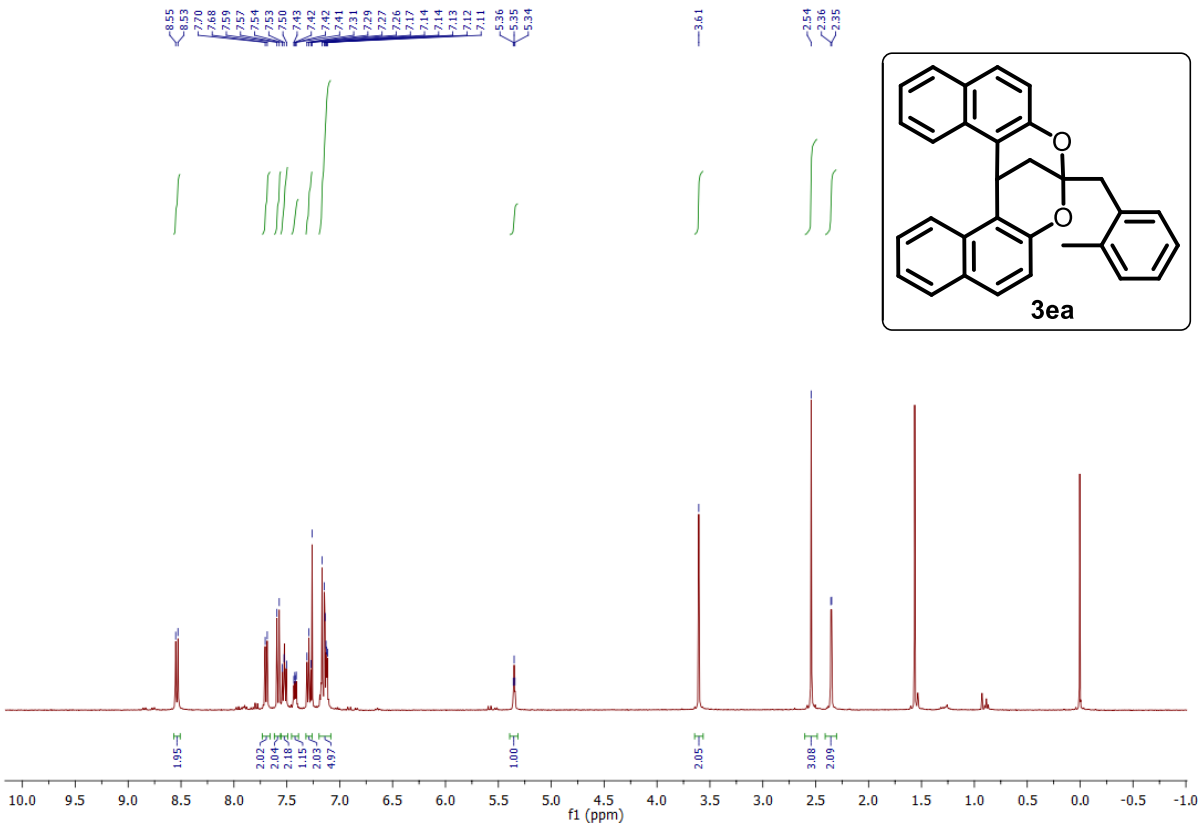

$^{13}C\{^{1}H\}$ -NMR ($CDCl_3$, 101MHz) of 3ea

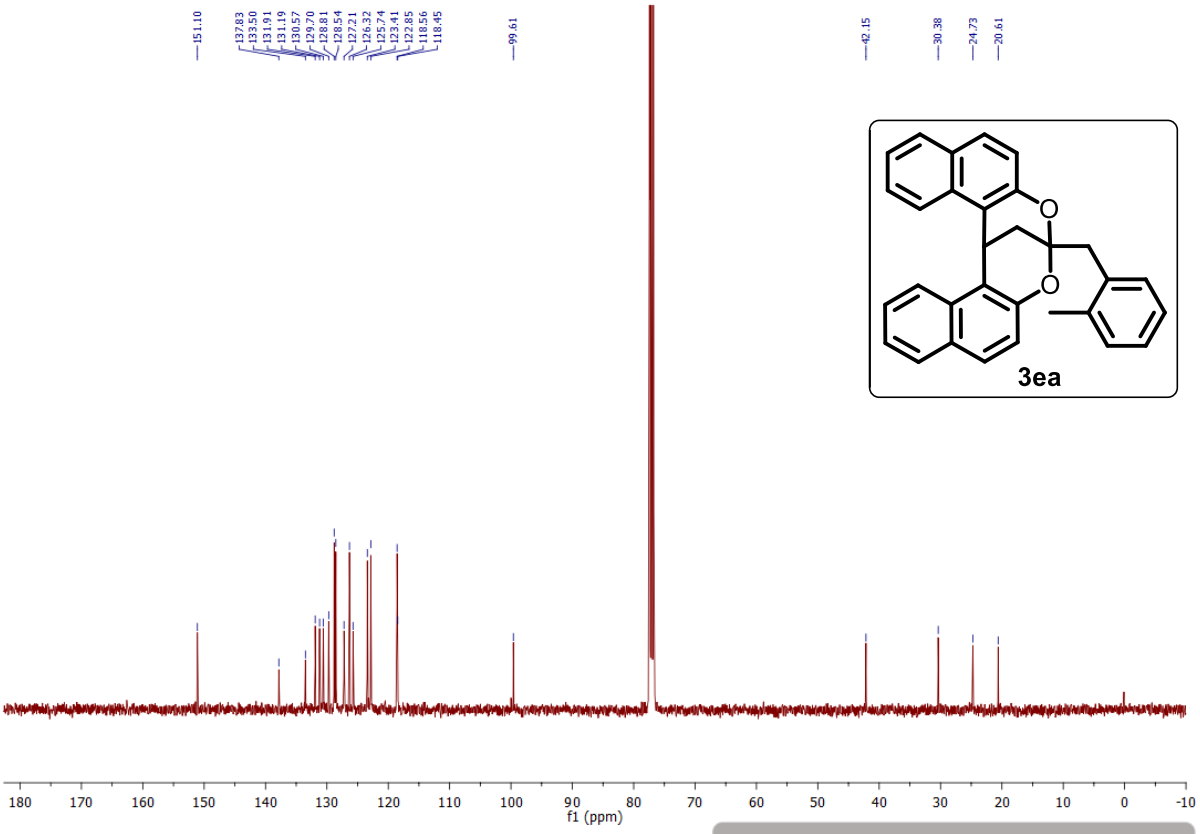

^{1}H-NMR ($CDCl_3$, 400MHz) of 3fa

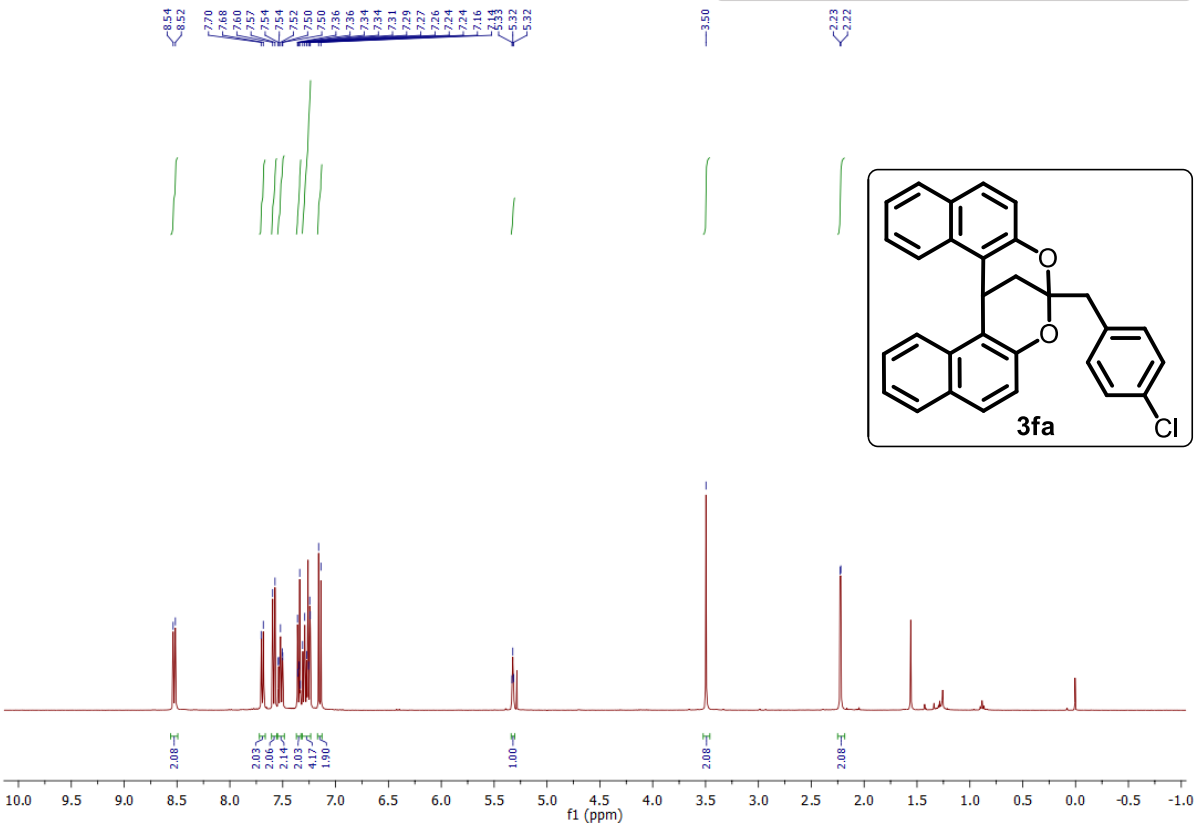

$^{13}C\{^{1}H\}$ -NMR ($CDCl_3$, 101MHz) of 3fa

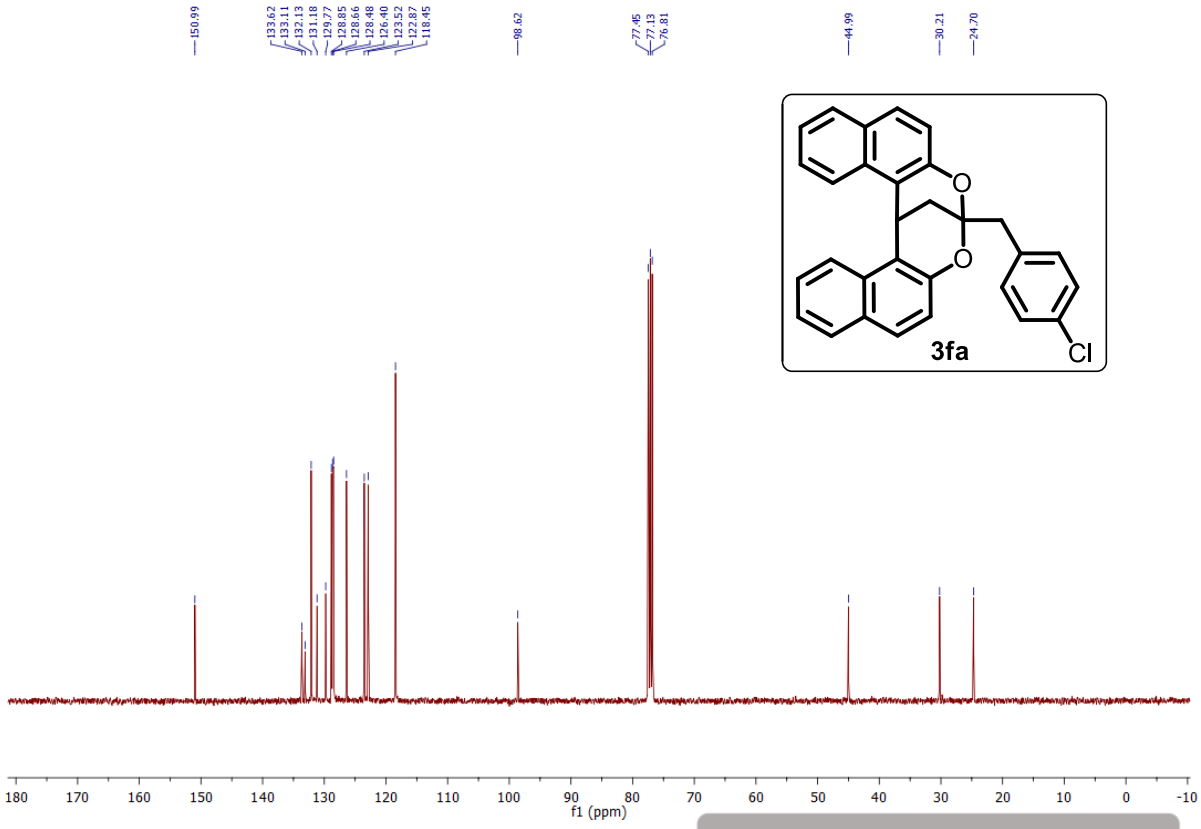

^{1}H-NMR ($CDCl_3$, 400MHz) of 3ga

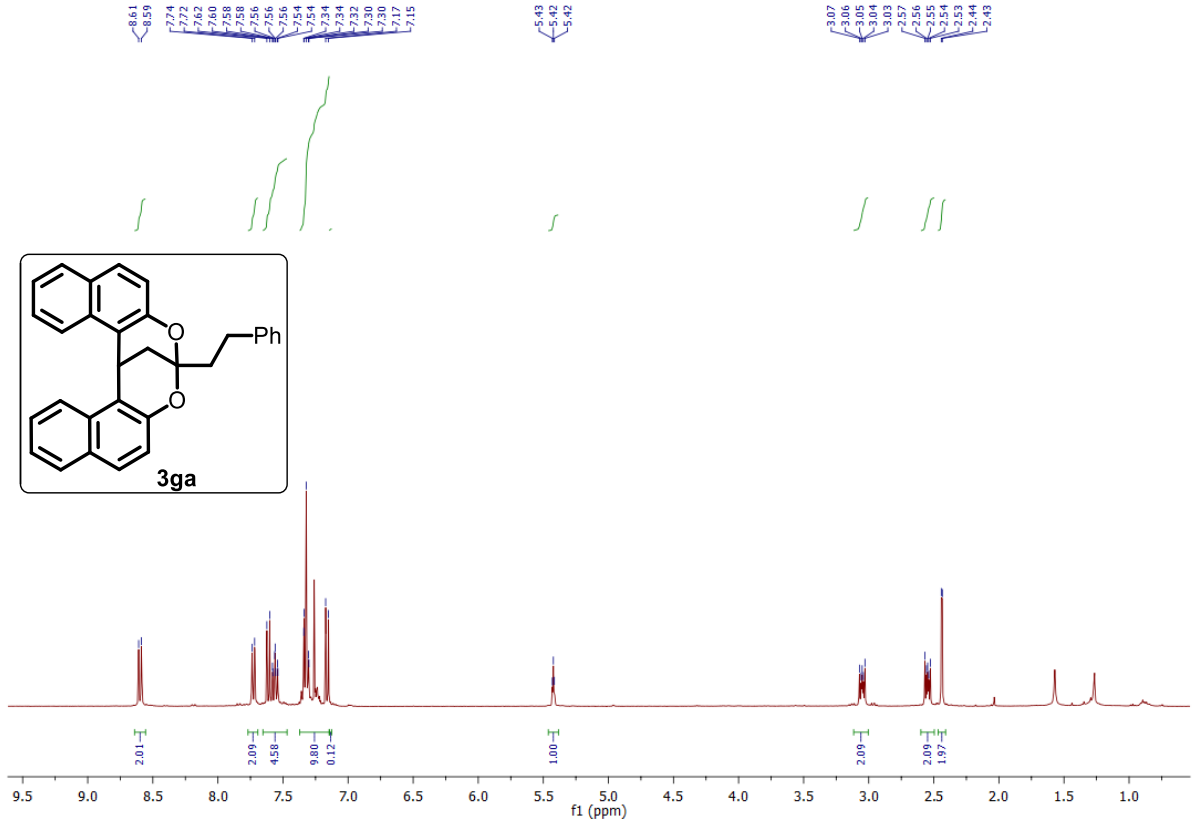

$^{13}C\{^{1}H\}$ -NMR ($CDCl_3$, 101MHz) of 3ga

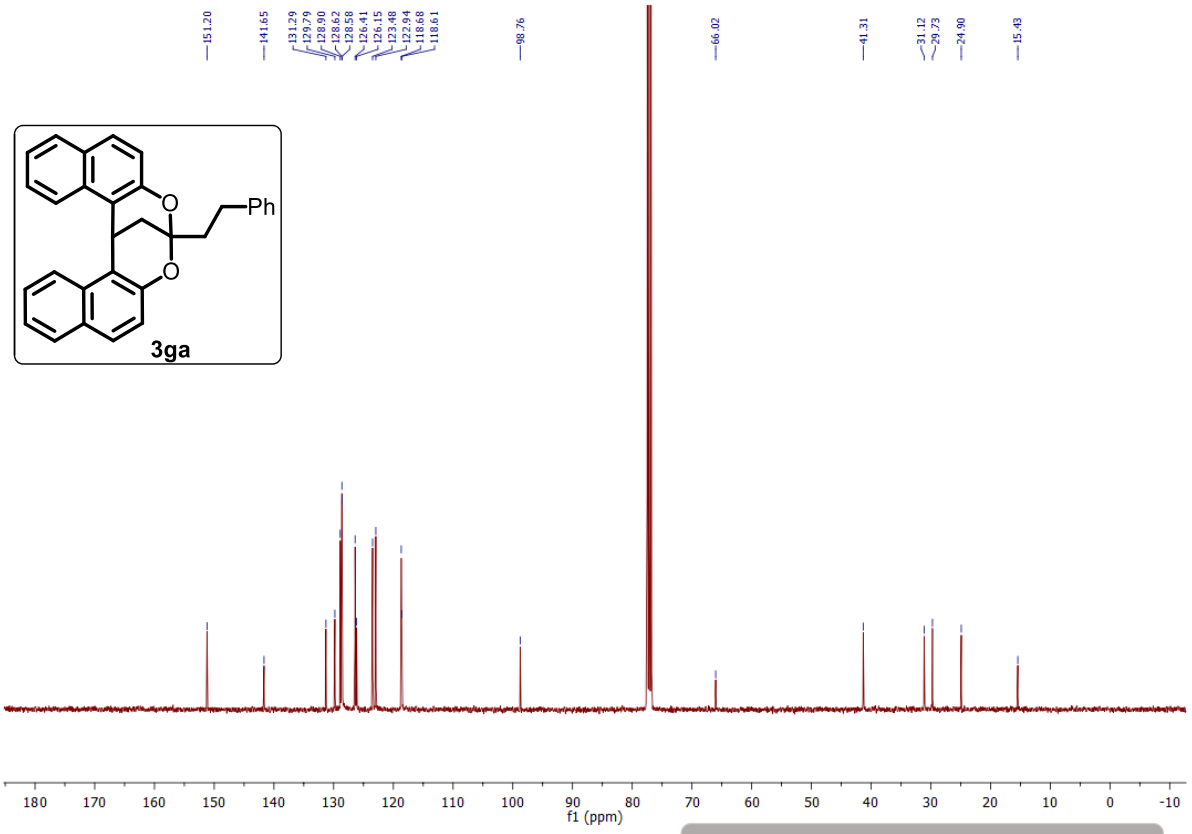

^{1}H-NMR ($CDCl_3$, 400MHz) of 3ha

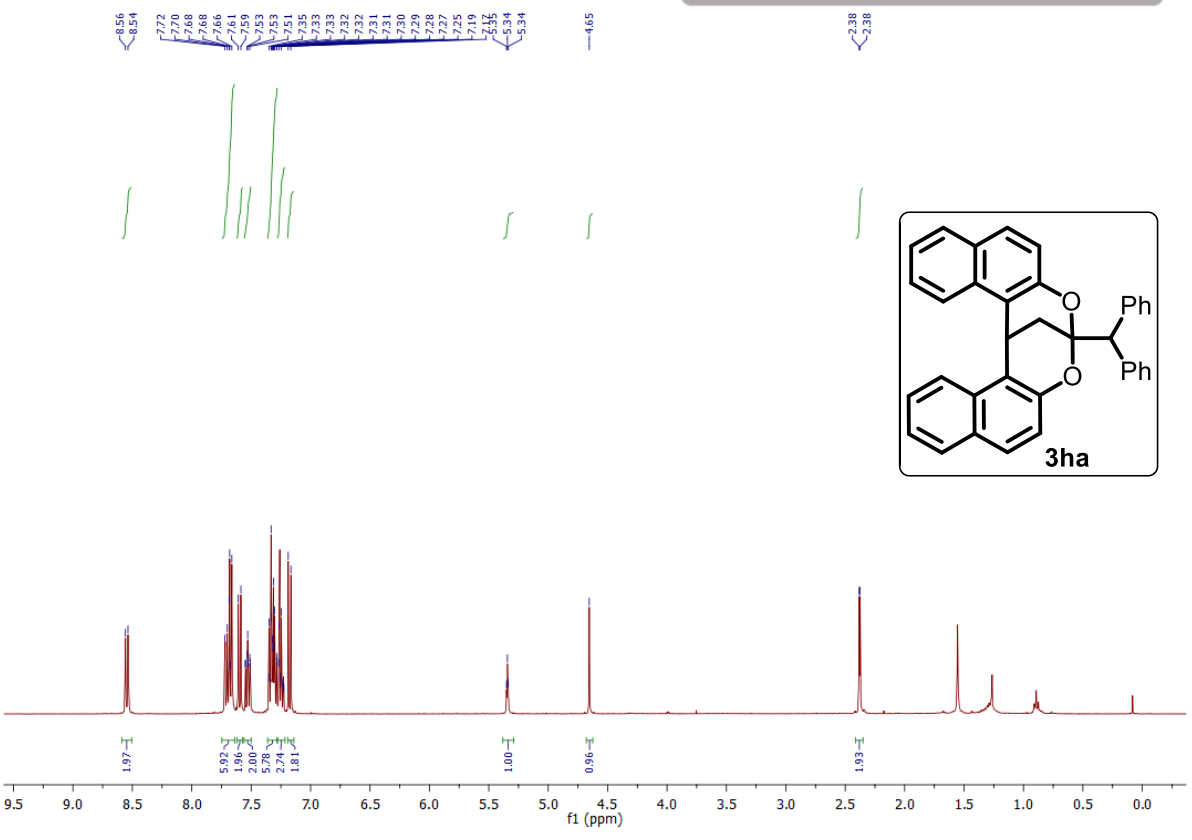

$^{13}C\{^{1}H\}$ -NMR ($CDCl_3$, 101MHz) of 3ha

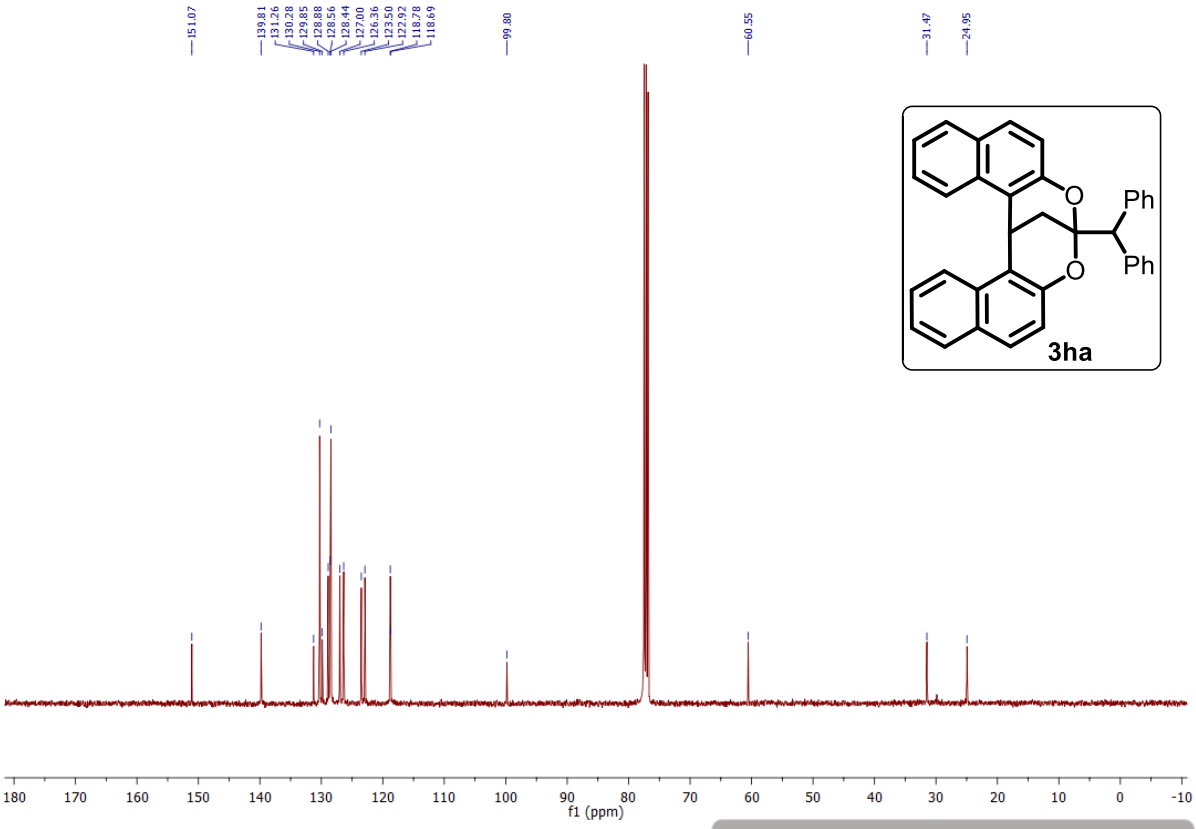

^{1}H-NMR ($CDCl_3$, 400MHz) of 3ab

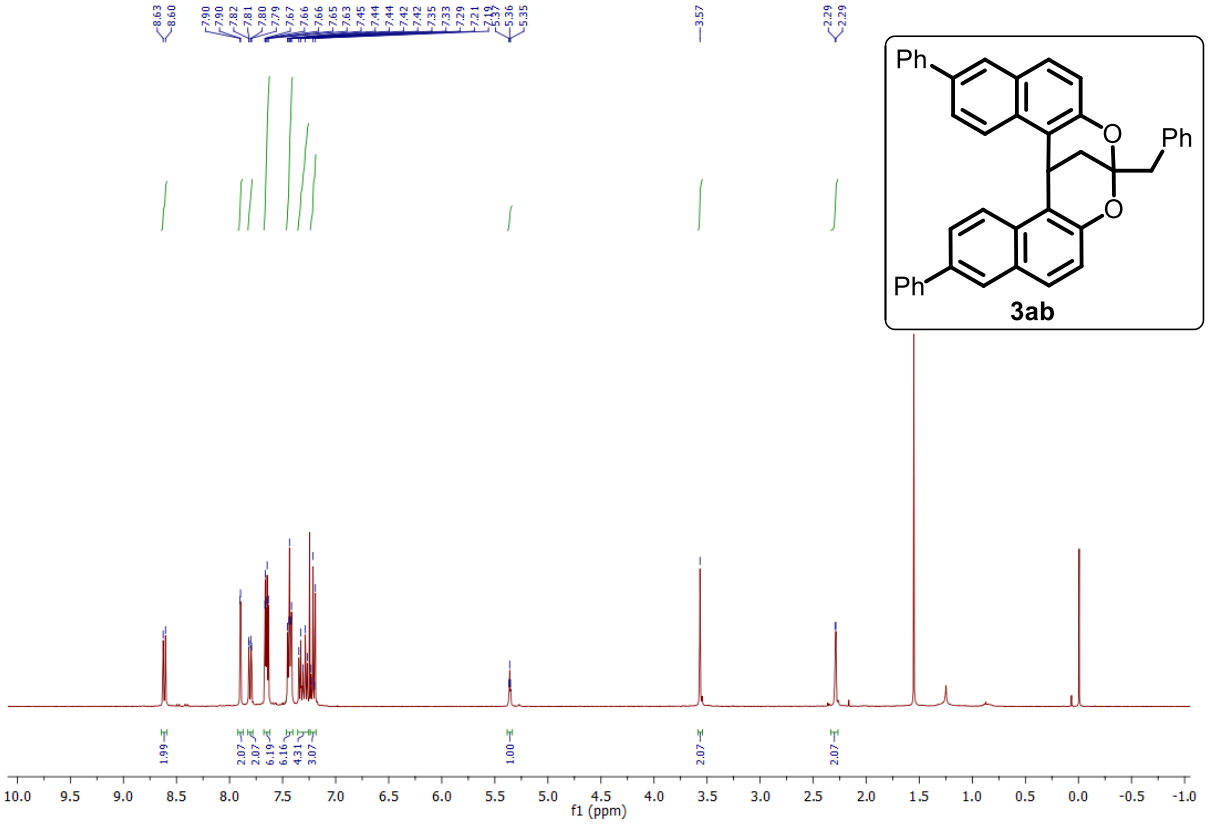

$^{13}C\{^{1}H\}$ -NMR ($CDCl_3$, 101MHz) of 3ab

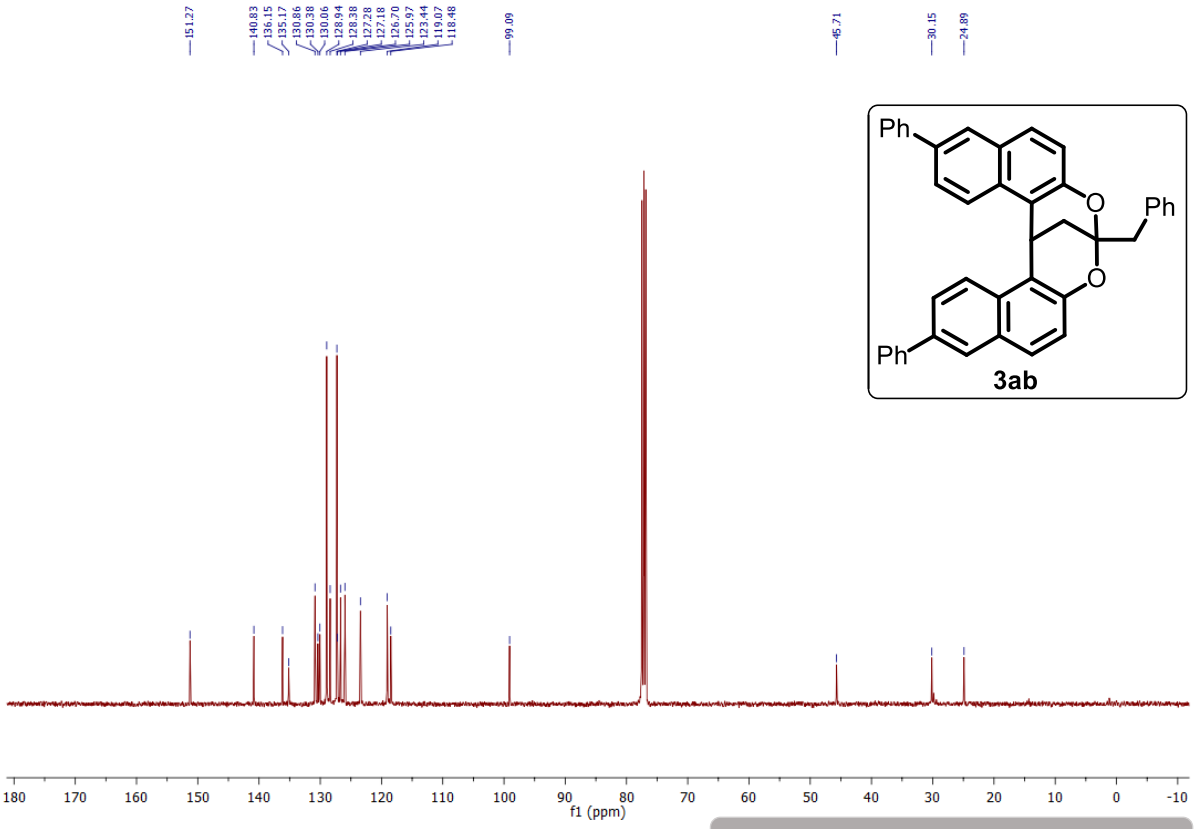

^{1}H-NMR ($CDCl_3$, 400MHz) of 3ac

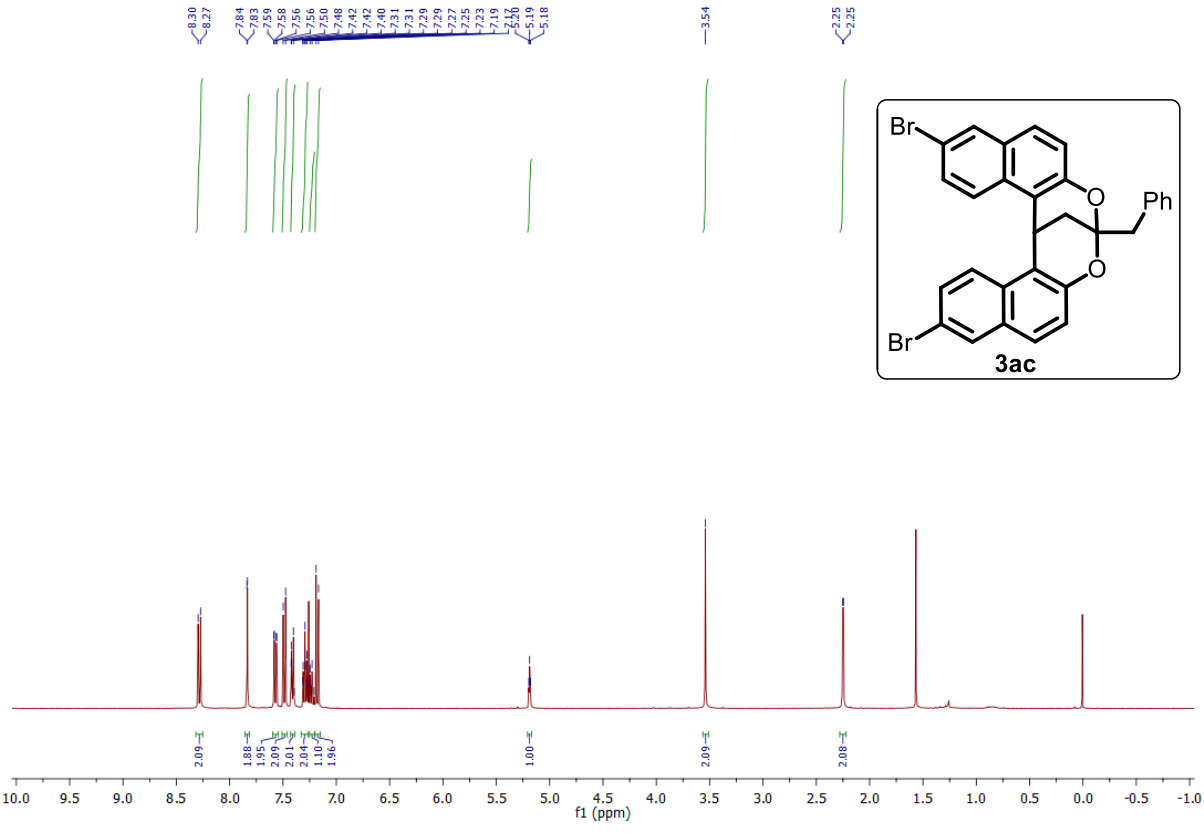

$^{13}C\{^{1}H\}$ -NMR ($CDCl_3$, 101MHz) of 3ac

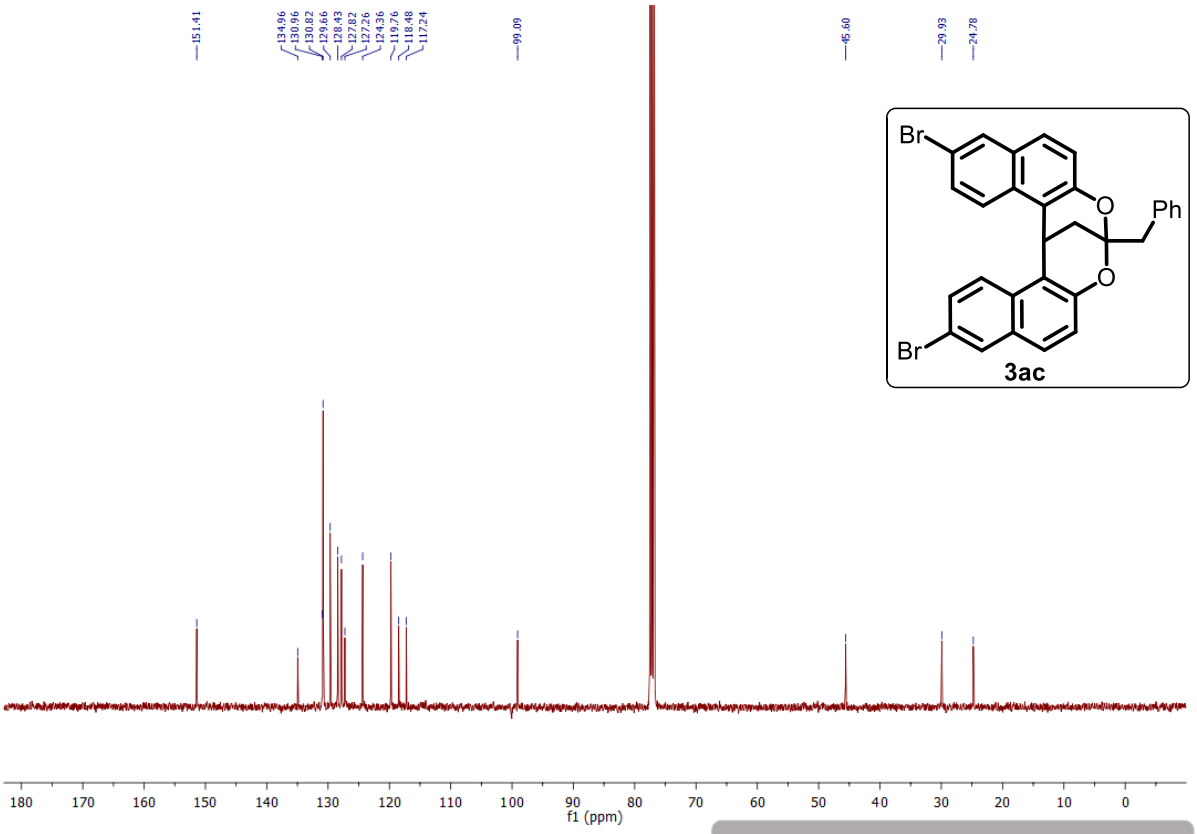

^{1}H-NMR ($CDCl_3$, 400MHz) of 3ad

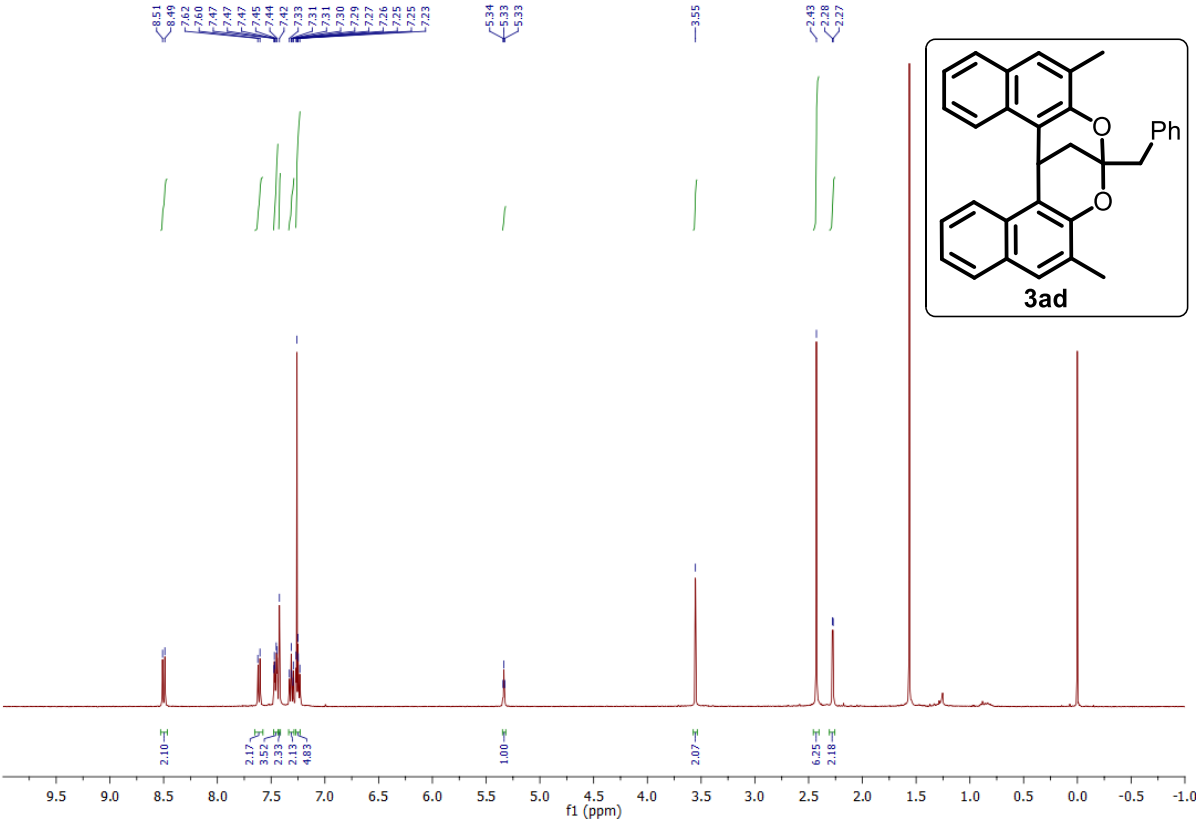

$^{13}C\{^{1}H\}$ -NMR ($CDCl_3$, 101MHz) of 3ad

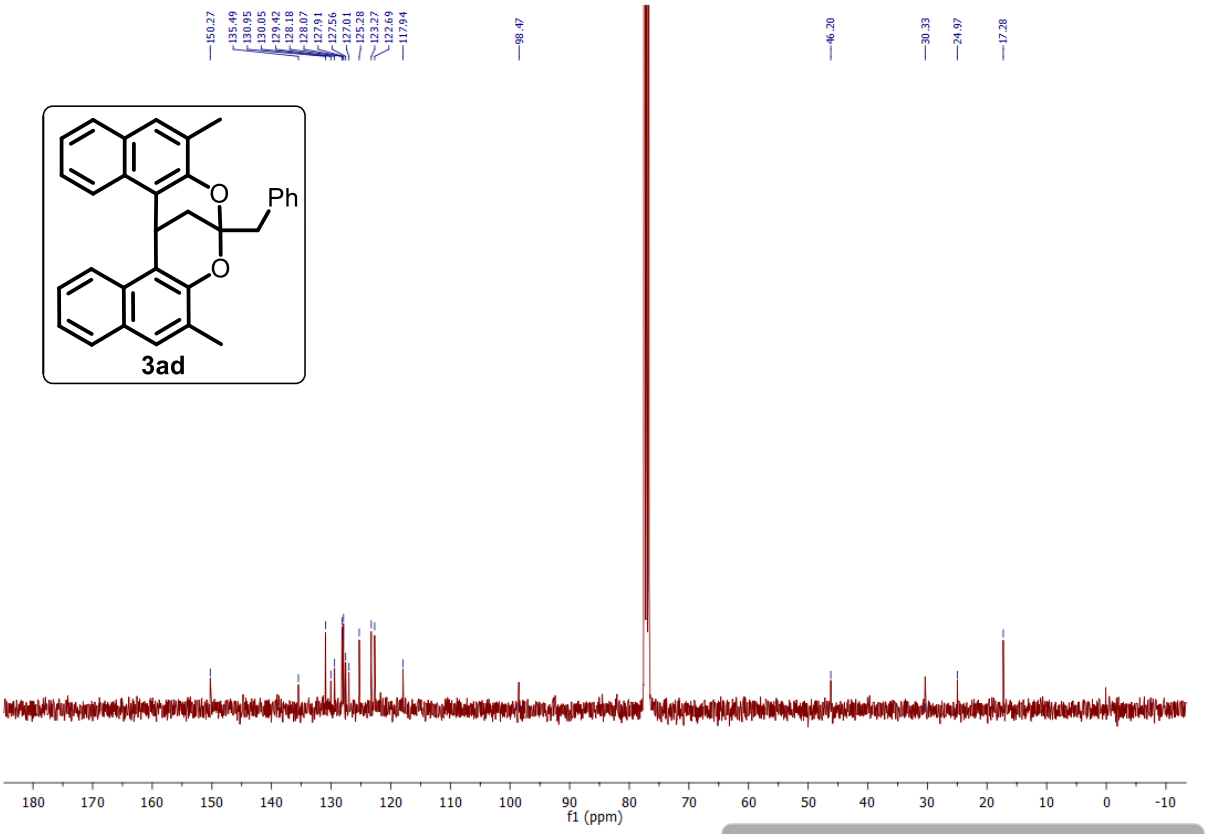

^{1}H-NMR ($CDCl_3$, 400MHz) of 3bd

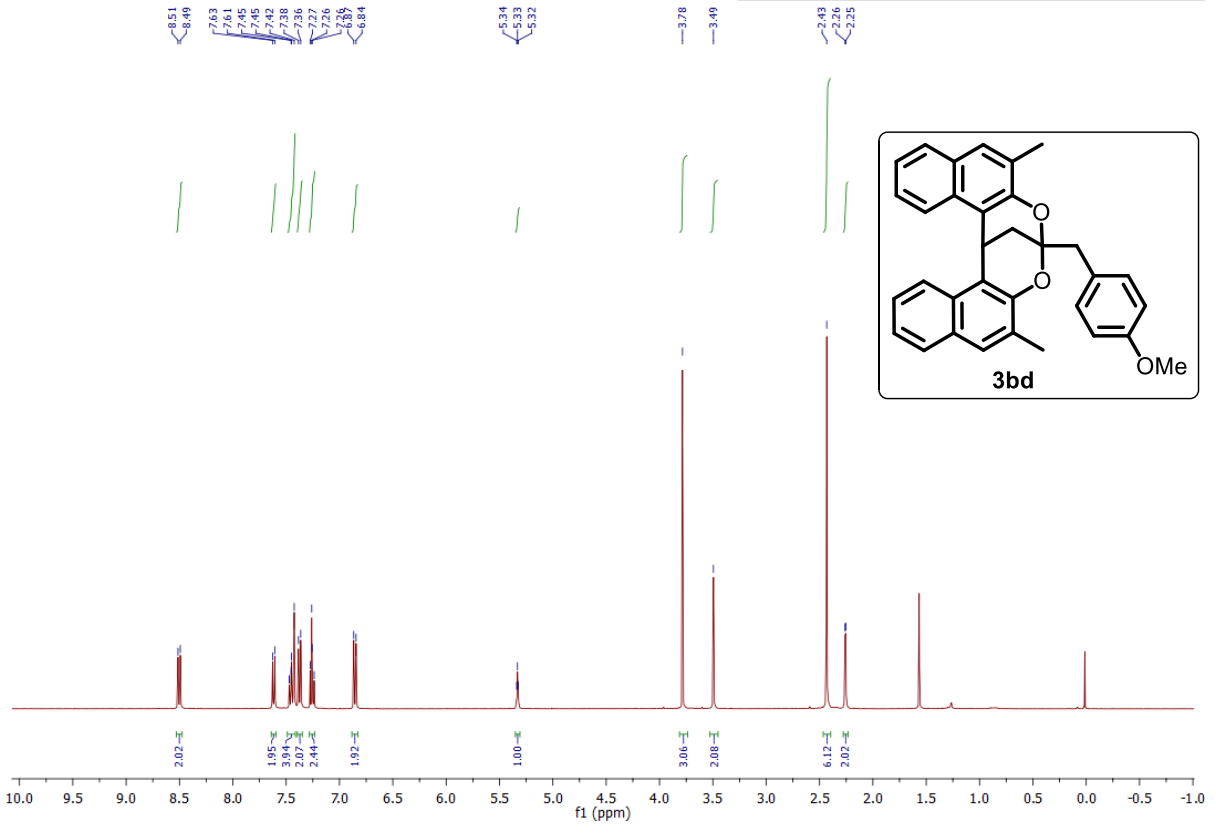

$^{13}C\{^{1}H\}$ -NMR ($CDCl_3$, 101MHz) of 3bd

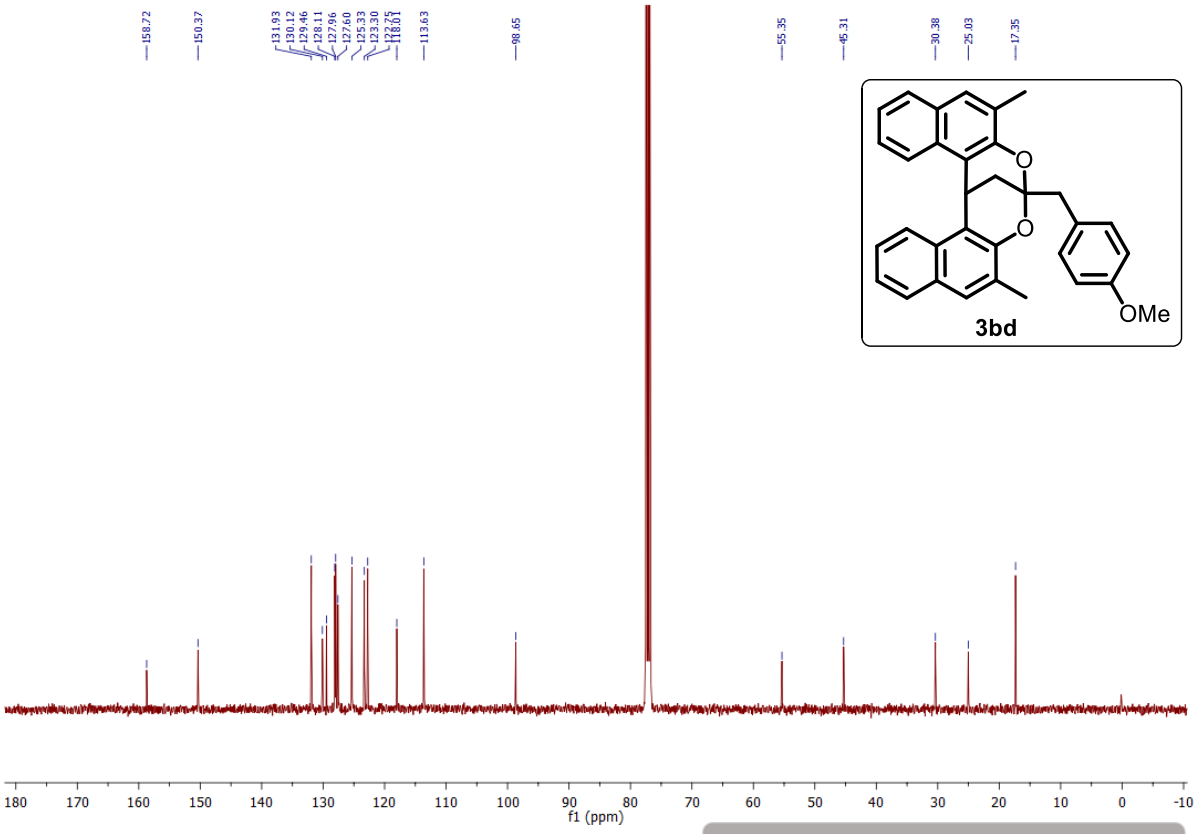

^{1}H-NMR ($CDCl_3$, 400MHz) of 3ae

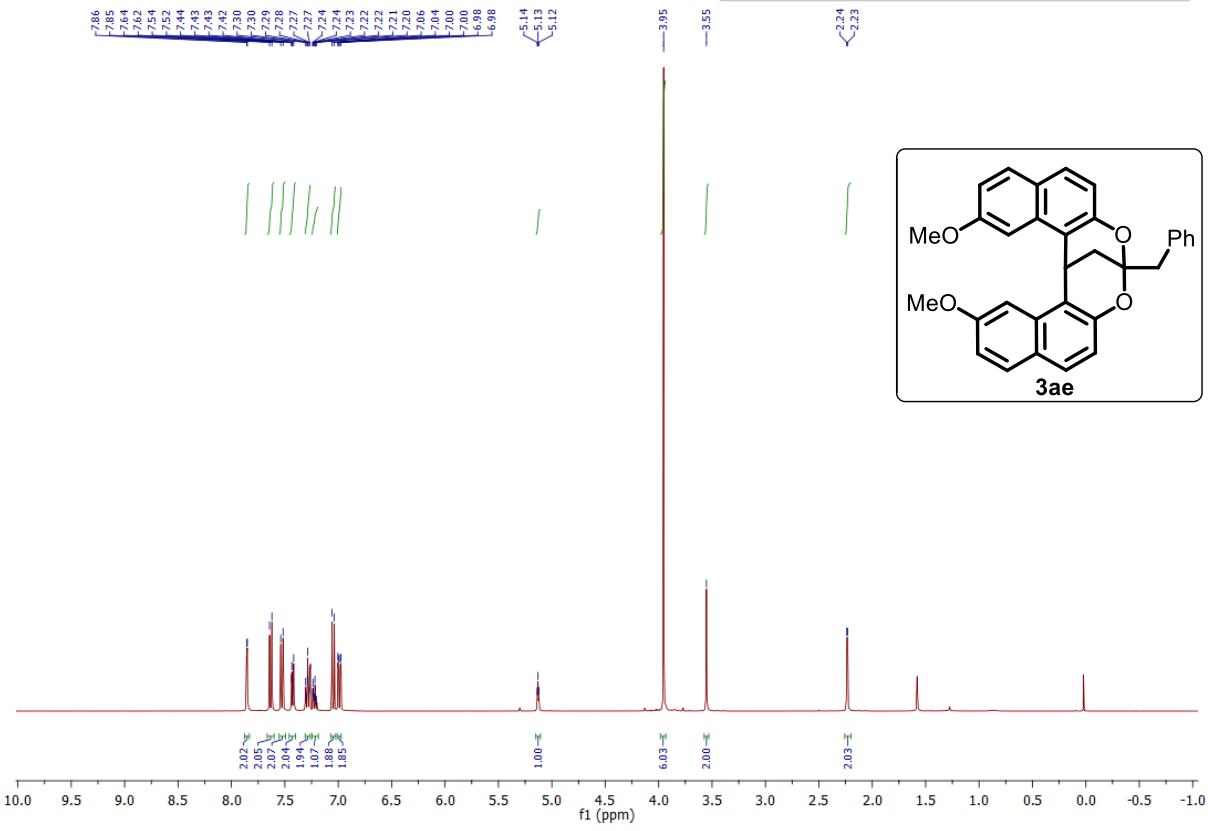

$^{13}C\{^{1}H\}$ -NMR ($CDCl_3$, 101MHz) of 3ae

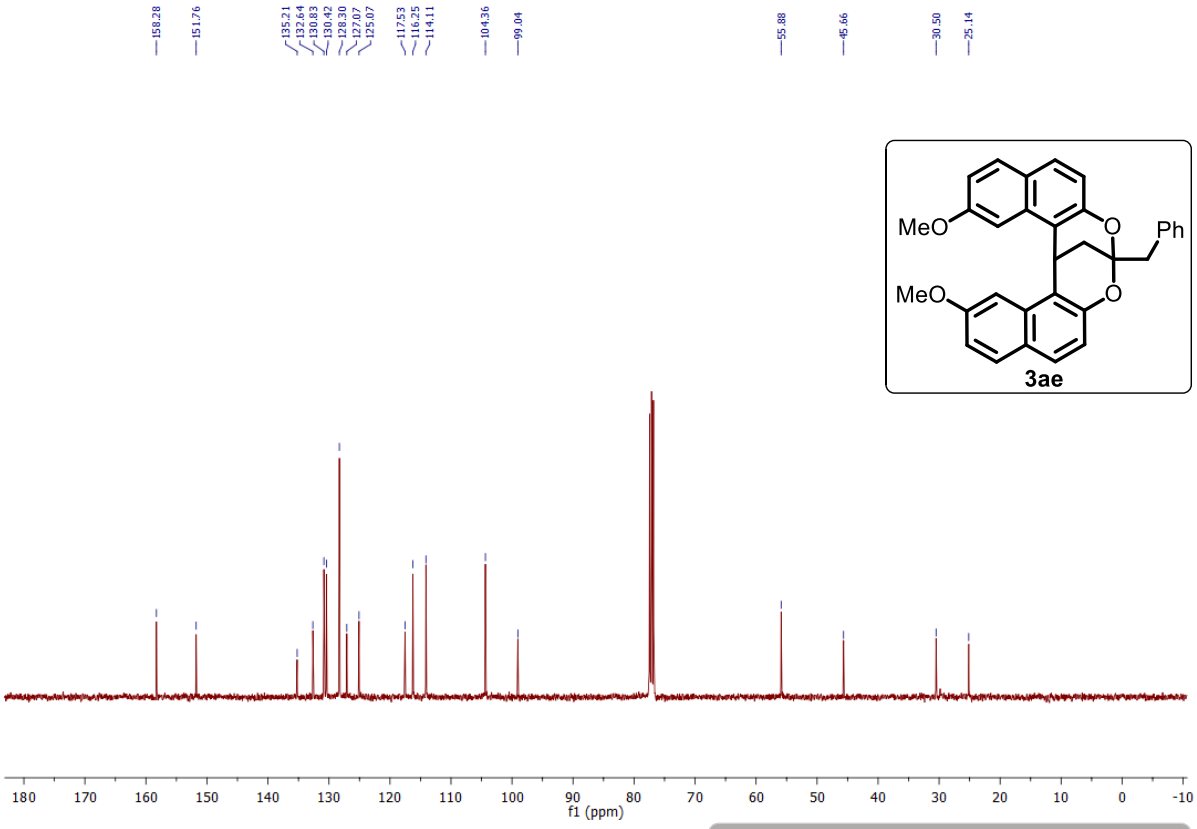

^{1}H-NMR ($CDCl_3$, 400MHz) of 3af

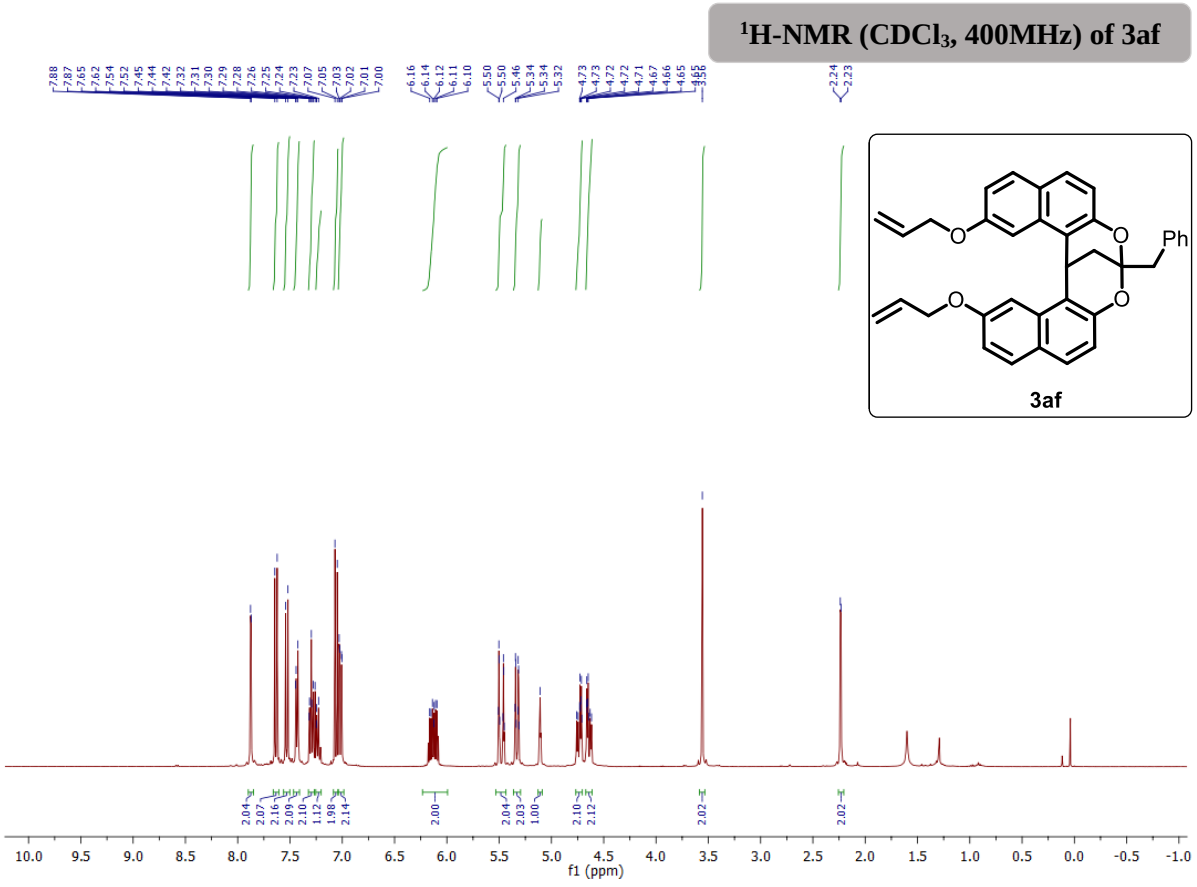

$^{13}C\{^{1}H\}$ -NMR ($CDCl_3$, 101MHz) of 3af

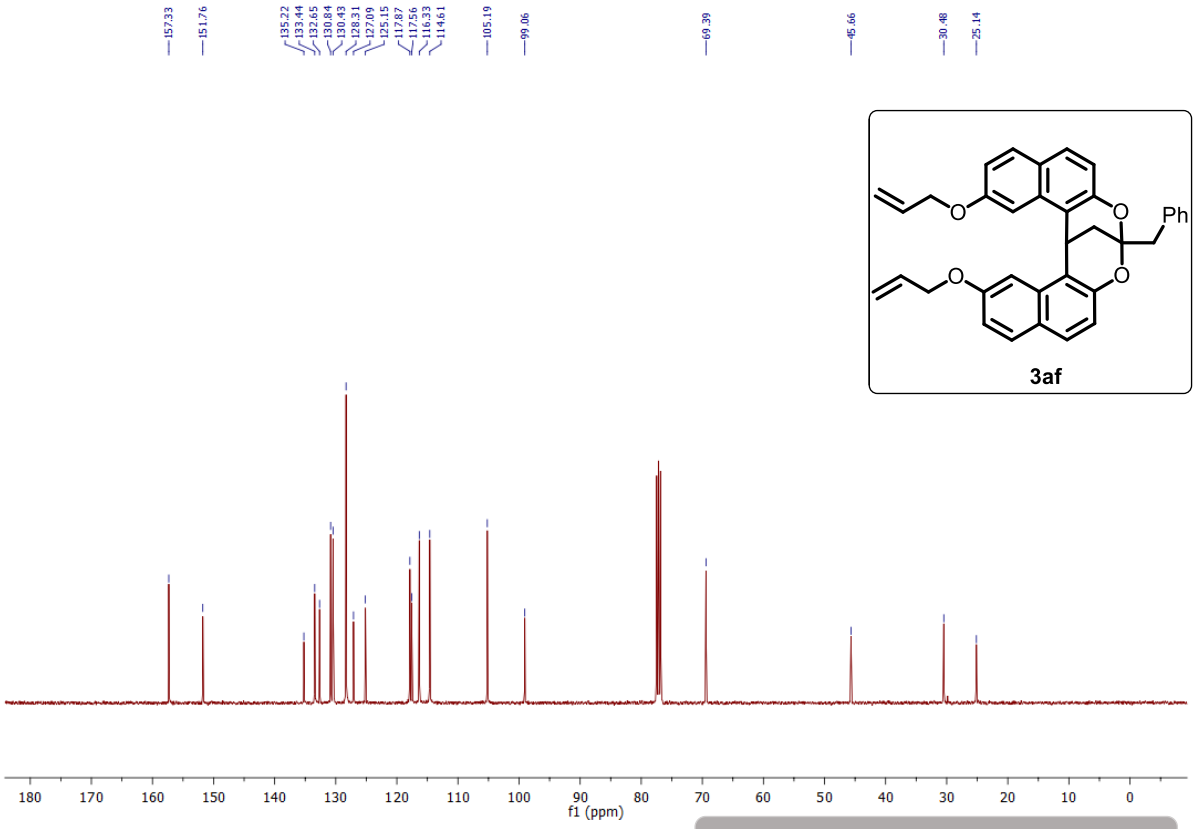

^{1}H-NMR ($CDCl_3$, 400MHz) of 3ag

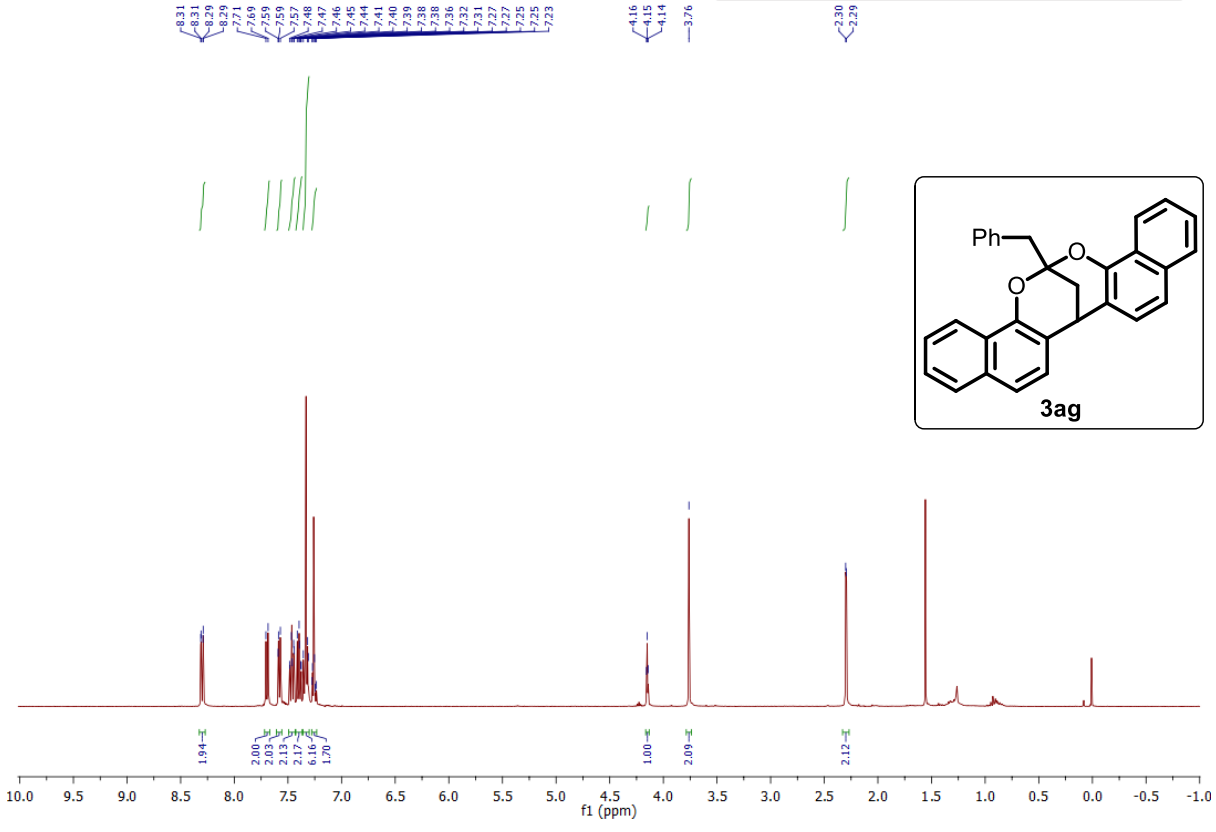

$^{13}C\{^{1}H\}$ -NMR ($CDCl_3$, 101MHz) of 3ag

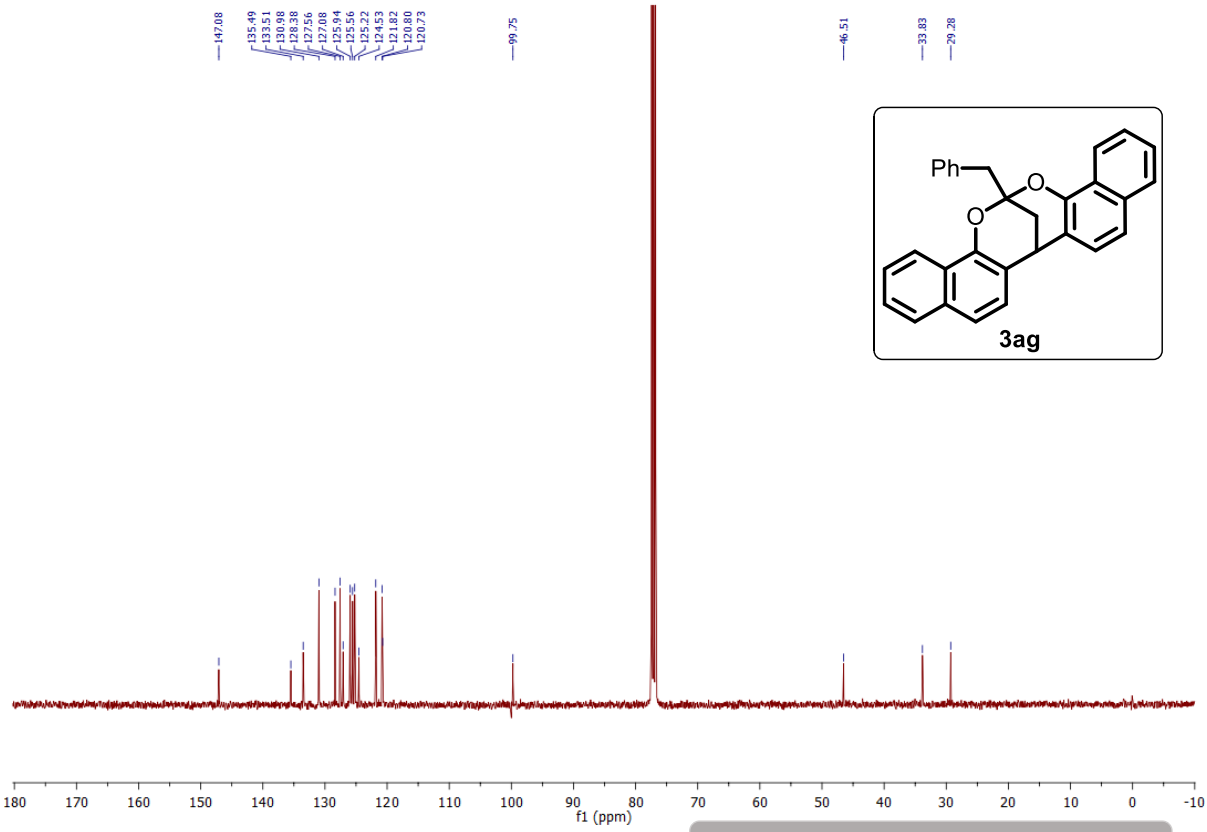

^{1}H-NMR ($CDCl_3$, 400MHz) of 3ah

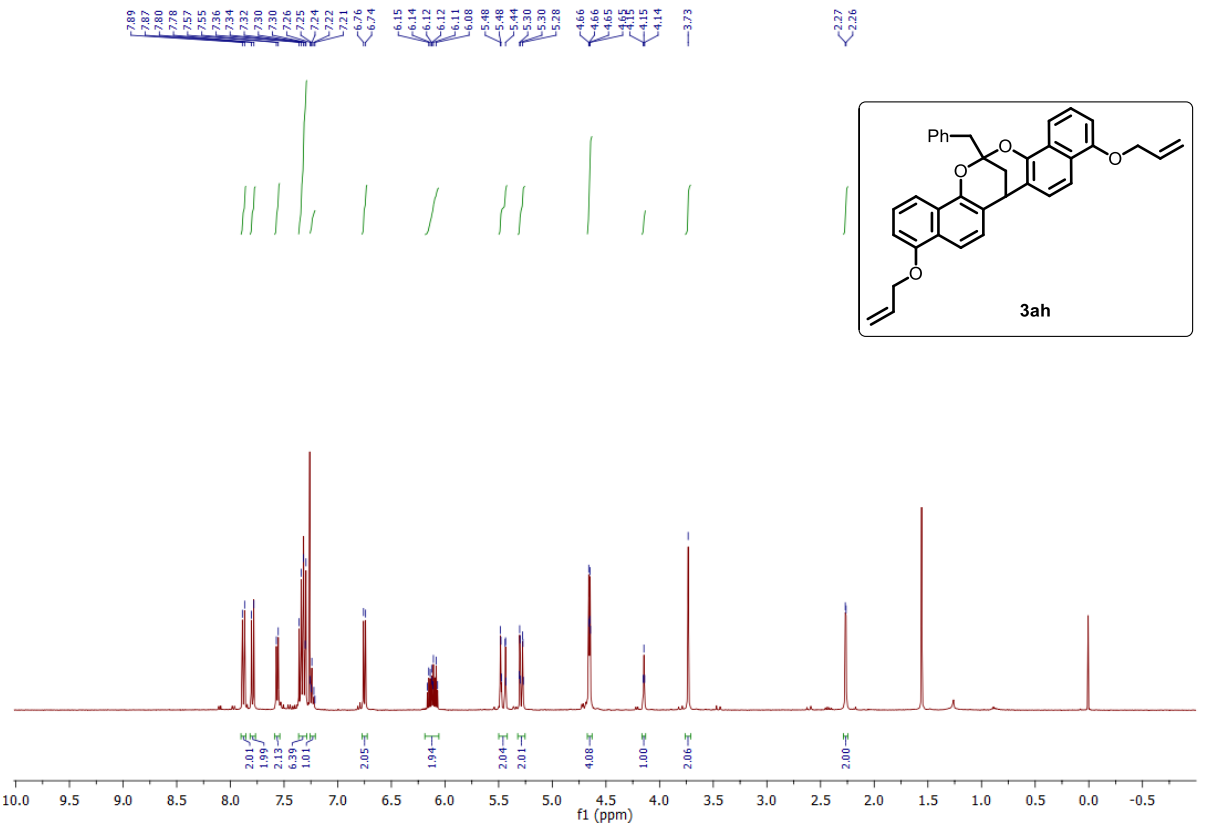

$^{13}C\{^{1}H\}$ -NMR ($CDCl_3$, 101MHz) of 3ah

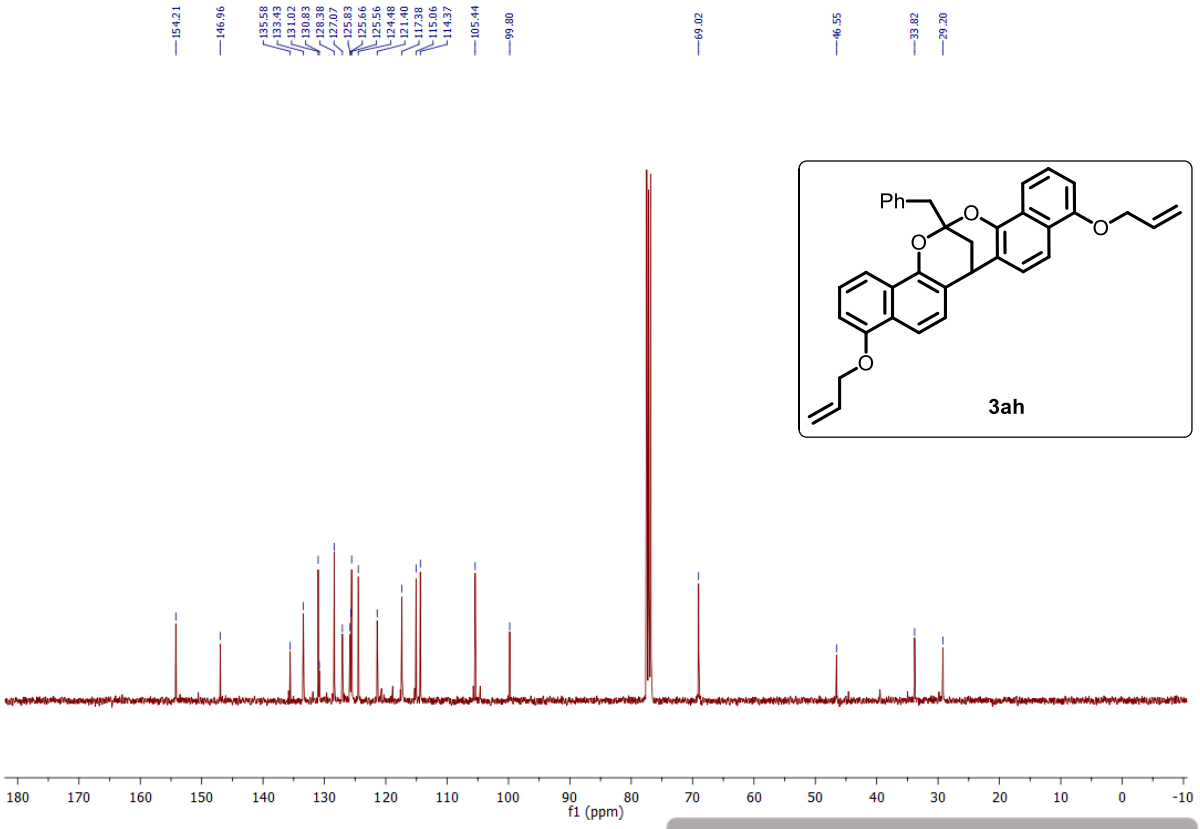

^{1}H-NMR ($CDCl_3$, 400MHz) of *cis*-3afa

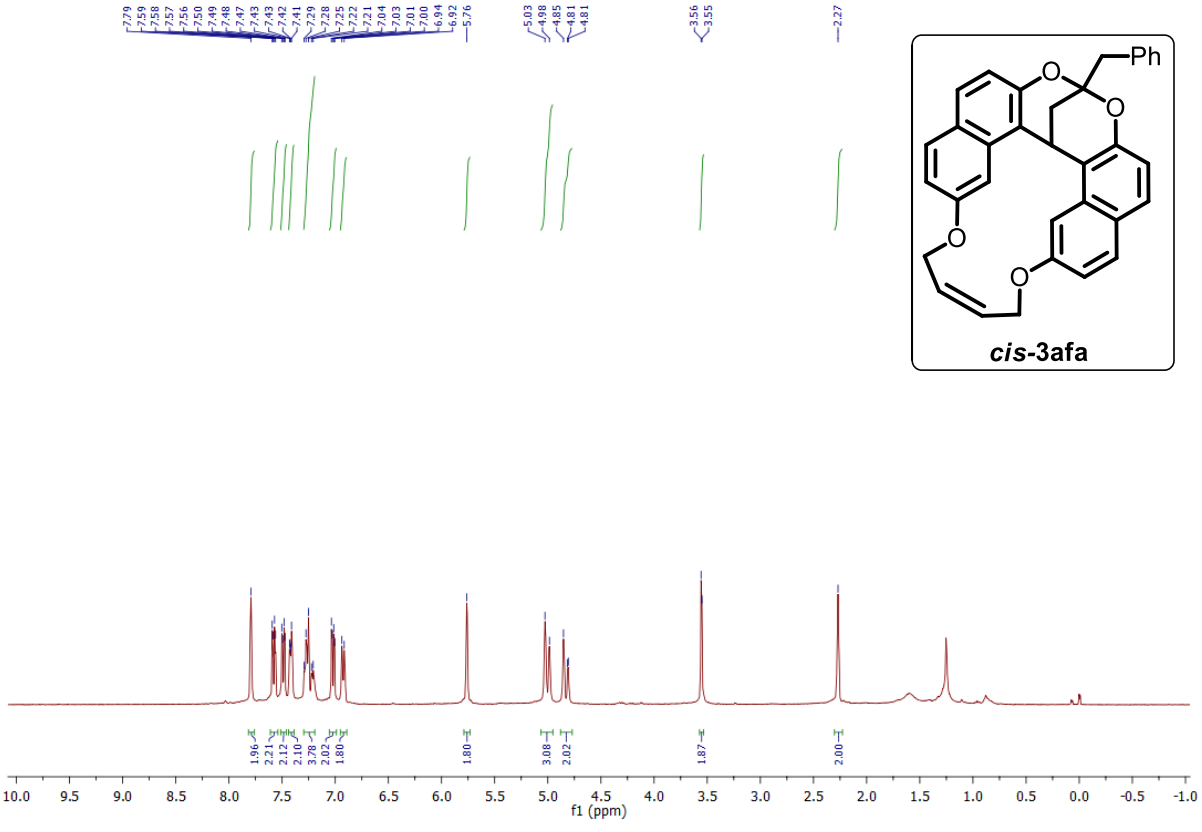

$^{13}C\{^{1}H\}$ -NMR ($CDCl_3$, 101MHz) of *cis*-3afa

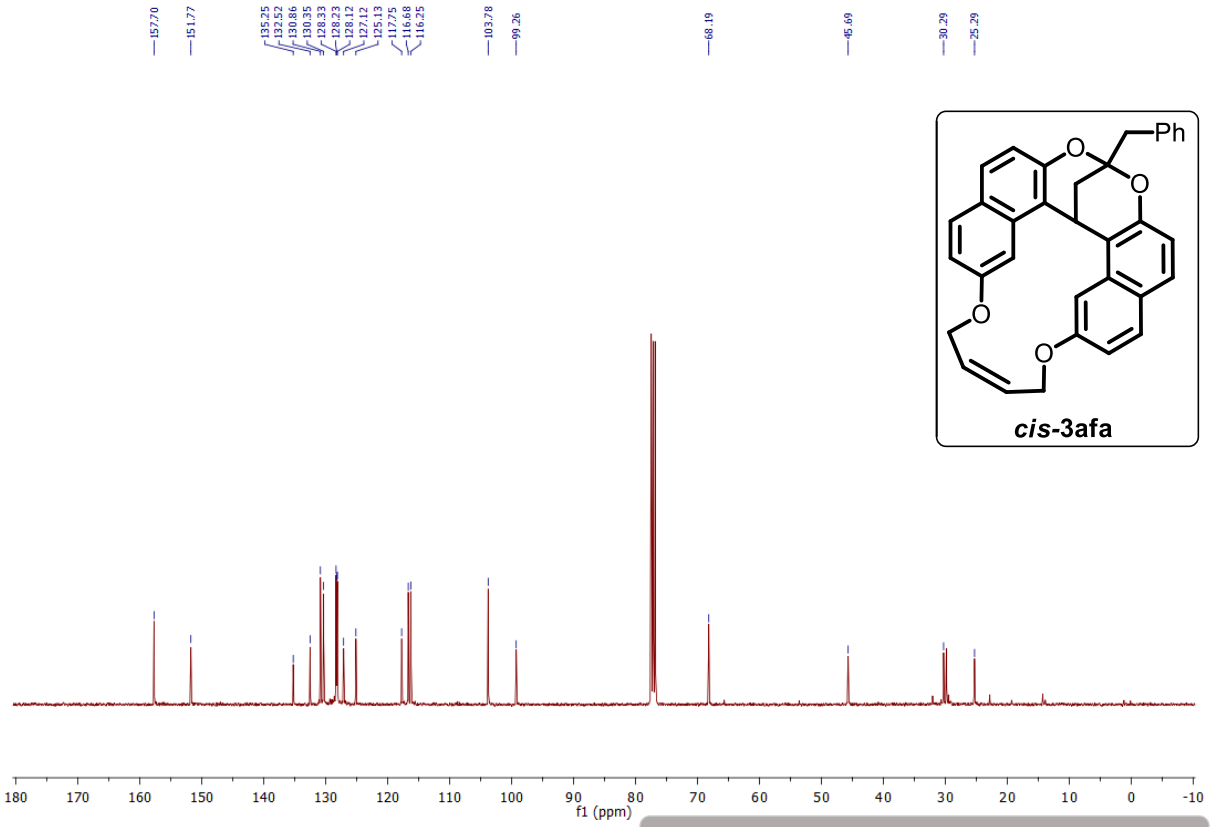

^{1}H-NMR ($CDCl_3$, 400MHz) of *trans*-3afa

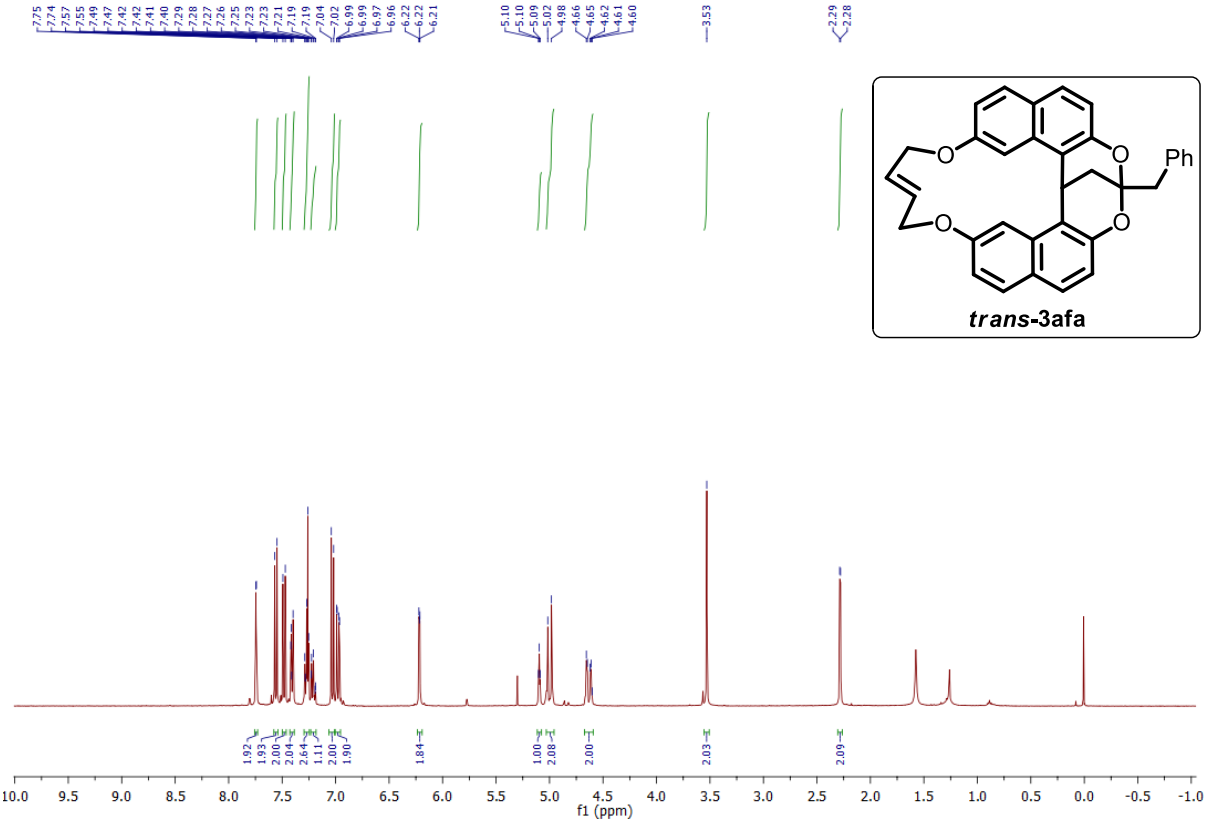

$^{13}C\{^{1}H\}$ -NMR ($CDCl_3$, 101MHz) of *trans*-3afa

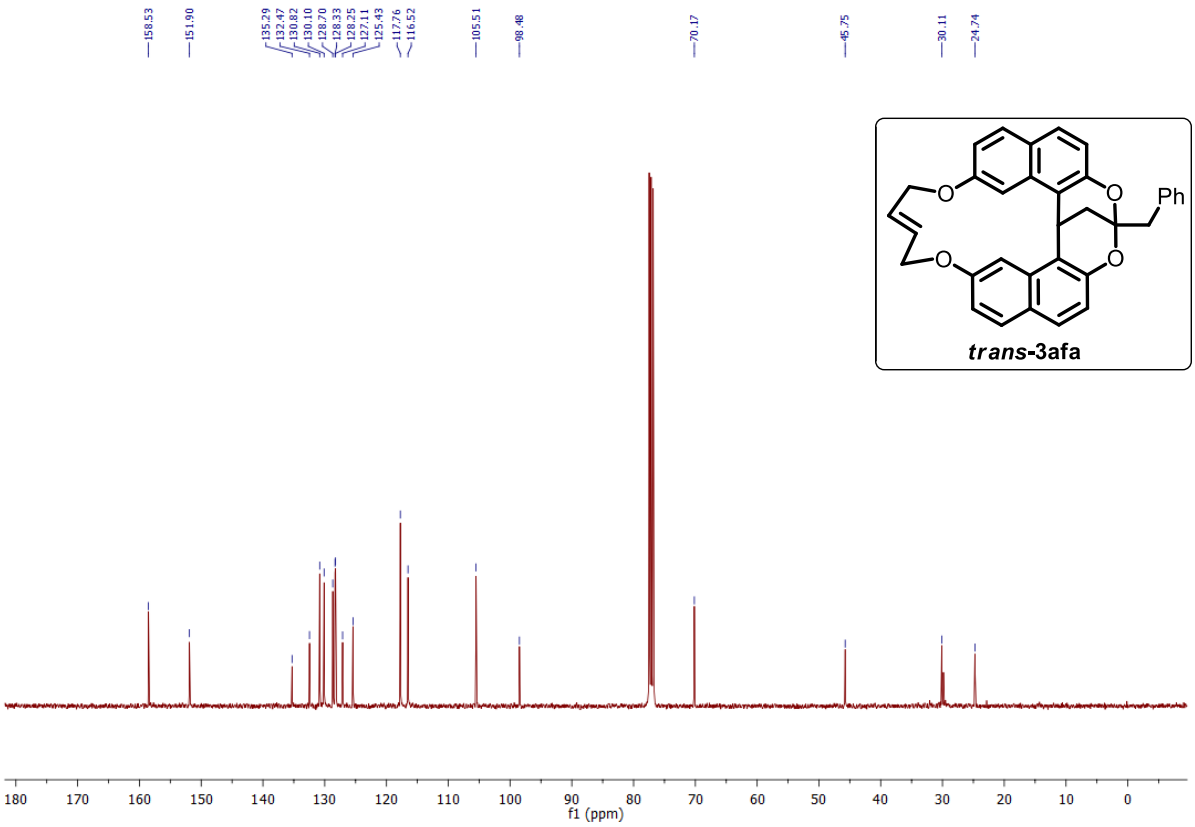

Summary and Future Aspects

Summary and Future Aspects

The work presented in this thesis features diverse catalytic activation strategies of two different smallest carbocycles for the construction of different valuable chiral and achiral organic molecules. Over the years, various catalytic activation strategies were developed from three and four-membered strained carbocycles cyclopropanes, and cyclobutanes respectively, to form numerous important cyclic and acyclic compounds. Organocatalysis gathered remarkable attention in the 21st century and its utilization for the small molecule activation towards enantioenriched complex organic frameworks became an alluring field of interest to the synthetic community. However, harnessing traditional catalytic systems like transition metal containing Lewis acid was also applied extensively to activate these two smallest carbocycles to achieve unprecedented methodology development. Surprisingly, the environmentally benign metal-free Brønsted acid catalytic activation of cyclobutane has remained underdeveloped till now. Therefore, the implementation of diverse catalytic strategies to activate these two strained cyclic systems and their exploration to develop new techniques in our laboratory has been the source of inspiration to execute various catalytic activations of these smallest carbocycles.

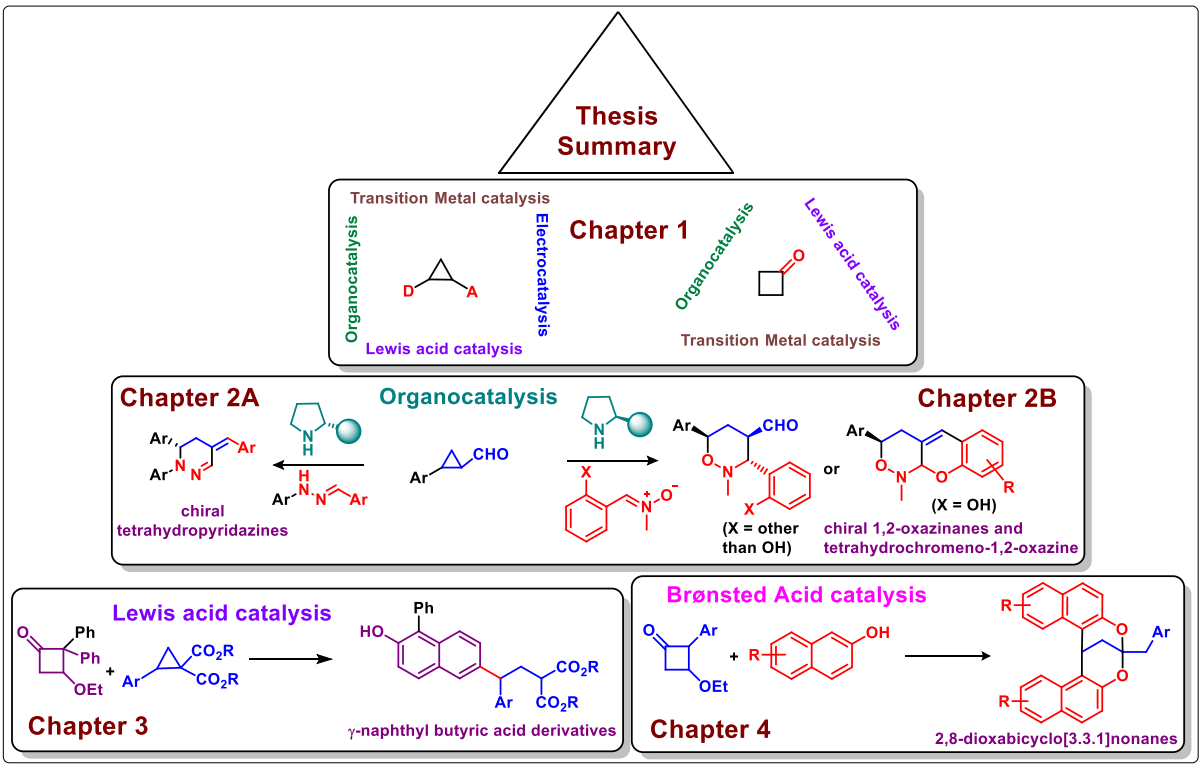

The research work in the thesis is divided into four chapters. Chapter 1 started with a brief discussion about the two smallest carbocycles and their classification. Further, activation of the donor-acceptor cyclopropane and 3-donor cyclobutanones via different types of catalysis have also been discussed.

Chapter 2A demonstrated the first organocatalytic activation of *racemic* cyclopropane carbaldehydes for the enantioselective (3 + 3) cycloaddition via a secondary amine catalyst. A wide range of enantioenriched tetrahydropyridazines was obtained in moderate to good yields with moderate to excellent enantioselectivities. Detailed mechanistic investigations revealed that an unconventional type of matched/mismatched kinetic resolution was the reason behind this asymmetric induction. The control experiment disclosed that the intriguing 1,3-aryl migration is intramolecular and concerted in nature. Further computational studies were also conducted to get insights into the mechanism which suggested that the aryl migration proceeds via a four-membered transition state.

Chapter 2B represented a secondary amine-catalyzed enantioselective (3+3)-cycloaddition reaction of *ortho*-substituted nitrones with aryl cyclopropane carbaldehydes for the first time. Only the electron-rich aryl-containing cyclopropanes undergo this reaction to render a range of 1,2-oxazinanes in moderate yields and enantioselectivities. Noticeably, in all the cases the corresponding aryl aldehydes were obtained with a considerable amount. Surprisingly, when *ortho*-hydroxy substituted nitrone was employed the unusual 1,3-aryl shift took place to furnish an unprecedented product tetrahydrochromeno[2,3- c][1,2]oxazine.

Chapter 3 developed the tandem activation of the two smallest carbocycles via Lewis acid catalysis. The diphenyl-substituted 3-ethoxy cyclobutanone led to the *in situ* formation of 1-phenyl 2-naphthol, which subsequently underwent the remote site-selective Friedel−Crafts alkylation with aryl cyclopropane diesters. The rearrangement of cyclobutanone and ring-opening of donor-acceptor cyclopropane has been achieved simultaneously in one pot. A series of γ-naphthyl butyric acid derivatives were obtained in good to excellent yields. Control experiments emphasize the role of diphenyl substitution on the cyclobutanone for this designed methodology and also confirm the site selectivity of the *β*-naphthol for the Friedel−Crafts reaction. Moreover, selective methylation and decarboxylation have been conducted smoothly for the synthetic transformation of the product.

Chapter 4 disclosed the Brønsted acid catalytic activation of 3-ethoxy cyclobutanone. A new methodology has been developed to construct 2,8-dioxabicyclo[3.3.1]nonanes from simple starting material. Both *α*- and *β*-naphthol derivatives were found to be tolerated for this transformation and rendered a series of bicyclic ketals in poor to good yields. However, other electron-rich arenes or phenols did not participate in rendering the corresponding cyclization products. Moreover, a gram-scale experiment has been conducted to showcase the practical utility of the designed protocol. Additionally, a 15-membered macrocyclic framework was also synthesized by ring-closing metathesis as a post-functional modification.

After the successful exploration of organocatalytic enantioselective (3+3) cycloadditions, similar strategies can also be utilized further to activate the cyclopropane carbaldehydes for the other types of cycloaddition reactions like (3+2), (4+3), etc. The asymmetric version of the Brønsted acid-catalyzed activation of the cyclobutanone derivatives to afford chiral bicyclic scaffolds could also open new avenues in the future. Apart from these, we also believe that the future generation will come up with modern burgeoning catalytic approaches like photocatalysis and electrocatalysis to activate these two smallest carbocycles which remain unexplored to date and a diverse array of new methodologies will flourish in the upcoming years.

Appendices: X-Ray Diffraction and Computational Studies

APPENDIX A: X-RAY DIFFRACTION

For the determination of X-ray crystal structures of the compounds, a single crystal was selected and mounted with paratone oil on a glass fiber using gum. The data was collected at 293K on a CMOS based Bruker D8 Venture PHOTON 100 diffractometer equipped with a INCOATEC micro-focus source with graphite monochromatic Mo Kα radiation (λ = 0.71073 Å) operation at 50 kV and 30 mA. For the integration of diffraction profiles SAINT program[1] was used. Absorption correction was done applying SADABS program.[2] The crystal structure was solved by SIR 92[3] and refined by full matrix least square method using SHELXL-97[4] WinGX system, Ver 1.70.01.[5] All the non-hydrogen atoms in the structure were located the Fourier map and refined anisotropically. The hydrogen atoms were fixed by HFIX in their ideal positions and refined using riding model with isotropic thermal parameters. The crystal structure (excluding structure factor) has been deposited to Cambridge Crystallographic Data Centre and allocated deposition numbers for each crystal are given in their respective table.

Chapter 2A

Single Crystal X-Ray Data of 3a

The CCDC number for the compound 3a is **CCDC 2078121**

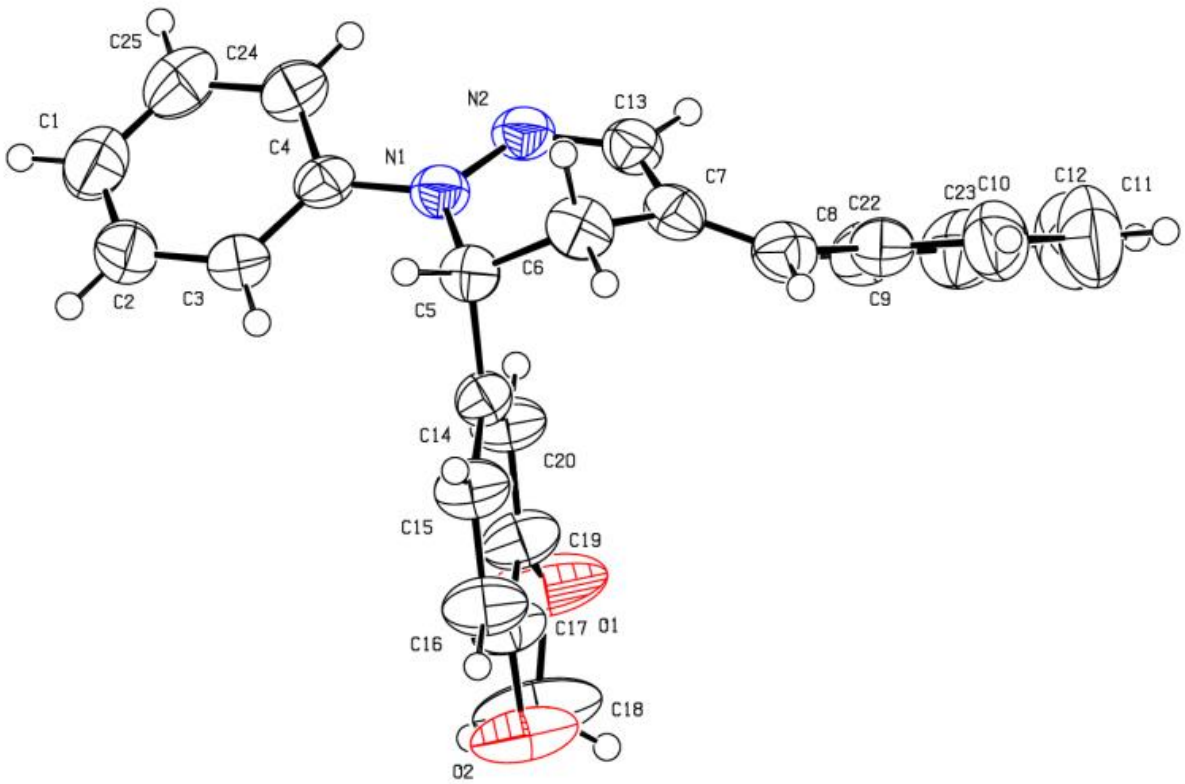

Figure 1: Single Crystal X-ray structure of compound **3a** with 50% ellipsoid probability.

Table 1. Crystal data and structure refinement for 3a.

CCDC No.	CCDC 2078121
Formula	C24 H20 N2 O2
Formula weight	368.42
Crystal System	Monoclinic
Space group	P21
a, b, c (Å)	10.228(2) 6.2956(14) 15.632(4)
α, β, γ (°)	90 90.900(8) 90
V ($Å^3$)	1006.4(4)
Z	2
Calculated Density (g/cm^3)	1.210
Absorption coefficient (mm^{-1})	0.078
F(000)	388
Crystal Size (mm^3)	0.25 x 0.31 x 0.36
Theta range for data collection:	2.4^o to 27.4°
Data set	-11: 13 ; -8: 8 ; -20: 19
Reflection	4430
Independent refl.	[R(int) = 0.021]
data [I > 2σ(I)]	3752
R indices (all data)	R = 0.0405, wR_2 = 0.1117
S	1.04
Min. and Max. Resd. Dens. ($e/Å^3$)	-0.19 and 0.17

Table 2: Selected bond lengths [Å] of 3a

Atoms	**Bond lengths [Å]**	**Atoms**	**Bond lengths [Å]**
O1-C18	1.425(5)	C15-C16	1.399(4)
O1-C19	1.374(3)	C16-C17	1.358(4)
O2-C17	1.380(3)	C17-C19	1.366(4)
O2-C18	1.415(5)	C19-C20	1.382(3)
N1-N2	1.369(3)	C22-C23	1.383(4)
N1-C4	1.414(3)	C24-C25	1.396(4)

N1-C5	1.464(3)	C1-H1	0.9300
N2-C13	1.298(3)	C2-H2	0.9300
C1-C2	1.373(5)	C3-H3	0.9300
C1-C25	1.381(4)	C5-H5	0.9800
C2-C3	1.389(4)	C6-H6A	0.9700
C3-C4	1.395(4)	C6-H6B	0.9700
C4-C24	1.397(3)	C8-H8	0.9300
C5-C6	1.537(3)	C10-H10	0.9300
C5-C14	1.522(3)	C11-H11	0.9300
C6-C7	1.504(3	C12-H12	0.9300
C7-C8	1.342(3)	C13-H13	0.9300
C7-C13	1.454(4)	C15-H15	0.9300
C8-C9	1.468(3)	C16-H16	0.9300
C9-C10	1.394(4)	C18-H18A	0.9700
C9-C22	1.400(4)	C18-H18B	0.9700
C10-C11	1.381(6)	C20-H20	0.9300
C11-C12	1.384(7)	C22-H22	0.9300
C12-C23	1.366(6)	C23-H23	0.9300
C14-C15	1.385(3)	C24-H24	0.9300
C14-C20	1.391(3)	C25-H25	0.9300

Table 3: Selected bond angles [º] of 3a

Atoms	Bond angles[º]	Atoms	Bond angles[º]
C18-O1-C19	105.3(2)	C5-C14-C20	121.51(18)
C17-O2-C18	105.1(2)	C15-C14-C20	119.68(19)

N2-N1-C4	115.59(18)	C14-C15-C16	122.1(2)
N2-N1-C5	122.17(17)	C15-C16-C17	116.5(2)
C4-N1-C5	121.60(18)	O2-C17-C16	127.9(2)
N1-N2-C13	118.90(19)	O2-C17-C19	110.3(2)
C2-C1-C25	118.9(3)	C16-C17-C19	121.9(2)
C1-C2-C3	121.1(3)	O1-C18-O2	108.8(3)
C2-C3-C4	120.3(3)	O1-C19-C17	109.8(2)
N1-C4-C3	120.8(2)	O1-C19-C20	127.7(2)
N1-C4-C24	120.3(2)	C17-C19-C20	122.5(2)
C3-C4-C24	118.9(2)	C14-C20-C19	117.3(2)
N1-C5-C6	108.30(17)	C9-C22-C23	120.5(3)
N1-C5-C14	113.13(16)	C12-C23-C22	120.6(4)
C6-C5-C14	112.17(17)	C4-C24-C25	119.5(2)
C5-C6-C7	108.76(19)	C1-C25-C24	121.4(3)
C6-C7-C8	123.7(2)	C2-C1-H1	121.00
C6-C7-C13	111.00(19)	C25-C1-H1	121.00
C8-C7-C13	125.3(2)	C1-C2-H2	119.00
C7-C8-C9	128.5(2)	C3-C2-H2	119.00
C8-C9-C10	119.1(3)	C2-C3-H3	120.00
C8-C9-C22	122.9(2)	C4-C3-H3	120.00
C10-C9-C22	118.0(3)	N1-C5-H5	108.00
C9-C10-C11	120.9(4)	C6-C5-H5	108.00
C10-C11-C12	120.1(4)	C14-C5-H5	108.00
C11-C12-C23	119.9(4)	C5-C6-H6A	110.00
N2-C13-C7	125.4(2)	C5-C6-H6B	110.00

C5-C14-C15	118.80(17)	C7-C6-H6A	110.00
C7-C6-H6B	110.00	O1-C18-H18A	110.00
H6A-C6-H6B	108.00	O1-C18-H18B	110.00
C7-C8-H8	116.00	O2-C18-H18A	110.00
C9-C8-H8	116.00	O2-C18-H18B	110.00
C9-C10-H10	120.00	H18A-C18-H18B	108.00
C11-C10-H10	120.00	C14-C20-H20	121.00
C10-C11-H11	120.00	C19-C20-H20	121.00
C12-C11-H11	120.00	C9-C22-H22	120.00
C11-C12-H12	120.00	C23-C22-H22	120.00
C23-C12-H12	120.00	C12-C23-H23	120.00
N2-C13-H13	117.00	C22-C23-H23	120.00
C7-C13-H13	117.00	C4-C24-H24	120.00
C14-C15-H15	119.00	C25-C24-H24	120.00
C16-C15-H15	119.00	C1-C25-H25	119.00
C15-C16-H16	122.00	C24-C25-H25	119.00
C17-C16-H16	122.00		

Table 4: Selected hydrogen bonding geometry [Å, º] for a compound 3a

D--H.. A	**D..H**	**H..A**	**D..A**	**D--H..A**
C16--H16..O1	0.9300	2.5200	3.380(4)	155.00

Single Crystal X-Ray Data of 3ab

The CCDC number for the compound **3ab** is **CCDC 2246737**

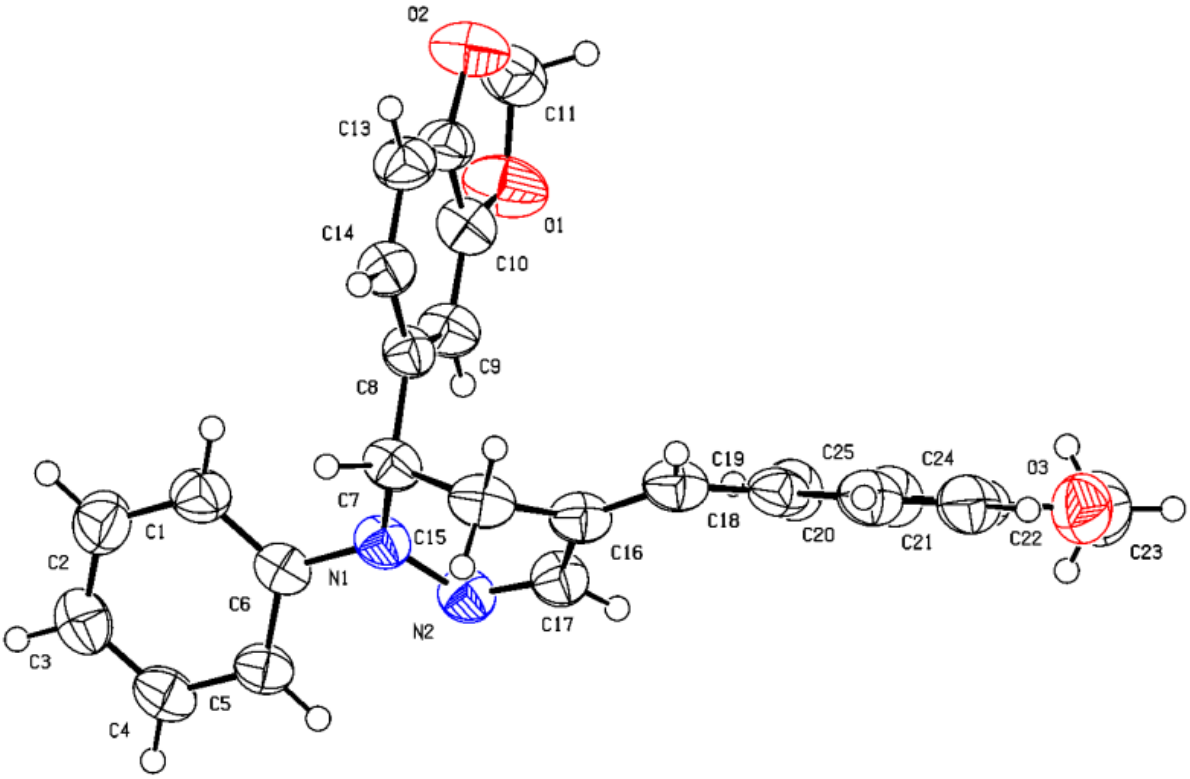

Figure 2: Single Crystal X-ray structure of compound **3ab** with 50% ellipsoid probability.

Table 5. Crystal data and structure refinement for 3ab.

CCDC No.	2246737
Formula	$C_{25}H_{22}N_2O_3$
Formula weight	398.44
Crystal System	Triclinic
Space group	P-1
a, b, c (Å)	6.2771(3) 10.5421(5) 15.6466(8)
α, β, γ (°)	100.831(2) 96.589(2) 90.664(2)
V ($Å^3$)	1009.65(9)
Z	2

Calculated Density (g/cm^3)	1.311
Absorption coefficient (mm^{-1})	0.087
F(000)	420.0
Crystal Size (mm^3)	0.315 × 0.256 × 0.214
Theta range for data collection:	3.936 to 56.664
Data set	$-8 \leq h \leq 8, -14 \leq k \leq 14, -20 \leq l \leq 20$
Reflection	22798
Independent refl.	[R(int) = 0.0367]
data [$I > 2\sigma(I)$]	4965
R indices (all data)	R = 0.0536, $wR_2 = 0.1231$
S	1.039
Min. and Max. Resd. Dens. ($e/Å^3$)	-0.12 and 0.18

Table 6: Selected bond lengths of 3ab

Atoms	Bond lengths [Å]	Atoms	Bond lengths [Å]
N1-N2	1.3595(14)	C8-C9	1.3975(16)
N1-C6	1.4056(15)	C17-C16	1.4539(16)
N1-C7	1.4731(13)	C5-C4	1.3834(18)
N2-C17	1.2962(16)	C12-C10	1.3755(18)
O2-C12	1.3801(16)	C12-C13	1.3656(19)
O2-C11	1.423(2)	C16-C18	1.3421(18)
O1- C10	1.3728(16)	C10-C9	1.3698(18)
O1-C11	1.4208(19)	C19-C25	1.3929(19)
O3-C22	1.3637(18)	C19-C18	1.459(2)
O3-C23	1.415(2)	C19-C20	1.4010(17)

C15-C16	1.4969(18)	C1-C2	1.385(2)
C15-C7	1.5274(18)	C22-C21	1.391(2)
C14-C8	1.3907(15)	C22-C24	1.3872(18)
C14-C13	1.3951(18)	C25-C24	1.382(2)
C6-C5	1.3938(15)	C21-C20	1.369(2)
C6-C1	1.3907(18)	C4-C3	1.377(2)
C8-C7	1.5211(16)	C3-C2	1.377(2)

Table 7: Selected bond angles of 3ab

Atoms			**Bond angles[º]**	**Atoms**			**Bond angles[º]**
N2	N1	C6	116.59(9)	N1	C7	C8	113.13(9)
N2	N1	C7	122.58(10)	C8	C7	C15	111.97(10)
C6	N1	C7	120.72(10)	O1	C10	C12	110.10(12)
C17	N2	N1	119.10(9)	C9	C10	O1	127.66(12)
C12	O2	C11	105.32(11)	C9	C10	C12	122.24(12)
C10	O1	C11	105.54(11)	C12	C13	C14	116.54(11)
C22	O3	C23	118.34(13)	C25	C19	C18	124.19(11)
C16	C15	C7	109.74(9)	C25	C19	C20	116.61(13)
C8	C14	C13	122.13(11)	C20	C19	C18	119.17(12)
C5	C6	N1	120.91(11)	C2	C1	C6	120.11(12)
C1	C6	N1	120.16(10)	O3	C22	C21	115.95(12)
C1	C6	C5	118.93(11)	O3	C22	C24	124.78(14)
C14	C8	C7	118.37(10)	C24	C22	C21	119.27(14)
C14	C8	C9	119.87(11)	C10	C9	C8	117.28(11)
C9	C8	C7	121.71(10)	C24	C25	C19	122.26(12)

N2	C17	C16	124.89(11)	C16	C18	C19	129.77(12)
C4	C5	C6	119.95(12)	C20	C21	C22	120.31(12)
C10	C12	O2	109.80(12)	C3	C4	C5	121.08(12)
C13	C12	O2	128.25(12)	C25	C24	C22	119.62(13)
C13	C12	C10	121.94(12)	C21	C20	C19	121.90(13)
C17	C16	C15	111.67(11)	C4	C3	C2	119.04(13)
C18	C16	C15	122.37(11)	C3	C2	C1	120.90(14)
C18	C16	C17	125.80(12)	O1	C11	O2	108.98(11)
N1	C7	C15	107.92(10)				

Chapter 2B

Single Crystal X-Ray Data of 5aa

The CCDC number for the compound **5aa** is **CCDC 2237741**

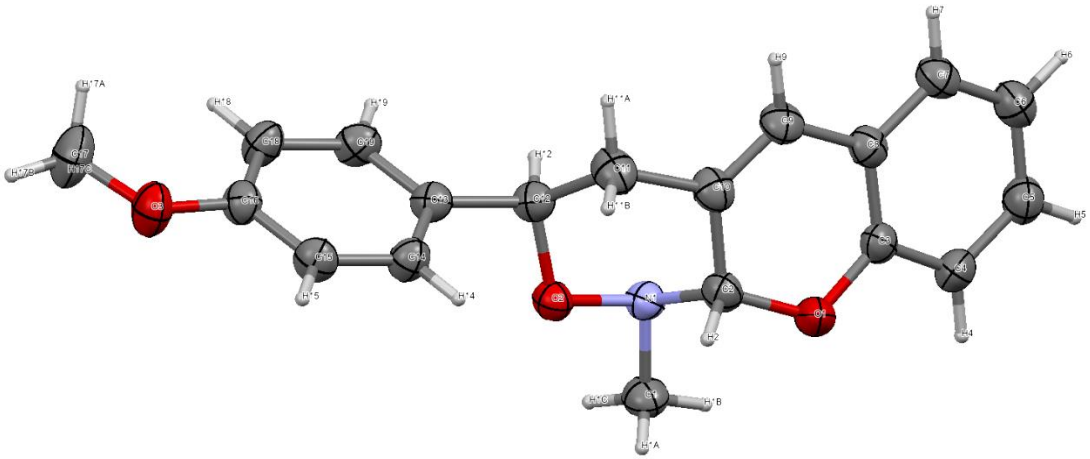

Figure 3: Single Crystal X-ray structure of compound **5aa** with 50% ellipsoid probability.

Table 8. Crystal data and structure refinement for 5aa.

Ccdc no.	2237741
Empirical formula	$C_{19}H_{19}NO_3$

Formula weight	309.35
Temperature/K	298.0
Crystal system	orthorhombic
Space group	$P2_12_12_1$
a/Å	5.8734(3)
b/Å	15.4556(7)
c/Å	17.6587(7)
α/°	90
β/°	90
γ/°	90
Volume/Å^3	1603.00(13)
Z	4
ρ_{calc}g/cm^3	1.282
μ/mm^{-1}	0.087
F(000)	656.0
Crystal size/mm^3	0.35 × 0.236 × 0.123
Radiation	MoKα (λ = 0.71073)
2Θ range for data collection/°	4.614 to 52.79
Index ranges	$-7 \leq h \leq 7$, $-19 \leq k \leq 19$, $-22 \leq l \leq 22$
Reflections collected	33944
Independent reflections	3289 [R_{int} = 0.0505, R_{sigma} = 0.0225]
Data/restraints/parameters	3289/0/210
Goodness-of-fit on F^2	1.087
Final R indexes [I>=2σ (I)]	R_1 = 0.0360, wR_2 = 0.0859

Final R indexes [all data]	R_1 = 0.0444, wR_2 = 0.0908
Largest diff. peak/hole / e Å^{-3}	0.12/-0.10
Flack parameter	0.2(5)

Table 9: Selected bond lengths of 5aa

Atoms	Length/Å	Atoms	Length/Å
O2- N1	1.475(2)	C13- C12	1.509(3)
O2- C12	1.435(3)	C13- C19	1.370(3)
O1- C3	1.377(3)	C14- C15	1.380(3)
O1- C2	1.417(3)	C7- C6	1.381(3)
N1- C1	1.455(3)	C15- C16	1.382(3)
N1- C2	1.481(3)	C10- C2	1.493(3)
O3- C16	1.366(3)	C10- C11	1.498(3)
O3- C17	1.418(4)	C3- C4	1.376(3)
C8- C9	1.453(3)	C12- C11	1.523(3)
C8- C9	1.390(3)	C18- C16	1.382(3)
C8- C3	1.390(3)	C18- C19	1.391(3)
C9- C10	1.320(3)	C4- C5	1.384(3)
C13- C14	1.393(3)	C5- C6	1.376(4)

Table 10: Selected bond angles of 5aa

Atom	Angle/°	Atom	Angle/°
C12- O2- N1	108.46(14)	O1- C3- C8	121.3(2)
C3- O1- C2	120.09(18)	C4- C3- O1	116.8(2)

O2- N1- C2	103.21(15)	C4- C3- C8	121.9(2)
C1- N1- O2	103.55(16)	O2- C12- C13	106.62(18)
C1- N1- C2	112.55(19)	O2- C12- C11	109.18(19)
C16- O3- C17	117.7(2)	C13- C12- C11	113.76(18)
C7- C8- C9	123.9(2)	C16- C18- C19	119.3(2)
C3- C8- C9	118.3(2)	O1- C2- N1	108.86(18)
C3- C8- C7	117.7(2)	O1- C2- C10	115.90(18)
C10- C9- C8	121.2(2)	N1- C2- C10	105.93(19)
C14- C13-	121.0(2)	C3- C4- C5	119.2(2)
C19- C12	117.9(2)	O3- C16- C15	115.6(2)
C19- C13- C12	121.2(2)	O3- C16- C18	124.8(2)
C15- C14- C13	121.0(2)	C15- C16- C18	119.6(2)
C6- C7- C8	120.8(2)	C13- C19-C18	122.0(2)
C14- C15- C16	120.2(2)	C10- C11- C12	109.39(18)
C9- C10- C2	120.6(2)	C6- C5- C4	120.1(2)
C9- C10- C11	126.3(2)	C5- C6- C7	120.3(2)
C2- C10- C11	112.3(2)		

Chapter 3

Single Crystal X-Ray Data of 3aa

The CCDC number for the compound 3aa is CCDC 2206200

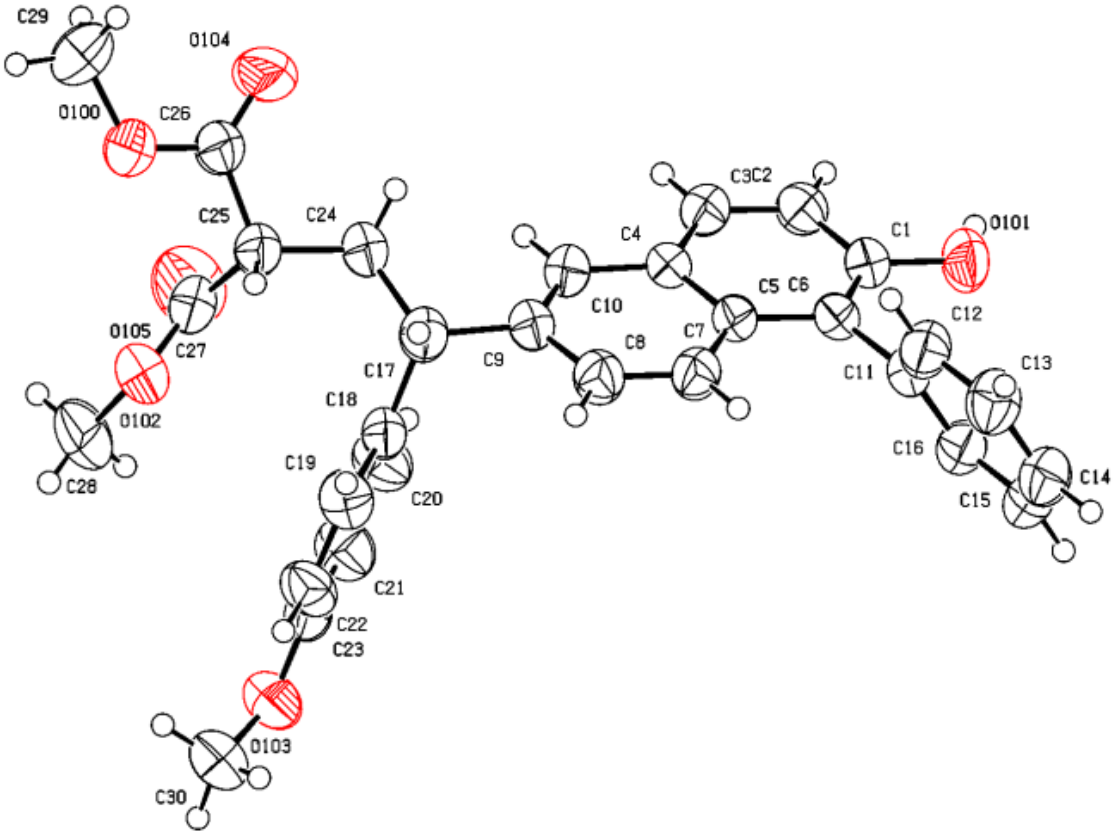

Figure 4: Single Crystal X-ray structure of compound **3aa** with 50% ellipsoid probability.

Table 10. Crystal data and structure refinement for 3aa.

CCDC No.	CCDC 2206200
Formula	C30 H28 O6
Formula weight	484.52
Crystal System	Monoclinic
Space group	P21/n
a, b, c (Å)	13.902(5), 6.052(5), 29.577(5)
α, β, γ (°)	90, 92.537(5), 90
V ($Å^3$)	2486(2)
Z	4
Calculated Density (g/cm^3)	1.290

Absorption coefficient (mm^{-1})	0.090
F(000)	1024
Crystal Size (mm^3)	0.27 x 0.28 x 0.29
Theta range for data collection:	2.5 °C to 25.7 °C
Data set	-16: 16 ; -7: 7 ; -35: 36
Reflection	30440
Independent refl.	4736 [R(int) = 0.115]
data [I > 2σ(I)]	2268
R indices (all data)	R = 0.0612, wR_2 = 0.1862
S	1.03
Min. and Max. Resd. Dens. ($e/Å^3$)	-0.19 and 0.26

Table 11: Selected bond lengths [Å] of 3aa

Atoms	Bond lengths [Å]	Atoms	Bond lengths [Å]
O100-C26	1.298(5)	C15-C16	1.385(5)
O100-C29	1.463(5)	C17-C18	1.525(4)
O101-C1	1.376(4)	C17-C24	1.512(5)
O102-C27	1.317(5)	C18-C19	1.376(5)
O102-C28	1.464(5)	C18-C20	1.386(5)
O103-C23	1.370(4)	C19-C22	1.384(5)
O103-C30	1.419(5)	C20-C21	1.373(6)
O104-C26	1.191(5)	C21-C23	1.381(5)
O105-C27	1.189(5)	C22-C23	1.371(5)
O101-H101	0.8200	C24-C25	1.543(4)
C1-C6	1.377(4)	C25-C26	1.509(5)

C1-C2	1.407(4)	C25-C27	1.516(5)
C2-C3	1.360(4)	C2-H2	0.9300
C3-C4	1.409(4)	C3-H3	0.9300
C4-C5	1.412(4)	C7-H7	0.9300
C4-C10	1.425(4)	C8-H8	0.9300
C5-C6	1.432(4)	C10-H10	0.9300
C5-C7	1.416(4)	C12-H12	0.9300
C6-C11	1.488(4)	C13-H13	0.9300
C7-C8	1.358(4)	C14-H14	0.9300
C8-C9	1.409(4)	C15-H15	0.9300
C9-C10	1.361(5)	C16-H16	0.9300
C9-C17	1.523(4)	C17-H17	0.9800
C11-C12	1.392(4)	C19-H19	0.9300
C11-C16	1.382(5)	C20-H20	0.9300
C12-C13	1.383(5)	C21-H21	0.9300
C13-C14	1.376(5)	C22-H22	0.9300
C14-C15	1.371(5)	C24-H24A	0.9700
C24-H24B	0.9700	C29-H29B	0.9600
C25-H25	0.9800	C29-H29C	0.9600
C28-H28A	0.9600	C30-H30A	0.9600
C28-H28B	0.9600	C30-H30B	0.9600
C28-H28C	0.9600	C30-H30C	0.9600
C29-H29A	0.9600		

Table 12: Selected bond angles [º] of 3aa

Atoms	Bond angles[º]	Atoms	Bond angles[º]
C26-O100-C29	118.2(3)	C12-C13-C14	121.1(3)
C27-O102-C28	115.1(3)	C13-C14-C15	119.4(3)
C23-O103-C30	117.4(3)	C14-C15-C16	119.8(3)
C1-O101-H101	109.00	C11-C16-C15	121.7(3)
O101-C1-C2	119.7(3)	C9-C17-C18	111.2(3)
O101-C1-C6	118.4(3)	C18-C17-C24	113.6(2)
C2-C1-C6	121.9(3)	C9-C17-C24	112.4(3)
C1-C2-C3	119.8(3)	C17-C18-C19	122.2(3)
C2-C3-C4	121.2(3)	C17-C18-C20	121.7(3)
C3-C4-C10	122.0(3)	C19-C18-C20	116.1(3)
C5-C4-C10	119.1(3)	C18-C19-C22	122.6(3)
C3-C4-C5	118.9(3)	C18-C20-C21	122.4(3)
C4-C5-C6	120.0(3)	C20-C21-C23	120.1(3)
C4-C5-C7	117.7(3)	C19-C22-C23	119.8(3)
C6-C5-C7	122.3(3)	O103-C23-C22	124.5(3)
C1-C6-C5	118.2(3)	C21-C23-C22	119.0(3)
C1-C6-C11	120.1(3)	O103-C23-C21	116.6(3)
C5-C6-C11	121.7(3)	C17-C24-C25	113.6(3)
C5-C7-C8	121.1(3)	C24-C25-C26	111.4(3)
C7-C8-C9	122.2(3)	C24-C25-C27	111.6(3)
C8-C9-C10	117.6(3)	C26-C25-C27	109.4(3)
C10-C9-C17	124.1(3)	O100-C26-C25	111.6(3)

C8-C9-C17	118.3(3)	O104-C26-C25	126.3(3)
C4-C10-C9	122.3(3)	O100-C26-O104	122.0(3)
C6-C11-C16	120.6(3)	O102-C27-C25	112.2(3)
C12-C11-C16	117.9(3)	O105-C27-C25	123.1(4)
C6-C11-C12	121.5(3)	O102-C27-O105	124.7(4)
C11-C12-C13	120.1(3)	C1-C2-H2	120.00
C3-C2-H2	120.00	C19-C22-H22	120.00
C2-C3-H3	119.00	C23-C22-H22	120.00
C4-C3-H3	119.00	C17-C24-H24A	109.00
C5-C7-H7	119.00	C17-C24-H24B	109.00
C8-C7-H7	119.00	C25-C24-H24A	109.00
C7-C8-H8	119.00	C25-C24-H24B	109.00
C9-C8-H8	119.00	H24A-C24-H24B	108.00
C4-C10-H10	119.00	C24-C25-H25	108.00
C9-C10-H10	119.00	C26-C25-H25	108.00
C11-C12-H12	120.00	C27-C25-H25	108.00
C13-C12-H12	120.00	O102-C28-H28A	109.00
C12-C13-H13	119.00	O102-C28-H28B	109.00
C14-C13-H13	119.00	O102-C28-H28C	109.00
C13-C14-H14	120.00	H28A-C28-H28B	110.00
C15-C14-H14	120.00	H28A-C28-H28C	110.00
C14-C15-H15	120.00	H28B-C28-H28C	109.00
C16-C15-H15	120.00	O100-C29-H29A	110.00
C11-C16-H16	119.00	O100-C29-H29B	109.00
C15-C16-H16	119.00	O100-C29-H29C	110.00

C9-C17-H17	106.00	H29A-C29-H29B	109.00
C18-C17-H17	106.00	H29A-C29-H29C	109.00
C24-C17-H17	106.00	H29B-C29-H29C	109.00
C18-C19-H19	119.00	O103-C30-H30A	109.00
C22-C19-H19	119.00	O103-C30-H30B	109.00
C18-C20-H20	119.00	O103-C30-H30C	109.00
C21-C20-H20	119.00	H30A-C30-H30B	109.00
C20-C21-H21	120.00	H30A-C30-H30C	110.00
C23-C21-H21	120.00	H30B-C30-H30C	110.00

Table 13: Selected hydrogen bonding geometry [Å, º] for a compound 3aa

D--H.. A	D..H	H..A	D..A	D--H..A
O101 -- H101 .. O104	0.8200	1.9700	2.760(4)	161.00
C24 -- H24A .. O105	0.9700	2.5800	2.975(5)	105.00
C24 -- H24B .. O104	0.9700	2.4000	2.817(5)	105.00

Chapter 4

Single Crystal X-Ray Data of 3aa

The CCDC number for the compound 3aa is CCDC 2220353

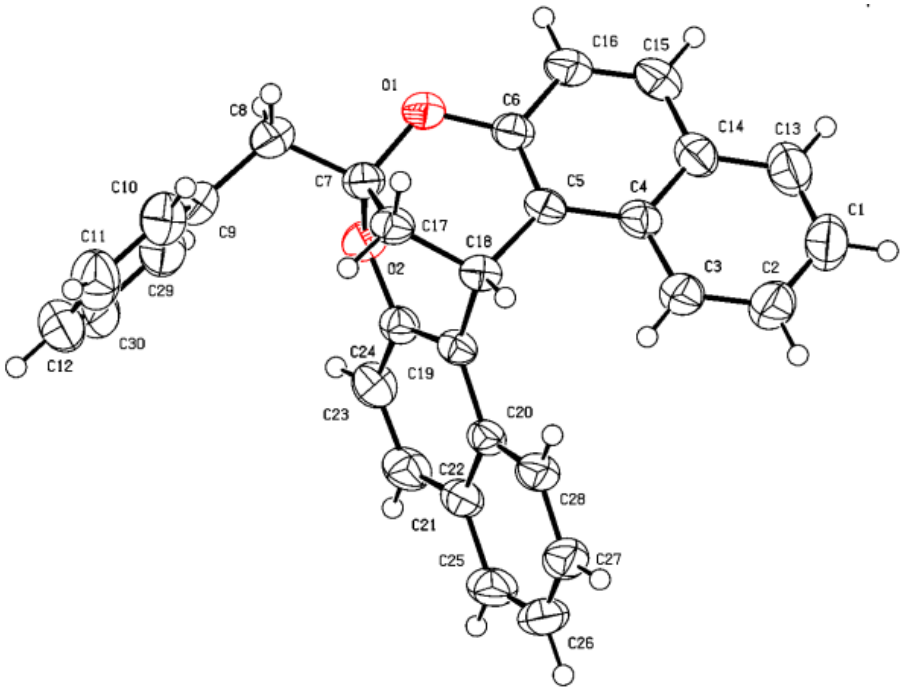

Figure 5: Single Crystal X-ray structure of compound **3aa** with 50% ellipsoid probability.

Table 14. Crystal data and structure refinement for 3aa.	
CCDC no.	2220353
Empirical formula	$C_{30}H_{22}O_2$
Formula weight	414.47
Temperature/K	298
Crystal system	orthorhombic
Space group	Pbca
a/Å	9.2112(4)
b/Å	11.4722(5)
c/Å	40.1618(16)
α/°	90
β/°	90
γ/°	90

Volume/Å^3	4244.0(3)
Z	8
ρ_{calc}g/cm^3	1.297
μ/mm^{-1}	0.080
F(000)	1744.0
Crystal size/mm^3	0.256 × 0.251 × 0.123
Radiation	MoKα (λ = 0.71073)
2Θ range for data collection/°	4.866 to 52.764
Index ranges	-11 ≤ h ≤ 11, -14 ≤ k ≤ 14, -49 ≤ l ≤ 50
Reflections collected	65512
Independent reflections	4334 [R_{int} = 0.0497, R_{sigma} = 0.0195]
Data/restraints/parameters	4334/0/289
Goodness-of-fit on F^2	1.095
Final R indexes [I>=2σ (I)]	R_1 = 0.0487, wR_2 = 0.1109
Final R indexes [all data]	R_1 = 0.0553, wR_2 = 0.1146
Largest diff. peak/hole / e Å^{-3}	0.18/-0.17

Table 15. Bond Lengths for 3aa.

Atom	Atom	Length/Å	Atom	Atom	Length/Å
O1	C6	1.3828(18)	C11	C12	1.370(3)
O1	C7	1.4252(17)	C12	C30	1.378(3)

O2	C7	1.4400(17)	C13	C14	1.414(2)
O2	C24	1.3803(17)	C14	C15	1.410(2)
C1	C2	1.397(3)	C15	C16	1.356(2)
C1	C13	1.355(3)	C17	C18	1.5320(19)
C2	C3	1.371(2)	C18	C19	1.5207(18)
C3	C4	1.412(2)	C19	C20	1.4310(19)
C4	C5	1.439(2)	C19	C24	1.3738(19)
C4	C14	1.425(2)	C20	C21	1.425(2)
C5	C6	1.371(2)	C20	C28	1.416(2)
C5	C18	1.5312(19)	C21	C22	1.414(2)
C6	C16	1.414(2)	C21	C25	1.412(2)
C7	C8	1.522(2)	C22	C23	1.357(2)
C7	C17	1.505(2)	C23	C24	1.405(2)
C8	C9	1.512(2)	C25	C26	1.355(3)
C9	C10	1.383(2)	C26	C27	1.398(3)
C9	C29	1.386(2)	C27	C28	1.373(2)
C10	C11	1.386(3)	C29	C30	1.378(3)

Table 16. Bond Angles for 3aa.

Atom	**Atom**	**Atom**	**Angle/°**	**Atom**	**Atom**	**Atom**	**Angle/°**
C6	O1	C7	115.69(11)	C15	C14	C4	119.25(14)
C24	O2	C7	120.10(11)	C15	C14	C13	121.27(16)
C13	C1	C2	119.51(17)	C16	C15	C14	120.95(15)
C3	C2	C1	120.82(18)	C15	C16	C6	119.68(15)
C2	C3	C4	121.50(17)	C7	C17	C18	107.64(12)

C3	C4	C5	123.08(14)	C5	C18	C17	108.54(11)
C3	C4	C14	117.20(14)	C19	C18	C5	112.13(11)
C14	C4	C5	119.72(14)	C19	C18	C17	105.19(11)
C4	C5	C18	123.01(13)	C20	C19	C18	125.93(12)
C6	C5	C4	117.60(13)	C24	C19	C18	115.51(12)
C6	C5	C18	119.36(13)	C24	C19	C20	118.49(13)
O1	C6	C16	113.02(13)	C21	C20	C19	118.70(13)
C5	C6	O1	124.18(13)	C28	C20	C19	124.38(13)
C5	C6	C16	122.79(14)	C28	C20	C21	116.91(13)
O1	C7	O2	106.25(11)	C22	C21	C20	119.51(14)
O1	C7	C8	105.00(12)	C25	C21	C20	119.62(15)
O1	C7	C17	109.87(12)	C25	C21	C22	120.86(15)
O2	C7	C8	107.07(12)	C23	C22	C21	121.06(14)
O2	C7	C17	112.12(12)	C22	C23	C24	119.28(15)
C17	C7	C8	115.89(13)	O2	C24	C23	114.59(13)
C9	C8	C7	112.94(13)	C19	C24	O2	122.72(12)
C10	C9	C8	120.98(16)	C19	C24	C23	122.62(14)
C10	C9	C29	118.30(17)	C26	C25	C21	121.65(16)
C29	C9	C8	120.72(16)	C25	C26	C27	119.42(16)
C9	C10	C11	120.67(19)	C28	C27	C26	120.75(17)
C12	C11	C10	120.4(2)	C27	C28	C20	121.57(16)
C11	C12	C30	119.5(2)	C30	C29	C9	120.83(19)
C1	C13	C14	121.49(18)	C12	C30	C29	120.3(2)
C13	C14	C4	119.47(16)				

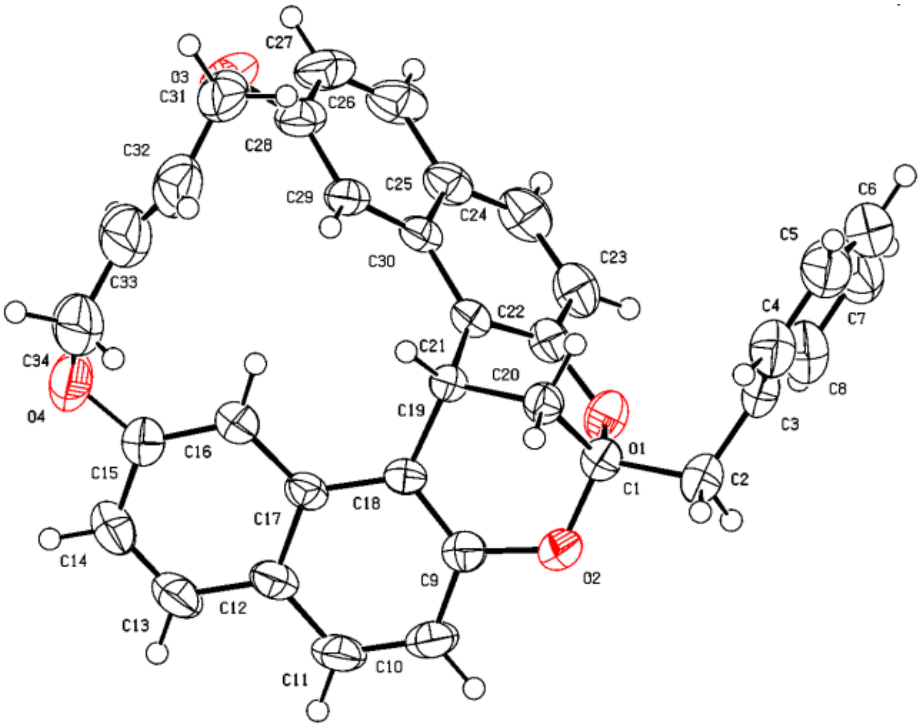

Figure 6: Single Crystal X-ray structure of compound *trans*-**3afa** with 50% ellipsoid probability.

Table 17. Crystal data and structure refinement for *trans*-3afa.	
CCDC no.	2294906
Empirical formula	$C_{34}H_{26}O_4$
Formula weight	498.39
Temperature/K	298
Crystal system	monoclinic
Space group	$P2_1/c$
a/Å	23.325(3)
b/Å	9.2221(10)
c/Å	11.5821(16)
α/°	90
β/°	97.078(4)

γ/°	90
Volume/Å^3	2472.4(5)
Z	4
ρ_{calc}g/cm^3	1.339
μ/mm^{-1}	0.087
F(000)	1048.0
Crystal size/mm^3	0.201 × 0.156 × 0.123
Radiation	MoKα (λ = 0.71073)
2Θ range for data collection/°	4.754 to 53.01
Index ranges	-29 ≤ h ≤ 28, -11 ≤ k ≤ 11, -14 ≤ l ≤ 14
Reflections collected	28242
Independent reflections	5103 [R_{int} = 0.0755, R_{sigma} = 0.0520]
Data/restraints/parameters	5103/0/343
Goodness-of-fit on F^2	1.035
Final R indexes [I>=2σ (I)]	R_1 = 0.0652, wR_2 = 0.1587
Final R indexes [all data]	R_1 = 0.0879, wR_2 = 0.1733
Largest diff. peak/hole / e Å^{-3}	0.70/-0.34

Table 18. Bond Lengths for *trans*-3afa.

Atom	Atom	Length/Å	Atom	Atom	Length/Å
O1	C1	1.436(3)	C3	C4	1.383(4)
O1	C22	1.379(3)	C8	C7	1.376(4)
O3	C28	1.371(3)	C7	C6	1.375(5)
O3	C31	1.410(3)	C6	C5	1.367(5)

O2	C1	1.422(3)	C32	C31	1.479(4)
O2	C9	1.377(3)	C5	C4	1.379(4)
O4	C34	1.444(5)	C22	C23	1.412(3)
O4	C15	1.371(3)	C22	C21	1.368(3)
C33	C34	1.466(5)	C23	C24	1.352(4)
C33	C32	1.280(5)	C24	C25	1.404(4)
C15	C16	1.373(3)	C25	C26	1.414(3)
C15	C14	1.393(4)	C25	C30	1.425(3)
C16	C17	1.415(3)	C26	C27	1.346(4)
C17	C18	1.435(3)	C27	C28	1.405(4)
C17	C12	1.422(3)	C28	C29	1.367(3)
C18	C19	1.529(3)	C29	C30	1.416(3)
C18	C9	1.374(3)	C30	C21	1.431(3)
C19	C20	1.533(3)	C9	C10	1.405(3)
C19	C21	1.517(3)	C10	C11	1.351(4)
C20	C1	1.502(3)	C11	C12	1.405(4)
C1	C2	1.518(3)	C12	C13	1.408(4)
C2	C3	1.502(4)	C13	C14	1.347(4)
C3	C8	1.384(4)			

Table 19. Bond Angles for *trans*-3afa.

Atom	Atom	Atom	Angle/°	Atom	Atom	Atom	Angle/°
C22	O1	C1	119.75(17)	C6	C5	C4	120.2(3)
C28	O3	C31	117.8(2)	C5	C4	C3	121.0(3)
C9	O2	C1	116.72(17)	O1	C22	C23	114.0(2)

C15	O4	C34	117.6(2)	C21	C22	O1	123.0(2)
C32	C33	C34	128.1(5)	C21	C22	C23	123.0(2)
O4	C34	C33	109.3(3)	C24	C23	C22	118.9(2)
O4	C15	C16	125.3(2)	C23	C24	C25	121.1(2)
O4	C15	C14	113.3(2)	C24	C25	C26	121.6(2)
C16	C15	C14	121.3(2)	C24	C25	C30	120.0(2)
C15	C16	C17	120.8(2)	C26	C25	C30	118.5(2)
C16	C17	C18	123.71(19)	C27	C26	C25	122.1(2)
C16	C17	C12	117.0(2)	C26	C27	C28	119.6(2)
C12	C17	C18	119.2(2)	O3	C28	C27	114.8(2)
C17	C18	C19	123.89(18)	C29	C28	O3	124.4(2)
C9	C18	C17	117.55(19)	C29	C28	C27	120.9(3)
C9	C18	C19	118.55(19)	O3	C31	C32	116.5(3)
C18	C19	C20	108.87(17)	C28	C29	C30	120.7(2)
C21	C19	C18	112.62(17)	C25	C30	C21	118.5(2)
C21	C19	C20	104.95(16)	C29	C30	C25	118.2(2)
C1	C20	C19	107.55(17)	C29	C30	C21	123.29(19)
O1	C1	C20	112.46(18)	C22	C21	C19	116.10(19)
O1	C1	C2	107.32(19)	C22	C21	C30	118.17(19)
O2	C1	O1	106.21(18)	C30	C21	C19	125.63(19)
O2	C1	C20	109.79(18)	O2	C9	C10	112.9(2)
O2	C1	C2	105.17(18)	C18	C9	O2	124.21(19)
C20	C1	C2	115.3(2)	C18	C9	C10	122.9(2)
C3	C2	C1	113.5(2)	C11	C10	C9	119.8(2)
C8	C3	C2	120.9(2)	C10	C11	C12	120.7(2)

C4	C3	C2	121.2(2)	C11	C12	C17	119.8(2)
C4	C3	C8	117.9(3)	C11	C12	C13	120.3(2)
C7	C8	C3	121.0(3)	C13	C12	C17	119.9(2)
C6	C7	C8	120.2(3)	C14	C13	C12	121.5(2)
C5	C6	C7	119.6(3)	C13	C14	C15	119.4(2)
C33	C32	C31	125.4(4)				

APPENDIX B: COMPUTATIONAL STUDIES

Computational Studies for Chapter 2A

All calculations are performed with **ONIOM (wB97XD/6-31G(d,p): PM6)** using the Gaussian 09 software[6]. The **wB97XD** functional is chosen for its ability to describe both long-range and short-range interactions with Pople double-zeta basis including both *d* and *p* polarization for accurate description of phenyl-migration. The **PM6** semi-empirical method is applied to the catalyst and two other aryl groups.

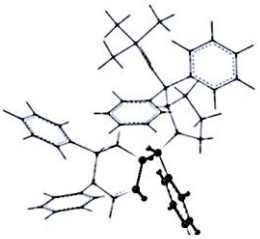

Figure 7: Species "C" representing high and low layers.

All structures (including minimum and transition states) and pathways have been first optimized and scanned using HF/STO-3G[7,8] which were used as guess geometries (input for the ONIOM model). The structures are then separated into a **high-layer (shown using wireframe)** using DFT functional wB97XD[9] with 6-31G(d,p)[10] basis set, and a **low-layer (shown using ball and stick)** using semi-empirical method PM6[11] as represented in Figure 7.

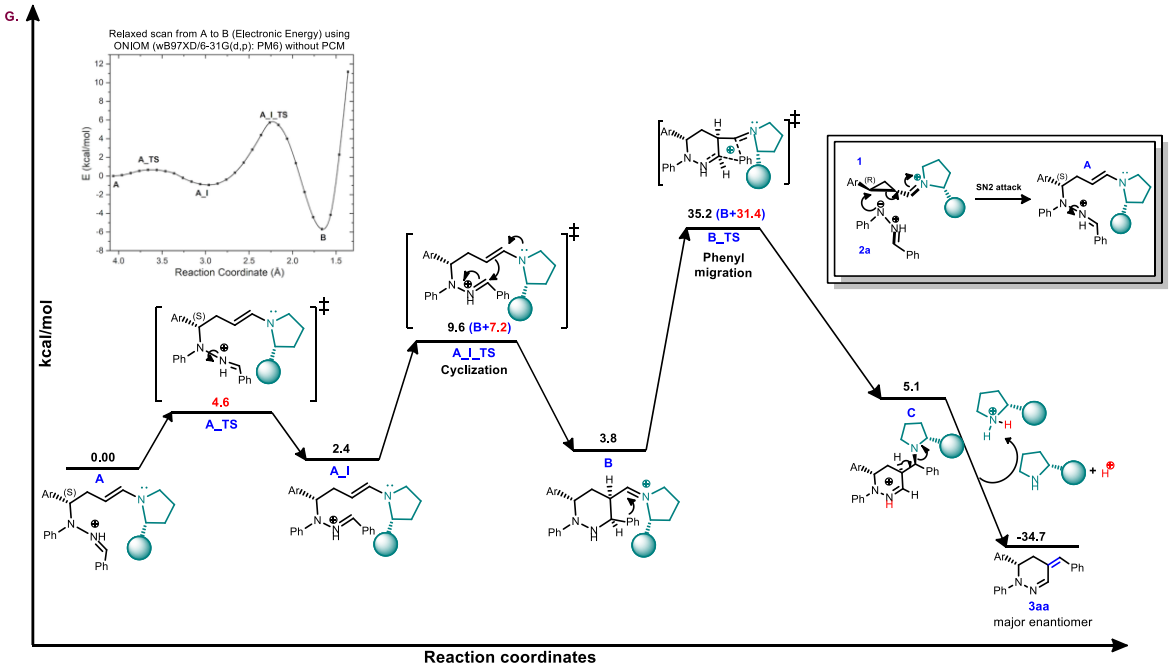

Figure 8: Reaction coordinates for cyclization and phenyl migration. All energies are in kcal/mol (Gibbs free energy). The relaxed scan shows electronic energy (without PCM) for cyclization of A to form B (Bond distance C-C from 4.2 - 1.4 Å).

The catalyst (bearing Si atom) and the two aryl groups (on the left) have been included in the low layer while the aryl group (the one that migrates on the right) along with adjacent carbon atoms have been included in the high layer.

The solvent effect has been incorporated through single-point frequency calculations using the Polarizable Continuum Model (PCM)[12] at 349.87 K (reflux temperature of CCl_4). All energies reported in reaction coordinate in Figure 8 are the Gibbs free energy (ΔG) of the molecules. The ΔG from A to C is calculated directly while ΔG of 3aa is obtained by subtracting the energy of the (catalyst + D) and adding the energy of the protonated catalyst.

All structures:

1 (R) + 2a	**A (S)**	**A_TS**
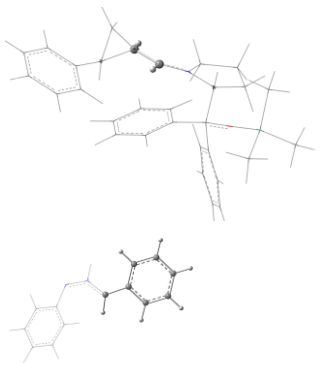	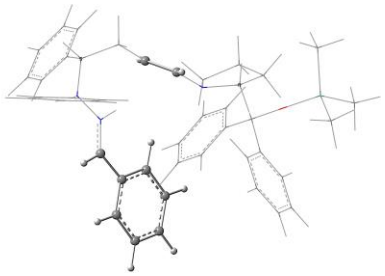	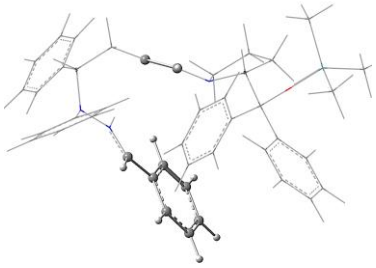
A_I	**A_I_TS**	**B**
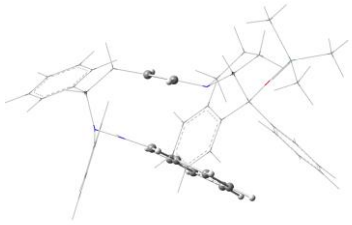	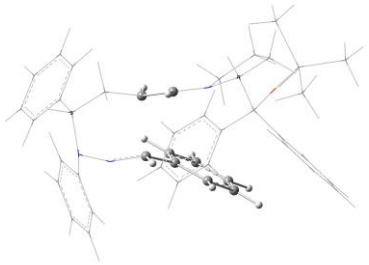	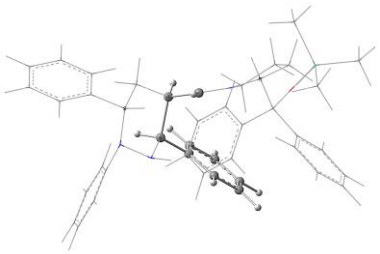
B_TS	**C**	**3aa**

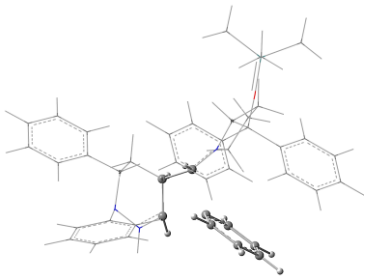	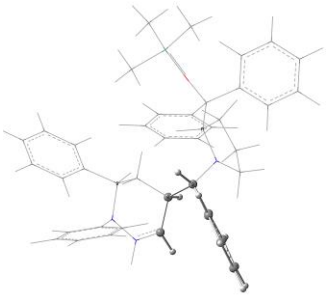	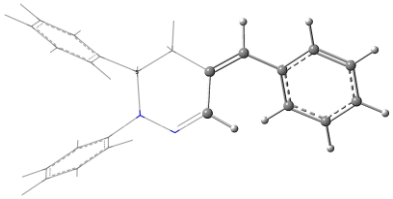
D (3aa + H^+)	**Catalyst**	**Catalyst (H^+)**
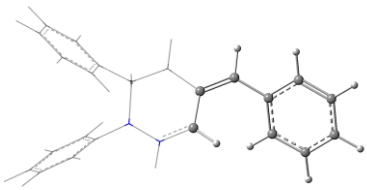	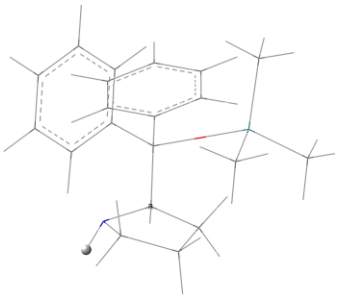	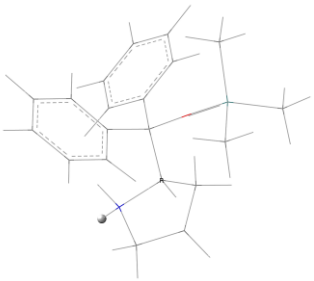

References

1. Bruker, SAINT V7.68A, Bruker AXS Inc., Madison (WI, USA) **2005**.

2. Sheldrick, G. M. SADABS 2008/2, Göttingen **2008**.

3. Altomare, A.; Cascarano, G.; Giacovazzo, C.; Guagliardi, A. *J. Appl. Cryst.,* **1993**, *26*, 343.

4. Sheldrick, G. M. SHELXL-97, Program for Crystal Structure Solution and Refinement, University of Göttingen, Göttingen, Germany 1997.

5. Farrugia, L. J.; WinGX-A Windows Program for Crystal Structure Analysis, *J. Appl. Cryst.* **1999**, *32*, 837.

6. M. J. Frisch, G. W. Trucks, H. B. Schlegel, G. E. Scuseria, M. A. Robb, J. R. Cheeseman, G. Scalmani, V. Barone, B. Mennucci, G. A. Petersson, H. Nakatsuji, M. Caricato, X. Li, H. P. Hratchian, A. F. Izmaylov, J. Bloino, G. Zheng, J. L. Sonnenberg, M. Hada, M. Ehara, K. Toyota, R. Fukuda, J. Hasegawa, M. Ishida, T. Nakajima, Y. Honda, O. Kitao, H. Nakai, T. Vreven, J. A. Montgomery, Jr., J. E. Peralta, F. Ogliaro, M. Bearpark, J. J. Heyd, E. Brothers, K. N. Kudin, V. N. Staroverov, R. Kobayashi, J. Normand, K. Raghavachari, A. Rendell, J. C. Burant, S. S. Iyengar, J.

Tomasi, M. Cossi, N. Rega, J. M. Millam, M. Klene, J. E. Knox, J. B. Cross, V. Bakken, C. Adamo, J. Jaramillo, R. Gomperts, R. E. Stratmann, O. Yazyev, A. J. Austin, R. Cammi, C. Pomelli, J. W. Ochterski, R. L. Martin, K. Morokuma, V. G. Zakrzewski, G. A. Voth, P. Salvador, J. J. Dannenberg, S. Dapprich, A. D. Daniels, Ö. Farkas, J. B. Foresman, J. V. Ortiz, J. Cioslowski, and D. J. Fox, Gaussian 09 (Gaussian, Inc., Wallingford CT, 2009).

7. C. C. J. Roothaan, *Rev. Mod. Phys*., **1951**, 23, 69-89. DOI: 10.1103/RevModPhys.23.69

8. W. J. Hehre, R. F. Stewart, and J. A. Pople, *J. Chem. Phys*., **1969**, 51, 2657-2664. DOI: 10.1063/1.1672392

9. J.-D. Chai, M. Head-Gordon, *Phys. Chem. Chem. Phys*., **2008**, 10, 6615-6620. DOI: 10.1039/B810189B

10. M. M. Francl, W. J. Pietro, W. J. Hehre, J. S. Binkley, D. J. DeFrees, J. A. Pople, M. S. Gordon, *J. Chem. Phys.,* **1982,** 77, 3654-3665. DOI: 10.1063/1.444267

11. J. J. P. Stewart, *J. Mol. Model.,* **2007**, 13, 1173-213. DOI: 10.1007/s00894-007-0233-4

12. T. Vreven, B. Mennucci, C. O. da Silva, K. Morokuma, J. Tomasi, *J. Chem. Phys.,* **2001**, 115, 62-72. DOI: 10.1063/1.1376127

Bio-Data

Name: Arijit Hazra

Date of Birth: 2nd November, 1993

Educational Qualification:

- **2016: Bachelor of Science** from the Department of Chemistry, Burdwan Raj College, Burdwan, West Bengal, India.
- **2018: Master of Science** from the Department of Chemistry, The University of Burdwan, West Bengal, India.
    - **Project:** Oxidation of β-cyclodextrin and its purification by size exclusion chromatography.

Achievements:

- Qualified **Graduate Aptitude Test for Engineering (GATE)** in 2019.